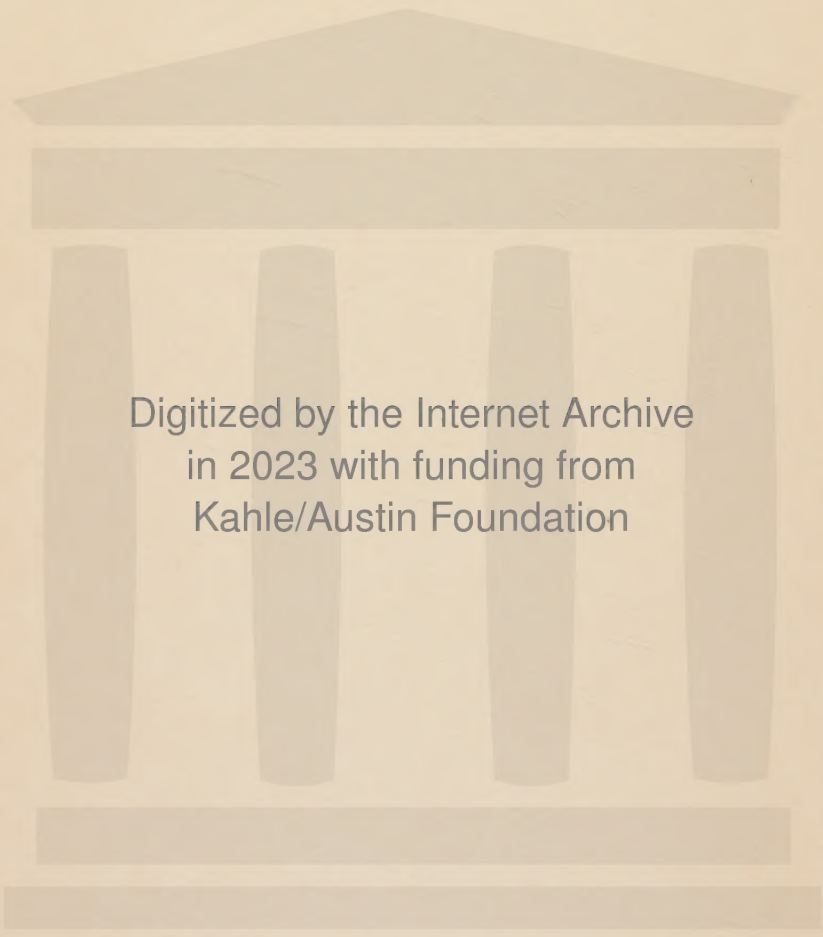
Digitized by the Internet Archive
in 2023 with funding from
Kahle/Austin Foundation

https://archive.org/details/contributionsfro0018unse

Carnegie Institution of Washington

UNIVERSITY OF ARIZONA
STEWARD OBSERVATORY
TUCSON, ARIZONA

CONTRIBUTIONS

FROM THE

MOUNT WILSON OBSERVATORY

VOLUME XVIII

NOS. 391–419

WITH FOURTEEN PLATES

DECEMBER, 1929—NOVEMBER, 1930

UNIVERSITY OF ARIZONA
LIBRARY

C28
V.18

CONTENTS

NO. PAGE

391. The Photographic Determination of Stellar Parallaxes with the 60-Inch and 100-Inch Reflectors. Eleventh Series. *Adriaan van Maanen* 1

392. Lunar Radiation and Temperatures. *Edison Pettit* and *Seth B. Nicholson* 21

393. The Spectrohelioscope and Its Work. Part II. The Motions of the Hydrogen Flocculi near Sun-Spots. *George E. Hale* . 55

394. On the Radial Velocity of R Lyrae. *Roscoe F. Sanford* . . 85

395. A Method for Determining the Distribution of Stellar Absolute Magnitudes from the Distributions of Angular and Linear Peculiar Velocities. *Gustaf Strömberg* 93

396. The Distribution of Absolute Magnitudes among K and M Stars Brighter than the Sixth Apparent Magnitude as Determined from Peculiar Velocities. *Gustaf Strömberg* . 105

397. Spectral Energy-Curve of Sun-Spots. *Edison Pettit* and *Seth B. Nicholson* 121

398. Distribution of Luminosity in Elliptical Nebulae. *Edwin Hubble* 131

399. Behavior of Bright Lines in the Spectra of Several Long-Period Variable Stars. *Paul W. Merrill* and *Cora G. Burwell* . 177

400. The Rayton Short-Focus Spectrographic Objective. *Milton L. Humason* 229

401. A Spectrographic Study of U Sagittae. *Alfred H. Joy* . . 235

402. Evidence from Band Spectra of the Existence of a Carbon Isotope of Mass 13. *Arthur S. King* and *Raymond T. Birge* . 251

403. The Spectrographic Orbit of RS Canum Venaticorum. *Alfred H. Joy* 273

404. Variations in Radial Velocity of the Cepheid Variables W Geminorum, U Aquilae, and DT Cygni. *Roscoe F. Sanford* . 279

405. Investigations on Proper Motion. Thirteenth Paper: The Proper Motion of N.G.C. 2264. *Adriaan van Maanen* . . . 293

406. Investigations on Proper Motion. Fourteenth Paper: The Proper Motions of Six Planetary Nebulae. *Adriaan van Maanen* 299

375503

CONTENTS

NO. PAGE

407. Investigations on Proper Motion. Fifteenth Paper: The Proper Motion of the Spiral Nebula N.G.C. 4051. *Adriaan van Maanen* 305

408. Investigations on Proper Motion. Sixteenth Paper: The Proper Motion of Messier 51, N.G.C. 5194. *Adriaan van Maanen* 311

409. Notes on the Spectra of Ten Bright-Line Stars of Classes B and A. *Paul W. Merrill* 315

410. A Method for Determining the Distribution of Stellar Absolute Magnitudes from the Distributions of Parallactic Motions and Radial Velocities. *Gustaf Strömberg* . . . 329

411. The Distribution of Absolute Magnitudes among M Stars Brighter than the Sixth Apparent Magnitude as Determined from Parallactic and Peculiar Velocities. *Gustaf Strömberg* 335

412. Investigations on Proper Motion. Seventeenth Paper: Proper Motions of Some Very Faint Stars. *Adriaan van Maanen* and *Howard C. Willis* 345

413. Multiplet Intensities in the Solar Spectrum. *R. van der R. Woolley* 361

414. Temperature Classification of the Spectra of Europium, Gadolinium, Terbium, Dysprosium, and Holmium, λ 3850 to λ 4700. *Arthur S. King* 373

415. Magnitudes of Southern Comparison Stars for Eros. *F. H. Seares, B. W. Sitterly,* and *Mary C. Joyner* 409

416. Temperature Classification of the Stronger Lines of Columbium, with Preliminary Notes on Their Hyperfine Structure. *Arthur S. King* 441

417. Positions, Orbit, and Mass of Pluto. *Seth B. Nicholson* and *Nicholas U. Mayall* 455

418. The Distribution of Absolute Magnitudes among K Stars Brighter than the Sixth Apparent Magnitude as Determined from Parallactic and Peculiar Velocities. *Gustaf Strömberg* 467

419. Photometric and Spectrographic Orbits of TT Aurigae. *Alfred H. Joy* and *Bancroft W. Sitterly* 481

LIST OF PLATES

NO.		FACING PAGE
I.	Photograph of Full Moon, Showing Points Measured To Obtain Distribution-Curves for Planetary Heat and Reflected Light	34
II.	Flocculi near Large Sun-Spot	56
III.	Bright and Dark Hydrogen Flocculi with Bipolar Sun-Spot	74
IV.	Bright and Dark Hydrogen Flocculi with Bipolar Sun-Spot	76
V.	Three Successive Photographs of a Prominence	82
VI.	Elliptical Nebulae Photographed with 100-Inch Reflector	135
VII.	Spectra Taken with Rayton Camera Lens	233
VIII.	Region of Cluster of Spirals in Perseus	234
IX.	Carbon Band λ 4737 and Isotope Band λ 4744.5	256
X.	Microphotometer Curves of the Carbon Band λ 4737 and Its Isotope λ 4744.5	256
XI.	Microphotometer Curves of Carbon and Cyanogen Bands and Their Isotopes	263
XII.	Band Structures with Isotopes	266
XIII.	Spectrograms of RS Canum Venaticorum	276
XIV.	Spectrum of Gadolinium	405

Contributions from the Mount Wilson Observatory, No. 391
Printed in the U.S.A.

STANFORD OBSERVATORY

THE PHOTOGRAPHIC DETERMINATION OF STELLAR PARALLAXES WITH THE 60- AND 100-INCH REFLECTORS[1]

ELEVENTH SERIES

By ADRIAAN VAN MAANEN

ABSTRACT

Trigonometric parallaxes determined with the 60- and 100-inch reflectors.—Detailed results are given for 25 fields, including 29 stars and nebulae. The list includes the large planetary nebula N.G.C. 246; two Cepheid variables, SU Draconis and XZ Cygni; several faint stars with large proper motion; and one nova, Nova Lyrae.

The present paper contains the results for 25 fields which have recently been measured for parallaxes. The work has been carried out in the same way as for the previously published series.[1]

Table I gives the results of these measures; the data for each field are collected in tables which are arranged as in the last five series. For the 17 fields observed at the Cassegrain focus (80 ft.) of the 60-inch reflector the mean probable error is $\pm 0''.0065$; for the 8 fields observed at the Newtonian focus (42 ft.) of the 100-inch reflector, $\pm 0''.0139$. The considerably larger error derived in the latter case is partly due to the shorter focal length; the principal source of uncertainty, however, is the fact that at the Newtonian focus the quality of the images falls off much more rapidly with distance from the center than at the Cassegrain focus.

After excluding N.G.C. 6891, for which the measures are probably vitiated by the surrounding nebulosity, the objects thus far measured at the 100-inch reflector total 46. The probable errors of the parallaxes were arranged in two ways: (*a*) according to the mean distance from the center of the comparison stars and (*b*) according to the largest distance of any of the comparison stars in each field. Table II gives the results.

This summary plainly indicates that in order to increase the re-

[1] *Mt. Wilson Contr.*, Nos. 111, 1916; 136, 1917; 158, 1918; 182, 1920; 204, 1921; 237, 1922; 270, 1923; 290, 1925; 321, 1926; 356, 1928.

liability of the results it will be necessary to avoid comparison stars which are farther from the center than 7′ or 8′, and that, in general,

TABLE I

Object	α 1900	δ 1900	Vis. Mag. Harvard	Mount Wilson Spectrum	Relative Parallax	μ_α	P.E.		No. of Exp.	Instrument
α Cassiopeiae	$0^h34^m50^s$	+55° 59′	2.47	G8	+0″.014	+0″.035	8	3	16	60
N.G.C. 246	0 42 0	−12 25	11.6*	Pl. Neb.	+0.006	−0.041	6	3	16	100
γ Andromedae A	1 57 45	+41 51	2.28	K2	+0.007	+0.038	4	2	18	60
γ Andromedae BC	1 57 46	+41 51	5.08	Ao‡	−0.004	+0.035	7	3	18	60
No. 190 in N.G.C. 1647	4 41 17	+18 58	12.40†	.....	+0.006	+0.004	5	9	18	60
I.C. 405	5 9 42	+34 12	5.81	Bop‡	−0.001	−0.013	4	3	16	60
βG.C. 2654	5 14 8	− 3 11	8.6	K5	+0.007	+0.717	35	16	14	100
N.G.C. II 2149	5 48 54	+46 6	10.2	Pl. Neb.	−0.018	−0.004	5	2	16	60
6 Lyncis	6 22 6	+58 14	5.96	G8	+0.037	−0.026	5	1	16	60
Boss 2410	8 53 32	+18 31	6.57	M4	−0.005	−0.049	14	7	16	60
SU Draconis	11 32 15	+67 53	Var.	A2‡	−0.019	−0.032	9	2	16	60
Σ 1835 BC	14 18 28	+ 8 54	6.64	F1s	+0.019	−0.068	10	2	16	60
Wolf 562	15 14 14	− 7 21	11.7‡	M5	+0.217	−1.308	23	11	18	100
49 Serpentis	16 8 39	+13 48	7.50§	Ko	+0.046	+0.194	7	3	20	60
49 Serpentis Comp.	16 8 39	+13 48	7.70§	Ko	+0.050	+0.186	7	4	20	60
W.B. 16^h 1259	16 41 23	+33 41	8.6	Mo	+0.106	−0.038	6	5	16	60
Wolf 636	17 0 2	− 4 55	10.4‖	M3	+0.015	−0.880	21	11	16	100
Furuhjelm 46	17 9 12	+45 50	9.6	M4	+0.150	+0.297	6	6	16	60
α Herculis	17 10 5	+14 30	3.48	M5	−0.001	+0.001	3	1	20	60
α Herculis Comp.	17 10 6	+14 30	5.39	F9	0.000	+0.002	4	1	20	60
Ross 136	18 17 12	+ 6 17	14.6‖	.....	+0.084	−1.261	6	6	20	100
βG.C. 8512	18 17 35	+11 24	8.9¶	.....	−0.015	−0.005	4	4	20	60
βG.C. 8512 Comp.	18 17 35	+11 24	9.9¶	.....	−0.007	−0.012	8	7	20	60
Nova Lyrae	18 49 31	+29 6	15.3‖	.....	+0.015	−0.006	7	3	16	100
XZ Cygni	19 30 25	+56 10	Var.	.....	+0.003	+0.083	8	2	16	60
Wolf 901	20 54 6	+ 3 10	13.2‖	.....	+0.032	+0.345	6	2	18	100
Anonymous	21 24 17	+11 43	11.1‖	.....	+0.028	+0.202	7	9	16	60
Lalande 42883	21 54 15	+29 21	6.83	F5s	+0.020	−0.392	6	4	18	60
Wolf 1337	21 54 49	− 1 8	13.7‖	.....	+0.015	−0.204	7	5	18	100

* Magnitude by Hubble.

† Photographic magnitude by Hertzsprung, *Mt. Wilson Contr.*, No. 100.

‡ Spectrum from *Henry Draper Catalogue.*

§ The combined magnitude in the *Henry Draper Catalogue* is 6.84.

‖ Photographic magnitude, derived from counts of the number of stars of equal and brighter magnitude and based on Table IV of *Groningen Publications*, No. 27.

¶ Magnitude from Burnham's *General Catalogue.*

TABLE II

Mean r	Mean P.E.	n	Maximum r	Mean P.E.	n
2′.2	0″.0053	6	≦5′	0″.0054	7
3.4	0.0070	8	5 −7	0.0086	8
4.7	0.0060	7	7 −9	0.0108	18
5.5	0.0129	17	9 −11	0.0108	11
6.2	0.0124	5	11 −14	0.0245	2
9.7	0.0197	3			

care should be taken that the mean distance does not exceed 5′. Both conditions can be fulfilled by using sufficiently faint comparison

stars, and the only fields to be avoided are those of bright stars which cannot be reduced adequately with the present arrangement of the rotating single sector.

Some of the fields given in Table I require special comment; in the following discussion the systematic errors published in *Mt. Wilson Contr.* No. 357 have been applied.

a) *The parallax and proper motion of N.G.C. 246.*—This object is one of the largest planetary nebulae in the sky, being $4' \times 3'.5$ in diameter. Curtis gives the magnitude of the central star as 9.5 and notes that it is bluish and considerably brighter photographically than visually. It is, in fact, a double star, having a companion at a distance of $4''$.

On Cramer Inst. Iso plates, taken through a yellow color-screen at the Newtonian focus of the 100-inch telescope, the magnitude of the principal star is between 11.5 and 12, while the companion is about 1.5 mag. fainter. These magnitudes are based on counts of stars of equal or brighter magnitude, but as the galactic latitude is $-75°$, the numbers are too small to allow great accuracy. For the principal star Hubble has found a magnitude of about 11.6 and a spectrum of about B0, while for the companion he has estimated from exposure ratios a color-index corresponding to a spectral type of G5–K. From 16 exposures I have derived a parallax for both stars, and have determined the proper motions from two pairs of exposures with a 7-year interval. The results are:

	Central Star	Companion
π_{rel}	$+0''.006 \pm 0''.006$	$+0''.011 \pm 0''.025$
μ_α	-0.041 ± 0.003	-0.041 ± 0.010
μ_δ	-0.014 ± 0.004	-0.011 ± 0.003

The proper motions are so large and so nearly equal as to leave little doubt that the stars form a physical pair. The weighted mean absolute parallax is $+0''.009$. If the apparent magnitudes are taken as 11.6 and 13.0, the absolute magnitudes will be +6.4 and +7.8.

It is hoped that it will be possible to obtain a spectrum of the companion when the field comes again within reach. This should make a determination of the absolute magnitude of the central star

of this nebula fairly reliable and may furnish a check on the trigonometric parallax.

b) *SU Draconis and XZ Cygni.*—This adds 2 more Cepheids to the Mount Wilson parallaxes, making a total of 14. While the individual values of the parallaxes for these stars are too small to be of much use, they afford valuable data for the determination of systematic errors. For the fields taken with the 100-inch reflector the material is still too scanty to derive such errors, but those for the 60-inch fields given in *Mt. Wilson Contr.* No. 357 are thought to be well founded. Of the 14 Cepheids, 2 were taken with the 100-inch, viz., Y Ophiuchi and Y Sagittarii; the mean distances of the comparison stars were 6'.2 and 7'.5, respectively, while the greatest distance in each case was 9'.2 and 10'.2, respectively. From what has been said above, both parallaxes are none too reliable. Comparing the 12 stars taken at the 60-inch reflector with the values determined by Shapley, we find

$$\bar{\pi} \text{ uncorrected} = +0''.0043;\ \bar{\pi} \text{ corrected} = +0''.0018;$$
$$\bar{\pi} \text{ Shapley} = +0''.0019.$$

For 9 of these stars Mr. Adams and his collaborators have determined spectroscopic parallaxes; a comparison with these gives

$$\bar{\pi} \text{ uncorrected} = +0.0080;\ \bar{\pi} \text{ corrected} = +0''.0031;$$
$$\bar{\pi} \text{ Spectr.} = +0''.0030.$$

Although the material is insufficient to permit final conclusions, it does strongly corroborate the validity of the investigation of the systematic errors already published.

c) *Wolf 562.*—The corrected absolute parallax is +0".0213, the spectroscopic parallax +0".200. In *Bulletin of the Astronomical Institutes of the Netherlands*, No. 5, Hertzsprung gives 29 stars with parallaxes exceeding 0".2, of which 8 are companions. In looking through my card catalogue I find 10 more objects which may now be added to Hertzsprung's list published in 1922. These are collected in Table III.

On the other hand, more recent determinations of the parallax of α Aquilae, which is included in Hertzsprung's list, reduces the parallax to +0".198, just below the adopted limit of 5 parsecs. At

present we therefore know 38 stars within this distance, 10 of which, however, are components of double stars. According to Kapteyn and van Rhijn, the number of stars (counting double stars as one) per cubic parsec in the vicinity of the sun is 0.0451,[1] while according to Seares the number of stars in our immediate neighborhood (again counting double stars as single) brighter than absolute magnitude +14.86 is 0.098 per cubic parsec.[2] The number required by Kapteyn and van Rhijn, viz., 24, is therefore already surpassed by 4; of the number required by Seares's formula, viz., 51, we know at present 25 (3 of the stars are fainter than +14.86).

TABLE III

Star	α 1900	δ 1900	Vis. Mag.	π	M	Sp.	μ
o_2 Eridani A.....	$4^h10^m40^s$	$-7°49'$	4.48	0".200	+6.0	G5	4".082
o_2 Eridani B.....	4 10 45	−7 49	9.7	0.200	+11.2	A	4.082
o_2 Eridani C.....	4 10 45	−7 49	10.8	0.200	+12.3	Md	4.082
Groomb. 1618....	10 5 15	+49 58	6.82	0.208	+8.4	K5	1.451
W.B. 10^h234.....	10 14 11	+20 22	9.2	0.217	+10.9	Mdp	0.49
Wolf 359.....	10 51 38	+7 36	13.5	0.407	+16.5	M4e	4.84
Lalande 25372...	13 40 40	+15 26	8.5	0.213	+10.1	M6	2.298
Wolf 562.....	15 14 14	−7 21	10.7	0.209	+12.3	M5	1.33
B.D.−12°4523...	16 24 45	−12 24	9.5	0.327	+12.1	M5	1.24
B.D.+43°4305...	22 42 31	+43 49	9.5	0.208*	+11.1	M5e	0.858

* Since this article was sent to the printer, I have found for the absolute parallax of this star 0".213±0.006.

d) *Wolf 636.*—This is one of the stars of a wide pair, which has been measured before. The field is apparently hard to measure, as the former values, published in *Mt. Wilson Contr.* No. 321, also had large probable errors. The mean of the three quite discordant values is exactly +0".100; the mean of the values obtained at McCormick, Yerkes, and Allegheny is +0".079; the mean of the spectroscopic determinations is +0".120.

e) *Furuhjelm 46, Ross 136, Wolf 901 and 1337* are four stars of large proper motion, whose photographic absolute magnitudes are +11.7, +14.2, +11.0, and +10.2, respectively. All these stars, as well as those under *c* and *d*, are additions to the rapidly growing number of stars fainter than absolute magnitude +10.

To this list should also be added the faint companion of the star

[1] *Mt. Wilson Contr.*, No. 188; *Astrophysical Journal*, **52**, 32, 1920.

[2] *Mt. Wilson Contr.*, No. 273; *Astrophysical Journal*, **59**, 337, 1924.

given in Table I as "anonymous" ($\alpha = 21^h24^m17^s$, $\delta = +11°43'$, $\Delta = 1''.13$, $p = 56°$), which undoubtedly has the same parallax as the principal star, as they have the same proper motion, $0''.499$. Its photographic absolute magnitude is +11.8. The faint companion is, according to Mr. Humason, well seen at the Cassegrain focus of the 100-inch telescope, and is redder than the bright component, the spectral type of which has been estimated as K5.

f) Nova Lyrae.—This nova was found on Harvard plates by Miss Mackie. Between December 4 and 6, 1919, its brightness increased from magnitude 16 to 6.5; in April, 1920, it had decreased to 9.5, while on the parallax plates taken in 1928 it was again as faint as 15.3. The absolute parallax is $+0''.016$, which would give absolute magnitudes of +2.5 and +12.0 at maximum and minimum, respectively.

Carnegie Institution of Washington
Mount Wilson Observatory
December 1929

α Cassiopeiae $\alpha = 0^h 34^m 50^s$ $\delta = +55°59'$

Mor.	Ev.	t_1	t_2	Δ_p	M	v
7.630	12.958	−14°.5	− 3°.2	+1.52	−68	− 3
7.630	12.906	−10.5	+ 2.0	+1.39	−66	− 1
13.606	12.958	+ 2.0	+ 3.5	+1.61	+29	+11
7.625	12.906	+ 3.0	+ 6.2	+1.41	−69	− 4
13.607	10.879	+ 6.0	+ 7.5	+1.38	+12	−34
7.625	10.882	+ 7.0	+ 7.5	+1.33	−30	+ 7
13.609	10.882	+ 7.5	+13.0	+1.38	+41	− 5
13.612	10.879	+10.2	+15.0	+1.36	+72	+26

$+117.57\,\mu_\alpha - 14.92\,\pi = +1533$
$-\ 14.92\,\mu_\alpha + 16.24\,\pi = -\ 113$
$\pi = +\ 5.7 = 0''.014 \pm 0''.008$
$\mu_\alpha = +13.8 = +0''.035 \pm 0''.003$

No.	Br.	x	y	π
1.....	f	+0'.1	+3'.8	−0''.001
2.....	f	+4.1	+0.5	−0.007
3.....	bf	+3.3	−4.8	+0.006
4.....	f	−1.6	−3.7	−0.004
5.....	f	−5.2	+2.2	0.000
6.....	f	−0.8	+2.7	+0.007

N.G.C. 246 $\alpha = 0^h 42^m 0^s$ $\delta = -12°25'$

Mor.	Ev.	t_1	t_2	Δ_p	M	M(Comp.)	v	v(Comp.)
6.586	12.903	−7°.0	−14°.0	+1.53	+54	+58	−1	+ 2
13.617	12.900	−6.7	−12.5	+1.43	− 8	−31	−4	−28
7.635	12.903	−5.0	−10.2	+1.37	+40	+31	−6	−16
13.617	12.900	−3.7	− 7.7	+1.43	+ 2	−25	+6	−22
11.674	8.852	−4.0	− 5.5	+0.98	−29	+ 5	−6	+27
6.586	8.849	−4.0	− 4.7	+1.29	+28	+46	+7	+24
7.636	9.903	−2.2	+ 1.0	+1.36	+27	+49	+6	+27
11.674	12.961	0.0	+11.2	+1.35	+ 8	+11	−5	− 3

$+88.62\,\mu_\alpha - 19.82\,\pi = -773$ } N.G.C.
$-19.82\,\mu_\alpha + 14.59\,\pi = +186$ } 246
$= -785$ } Comp.
$= +197$ }
$\pi = +1.3 = +0''.006 \pm 0''.006$ } N.G.C.
$\mu_\alpha = -8.4 = -0''.041 \pm 0''.003$ } 246
$\pi = +2.2 = +0''.011 \pm 0''.025$ } Comp.
$\mu_\alpha = -8.4 = -0''.041 \pm 0''.010$ }

No.	Br.	x	y	π
1.....	bf	−1'.3	+1'.7	+0''.003
2.....	bf	−0.8	−0.5	−0.012
3.....	f	−1.8	−2.2	+0.009
4.....	f	+1.4	−0.6	+0.001

γ Andromedae $\alpha = 1^h57^m45^s$ $\delta = +41°51'$

Mor.	Ev.	l_1	l_2	Δ_p	$M(A)$	$M(BC)$	$v(A)$	$v(BC)$
7.625	12.958	− 8°0	−10°0	+1.61	−61	−61	+14	+15
13.705	12.906	− 7.0	− 8.2	+1.12	+13	+19	− 2	+10
7.627	12.906	− 5.7	− 4.0	+1.38	−73	−62	+ 2	+13
7.625	11.032	− 3.5	+ 2.5	+1.79	−51	−66	− 5	−16
13.705	11.043	− 2.7	+ 9.0	+1.53	+44	+28	0	− 7
7.627	11.032	− 1.0	+ 9.2	+1.78	−64	−72	−18	−22
13.710	13.054	+ 2.5	+ 9.5	+1.51	+12	− 3	− 2	−10
13.707	11.043	+ 3.2	+15.5	+1.52	+48	+44	+ 4	+ 9
13.708	13.054	+10.2	+15.7	+1.52	+23	+24	+ 9	+17

$$\left.\begin{aligned} +95.14\,\mu_a - 17.02\,\pi &= +1380 \\ -17.02\,\mu_a + 21.35\,\pi &= - 196 \end{aligned}\right\}(A)$$

$$\left.\begin{aligned} &= +1342 \\ &= - 268 \end{aligned}\right\}(BC)$$

$$\left.\begin{aligned} \pi &= + 2.8 = +0''.007 \pm 0''.004 \\ \mu_a &= +15.0 = +0''.038 \pm 0''.002 \end{aligned}\right\}(A)$$

$$\left.\begin{aligned} \pi &= - 1.5 = -0''.004 \pm 0''.007 \\ \mu_a &= +13.8 = +0''.035 \pm 0''.003 \end{aligned}\right\}(BC)$$

No.	Br.	x	y	π
1.....	f	+3'.8	+1'.6	−0''.009
2.....	f	+5.4	+3.7	+0.004
3.....	f	+1.8	−4.9	+0.008
4.....	f	−0.3	−3.7	−0.007
5.....	bf	−2.6	−1.6	0.000
6.....	b	−4.5	+1.9	−0.001
7.....	bf	−1.1	+3.2	+0.007

No. 190 in N.G.C. 1647 $\alpha = 4^h41^m17^s$ $\delta = +18°58'$

Mor.	Ev.	l_1	l_2	Δ_p	M	v
12.721	12.092	−7°2	−5°2	+1.82	+ 1	− 5
11.778	13.054	−6.7	−4.5	+1.52	− 6	− 8
12.723	13.051	−6.5	−4.0	+1.66	+16	+12
11.775	13.141	−6.2	−0.2	+1.78	+19	+17
11.781	13.054	−4.5	+1.2	+1.51	−16	−18
12.721	12.092	−3.0	+0.5	+1.82	+ 6	0
12.723	13.141	−2.5	+4.0	+1.92	+ 7	+ 3
11.775	11.109	−1.0	+3.7	+1.72	+17	+12
11.781	11.109	+1.0	+9.5	+1.70	−12	−17

$$+7.12\,\mu_a - 3.08\,\pi = + 2$$
$$-3.08\,\mu_a + 26.68\,\pi = +63$$
$$\pi = +2.5 = +0''.006 \pm 0''.005$$
$$\mu_a = +1.4 = +0''.004 \pm 0''.009$$

No.	Br.	x	y	π
1.....	bf	+5'.1	+4'.9	0''.000
2.....	f	+4.3	+1.8	−0.003
3.....	f	+2.5	−4.0	−0.001
4.....	f	−1.5	−1.5	+0.004
5.....	f	−3.0	−4.0	−0.007
6.....	f	−4.3	+0.3	+0.003
7.....	f	−2.7	+0 5	−0.013
8.....	b	−1.4	−0.1	+0.016

I.C. 405 $\alpha = 5^h 9^m 42^s$ $\delta = +34^\circ 12'$

Mor.	Ev.	t_1	t_2	Δ_p	M	v
9.811	12.090	−14°.0	− 4°.0	+1.54	+22	+10
9.806	12.090	− 5.5	+ 1.2	+1.56	+18	+ 6
12.830	12.087	− 0.2	+ 2.5	+1.45	−14	−10
12.830	12.092	+ 4.0	+ 4.0	+1.47	−12	− 8
10.795	11.032	+ 4.0	+ 7.5	+1.34	− 6	− 7
13.795	12.087	+ 8.0	+ 8.2	+1.59	− 1	+ 8
10.795	12.092	+ 8.2	+11.5	+1.62	− 3	−10
13.795	11.032	+12.0	+14.0	+1.34	− 6	+ 8

$+23.79\ \mu_\alpha - 0.92\ \pi = -124$
$-\ 0.92\ \mu_\alpha + 17.81\ \pi = +\ 1$
$\pi = -0.2 = -0''.001 \pm 0''.004$
$\mu_\alpha = -5.2 = -0''.013 \pm 0''.003$

No.	Br.	x	y	π
1.....	bf	+1'.5	+3'.2	+0".015
2.....	f	+3.2	+1.8	−0.012
3.....	f	+5.8	+1.6	−0.002
4.....	f	+1.6	−6.5	+0.006
5.....	bf	−2.1	−2.1	−0.009
6.....	b	−3.6	−0.4	+0.008
7.....	bf	−5.9	+1.1	−0.007

βG.C. 2654 $\alpha = 5^h 14^m 8^s$ $\delta = -3^\circ 11'$

Mor.	Ev.	t_1	t_2	Δ_p	M	v
9.817	14.035	−12°.0	−14°.0	+1.26	−617	− 2
11.860	14.035	−10.7	−11.0	+1.06	−348	−30
9.817	13.133	− 8.7	− 7.0	+1.65	−447	+37
14.759	11.040	− 8.5	− 0.5	+1.49	+604	+58
11.855	11.040	− 5.2	+ 3.5	+1.12	+101	−21
12.756	10.065	+ 1.5	+ 7.5	+1.62	+360	−36
12.756	10.065	+ 4.7	+10.5	+1.62	+377	−19

$+62.57\ \mu_\alpha + 2.07\ \pi = +9159$
$+\ 2.07\ \mu_\alpha + 14.14\ \pi = +\ 323$
$\pi = +\ 1.4 = +0''.007 \pm 0''.035$
$\mu_\alpha = +146.3 = +0''.717 \pm 0''.016$
The 12.5-mag. companion, occulted by the sector, does not show images on the plates.

No.	Br.	x	y	π
1.....	f	−3'.7	+3'.0	+0".004
2.....	f	−5.2	+2.5	−0.009
3.....	bf	−1.2	−6.0	−0.008
4.....	f	−0.4	−3.4	+0.022
5.....	bf	+5.9	−5.5	−0.003
6.....	f	+3.8	+1.2	−0.003
7.....	bf	+1.5	+7.1	0.000

N.G.C. II 2149 $\alpha = 5^h48^m54^s$ $\delta = +46°6'$

Mor.	Ev.	t_1	t_2	Δ_p	M	v
11.852	5.122	−13°.7	−12°.5	+1.51	−31	−11
11.852	5.125	− 8.0	−10.2	+1.52	0	+20
7.789	5.122	− 4.7	− 8.5	+1.74	−28	−11
12.830	5.125	− 0.5	− 6.2	+1.61	−22	+ 1
7.789	14.131	− 0.5	− 1.2	+1.77	+ 6	+10
12.830	13.141	+ 3.7	+ 3.0	+1.66	−14	− 2
10.795	14.131	+ 4.2	+ 5.0	+1.75	−25	−17
10.795	13.141	+ 8.5	+ 7.0	+1.78	+ 1	+11

$+213.98\ \mu_a + 15.69\ \pi = -405$
$+\ 15.69\ \mu_a + 22.33\ \pi = -185$
$\pi = -7.3 = -0''.018 \pm 0''.005$
$\mu_a = -1.4 = -0''.004 \pm 0''.002$

No.	Br.	x	y	π
1.....	bf	+4'.9	+2'.5	+0''.002
2.....	f	+3.6	−5.1	−0.001
3.....	f	+0.1	−3.6	−0.006
4.....	bf	−3.3	−2.3	+0.009
5.....	bf	−3.3	+2.6	+0.004
6.....	f	−2.3	+3.4	−0.011
7.....	bf	−0.4	+2.9	+0.004

6 Lyncis $\alpha = 6^h22^m6^s$ $\delta = +58°14'$

Mor.	Ev.	t_1	t_2	Δ_p	M	v
4.885	14.130	−16°.5	−16°.0	+1.41	+110	− 7
4.885	12.087	−11.0	− 2.5	+1.20	+ 78	−15
5.762	12.090	− 7.5	+ 2.5	+1.58	+ 91	+ 2
5.844	13.141	− 5.0	+ 4.0	+1.62	+118	+18
13.798	9.087	− 4.0	+ 6.2	+1.51	− 35	− 8
13.795	12.087	0.0	+ 4.0	+1.52	+ 12	+ 8
13.798	13.141	+ 0.2	+ 8.0	+1.76	+ 14	− 5
13.795	9.087	+ 4.0	+10.5	+1.52	− 24	+ 3

$+278.30\ \mu_a - 25.47\ \pi = -3263$
$-\ 25.47\ \mu_a + 18.55\ \pi = +\ 538$
$\pi = +14.8 = +0''.037 \pm 0''.005$
$\mu_a = -10.4 = -0''.026 \pm 0''.001$

No.	Br.	x	y	π
1.....	f	+1'.9	+1'.9	−0''.002
2.....	bf	+2.5	+4.3	−0.001
3.....	bf	+3.4	+2.6	−0.003
4.....	bf	+3.0	−4.0	−0.001
5.....	f	−0.8	−3.2	+0.010
6.....	f	−6.0	−4.1	−0.010
7.....	f	−3.3	+1.6	+0.007

Boss 2410 $\alpha = 8^h 53^m 32^s$ $\delta = +18° 31'$

Mor.	Ev.	t_1	t_2	Δ_p	M	v
3.866	4.229	−9°.5	0°.0	+1.70	− 2	− 6
3.945	5.199	−9.0	+ 1.2	+1.38	− 1	−22
3.866	4.232	−5.2	+ 2.0	+1.71	+ 7	+ 3
3.989	4.229	−3.0	+ 4.7	+1.32	− 4	− 6
6.934	4.232	−2.2	+ 6.5	+1.55	− 95	−39
12.959	5.199	−0.2	+ 6.5	+1.33	−163	− 9
12.959	11.186	+6.2	+ 7.0	+1.27	+ 4	+41
12.907	11.186	+8.2	+14.5	+1.44	+ 9	+46

$+75.49\ \mu_a + 15.95\ \pi = -1499$
$+15.95\ \mu_a + 17.30\ \pi = -\ 343$
$\pi = -\ 1.9 = -0''.005 \pm 0''.014$
$\mu_a = -19.5 = -0''.049 \pm 0''.007$

No.	Br.	x	y	π
1.....	f	+1'.0	+6'.3	+0".005
2.....	f	+4 4	+3 8	+0 004
3.....	f	+1.5	0.0	+0.006
4.....	b	+2.1	−0.5	−0.012
5.....	f	+2.7	−3.8	−0.002
6.....	bf	−4.1	−7.8	+0.007
7.....	f	−4.3	−1.8	−0.001
8.....	f	−3.2	+2.5	−0.006

SU Draconis $\alpha = 11^h 32^m 15^s$ $\delta = +67° 53'$

Mor.	Ev.	t_1	t_2	Δ_p	M	v
6.005	13.319	− 3°.0	− 5°.0	+1.48	+103	+23
6.003	13.319	− 0.5	− 0.2	+1.49	+ 71	−10
6.006	7.301	+ 1.0	+ 1.5	+1.40	− 5	−10
6.003	7.317	+ 3.5	+ 4.2	+1.48	− 7	−12
14.129	7.301	+ 5.2	+ 5.7	+0.94	−117	−25
14.131	6.331	+ 5.2	+ 7.0	+1.06	− 89	+17
14.131	7.317	+12.0	+10.5	+1.00	− 79	+14
14.129	6.331	+12.0	+11.5	+1.07	−103	+ 3

$+325.14\ \ \mu_a + 4.36\ \pi = -4092$
$+\ 4.36\ \ \mu_a + 12.70\ \pi = -\ 152$
$\pi = -\ 7.7 = -0''.019 \pm 0''.009$
$\mu_a = -12.5 = -0''.032 \pm 0''.002$

No.	Br.	x	y	π
1.....	f	+1'.6	+2'.5	+0".005
2.....	f	+8.8	+1.9	−0.007
3.....	ff	−2.7	−3.3	+0.010
4.....	f	−7.1	−3.4	−0.011
5.....	f	−1.2	+0.4	+0.001

Σ 1835 = βG.C. 6842 BC $\alpha = 14^h18^m28^s$ $\delta = +8°54'$

Mor.	Ev.	l_1	l_2	Δ_p	M	v
8.227	14.424	−14°.7	−11°.7	+1.10	+167	− 9
8.227	14.418	−10.5	−11.2	+1.07	+164	−12
13.139	14.424	− 4.5	− 7.5	+1.42	+ 65	+19
13.216	4.391	− 2.2	− 8.0	+0.95	−261	−30
13.139	4.391	+ 2.2	− 2.2	+1.24	−204	+24
13.216	13.461	+ 4.2	+ 2.5	+1.32	+ 21	+ 4
11.192	5.450	+ 5.7	+ 7.2	+1.36	−145	+ 1
11.192	4.427	+11.2	+11.5	+1.26	−184	−11

$+311.46\ \mu_a + 20.33\ \pi = -8301$
$+\ 20.33\ \mu_a + 12.07\ \pi = -\ 461$
$\pi = +\ 7.6 = +0''.019 \pm 0''.010$
$\mu_a = -\ 27.1 = -0''.068 \pm 0''.002$

For A, which is too bright for accurate measures, we derive:

$\pi = +11.6 = +0''.029 \pm 0''.021$
$\mu_a = -26.7 = -0''.067 \pm 0''.004$

No	Br.	x	y	π
1.....	f	+1'.0	+7'.4	−0''.025
2.....	f	+6.3	−0.5	+0.004
3.....	bf	+4.1	−8.9	−0.001
4.....	ff	−6.3	−4.7	−0.011
5.....	bf	−2.5	+4.5	+0.032

Wolf 562 $\alpha = 15^h14^m14^s$ $\delta = -7°21'$

Mor.	Ev.	l_1	l_2	Δ_p	M	v
12.255	13.455	+1°.0	− 2°.0	+1.13	+ 375	+ 5
13.216	13.453	+2.0	+ 2.0	+1.28	+ 109	−12
12.263	12.487	+5.2	+ 4.2	+1.24	+ 134	+20
13.219	13.453	+3.2	+ 5.7	+1.27	+ 112	− 5
12.255	8.533	+6.5	+ 6.0	+1.45	− 905	+24
13.219	8.528	+6.5	+ 6.2	+1.58	−1197	−15
13.216	12.487	+6.7	+ 7.0	+1.44	− 134	− 3
12.257	8.528	+8.0	+ 9.7	+1.42	− 963	−30
12.263	8.443	+9.7	+11.0	+1.02	− 946	+29

$+66.47\ \mu_a + 20.82\ \pi = -16816$
$+20.82\ \mu_a + 15.80\ \pi = -\ 4856$
$\pi = +\ 44.3 = +0''.217 \pm 0''.023$
$\mu_a = -266.9 = -1''.308 \pm 0''.011$

No.	Br.	x	y	π
1.....	f	−0'.2	+5'.6	+0''.005
2.....	f	−2.8	−3.6	−0.023
3.....	bf	−4.2	−5.9	+0.013
4.....	bf	−2.0	−4.8	+0.006
5.....	f	+3.6	−2.7	+0.002
6.....	f	+2.5	+5.0	−0.009
7.....	f	+1.5	+6.0	+0.005

49 Serpentis = βG.C. 7551 $\alpha = 16^h 8^m 30^s$ $\delta = +13°48'$

Mor.	Ev.	t_1	t_2	Δ_p	$M(49)$	M(Comp.)	$v(49)$	v(Comp.)
7.307	10.547	− 9°.7	− 1°.5	+1.33	−207	−193	+18	+20
13.210	11.520	− 4.5	+ 3.2	+1.57	+182	+179	+23	+23
8.279	10.550	− 3.2	+ 4.5	+1.48	−143	−130	+ 5	+ 9
7.312	10.547	− 1.0	+ 4.5	+1.30	−225	−213	0	0
13.213	9.508	+ 0.7	+ 5.5	+1.51	+306	+292	− 7	−11
13 210	11 517	+ 0.7	+ 7 2	+1.56	+155	+149	− 4	− 7
13.319	11.520	+ 2.2	+ 9.0	+1.14	+145	+150	−15	− 6
7.312	9.505	+ 3.5	+ 9.5	+1.11	−152	−148	− 3	− 8
13.319	9.508	+ 6.5	+10.7	+1.08	+323	+316	+10	+14
8.227	9.505	+11.0	+15.0	+1.46	−103	− 98	−31	−33

+69.76 μ_a + 0.86 π = +5384 } 49
+ 0.86 μ_a + 18.65 π = + 406 } Serp.
= +5168 } Comp.
= + 433 }

$\pi = +18.3 = +0''.046 \pm 0''.007$ } 49
$\mu_a = +77.0 = +0''.194 \pm 0''.003$ } Serp.
$\pi = +19.8 = +0''.050 \pm 0''.007$ } Comp.
$\mu_a = +73.8 = +0''.186 \pm 0''.004$ }

Stars 4 and 8 were measured on only four pairs of plates.

No.	Br.	x	y	π
1.....	bf	+0'.7	+3'.2	+0''.002
2.....	f	+1.5	+6.6	+0.014
3.....	f	+5.9	+0.1	−0.002
4.....	bf	+3.3	−2.2	−0.048
5.....	f	+1.1	−6.6	+0.011
6.....	f	−2.1	−4.3	+0.014
7.....	f	−8.4	−0.8	−0.008
8.....	b	−5.1	+3.7	−0.011

W.B. 16^h1259 $\alpha = 16^h 41^m 23^s$ $\delta = +33°41'$

Mor.	Ev.	t_1	t_2	Δ_p	M	v
10.323	11.531	−13°.0	− 7°.7	+1.19	+57	−11
10.323	11.531	− 9.2	− 3.2	+1.19	+68	0
12.326	12.580	− 9.7	+ 1.2	+1.38	+71	+ 9
12.323	12.580	− 5.5	+ 5.2	+1.40	+72	+ 9
12.326	10.550	− 4.5	+ 5.0	+1.27	+24	− 2
14.279	11.605	+ 1.0	+ 7.5	+1.66	+11	−18
13.320	10.550	+ 4.5	+10.5	+1.30	+26	+13
13.320	11.605	+ 9.0	+11.5	+1.49	+40	+ 3

+23.98 μ_a + 9.27 π = + 25
+ 9.27 μ_a + 14.98 π = +490
$\pi = +42.1 = +0''.106 \pm 0''.006$
$\mu_a = -15.2 = +0''.038 \pm 0''.005$

No.	Br.	x	y	π
1.....	f	+5'.2	+3'.4	+0''.003
2.....	bf	+6.2	+1.9	−0.012
3.....	f	+6.9	−6.3	−0.002
4.....	f	−1.8	−2.2	+0.015
5.....	bf	−4.8	−0.8	−0.006
6.....	bf	−9.6	−1.5	−0.011
7.....	b	−2.2	+2.1	+0.013
8.....	f	−0.8	+4.4	+0.000

Wolf 636 $\alpha = 17^h0^m2^s$ $\delta = -4°55'$

Mor.	Ev.	t_1	t_2	Δ_p	M	v
12.334	13.556	−14.°0	−10.°5	+1.27	+215	− 8
12.337	13.559	−13.7	−10.5	+1.26	+221	− 2
12.337	13.557	− 9.0	− 4.7	+1.25	+218	− 5
12.334	13.559	− 8.7	− 6.0	+1.28	+238	+13
10.315	7.558	+ 2.2	+10.5	+1.36	−502	−11
11.288	7.555	+11.7	+11.5	+1.46	−698	−33
11.288	7.558	+14.7	+14.2	+1.47	−632	+33
10.321	7.555	+15.2	+14.2	+1.32	−482	+11

$+49.09\ \mu_a + 12.16\ \pi = -8773$
$+12.16\ \mu_a + 14.28\ \pi = -2139$
$\pi = +\ 3.0 = +0''.015 \pm 0''.021$
$\mu_a = -179.5 = -0''.880 \pm 0''.011$

No.	Br.	x	y	π
1.....	f	−2'.4	+5'.3	0''.000
2.....	f	−6.0	−1.1	+0.008
3.....	bf	−2.9	−3.7	−0.013
4.....	f	+2.1	−3.6	−0.004
5.....	f	+3.2	+0.2	+0.021
6.....	f	+4.6	+4.2	−0.014

Furuhjelm 46 $\alpha = 17^h9^m12^s$ $\delta = +45°50'$

Mor.	Ev.	t_1	t_2	Δ_p	M	v
14.339	13.540	−14.°2	−12.°2	+1.16	+171	+ 8
14.350	13.537	−14.5	− 8.7	+1.08	+177	+18
14.353	13.540	−10.5	− 8.2	+1.08	+157	− 2
14.353	12.583	− 5.0	− 4.7	+1.27	+272	−13
12.326	13.551	− 3.0	− 5.0	+1.29	− 81	−14
12.323	13.537	− 2.5	− 4.2	+1.23	− 66	+ 4
12.326	12.583	+ 2.7	− 1.0	+1.42	+ 53	− 1
12.323	13.551	+ 4.2	− 0.7	+1.30	− 62	+ 5

$+\ 9.62\ \mu_a - 0.11\ \pi = +1129$
$-\ 0.11\ \mu_a + 12.18\ \pi = +\ 713$
$\pi = +\ 59.6 = +0''.150 \pm 0''.006$
$\mu_a = +117.8 = +0''.297 \pm 0''.006$

No.	Br.	x	y	π
1.....	ff	+4'.9	+4'.1	−0''.013
2.....	bf	+5.8	−2.9	+0.003
3.....	bf	+7.5	−5.4	+0.021
4.....	f	−5.2	−3.2	−0.024
5.....	bf	−4.1	−0.8	+0.032
6.....	f	−5.4	+6.0	+0.024
7.....	f	−0.4	+0.3	−0.044

α Herculis = βG.C. 7914 $\quad \alpha = 17^h 10^m 5^s \quad \delta = +14^\circ 30'$

Mor.	Ev.	t_1	t_2	Δ_p	M	M(Comp.)	v	v(Comp.)
9.249	13.606	−3°.0	0°.0	+1.78	−15	−20	−14	−17
14.350	3.613	−2.7	0.0	+1.40	+ 7	+ 8	+ 4	+ 1
9.339	13.611	−1.7	+ 0.5	+1.46	+ 5	+ 7	+ 6	+10
9.341	13.608	+0.2	+ 1.7	+1.43	0	− 7	+ 1	− 4
14.279	3.616	+2.0	+ 1.5	+1.72	− 1	+ 8	− 4	+ 1
14.350	3.618	+2.2	+ 2.5	+1.42	+17	+20	+14	+13
5.284	13.611	+3.0	+ 4.7	+1.69	+ 7	+ 8	+ 9	+14
9.339	3.616	+5.0	+ 6.0	+1.47	− 1	+ 1	− 2	− 3
5.284	13.608	+7.5	+ 6.5	+1.68	− 6	− 8	− 4	− 2
14.279	2.534	+8.0	+12.0	+1.38	− 9	0	−12	− 8

$+708.75\mu_a + 25.07\pi = +170$ } α
$+ 25.07\mu_a + 24.02\pi = + 1$ } Herc.
$= +479$ } Comp.
$= + 19$ }

$\pi = -0.2 = -0''.001 \pm 0''.003$ } α
$\mu_a = +0.2 = +0''.001 \pm 0''.001$ } Herc.
$\pi = +0.1 = 0''.000 \pm 0''.004$ } Comp.
$\mu_a = +0.7 = +0''.002 \pm 0''.001$ }

No.	Br.	x	y	π
1.....	bf	+0'.8	+1'.1	+0".011
2.....	bf	+2.5	+6.2	+0.005
3.....	f	+2.6	+1.1	0.000
4.....	bf	+5.9	−4.5	0.000
5.....	f	+5.5	−6.2	−0.009
6.....	b	−5.6	−5.4	+0.014
7.....	f	−4.0	+1.0	−0.010
8.....	f	−8.2	+2.1	−0.008
9.....	f	−1.9	+5.9	−0.001

Ross 136 $\quad \alpha = 18^h 17^m 12^s \quad \delta = +6^\circ 17'$

Mor.	Ev.	t_1	t_2	Δ_p	M	v
12.337	13.617	−11°.0	−12°.5	+1.53	+349	− 6
12.337	13.614	− 8.0	− 7.5	+1.52	+347	− 8
12.411	13.619	− 6.7	− 4.2	+1.19	+345	+14
12.411	13.614	− 4.7	− 3.7	+1.16	+335	+ 7
12.334	13.619	− 2.0	− 2.0	+1.54	+352	− 3
13.385	11.695	− 0.5	+ 6.2	+1.54	−416	− 8
12.334	11.692	+ 1.7	+ 6.7	+1.76	−140	− 6
13.385	11.670	+ 2.5	+10.5	+1.49	−410	+ 7
13.388	11.692	+ 6.5	+ 9.2	+1.53	−412	− 1
13.388	11.670	+ 9.7	+15.0	+1.48	−416	+ 1

$+19.90\,\mu_a + 2.73\,\pi = -5075$
$+ 2.73\,\mu_a + 22.01\,\pi = - 325$
$\pi = + 17.1 = +0''.084 \pm 0''.006$
$\mu_a = -257.4 = -1''.261 \pm 0''.006$

No.	Br.	x	y	π
1.....	f	−0'.1	+1'.6	0".000
2.....	f	−2.4	+3.5	+0.011
3.....	f	−3.9	+1.8	−0.007
4.....	bf	−1.4	−1.1	−0.010
5.....	f	+0.6	−4.7	−0.005
6.....	f	+1.2	−3.2	+0.020
7.....	bf	+3.5	+0.7	−0.009
8.....	bf	+2.4	+2.0	0.000

βG.C. 8512 $\alpha = 18^h17^m35^s$ $\delta = +11°24'$

Mor.	Ev.	t_1	t_2	Δ_p	M(8512)	M(Comp.)	v(8512)	v(Comp.)
12.329	12.583	− 9°.0	−11°.2	+1.39	− 6	+17	+ 1	+20
13.320	10.648	− 7.0	− 6.0	+1.71	−20	−15	− 4	+ 3
12.326	12.583	− 5.7	− 7.0	+1.40	0	+13	+ 7	+16
13.377	11.602	− 3.2	− 4.7	+1.28	−25	− 8	−13	+ 4
13.329	10.648	− 2.5	− 2.0	+1.67	−16	−16	− 2	− 3
13.320	10.643	− 1.0	− 0.5	+1.69	− 3	0	+13	+18
12.326	11.602	− 0.5	− 0.5	+1.49	− 7	−14	+ 4	− 7
13.377	10.643	+ 2.7	+ 4.2	+1.45	−13	−36	+ 2	−19
10.397	10.698	+ 5.0	+ 5.2	+1.48	−20	−13	−12	−10
10.397	10.703	+10.5	+ 6.2	+1.49	− 4	−22	+ 4	−19

$+28.59\,\mu_a + 17.61\,\pi = -163$ } βG.C.
$+17.61\,\mu_a + 22.84\,\pi = -171$ } 8512
$= -185$ } Comp.
$= -146$ }

$\pi = -5.9 = -0''.015 \pm 0''.004$ } βG.C.
$\mu_a = -2.1 = -0''.005 \pm 0''.004$ } 8512
$\pi = -2.7 = -0''.007 \pm 0''.008$ } Comp.
$\mu_a = -4.8 = -0''.012 \pm 0''.007$ }

No.	Br.	x	y	π
1.....	f	+3'.8	+1'.2	−0".004
2.....	bf	+3.4	−1.0	+0.001
3.....	f	+2.7	−3.4	+0.004
4.....	bf	−0.5	−3.4	−0.007
5.....	f	−3.4	+0.5	0.000
6.....	f	−4.1	+1.2	0.000
7.....	f	−1.4	+2.9	0.000
8.....	b	−1.1	+2.2	0.000

Nova Lyrae $\alpha = 18^h49^m31^s$ $\delta = +29°6'$

Mor.	Ev.	t_1	t_2	Δ_p	M	v
12.337	13.617	− 8°.2	−11°.5	+1.50	+ 9	+ 2
12.337	13.617	− 4.5	− 8.2	+1.50	+ 6	0
13.385	13.614	+ 1.7	+ 2.0	+1.30	+ 7	+ 3
13.385	9.668	+ 6.0	+ 2.5	+1.52	− 8	− 8
13.388	13.614	+ 6.7	+ 5.2	+1.28	− 2	− 6
12.411	7.711	+ 7.0	+11.2	+1.51	+ 1	+ 2
13.388	7.711	+10.0	+14.0	+1.62	− 9	− 7
12.411	7.714	+10.0	+15.5	+1.52	+12	+13

$+93.66\,\mu_a + 24.66\,\pi = -42$
$+24.66\,\mu_a + 17.35\,\pi = +22$
$\pi = +3.0 = +0''.015 \pm 0''.007$
$\mu_a = -1.2 = -0''.006 \pm 0''.003$

No.	Br.	x	y	π
1.....	f	−0'.5	+1'.4	−0".018
2.....	bf	−2.1	+2.0	+0.008
3.....	bf	−3.5	−0.5	−0.002
4.....	f	−3.4	−1.5	−0.007
5.....	f	+1.0	−0.4	+0.028
6.....	b	+1.7	−1.9	+0.012
7.....	f	+3.7	−2.1	−0.014
8.....	f	+2.7	+3.0	−0.004

XZ Cygni $\alpha = 19^h30^m25^s$ $\delta = +56°10'$

Mor.	Ev.	t_1	t_2	Δ_p	M	v
13.377	6.657	−8°.0	− 5°.7	+1.50	+220	− 2
13.380	6.657	−8.0	0.0	+1.49	+211	−11
13.462	13.709	−6.5	+ 1.0	+1.30	+ 9	+16
13.459	13.709	−4.2	+ 5.2	+1.32	+ 2	+ 9
13.377	5.769	−2.7	+ 6.0	+1.80	+267	+15
13.380	5.641	−2.5	+10.5	+1.42	+251	− 5
13.462	13.794	−1.2	+12.2	+1.41	− 26	−17
13.459	13.797	0.0	+15.7	+1.42	− 17	− 8

$+208.49\ \mu_a + 43.18\ \pi = +6884$
$+\ 43.18\ \mu_a + 17.17\ \pi = +1435$
$\pi = +\ 1.1 + 0''.003 \pm 0''.008$
$\mu_a = +32.8 + 0''.083 \pm 0''.002$

No.	Br.	x	y	π
1.....	bf	−0'.5	+1'.4	+0".008
2.....	f	+3.7	+1.4	0.000
3.....	f	+3.2	+0.5	−0.016
4.....	f	+3.2	−0.4	+0.012
5.....	f	−1.1	−2.5	+0.003
6.....	f	−2.3	−3.0	−0.005
7.....	f	−4.0	−0.8	−0.008
8.....	f	−2.9	+3.2	+0.002

Wolf 901 $\alpha = 20^h54^m6^s$ $\delta = +3°10'$

Mor.	Ev.	t_1	t_2	Δ_p	M	v
13.470	7.799	−11°.2	− 7°.7	+1.58	+406	− 4
13.470	13.699	− 8.0	− 3.2	+1.26	− 7	+ 1
9.511	7.799	− 5.7	− 6.2	+1.38	+138	+ 8
9.511	13.699	− 4.2	− 1.0	+1.06	−287	+ 1
9.500	7.712	+ 0.2	+ 3.7	+1.17	+142	+ 8
14.507	7.712	+ 0.5	+ 5.5	+1.16	+480	− 7
9.513	13.701	+ 1.5	+ 5.7	+1.06	−287	+ 1
9.513	13.696	+ 3.0	+13.0	+1.03	−300	−12
14.507	13.696	+ 2.7	+14.7	+1.09	+ 65	+ 1

$+137.81\ \mu_a + 8.70\ \pi = +9771$
$+\ 8.70\ \mu_a + 13.20\ \pi = +\ 699$
$\pi = +\ 6.5 = +0''.032 \pm 0''.006$
$\mu_a = +70.5 = +0''.345 \pm 0''.002$

No.	Br.	x	y	π
1.....	f	−0'.2	+2'.9	−0".009
2.....	bf	−1.9	+2.1	−0.022
3.....	f	−3.7	−0.9	+0.028
4.....	b	−1.1	−1.6	+0.013
5.....	ff	−0.5	−5.3	−0.011
6.....	f	+1.9	−2.1	−0.030
7.....	bf	+3.3	+1.3	+0.044
8.....	f	+2.5	+2.9	−0.011

Anonymous $\alpha = 21^h24^m17^s$ $\delta = +11°43'$

Mor.	Ev.	t_1	t_2	Δ_p	M	v
13.467	12.717	−13°.2	−13°.5	+1.32	+ 73	− 1
13.459	12.720	−11.5	− 9.2	+1.36	+ 62	−12
12.496	12.717	− 9.5	− 9.0	+1.21	− 6	− 1
11.531	11.701	− 9.0	− 7.0	+0.95	+ 12	+16
13.467	11.698	− 6.5	− 5.0	+1.23	+171	+16
13.459	11.701	− 6.5	− 2.7	+1.27	+146	− 9
12.496	12.720	− 4.7	− 3.5	+1.22	− 4	+ 1
11.531	11.698	− 4.2	− 0.2	+0.94	− 3	+ 1

$+7.50\ \mu_a + 5.56\ \pi = +662$
$+5.56\ \mu_a + 11.44\ \pi = +571$
$\pi = +10.9 = +0''.028 \pm 0''.007$
$\mu_a = +80.2 = +0''.202 \pm 0''.009$

No.	Br.	x	y	π
1.....	b	+1'.8	+2'.5	+0''.011
2.....	bf	+7.3	0.0	−0.002
3.....	f	+1.5	−0.7	−0.002
4.....	f	+0.5	−2.3	−0.004
5.....	bf	−5.1	−2.3	+0.011
6.....	bf	−7.0	+3.2	−0.007
7.....	bf	−0.4	+3.3	−0.005

Lalande 42883 $\alpha = 21^h54^m15^s$ $\delta = +29°21'$

Mor.	Ev.	t_1	t_2	Δ_p	M	v
13.552	12.829	−12°.0	−10°.2	+1.34	−128	−26
13.552	9.805	− 8.0	− 8.5	+1.29	−574	− 7
9.508	9.748	− 7.7	− 6.5	+1.28	+ 51	+ 5
12.496	12.829	− 6.5	− 5.5	+1.60	+ 71	+ 8
13.538	9.748	− 4.2	− 2.2	+1.14	−589	− 9
9.508	9.805	− 1.0	− 2.0	+1.49	+ 61	0
12.496	13.794	− 1.0	0.0	+1.51	+209	− 4
13.538	8.840	+ 1.7	+ 2.5	+1.42	−702	+16
13.541	13.794	+13.2	+ 4.7	+1.31	+ 64	+15

$+53.04\ \mu_a + 13.21\ \pi = -8116$
$+13.21\ \mu_a + 17.20\ \pi = -1910$
$\pi = +\ 8.0 = +0''.020 \pm 0''.006$
$\mu_a = -155.1 = -0''.392 \pm 0''.004$

No.	Br.	x	y	π
1.....	f	+2'.1	+1'.0	−0''.015
2.....	f	+3.2	+0.5	+0.003
3.....	f	+2.6	−3.7	+0.003
4.....	f	−0.3	−3.2	+0.006
5.....	f	−4.4	−2.3	+0.002
6.....	bf	−2.3	+2.7	−0.020
7.....	f	−0.8	+5.4	+0.019

Wolf 1337 $\alpha = 21^h 54^m 49^s$ $\delta = -1°8'$

Mor.	Ev.	t_1	t_2	Δ_p	M	v
11.529	12.753	−12°.5	− 4°.5	+1.20	+ 58	+ 3
11.526	10.796	−10.7	− 2.5	+1.38	− 19	+ 7
11.526	12.753	− 8.0	0.0	+1.22	+ 48	− 7
11.529	10.796	− 9.0	+ 2.0	+1.37	− 28	− 2
9.514	12.755	+ 4.5	+ 5.7	+1.28	+149	+10
9.514	12.755	+ 8.5	+ 8.2	+1.28	+129	−10
13.577	11.857	+ 1.5	+ 8.2	+1.36	− 79	−12
13.557	11.859	+ 5.2	+ 9.7	+1.36	− 66	+ 1
13.560	11.857	+ 6.7	+14.0	+1.34	− 59	+ 8

$+33.73\,\mu_a - 2.35\,\pi = -1411$
$-2.35\,\mu_a + 15.49\,\pi = +145$
$\pi = +3.1 = +0''.015 \pm 0''.007$
$\mu_a = -41.6 = -0''.204 \pm 0''.005$

No.	Br.	x	y	π
1.....	bf	−0'.7	+2'.2	+0''.005
2.....	f	−1.8	+3.4	0.000
3.....	f	−5.0	−1.0	+0.002
4.....	bf	−3.5	−2.8	−0.003
5.....	bf	+1.4	−5.0	−0.006
6.....	f	+3.5	−3.6	+0.001
7.....	f	+3.1	−1.6	+0.007
8.....	bf	+1.2	+8.9	−0.002

Contributions from the Mount Wilson Observatory, No. 392
Reprinted from the *Astrophysical Journal*, Vol. LXXI, pp. 102–135, 1930
Printed in the U.S.A.

STEWARD OBSERVATORY

LUNAR RADIATION AND TEMPERATURES

By EDISON PETTIT and SETH B. NICHOLSON

ABSTRACT

Methods of observing.—The vacuum thermocouple attached to the 100-inch telescope was used as in measuring stellar radiation. A microscope cover-glass was used to separate the reflected light from the planetary heat. A fluorite screen and water-cell were used for special purposes.

Reduction of the measurements.—Comparison stars, whose radiometric magnitudes we have already determined, were used to reduce the galvanometer deflections to absolute intensities. These are expressed in terms of the radiometric magnitude of the planetary heat in a solid angle of 1 sq. sec. of arc. The relation of radiometric magnitude to absolute temperature is given by the equation

$$\log T = 2.612 - 0.1\,(\overline{m}_r - \Delta m_r)\,.$$

An expression applicable to the screens used and to the conditions of observing is derived from this equation.

Limiting measurable temperature.—Temperatures below 100° K are measured with difficulty, since the value of m'_r for that temperature is 12.47 mag.; and it is probably not feasible to detect planetary radiation from a celestial body whose temperature is below 70° K.

Reflection of solar radiation between 8 and 14 μ.—Even if the moon reflected all the solar radiation in this region, it would add only 1½ per cent to the planetary heat and affect the computed temperature by only 1°. With the fluorite screen the emissivity between 8 and 10 μ is shown to be the same as between 8 and 14 μ, which indicates that the silicates, if present in the lunar crust, cannot be detected by the selective emissivity between 8 and 10 μ as in laboratory tests, probably because they are in a finely divided or porous state for which the emissivity would be more like that of a black body.

Distribution of radiation over the disk.—From drift-curves it is found that the distribution of planetary heat over the disk at full moon does not follow the formula

$$E = a \cos\theta\,,$$

derived from the Lommel-Seeliger law, but more nearly the formula

$$E = a \cos^{3/2}\theta\,.$$

This is explained by the rough surface. From the water-cell drift-curve it appears that the general trend of reflected light at full moon is uniform, but that at the limb in the E–W direction the intensity is 60 per cent greater than that of the neighboring *maria*.

Temperature of the subsolar point.—The measures indicate that at full moon, when the subsolar point is nearly central on the disk, its temperature is 407° K, but that at quarter-phase, when it is on the limb, they show a temperature of 358° K. The directive effect of the rough surface on the planetary heat probably accounts for this difference.

Temperatures during a lunar eclipse.—Measurements made near the south limb on June 14, 1927, show that the temperature fell from 342° to 175° K during the first partial phase, continued to drop to 156° K during totality, and rose again abruptly to nearly the original temperature during the last partial phase. From these data it is estimated that less than 0.1 cal cm^{-2} min^{-1} is conducted into the moon from the surface.

Distribution of planetary heat and reflected light about the subsolar point.—With special equipment the night-to-night values of the reflected light transmitted by the cover-

glass and of the planetary heat eliminated by it were determined for the subsolar point as it passed over the earthward side of the moon. The mean spherical distribution of light over the hemisphere about the subsolar point is 0.85 mag. fainter and the planetary heat 0.15 mag. fainter than the corresponding intensities at full moon.

The theoretical lunar temperature.—From the water-cell measurements and the distribution-curve, the light reflected from the subsolar point is estimated to be 0.24 cal cm^{-2} min^{-1}; and combining this with the amount conducted and with the solar constant, we find the mean spherical rate of lunar emission to be 1.61 cal cm^{-2} min^{-1} and the computed black-body temperature to be 374° K. From the distribution-curve of planetary heat about the subsolar point the mean spherical rate of emission is found to be 1.93 cal cm^{-2} min^{-1} and the corresponding temperature 391° K, which is to be compared with the theoretical temperature of 374° K.

Atmospheric absorption.—A discussion of the discrepancy between the observed and theoretical rate of lunar emission gives a set of corrections to the atmospheric absorption constants, derived on the assumption that the entire difference is due to errors in these quantities.

Reflection of solar radiation from the lunar surface.—From the distribution-curve of reflected light about the subsolar point and the drift-curve made with the water-cell in the beam the formula

$$E_r = K \frac{0.46 \sec^2 i/2}{0.46 \cos\theta + \sin\theta} \qquad (22)$$

was derived, where i and θ are the angles of incidence and reflection, respectively. The laws of Lambert, Lommel and Seeliger, and Euler cannot be made to fit the observational material.

Radiometric albedo.—The radiometric magnitude of the reflected light is found to be −13.3, and of the whole lunar radiation −14.8. The radiometric albedo of the reflected light is 0.093.

Temperature of the dark side.—This was found to be 120° K. The temperature is so low that considerable observing will be necessary to establish a good value.

The radiation from a planet consists of two parts: reflected sunlight which, when it reaches us, is confined practically to the limits of wave-length 0.3 to 5 μ, and the low-temperature radiation called "planetary heat," which is emitted by the warmed surface and which reaches us principally through the great water-vapor transmission band between 8 and 14 μ. The small amount of planetary heat transmitted between 0.3 and 8 μ is nearly negligible except in the case of the planet Mercury. To separate these radiations a microscope cover-glass 0.165 mm thick is superior to a water-cell, since any errors in the spectral reflection coefficients for the planet enter into the results very much less with the former screen than with the latter.

TRANSMISSION COEFFICIENTS

The transmission-curves of the microscope cover-glass,[1] fluorite screen,[2] rock-salt window,[2] and the atmosphere[3] are shown in

[1] *Mt. Wilson Contr.*, No. 336; *Astrophysical Journal*, **66**, 43, 1927.

[2] *Smithsonian Physical Tables* (7th ed.), p. 305, 1921.

[3] *Smithsonian Miscellaneous Collections*, **68**, No. 8, 1917.

Figure 1. All of these are well determined except that of the atmosphere. The only complete data on the transmission of water vapor and the atmosphere in long wave-lengths where planetary heat is radiated most abundantly are those obtained by F. E. Fowle.[1] The admirable experimental data from which these transmission coefficients were determined cover the range 0.001 to 0.082 cm of precipitable water, whereas the amount between an observer on Mount Wilson and a celestial object in the zenith is 0.7

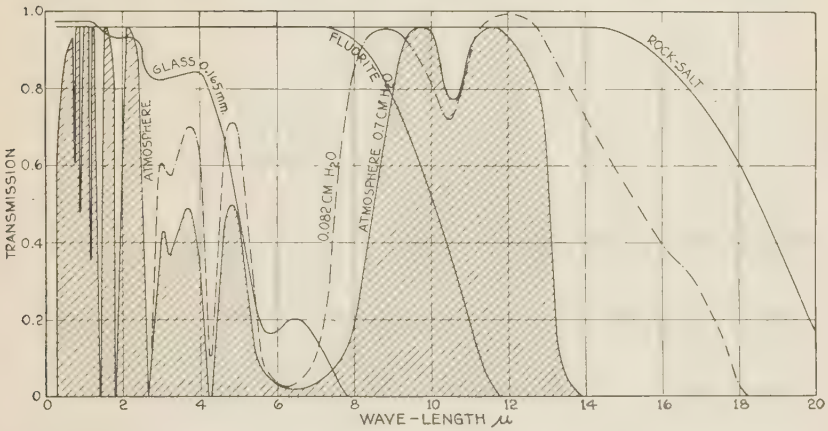

FIG. 1.—Transmission curves of (*a*) the atmosphere above Mount Wilson (the shaded curve); (*b*) water vapor, 0.082 cm precipitable water; (*c*) microscope coverglass, 0.165 mm thick; (*d*) fluorite, 4 mm; and (*e*) rock salt, 2 mm.

cm,[2] which necessitates an extrapolation of the observational data over a range 900 per cent greater than that observed. Probably no greater contribution to our knowledge of planetary temperatures could be made than a determination of the transmission coefficients of water vapor between 2.7 and 20 μ for amounts in the neighborhood of 1 cm of precipitable water, which is equivalent to a column of steam 16.7 m long at normal atmospheric pressure.

The shaded curve in Figure 1 is that for the atmosphere having 0.7 cm of precipitable water as recommended by Fowle,[3] with details

[1] *Ibid.*, p. 23, 1917.

[2] *Astrophysical Journal*, **35**, 149, 1912; *Annals of the Astrophysical Observatory, Smithsonian Institution*, **3**, 171, 1913.

[3] *Smithsonian Miscellaneous Collections*, **68**, No. 8, 1917.

in the near infra-red from radiation-curves which we observed for the purpose. That portion of the curve between 2 and 14 μ was made as nearly symmetrical as possible with Fowle's laboratory curve (the broken line) for 0.082 cm of precipitable water, the data for which are given in his table only in steps of 1 μ.

Variation in the amount of atmospheric water vapor will, of course, affect the atmospheric transmission. According to the shaded curve, a variation of 50 per cent[1] in the water vapor changes the transmission of the atmosphere 11 per cent. The formula of Hann,

$$p = 1.7\, e_w \sec z, \qquad (1)$$

gives the precipitable water p in the optical path for a given vapor pressure e_w. Fowle[2] has shown that in actual practice the coefficient 1.7 varies over a large range. On account of this and the uncertainty in the transmissions themselves it was thought better not to include observations when p differed largely from the mean value 0.7 cm than to apply corrections which could be of little certainty. From Fowle's extrapolations, which apply to the shaded curve only, it follows that the correction due to a variation of p, to be applied to a galvanometer deflection, B, for planetary heat from a celestial object between 300° and 500° K, is

$$\delta B = \frac{p - 0.7}{3} B, \qquad (0.3 < p < 1.5 \text{ cm}). \qquad (2)$$

OBSERVATIONAL DATA

The general method which we have used for measuring radiation from celestial objects has already been discussed.[3] The vacuum thermocouple employed for most of the lunar observations had a silver shield covering all the thermocouple and the platinum lead-wires except the receiver, 0.62 mm square, over one junction. The cell of the thermocouple was provided with a rock-salt window 2 mm thick.

[1] See also *Annals of the Astrophysical Observatory, Smithsonian Institution*, **4**, 284–285, 1922.

[2] *Astrophysical Journal*, **35**, 149, 1912; *Annals of the Astrophysical Observatory, Smithsonian Institution*, **3**, 171, 1913.

[3] *Mt. Wilson Contr.*, No. 369; *Astrophysical Journal*, **68**, 279, 1928.

The general scheme of observing was to make (1) a series of measurements on the moon with the microscope cover-glass, water-cell, and fluorite screen, and without any screen at all (free deflection); (2) a set of free deflections on a star whose radiometric magnitude we had previously determined;[1] and (3) a reading of the sling psychrometer. All the measurements were made at the Newtonian focus of the 100-inch telescope, where the mean diameter of the lunar image is 116.6 mm. The width of the receiver of the thermocouple is only 0.0055 of this image.

REDUCTION OF THE MEASUREMENTS

We have already pointed out[2] that the temperature of a star computed from the total radiation is given by

$$\log T = 2.638 - 0.1\,(m_r - \Delta m_r) - \tfrac{1}{2}\log d\,, \qquad (3)$$

where T is the absolute temperature, m_r the radiometric magnitude, Δm_r the loss, in magnitudes, due to the atmosphere and silvered surfaces of the telescope, and d the diameter of the star in seconds of arc. This formula assumes that the star radiates uniformly over its apparent surface—a condition which is approximately satisfied for the total radiation from the sun. From drift-curves on the sun taken in the Pasadena laboratory we have found that d from (3) should be multiplied by 1.07 for dG-type stars. In the case of a planet, d is the angular diameter of the receiver as seen from the mirror of the telescope, provided that the receiver is so small that the temperature of that part of the disk covered by it is practically constant. If the image of the planet approaches or is smaller than the diameter of the receiver, the condition of uniform distribution of radiation over the receiver no longer holds, and d is then the angular diameter of the receiver, on the one hand, or the angular diameter of the planet, on the other, corrected for distribution of radiation. Since either of these cases may occur for a planet, the last term of equation (3) has been changed to correspond to the diameter of a solid angle of 1 sq. sec. of arc of planetary heat and

[1] *Ibid.*, Table III.

[2] *Ibid.*, equation 4.

all observations have been reduced to this unit. Equation (3) then becomes

$$\log T = 2.612 - 0.1\ (\bar{m}_r - \Delta m_r)\ , \tag{4}$$

where $\bar{m}_r$ is the radiometric magnitude of a solid angle of 1 sq. sec. of arc of planetary heat. This equation gives the temperature corresponding to the mean radiation from the portion of the planet's surface, the image of which falls on the thermocouple, and assumes that the spectral distribution of energy is like that of a black body.

The values of Δm_r (Table I) have been obtained for various temperatures by combining the black-body curves with the atmospheric transmission-curves in Figure 1 and the reflecting power of silver, which for two reflections is 0.97 throughout the region of planetary heat.

The values of $\bar{m}_r$ are obtained from

$$\left.\begin{aligned} \bar{m}_r = m_r + (C-c) + 10/4 \log b - 10/4 \log B \\ -(a \sec Z - 0.16 \sec z) - P + 10/4 \log As^2\ , \end{aligned}\right\} \tag{5}$$

where m_r is the radiometric magnitude of the comparison star, $C-c$ the correction to m_r due to tarnishing of the silver, b the deflection for the star, B that part of the deflection for the planet due to planetary heat, Z and z the zenith distances of the moon and the star, respectively, a the coefficient of atmospheric extinction for planetary heat, P the correction in magnitudes from equation (2) due to the deviation of the water-vapor content of the atmosphere from the average, A the area of the thermocouple receiver in square millimeters, and s the scale of the telescope field in seconds of arc per millimeter. We will consider these quantities in the order in which they occur in equation (5).

The values of m_r for a number of stars have already been published.[1] The correction to m_r due to the differential absorption of radiation from the star and planetary heat by tarnished silver is

$$C - c = D\ (S_p - S_s)\ , \tag{6}$$

[1] *Ibid.*, Table III.

where D is the number of days since silvering, S_p the coefficient for planetary heat, and S_s the coefficient for the comparison star. S increases with spectral class[1] but becomes nearly constant at 205×10^{-6} mag. per day for the radiation from M-type stars, and, since planetary heat is of still longer wave-length, we may substitute this value for S_p in equation (6).

In obtaining B, that part of the deflection due to planetary heat, the free deflection, F, is combined as follows with Cg, the deflection observed with the cover-glass screen. Let R be that part of the light reflected from the planet, Tr the transmission of planetary heat through the cover-glass, and tr the transmission of the reflected light from the planet through the cover-glass. Then,

$$F=B+R\,, \tag{7a}$$

$$Cg=BTr+Rtr\,, \tag{7b}$$

$$B=\frac{F-\frac{Cg}{tr}}{1-\frac{Tr}{tr}}\,. \tag{7c}$$

The coefficient, a, of sec Z was determined from a series of measurements on the moon and Mars which gave a value of 0.16 mag., the same as the mean value for stellar radiation.

P is equivalent to δB in equation (2) expressed in magnitudes, and $s^2=256$ sq. sec. of arc at the Newtonian focus of the 100-inch telescope.

For planets in general we substitute B from equation (7c) into equation (5) and obtain (8):

$$\left.\begin{aligned}\bar{m}_r=m_r&+D(205\times 10^{-6}-S_s)+10/4\log b-10/4\log\left(F-\frac{Cg}{tr}\right)\\&+10/4\log\left(1-\frac{Tr}{tr}\right)-0.16\,(\sec Z-\sec z)-10/4\log\frac{p+2.3}{3}\\&+10/4\log As^2\,.\end{aligned}\right\} \tag{8}$$

[1] *Ibid*, Table I.

If we substitute the value of $\bar{m}_r$ from (8) into equation (4) and collect the constants and those variables which are functions of the planetary temperature, T, we obtain

$$\left.\begin{aligned} m_r + D\,(205\times 10^{-6} - S_s) + 10/4\,\log b - 10/4\,\log\left(F - \frac{Cg}{tr}\right) \\ - 0.16\,(\sec Z - \sec z) - 10/4\,\log\frac{p+2.3}{3} + 10/4\,\log As^2 \\ = 26.12 - 10\,\log T + \Delta m_r - 10/4\,\log\left(1 - \frac{Tr}{tr}\right) = m_r' \,, \end{aligned}\right\} \quad (9)$$

which applies to any planet for which the spectral distribution of the reflected light is known. This equation represents the radiometric magnitude of the planetary heat eliminated by the cover-glass for a solid angle of 1 sq. sec. of arc; the second member can be calculated for any planetary temperature, T, and the first member, which will be called m_r', can be obtained from observations.

It has already been shown[1] that, in the visible spectrum at least, the energy-curve of moonlight gives a color-index on the Mount Wilson scale[2] of 0.92 mag., which corresponds approximately to that of a Ko dwarf star. The absorption of the cover-glass screen for a star of this type[3] is 0.03 mag. with sufficient approximation, and the radiation reflected by it is 0.08 mag. Hence, the value of tr for the moon is 0.90. Substituting this value of tr into equation (9), we have equation (10), which applies to observations of the moon:

$$\left.\begin{aligned} m_r + D\,(205\times 10^{-6} - S_s) + 10/4\,\log b - 10/4\,\log\,(F - 1.11Cg) \\ - 0.16\,(\sec Z - \sec z) - 10/4\,\log\frac{p+2.3}{3} + 10/4\,\log As^2 \\ = 26.12 - 10\,\log T + \Delta m_r - 10/4\,\log\,(1 - 1.11Tr) = m_r' \,. \end{aligned}\right\} \quad (10)$$

From the atmospheric transmission-curves in Figure 1, the black-body energy-curves for various temperatures, and the reflecting power of silver, we have computed Table I for different values of T. The application of $\Delta m_r'$ will be discussed later.

[1] *Publications of the Astronomical Society of the Pacific*, **38**, 242, 1926.

[2] *Mt. Wilson Contr.*, No. 226; *Astrophysical Journal*, **55**, 165, 1922.

[3] *Mt. Wilson Contr.*, No. 369; *Astrophysical Journal*, **68**, 279, 1928.

In equation (10) the first and third terms of the left-hand member are fixed by the conditions of observing. The correction due to tarnished silver given by the second term did not exceed 0.05 mag. The reduction for air mass given by the fifth term did not exceed 0.16 mag. The correction for atmospheric water vapor given by the sixth term would not have exceeded 0.1 mag. The last term, which depends on the area of the thermocouple receiver and the scale of the telescope, was 5.07 mag. for the thermocouple previously described when used at the Newtonian focus of the 100-inch reflector.

TABLE I

T	Δm_T	T_T	m'_T	$\Delta m'_T$
100° K	6.35	0.000	+12.47	−0.49
150	.....	.....	7.80	.38
200	2.12	.000	5.23	.28
250	.....	.....	3.76	.24
300	1.39	.013	2.76	.20
350	.....	.....	2.01	.19
400	1.28	.063	1.45	.18
450	.....	.....	0.99	.18
500	1.28	.147	.60	.18
550	.....	.....	+ .27	.17
600	1.30	.249	− .01	.17
650	.....	.....	.25	.17
700	1.31	.364	.46	.17
750	.....	.....	.67	.16
800	1.25	0.468	− 0.85	−0.16

The lower limit of planetary temperature which can be measured is fixed by the sensitiveness of the thermocouple circuit and the area of the receiver, if the receiver is smaller than the image of the planet. As has been pointed out,[1] stars of radiometric magnitude +7 can be observed with the routine equipment which we have used; and with especially constructed thermocouples a gain of two additional magnitudes can be made. By adding the last term of equation (8) for the thermocouple described above, planetary heat of radiometric magnitude +12 could be measured with an accuracy of about 10 per cent, and with effort this might be increased to +15 or +16 if a large surface were available. Table I shows that planetary heat eliminated by the cover-glass of radiometric magnitude

[1] *Ibid.*

+12 corresponds to a temperature of 100° K, and of magnitude +16 to 70° K. From this it is seen that the temperatures of celestial objects much below 100° K can be determined only with difficulty.

REFLECTION OF SOLAR RADIATION OF WAVE-LENGTH 8–14 μ

It is well known that silica and to a less extent the silicates, of which the lunar crust may contain a large percentage, have high reflecting power in the region 8–14 μ. If these substances are present, it might be supposed that the solar radiation reflected from the lunar surface would be great enough to affect the temperatures calculated on the assumption that all the radiation in these wave-lengths is planetary heat radiated by the warmed surface of the moon. A simple calculation from Planck's black-body formula shows, however, that the reflected solar radiation would be less than $1\frac{1}{2}$ per cent of the planetary heat, even if the reflecting power of the lunar surface were perfect over the whole atmospheric transmission band 8–14 μ. This would decrease the computed temperature about 1°, which is less than the uncertainty arising from other sources. It is not easy, therefore, to determine by this means whether the lunar crust has a high silicate content.

Since the emissivity of silica (and to a less extent of the silicates) is abnormally low between 8 and 10 μ,[1] some indication of its presence should be revealed by the transmission of planetary heat through a fluorite screen, which, as an examination of Figures 1 and 2 will show, isolates just this spectral region. We will now compare the ratio, H, of the observed planetary heat transmitted by the fluorite screen to that without a screen and the similar ratio computed (*a*) by assuming unit emissivity and (*b*) by assuming the emissivity to be that of silica. From the curves in Figure 1 it will be seen that this ratio is essentially that of fluorite *minus* cover-glass to free deflection *minus* cover-glass, or of the energy between 8 and 10 μ to that between 8 and 14 μ.

From drift-curves in Figure 3 we find the following data, which

[1] Wood, *Physical Optics*, p. 602, 1911; Sosman, *The Properties of Silica*, p. 738, 1927.

apply to the subsolar point where the temperature is approximately 400° K:

$$F = 145 \text{ mm},$$
$$Fl = 79 \text{ mm},$$
$$Cg = 41 \text{ mm},$$
$$H = \frac{Fl - Cg}{F - Cg} = 0.37,$$

where Fl is the deflection with the fluorite screen in place.

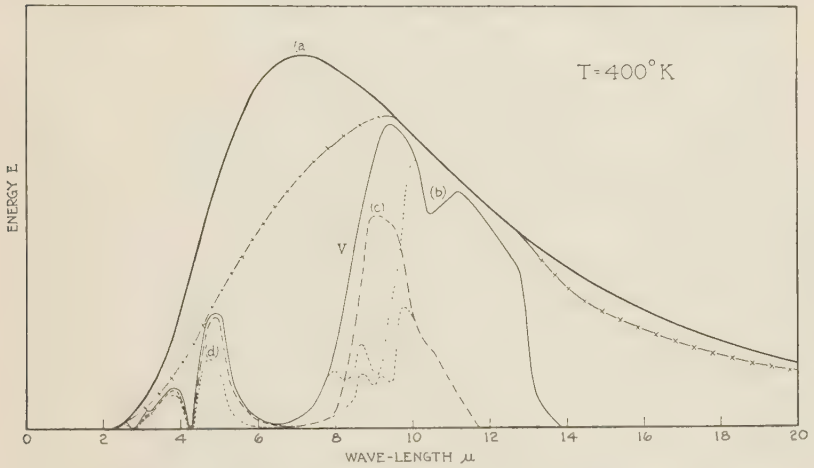

FIG. 2.—Energy-curve (*a*) of a black body at 400° K; (*b*) the same after the radiation has passed through the earth's atmosphere, the dotted line between 8 and 10 μ being the deformation due to presence of silica; (*c*) after passage through fluorite screen, the dotted line between 8 and 10 μ being the deformation due to presence of silica; (*d*) after passage through microscope cover-glass (red limit at 6 μ). The dash-and-cross line is the deformation of (*a*) necessary to explain the discrepancy between the observed and theoretical lunar temperatures.

From these data it can also be seen that the reflected light, R, which is essentially represented by Cg, is 0.39 as great as the planetary heat represented by $F - Cg$.

From the ordinates of the curves in Figure 1 multiplied into those of a black body at 400° K, we obtain Figure 2, where (*a*) is the spectral energy-curve for a black body at 400° K, (*b*) the same after transmission by the atmosphere, (*c*) after further transmission by the fluorite screen, and (*d*) after transmission by the cover-glass.

From this we find that the area which represents planetary heat in the free deflection is 2054, and that when the fluorite screen is in place it is 773. The ratio of these numbers represents H approximately, but to get a more exact value we must apply equations (7*a*) and (7*b*), which allow for the small amount of planetary light lost by the cover-glass. From these we find

$$Fl-Cg=0.05R+\ 773\ ,$$
$$F-Cg=0.10R+2054\ ,$$

whence

$$H=\frac{Fl-Cg}{F-Cg}=\frac{41+\ 773}{82+2054}=0.38\ ,$$

where R is 0.39 $(F–Cg)$ as above, and the reflecting power used for fluorite is 0.05. While the observed value $H=0.37$ is less than the 0.38 computed from the transmissions on the assumption of equal emissivities in the regions 8–10 μ and 8–14 μ, it can scarcely be interpreted as implying the presence of silicates, since with such a close agreement no surprise would have been caused had the figures been interchanged. From this, together with the nature of the lunar surface indicated by the low conductivity as shown in the discussion of eclipse observations to follow, it appears that practically all the planetary heat in the region 8–10 μ is accounted for by the assumption of unit emissivity.

We will now compute H on the assumption that the moon has a relatively smooth silica surface. The computed spectral energy-curves of planetary heat transmitted by the atmosphere and by the fluorite used above must be multiplied by the emissivity coefficients of silica before the ratio H is determined. The adopted coefficients, e, are as follows:[1]

λ	e	λ	e
7.75 μ	1.00	9.0 μ	0.20
8.0	0.76	9.25	.24
8.25	.38	9.5	.42
8.5	.30	9.75	.68
8.62	.40	10.0	0.98
8.75	0.32	10.25	1.00

[1] *Ibid.*

From these data we find

$$H = \frac{41 + 505}{82 + 1691} = 0.30 .$$

This value of H is so radically different from the observed value that we conclude that the emissivity of the lunar surface in the region 8–10 μ is unity for practical purposes and unaffected by any silica content it may have. This does not necessarily mean that the silica content of the lunar crust is small, for if it were finely divided like sand or porous like pumice, which probably would be its state if present, its radiating properties would be nearly those of a black body.[1] We can only say then that if silica or silicates are present, they are probably in the finely divided or porous state. It is possible that spectroscopic examination of the violet slope V (Fig. 2) of the band at 8–14 μ might reveal a deformation due to the emissivity of small amounts of non-porous silicates which would escape detection by the foregoing methods. It will be recalled, however, that the energy-curve[2] of lunar radiation obtained by Langley and Very showed no effect of this kind.

DISTRIBUTION OF RADIATION OVER THE DISK

Figure 3 shows drift-curves along a parallel of declination passing through the center of the disk of the full moon on June 16, 1924, when the phase angle was 0°. The curves were made by unclamping the telescope and allowing the image of the moon to transit the thermocouple. They represent (1) free radiation, that is, without filters, (2) radiation transmitted by 4 mm of fluorite, (3) radiation transmitted by 0.165 mm of glass, and (4) radiation transmitted by 1 cm of water. Number 1 represents all the planetary heat and all the reflected light transmitted by our atmosphere and reflected by the telescope mirrors. Number 2 represents about 35 per cent of the planetary heat and about 90 per cent of the reflected light. Number 3 represents about 11 per cent of the planetary heat and about 95 per cent of the reflected light, while No. 4 represents about 60 per

[1] *Ibid.*, p. 740.

[2] *Memoirs of the National Academy of Sciences*, 4, Part II, 193 ff., 1889.

cent of the reflected light. The principal features of the moon corresponding to points on the curve are indicated below.

Plate I is a photograph of the full moon made at the Lick Observatory, upon which are plotted the axes of co-ordinates (in

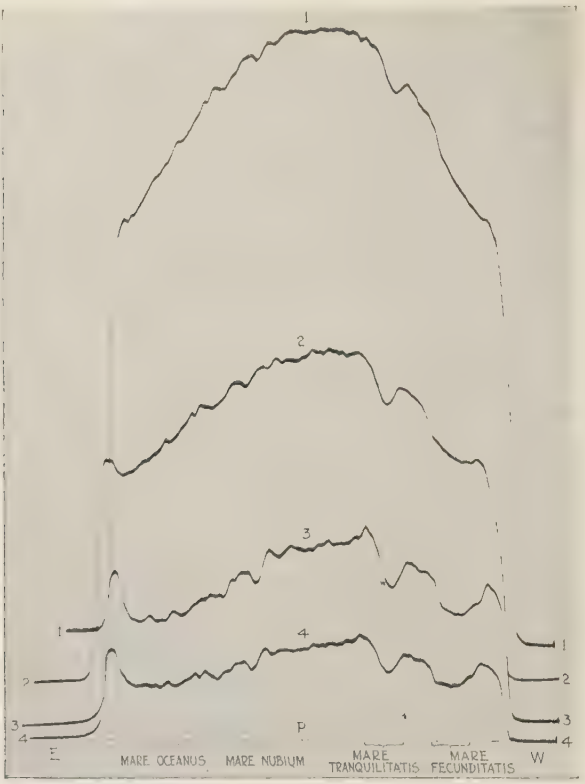

FIG. 3.—Drift-curves across full moon: (1) free radiation; (2) fluorite screen; (3) cover-glass; (4) water-cell.

black) and the paths (in white) traversed by the thermocouple junction on the three dates when drift-curves were taken. The width of the white lines is that of the thermocouple-receiver as used at the 100-inch telescope in making the drift-curves. The black squares refer to the dimensions of the thermocouple-receiver as used at the Snow telescope in the focus of a 27-inch mirror of 67 inches focal

PLATE I

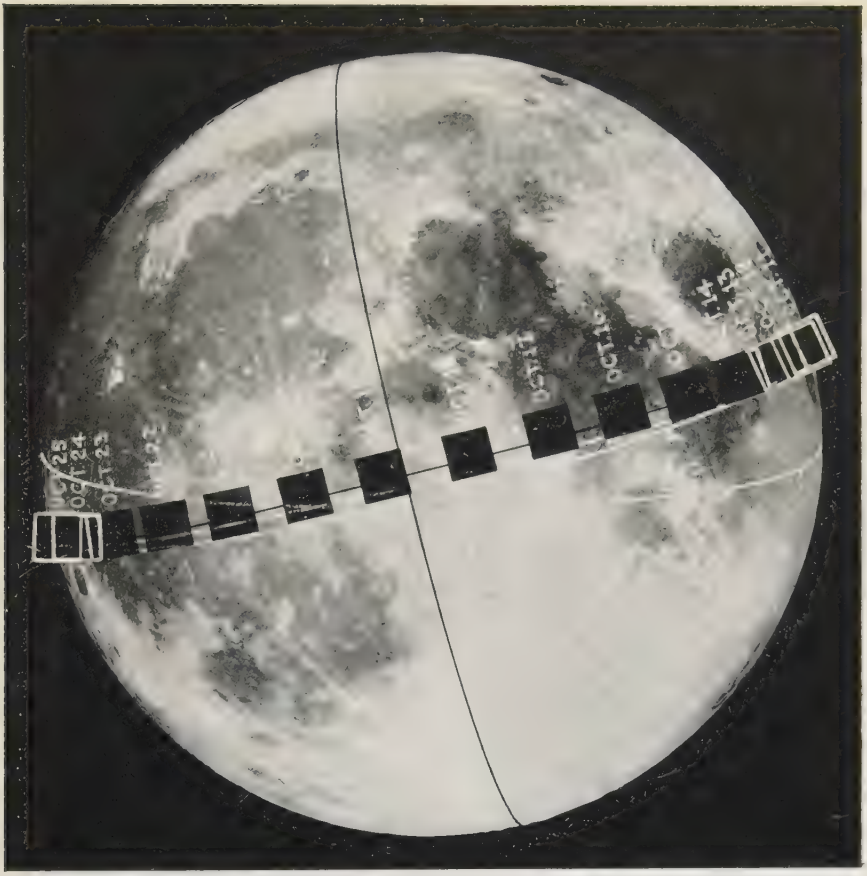

The white lines represent the width of path traversed by the thermocouple-receiver in recording drift-curves such as in Figure 3; the black lines are the axes of lunar co-ordinates. The black squares represent the size and position of the receiver in measuring the energy from the subsolar point between first and last quarters. These measures were used to obtain the distribution-curves in Figure 7.

length in the study of the distribution of energy about the subsolar point to be described later. We will first discuss the distribution of planetary heat over the disk.

DISTRIBUTION OF PLANETARY HEAT OVER THE DISK

As has been known from experimental observations for more than a hundred years, the radiation incident on the thermocouple-receiver from a given solid angle presented by a uniformly heated surface is independent of the angle of projection.[1] If we consider a smooth sphere, not in rapid rotation, exposed to parallel sunlight, the amount of solar radiation which is incident on and can be absorbed by any small-unit area and converted into heat will vary with the cosine of its angular distance from the subsolar point. The amount of planetary heat radiated by the small area in any directed unit solid angle, if it is a constant fraction of that absorbed, will follow the same law. Hence, if we pass a thermocouple junction over an image of this sphere as seen from any direction, the galvanometer deflections due to planetary heat emitted by it will follow the cosine law (eq. [13]).

Two circumstances modify this principle as applied to the moon. The increasing absorption, Δm_r, of the earth's atmosphere for planetary heat from the moon as the receiver moves away from the subsolar point, due to the falling temperature, causes the deflection observed toward the limb or terminator to be too low. A more serious difficulty is the roughness of the lunar surface, which makes the deflections anywhere on the disk near full moon higher, but near quarter-phase lower, than those calculated from the cosine law. The first consideration is obvious from an examination of Table I, but the second may need added explanation.

Two factors which unfortunately cannot be separated appear to explain the effect of roughness. Consider a cavity or bowl-shaped crater. Reflection of planetary heat from the interior by the sides of this depression, or re-emission of absorbed radiation, will tend to make the radiation toward the selenographic zenith greater, and toward the horizon less than it should be, thus making deflections at the center of the disk higher and at the limb lower than the cosine

[1] *Mémoires de l'Académie des Sciences, Paris*, **5**, 179–213, 1826.

law predicts. Again, if we consider an almost vertical mountain side near the terminator and facing the sun, it is clear that its temperature ought to be equal to that of the subsolar point, and its radiation, measured at full moon with a thermocouple-receiver smaller than its image in the field of the telescope, will give the same deflection as that from the subsolar point. At quarter-phase, however, such a mountain face at the terminator is invisible, and the area covered by its shadow will give no deflection. Thus arises the idea of directional temperature. The thermocouple measures the mean radiation of a small area of the moon as seen from the particular direction of the earth at the time, and this is interpreted in terms of temperature. Viewed from a different direction, the mean surface involved would not be the same because of its rough character.

The apparent distribution of planetary heat over the lunar surface can be obtained from the ordinates of curves Nos. 1 and 3 in Figure 3 by applying equation (7*c*) where $tr = 0.90$. The distribution of temperature can be obtained from equation (10). The real distribution of planetary heat over the lunar surface can be obtained from the distribution of temperature. This has been done for plates taken on April 19 and June 16, 1924, and June 14, 1927. The measurements were made for points located at intervals of 0.025 diameter of the apparent disk, and were plotted after reducing the positions of the measured points to the positions they would have for equatorial phase angle 0° when the subsolar point is on the hour circle passing through the center. This may be done by the usual formulae for the measurement of positions on a sphere; but, since the paths in every case pass very close to the subsolar point, the simpler formula of projection in one plane applies:

$$Y = \sin\,(\sin^{-1} Y_0 - i_0)\,, \qquad (11)$$

where Y is the distance in lunar radii from the subsolar meridian, Y_0 the observed distance from the central meridian in the same units, and i_0 the component of the phase angle in right ascension given by $i_0 = 180° - (\alpha\odot - \alpha\leftmoon)$. Y and Y_0 are positive west of the subsolar and central meridians, respectively.

The results of such measurements are plotted in Figure 4. The

scale of abscissae gives fractional parts of a radius of the lunar disk, the center of which is on the subsolar meridian indicated in the middle of the figure. The scales of ordinates show the galvanometer deflection B in millimeters due to apparent planetary heat, the radiometric magnitude m_r' of a square second of arc of planetary heat eliminated by the cover-glass, the absolute temperature T, and the energy E emitted by the lunar surface in cal cm^{-2} min^{-1}. The temperatures are computed from the data in Table I.

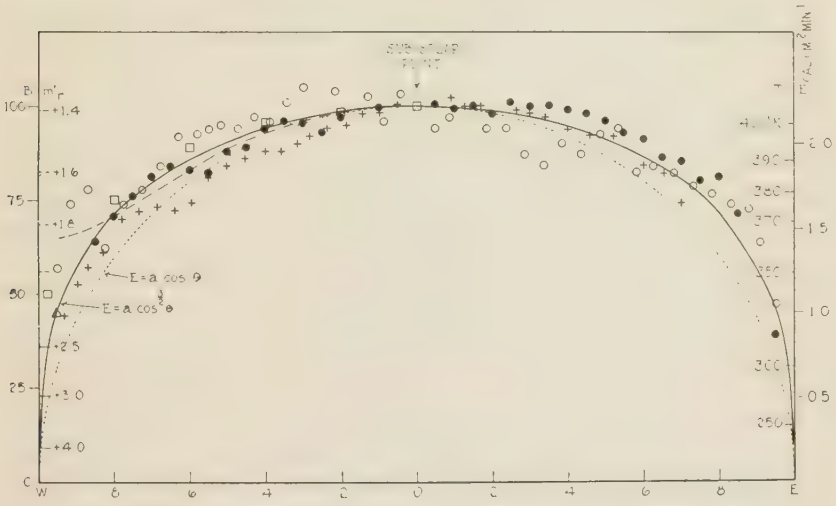

FIG. 4.—Distribution of planetary heat over the disk at full moon

The heavy full line in Figure 4 which represents the plotted observations is also the locus of the equation

$$E = a \cos^{3/2} \theta , \qquad (12)$$

and, as the observed points show, represents the apparent distribution of planetary heat over the lunar disk. An inspection of Figure 4 shows that from the center to 0.95 radius from the center the temperature varies only between 400° and 320° K, and since Δm_r is nearly constant over this range (Table I), the apparent distribution of radiation over most of the lunar surface at full moon is nearly the real one and is practically represented by equation (12).

The semicircle (dotted line) is that which represents the ideal

distribution of planetary heat emitted by a smooth, slowly rotating sphere without atmosphere exposed to sunlight according to the simple formula

$$E = a \cos \theta , \tag{13}$$

where θ is the angular distance of a point from the subsolar point and a is a constant, made equal to the radius of the sphere in this plot.

That roughness of the lunar surface will explain qualitatively, in part at least, the deviation of the drift-curve of planetary heat from the cosine-curve is illustrated by the following simple consideration. If the roughness on the moon is due to non-conducting spheres uniformly distributed over its surface, each sphere will present at full moon a distribution of energy approximating the cosine law, and its radiation in the direction of the earth at that phase will be two-thirds that which the surface it occults would have radiated. It is easily seen then that the energy E emitted in an earthward beam of unit cross-section, small compared to the radius of the moon, will be given by

$$E = E_0 \left[\cos \theta + \frac{na}{k} \left(\frac{2}{3 \cos \theta} - 1 \right) \right] , \tag{14}$$

where E_0 is the energy from the area k in the beam at the subsolar point, θ the angular distance from the subsolar point, n the number of spheres of sectional area a in the area k (at the subsolar point). This equation will hold to a value $\theta = \theta'$, where the spheres would begin to occult each other. The constant na/k was determined from Figure 4 by inserting the observed value of E for $\cos \theta = 0.6$ in equation (14) and was found to be 0.316. From this it appears that the spheres would be separated 3.39 radii, which gives $\theta' = 53^\circ\ 50'$. The locus of this equation appears in Figure 4 as a broken line. An additional point was found for the case where for one orientation of the field the spheres appear mutually tangent, while for another orientation their maximum occultation is 0.78 radius.

In an extended series of measurements during the lunar eclipse of June 24, 1927, a point 0.05 radius from the south limb of the

moon was selected for continuous observation. This gave the point indicated in Figure 4 by a triangle, which agrees fairly well with similar points obtained from the drift-curves above.

DISTRIBUTION OF REFLECTED SOLAR RADIATION OVER THE DISK

Several conclusions concerning the reflected light from the moon follow directly from an examination of curve No. 4 of Figure 3 taken through the water-cell: (*a*) the limb of the moon is 60 per cent brighter than the neighboring surface, which in this case consists of *maria;* (*b*) the center of the moon is 10 to 15 per cent brighter than the limb; (*c*) the brightest point on the E–W diameter is on the eastern boundary of Mare Tranquilitatis near longitude 17° W; (*d*) the *maria* are only three-fourths as bright as the mountainous regions; (*e*) the general trend of the curve is toward uniform brightness, which would be expected from the Lommel-Seeliger or Euler laws of diffuse reflectivity,[1] but not from Lambert's law, which would give a distribution more like that obtained above for planetary heat. A discussion of the laws of diffuse reflection which apply to the moon will be given in another section.

TEMPERATURE OF THE SUBSOLAR POINT

The temperature of the subsolar point has been determined at full moon from the drift-curves described above, and at quarter-phase by observing deflections on the middle of the limb. When the phase angle in the latter case was not exactly 90°, the deflections due to planetary heat were reduced to quarter-phase by equation (13). The results are given in Table II, where m_r° is the radiometric magnitude of the moonlight transmitted by the water-cell and the other symbols have the meanings previously defined.

The solar constant has been reduced to the heliocentric distance of the moon at the time of observation, and the average temperatures to 1.93 cal cm^{-2} min^{-1} by the fourth-power law. That the temperature of the subsolar point measured at first quarter is 49° C. lower than that measured at full moon may be explained by the rough surface. The work of Rosse[2] and of Langley[3] showed that the

[1] Müller, *Photometrie der Gestirne*, p. 68, 1897.

[2] *Philosophical Transactions of the Royal Society*, **163**, 587, 1873.

[3] *Memoirs of the National Academy of Sciences*, **4**, Part II, 107, 1889.

lunar temperature was probably as high as boiling water, and the value of 407° K obtained by us for the subsolar point at full moon is in substantial agreement with that found by Menzel[1] from the water-cell observations of Coblentz,[2] the known visual albedo of the moon being used to interpret the eliminated planetary heat in terms of temperature.

TABLE II

TEMPERATURE OF THE MOON'S SUBSOLAR POINT

Date P.S.T.	Solar Const.	W.C.	m_r°	m_r'	T	E
	Full Moon					
1924 Apr. 19	1.92	2.42	+3.44	+1.37	408°K	.....
Apr. 20	1.92	2.50	3.55	1.35	410	.....
June 16	.....	2.01	.....	.....	.....	.....
1927 June 14	1.87	2.00	+3.05	1.44	401	.....
1929 Oct. 17*	1.93	.....	.....	+1.40	405	.....
Corrected average	1.93	2.23	+3.35	+1.39	407	2.24
	Quarter-Phase					
1923 Mar. 24†	1.93	2.49	+4.18	+1.69	377	.....
July 19†	1.85	2.35	3.99	1.96	354	.....
Oct. 14†	1.95	2.30	4.28	2.02	349	.....
Nov. 14†	1.98	2.89	3.80	1.80	367	.....
1924 June 9†	1.90	2.36	4.20	1.81	366	.....
July 24‡	1.88	1.90	+4.05	+2.21	335	.....
Corrected average	1.93	2.38	+4.08	+1.92	358	1.36

* Corresponds to Greenwich Civil date, Oct. 18, on Plate I.
† First quarter.
‡ Last quarter.

TEMPERATURES DURING A LUNAR ECLIPSE

A continuous series of measurements of lunar radiation was made during the eclipse of June 14, 1927. A point 48″ (0.05 radius) from the south limb was chosen, since this limb passed nearest to the center of the earth's shadow, the distance at mid-totality being 11′ north. The duration of total phase for this point was 2^h40^m,

[1] *Astrophysical Journal*, **58**, 65, 1923.

[2] *Scientific Papers, Bureau of Standards*, **18**, 535 (No. 438), 1922.

and the partial phases were 1^h each. For the point selected the time of mid-totality was 12^h16^m A.M., P.S.T., which made it a favorable eclipse for continuous measurement. Figure 5 shows the circumstances of the eclipse, *P* being the position of the thermocouple junction.

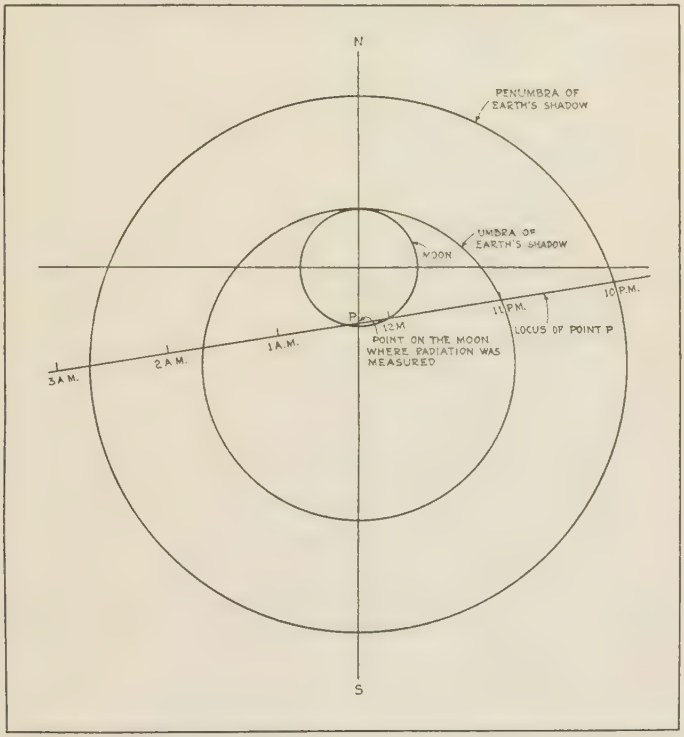

FIG. 5.—Circumstances of the total lunar eclipse of June 14, 1927. The radiation measurements were made at the point *P*.

The program of observation included several drift-curves before and after eclipse, and deflections on and off the south limb for free radiation, and with the cover-glass and the water-cell in the beam, all taken in the usual manner. Arcturus and Vega were used as comparison stars.

The deflections have been reduced to the zenith as previously described. Since the radiation varied greatly during the eclipse, the

sensitivity used in the electrical circuit was changed in four steps, so that during totality it was 4.2 times as great as before and after the eclipse. The time required to obtain a single set of deflections for free radiation or for that through water-cell or cover-glass was 3 minutes. To simplify the record in Table III the deflections have been read for the same instant (the time of free deflection) from a plot of the observed deflections against the time.

TABLE III

RADIATION DURING LUNAR ECLIPSE

TIME P.S.T.	OBSERVED DEFLECTIONS			m'_r	T	E	E_R
	Free	Cg	Wc				
	mm	mm	mm			cal cm^{-2}min^{-1}	
9h22m*	617	289	191	+2.09	342°	1.13	1.85
10 04	617	289	182	2.09	342	1.13	1.85
10 30	347	166	113	2.74	300	0.67	1.00
10 52	79.5	33.9	20	4.2	231	.24	0.19
11 13	6.46	1.00	0.80	6.4	174	.08	.00
11 34	4.47	0.07	.64	6.7	170	.07	.00
11 47	5.13	.12	.07	6.5	173	.07	.00
12 02†	2.57	.09	.07	7.3	160	.05	.00
12 28	4.08	.01	.14	6.8	169	.07	.00
12 58	1.48	.20	.16	8.0	149	.04	.00
1 22	2.89	0.42	0.20	7.3	160	.05	.00
1 46	8.92	.....	6.31	7.6	156	.05	.09
1 54	55.0	31.6	21.9	5.0	205	.15	.28
1 59	100	63.1	39.8	4.6	219	.19	0.48
2 28	513	263	174	2.41	320	0.87	1.63
2 41	617	302	200	2.15	339	1.09	1.85
3 04	603	309	204	+2.23	333	1.02	1.85

* P.M. † A.M.

The values of m'_r were computed from equation (10), and the absolute temperatures, T, were read from Table I. E, the radiation emitted by the moon in cal cm^{-2} min^{-1}, was obtained from the black-body formula by using the temperature T. The energy, E_R, received by the moon from the sun, was calculated from the conditions of the eclipse and the distribution of energy on the solar disk.

The total radiation along a radius of the sun is expressed by the formula given by Jeans:[1]

$$\frac{J}{J_0}=0.465+0.535\sqrt{1-r^2}\,, \qquad (15)$$

[1] *Monthly Notices of the Royal Astronomical Society*, **78**, 35, 1917.

where J_0 is the total radiation at the center of the disk and r the distance in radii from the center to the point where the total radiation is J; the constants have been derived from Abbot's data.[1] The total radiation which reaches the moon at any instant as the sun is eclipsed by the earth is the summation over all the uneclipsed area, each element of which is to be weighted according to equation (15). Table IV gives the resulting intensity of solar radiation on the moon as a function of the fraction of a solar diameter occulted by the earth.

TABLE IV

Fraction of Solar Diameter Occulted by Earth	Fraction of Total Solar Radiation Received by Moon
0.1	0.96
.2	.89
.3	.79
.4	.67
.5	.54
.6	.41
.7	.27
.8	.15
0.9	0.05

Figure 6 is a plot of the data in the last three columns of Table III. The full line indicates the absolute temperature, T, of the point P in Figure 5 obtained from the data in Table I. The dotted line represents the solar radiation E_R received, and the broken line the energy E radiated by the moon in cal cm^{-2} min^{-1}.

In general, the fall and rise in temperature lags behind E_R, the energy received by the moon, as might be expected.

The temperature falls from 342° to a value between 200° and 175° K during the first partial phase, and during totality continues to fall slowly, reaching 156° K at the end. For a few minutes after totality the temperature does not change materially, then it rises abruptly during the next 20 minutes. From this it follows that the surface materials of the moon have low heat conductivity.

DISTRIBUTION OF PLANETARY HEAT AND REFLECTED LIGHT ABOUT THE SUBSOLAR POINT

It will now be our purpose to compare the radiation and temperature of the moon as determined from direct observations with

[1] Abbot, *The Sun*, 2d ed., p. 107, 1929.

the thermocouple (Table II) with the values derived theoretically from the solar constant by making suitable allowances for reflected light and conducted heat. Before this can be done the distribution of both reflected light and planetary heat over the hemisphere about the subsolar point must be investigated in much the same manner as we study the distribution of radiation about an electric light. This was accomplished by a continuous series of measurements on the subsolar point made throughout the lunation between first and last quarters in October, 1929.

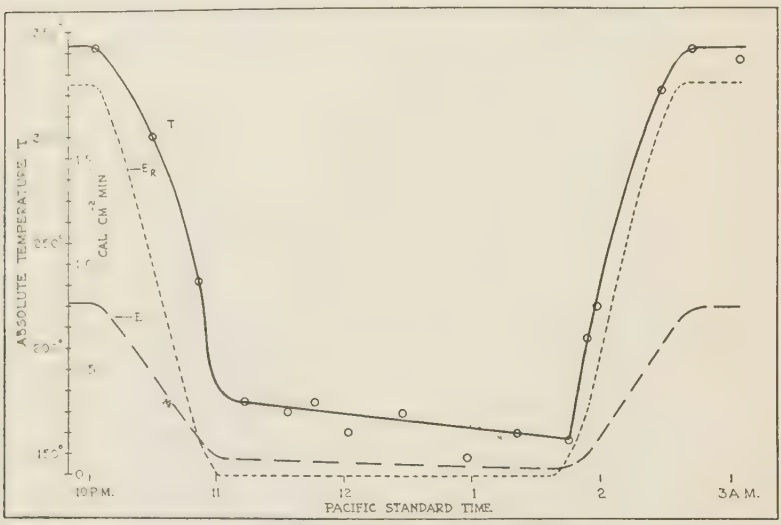

FIG. 6.—March of absolute temperature, T, of energy received from the sun by the moon, E_R, and of energy radiated, E, during the total lunar eclipse of June 14, 1927.

The apparatus employed was a reflecting telescope of 27 inches aperture and 67 inches focal length fed by the coelostat of the Snow telescope.[1] The image of the moon was approximately 15.5 mm in diameter. The deflections, which were of the order of 200 mm for free radiation and 50 mm with the cover-glass, were read visually at intervals during the night. The planetary heat eliminated by the cover-glass and the light transmitted by it were reduced to the zenith by Bouguer's formula in the usual manner.

Simultaneous observations made with the 100-inch telescope at

[1] *Mt. Wilson Contr.*, No. 4; *Astrophysical Journal*, **23**, 6, 1906.

the time of full moon, with suitable comparison stars, furnished the scale of absolute units. The settings of the thermocouple upon the subsolar point were made from the photograph in Plate I, upon which were plotted the night-to-night positions of the subsolar

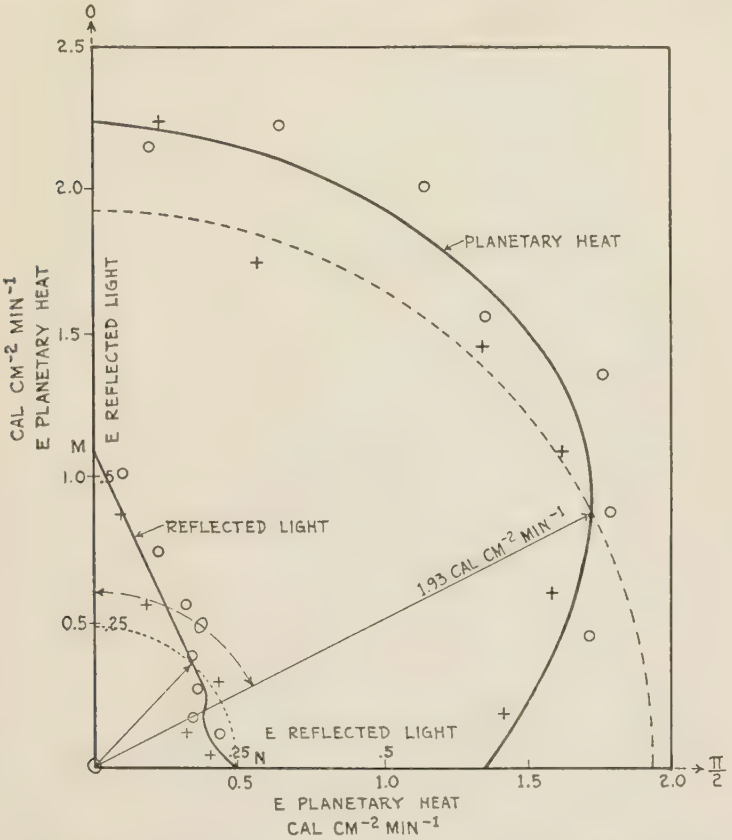

FIG. 7.—Distribution of planetary heat and reflected solar radiation about the subsolar point on the moon.

point. These are shown by the black squares which give the size and position of the thermocouple-receiver for each Greenwich Civil date. The angle between the sun and earth as seen from the subsolar point (which is equivalent to the zenith distance of the earth) was computed by the usual formula. The resulting distribution-curves of planetary heat and reflected light about the subsolar point are

plotted in polar co-ordinates in Figure 7. The intensity scales E on the outside of the figure are for planetary heat and on the inside for reflected light outside the atmosphere and were calibrated by the 100-inch measurements in Table II.

Curiously, the intensities of both planetary heat and reflected light from the subsolar point after full moon (indicated by circles) are somewhat greater than the corresponding intensities before full moon (indicated by crosses). As these observations are all on the subsolar point, this difference can have no relation to accumulation of heat by the moon, which might tend to make the maximum temperature of a fixed point on the surface occur in the lunar afternoon.

It will be noted that the values of the planetary heat E in absolute units at full moon and first quarter in Table II agree with the corresponding values read from the distribution-curve of planetary heat for $\theta=0$ and $\theta=\pi/2$ given in Figure 7. The distribution of reflected light shows a sharp drop from full moon ($\theta=0$) to $\theta=75^\circ$, and a definite increase again near quarter-phase ($\theta=\pi/2$).

Simple considerations show that the mean value of the intensity of both planetary heat and reflected light about the subsolar point is the radius of the hemisphere having the volume generated by revolution of the curves in Figure 7 about the axis $\theta=0$. The arc quadrants of these hemispheres and their radii, which represent the mean spherical intensities, are also shown in Figure 7.

THEORETICAL LUNAR TEMPERATURE

The temperature of the subsolar point on the moon may be computed from the solar radiation received, E_R, if that part of it reflected from the lunar surface, E_r, and that part conducted into it, E_c, are known. The radiated energy E can then be found from the equation

$$E_R-E_r-E_c=E=\eta\sigma T^4\,. \qquad (16)$$

Here η is the emissivity, which will be taken as unity in the calculation following. The value of E_R is the solar constant for the times of observation, reduced from the mean distance of the sun to the heliocentric distance of the moon by the inverse-square law. The error in the measurement of this quantity arising from uncer-

tainties in the atmospheric transmission is small, since it depends on atmospheric transmissions principally to the violet of λ 3 μ, beyond which there is only about 1 per cent of the solar radiation. These transmissions are easily determined, while those in the region 8–14 μ are determined only with great difficulty.

E_r may be obtained from the average value of m_r° in Table II, which is +3.35 mag. This quantity is the radiometric magnitude of a solid angle of 1 sq. sec. of arc of moonlight from the subsolar point transmitted by the water-cell. Since the energy-curve of moonlight is approximately that of a Ko dwarf star, as has already been pointed out, it would be 0.41 mag. brighter[1] outside the atmosphere; and since the water-cell absorption for a Ko dwarf star is 0.54[2] mag., the radiometric magnitude of 1 sq. sec. of reflected moonlight outside the atmosphere would be +2.40. A similar reduction for the subsolar point at quarter-phase gives +3.13 mag. for a point outside the atmosphere.

From the distribution-curve of reflected light in Figure 7 we find that the mean intensity is 0.85 mag. greater (fainter) than the intensity at full moon, which makes the radiometric magnitude of a square second of reflected moonlight outside the atmosphere +3.25 (mean spherical intensity). This is nearly the observed value at quarter-phase given above, and Figure 7 shows that the actual observed distribution-curve crosses the mean spherical distribution-curve near quarter-phase ($\theta = \pi/2$).

Since the ratio of the whole hemisphere to 1 sq. sec. is −28.57 mag., the magnitude of the total reflected light is −25.32. This, reduced to terms of energy,[3] gives

$$\begin{aligned} E_r &= 17.3 \times 10^{-12} \times 2.51^{25.32} \text{ cal cm}^{-2} \text{ min}^{-1}, \\ E_r &= 0.24 \text{ cal cm}^{-2} \text{ min}^{-1}. \end{aligned} \qquad (17)$$

The data in Table III may be used to estimate the amount of heat, E_c, conducted into the interior of the moon. Let us assume that before a stable condition, such as existed previous to the eclipse, can be restored, approximately the same amount of heat must be

[1] *Mt. Wilson Contr.*, No. 369; *Astrophysical Journal*, **68**, 279, 1928.

[2] *Ibid.*, p. 297. [3] *Ibid.*, p. 300.

returned to the moon as was given up by it during the eclipse. Hence, if we interpolate E and E_R from Table III for uniform time-intervals and compute E_c from equation (16), using the temperatures to determine E and various arbitrary values for E_r, until the sum of the values of E_c for the period of the eclipse is zero, we find that to fulfil this condition 52 per cent of the solar energy incident on the area observed must have been reflected, and of the remainder less than 0.1 cal cm^{-2} min^{-1} could have been conducted into the interior of the moon before and after the eclipse. At the subsolar point, where the surface temperature is higher, the conducted heat would be somewhat greater, but even there probably does not exceed 0.1 cal cm^{-2} min^{-1}.

The large value of the reflected light assumed here is borne out by the large fraction of lunar radiation transmitted by the water-cell (0.33) and cover-glass (0.50) shown in Table III, before and after the eclipse.

From the data in Figure 6, Epstein[1] has shown that $(\kappa\rho c)^{-1/2}$, in which κ is the conductivity, ρ the density, and c the specific heat of the lunar crust, is in the neighborhood of 120. This value corresponds to that of pumice or volcanic ash, for which the conductivity is about 0.001. This would indicate that at a temperature of 373° K on the moon, the temperature 1 cm below the surface is 100° C. lower, that is, about at the freezing-point of water. It is therefore probably safe to assume that E_c does not exceed 0.1 cal cm^{-2} min^{-1}.

Taking the solar constant on the moon to be 1.95 cal cm^{-2} min^{-1} and applying equation (16), we find

$$\begin{aligned} E &= 1.61 \text{ cal cm}^{-2} \text{ min}^{-1}, \\ T &= 374^\circ \text{ K}. \end{aligned} \tag{18}$$

If E_c is 0.05 cal cm^{-2} min^{-1}, $T = 377°$ K, while if E_c is negligible, $T = 379°$ K.

Since the solar constant probably varies from 1.91 to 1.965 cal cm^{-2} min^{-1}, and the reciprocal square of the heliocentric distance of the moon ranges from 0.962 to 1.039, E_R may vary from 1.84 to

[1] *Physical Review*, **33**, 269, 1929.

2.04 cal cm^{-2} min^{-1}. If we assume that E_r is proportional to E_R and that E_c is practically constant, E varies from 1.52 to 1.69 cal cm^{-2} min^{-1}, and T for the subsolar point would vary from 368° to 378° K.

From the distribution-curve of planetary heat in Figure 7 we find that the mean spherical intensity which is to be compared with the theoretical value in equation (18) is

$$\begin{aligned} E &= 1.93 \text{ cal cm}^{-2} \text{ min}^{-1}, \\ T &= 391^\circ \text{ K}, \\ m'_r &= +1.54 \text{ mag.} \end{aligned} \tag{19}$$

The planetary heat emitted by the lunar surface is therefore 0.32 cal cm^{-2} min^{-1}, or 20 per cent in excess of that which can be accounted for by the theory, and corresponds to a temperature 17° higher than the solar constant permits after reflection of solar radiation and conducted surface heat on the moon have been deducted.

This result can be explained by any one or by a combination of the following conditions: (1) The solar constant is greater than 1.93 cal cm^{-2} min^{-1}; (2) the emissivity η is greater than unity in the region 8–14 μ; (3) the atmosphere is more transparent in the region 8–14 μ than Fowle's extrapolated coefficients show.

In view of the careful work on the solar constant in spectral regions and under climatic conditions where the atmospheric transmissions which affect the problem are relatively easy to determine, it is hardly possible to allow the increase of 20 per cent necessary to account for the foregoing discrepancy between the theoretical and the observed temperatures of the moon.

As to the second postulate, we have already found, in the section on "Reflection of Solar Radiation of Wave-Length 8–14 μ," evidence that in this region of the spectrum the moon radiates like a black body. The deformation of the energy-curve of the moon necessary to satisfy the observed planetary heat is shown by the dash-and-cross line in Figure 2. We do not regard this deformation as very probable.

This leaves us with the third postulate, which requires that the atmospheric transmissions in the region 8–14 μ be increased about

19 per cent. This can be done easily without seriously encroaching on the transmission-curve for the maximum water-vapor content used in the laboratory determinations and, in view of the large extrapolation from the observed data, would not be regarded as presuming an unreasonable systematic error. Formally then, we compute the magnitude $\Delta m'_r$, which must be added to m'_r in Table I, or to Δm_r, from which m'_r is computed, to make the observed value of T agree with that deduced from the solar constant. To do this it is necessary to assign to the theoretical temperature $T=374°$ K in equation (18) the value $m'_r=1.54$ mag. found from direct measurement in equation (19). The atmospheric transmission-curve in Figure 1 was accordingly symmetrically adjusted between 8 and 14 μ to give this result for a black body at 374° K, and from these data a new set of values of m'_r was computed which appear as corrections, $\Delta m'_r$, to be added to the original values of m'_r in order to make the theoretical and observed temperatures agree. In computing the temperatures of planets with equation (9), $\Delta m'_r$ should be added to m'_r in Table I unless circumstances are found which modify this conclusion.

The effect of $\Delta m'_r$ is to lower the temperature computed from the radiation measurements of Mercury[1] about 45° C., Venus[2] 9°, Mars[3] 10°, and the moon 17°.

REFLECTION OF SOLAR RADIATION FROM THE LUNAR SURFACE

In general, three different theoretical laws of diffuse reflection have been used in discussions of the photometric properties of planets. As applied to apparent solid angles of radiation they are[4]

$$E_1=K_1\cos i \qquad \text{(Lambert)}, \qquad (20a)$$

$$E_2=K_2\frac{\cos i}{\cos i+\cos\theta} \qquad \text{(Lommel-Seeliger)}, \qquad (20b)$$

$$E_3=K_3\frac{\cos i}{\cos\theta} \qquad \text{(Euler)}, \qquad (20c)$$

[1] *Popular Astronomy*, **33**, 299, 1925.

[2] *Ibid.*, **32**, 614, 1924.

[3] *Ibid.*, p. 601, 1924.

[4] Müller, *Photometrie der Gestirne*, p. 68, 1897.

where i is the angle of incidence, θ the angle of reflection, and the K's are constants. We will compare these equations with the observed distribution of reflected light about the subsolar point in Figure 7, and the drift-curve (No. 4 in Figure 3) taken through the water-cell across the full moon.

We may consider the curve of distribution MN about the subsolar point O in Figure 7 to be a straight line. Its intercept N on the axis of $\pi/2$ is 0.46 of the intercept M on the axis of 0°, and since for this curve the angle of incidence i is always zero, the equation which represents it is

$$E' = K_4 \frac{0.46}{0.46 \cos \theta + \sin \theta}. \tag{21}$$

This equation gives us no knowledge as to the effect of varying the angle of incidence i, but we can determine this from drift-curve No. 4 in Figure 3.

The distribution of reflected solar radiation across the disk of the full moon shown in this curve has a general uniform trend, but is high in the middle near the subsolar point, decreases toward the limb, and then rises again at the limb itself. For this curve the values of i and θ are always equal, and their sines are proportional to the abscissae measured from the subsolar point P (Fig. 3). By multiplying E_r' in equation (21) by a power of the secant of a function of i, it may be made to fit both the drift-curve in Figure 3 and the distribution-curve in Figure 7, since i is zero for the latter case. By trial we find that

$$E_r = K \frac{0.46 \sec^2 i/2}{0.46 \cos \theta + \sin \theta} \tag{22}$$

fits both the drift-curve and the distribution-curve fairly well and therefore represents the law of diffuse reflectivity for the moon as derived from these radiometric observations. More complicated functions of i can be found which give better agreement with the observed drift-curve; but as the surface features of the moon probably affect the drift-curve in a manner not entirely dependent on i, such a procedure seems unjustified until more extended observations are obtained.

For $i=0$, equation (22) reduces to the straight line (21) and therefore deviates from the mean curve MN of Figure 7 only in the curved portion of this line. Equation (20*a*) would give a quadrant of a circle of radius OM centered about the origin O. Equation (20*b*) would be a curve intercepting the 0° axis halfway between the origin O and M and the $\pi/2$ axis at a distance from the origin equal to OM. Equation (20*c*) is the locus of a straight line parallel to the axis of $\pi/2$ and passing through M. It is therefore easy to see that equations (20*a*), (20*b*), and (20*c*) do not fit the observed curve at all, while equation (22) agrees fairly well. Table V gives a comparison

TABLE V

INTENSITY OF REFLECTED SUNLIGHT

$i=\theta$	Obs.	Eq. (22)	Eq. (20*a*)	Eq. (20*b*)	Eq. (20*c*)
0°	51	51	50	50	50
15	46	34	48	50	50
30	41	28	43	50	50
45	32	26	35	50	50
60	32	28	25	50	50
75	41	34	13	50	50
90	44	47	0	50	50

of the intensities on an arbitrary scale for various values of $i=\theta$ read from the drift-curve in Figure 3 with those computed from formulae (22), (20*a*), (20*b*), and (20*c*). Here again formula (22) perhaps represents the observations better than formulae (20*a*), (20*b*), and (20*c*.)

RADIOMETRIC MAGNITUDE AND ALBEDO OF THE MOON

Since the radiometric magnitude of a solid angle of 1 sq. sec. of moonlight from the subsolar point at full moon transmitted by the water-cell is +3.35 and the water-cell absorption 0.54 mag., the radiometric magnitude of 1 sq. sec. of reflected full moonlight transmitted by the atmosphere is +2.81. This gives −13.3 for the radiometric magnitude of the reflected light from the whole full moon at mean distance. From the areas under the water-cell and free curves in Figure 3 we find the radiometric magnitude of the whole radiation from the full moon to be −14.8.

The ratio of the solar energy reflected from the subsolar point to that received by it is 0.124. This may be considered as the albedo of the subsolar point but should not be confused with the albedo[1] of the moon, 0.073, which is the ratio of light reflected by the whole hemisphere to that received by it. The albedo, A, may be expressed as

$$A = pq ,$$

where p is the ratio of actual brightness of the moon at full phase to that of a self-luminous body of the same size and position, which radiates as much light from each unit of its surface as the moon receives from the sun under normal illumination, and q is a factor depending on the law of diffuse reflection from the moon. For visual light[2] the value of q is 0.694 and $p = 0.105$. The ratio p for light transmitted by the earth's atmosphere may be obtained from the equation

$$\log p = 0.4[m_r \text{ (sun)} - m_r'' \text{ (moon)}] + \log \pi - 2 \log \sin 1'' .$$

The radiometric magnitude, m_r'', of a solid angle of 1 sq. sec. of the sunlight reflected from the full moon is practically constant over the lunar disk, as may be seen from Figure 3. The mean ordinate of curve No. 4 is 15 per cent lower than at the subsolar point, but since the *maria*, which seem to be responsible for the depressions, cover only one-third of the apparent disk of the full moon, the error in this assumption is probably only 5 per cent, i.e., 0.05 mag. Substituting for m_r'' the value $+2.8$ found above, and for m_r the value -27.18 mag. found for the radiometric magnitude of the sun,[3] we find

$$p = 0.135 ;$$

and if q is the same for all wave-lengths the radiometric albedo of the moon is

$$A = 0.093 .$$

[1] Russell, *Astrophysical Journal*, **43**, 179, 1916.

[2] *Ibid.*

[3] *Mt. Wilson Contr.*, No. 369; *Astrophysical Journal*, **68**, 308, 1928.

TEMPERATURE OF THE DARK SIDE OF THE MOON

Measurements of the radiation from the dark side of the moon 48″ from the east limb were made on July 5, 1927, when this point was nearly opposite the sun on the midnight meridian. The sensitivity used was such that a star of radiometric magnitude 0 would produce 19 mm deflection. Our result was a deflection of 0.09 ± 0.05 mm. This gives radiometric magnitude 10.6 per square second of arc, which corresponds to a temperature of about 120° K. The temperature corresponding to the deflection *plus* its probable error is 125° K, which may be considered its upper limit. Considerable observing will be required to establish a good value of this temperature.

We wish to acknowledge the assistance of Miss Richmond in the rather involved processes of reduction and also in much of the observing program.

Carnegie Institution of Washington
Mount Wilson Observatory
December 1929

Contributions from the Mount Wilson Observatory, No. 393
Reprinted from the *Astrophysical Journal*, Vol. LXXI, pp. 73–101, 1930
Printed in the U.S.A.

STEWARD OBSERVATORY

THE SPECTROHELIOSCOPE AND ITS WORK

PART II. THE MOTIONS OF THE HYDROGEN FLOCCULI NEAR SUN-SPOTS

By GEORGE E. HALE

ABSTRACT

The purpose of this paper is to describe in detail some of the rapid motions of hydrogen flocculi near sun-spots. The observations, to be discussed in a future article of this series, were made visually by the author with a spectrohelioscope, which in certain respects is better adapted than other instruments for work of this nature.

In the first part of this paper[1] I have described some of the motions of hydrogen flocculi seen with the spectrohelioscope, without going into the details of many observations recorded in my notebooks. The subject is not a simple one, as the diverse views of experienced astronomers on the similar problem of the motions of prominences indicate. Although the results given in the present paper are fragmentary, I hope they may serve in some measure to stimulate future work by observers adequately equipped for either visual or photographic studies.

An examination of the series of spectroheliograms reproduced in Plate II will show that the most conspicuous phenomena here recorded by Ellerman are two dark ($H\alpha$) flocculi, rapidly changing in form as they are shot outward from a region, in some cases (especially at $6^h\ 39^m$) appearing as a bright flocculus, on the preceding edge of a large sun-spot.

By way of contrast, another series of spectroheliograms, also taken on Mount Wilson in 1908, may be found in my first paper on "Solar Vortices."[2] A long dark hydrogen flocculus, which had been

[1] *Mt. Wilson Contr.*, No. 388; *Astrophysical Journal*, **70**, 265, 1929.

[2] *Mt. Wilson Contr.*, No. 26, Plates XXXVIII and XXXIX; *Astrophysical Journal*, **28**, 100, Plates XI and XII, 1908.

photographed on several days with comparatively little change of form, lying at a distance of about 150,000 km from a sun-spot, was suddenly drawn toward the spot at a velocity of the order of 100 km/sec. Four spectroheliograms were fortunately taken by St. John during the fifteen or twenty minutes while the rapid inflow was in progress. Such photographs, which are very rarely obtained, leave no doubt regarding the direction of flow or its approximate velocity. But, as my observations with the spectrohelioscope cited below illustrate, they fail to record some of the most important phases of such phenomena whenever the high radial velocities throw parts of the *Hα* line completely off the second slit of the spectroheliograph.

Spectroheliograms of prominences at the limb have been shown by Pettit to indicate accelerating inflow in most cases and outflow in others:

> Occasionally a streamer may be projected from one of the wings away from the spot, or a spike rise from the region of the spot. This is not the normal condition, however.[1]

Evershed, whose long experience with the solar spectroscope and spectroheliograph renders his conclusions of great value, gives a discussion of his work in the Kodaikanal *Memoirs*.[2] After stating that "all our experience at Kodaikanal goes to prove the essential identity of the filaments (long dark flocculi on the disc) and the prominences which have been photographed here" (p. 111), he gives many other conclusions, some of which will be referred to later. Among these one may be cited now: "The prevailing type of prominence found above sun-spots is the Rocket, called by Fényi 'Fleckenkrone,' which consists of jets and streamers radiating from the sun-spot."

In this type of prominence, as Fényi showed in 1892, the changes are rapid and the motion outward.

[1] "The Forms and Motions of the Solar Prominences," *Publications of the Yerkes Observatory*, **3**, Part IV, 232, 1925. See also Part I of the present article, *Mt. Wilson Contr.*, No. 388; *Astrophysical Journal*, **70**, 300, 1929.

[2] John Evershed and Mary Acworth Evershed, "Results of Prominence Observations," *Memoirs of the Kodaikanal Observatory*, **1**, Part II, 1917.

PLATE II

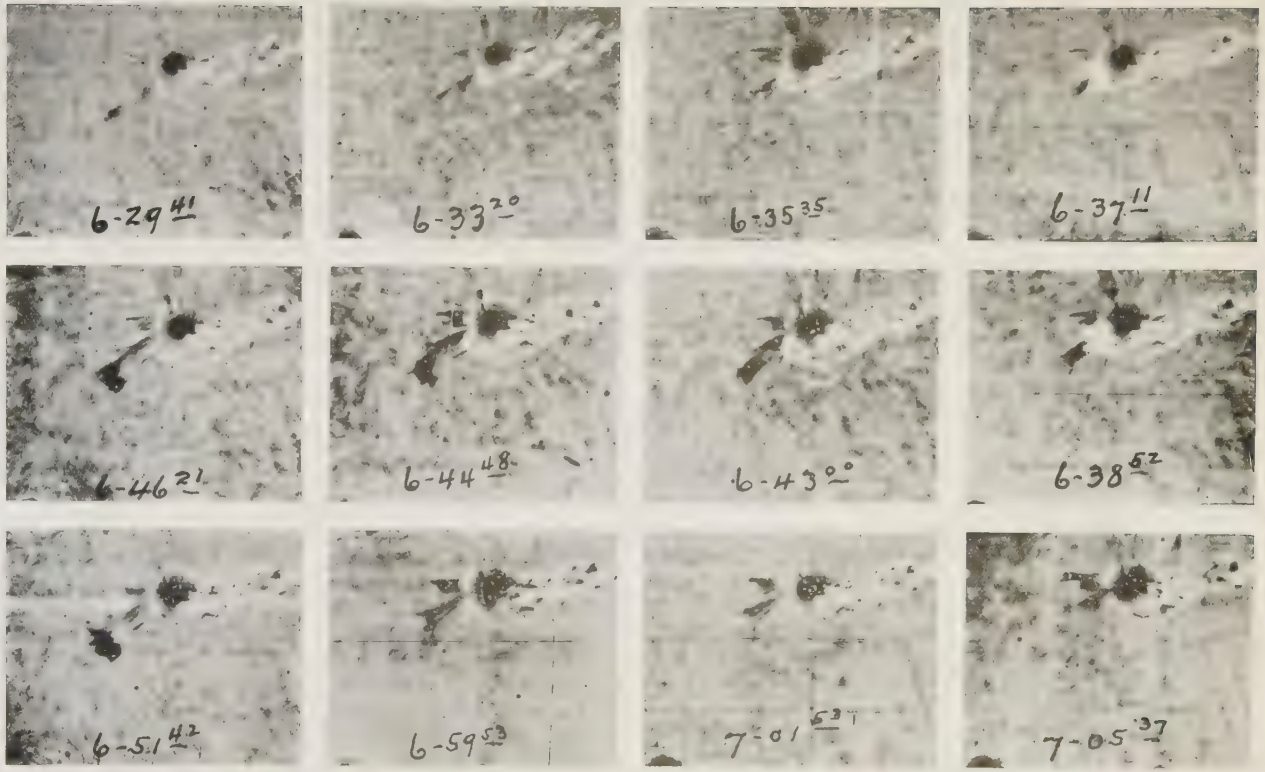

RAPIDLY CHANGING FLOCCULI NEAR LARGE SUN-SPOT, SEPTEMBER 10, 1908

Evershed's general conclusion (p. 123) will also be of interest here: "Sixty thousand Kodaikanal prominences, and eleven thousand from Kenley, and other thousands from Rome, Sicily, Kalocsa, yet we cannot take one prominence and say: This caused it, thus and thus it began, and developed, and ended."

The fact is that the problem, both observational and theoretical, is complicated and important enough to call for the widespread application of any promising devices that may aid in its solution. The score of spectrohelioscopes already constructed or ordered, after the designs given in my last paper,[1] are especially adapted for this work, because they show many prominences on the disk and also at the limb, render visible masses of hydrogen moving at high speeds which are frequently not recorded by the spectroheliograph, and give an instant measure of the radial velocities of their various parts. It should be remembered, however, that the spectroheliograph is much better adapted for recording the forms of most of the flocculi, especially the fainter ones and those of minute and complex structure. The chief uses of the spectrohelioscope are the detection and study of intense and rapidly moving flocculi and the velocity analysis of prominences.

OBSERVATIONS WITH THE SPECTROHELIOSCOPE

The first satisfactory observations of hydrogen flocculi with a spectrohelioscope were made at my Solar Laboratory in Pasadena on January 16, 1924. On January 18 I tried moving the second slits across $H\alpha$ while observing (five slits were then used at each end of the oscillating bar, as described in the paper just cited), and found that the widely different forms of the flocculi corresponding to different wave-lengths could be beautifully seen in this way. On January 22, after further observations by this method, it became evident that it would serve as a very quick and effective means of distinguishing between approaching and receding flocculi. On January 23 vortex phenomena in a spot group were clearly seen and partially analyzed. The next day the distortions of $H\alpha$ near a brilliant erup-

[1] "The Spectrohelioscope and Its Work: Part I," *Mt. Wilson Contr.*, No. 388; *Astrophysical Journal*, **70**, 265, 1929.

tion on the sun's disk were so pronounced that the forms of dark descending masses could be seen when the second slits were well beyond the extreme (red) boundary of the dark wings of *Hα*. On January 25 the eruption was very large and brilliant, and beyond it dark flocculi were descending at high velocities toward the largest spot in the accompanying group. The following day the large eruption had subsided, but a very small brilliant flocculus was seen at $12^h\ 10^m$ P.S.T. on the outer edge of the bridge separating the umbrae of the largest spot. This lasted only a few minutes, after which a long slender dark flocculus appeared, moving outward from the same point, evidently similar in type to the outflowing dark flocculi shown in Plate II. Small short-lived bright flocculi also developed intermittently near this spot on January 27, where dark vortex structure could also be seen by setting the second slits at the wave-lengths corresponding to the radial velocities of the moving gases.

During this period, though the oscillating slits were still crude and my observations necessarily fragmentary, I could thus appreciate some of the possibilities of the spectrohelioscope, with which I also observed the tips of prominences moving rapidly toward spots at the sun's limb (as in the photographs reproduced by Slocum and Pettit), the remarkable effects of radial velocity in prominences projecting partly beyond the limb and partly (as dark flocculi) upon the disk, and the rapid flow (on Feb. 17) of such a flocculus toward a spot. Passing over some curious observations of radial motion and apparent absorption effects in prominences at the limb, of the appearance of spots in the light of the D lines, of bright eruptive regions observed with nicol and revolving half-wave plate, and of vortices associated with sun-spots, I come to an observation that bears directly upon the subject of this paper. My instrument, not yet completed, had been equipped with a pair of single oscillating slits and a plane-parallel glass plate below them (the "line-shifter" previously described) for setting any part of the *Hα* line or neighboring wave-lengths on the oscillating second slit while the sun was under observation.

I referred in Part I of this paper to a typical dark arch seen on

May 31, 1926, near the spot Mount Wilson No. 2571, then not far from the center of the sun. The appearance in the spectrohelioscope was approximately as shown in Figure 1, which is copied from a rough sketch in my notebook, made at $2^h\ 40^m$ P.S.T. The spot was at *A* and the small bright flocculus at *B*. The portion of the dark arch *C* was of maximum intensity when the second slit was off the *Hα* line to the violet. As *Hα* was moved across the slit with the line-shifter the following portion of the arch appeared. When the maximum of intensity in the arch reached *D*, the line was nearly central on the second slit. The rest of the arch did not appear until the red side of *Hα* was brought on to the slit. This terminated in a small black head at *E*, which was blackest when the second slit was well beyond the visible wing of the line to the red. This effect was repeatedly observed by turning the line-shifter, but at $2^h\ 55^m$ it was much less marked.

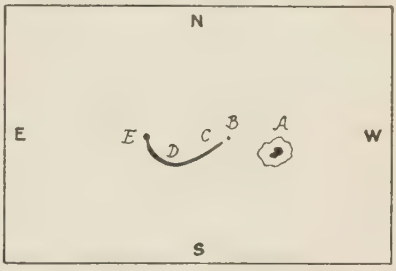

FIG. 1.—Arched flocculus observed on May 31, 1926, near the unipolar spot Mt. Wilson No. 2571.

The inference is plain. Hydrogen, rising from the bright flocculus at *B*, with a radial velocity sufficient to displace *Hα* well to the violet, followed a trajectory which was nearly at right angles to the line of sight at *D* and descended with high radial velocity at *E*. The termination of the arch in a small black head is an interesting phenomenon, frequently observed since that time, especially on the outer edge of the penumbra of spots, at the extremity of an inflowing flocculus.

Such an inflowing flocculus, typical in behavior and important in its bearing on the nature of the currents in the solar atmosphere, was seen in several of its phases on June 26, 1926. When observing at $4^h\ 45^m$ the preceding member of the large bipolar spot Mount Wilson No. 2598 (N 21°, E 26°, approx.), I noticed west of it a strong dark flocculus which I had not seen at 3^h. The glass plate used for a line-shifter was a provisional one, and was not yet equipped with

a divided circle. Thus I had to estimate displacements of the slit from the center of *Hα*, and as I was not then accustomed to the observation of rapidly changing flocculi, my record is imperfect. Nevertheless, it will serve to give an idea of what to look for in a case of this kind.

At $4^h\ 52^m$, with a second slit half again as wide as *Hα*, the flocculus appeared nearly as in the composite sketch reproduced in Figure 2.

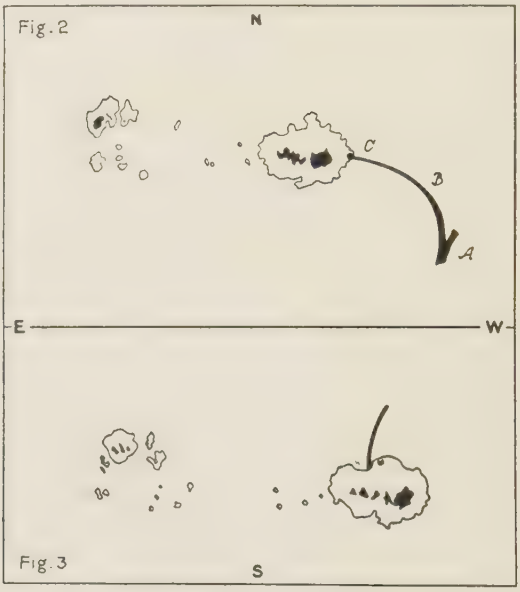

FIG. 2.—Flocculus observed on June 26, 1926, approaching preceding spot of large bipolar group Mt. Wilson No. 2598.

FIG. 3.—Flocculus observed on June 28, 1926, receding from preceding spot of bipolar group Mt. Wilson No. 2598.

The outer extremity was most intense when the center of the slit was more than an angstrom from the center of *Hα* toward the violet, and at this slit position the inner end of the flocculus did not reach the penumbra. When the center of the slit was nearly an angstrom to the red of *Hα* the appearance was similar, but the tip now touched the penumbra, though the small black dot noticed later at *C* was

not then seen. Puzzled at first by these phenomena, I soon recognized that the second slit was too wide, and closed it to about half its previous width, or about 0.8 the width of *Hα*. At 5^h 10^m, with the slit well beyond *Hα* to the violet, the flocculus had shortened, as though the outer hydrogen had flowed toward the spot. At 5^h 18^m the whole flocculus was faint with the slit central on *Hα*, and became very faint or disappeared at shorter wave-lengths. Three minutes later, with the slit about an angstrom toward the red of the center of *Hα*, nothing was observed but a small black dot at *C*, which fell exactly on the outer boundary of the spot's penumbra. After this time a portion of the curved flocculus could be faintly seen by moving toward *Hα* (slit overlapping its red edge). At 5^h 34^m the black dot on the penumbra appeared to be of maximum intensity at a slit position about half an angstrom to the red of *Hα*, and this was the condition at 6^h 10^m, when the rest of the flocculus had practically disappeared (for any slit position).

According to Rowland, the width of the normal dark *Hα* line is 0.963 A, or, including the extreme shading, 1.240 A. Judged from the width of the bright *Hα* at the base of the chromosphere, the shading is actually wider than this. Therefore, a dark hydrogen flocculus without motion in the line of sight may be visible when the second slit, even if extremely narrow, is anywhere within 0.5 or 0.6 A, or even more, from the center of the line.

The flocculus appears of greatest intensity when the slit coincides with the position of maximum absorption of the portion of the *Hα* line corresponding to the region in question. If, because of local radial velocity or other cause, this position of maximum absorption is shifted toward red or violet, the second slit must be displaced an equal amount in order to show such parts of the flocculus with maximum contrast. With a wide second slit (on the assumption that the flocculus is exceptionally intense), even those parts moving toward or away from the observer at considerable velocity may be visible at the same time.

With these points in mind it is easy to include the foregoing observations in a single progressive picture. At some time after 3^h an intensely dark flocculus was shot upward near the point *A*. At 4^h 45^m it was still rising rapidly, but the absorbing gas had been drawn

toward the spot and its narrowed tip was already descending toward the outer edge of the penumbra. At $5^h\ 10^m$ the dark mass at *A* had disappeared and the maximum of intensity had moved about halfway toward the spot to *B*. The outer part of the flocculus continued to fade and by $5^h\ 21^m$ the maximum of intensity had shifted to the round black dot at *C*, moving downward with a radial component of some 60 km/sec. At $6^h\ 10^m$ the dot on the penumbra was still black, though apparently descending less rapidly, and the rest of the flocculus had almost completely faded away.

This observation, which recalls the almost unique spectroheliographic results of June 3, 1908, was followed on June 28 by an eruptive outflow from a different part of the same (preceding) spot of the bipolar group. A small bright region appears at the north side of the penumbra of this spot on a direct photograph taken by Ellerman with the 60-foot tower telescope the same morning (June 28, about 6^h). At $10^h\ 09^m$, I saw with my spectrohelioscope in Pasadena a bright flocculus at this point, when the inner edge of the second slit was just touching the violet edge of *Hα*. Eight minutes later a narrow dark flocculus, nearly straight, extended from the same point to a distance about equal to the width of the penumbra of the large spot (Fig. 3). At $10^h\ 20^m$ only the outer extremity of the flocculus could be seen with the second slit in the same position as in the two previous observations. When the slit was moved farther toward the violet, the maximum of intensity advanced along the dark flocculus toward the spot, ending at the edge of the penumbra. Intermittent renewals of this outflow, bright and dark, appeared later in the day. The hydrogen, rising at intervals from the bright point near the end of the bridge, traveled outward toward the north, reaching its maximum distance at about $3^h\ 30^m$, at a point where a short, somewhat elongated dark flocculus was seen descending with a radial component of about +60 km/sec.

Omitting various observations of outflow and inflow, made during a period chiefly devoted to experiments with various forms of spectrohelioscopes, we come to some results obtained on August 15, 1926, when improved optical and mechanical parts had been installed and the parallel-plate line-shifter provided with a divided circle for radial-velocity measures. In the first part of this paper

one of these inflowing flocculi (here shown as Fig. 4, *GHI*) was illustrated to explain the method of observation, but the others also deserve mention.[1]

The first inflow (Fig. 4, *ABC*) was seen at $10^h\ 15^m$, rising at some distance from the following spot of the pair (Mt. W. No. 2656) and terminating in a small black head descending with moderate velocity toward the outer edge of the penumbra. At $10^h\ 22^m$ another curved

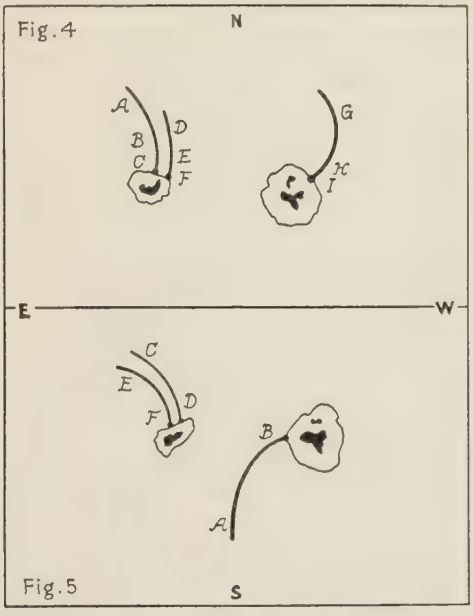

FIGS. 4, 5.—Flocculi observed on August 15 and 16, respectively, approaching both spots of the bipolar group Mt. Wilson No. 2656.

flocculus (Fig. 4, *DEF*) was sketched near the first one. The effect was precisely similar, except that the final black head was descending with higher velocity in this case, and could be seen alone on the edge of the penumbra, when the second slit was well beyond the normal *Hα* line toward the red, at a wave-length where the whole of the first flocculus had disappeared. In both cases, as the line-shifter was rotated, the outer ends of the curved flocculi appeared when the second slit was on the violet side of *Hα* and the maximum

[1] *Op. cit.*

of intensity moved steadily along them as the wave-length of the light entering the second slit increased. I was so absorbed in the observations that I forgot to determine the slit zero, and therefore cannot give the radial velocities, though my sketches corresponding to four different line-shifter records show the effects described. At $10^h\ 44^m$ the first flocculus had nearly faded out and *DEF* was weak. At $10^h\ 51^m$ traces of the extremities of both flocculi close to the spot could be seen on the red side of *Hα*, but neither flocculus was visible with the second slit on the center of the line.

A still finer effect of inflow, first observed near the preceding spot at $10^h\ 57^m$, which was described (with its radial velocities) in my last paper, is also shown here in Figure 4 (*GHI*).

On the following day a beautiful case of the same kind was observed at $10^h\ 0^m$. A long curved flocculus (Fig. 5, *AB*), originating in a bright eruptive region south following the preceding spot of the same group, terminated in a black head exactly on the following edge of the penumbra, where its radial velocity approached +30 km sec. A nearly parallel flocculus (not shown in Fig. 5) gave the same effect, which was also given to even better advantage by two parallel curved flocculi (*CD* and *EF*) seen descending toward the following spot at $10^h\ 25^m$. All of these showed the same characteristic appearance, again confirmed on August 17: the apparent advance toward the spot of the inner extremity of the flocculus as the line-shifter was turned so as to bring light of greater wave-length upon the oscillating second slit.

As already remarked, a notable fact, true for all these cases of inflow and for many others since observed, is the termination of each flocculus in a definite black head, usually nearly circular when observed alone well to the red of *Hα*, but sometimes accompanied (at the slit position giving maximum intensity) by a short tail. In many instances this head falls precisely above the outer edge of the penumbra of the spot, which is perfectly visible when the second slit is beyond the wings of *Hα*. This head, the advance of the maximum of intensity, and the considerable velocity of descent are the most striking features of such phenomena.

On September 11, 1926, having returned to Pasadena after an absence of several weeks, I again confirmed the foregoing effects.

In some instances, as illustrated below, the tip of the inflowing flocculus undoubtedly reaches a point above the edge of the umbra of the spot; but when the second slit is so placed in wave-length as to show the head at its blackest, its center will often be found to lie above the narrow outer boundary of the penumbra. As the seeing in Pasadena is rarely or never good enough to permit the use of high magnifying powers in solar observations, I hope this phenomenon will ultimately be studied minutely elsewhere under more perfect atmospheric conditions.

On September 13 two interesting cases of inflow were observed in conjunction with the spots of a bipolar group, the following member of which was very close to the east limb. A small, curved, dark flocculus was first noticed at $10^h\ 15^m$ just behind the following spot, extending from it to the limb. It could not be seen at circle readings from +10 (red) to −15 (violet), but first appeared at −15 as a dot almost touching the limb. As the line-shifter was turned farther toward the violet a curved extension from this dot approached the spot, appearing as a point on the penumbra when the circle indicated a (tangential) velocity of approach of some 50 km/sec. At $11^h\ 30^m$, just behind the preceding spot of the pair, a flocculus, appearing bright on the disk and extending beyond the limb as a curved prominence, was also seen to be approaching the spot.

I reserve for another section of this paper a discussion of hydrogen vortices in the solar atmosphere, which are usually best studied in their simplest form, associated with single spots.[1] The hydrogen arches and inflows accompanying active bipolar groups, however, often present very striking phenomena, some of which will be described here.

The great bipolar spot group Mount Wilson No. 2686, at about 24° north latitude, was well advanced on the sun's disk when examined with the spectrohelioscope on September 16, 1926. The accompanying outline of the spots was traced from the polarity record made by Nicholson with the 150-foot tower telescope on Mount Wilson at $9^h\ 10^m$, and some of my own later observations of inflowing flocculi have been sketched in at their different positions (Fig. 6).

[1] For a preliminary discussion see "The Fields of Force in the Atmosphere of the Sun," *Nature*, **119**, 708, 1927.

At $12^h\ 15^m$ I observed a clearly defined (dark) hydrogen inflow *AB*, which seemed to reach the central umbra of the following spot. Before I could complete a satisfactory set of measures my attention was attracted by a forked flocculus *CD* reaching the preceding umbra in this spot, which it certainly seemed to touch at $12^h\ 32^m$, when its inner end showed a marked radial velocity of recession. The

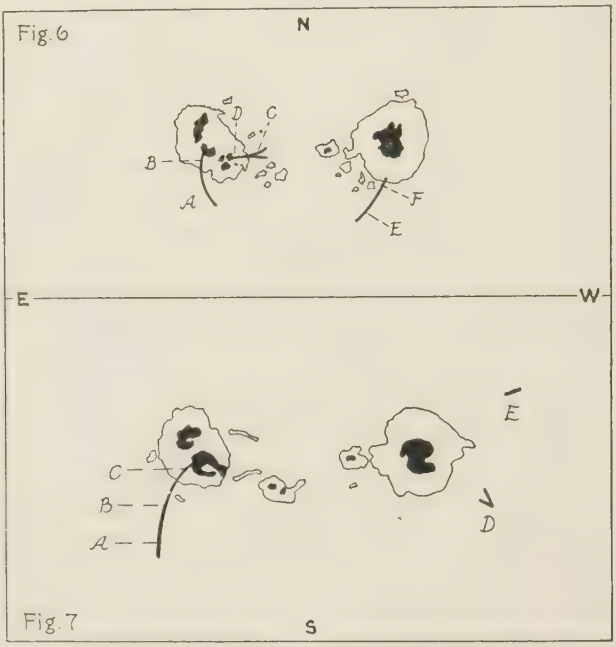

FIG. 6.—Flocculi observed on September 16, 1926, approaching both spots of the large bipolar group Mt. Wilson No. 2686.

FIG. 7.—Flocculi observed on September 17, 1926, near bipolar spot group Mt. Wilson No. 2686.

outer forked end *C*, the southern branch of which was darker than the northern, appeared to be nearly stationary in the line of sight. At $2^h\ 36^m$ another fainter inflow, which also seemed to reach the umbra, occurred near the same point. Several active bright flocculi appeared at various times during the day between the preceding and following spots of the bipolar group, two of which were very bright at $2^h\ 58^m$, when they gave a width of 1.8 A for *Hα*.

At 2^h a dark linear inflowing flocculus *EF* was seen south of the preceding spot. Its outer part *E* was seen alone on the violet side of *Hα*. Nearer the spot the radial component reached zero and attained a positive value of some 30 km/sec. in the black, slightly elongated head *F*, which centered exactly upon the outer boundary of the penumbra. This was apparently a case of an arch, composed of absorbing hydrogen, which rose south of the spot and descended toward the penumbra. Later in the afternoon the active bright flocculi fluctuated in intensity, but had disappeared at 5^h. A dark linear arc was then seen, rising near the east boundary of the large preceding spot and descending toward the west umbra of the following spot, but the sun was too low for satisfactory measurements.

On September 17 the same spot group showed some additional cases of inflow, two of which are sketched in Figure 7 on a tracing of the polarity drawing made on Mount Wilson at $8^h\ 30^m$ that morning by Pettit. At $11^h\ 05^m$ a very dark linear flocculus, which had not been noticed before, was suddenly seen as a short black line at *A*, with a radial velocity of about -20 km/sec. As the wave-length of the transmitted light was increased by the line-shifter, the flocculus was seen to lengthen toward the spot, though its maximum intensity just outside the penumbra could not be well determined because of a bright flocculus there. A series of measurements was made at six points along the flocculus, however, showing velocities changing from approach to recession, and indicating a faint extension to the central umbra of the following spot at $11^h\ 28^m$. Two minutes later I found that changes of intensity (for the same wave-length) had occurred near the point *B*, where the radial component was about $+40$ km/sec. At $11^h\ 35^m$ the tip was noted as apparently reaching the umbra, with a higher velocity of recession. One minute later nothing but a short length at the inner extremity *C* could be seen with the second slit well to the red of *Hα*. Another similar inflow, along a closely adjacent path, from a point somewhat farther from the spot, was observed about fifteen minutes later. The values of the radial velocities are uncertain, because the slit zero did not at that time always remain constant, owing to some instability in the parts of the spectrohelioscope. No very bright flocculi were then seen in or near the group. At $2^h\ 32^m$ two short dark flocculi (Fig. 7,

D and *E*), both rising rapidly, were seen west of the preceding spot. I was called away at that time, and could do no more than to note the fact of their ascent and also that one of them was forked, as indicated roughly in the sketch at *D*, where their positions are only approximate.

On September 18 I observed some of the phases of a striking phenomenon, repeatedly seen in slightly varying form on several successive days. After noting an apparent case of inflow near the preceding spot of the bipolar group, I saw at $11^h\ 56^m$ a very strong black flocculus *A* with a velocity of approach of about -40 km/sec., which had appeared very suddenly. It showed the beginnings of a forked structure, more fully developed four minutes later, when the general appearance of the flocculus was as shown in Figure 8, at a setting of the line-shifter corresponding to -30 km/sec. The faint curved arc, apparently extending from the point of the fork to the western extremity of the umbra of the following spot, was not seen in the first observation. At $12^h\ 03^m$, at the same wave-length, the flocculus was noted to be fading. At $12^h\ 12^m$ the fork, at a setting corresponding to $+16$ km/sec., no longer retained its form or position, but seemed to have split into two faint arcs, with an open space between them, moving in opposite directions toward the preceding and following spots (not shown in the figure, but at the approximate positions *B* and *C*). At $12^h\ 21^m$ nothing was seen (at any wave-length) excepting the two inflowing flocculi shown at *D* near the following spot in Figure 9 (radial component about $+20$ km/sec.). At $12^h\ 25^m$ these were fainter and had apparently reached a point above the western tip of the umbra (Fig. 9, *E*, radial component about $+26$ km/sec.). A minute later these flocculi at *E* had disappeared, but another single curved dark flocculus, with a radial component indicating ascent, had arisen at about the position *D*.

Even with the spectrohelioscope, constantly aided by the line-shifter, it is difficult to follow these varying phenomena. Their quick changes in position and wave-length, and the recurrence of new flocculi, rapidly ascending at nearly the same points, show what difficulty there would be in photographing and analyzing them satisfactorily with a spectroheliograph, even with visual guidance by an observer at the spectrohelioscope. As the scale of the photographed

image should be large enough to show sharply the slender details of the flocculi, and repeated exposures (necessarily rather long with most existing instruments) must be made at different settings of *Hα* on the second slit, the tasks of photography and measurement

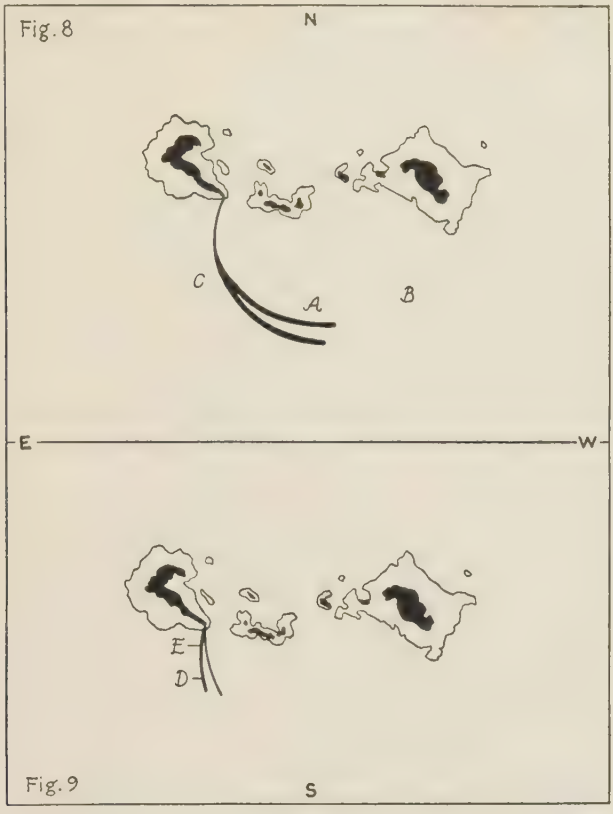

FIGS. 8, 9.—Flocculi observed on September 18, 1926, near bipolar spot group Mt. Wilson No. 2686.

are not easy.[1] On the other hand, it is very difficult with the spectrohelioscope alone to make accurate records of what one readily sees. All of the drawings reproduced in this paper are rough and

[1] I think that an optical combination of comparatively large angular aperture, such as the 40-inch Yerkes refractor and the Rumford spectroheliograph, could be adapted for making good photographic records of the phases of phenomena like those shown in Figs. 8 and 9.

schematic, but they will at least serve to indicate the general character of the phenomena. It is of course to be understood in every case that only a few flocculi of special interest have been picked out for record, though many others were seen; we must turn to the

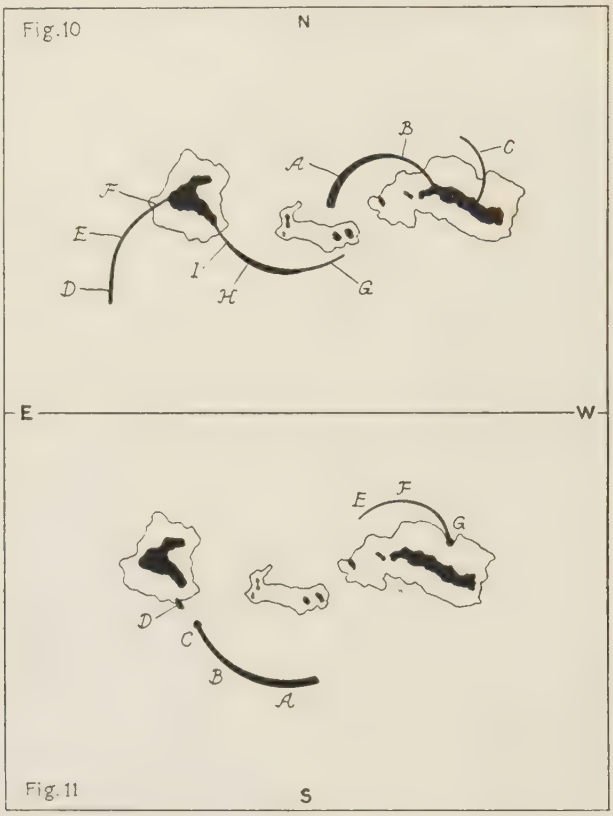

FIGS. 10, 11.—Flocculi observed on September 19, 1926, near bipolar spot group Mt. Wilson No. 2686.

spectroheliograph for the best means of showing the complex structure of the flocculi always present on the sun.

On September 19 the large bipolar group, as shown by Pettit's polarity sketch at $10^h\ 45^m$, was crossing the central meridian of the sun (Figs. 10 and 11). Soon after ten o'clock I saw at Pasadena with the spectrohelioscope a strongly marked dark flocculus, not

very intense at its inner end, which reached the umbra of the preceding spot (*B*, Fig. 10, radial component from +80 to +100 km/sec.), but broader and very black at its point of maximum intensity (*A*, Fig. 10, radial component +60 km/sec. at $10^h\ 12^m$). A nearly parallel faint slender curved flocculus was seen at $10^h\ 15^m$ near *A*, at a slit position corresponding to a radial component of about +40 km/sec., where the first flocculus at *A* was much fainter. At about the middle of *Hα* both of the parallel flocculi extended farther south than *A* is carried in the sketch. At $10^h\ 26^m$, and again four minutes later, I repeated the observation of the inner tip touching the umbra, and found it very short (reaching only to about *B*) and more intense than at first, with a radial component of about +110 km/sec. The line-shifter was then turned back and forth, permitting the whole length of the flocculus (*A* to umbra) to be repeatedly observed. At $10^h\ 38^m$ it had almost completely disappeared (for any wave-length), though the inner end could be faintly seen, still rapidly descending. Both of the oscillating slits, it may be added, were 0.003 inch wide, less than half the width of the normal dark *Hα* line.

Another faint curved inflow *C*, also descending rapidly and reaching the long umbra of the preceding spot farther to the east, was suspected at $10^h\ 26^m$ and definitely confirmed at $11^h\ 03^m$.

I then turned my attention to the following spot and saw another fine inflow at $11^h\ 12^m$. The maxima of intensity at different parts of the arc corresponded to the following approximate radial components: *D*, +14; *E*, +32; *F*, +54 km/sec. The inner end, which appeared to reach the umbra, was darker than that of the flocculus *AB*. Another inflow *GHI*, showing a greater range of velocity, was noticed at $11^h\ 24^m$, with the following approximate radial components: *G*, +8; *H* (very dark), +26; *I*, +86; tip touching umbra, +114 km/sec. The last measurement was made at $11^h\ 30^m$. Ten minutes later the descending tip at the umbra had about the same radial velocity, but was fainter.

Another inflowing flocculus, which suddenly developed about $11^h\ 50^m$, is shown in a separate sketch (Fig. 11, *AC*), to avoid confusion. At $11^h\ 57^m$ it appeared approximately as from *A* to *B* (very black, radial component about +12 km/sec.), but the black head *C* showed

with maximum intensity at +36 km/sec. Four minutes later the black head was seen as a short line *D* on the edge of the penumbra (radial component about +50 km/sec.). In this position of the second slit the outer part *A* could also be seen (indicating a greatly widened *Hα* line at this point), but the intermediate region *B* was invisible. At $12^h\ 01^m$, at a wave-length corresponding to a radial component of +74 km/sec., nothing was visible but a very black dot on the edge of the penumbra. Another very black curved flocculus, seen at $4^h\ 15^m$, flowed toward the following spot, but it faded so rapidly that satisfactory measures could not be made. At one position of the second slit the inner end seemed to reach the umbra, but farther toward the red (radial component about +52 km/sec.) it was seen to terminate as a dot (now fainter) on the edge of the penumbra. At $4^h\ 53^m$ another dot (inflow), with about the same radial velocity, was observed at the same point.

The last inflow seen on September 19 is shown at *EFG*. The outer part *E* was darkest, with a radial component of about −32 km/sec., but farther toward the red (−8 km/sec.), the arc advanced toward the penumbra. Still farther (about +34 km/sec.), nothing remained but the very black point *G*, descending toward the edge of the penumbra.

On September 20 the seeing was better than usual in Pasadena. A well-defined inflowing flocculus *ABC*, sketched in Figure 12 on a tracing of the polarity drawing made by Pettit at $11^h\ 15^m$ the same day on Mount Wilson, was observed at $9^h\ 10^m$ with the spectrohelioscope. Its inner end met the umbra exactly at the end of a narrow bridge recorded in my notes as extending across the umbra (when seen with the light of the continuous spectrum far from *Hα*), but not shown in Pettit's later direct image. The tip *C* was descending at $9^h\ 23^m$ toward the umbra with a radial component of about +60 km/sec. Near the center of *Hα* the tip could not be seen, but the part of the arc at *B* (not visible at the previous wave-length) was observed alone. Farther toward the violet were the fainter ascending parallel arcs indicated at *A*, which very likely had previously been more intense, if we may judge from earlier observations of this character. At $10^h\ 13^m$, and also at $12^h\ 08^m$, the tip *C* was visible, again noted as meeting the end of the bridge across the umbra and

as very black across the penumbra when the line-shifter indicated a radial component of between +40 and +50 km/sec. At $12^h\ 13^m$ two cases of inflow, having a smaller radial component of recession

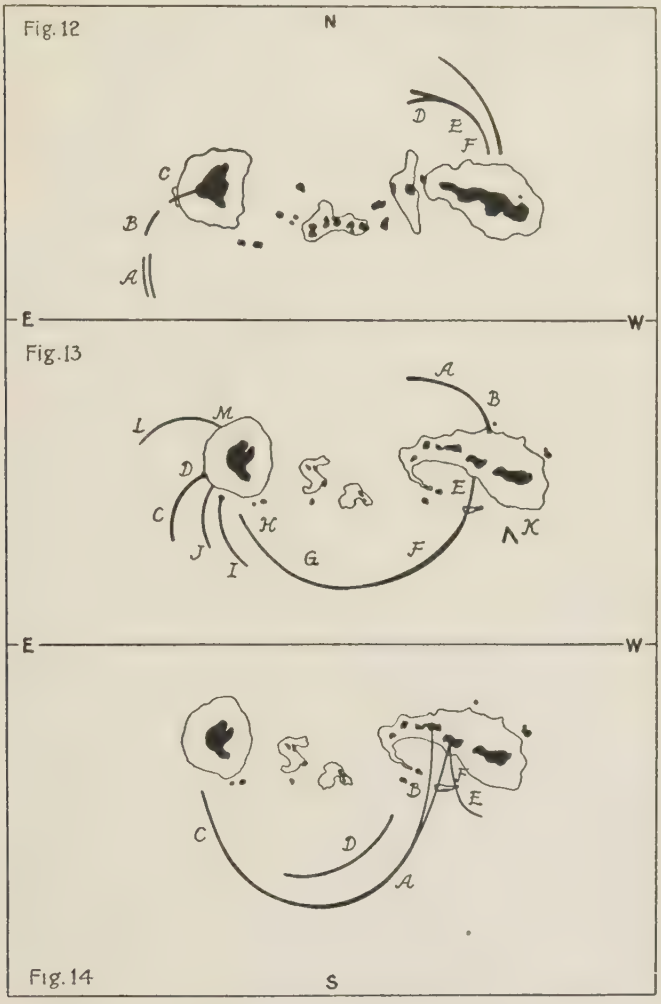

FIG. 12.—Flocculi observed on September 20, 1926, near bipolar spot group Mt. Wilson No. 2686.

FIGS. 13, 14.—Flocculi observed on September 21, 1926, near bipolar spot group Mt. Wilson No. 2686.

at the inner end, were seen reaching the preceding umbra on its north side, near the middle of its length.

In the afternoon, when the seeing was again recorded as exceptionally good, the fine structure of the field of force shown by the less intense flocculi on a spectroheliogram taken at $8^h\ 45^m$ that morning at Mount Wilson was plainly visible, approximately as in Plate III. The curvature of these flocculi on the south side of the preceding spot was noted to be as in the photograph, but no inflow (displacement of the maximum of intensity) could be detected along them with the line-shifter, though definite inflow of the opposite direction of whirl was seen on the north side of the umbra. Two brilliant small flocculi, first detected by my assistant, Mr. Hitchcock, about $12^h\ 30^m$, were recorded at $2^h\ 46^m$ on the penumbra of the preceding spot, a short distance northwest of the western end of the umbra. The width of the bright *Hα* line at these two points was then nearly 1.4 A, or about twice the normal for ordinary bright flocculi. But these bright flocculi, as is so often true, indicated little or no radial motion. At $3^h\ 41^m$ they were decidedly fainter, with a bright *Hα* line about 1 A wide.

At $3^h\ 50^m$, two inflowing curved flocculi were seen north following the preceding spot (Fig. 12, *DEF*). My rough sketch shows them approximately as they appeared five minutes later, when the line-shifter indicated a radial component of about +30 km/sec. At this setting the lower (southern) flocculus was more intense than the northern and forked at the outer end. The northern flocculus, faint at this time at its outer end, was visible alone at about the same setting at $4^h\ 10^m$, when the outer end had become stronger and the southern flocculus had disappeared. When first seen both flocculi extended farther southeast in longer arcs (as observed at the center of *Hα* and to the violet), curving down to reach a line prolonging the preceding umbra to the east.

At $3^h\ 28^m$, and again at 4^h, nearly linear dark flocculi, of a type (to be described later) which appears strong on both sides of *Hα*, were seen for short periods southwest of the large preceding umbra.

On September 21, as Nicholson's polarity drawing of the spot group made at $12^h\ 35^m$ shows (Fig. 13), the preceding umbra had divided into several parts. It is interesting to note, though perhaps

PLATE III

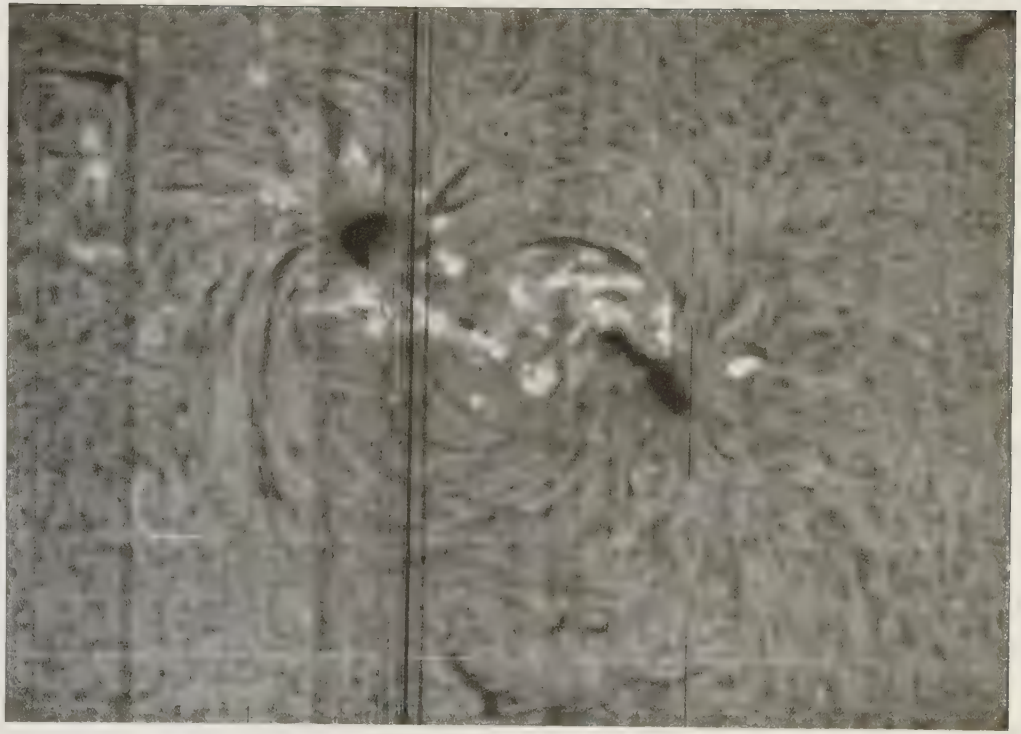

Bright and Dark Hydrogen (*H*α) Flocculi Associated with the Bipolar Sun-Spot Mt. Wilson No. 2686

Photographed on September 20, 1926, $8^h\ 45^m$, by Edison Pettit with the 60-Foot Tower Telescope and 13-Foot Spectroheliograph.

merely as a coincidence, that two very small spots had appeared on or near its north penumbra, close to the terminations of the dark descending flocculi *FED* in Figure 12. At 9^h I noticed an inflowing curved flocculus (Fig. 13, *AB*), the head of which reached the penumbra, apparently at one of these small spots, with a radial component of about +28 km/sec. Its outer half *A* was seen alone, of maximum intensity at the center of *Hα*, where the inner part *B* was invisible. At 9^h 16^m another inflow (Fig. 13, *CD*) was seen terminating in a black dot (radial component about +34 km/sec.) on the outer edge of the penumbra of the following spot, near the position of the inflowing flocculus seen on September 20 (Fig. 12, *ABC*). Its outer part *C* was of maximum intensity at about −16 km/sec.

A curved dark flocculus (Fig. 13, *EF*), extending from the south and east toward the central umbra of the preceding spot, was observed at 9^h 54^m, but no satisfactory measurements could be made because my instruments were set into vibration by a tractor in motion not far from the Solar Laboratory. The inner end, though faint, seemed to touch the spot when observed at 10^h. Ten minutes later rapid changes of intensity were noted, the part near *F* appearing very dark on the violet side of *Hα*. At 10^h 31^m only the broader and rather fainter section of the arc at *G* was seen (radial component roughly −12 km/sec.). At 11^h 13^m the arc, as observed at the center of *Hα*, included *G* and a narrower extension toward *H*. At 11^h 21^m (radial component about +8 km/sec.), three or four curved dark flocculi (*H*, *I*, *J*), two of which showed definite inflow, were observed south of the following spot; the maximum of *I* moved toward the penumbra, though it did not reach it (11^h 24^m), when the line-shifter was turned, while the tip of *J* did reach the penumbra when the circle indicated a radial component of +38 km/sec. Seven minutes later *I* terminated in a black dot just outside of the penumbra, of maximum intensity at +18 km/sec.

It should be added that a small brilliant point flocculus (bright *Hα* about 1.5 A wide) was observed at 10^h 36^m. When examined on the violet side of *Hα* it was seen to be accompanied by two dark wings, which diverged from it, as indicated at *K*.

At 4^h 09^m another curved flocculus *LM* was seen approaching the large following spot of the pair. Its inner extremity *M* appeared

alone as a short, narrow, black line, crossed centrally by the outer edge of the penumbra, with a radial component of about +27 km/sec., while its outer part *L* was visible without this tip, when the second slit was nearly central on *Hα*.

Another sketch (Fig. 14) is needed to show the phenomena noted soon afterward. At $4^h\ 23^m$, on the red edge of *Hα*, the slender dark flocculus *AB* was seen, forked as indicated, the branches extending to the two principal following umbrae of the large preceding spot. Eight minutes later, at a setting near the center of *Hα*, the entire arc *BAC* was visible, accompanied by a shorter arc *D*. I was unable to make a satisfactory set of measurements, especially as some small bright flocculi appeared within a few minutes south of the preceding spot, about on the line of the western branch of the dark fork. At $4^h\ 49^m$ a dark flocculus *EF* was found to extend from these bright flocculi to the third umbra in the preceding spot. There were definite signs of inflow, and I was struck by the fact that the direction of the curvature was opposite to that of the arc *AB*. The seeing was excellent, and there seemed to be no doubt about the reality of these phenomena.

On September 22 the spot group, as shown by Ellerman's polarity sketch made on Mount Wilson at $6^h\ 45^m$, appeared as in Figure 15. At $9^h\ 02^m$ I saw in Pasadena the curved dark flocculus *ABC*, with a maximum radial component of about +38 km/sec. at the point *C* on the edge of the penumbra. As the line-shifter was rotated toward the violet the curve lengthened toward *B*, so that the arc *BC* was seen at about +20 km/sec. Farther to the violet the head *C* disappeared and the arc lengthened to *A*. It was seen at nearly its full length, though not quite reaching the penumbra, at about −6 km/sec. This was at $9^h\ 12^m$. At $9^h\ 45^m$ the inner extremity, from about *B* to *C*, was seen near the center of *Hα* to be split from *B* to *C* into a fork (similar to that shown in Fig. 14). The arms of the fork were faint but unmistakable at −12 km/sec., but were stronger at +20 km/sec. At $9^h\ 48^m$ both branches terminated on the penumbra at a setting corresponding to a radial component of about +48 km/sec. The preceding branch was very faint, without head, while the stronger following branch ended in a definite pointlike head, precisely on the outer rim of the penumbra.

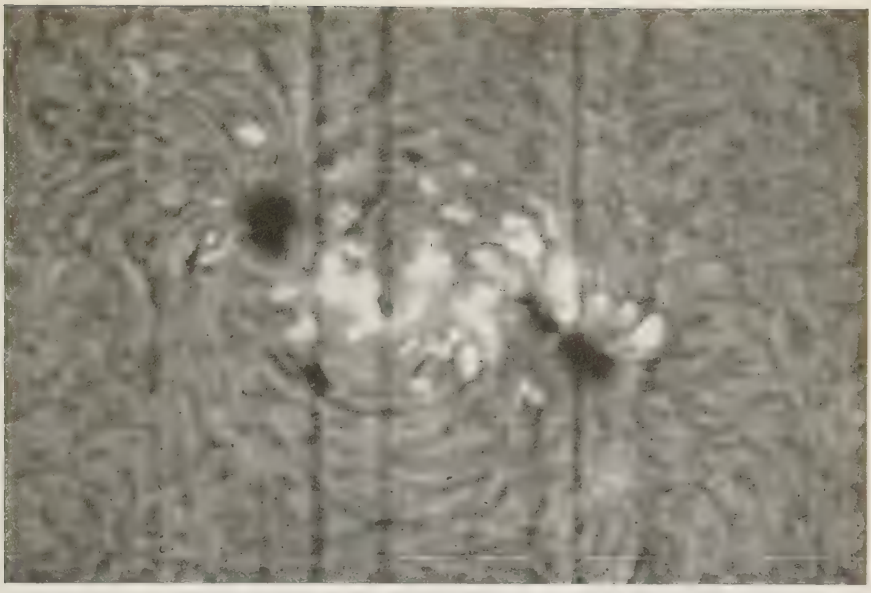

September 21, 1926, $6^h\,40^m$

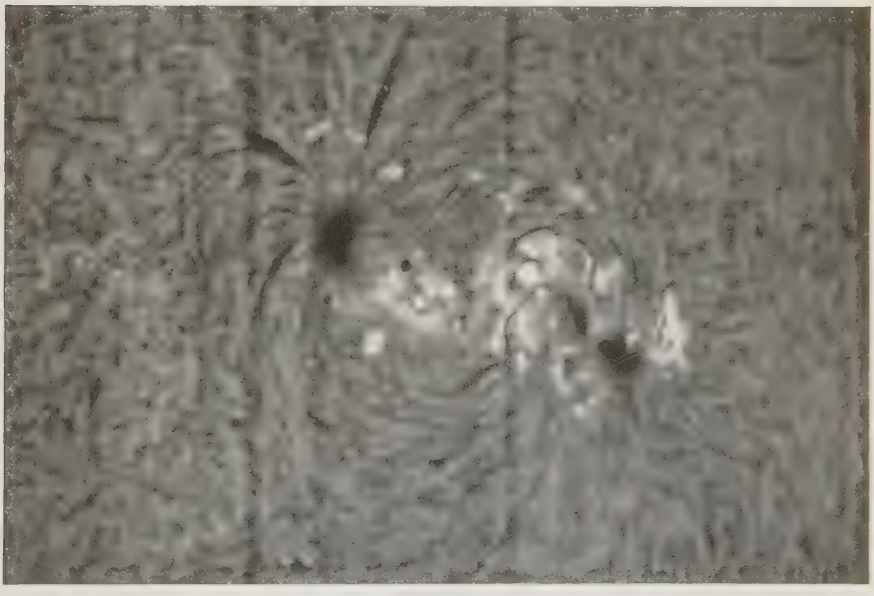

September 22, 1926, $6^h\,49^m$

BRIGHT AND DARK HYDROGEN ($H\alpha$) FLOCCULI ASSOCIATED WITH THE BIPOLAR SUN-SPOT MT. WILSON NO. 2686

Photographed by Lewis Humason with the 60-Foot Tower Telescope and 13-Foot Spectro-heliograph.

At this time the seeing was excellent, and the complex structure of the field of force in the flocculi surrounding the group could be

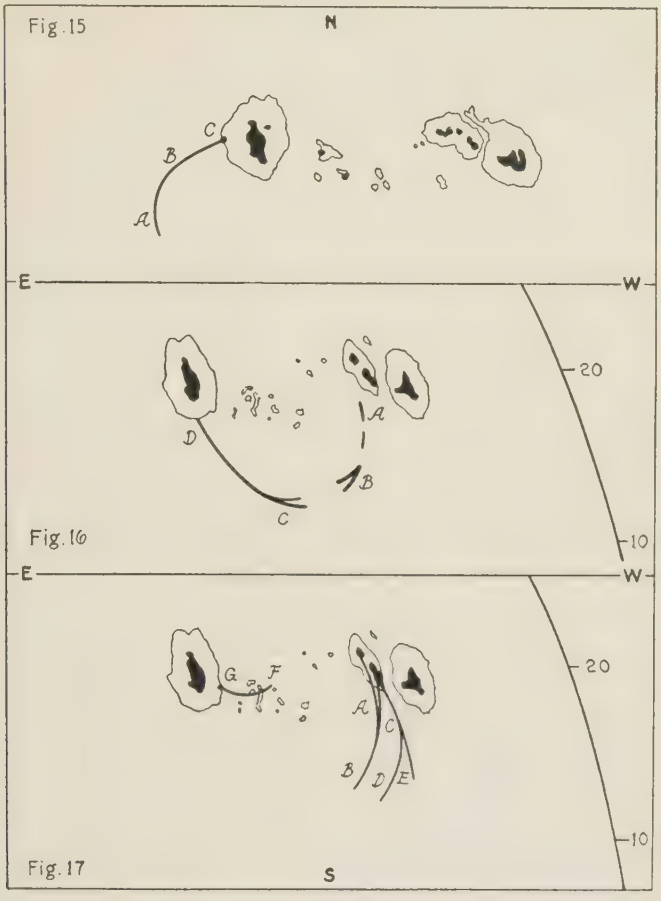

FIG. 15.—Flocculus observed on September 22, 1926, near bipolar spot group Mt. Wilson No. 2686.

FIGS. 16, 17.—Flocculi observed on September 23, 1926, near bipolar spot group Mt. Wilson No. 2686.

seen nearly as well as on the best spectroheliograms. North and south of the following spot the apparently inflowing slender flocculi appeared to be curved in opposite directions (clockwise and counter-

clockwise), a fact to be noted in my future discussion of the fields of force.

Passing over some other observations, to be mentioned later, we come to the phenomena seen on September 23. The preceding spot was 60° W and the following spot 41° W of the central meridian when Ellerman's polarity sketch was made on Mount Wilson at 6^h 36^m. At 10^h 12^m, after recording three fine cases of inflow on the south side of the preceding spots, I saw a long curved flocculus almost reaching the western member of the preceding pair and extending nearly to the following spot of the bipolar group (Fig. 16). The circle reading of the line-shifter was −15 (corresponding to a radial component of about −30 km/sec.), and when this was changed to −20, the maximum of intensity moved out along the arc from *A* toward *B*. At 10^h 38^m two forks not seen before had developed at *B* and *C*, one of which (*B*) was very black with the line-shifter at −23; at this setting only the arc from *B* to *D* was recorded. The forks weakened toward the red and were hardly visible beyond +10. My attention was diverted for a few minutes by another very black flocculus, first noticed at 10^h 31^m north of the following spot at a circle reading of +13, which seemed to originate in a bright flocculus and rapidly extended outward in two branches toward the north. At 10^h 47^m the crown of the arc *BC*, no longer forked, was very intense at −31, but invisible toward the red beyond the center of *Hα*. The rest of the arc (*CD*) was faint. At 10^h 56^m the crown of the arc appeared at −15 in two overlapping parts, not forked, the inner one now fading (though somewhat more intense at −19), while the outer arc extended to the western spot of the preceding pair, but disappeared east of *C*. At 11^h 20^m an arc of the opposite curvature (not shown in Fig. 16) was seen extending from a point near the center of the bipolar group toward the north following side of the western spot of the preceding pair.

Another cut (Fig. 17) is needed to show clearly my later observations on the same day. At 12^h 05^m, with the second slit nearly central on *Hα*, the three arcs *AB*, *CD*, and *CE* were seen. *AB* was split into a fork, the two branches of which appeared to reach the two umbrae of the western spot of the preceding pair. *DC* and *EC* united at *C*, from which point they continued as a slender dark line

to the nearer of these umbrae. Two minutes later, at a circle reading of −19, the fork (from *A* to the umbrae) was invisible, and the maximum of intensity of the arc was at *B*. The arc extending from *E* through *C* to the other umbra persisted faintly, but the arc *CD* was not seen.

In the afternoon, at $3^h\ 16^m$, the arc *FG* was observed. The outer extremity *F* was seen alone near the center of *Hα*. At a circle reading of −6 only the crown of the arc, curving about a small sun-spot, was visible. At $3^h\ 19^m$, when the line-shifter was set at −26, no trace of the arc could be seen excepting the black dot at *G* on the edge of the penumbra of the large following spot.

The arcs south of the bipolar group were renewed on September 24, and on the following day, when the preceding spot had almost reached the west limb, several slender prominences were seen projecting to heights of from 30,000 to 40,000 km. The first of these, observed at $10^h\ 30^m$ with first and second slits 0.006 and 0.004 inch in width, respectively, is shown in Figure 18. It had disappeared within a few minutes, before satisfactory measurements could be completed. At $10^h\ 58^m$ this prominence reappeared at about the same position, somewhat higher and brighter than before. With the comparatively wide slits employed its entire length was visible near the center of *Hα*, but the line-shifter showed that the maximum of intensity of its upper part was to the violet of that at the base, implying for its summit a relative motion of approach. At the same time a small brilliant spike, giving a broad, bright *Hα* line, was seen on the disk between the two members of the preceding spot.

At $11^h\ 12^m$ the slender prominence, now apparently higher, was forked, as in *A*, Figure 19. Five minutes later the fork had vanished, and the prominence appeared nearly as in Figure 18 at the center of *Hα*; a faint slender arc (*C*, Fig. 19), directed toward the second member of the preceding pair of spots, was also seen to the north. When the line-shifter was turned to admit longer wave-lengths, another slender linear prominence (*B*, Fig. 19) appeared well toward the red. These fleeting phenomena were gone before they could be carefully measured and sketched. At $11^h\ 42^m$ two linear prominences could be seen, as indicated in Figure 20. The southern (*A*)

was of maximum intensity near the middle of *IIa* (about +3), while the maximum brightness of the northern one (*B*) was at −24, where *A* was not visible. Similar intermittent phenomena, changing as

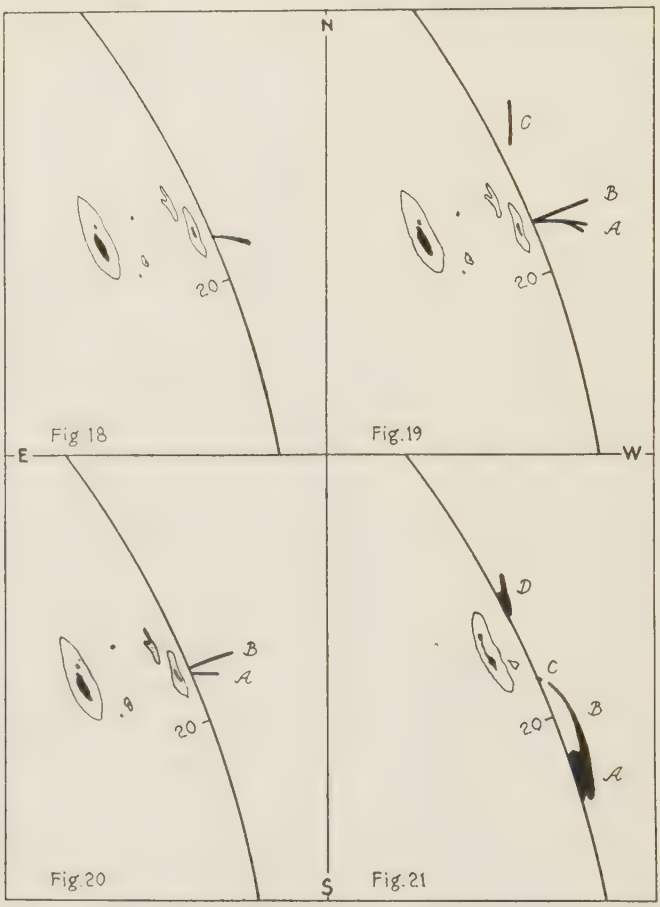

FIGS. 18, 19, 20.—Prominences observed on September 24, 1926, near preceding spot of Mt. Wilson No. 2686.

FIG. 21.—Prominences observed on September 26, 1926, between spots of Mt. Wilson No. 2686.

rapidly in intensity and radial velocity, were observed later in the morning, in spite of a very thick atmosphere, the forerunner of a fog.

On September 26, as Ellerman's polarity sketch at $6^h\ 40^m$ shows,

the preceding spots of the bipolar group were beyond the limb, while the following spot was approaching it. I cannot attempt to illustrate the rapidly changing prominences seen at the limb with the spectrohelioscope on this date, but Figure 21 will serve roughly to indicate the general character of the most significant of them. At $10^h\ 27^m$, after a heavy ground fog had cleared away, I saw at *A* a comparatively low prominence, which already extended toward the spot nearly to *B*, with a minute pointlike tip in advance of the slender extension behind it. About fifteen minutes later the tip had curved down to meet the limb not far from *C*. At this moment I noticed a short bright eruptive spike *D* just north of the spot, characterized by a very broad *Hα* line. I tested the image of the spike given by the edges of this bright line with a nicol prism and half-wave plate, but could detect no evidence of polarization. At $11^h\ 03^m$ the prominence *A* was nearly twice as high as when first seen, but the slender extension *BC* toward the spot had disappeared. Meanwhile, the spike *D* had thrown out toward the north an intensely bright extension, partly overlapped by a bright arch, which had enlarged and grown fainter as it moved away from the spot. At $11^h\ 10^m$ the prominence *A* had begun to develop a new slender extension advancing toward *B*, while an arch overlapping *D* (not shown in Fig. 21) had brightened and lengthened toward the north. Its brilliant top had little or no radial motion, but its lower end, which now curved down nearly to the limb, showed a rapid velocity of recession. At $11^h\ 35^m$ the extension from *A* reached beyond *B* and another smaller prominence similar in form to *ABC* had appeared beneath it. Other changes had occurred, including the formation of an arch extending south from above the spike *B*, with which it seemed to have no connection. Similar rapid changes continued, but at $12^h\ 20^m$ little remained excepting two low prominences at *A* and *D*.

On September 27 a prominence closely similar to *ABC* in Figure 21 was seen at $10^h\ 40^m$, near the same position angle. This is a typical form near sun-spots, which I have often observed with the spectrohelioscope. In our photographic records it goes back as far as my early wide-slit photographs of a prominence with the K line of calcium, made at the Kenwood Observatory, Chicago, on October

20, 1891,[1] and the three successive photographs of a prominence, showing the growth of its long slender extension, taken at Kenwood with my first spectroheliograph in 1893 (Plate V*a*, *b*, *c*). Other Kenwood negatives and many made with the 40-inch Yerkes telescope and the Rumford spectroheliograph show prominences of the same type, some of which have been mentioned in references to the work of Slocum and Pettit.

It is not my purpose to enter here into a detailed examination of the observations described above, as these will be supplemented by other observations and discussed in my next paper on whirls and arches in the solar atmosphere. I wish, however, to emphasize a few conclusions bearing on the effective use of the spectrohelioscope and the nature of the phenomena it discloses.

1. As remarked in one of my early papers on the spectroheliograph, in cases of considerable local motion in the line of sight "the portion of a prominence moving with sufficient radial velocity to produce so large a displacement (i.e., great enough to throw the line completely off the second slit) would not appear in the photograph."[2] This accounts for the absence of large and often very significant portions of prominences and flocculi from spectroheliograms, and illustrates the value of the spectrohelioscope for the study of such phenomena.

2. On the other hand, as such photographs as those reproduced in Plates II, III, and IV indicate, the spectroheliograph is incomparably superior to the spectrohelioscope for recording most of the intricate details of the *Hα* fields of force surrounding sun-spots. My rough schematic sketches hurriedly made with the latter instrument make no pretense to accuracy, but will serve to show the nature of the velocity analyses of certain outstanding phenomena.

3. The advantages and disadvantages of the spectrohelioscope for velocity measures and thus for the analysis of the flocculi should be borne in mind while observing. Its limitations depend upon the width of the second slit, the dispersion employed, and the nature of the intensity-curve of the *Hα* line. It is important to remember, as already stated, that a flocculus may be seen even when the second

[1] *Astronomy and Astrophysics*, 11, 77, 1892.

[2] "The Spectroheliograph," *Astronomy and Astrophysics*, **12**, 256, 1893.

PLATE V

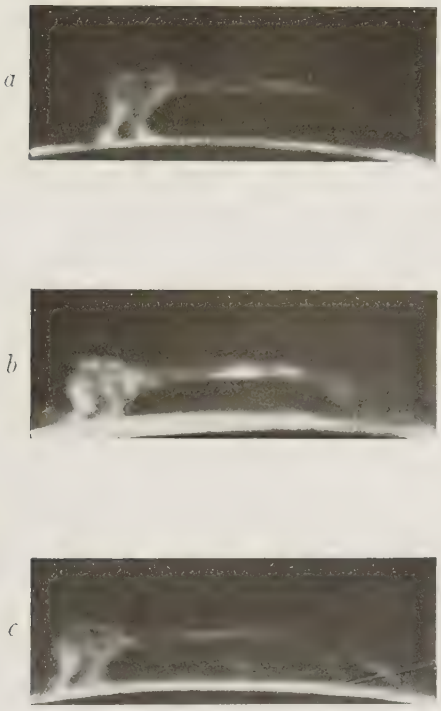

THREE SUCCESSIVE PHOTOGRAPHS OF A PROMINENCE

Taken with the Kenwood Spectroheliograph (K line) in 1893

slit of the spectrohelioscope falls near the extreme outer edge of its *Hα* line, though it may be very faint under these conditions. On this account, and in view of the fact that the intensity-curve of the line may be materially altered by the physical condition of the absorbing or radiating hydrogen, caution must always be observed in interpreting the results. In general, however, the circle of the line-shifter, when set for a position of maximum intensity, affords a quick and dependable means of analysis.

Carnegie Institution of Washington
Mount Wilson Observatory
January 1930

Contributions from the Mount Wilson Observatory, No. 394
Reprinted from the *Astrophysical Journal*, Vol. LXXI, pp. 209–210, 1930
Printed in the U.S.A

ON THE RADIAL VELOCITY OF R LYRAE

By ROSCOE F. SANFORD

ABSTRACT

Observations.—Table I gives thirty-nine radial velocities from one-prism spectrograms of R Lyrae obtained at Mount Wilson in 1917, 1923, 1924, 1925, and 1929.

Radial-velocity variation.—Consistent seasonal values of the phases of maximum and minimum velocity (Table II) are given by the formula

Phase = Julian Day of observation
$-[\text{J.D. } 2423600.000 + 43^d.48E + 6^d.5 \sin (2°.7E - 47°.2)]$ G.M.T.

The nature of the mean variation of the radial velocity is shown by the plots in Fig. 1, for Lick, Allegheny, and Mount Wilson observations. Mrazek's period does not fit the complete data.

The scattering of the observations, the difference in amplitude apparent in different series, and some difference in systemic velocity may indicate a velocity variation other than that corresponding to a period of 43.48 days. This, however, can hardly be the five-year variation in the center-of-mass velocity found by Mrazek. The most serious objections to this are (*a*) the presence of a systematic difference between the Allegheny and Mount Wilson wave-lengths that would reduce the amplitude of Mrazek's long-period variation to 5 km/sec. (one-half his value) and (*b*) the failure of the Mount Wilson observations of 1925 to verify a predicted minimum velocity.

Spectrum.—There are at least no outstanding spectral changes which follow the period of 43.48 days.

The variability in light of the star now designated as R Lyrae[1] was discovered by Baxendell in 1855.[2] The very numerous photometric observations which have been accumulated since then indicate that, if periodic, the variation in light takes place in a cycle of 45± days, with an amplitude that does not exceed 0.7 of a magnitude and is often not more than 0.3 or 0.4. No one, however, has been able to find a law of variation which is competent to represent at all satisfactorily the complete photometric data. The star is interesting because it is one of those variables whose periods lie between those of the Cepheids and the long-period variables.

The variation in the radial velocity of R Lyrae was announced by Adams, Joy, and Sanford[3] from measures of spectrograms made at Mount Wilson. Daniels[4] had previously concluded that eighteen ob-

[1] B.D.+43°3117, H.D. 175865, Boss 4814, α $18^h52^m.3$, δ +43°48′.8 (1900); sp. Mb; mean mag. 4.3.

[2] *Monthly Notices, Royal Astronomical Society*, **16**, 201, 1856.

[3] *Publications of the Astronomical Society of the Pacific*, **36**, 137, 1924.

[4] *Publications of the Allegheny Observatory*, **2**, 125, 1910.

servations, which he made at Allegheny over an interval of 39 days in 1910, gave no evidence of a variation in radial velocity because the probable error of their mean was quite as small as could be expected in view of the type of photographic plate and the dispersion employed. The only additional observations thus far published are those from the Lick Observatory.[1] These comprise three groups, 1899–1901, 1907, and 1912, and are all from measures of three-prism spectrograms.

Mrazek[2] has discussed the Lick radial velocities of 1899–1901 and 1907 and those obtained at the Allegheny Observatory and certain contemporary observations of light variation. He concludes that both velocity variation and light variation are satisfied by a period of 41.3 days, and that light maximum precedes velocity minimum in the three cases by 4.6, 6, and 4.6 days, respectively. He also finds a difference of nearly 10 km/sec. in the systemic velocity, which suggests a periodic change. Meridian-circle observations of the right ascension of R Lyrae made at Munich[3] over an interval of years furnish values of $\Delta\alpha$ which not only give the proper motion in that coordinate but also indicate a periodicity of five years in the motion. He draws attention to this as possible evidence of orbital motion about an invisible companion and then derives a curve for the variation in the velocity of the system on the assumption that the Allegheny observations are at the minimum and the Lick observations of 1901 at the maximum of this velocity variation and correspond to the points of maximum and minimum, respectively, of the $\Delta\alpha$-curve. Intermediate values of the radial velocity are inferred by interpolating values on the supposition that the form of the velocity-curve is the same as that of the $\Delta\alpha$-curve. The result is a variation in the velocity of the system with a period of five years and a semi-amplitude of 4.55 km/sec. The form of the velocity-curve corresponds to motion in an orbit with an eccentricity of 0.52.

It is now possible to add thirty-nine more radial velocities, obtained at the Mount Wilson Observatory, mostly with the 60-inch reflector, in 1917, 1923, 1924, 1925, and 1929. Practically all are from spectrograms having a dispersion of 37 A per millimeter at $H\gamma$,

[1] *Publications of the Lick Observatory*, **16**, 278, 1928.

[2] *Astronomische Nachrichten*, **236**, 281, 1929. [3] *Ibid.*, **209**, 55, 1919.

which were reduced with the aid of a table of stellar wave-lengths derived by Merrill[1] from measures of absorption lines in the spectra

TABLE I

MOUNT WILSON OBSERVATIONS OF R LYRAE

No.	Plate	Date	G.M.T.	Vel.	Wt.
				km/sec.	
1	γ 5804	1917 May 11	23^h40^m	−26.7	.....
2	5957	July 7	20 20	27.6	.....
3	6011	July 30	20 59	29.0	.....
4	11752	1923 May 2	22 4	30.4	.....
5	11764	May 5	21 43	30.4	.....
6	11769	May 6	20 5	34.8	.....
7	11813	May 28	22 26	23.8	.....
8	11819	May 29	21 12	21.8	.....
9	11901	June 28	19 58	20.8	0.5
10	11906	June 29	19 30	26.9	.....
11	11995	Aug. 3	19 15	29.0	.5
12	12088	Sept. 1	15 15	27.6	.....
13	12172	Oct. 3	14 42	28.4	.....
14	C 2497	Oct. 22	15 10	31.5	.....
15	γ 12242	Oct. 28	14 36	28.2	.....
16	12298	Nov. 25	14 58	30.0	.....
17	12642	1924 May 15	21 1	24.1	.....
18	12644	May 15	22 32	23.3	.....
19	12745	June 18	19 38	27.2	.....
20	12783	July 13	16 14	32.4	.....
21	12893	Aug. 20	15 28	31.7	.5
22	12938	Sept. 10	16 2	25.6	.....
23	13022	Oct. 15	14 53	29.0	.5
24	13094	Nov. 11	15 01	27.7	.....
25	13264	1925 Feb. 10	1 30	26.5	.5
26	13305	Mar. 11	1 10	22.7	.....
27	13347	Apr. 3	0 57	22.6	.5
28	13441	June 7	21 4	26.4	.....
29	13516	July 5	16 57	34.2	.....
30	13621	Aug. 6	16 27	25.0	.....
31	13710	Sept. 8	14 57	20.9	.....
32	13729	Sept. 23	15 10	33.9	.5
33	16600	1929 May 22	23 43	25.0	.5
34	16603	May 23	19 45	28.2	.5
35	16606	May 23	23 52	28.8	0.5
36	16635	June 16	22 10	31.6	.....
37	16723	July 18	23 52	30.4	.....
38	16832	Aug. 20	19 27	26.1	.....
39	16900	Sept. 12	14 47	−32.1	.....

of Me-type stars. All the results for lines on a single plate are very consistent. About half of the velocities are the means of two or more measures. The agreement for repeated measures was found to be

[1] *Mt. Wilson Contr.*, No. 265; *Astrophysical Journal*, **58**, 195, 1923.

such that little would have been gained by remeasuring spectrograms for which the velocity already derived depended on a large number of lines. Table I gives the data of observation and measurement for this series of velocities. The only comment required is that plates of inferior quality which still seemed useful were assigned weight one-half; the remainder have unit weight.

It is evident from this table and from the Lick and Allegheny observations that the variation in radial velocity is small and that an adequate discussion therefore calls for spectrograms of at least as high an order of accuracy as those made at the Lick Observatory. Nevertheless it seems best to present the additional Mount Wilson data and consider their consistency with Mrazek's conclusions.

TABLE II

PHASES OF MAXIMUM AND MINIMUM VELOCITY

Series	Observatory	Phase of Max.	Phase of Min.
1901	Lick	17^d	38^d
1907	Lick	19	38
1910	Allegheny	18	37
1912	Lick	16	35
1923	Mt. Wilson	19	35
1924	Mt. Wilson	16	33
1925	Mt. Wilson	15	35
1929	Mt. Wilson	20	40

Julian Day 2423600.000, which is approximately in the middle of the interval covered by the Mount Wilson observations, is the epoch to which they have been reduced by means of Mrazek's period. When thus reduced to a single cycle and grouped according to seasons (1923, 1924, 1925, and 1929), some evidence of a periodicity appears, but the phases of maximum and minimum velocity for the different seasons do not agree. Since this disagreement is very marked between 1923 and 1924, the period evidently needs considerable change. Trials with periods smaller than 41.3 days proved futile. The best agreement was found with 43.48 days, which also gives fairly consistent results for the phases of maximum and minimum velocity for the seasons involved in the earlier observations (1901, 1907, 1910, and 1912). There remains, however, some spread in these phases, and, when plotted, they show a periodic variation which can

be represented by a sine term. If this variation be taken into account by computing anew all phases by means of the formula

$$\text{Phase} = \text{Julian Day of observation} - [\text{J.D. } 2423600.000 + 43^d.48E + 6^d.5 \sin (2^\circ.7E - 47^\circ.2)] \text{ G.M.T.}, \quad (1)$$

the results for maximum and minimum velocity for the different seasons are approximately as given in Table II.

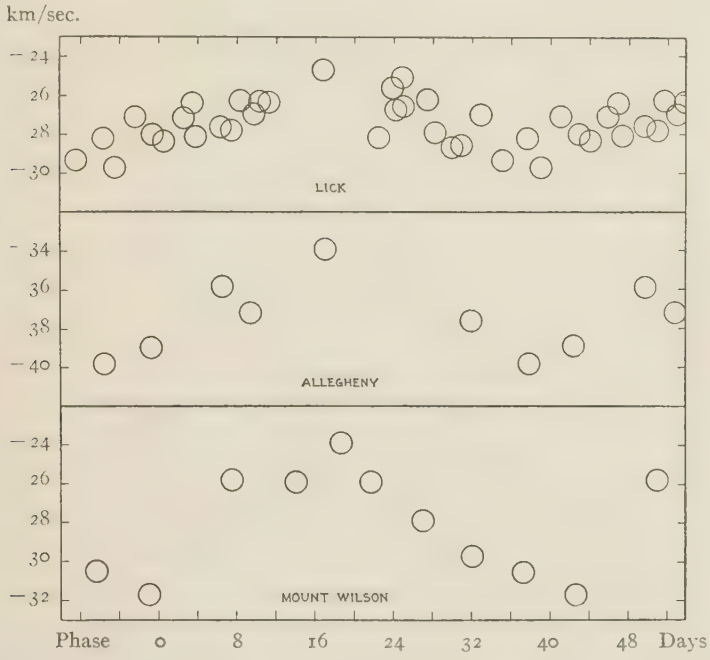

FIG. 1.—Radial-velocity diagrams derived by means of formula (1) from the Lick observations of 1901, 1907, and 1912, the Allegheny observations of 1910, and the Mount Wilson observations of 1923, 1924, 1925, and 1929. Normal places are plotted for Allegheny and Mount Wilson, but individual velocities for the Lick Observatory measures. The radius of the circles corresponds to 0.5 km/sec., which is of the order of the probable error of a plotted velocity.

No further attempt at refinement with this mode of computing the phases seems warranted, since, for the low-dispersion observations at least, the accidental errors in the radial velocities are probably a large percentage of the total amplitude involved. Figure 1 shows the variation in radial velocity derived from the Lick, Al-

legheny, and Mount Wilson observations, respectively. On account of their relatively higher accuracy, individual radial velocities are plotted on the Lick Observatory diagram. The Allegheny observations cover less than a single period, and each plotted point is the mean of three successive values. The points on the Mount Wilson diagram are means of velocities falling within intervals of five days in phase, the grouping being that shown in Table III.

It is evident from the Lick Observatory diagram, where the determinations are of relatively high weight, that the scatter is more than would be anticipated if simple periodic velocity variation alone is involved, and the individual observations made at both Allegheny

TABLE III

MOUNT WILSON NORMAL PLACES

No.	Phase	Radial Vel.	Observation No. from Table I, Col. 1
		km/sec.	
I	$7^d.449$	−25.8	9, 10, 19, 22
II	14.033	25.8	13, 26, 28
III	18.576	23.9	7, 8, 31, 33, 34, 35
IV	21.602	25.9	16, 17, 18, 38
V	26.896	27.9	12, 21, 24, 25
VI	32.000	29.7	14, 30, 32, 37
VII	37.236	30.5	4, 5, 6, 15, 20, 27
VIII	42.588	−31.7	11, 23, 29, 36, 39

and Mount Wilson bear this out. It is hard, therefore, to escape the conclusion that other variations, either erratic or periodic, may also be involved.

As already stated, Mrazek has concluded that a variation in the velocity of the center of mass with a period of five years is also present. Although a long-period variation may be involved, several points may be urged against Mrazek's value. In the first place, his long-period velocity-curve requires a minimum in 1925. The mean velocity for the eight observations made at Mount Wilson in 1925 is −26.6 km/sec., which is nearly 10 km/sec. higher than the predicted minimum. Second, the seasonal means are in substantial agreement except for the Allegheny observations. This suggests the possibility of a systematic difference between Allegheny determinations and those made at the Lick and Mount Wilson Observatories. Such a

difference really exists, and explains at least a part of the discrepancy. Daniels has published the wave-lengths which he used; and a sufficient number of his lines appear in Merrill's list to show that, if he had used Merrill's wave-lengths instead of his own, his radial velocities would have been larger algebraically by approximately 5 km/sec. Proper attention was given in the comparison to the fact that Daniels' wave-lengths are on the Rowland system and Merrill's on the international system. It is safe to say, therefore, that, if the total amplitude of long-period variation in the γ-velocity is involved in the difference between Allegheny, on the one hand, and the Lick and Mount Wilson observations, on the other, it can only be about one-half what Mrazek inferred.[1] It seems equally evident that the period is not five years.

The amplitudes of the velocity variation of the Lick, Allegheny, and Mount Wilson observations differ somewhat, as may be seen from Figure 1, although in kilometers per second the differences are not large. Nevertheless, they may be taken as further evidence of a variation additional to that in the period of 43.48 days.

The small amplitude of variation found with this period, together with the scattering still remaining in the individual observations, may suggest to some that the real period has not yet been found. Such a possibility is recognized, but perhaps is offset by the following facts: (1) the period is of the order of magnitude found many times by photometric observers; (2) the three series are harmoniously periodic; and (3) the probable errors derived with the residuals from simple means of the respective series are larger than would be expected from spectrograms as easily measurable as these.

The Mount Wilson spectrograms have been examined for any outstanding changes in the spectrum synchronous with the period of velocity variation, but none was found.

While most photometric observers assign a period in the neighborhood of 45 days, no one has yet had complete success in devising a formula which represents the great mass of photometric data that

[1] The possibility that the difference of 5 km/sec. which still remains is a systematic difference of instrumental origin has not been overlooked, but other evidence is lacking. It hardly seems reasonable. It is equally unlikely that Campbell's K-term for stars of spectral class M (+4 km/sec.) affects the Lick and Mount Wilson values and not those of Allegheny.

has been accumulated. It has seemed preferable, therefore, to discuss the radial velocities independently of the photometric observations. When the photometric data are later brought into harmony some definite relation may be forthcoming.

Briefly, the radial velocities of R Lyrae show that in the mean, at least, they are consistently represented in phase by formula (1). The mean amplitude is small. The scattering of the observations, the difference in amplitude for the curves of different series, and the difference in systemic velocity given by the Allegheny observations and by the Lick and Mount Wilson measures suggest a superposed velocity variation which may be either erratic or periodic, but which cannot be established from the present observations. Spectral changes synchronous with the period, if present, are not at all outstanding.

Carnegie Institution of Washington
Mount Wilson Observatory
February 1930

Contributions from the Mount Wilson Observatory, No. 395
Reprinted from the *Astrophysical Journal*, Vol. LXXI, pp. 163–174, 1930
Printed in the U.S.A.

A METHOD FOR DETERMINING THE DISTRIBUTION OF STELLAR ABSOLUTE MAGNITUDES FROM THE DISTRIBUTIONS OF ANGULAR AND LINEAR PECULIAR VELOCITIES

By GUSTAF STRÖMBERG

ABSTRACT

The method described was devised for the purpose of finding the *distribution of stellar absolute magnitudes* with high *accuracy* and with the greatest possible "*resolution*," however complex this distribution may be. It avoids use of analytical distribution functions, as well as means and dispersions, and is *inductive* and entirely *numerical*. The procedure depends on a knowledge of the distributions of reduced τ-components and peculiar radial velocities V' for the group of stars studied. The distributions are converted into logarithmic distributions, account being taken of the effect of errors, which is greatest in the case of the smallest values. The new variables are $x=\log \tau + 0.2m$ and $y=\log V'-1.6756$. Each distribution is defined by a sequence of frequencies within constant intervals. The unknown distribution of absolute magnitudes is determined by an integral equation. To solve this an approximate distribution of absolute magnitudes M is combined with that of y to give a computed distribution of x. The differences between the observed and the computed distributions of x are formed and used to derive by least-squares corrections to the assumed distribution of M. The corrected distribution of M is again combined with the distribution of y, and the computed distribution of x compared with the observed distribution. The process is repeated until a satisfactory reproduction is obtained of the distribution of x.

1. In the derivation of stellar absolute magnitudes we may distinguish between individual and statistical determinations, the former giving the absolute magnitude for a particular star with a certain probable error, which may be small or large, the latter usually giving the mean absolute magnitude for a group of stars.

Individual determinations are possible in the following cases: (1) when the trigonometric parallaxes can be determined with small percentage errors; (2) when several stars in a group have strictly parallel motions and their proper motions and some of their radial velocities are known; (3) when an observable physical characteristic of the star is correlated with its intrinsic brightness, the accidental errors being dependent upon the degree of correlation; (4) when the stars in a group are all at approximately the same distance (on a logarithmic scale). In the third and fourth cases it is necessary to determine certain constants in the reduction formulae either from

individual stars or by statistical methods, and any errors in these constants will introduce systematic errors in the absolute magnitudes.

The statistical methods in use are based on (1) the determination of mean trigonometric parallaxes; (2) comparison between angular and linear motion, usually a comparison between their means (parallactic motion) or their dispersions (mean peculiar motion).

In most cases, however, the ultimate purpose is not to determine the absolute magnitude of a particular star or the mean absolute magnitude of a group of stars, but rather the distribution of absolute magnitudes within a group, which may contain stars of a certain spectral type or the whole galactic system, and which may or may not be confined within definite limits of apparent magnitude. Particularly since the discovery of giants and dwarfs, many attempts based on both individual and statistical determinations have been made to find in a unique way the distribution in absolute magnitude among groups of stars. Much success has been attained by Kapteyn and van Rhijn,[1] who have combined and extrapolated the data for a number of smaller groups, usually the mean absolute magnitudes and estimates of the spread, into a distribution covering the whole galactic system. But any introduction of means and of "spread" or "dispersion" may obliterate the finer details of the absolute-magnitude distribution. These details are very important since they may give information on the existence of separate maxima and minima, which may be expected if the actual absolute magnitudes correspond to different states of stable equilibrium of radiation. A method capable of giving the absolute-magnitude distribution with a certain degree of "resolution" is accordingly needed. It might be thought that individual absolute-magnitude determinations would be best suited to such a study, but that is not necessarily the case, since the errors in the determinations, particularly in method (3) above, may tend to smooth out less prominent maxima and minima—a tendency which, of course, is not removed by increasing the number of stars. A particular aim of the present study has been to ascertain if the supergiants are separated from the ordinary

[1] *Publications of the Kapteyn Astronomical Laboratory*, No. 38, and previous publications.

giants by a distinct frequency minimum, or if the distribution shows a certain amount of asymmetry, as is indicated by the spectroscopically determined absolute magnitudes.

2. If we may regard the absolute-magnitude distribution as similar to that represented by a normal error function, the dispersion in absolute magnitude may be determined from the "excess" in the distribution of peculiar angular motions, as has been done by Gyllenberg.[1] It is also possible to determine the constants of two error-curves, which has also been done by Gyllenberg,[2] but the determination, which is based on the method of moments, is very uncertain, for reasons which will be explained later.

The present method developed from an attempt to find if the distribution of absolute magnitudes is a definite function of the distribution of angular and linear tangential motions, the angular motions being reduced to a constant apparent magnitude. Since, under certain conditions, the distribution of linear tangential motions may be replaced by that of radial velocities, the main problem is to handle complex distributions properly without introducing simplifying assumptions which may obliterate important features of the unknown absolute-magnitude distribution. Complex distributions have been studied, particularly by Charlier, Wicksell, Gyllenberg, Malmquist, and others at the Lund Observatory, by the use of moments, and many valuable results have been obtained. But it is clear that a distribution with many characteristic features can be analytically described only by the use of many parameters. To determine these it is necessary to compute moments of high order, which obviously are extremely uncertain because they involve means of observed quantities raised to a high power. Even with moments of third and fourth order there is always doubt whether the outstanding values ought to be included or not. The effect of the inclusion of a single star may be overwhelming.

3. The method here developed consists in relinquishing all attempts to represent the distributions involved by analytical func-

[1] *Meddelanden från Lunds Observatorium* (2d ser.), No. 41*a*, Charlier Festskrift, 1928. See also Strömberg, *Mt. Wilson Communications*, No. 103; *National Academy Proceedings*, **14**, 834, 1928.

[2] *Meddelanden från Lunds Observatorium* (2d ser.), No. 41*b*, Charlier Festskrift, 1928.

tions, at least until the distributions are known numerically, and in characterizing each distribution simply by a sequence of numbers representing the number of values occurring within definite intervals. The whole computation is thus strictly numerical; the observations are left free to speak for themselves with the least amount of interference from the investigator. The only interference introduced is that of arranging the observed values in intervals of rather narrow class breadths and of assuming a certain degree of continuity in the distributions. All moments are regarded as artificial and thus to be avoided; even the use of means is prohibited except within definite narrow limits when their introduction has no tendency to smooth out unduly the unknown distribution.

The problem is simplest in the case of peculiar motions, and the method has so far been developed only for this case. It has been applied to the determination of absolute magnitudes among stars of spectral classes K and M and of apparent magnitude brighter than 6.0. The results will be published in the following *Contribution*, No. 396.

4. The proper motion, supposed to be known for each star, is projected on a great circle passing through the star and the antapex, and on another great circle perpendicular to the first. The latter projection is the τ-component and is the only part of the proper motion used in the present investigation. It is expressed in seconds of arc per year. The radial velocities of the stars are also supposed to be known, but it is not necessary that radial velocities and τ-components be known for exactly the same stars. The main thing is that the distribution of the τ-components and of the radial velocities be representative for the stars studied.

For any star the relation between parallax π, apparent magnitude m, and absolute magnitude M is

$$M = m + 5 + 5 \log \pi , \tag{1}$$

which defines the absolute magnitude as the value of the apparent magnitude at a distance of 10 parsecs. The relation between the angular tangential motion τ and the linear tangential motion T in the direction of τ is

$$k\tau = T\pi , \tag{2}$$

where k is dependent on the units employed. T is expressed in kilometers per second; numerically, therefore, k is the ratio of the mean distance earth-sun, expressed in kilometers, to the number of seconds in a year, whence

$$k = 4.738 \text{ km year/sec.}$$

Eliminating π from equations (1) and (2), we find

$$M = m + 5 \log \tau - 5(\log T - \log k - 1) , \tag{3}$$

or, expressed in other terms,

$$M' = x - y , \tag{4}$$

where

$$\left.\begin{aligned} M' &= 0.2\, M , \\ x &= \log \tau + 0.2\, m = \log \tau' , \\ y &= \log T - \log k - 1 = \log T - 1.6756 . \end{aligned}\right\} \tag{5}$$

The quantity $\tau' = \tau 10^{0.2m}$ is often referred to as the reduced τ-component.

We have now to deal, not with individual stars, but with three distribution functions, viz., those of x, y, and M', denoted by $F_1(x)dx$, $F_2(y)dy$, and $F_3(M')dM'$, respectively. The velocities T are not known; but, being one-dimensional, that is, projected on axes independent of the direction of motion of the individual stars, they are statistically comparable with the peculiar radial velocities. If the peculiar velocities depend on the direction of motion, as, for instance, in an ellipsoidal velocity distribution, the stars must be well distributed over the sky. If this condition is fulfilled, we may thus replace the distribution of T by that of the peculiar radial velocities V', and thereby determine the distribution $F_2(y)dy$.

5. The distributions $F_1(x)dx$ and $F_2(y)dy$ must first be corrected for the effect of errors in the τ-components and in the peculiar radial velocities V', which is very great when τ' and V' approach zero. Although rather obvious, it may be mentioned here that these quantities are to be used without regard to signs. The probability of infinite values of x and y must be infinitely small, because a value of τ' or V' exactly equal to zero has an infinitely small probability.

For the intervals $d\tau'$ and dV' must then also be zero and the probabilities $F(\tau')d\tau'$ and $F(V')dV'$ must vanish, in spite of the fact that $F(\tau')$ and $F(V')$ may have their maximum values.[1]

To find the distribution of x and y for small values of τ' and V' I have assumed that the distributions of these quantities, for uniform intervals $d\tau'$ and dV', are of such types that for values numerically less than certain limits the frequency is constant. That is, if signs were retained, the distributions would have flat tops and maxima around $\tau'=V'=0$. Even if the most frequent value of τ' or V' should differ slightly from zero because of uncertainties in the apex direction or from systematic errors, the effect on the distribution of the logarithms would be quite insignificant. In the case of the radial velocities I assume that the distribution is constant for $V' \leq a$. Below this limit the frequency of V' is thus given by the equation

$$F(V')dV'=\frac{n_1}{a}\,dV'\,,$$

where n_1 is the number of values of V' numerically less than a.

From equations (5) we find, replacing T by V',

$$V'=47.38\ 10^{y}\,,$$

and thus

$$dV'=\frac{47.38}{\text{mod}}\ 10^{y}\,dy\,.$$

Consequently

$$F_2(y)dy=\frac{n_1}{a}\,\frac{47.38}{\text{mod}}\ 10^{y}\,dy\,,$$

and for any value of y less than $\log a-1.6756$,

$$\int_{y_1}^{y_2} F_2(y)dy=47.38\,\frac{n_1}{a}\,(10^{y_2}-10^{y_1})\,. \qquad (6)$$

The n_1 values of y can thus be distributed in uniform intervals dy from $y=\log a-1.6756$ backward until the frequency falls to practically zero, when the table stops.

[1] In this connection a reference may be made to a note by Russell regarding the computation of geometrical mean parallaxes (*Publications of the Astronomical Society of the Pacific*, **32**, 243, 1920) and also a note by the writer (*ibid.*, p. 244).

A similar procedure is used for the τ-components. The distribution of the reduced components $\tau' = \tau \cdot 10^{0.2m}$ less than or equal to a certain value β is supposed to be constant, and we find as before

$$\int_{x_1}^{x_2} F_1(x)dx = \frac{n_2}{\beta}\,(10^{x_2} - 10^{x_1})\,, \tag{7}$$

where n_2 is the number of values of $\tau' \leq \beta$.

If the values of α and β can be so chosen that they are of the order of magnitude of the mean errors in V' and τ', the main effect of these errors is automatically corrected. A small effect is still left in the distributions $F_1(x)dx$ and $F_2(y)dy$, which could well be neglected. The additional corrections were, however, actually applied, and for completeness I shall here derive the necessary formulae.

In the general case denote true values by subscripts, the errors by ϵ, and the measured quantities by V. Thus

$$V_1 = V + \epsilon\,. \tag{8}$$

V_1 and ϵ can be regarded as mutually independent quantities. Denote the probabilities of true V, observed V, and errors by $F(V)dV$, $f(V)dV$, and $g(\epsilon)d\epsilon$, respectively. A little consideration shows that the following relation holds:

$$f(V)dV = dV \int_{-\infty}^{+\infty} F(V+\epsilon)g(\epsilon)d\epsilon\,. \tag{9}$$

Develop $F(V+\epsilon)$ in a power series retaining terms up to second order.

$$F(V+\epsilon) = F(V) + \frac{\epsilon dF}{dV} + \frac{\epsilon^2}{2}\frac{d^2F}{dV^2}\,. \tag{10}$$

It is here supposed that the convergence of this series is sufficiently rapid. Thus

$$f(V)dV = dV\left[F(V)\int_{-\infty}^{+\infty} g(\epsilon)d\epsilon + \frac{dF}{dV}\int_{-\infty}^{+\infty} \epsilon g(\epsilon) + \tfrac{1}{2}\frac{d^2F}{dV^2}\int_{-\infty}^{+\infty} \epsilon^2 g(\epsilon)d\epsilon\right]$$

or

$$f(V)dV = dV\left[F(V) + \bar{\epsilon}\,\frac{dF}{dV} + \frac{\overline{\epsilon^2}}{2}\frac{d^2F}{dV^2}\right]\,.$$

175593

Replacing the derivatives of the function of true values with those of observed values, we have approximately

$$F(V)dV = dV\left[f(V) - \bar{\epsilon}\frac{df}{dV} - \frac{\bar{\epsilon}^2}{2}\frac{d^2f}{dV^2}\right]. \tag{11}$$

This procedure has often been used and is practically the same as that employed in *Contribution* No. 332.[1]

The numerical values of the derivatives may be found by either the graphical or the numerical method. In the present case, when the mean errors in τ' and V' are small compared with the dispersions themselves, we may with sufficient accuracy assume the distributions of V' and τ' to be normal error distributions. Denoting the dispersion in V' by σ_1 and the mean error in a determination of radial velocities by σ_2, we find, after taking into account that we are considering all values as positive,

$$\int_0^{V'} F(V')dV' - \int_0^{V'} f(V')dV' = \frac{N}{\sqrt{\pi}}\frac{\sigma_2^2}{\sigma_1^2} z e^{-z^2}, \tag{12}$$

where

$$z = \frac{V'}{\sqrt{2}\sigma_1}.$$

N is here the total number of stars in the group studied.

The limits in equation (12) are now chosen so as to conform to uniform intervals in $y = \log V' - 1.6756$, and the corrections thus derived are applied to the observed distribution $F_2(y)dy$.

The corrections to the distribution $F_1(x)dx$ are derived in exactly the same way from the mean error and the dispersion in τ'.

6. After the two distributions $F_1(x)dx$ and $F_2(y)dy$ have been found, the mean values of x and y might be formed, and the difference $\bar{x} - \bar{y}$ would give us the mean absolute magnitude immediately. This procedure would be identical with that proposed in 1918 in *Contribution* No. 144.[2] But we are not now interested in means; we want, if possible, to find the actual shape of the distribution-curve of absolute magnitudes.

[1] *Astrophysical Journal*, **65**, 238, 1927.

[2] *Ibid.*, **47**, 7, 1918.

If x and y were independent of each other, that is, if there were no correlation between them, the compounded distribution could be computed directly. But, since the angular motion is dependent on the linear tangential motion, there clearly must be a strong correlation between individual values of x and y. The independent variables on which the angular motion depends are linear tangential motion and distance, or, if the angular motions have been multiplied by $10^{0.2m}$, the independent variables are linear tangential motion and absolute magnitude, that is, y and M'. The dependence of linear motion upon absolute magnitude can be taken care of by using several distributions $F_2(y)dy$ for different limits in absolute magnitude.

As will be shown presently, the unknown distribution $F_3(M')dM'$ is determined by an integral equation ([15] below). The method used for solving it is an indirect one. At first a guess based on present knowledge is made of the distribution of absolute magnitudes, and then an expected distribution of x is computed from the assumed distribution of M' and the observed distribution of y. From the differences between the computed and the observed distributions of x, corrections to the assumed distribution of absolute magnitudes are derived and applied, and the process repeated until the observed distribution of reduced proper motion is well reproduced. The necessary formulae will now be derived.

We have the fundamental relation

$$x=M'+y\,, \tag{13}$$

where we may now assume M' and y to be independent variables. We can therefore compute the expected distribution $f_1(x)dx$ from the equation

$$\frac{1}{N_1}f_1(x)dx=\frac{dx}{N_2N_3}\int_{-\infty}^{+\infty}F_2(x-M')f_3(M')dM'\,. \tag{14}$$

The approximate distribution of M' is here denoted by $f_3(M')dM'$, and N_1, N_2, N_3 are the total numbers of stars in the three distributions $F_1(x)dx$, $F_2(y)dy$, and $f_3(M')dM'$, respectively. Equation (14) is simply a combination of partial probabilities summed for

all values of M' and expressed as a function of x. Numerically it means that each of the numbers occurring in the sequence $F_2(y)dy$ is to be multiplied by each of the numbers in the sequence $f_3(M')dM'$ and the products grouped according to the values of $x=M'+y$, and then summed for each interval of x. It is practical to have the intervals dy and dM' equal, and then the interval dx will be the same as the other two. The numbers N_1, N_2, and N_3 can be chosen equal and the distributions reduced to this number beforehand.

A relation similar to equation (14) exists for the true distributions, $F_1(x)dx$ and $F_3(M')dM'$. Thus

$$\frac{1}{N_1}F_1(x)dx=\frac{dx}{N_2N_3}\int_{-\infty}^{+\infty}F_2(x-M')F_3(M')dM'\,. \tag{15}$$

This is the integral equation which must be solved numerically for $F_3(M')$. From (14) and (15) we find

$$[F_1(x)-f_1(x)]dx=\frac{N_1}{N_2N_3}\,dx\int_{-\infty}^{+\infty}[F_3(M')-f_3(M')]F_2(x-M')dM'\,. \tag{16}$$

Denote

$$[F_1(x)-f_1(x)]dx \text{ by } \Delta f_1(x)dx\,,$$

and

$$[F_3(M')-f_3(M')]dM' \text{ by } \Delta f_3(M')dM'\,,$$

and we have

$$\frac{N_1}{N_2N_3}\,dx\int_{-\infty}^{+\infty}F_2(x-M')\Delta f_3(M')dM'=\Delta f_1(x)dx\,. \tag{17}$$

We will now assume that $\Delta f_3(M')$ is approximately constant for a certain small range in M'. The limits used are M_1', M_2', M_3', etc., and the corresponding means M_{12}', M_{23}', etc.

We have then

$$\frac{N_1}{N_2N_3}\,dx\left[\Delta f_3(M_{12}')\int_{M_1'}^{M_2'}F_2(x-M')dM'+\Delta f_3(M_{23}')\int_{M_2'}^{M_3'}F_2(x-M')dM'\right.$$
$$\left.+\text{etc.}\right]=\Delta f_1(x)dx\,.$$

But

$$\int_{M_1'}^{M_2'} F_2(x-M')dM' = \int_{x-M_1'}^{x-M_2'} F_2(y)dy\,,$$

and for other integrals we have similar equations. Hence

$$\left.\begin{aligned}\frac{N_1}{N_2N_3}\,dx\Big[\Delta f_3(M_{12}')\int_{x-M_1'}^{x-M_1'}F_2(y)dy+\Delta f_3(M_{23}')\int_{x-M_3'}^{x-M_2'}F_2(y)dy\\ +\text{etc.}\Big]=\Delta f_1(x)dx\,.\end{aligned}\right\}\quad(18)$$

For a range in x from x_1 to x_2, the mean of which is denoted by x_{12}, we may write the last equation in the form

$$\left.\begin{aligned}\frac{N_1}{N_2N_3}\,(x_2-x_1)\Big[\Delta f_3(M_{12}')\sum_{x_{12}-M_2'}^{x_{12}-M_1'}F_2(y)dy+\Delta f_3(M_{23}')\sum_{x_{12}-M_3'}^{x_{12}-M_2'}F_2(y)dy\\ +\text{etc.}\Big]=\sum_{x_1}^{x_2}\Delta f_1(x)dx\,.\end{aligned}\right\}\quad(19)$$

This equation may be regarded as an equation of condition for determining the unknown corrections $\Delta f_3(M')$ from the differences between observed and computed frequencies between the limits x_1 and x_2. For the next interval x_2 to x_3 a similar equation of condition may be obtained, and so on, until the whole range in x has been used.

The values of the absolute magnitude for which the corrections $\Delta f_3(M')$ are to be determined must not be taken too close together, for the least-squares solution will then become indeterminate. But by using overlapping intervals in x and in M' such that the means of x and M' are shifted the same amount, the corresponding y remains unchanged. The same coefficients in the equations of condition and in the normal equations can then be used for many determinations of $\Delta f_3(M')$ for as closely distributed values of M' as one may desire. The different solutions are, of course, not independent, but furnish corrections to the assumed distribution of absolute magnitude at points numerous enough to derive the corrected distribution with high precision and without excessive smoothing effect,

even though the true absolute-magnitude distribution changes rapidly.

It is clear that the different equations of condition (19) have greatly different weights, depending on the size of $F_1(x)dx$. It was found practical to apply to these equations weights inversely proportional to $F_1(x)dx$ after this distribution had been smoothed out.

When the improved absolute-magnitude distribution has been obtained, a new expected distribution of x is derived and compared with the observed distribution. If any systematic differences still exist, the process can be repeated. In general, two approximations have been found sufficient, even when the first approximation was very poor.

7. The integral equation (15) may not always have a definite solution. This depends upon the value of a certain determinant. If the value of this determinant is small, the solution becomes uncertain and may easily become unstable and indeterminate. The assumption of constant corrections $\Delta f_3(M')$ for a finite range in M' automatically eliminates very rapid oscillations in $F_3(M')$, which have no effect on the computed distribution of x and are thus indeterminate. The least-squares solution itself will tell if the intervals $M_2'-M_1'$, $M_3'-M_2'$, etc., have been chosen too small, for in this case the solution will become unstable. In this way a limit is set to the degree of resolution which can be obtained.

With slight modification the method can be applied to parallactic motions, and the necessary formulae and their application to K and M stars will be published in a future *Contribution*.

Carnegie Institution of Washington
Mount Wilson Observatory
January 1930

Contributions from the Mount Wilson Observatory, No. 396
Reprinted from the *Astrophysical Journal*, Vol. LXXI, pp. 175-190, 1930
Printed in the U.S.A.

THE DISTRIBUTION OF ABSOLUTE MAGNITUDES AMONG K AND M STARS BRIGHTER THAN THE SIXTH APPARENT MAGNITUDE AS DETERMINED FROM PECULIAR VELOCITIES

By GUSTAF STRÖMBERG

ABSTRACT

1. The *statistical method of determining the distribution of absolute magnitudes* from the reduced τ-*components and peculiar radial velocities* given in the preceding *Contribution* has been applied to the K and M stars in Boss's *Catalogue* brighter than *6 mag.* The stars were divided into three spectral groups, the number in each group being 659, 330, and 253, respectively.

Table I shows the distribution of $x = \log \tau + 0.2m$, as observed and also after correction for the effect of errors. It also shows the distribution of x computed from the adopted distribution of absolute magnitudes and of peculiar radial velocities V', and the differences between the observed and the computed distributions. The distributions of x are shown graphically in Figs. 1, 2, and 3.

The distribution of $y = \log V' - 1.6756$, as observed and after correction for the effect of errors in the radial velocities, is given in Table II for different absolute magnitudes.

The final distributions of absolute magnitudes are shown in Table IV and in Figs. 4, 5, and 6 with a class interval of 0.2 mag.

2. Among stars of spectral classes Ko–K2 the absolute-magnitude distribution shows four distinct maxima, occurring at absolute magnitudes -1.8, $+0.2$, $+2.9$, and $+6.7$. The proportions of stars in the four groups are 9, 78, 12, and 1 per cent, respectively; these stars are designated by the terms "supergiants," "ordinary giants," "subgiants," and "dwarfs."

In the spectral interval K3–K9 three distinct frequency maxima occur, at -2.4, -0.1, and between 4 and 9, with relative proportions of 19, 78, and 3 per cent. These groups are identified as supergiants, ordinary giants, and dwarfs. No subgiants exist in this spectral interval.

Among the M stars only supergiants and ordinary giants appear. The frequency maxima occur at -1.6 and -0.1, and the relative proportions are 44 and 56 per cent.

3. Stable conditions in the stars and relatively rapid transitions from one stable state to another are suggested as the probable cause of the frequency maxima and minima.

The preceding *Contribution*, No. 395,[1] describes a method for determining as closely as possible the general shape of the distribution-curve of absolute magnitudes from the distribution of reduced τ-components and of peculiar radial velocities. This method has been applied to all the stars in Boss's *Catalogue*, excepting variables, equal to or brighter than Harvard apparent magnitude 5.99 and of spectral classes K–M. During the computation the method was

[1] *Astrophysical Journal*, 71, 163, 1930.

found to be more powerful than had been anticipated and capable of giving the distribution of absolute magnitude with high precision and great resolution, provided the distributions for the τ-components and the radial velocities are themselves well known.

The stars were divided into three spectral groups, K0–K2, K3–K9, and M0–M9, according to the Harvard classification. In some cases, however, Mount Wilson classifications were used, which in the mean give the type one or two subdivisions earlier than the Harvard classification. The numbers of stars in the three groups are 659, 330, and 253, or 53, 27, and 20 per cent, respectively.

The τ-components were taken from a typewritten copy prepared by prisoners in Holland under Kapteyn's direction. The second, third, and fourth columns of Table I give the distribution of $x = \log \tau + 0.2m$, as obtained directly from the original data, reduced to a total of one thousand stars. For convenience the interval is made uniform throughout and equal to 0.1. All the values of x less than -1.7 were combined in one group and then distributed according to the logarithmic scale. The distributions have also been corrected for the effect of errors in accordance with the formulae derived in the preceding *Contribution*. The mean error in a τ-component was assumed to be $\pm 0''.005$. The final distributions are given in the fifth, sixth, and seventh columns of Table I.

The computed distributions are given in the eighth, ninth, and tenth columns. These were derived from the last approximation for the absolute-magnitude distribution, which appears in Table IV, combined with the distribution of y in Table II. The last three columns of Table I give the differences between observed and computed distributions. The computed distribution-curves for the three spectral groups are shown graphically in Figures 1, 2, and 3. The observed values for the distribution are indicated by dots connected by straight lines.

The distributions of the linear velocities are in the second, third, and fourth columns of Table II between limits of $y = \log V' - 1.6756$, where V' is the peculiar radial velocity. To increase the data, the radial velocities for some stars fainter than sixth magnitude were included. This does not change the distribution of peculiar velocities, provided the fainter stars are not selected on the basis of large

proper motion, which would produce a certain increase in the mean linear motion. The numbers of stars used in the three groups were 447, 273, and 306, respectively.

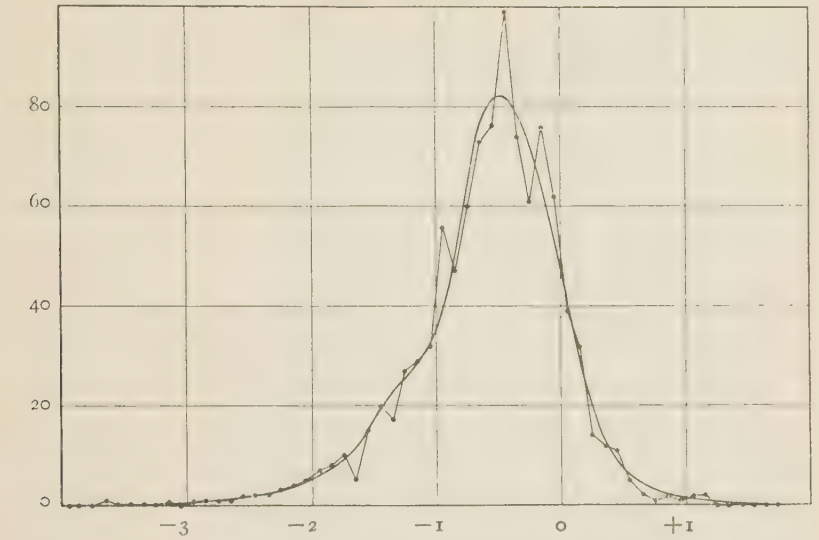

FIG. 1.—Distribution of $x = \log \tau + 0.2m$ for stars of spectral types K0 to K2. The dots joined by straight lines represent observed numbers within intervals $dx = 0.1$. The smooth curve is computed from the distributions of absolute magnitudes and peculiar radial velocities.

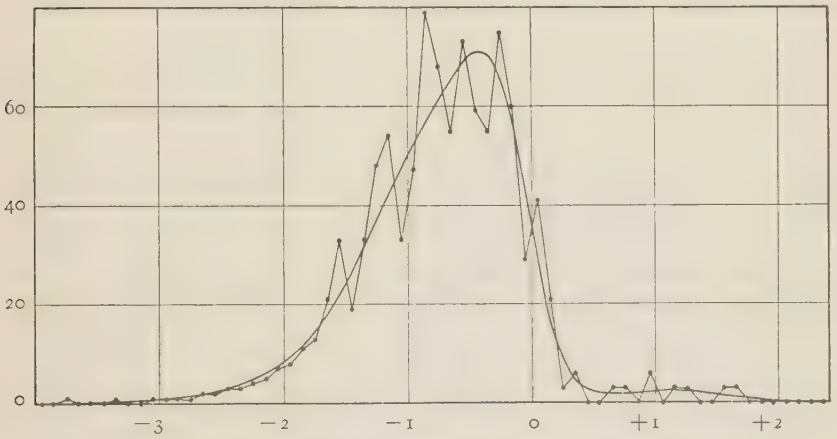

FIG. 2.—Same as Fig. 1 for stars of spectral types K3 to K9

The radial velocities, determined mainly at the Lick and Mount Wilson Observatories, were corrected for a constant solar motion of 20 km/sec. toward the apex $\alpha = 270°$, $\delta = +30°$. A moderate change in the solar motion does not appreciably influence the distribution of peculiar radial velocities.

The frequencies are reduced to a total of one thousand stars, those for $y < -1.2$, that is, for V' less than 3.0 km/sec., being grouped to-

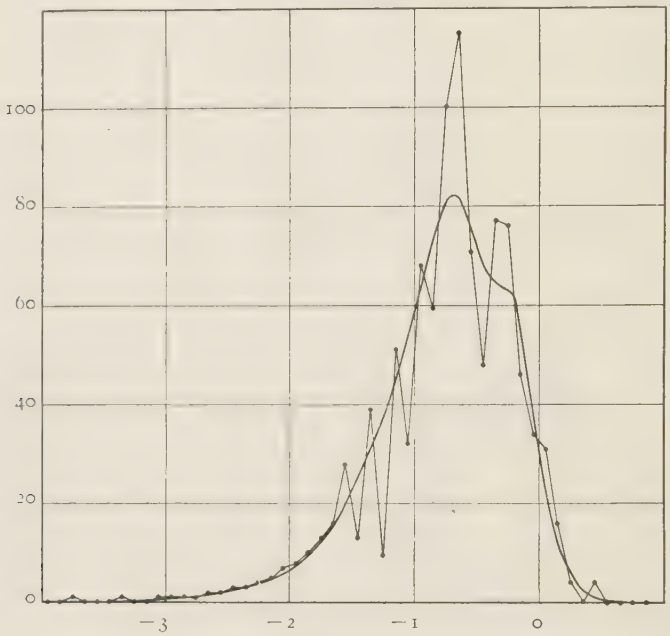

FIG. 3.—Same as Fig. 1 for stars of spectral type M

gether. The frequencies for the small values of V' were then found as before. The distributions were corrected for errors on the basis of a mean error of ± 3.0 km/sec. in the radial velocities, which is supposed to include systematic errors and errors in the assumed solar motion as well as accidental errors. The distributions of y were also smoothed graphically without losing the peculiarities in the distribution-curves.

The dependence of velocity distribution on absolute magnitude was derived from spectroscopic absolute magnitudes. This was done

TABLE I

$F(x)dx$

x	Observed Distribution			Observed Distribution Corrected for Errors			Computed Distribution			Observed *minus* Computed Distribution		
	K0–K2	K3–K9	M0–M9	K0–K2	K3–K9	M0–M9	K0–K2	K3–K9	M0–M9	K0–K2	K3–K9	M0–M9
−4.4				...	...	...	0.0	0.1	0.0	.....	− 0.1	0.0
−4.3				...	...	...	.0	.1	.0	.....	− .1	.0
−4.2				...	...	...	.0	.0	.0	.....	0.0	.0
−4.1				...	...	...	.1	.1	.1	− 0.1	− .1	− .1
−4.0				...	...	...	.0	.1	.1	.0	− .1	− .1
−3.9				...	...	...	.1	.1	.1	− .1	− .1	− .1
−3.8				...	1	1	.1	.2	.1	− .1	+ .8	+ .9
−3.7				1	0	0	.2	.3	.2	+ .8	− .3	− .2
−3.6				0	0	0	.2	.4	.3	− .2	− .4	− .3
−3.5				0	0	0	.2	.3	.3	− .2	− .3	− .3
−3.4				0	1	1	.3	.4	.4	− .3	+ .6	+ .6
−3.3				0	0	0	.3	.4	.5	− .3	− .4	− .5
−3.2				1	0	0	.5	.6	.6	+ .5	− .6	− .6
−3.1	49	64	63	0	1	1	.5	.9	.7	− .5	+ .1	+ .3
−3.0				1	1	1	.5	.9	.6	+ .5	+ .1	+ .4
−2.9				1	1	1	0.7	1.2	0.9	+ .3	− .2	+ .1
−2.8				1	1	1	1.1	1.6	1.3	− .1	− .6	− .3
−2.7				1	2	2	1.4	2.1	1.6	− .4	− .1	+ .4
−2.6				2	2	2	1.5	2.5	2.1	+ .5	− .5	− .1
−2.5				2	3	3	2.0	3.2	2.6	.0	− 0.2	+ .4
−2.4				2	3	3	2.6	4.0	3.2	− .6	− 1.0	− .2
−2.3				3	4	4	3.0	5.0	3.9	.0	− 1.0	+ .1
−2.2				4	5	5	3.8	6.1	4.9	+ .2	− 1.1	+ 0.1
−2.1				5	7	7	4.7	7.6	5.8	+ 0.3	− 0.6	+ 1.2
−2.0				7	8	8	6.0	9.6	7.3	+ 1.0	− 1.6	+ 0.7
−1.9				8	11	10	7.5	11.8	9.3	+ 0.5	− 0.8	+ 0.7
−1.8				10	13	13	9.4	14.6	12.0	+ 0.6	− 1.6	+ 1.0
−1.7	5	21	16	5	21	16	11.7	18.1	15.5	− 6.7	+ 2.9	+ 0.5
−1.6	15	33	28	15	33	28	15.3	22.1	19.9	− 0.3	+10.9	+ 8.1
−1.5	20	18	12	20	19	13	19.4	26.5	25.0	+ 0.6	− 7.5	−12.0
−1.4	17	33	39	17	33	39	22.9	31.8	31.0	− 5.9	+ 1.2	+ 8.0
−1.3	27	48	9	27	48	9	25.8	36.9	37.5	+ 1.2	+11.1	−28.5
−1.2	29	54	51	29	54	51	29.0	42.1	45.2	0.0	+11.9	+ 5.8
−1.1	32	33	32	32	33	32	32.7	47.4	54.1	− 0.7	−14.4	−22.1
−1.0	56	46	67	56	47	68	38.9	52.3	63.4	+17.1	− 5.3	+ 4.6
−0.9	47	79	59	47	79	59	49.8	56.6	72.9	− 2.8	+22.4	−13.9
−0.8	59	67	99	60	68	100	64.6	60.8	80.4	− 4.6	+ 7.2	+19.6
−0.7	73	55	115	73	55	115	76.5	64.9	81.8	− 3.5	− 9.9	+33.2
−0.6	76	73	71	76	73	71	81.4	68.4	75.7	− 5.4	+ 4.6	− 4.7
−0.5	99	58	47	99	59	48	81.7	70.8	68.0	+17.3	−11.8	−20.0
−0.4	74	55	77	74	55	77	78.5	70.2	64.7	− 4.5	−15.2	+12.3
−0.3	61	76	77	61	75	76	72.3	65.5	63.2	−11.3	+ 9.5	+12.8
−0.2	76	61	47	76	60	46	63.7	56.6	54.9	+12.3	+ 3.4	− 8.9
−0.1	62	30	35	62	29	34	52.9	44.0	39.9	+ 9.1	−15.0	− 5.9
0.0	38	42	32	38	41	31	41.3	29.2	24.5	− 3.3	+11.8	+ 6.5
+0.1	33	21	16	32	21	16	29.9	16.9	12.9	+ 2.1	+ 4.1	+ 3.1
+0.2	14	3	4	14	3	4	20.3	9.2	6.2	− 6.3	− 6.2	− 2.2
+0.3	12	6	0	12	6	0	13.4	5.1	2.7	− 1.4	+ 0.9	− 2.7
+0.4												

TABLE I—*Continued*

x	Observed Distribution			Observed Distribution Corrected for Errors			Computed Distribution			Observed *minus* Computed Distribution		
	Ko–K2	K3–K9	Mo–M9	Ko–K2	K3–K9	Mo–M9	Ko–K2	K3–K9	Mo–M9	Ko–K2	K3–K9	Mo–M9
+0.4	11	0	4	11	0	4	8.9	3.0	1.2	+ 2.1	− 3.0	+ 2.8
+0.5	5	0	0	5	0	0	6.4	2.2	0.4	− 1.4	− 2.2	− 0.4
+0.6	2	3	0	2	3	0	4.5	1.9	.1	− 2.5	+ 1.1	− .1
+0.7	1	3	0	1	3	0	3.2	1.8	0.0	− 2.2	+ 1.2	0.0
+0.8	2	0	0	2	0	0	2.3	2.0	.....	− 0.3	− 2.0	.....
+0.9	1	6	0	1	6	0	1.6	2.2	.....	− .6	+ 3.8	.....
+1.0	2	0	0	2	0	0	1.3	2.4	.....	+ .7	− 2.4	.....
+1.1	0	3	0	0	3	0	0.9	2.5	.....	− .9	+ 0.5	.....
+1.2	0	3	0	0	3	0	.8	2.4	.....	− .8	+ 0.6	.....
+1.3	0	0	0	0	0	0	.6	2.2	.....	− 0.6	− 2.2	.....
+1.4	2	0	0	2	0	0	.4	1.9	.....	+ 1.6	− 1.9	.....
+1.5	0	3	0	0	3	0	.2	1.6	.....	− 0.2	+ 1.4	.....
+1.6	0	3	0	0	3	0	.1	1.3	.....	− .1	+ 1.7	.....
+1.7	0	0	0	0	0	0	.1	1.1	.....	− .1	− 1.1	.....
+1.8	0	0	0	0	0	0	.0	0.7	.....	0.0	− 0.7	.....
+1.9	0	0	0	0	0	0	.0	.5	.....	.....	− .5	.....
+2.0	0	0	0	0	0	0	.0	.2	.....	.....	− .2	.....
+2.1	0	0	0	0	0	0	.0	.2	.....	.....	− .2	.....
+2.2	0	0	0	0	0	0	0.0	0.1	.....	.....	− 0.1	.....
+2.3												

by forming the means of the logarithms of the peculiar radial velocities for different absolute-magnitude groups. It was assumed that the shape of the distribution-curve of y for each spectral group was the same for different absolute magnitudes. By simply shifting the whole distribution-curve by an amount determined from the means of y it was thus possible to find the distribution for each absolute magnitude. The final distributions are given in Table II, the absolute magnitude at which the transition from one distribution to another takes place being given on top between the columns.

In the first approximation for the M stars it was assumed that the linear velocities are independent of the absolute magnitudes. It was then found that the absolute-magnitude distribution showed a separation into two distinct groups, and the mean velocity in each of these was found by using reduced proper motion as well as spectroscopic evidence as criteria for absolute magnitude. The data for reduced proper motion are given in *Contribution* No. 293.[1]

At the bottom of each column in Table II is given the arithmetical

[1] *Astrophysical Journal*, **61**, 363, 1925.

TABLE II

$F(y)dy$

y	K0–K2	K3–K9	M0–M9	K0–K2			K3–K9						M0–M9	
				−1.4		+5.0	−2.4	−2.0	−1.4	−0.6	+2		−0.9	
−4.0				1	.....	.....	1							
−3.9				0	.....	.....	0	1						
−3.8				0	.....	.....	0	0	1	.....	.....	.....	1	0
−3.7				0	1	1	0	0	0	1	.....	.....	0	0
−3.6				0	0	0	0	0	0	0	1	.....	0	1
−3.5				1	0	0	1	0	0	0	0	1	0	0
−3.4				0	0	0	0	1	0	0	0	0	0	0
−3.3				0	0	0	0	0	1	0	0	0	1	0
−3.2				1	1	1	1	0	0	1	0	0	0	0
−3.1				1	0	0	1	1	0	0	1	0	0	1
−3.0				1	0	0	1	1	1	0	0	1	1	0
−2.9				1	1	1	1	1	1	1	0	0	1	0
−2.8	123	121	111	2	1	1	2	1	1	1	1	0	1	1
−2.7				2	1	1	2	2	1	1	1	1	1	1
−2.6				2	1	1	2	2	2	1	1	1	1	1
−2.5				3	2	2	3	2	2	2	1	1	2	1
−2.4				4	2	2	4	3	2	2	2	1	2	1
−2.3				5	2	2	5	4	3	2	2	2	3	2
−2.2				7	3	3	6	5	4	3	2	2	4	3
−2.1				8	4	3	8	6	5	4	3	2	5	3
−2.0				10	5	4	10	8	6	5	4	3	6	4
−1.9				13	7	6	12	10	8	6	5	4	7	5
−1.8				16	8	7	17	12	10	8	6	5	8	6
−1.7				18	10	9	20	17	12	10	8	6	10	7
−1.6				22	13	11	23	20	17	12	10	8	12	9
−1.5				25	16	14	28	23	20	17	12	10	17	12
−1.4				29	18	17	34	28	23	20	17	12	22	16
−1.3				36	22	20	43	34	28	23	20	17	29	20
−1.2				58	25	23	53	43	34	28	23	20	37	26
−1.1	22	33	42											

TABLE II—*Continued*

y	K_0–K_2	K_3–K_9	M_0–M_9	K_0–K_2		K_3–K_9					M_0–M_9	
				-1.4	$+5.0$	-2.4	-2.0	-1.4	-0.6	$+2$	-0.9	
-1.1		47	43	84	27	63	53	43	34	23	46	34
-1.0	29	26	43	97	32	73	63	53	43	28	54	42
-0.9	31	44	62	101	42	84	73	63	53	43	64	50
-0.8	63	73	62	100	74	95	84	73	63	53	75	60
-0.7	94	60	65	92	92	99	95	84	73	63	86	70
-0.6	89	90	82	81	100	99	99	95	84	73	97	82
-0.5	101	92	92	65	101	87	99	99	95	84	111	92
-0.4	96	99	118	50	98	58	87	99	99	95	116	106
-0.3	92	99	114	33	86	32	58	87	99	99	92	116
-0.2	65	88	82	19	73	17	32	58	87	99	48	109
-0.1	65	59	39	8	58	8	17	32	58	87	24	64
0.0	72	33	23	3	41	4	8	17	32	58	10	32
$+0.1$	25	18	16	1	26	2	4	8	17	32	4	14
$+0.2$	27	11	3	0	14	1	2	4	8	17	2	5
$+0.3$	2	0	3	0	5	0	1	2	4	8	0	3
$+0.4$	2	4	0	0	2	0	0	1	2	4	0	1
$+0.5$	0	3	0	0	0	0	0	0	1	2	0	0
$+0.6$	2	0	0	0	0	0	0	0	0	1	0	0
$+0.7$	0	0	0	0	0	0	0	0	0	0	0	0
$+0.8$	0											
$\bar{y}$	-0.624	-0.600	-0.625	-0.921	-0.621	-0.570	-0.900	-0.800	-0.700	-0.600	-0.500	-0.400	-0.703	-0.558
V'	11.25	11.89	11.24	5.69	11.35	12.76	5.96	7.51	9.45	11.90	14.98	18.86	9.40	13.12

mean $\bar{y}$ and the geometric mean $\underline{V}'$ of the peculiar radial velocities for the different types and absolute magnitudes. These means are connected by the relation

$$\bar{y} = \log \underline{V}' - 1.6756 .$$

TABLE III

F(M)dM

M	K0–K2	K3–K9	M0–M9
−6.0	0.3	− 4.7	.....
−5.5	.6	− 3.3	.....
−5.0	.8	− 2.9	− 2.6
−4.5	− .5	− 5.2	− 1.8
−4.0	− .4	8.4	0.0
−3.5	0.2	6.3	− 6.2
−3.0	3.1	11.7	−10.3
−2.5	6.8	35.7	20.0
−2.0	14.4	21.8	58.7
−1.5	14.3	26.9	80.4
−1.0	14.0	59.5	21.7
−0.5	42.0	93.7	61.4
0.0	127.6	112.6	84.8
+0.5	132.4	33.0	49.8
+1.0	8.3	− 4.6	22.3
+1.5	6.3	− 1.7	5.3
+2.0	6.9	− 1.7	1.0
+2.5	14.2	− 6.1	− 0.3
+3.0	14.4	− 1.5	− .6
+3.5	7.5	− 1.2	− .4
+4.0	3.7	− 0.8	− .2
+4.5	− 0.8	3.2	+ 0.5
+5.0	− 4.0	1.8	.....
+5.5	− 1.1	1.1	.....
+6.0	0.1	1.5	.....
+6.5	1.8	− 0.6	.....
+7.0	2.0	4.4	.....
+7.5	0.2	0.2	.....
+8.0	.2	− 1.0	.....
+8.5	.4	0.7	.....
+9.0	.2	1.3	.....
+9.5	− 0.1	0.7	.....

The assumed absolute-magnitude distributions used as first approximations in deriving the final distributions were in general taken from the spectroscopic data. The actual values used are of no importance, since several approximations were made before the representation of the observed distribution of x was regarded as satisfactory. The method is described in detail in the preceding *Contribution* and consists in combining the assumed absolute-magnitude distribu-

tion with the distribution of y to obtain a computed distribution $f(x)dx$, and then, from the differences between computed and observed distributions of x, in finding corrections to the assumed distribution of absolute magnitudes. The frequencies $F(M)dM$ thus derived from the final least-squares solution, referred to an interval of

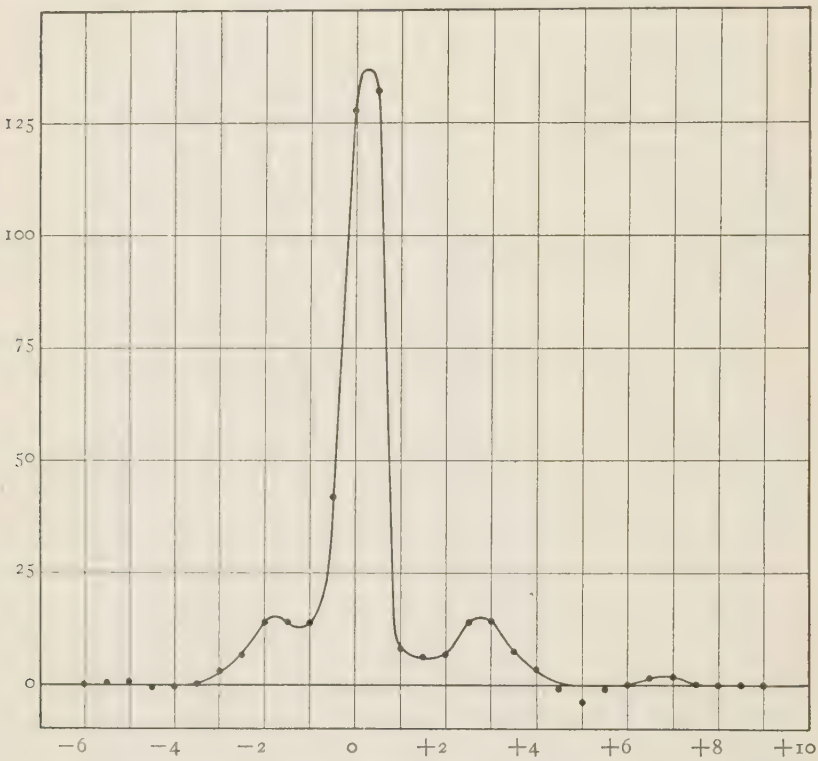

FIG. 4.—Distribution of absolute magnitudes for stars of spectral types Ko to K2. The points are computed from the distribution of reduced π-components and peculiar radial velocities. Notice four frequency maxima.

0.2 mag. in dM, are given in Table III. The final distributions of absolute magnitude are shown graphically in Figures 4, 5, and 6, where the computed values are indicated by dots. Negative frequencies have been replaced by zero values, and the total numbers adjusted with the least amount of smoothing. The final distributions are shown by the curves, and the corresponding numbers appear in Table IV.

A study of the distribution of absolute magnitudes shown in Figures 4, 5, and 6 and in Table IV is of great interest. The Ko–K2 stars show four distinct maxima, at −1.8, +0.2, +2.9, and +6.7 mags. The proportions of stars in the four groups are 9, 78, 12, and 1 per cent. The stars in these groups will here be designated "supergiants," "ordinary giants," "subgiants," and "dwarfs." The existence of supergiants was not unexpected, since spectroscopic criteria

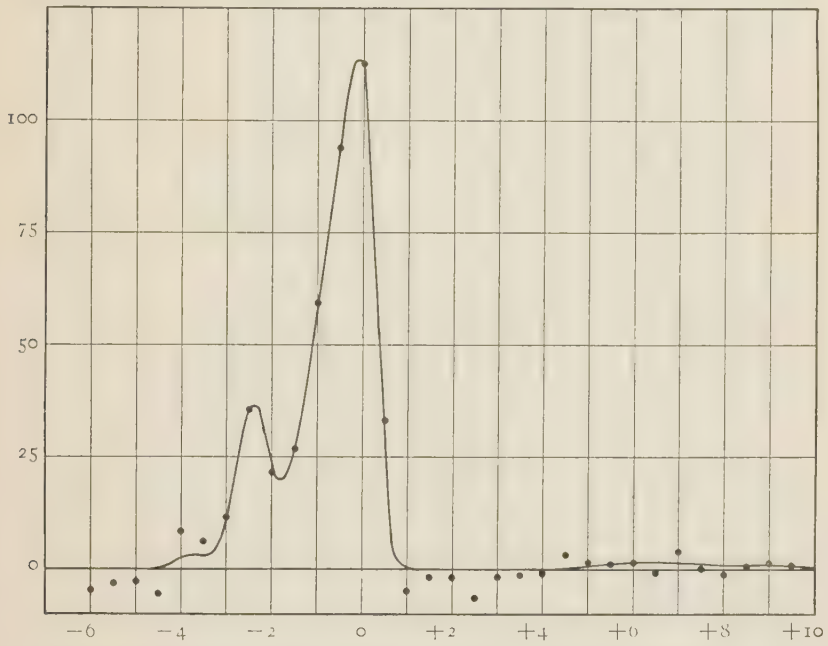

FIG. 5.—Absolute-magnitude distribution for stars of spectral types K3 to K9

have indicated their presence among stars of all types between F and M; but it is interesting to find that they are separated from the ordinary giants by a frequency minimum at −1.0. The most interesting feature of the distribution is the extremely rapid rise and fall around the maximum at +0.2. In spite of their great number, all the ordinary giants seem to be confined within an interval of 2 mags. The small range in M has also been indicated by the spectroscopic criteria, but additional evidence was desirable. The subgiants, as a distinct group of stars, were entirely unexpected. It has been known

that stars of an absolute magnitude intermediate between giants and dwarfs exist, but the presence of an intermediate group, separated on both sides by frequency minima, was not suspected. This group is probably rather prominent among the G stars, but does not seem to occur among other spectral classes. The dwarfs lie between absolute magnitudes 6 and 7.5, the fainter ones being excluded by the limitation in apparent magnitude.

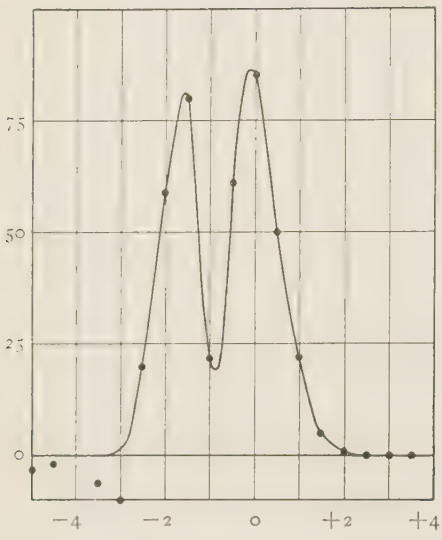

FIG. 6.—Absolute-magnitude distribution for stars of spectral type M.

Among stars of spectral class K3–K9 subgiants do not seem to occur. The maxima are at −2.4 for the supergiants, −0.1 for the ordinary giants, and between 5 and 9 for the dwarfs. The relative proportions are 19, 78, and 3 per cent, respectively, the supergiants thus being relatively more numerous than in the K0–K2 group. The minimum separating supergiants from the ordinary giants is now clearly marked. The rapid drop in frequency from absolute magnitude 0 to +1 is also here very pronounced, and no star seems to exist between absolute magnitudes +1 and +4.

The absolute magnitudes of the M stars fall into two distinct groups, the maximum frequencies occurring at −1.6 and −0.1. The relative proportions of supergiants and ordinary giants are 44 and 56 per cent. No subgiants or dwarfs seem to exist within the chosen limits of apparent magnitude. Because of the more evenly divided distribution, the minimum between the groups is now well marked.

The reality of these maxima and minima can, to a certain extent, be judged from the distributions of x in Figures 1, 2, and 3. The details in the absolute-magnitude distributions are, of course, much obscured by having been combined with the distributions of linear motion; but traces of the different maxima are left, in the form of

humps, on the curves. For the M stars the maximum in $F(x)dx$ corresponding to the supergiants is very pronounced in the observations, that corresponding to the ordinary giants less so. The whole

TABLE IV

$F(M)dM$

M	Ko–K2	K3–K9	Mo–M9	M	Ko–K2	K3–K9	Mo–M9
−4.2	0	2	0	+ 3.0	13	0	0
−4.0	0	3	0	+ 3.2	10	0	0
−3.8	0	3	0	+ 3.4	8	0	0
−3.6	0	3	0	+ 3.6	6	0	0
−3.4	1	4	0	+ 3.8	4	0	0
−3.2	2	8	0	+ 4.0	2	0	0
−3.0	4	17	2	+ 4.2	1	0	0
−2.8	5	27	9	+ 4.4	0	0	0
−2.6	7	36	20	+ 4.6	0	0	0
−2.4	10	36	37	+ 4.8	0	1	0
−2.2	13	27	52	+ 5.0	0	2	0
−2.0	15	20	67	+ 5.2	0	2	0
−1.8	15	21	78	+ 5.4	0	1	0
−1.6	14	27	80	+ 5.6	0	1	0
−1.4	13	38	55	+ 5.8	0	2	0
−1.2	13	51	31	+ 6.0	1	1	0
−1.0	15	67	19	+ 6.2	2	2	0
−0.8	19	82	30	+ 6.4	2	1	0
−0.6	39	95	61	+ 6.6	2	2	0
−0.4	74	107	82	+ 6.8	2	2	0
−0.2	111	113	86	+ 7.0	2	1	0
−0.0	135	94	79	+ 7.2	1	2	0
+0.2	137	59	65	+ 7.4	0	1	0
+0.4	129	25	50	+ 7.6	0	1	0
+0.6	70	4	36	+ 7.8	0	1	0
+0.8	11	0	26	+ 8.0	0	1	0
+1.0	7	0	17	+ 8.2	0	1	0
+1.2	6	0	9	+ 8.4	0	1	0
+1.4	5	0	5	+ 8.6	0	1	0
+1.6	5	0	3	+ 8.8	0	1	0
+1.8	6	0	1	+ 9.0	0	1	0
+2.0	8	0	0	+ 9.2	0	1	0
+2.2	11	0	0	+ 9.4	0	0	0
+2.4	14	0	0	+ 9.6	0	1	0
+2.6	15	0	0	+ 9.8	0	0	0
+2.8	15	0	0	+10.0			
+3.0							

run is, however, in this case rather erratic, because of the small number of stars and the small intervals used.

It is clear that the process of deriving the absolute-magnitude distribution from the distribution of reduced τ-components implies that humps of small amplitude and large extension in $F_1(x)dx$ determine humps of large amplitude and small extension in the absolute-

magnitude distribution. Since the reality of the small humps in $F_1(x)dx$ is difficult to prove or disprove, the demonstration of the existence of the maxima and minima in the absolute-magnitude distribution must be based principally on the smooth running of the curves and the general consistency of the results for different spectral types. Additional evidence may be forthcoming when the results from parallactic motions become available.

The effect of systematic errors in the proper motions was investigated by applying Raymond's corrections[1] to the proper motions in declination and computing the effect on the τ-components. It was found that the influence is entirely negligible and may be regarded as taken into account by the correction for accidental errors.

A comparison with the spectroscopic absolute magnitudes shows a very good agreement, except for the supergiants. There are several reasons for this discrepancy. One is that the stars in the present investigation are distributed all over the sky, whereas the spectroscopic data are limited to stars north of -25° declination. This limitation is significant since there is reason to believe that the supergiants are particularly numerous in the Southern Hemisphere. This selective effect might be expected to be most pronounced among the M stars which, according to the present study, include a large percentage of supergiants.

It has been known for some time that the mean error in the spectroscopic absolute magnitudes is considerably larger for the supergiants than for stars in general. For the M stars the writer found[2] the probable errors for the two classes of stars to be 0.63 and 0.45, respectively. The reason for this may be partly a smaller coefficient of correlation between line intensity and absolute magnitude and partly the fact that different reduction-curves are used for the two classes of stars, and it may be uncertain which reduction-curve should be used for stars with intermediate line intensities. It must be noted that the minimum separating the two classes is extremely narrow, and even a small extra dispersion may obliterate it.

The existence of a numerous group of supergiant M stars has been

[1] *Astronomical Journal*, **36**, 129, 1926.

[2] *Mt. Wilson Contr.*, No. 327; *Astrophysical Journal*, **65**, 108, 1927.

foreshadowed by certain discoveries. Adams, Joy, and Humason[1] first called attention to the fact that the M stars brighter than absolute magnitude −1.0 show a pronounced galactic concentration; and Luyten,[2] using spectroscopic absolute magnitudes, has shown that the giant M stars in galactic latitudes less than 20° are 0.5 mag. brighter than those in higher latitudes. Finally, as mentioned above, I have found a large difference in peculiar and solar motions for two groups of giant M stars, selected on the basis of $m+5 \log \mu$. All these phenomena are most easily explained by the existence of two distinct groups of different absolute magnitudes and different galactic concentrations.

A particular advantage of the present method of determining the distribution of absolute magnitudes is that the distribution is determined directly, without introducing extra spread or losing inherent spread in the distribution of true absolute magnitudes. This is in contradistinction to methods based on the existence of a correlation between physical characteristics of a star and its intrinsic brightness, which, while giving individual absolute magnitudes, may not give the distribution of absolute magnitudes as accurately as the present statistical method. With such methods minor frequency maxima and minima may be blotted out by the extra dispersion introduced by the circumstance that we are dealing with correlations and not with direct observations of absolute magnitude. On the other hand, the methods which give individual absolute magnitudes may be applied to faint and distant stars for which adequate proper-motion data may never be available.

It has often been suggested that the existence of giants and dwarfs is due to the fact that certain absolute magnitudes are connected with stable conditions in the stars. The existence of additional frequency maxima, as indicated by the present study, can similarly be explained, since several stable states with different degrees of stability can well be imagined, the degree being represented by the relative abundance and the duration in any given state. Transitions between different states may occur, but the stars do not remain long

[1] *Mt. Wilson Contr.*, No. 319; *Astrophysical Journal*, **64**, 225, 1926.

[2] *Proceedings of the National Academy of Sciences*, **14**, 488, 1928.

in the intermediate states. The proof of the existence of new frequency maxima and minima may thus be of importance for the solution of the problem of stellar evolution.

It is to be noted, however, that in order to derive the relative duration of different states in stellar evolution the frequencies here derived must first be converted into frequencies per unit of volume. Since the present investigation refers only to stars brighter than sixth magnitude it is necessary first to find the distribution in absolute magnitude among stars of fainter apparent magnitudes.

Carnegie Institution of Washington
Mount Wilson Observatory
January 1930

Contributions from the Mount Wilson Observatory, No. 397
Reprinted from the *Astrophysical Journal*, Vol. LXXI, pp. 153–162, 1930
Printed in the U.S.A.

SPECTRAL ENERGY-CURVE OF SUN-SPOTS

By EDISON PETTIT and SETH B. NICHOLSON

ABSTRACT

Ratio of the energy in the umbra of the spot to that in the photosphere.—This was measured between λ 0.4 μ and λ 2.2 μ by a thermocouple attached to a monochromator mounted in the focal plane of the 150-foot tower-telescope. That portion to the violet of λ 0.4 μ was determined by photographic photometry with an all-speculum optical system, the image-forming mirror being of 60 feet focal length. The mean curve shows that the spot-photosphere ratio varies in a nearly linear manner from 0.21 at λ 0.3 μ to 0.80 at λ 1.7 μ, after which it is nearly constant.

Sources of error.—Depressions at λ 1.38 μ and λ 1.9 μ may possibly be reflected errors due to the deep water-vapor bands at these points. The color-curve of the objective of the tower-telescope being unknown in the red, no corrections could be made for focus. The great focal ratio of this objective (150/1) probably gave sufficient depth of focus to offset this effect partially. The same argument applies to the stigmatic focus of the concave-grating spectrograph used in the measurements to the violet of λ 0.4 μ.

Spectral energy-curve of sun-spots.—This was obtained by multiplying the solar energy-curve for the center of the disk by the spot-photosphere ratios in different wave-lengths. The resulting spectral energy-curve is much like that for the photosphere and corresponds in total energy to a black body at 4860° K.

Temperature of the sun from the solar constant.—The rate of radiation at the center of the disk is 16 per cent greater than that of integrated sunlight, which makes the rate for this point 2.25 cal cm^{-2} min^{-1} and the corresponding temperature from the fourth-power law 5955° K.

Scattered radiation.—The total scattered radiation from the sky and instrument was measured at a point 15″ off the limb of the sun and found to be 0.037 of the intensity at the limb, or, at the center of the disk, 8 per cent of the photospheric light. If the solar energy-curve is assumed to be that of a black body at 5955° K, the energy-curve of the spot fits that of a black body at 4750° K fairly well except to the violet of λ 0.7 μ, where it is in excess. This amounts to 6 per cent of the area of the curve; hence the measured scattered radiation from the sky and instrument is more than double that necessary to explain this excess.

Total energy in the umbra.—This was measured directly with the thermocouple and found to be 0.471 that of the photosphere. The value computed from the curve of the ratio of spot to photosphere is 0.477.

Distribution of energy over a spot.—A thermocouple was mounted on a moving plate connected with the registering device. This traced the distribution of energy across

the spot. In all cases the energy falls continuously from the photosphere to about half-intensity at the umbra and shows no tendency to increase there. Microphotometer runs across spots with connecting bridges show some of this effect however.

Temperature of sun-spots from water-cell measurements.—The water-cell absorption of a spot is 0.50 mag. for average position on the disk, which corresponds to spectral classification dG7 and temperature 4720° K.

An investigation of the spectral energy-curve of sun-spots between 0.4 μ and 2.2 μ was undertaken at the 150-foot tower-telescope in July, 1922, and completed in September, 1922. The apparatus consisted of a Hilger constant-deviation spectroscope arranged as a monochromator with vacuum thermocouple attached and has already been briefly described.[1] The 17-inch solar image was projected horizontally by means of a plane mirror upon a white cardboard screen over the first slit of the monochromator. A pinhole in this screen admitted light to the slit, making it possible to set an image of a sun-spot or a definite point on the photosphere upon the slit with the electric slow motions of the coelostat. For more accurate guiding during an exposure the whole monochromator was mounted on a double slide so that it could be moved in rectangular co-ordinates in the focal plane, by means of two screws, to follow the spot image while an energy-curve was being traced.

The tangent screw of the monochromator prism table was connected through rods and gearing to a photographic recording device[2] which registered a trace from the D'Arsonval galvanometer connected with the thermocouple. The 7×17-inch plate in the registering device was driven at the rate of approximately 1 inch per minute, an entire trace from λ 0.4 μ to λ 2 μ requiring about 15 minutes.

The general procedure consisted in taking a trace with the slit of the monochromator set on a point of the photosphere just north of the penumbra of the spot, a second trace on the umbra, and a third on a point just south of the penumbra, all curves being recorded on the same plate. In other cases two traces were made on the umbra of the spot and one on the photosphere. Figure 1 illustrates such a record.

The plate was then placed on a comparator and the ordinates were

[1] *Mt. Wilson Contr.*, No. 336; *Astrophysical Journal*, **66**, 43, 1927.

[2] *Journal of the Optical Society of America*, 10, 267, 1925.

measured in steps of 0.05 μ, and the ratio of the ordinates of the spot-curve to the average of the corresponding ordinates of the two curves from the photosphere or the average of the ordinates of the two spot-curves to that of the curve from the photosphere, as the case might be, was formed for each wave-length. Figure 2 is a plot of these ratios of spot umbra to photosphere for six plates on two spots thus obtained in September, 1922, under good conditions of seeing. The open circles are observations made by Abbot with the bolometer in the Snow telescope in August, 1905.[1] His method consisted in setting the spectrobolometer for a given wave-length and causing the spot to drift across the slit with the lunar gears of the coelostat. The ratios for five wave-lengths were determined from drift-curves traced in this way.

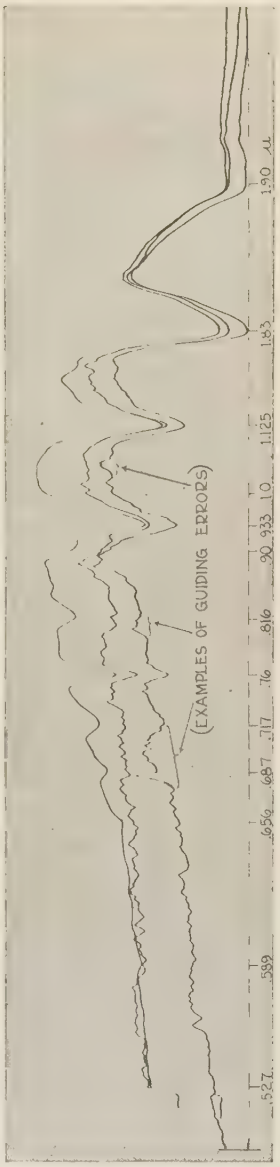

FIG. 1

That part of Figure 2 to the violet of λ 0.4 μ was determined by photographic photometry[2] with a 1-meter concave-grating spectrograph mounted Eagle fashion. A 6-inch concave speculum mirror of 60 feet focal length formed the image for this spectrograph and was fed by one reflection from a speculum-mirror coelostat. The 6-inch solar image fell upon a card in front of the slit, light being admitted to the latter through a pinhole. In some cases a quartz enlarging lens which gave an

[1] *Annals of the Astrophysical Observatory, Smithsonian Institution*, **2**, 233, 1908.

[2] *Mt. Wilson Contr.*, No. 336; *Astrophysical Journal*, **66**, 43, 1927.

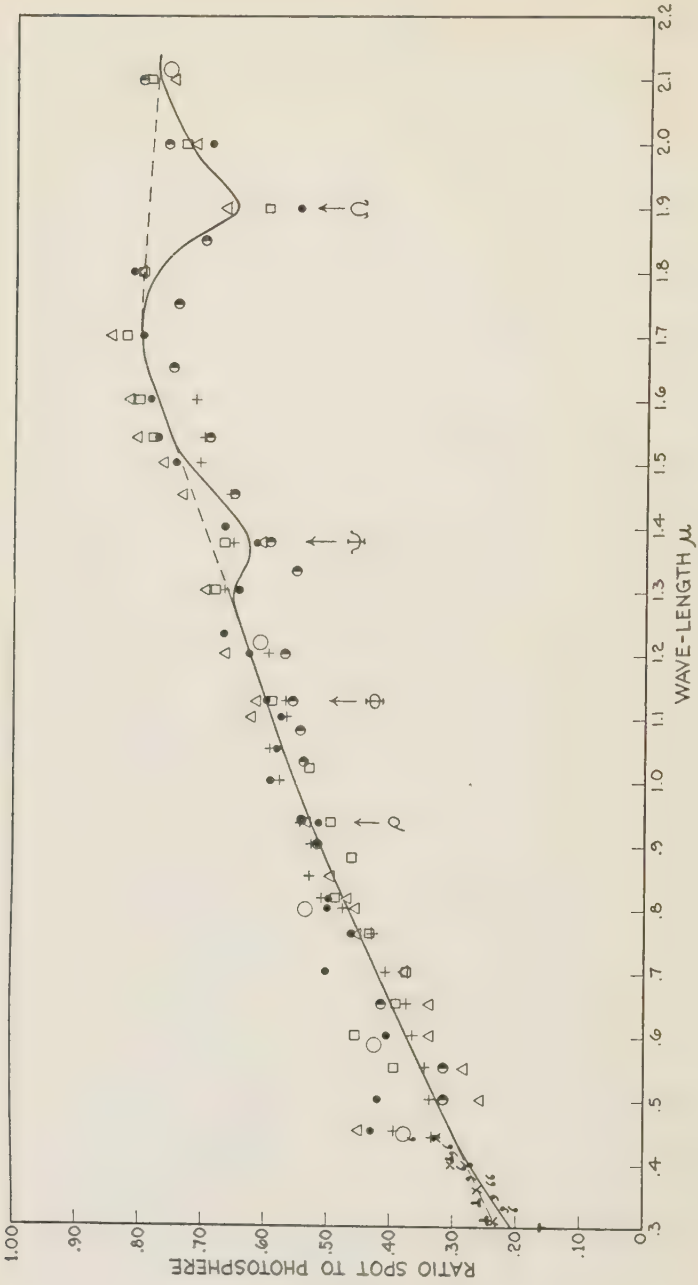
RATIO SPOT TO PHOTOSPHERE
1.00
.90
.80
.70
.60
.50
.40
.30
.20
.10
0
.3
.4
.5
.6
.7
.8
.9
1.0
1.1
1.2
1.3
1.4
1.5
1.6
1.7
1.8
1.9
2.0
2.1
2.2
WAVE-LENGTH μ
Ω
Ψ
Φ
ρ

FIG. 2

equivalent focal length of 150 feet was used. The spectrograph was mounted on a stand which permitted slow motion in rectangular co-ordinates in the focal plane for guiding on the spot during the exposure. The method of timed exposures was used with plates and development as already described.[1] When the spectrograph is used in the ultra-violet of the first order the stigmatic focus of the solar image is about 5 cm in front of the slit, but since the ratio of focal length to aperture of the image-forming mirrors is 120 to 300, only a small area about 1 cm in diameter on the grating was used; hence the great depth of focus of the spectrograph made this stigmatic effect practically ineffective. The points shown in Figure 2 to the violet of λ 0.4 μ were obtained on a spot in August, 1927.

The curve in Figure 2 is nearly linear, being slightly convex between λ 0.3 μ and λ 1.7 μ; for greater wave-lengths the ratio, spot to photosphere, appears to be nearly constant. The positions of the atmospheric water-vapor absorption bands are indicated by their symbols. Rather marked drops in the curve will be seen at Ψ and Ω, although none show for the other bands. Whether these are real or merely reflected effects of these deep bands on the measurement of the relatively small quantities is difficult to decide until additional data are available.

Since the color-curve of the objective of the tower-telescope is unknown in the infra-red, it is possible that the curve in Figure 2 to the red of λ 0.8 μ is somewhat too high owing to a mixture of partial pencils of photospheric light in this region with that from the umbra of the spot. No attempt was made to correct the focus, but the great focal-length aperture ratio, 150, of the objective in the tower-telescope probably gave a depth of focus sufficient to offset this effect somewhat. On the other hand, the observations in the infra-red agree well with those of Abbot made with a mirror telescope, and in the visual region run even somewhat less than those of Abbot. The photographic measures in the ultra-violet, which were made with a mirror telescope, show no pronounced discontinuity and check the overlapping radiometric measures between λ 0.4 μ and λ 0.45 μ fairly well. It is hoped that further work may be done with an all-mirror system.

[1] *Ibid.*

Energy-curve of sun-spots.—Curve *A* in Figure 3 is Abbot's solar energy-curve[1] for the center of the disk to which our spot measurements refer. Curve *C* is obtained by multiplying the ordinates of curve *A* by the ratio of the energy in the umbra of the spot to that in the photosphere read from Figure 2 for the corresponding wave-lengths.

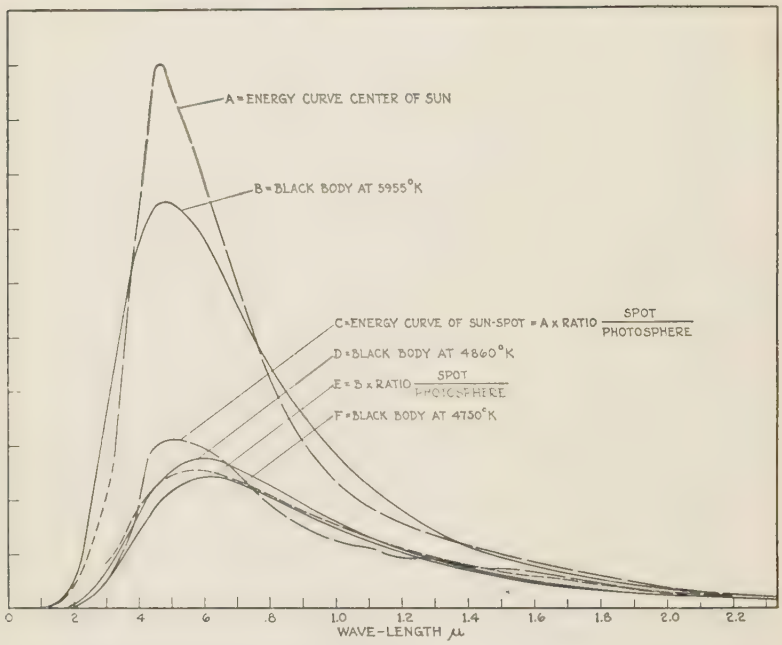

FIG. 3

That the energy-curve *C* of a sun-spot is not that of a black body is seen by the following argument. The ratio of the area of curve *C* to curve *A* should be the ratio of their total energies and is 0.445. The total energy of integrated sunlight is the solar constant, 1.94 cal cm^{-2} min^{-1}. The rate of radiation from the center of the disk where the sun-spot measurements were made is 1.16 times this quantity,[2] or 2.25 cal cm^{-2} min^{-1}, which corresponds to a black-body temperature of 5955° K. This is the temperature of the photosphere given by total radiation measurements and would appear to

[1] *The Sun* (1929), p. 107; *Annals of the Astrophysical Observatory, Smithsonian Institution*, **3**, 159, 1913.

[2] *Mt. Wilson Contr.*, No. 299; *Astrophysical Journal*, **62**, 210, 1925.

be the best value of the temperature of the sun derived from the solar constant. If the spot radiates like a black body, its temperature is therefore

$$T = 5955^\circ \text{ K} \times \sqrt[4]{0.445} = 4860^\circ \text{ K}.$$

Curve *D* in Figure 3 is a black-body energy-curve for this temperature having the same area as the sun-spot energy-curve *C*. It appears from curves *D* and *C* that, generally speaking, the sun-spot has more energy than the black-body curve for wave-lengths to the violet of λ 0.7 μ, and correspondingly less for wave-lengths to the red. A considerable part of the deviation of the sun-spot energy-curve *C* from a black-body curve such as *D* is due to the deviation of the solar energy-curve *A* from the black-body curve. To demonstrate this the black-body curve *B* for 5955° K has been drawn with the same area as the solar energy-curve *A*, and from it the energy-curve *E* has been drawn by multiplying *B* by the ratio, spot to photosphere, as was done to obtain curve *C*. It will be seen that this curve lies for the most part between the black-body curve *F* for 4750° K and *D* for 4860° K, agreeing to some extent with the former in wave-lengths greater than about 0.7 μ.

Scattered photospheric light.—A comparison of the spectra of photospheric light with those of sun-spots used to obtain the ultra-violet portion of the curve in Figure 2 shows little difference between the two in the region below the calcium lines H and K. This suggests that the spot spectrum has superposed upon it a considerable amount of photospheric light which would in turn explain the deviation of the energy-curve *E* of the spot spectrum (computed from the black-body curve *B*) in the visual and ultra-violet region from the energy-curve *F* of a black body at 4750° K. The area between these two curves to the violet of λ 0.7 μ is only 0.06 of the area of curve *E;* hence it might be thought that this represents the order of magnitude of the total scattered photospheric radiation. This scattered photospheric light may be from the sky, the instruments, and from the spot itself, where the photospheric light projected into the spot is scattered by the gases there to the observer along with the intrinsic light of the spot.

The total scattered radiation in the instrument and sky was

measured at the limb of the sun with the thermocouple behind a pinhole diaphragm as described below. The radiation from the sky and the instrument 15″ outside the limb of the sun was found to be 0.037 of that 15″ inside the limb of the sun. In order to approximate the conditions of scattering in a spot we may imagine another sun placed on the other side of the point, 15″ away, so that it would be practically surrounded by the two solar disks, whence the scattered light would have been 0.074 of the intensity 15″ inside the limb. After allowing for the increase in scattered light toward the center of the disk it appears from this rough estimate that scattering in the earth's atmosphere and the telescope will amount to fully 8 per cent or more of the photospheric radiation or 16 per cent of the total radiation received from the spot, which is approximately half that of the photosphere, as will be shown shortly. The radiation scattered by the sky and instrument is therefore more than twice as much as that necessary to explain the deviation of curve *E* from curve *F*.

Total energy in the umbra.—We may measure the whole radiation in the spot directly with the thermocouple and compare the result with that obtained from spectral distribution of energy. For this purpose the thermocouple was placed directly behind a pinhole in a card and mounted in the focal plane of the 150-foot tower-telescope. With this arrangement the ratio of the whole radiation received from a small area of the photosphere on each side of the spot was compared with the same area of the umbra. From twenty measures on six different spots in October, 1921, this ratio was found to be 0.471. The greatest value was 0.521 and the least 0.428. The solar energy-curve at the earth's surface on Mount Wilson was then multiplied by the transmission of the objective and the reflecting power of the silvered mirrors of the tower-telescope, ordinate by ordinate, and the resulting area compared with that obtained by multiplying this same curve by the ordinates of the curve in Figure 2. The ratio of the latter to the former, which should be that of the observable total energies in spot and photosphere, is 0.477, which agrees quite well with that (0.471) determined above from direct measurement. The very small pinhole, approximately 0.01 mm in diameter, which could be used in these measurements made the check the more rigorous, since the aperture used over the slit of the

monochromator was approximately 0.5 mm in diameter, which gave a usable slit about 0.5×0.1 mm.

In order to study the distribution of total energy over the spot, the thermocouple with its pinhole diaphragm as used above was mounted on a screw-driven plate which was connected with the photographic registering device by a rod and gears, as in the case of observations of the spectral energy-curve. In this manner the thermocouple with its pinhole diaphragm was made to move across the spot

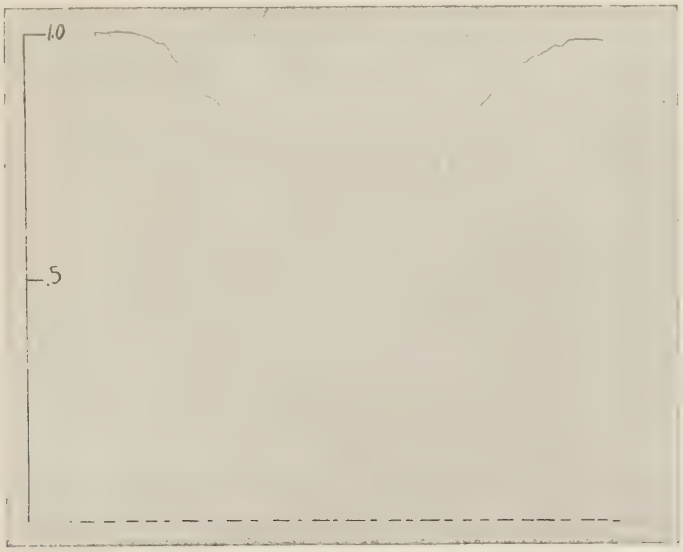

FIG. 4

while the galvanometer traced the corresponding distribution-curve in the registering device. Figure 4 is a reproduction of such a trace.

It will be noted that in Figure 4 the total energy falls continuously from the photosphere throughout the penumbra to the umbra, where it remains fairly constant at about half the photospheric intensity, as was found from the deflections described above. It will be recalled that Secchi[1] believed that the penumbra actually became brighter toward the periphery of the umbra, which his drawings strongly represent, and explained it by the convergence of the penumbral filaments toward the umbra.[2] None of our curves shows

[1] *Le soleil*, 1, 81, 1875.

[2] Russell, Dugan, and Stewart, *Astronomy*, 1, 200, 1926; Young, *The Sun* (1910), p. 116.

this effect, and considerable experience in drawing the daily polarity charts at the 150-foot tower gives visual confirmation of this result. Secchi's observation is possibly an effect of contrast. Some microphotometer runs made on a photograph of spots crossed by penumbral bridges show, however, something of the effect along the bridge. How much photographic contrast is involved is difficult to estimate.

The temperature of a sun-spot from water-cell measurements.—The water-cell absorption of the umbra of a spot near the center of the disk measured at the 150-foot tower-telescope is 0.47 mag., while the photosphere at the center of the disk gives 0.38 mag. The water-cell absorption for integrated sunlight[1] with two reflections from silver, but without the lens of the tower-telescope, is 0.41 mag. The difference of 0.03 mag. is probably due to the difference between the center of the disk and integrated sunlight. This would make the water-cell absorption for spots in an average position on the sun 0.50 mag., the corresponding spectral classification[2] dG7, and the temperature 4720° K. That the water-cell absorption of a spot should be affected in this manner by its position on the solar disk is indicated by measurements made on a spot in solar longitude 75° west of the central meridian and 8° north latitude, which gave a water-cell absorption of 0.7 mag. Such measurements are difficult, however, on account of the steep energy distribution-curve of the photosphere at the limb of the sun, and further observations will be necessary to determine accurately the water-cell absorption of a spot so near the limb.

We have finally the following comparative temperature data:

Temperature of the photosphere at center of disk	5955° K
Temperature of sun-spot umbra from spectral distribution of energy	4860°
Temperature of sun-spot umbra from spectral distribution of energy corrected for scattered light	4750°
Temperature of sun-spot umbra from water-cell absorption	4720°

From these data it appears that the temperature of the umbra of a sun-spot is probably near 4800° K, or possibly a little less.

Carnegie Institution of Washington
Mount Wilson Observatory
January 1930

[1] *Mt. Wilson Contr.*, No. 369; *Astrophysical Journal*, **68**, 289, 1928.
[2] *Ibid.*, p. 297, Table V.

Contributions from the Mount Wilson Observatory, No. 398
Reprinted from the *Astrophysical Journal*, Vol. LXXI, pp. 231–276, 1930
Printed in the U.S.A.

DISTRIBUTION OF LUMINOSITY IN ELLIPTICAL NEBULAE

By EDWIN HUBBLE

ABSTRACT

Luminosity-curves for fifteen elliptical nebulae have been derived from *transparency-curves of photographic images* measured with a *Koch registering microphotometer*. The transparencies were reduced to luminosities by means of empirical reduction-curves derived in the laboratory under conditions similar to those affecting the nebular photographs, namely, integrated sunlight, Eastman 40 plates, and X-ray developer.

The curves of luminosity *along various axes* of the different nebulae follow the general trend of the formula

$$\log I = \log I_0 - 2 \log \left(\frac{r}{a}+1\right) ,$$

where I is the luminosity, I_0 the central luminosity, r the distance from the center, and a a parameter varying from nebula to nebula, and, in any one nebula, directly with the radii along which the luminosities are measured.

With r/a as the unit of distance, the curves for all nebulae are parallel and may be shifted into coincidence to form a standard luminosity-curve referring to a standard central luminosity. With these units all *isophotal contours approximate circles*, although for very elliptical or lenticular images the fainter contours are noticeably elongated.

The luminosity formula, derived in the first instance from series of exposures generally up to fifteen minutes, has been further tested in the outer regions by luminosity-curves obtained from seven long exposures, ranging from one to two hours. Moreover, the formula has also been tested at the threshold of the plates, where $\log I$ is constant for a given exposure time, by plotting $\log (r/a+1)$, a function of the measured diameters, against $\log I_0$; and, finally, with the help of the time scale, $\log I_0 = m_1 \log t + C$, by plotting $\log (r/a+1)$ against $\log t$. The *correlations of the three independently observed quantities, diameters, central luminosities, and exposure times*, are supported by long exposures and indicate that the *formula represents the general trend* of the luminosity-curves out to the limit of the measures.

Integration of the luminosity formula leads to the expression for total luminosity:

$$I_t = I_0 a_1 a_2 \left\{ \log \left(\frac{r}{a}+1\right) - \frac{r/a}{r/a+1} \right\} ,$$

where a_1 and a_2 refer to the major and minor axes. Total luminosity thus varies with exposure time in a manner which differs from nebula to nebula. For moderate exposures, however, the formula leads to integrated magnitudes of the same order as those actually measured.

The *corresponding curve* which represents the distribution of luminosity in the nebulae themselves (the three-dimensional bodies) *has been derived* in a manner *analogous to that used in the case of globular clusters*. The mathematical expressions are complicated (probably by the introduction of an empirical formula into an integral equation), but the curve itself exhibits a suggestive similarity, over a considerable range, with that expressing the distribution of density in an isothermal gaseous sphere. The *nuclei* of the nebulae appear to be *relatively more concentrated*, and in the *outer regions* the luminosity *falls off faster than the density*, as would be expected in the case of finite rotating bodies such as the nebulae.

Extra-galactic nebulae, aside from the 2 or 3 per cent of irregular objects, fall into a progressive sequence of types composed of two sections, the elliptical nebulae and the spirals, which merge into each other.[1] The division point is rather well defined, and few transition cases are known.[2] The spiral section is composed of a main sequence of normal spirals and a secondary branch of barred spirals. There is some intermingling of characteristics, and further investigation will be required to determine the full significance of variations in structural detail.

The sequence of elliptical nebulae appears to offer a simpler problem, for the individual objects at any given stage in the sequence are curiously similar. There are, in general, no structural details whatsoever beyond the general appearance of rotational symmetry.[3] From the relatively bright semi-stellar nuclei the luminosity falls away smoothly to undefined borders. As far as the observations can be pushed the diameters increase with the exposure.

The sequence ranges from round images through successive degrees of elongation to the limiting lenticular form with a ratio of axes about 1 to 3. The preponderance of round and nearly round images indicates that we observe the projections of nebulae ranging from globular to lenticular, oriented more or less at random in space. Among the projected images only one pure type can be identified with certainty, namely, the occasional lenticular nebulae, at the very end of the sequence, which happen to be oriented with their minor axes perpendicular to the line of sight. The luminosity distribution in these images is remarkably uniform. As the ellipticities of the projected images decrease, the dispersion in luminosity distribution increases but does not become conspicuous until the round and nearly round images are reached. This suggests a confusion due to random orientation of different forms. When the effects of orientation are eliminated by statistical analysis of extensive material, the nebulae

[1] For the complete classification see *Mt. Wilson Contr.*, No. 324; *Astrophysical Journal*, 64, 321, 1926.

[2] N.G.C. 4274 and 5750 are good examples. Arms appear to be forming along the periphery in two segments separated by tapering rifts which curve inward toward the nuclei.

[3] Occasionally, small dark markings, generally arcs or crescents, are found near the nuclei (e.g., N.G.C. 383, etc.), and in one case, M 87, exceedingly faint stars appear to crowd around the periphery.

having any given degree of flattening appear to exhibit the uniformity in luminosity distribution which is found among the lenticular images. So insignificant are the deviations from the standard forms that, were it not for the confusion introduced by the orientation, either the degree of flattening (the ratio of axes) or the luminosity gradient could be used indiscriminately to determine positions in the sequence.

The ideal classification should indicate the position of individual objects in the sequence of actual forms, independent of orientation. Theoretically this might be accomplished by a combination of the only two criteria available, the ellipticity of the projected images and the luminosity distribution. In practice, however, the application of the latter criterion to individual images is unsatisfactory. A round image may represent a nebula at any stage in the sequence, provided the minor axis is oriented in the line of sight, and the proper assignment by means of the luminosity distribution is still highly speculative. For this reason the images have been provisionally classified according to their ellipticities alone—criteria which are readily and rather accurately estimated from simple inspection of photographic plates and which furnish numerical symbols, on a decimal scale, so desirable in all classifications. This procedure presents the data ready for statistical discussion. Later, when the significance of the luminosity distribution is more fully established, symbols describing the luminosity gradients may be added as postscripts in order to complete the classification.

These considerations have led to the present investigations, which form a preliminary attempt to determine the actual luminosity distribution in the images of a selected list of elliptical nebulae. The results emphasize the homogeneity of elliptical nebulae as a group and suggest the dynamical pattern on which they are constructed.

The pioneer investigations along this line are due to J. H. Reynolds, who, in 1913,[1] found that the luminosity along the major axis of M 31, out to 7′ from the nucleus, could be represented by the formula

$$\text{Luminosity} = \frac{\text{Constant}}{(x+1)^2},$$

[1] *Monthly Notices of the Royal Astronomical Society*, 74, 132, 1913.

where x, the distance from the nucleus, was expressed in a unit equal to 34".5. The measures were restricted to the unresolved nuclear region and did not extend to the well-defined spiral arms. The result bears on the present investigations in view of the similarity between the nuclear regions of the earlier-type spirals and the later stages of the sequence of elliptical nebulae. Luminosity-curves derived at Mount Wilson for both classes of nebulae are expressed by the same type of formula as that found by Reynolds, although for M 31 the numerical values differ considerably from his.

In a second paper[1] Reynolds published curves for five other spirals representing wide variations in structure and resolution. With the scale employed the nuclear regions were rather small, however, and the results, which varied considerably from those for M 31, do not bear so directly on the problem of the elliptical nebulae.

METHOD OF INVESTIGATION

The procedure in the present investigation was as follows: For each nebula a series of exposures, usually from 15 minutes to 5 seconds, was made on a single Seed 30 or Eastman 40 plate at the Newtonian focus of the 100-inch reflector. Transparency-curves were then derived with the aid of a Koch registering microphotometer. For sensibly round images runs were made along one diameter only, but for elongated images, along both major and minor axes. Curves for the various images in a given series were then combined into single curves representing transparencies against distances from the nuclei. Finally, these curves were transformed into others representing luminosities as functions of nuclear distances.

The sensitive element in the microphotometer is a thermocouple constructed by Pettit.[2] Galvanometer deflections, strictly proportional to transparencies, were recorded as continuous curves on photographic plates geared to move at twenty times the speed with which the images moved across the aperture admitting the light-beam into the thermocouple. The aperture was square and of the order of 0.1 mm, or about 1".6, on a side. The range in galvanometer deflection, i.e., the deflection for the free film, was maintained at

[1] *Ibid.*, **80**, 746, 1920.

[2] *Journal of the Optical Society of America*, **7**, 137, 1923.

PLATE VI

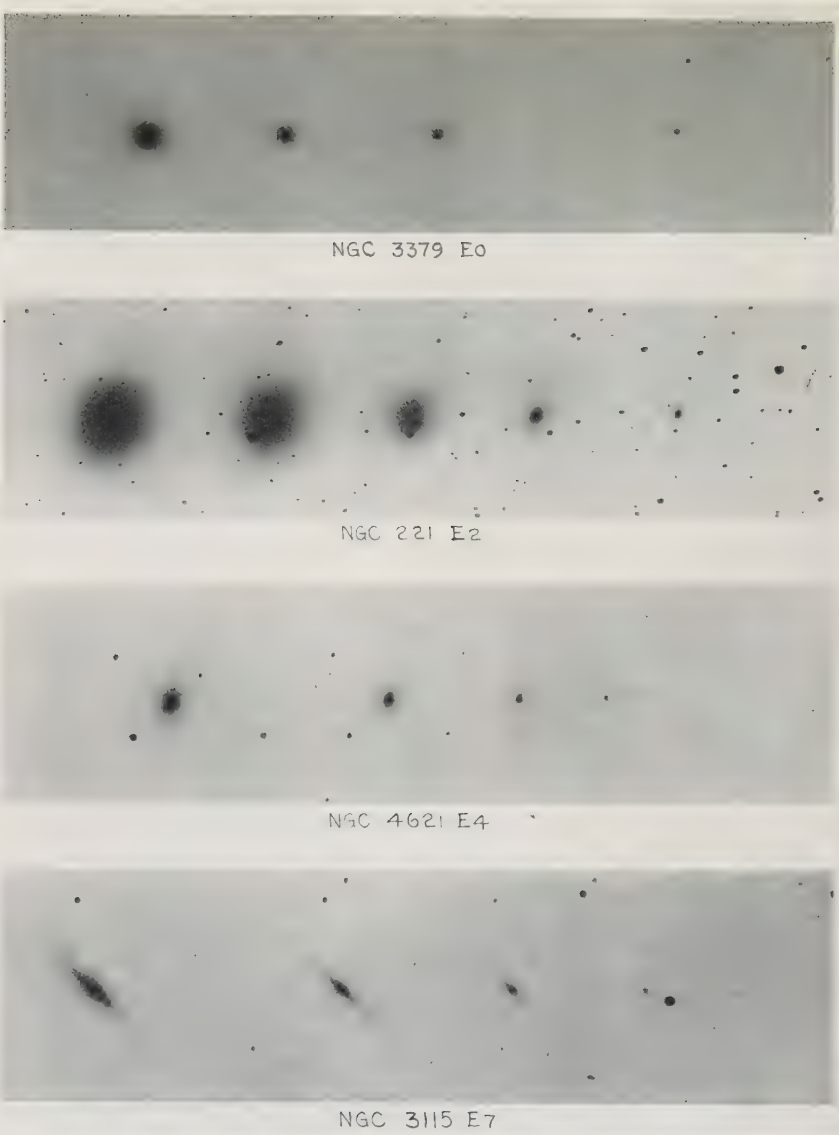

SUCCESSIVE EXPOSURES OF ELLIPTICAL NEBULAE PHOTOGRAPHED WITH THE 100-INCH REFLECTOR

about 4 inches. The linear scale of the recorded curves was, of course, twenty times the scale of the measured plates, or 1 mm = 0″.8.

MEASURES FOR N.G.C. 3379

The measures and reductions of N.G.C. 3379, an Eo nebula, furnish a typical example of the procedure. The series of images representing exposures of 15, 5, and 2 minutes, and 45 and 15 seconds, is illustrated in Plate VI. Figure 1*a* shows the transparency-curves along diameters parallel with the equator, as photographically re-

TABLE I

CORRECTIONS TO REDUCE *A* TO A LINEAR FUNCTION OF LOG *I*

TOE OF CURVE				SHOULDER OF CURVE	
A	Corr.	A	Corr.	A	Corr.
0.300.....	0.000	0.150	−0.077	0.760.....	0.000
.290.....	−0.002	.140	.087	.770.....	+0.001
.280.....	.004	.130	.098	.780.....	.003
.270.....	.007	.120	.111	.790.....	.007
.260.....	.010	.110	.127	.800.....	.011
.250.....	.013	.100	.146	.810.....	.016
.240.....	.017	.090	.168	.820.....	.021
.230.....	.021	.080	.193	.830.....	.026
.220.....	.026	.070	.222	.840.....	.032
.210.....	.031	.060	.254	.850.....	.039
.200.....	.037	.050	.290	.860.....	.048
.190.....	.043	.040	.331	.870.....	.057
.180.....	.050	.030	.382	.880.....	.067
.170.....	.058	0.020	−0.445	.890.....	.078
0.160.....	−0.067			0.900.....	+0.090

corded by the Koch microphotometer. These were measured by laying the plate, film down, on accurately ruled co-ordinate paper, the intervals on which, 0.1 inch, furnished a convenient unit. In the horizontal direction this unit represented 2″.03 on the original negatives of the nebulae, while in the vertical direction the scale was arbitrary. Eventually, however, the vertical readings were transformed into decimals of the galvanometer deflection for the free film, in this case 36.2 units or 3.62 inches. The transparencies thus ranged from zero for complete blackening to 1.0 for the free film. Measures at the same distance on either side of the nuclei were combined, and in the outer regions of the images where the grain of the plate introduced irregularities some smoothing was necessary.

The measures are shown in Table II. In order to make larger readings correspond with greater luminosities in the nebula, the transparency-curves were inverted for measurement, and hence the tabulated values represent, not transparencies, but absorptions. By current definition, $A = 1 - T$. The problem of combining the absorption-curves for the various images of the series into a single curve representing the distribution of luminosity in the image with the longest exposure was solved in an empirical manner.

TABLE II

MEASURES OF N.G.C. 3379
(Values of 36.2—Galvanometer Deflection)*

r†	Exposure Time				
	15m	5m	2m	45s	15s
0	36.2	34.05	31.25	23.55	10.15
0.5	.....	33.75	30.7	21.5	8.7
1	35.8	33.3	28.4	17.85	5.9
1.5	.....	32.35	24.8	14.1	3.7
2	35.4	30.7	21.3	10.75	2.35
3	34.7	26.1	14.95	6.3	1.6
4	32.65	21.2	9.85	3.3	1.0
5	29 8	16.45	6.5	2.4	0.65
6	26.2	12.8	4.45	1.6	.4
7	22.75	9.4	3.15	1.1	.25
8	19.15	6.8	2.4	0.7	.1
9	16.25	5.3	1.6	.5	0.0
10	14.0	4.45	1.1	.3	
11	11.4	3.75	0.8	.2	
12	9.9	3.15	.6	.1	
13	8.9	2.8	.4	0.0	
14	7.45	2.4	.3		
15	6.8	2.15	.2		
16	5.9	1.85	.1		
17	5.45	1.65	0.0		
18	4.85	1.45			
19	4.25	1.25			
20	3.7	1.15			
22	2.8	0.8			
24	2.05	.6			
26	1.5	.3			
28	1.0	.1			
30	0.65	0.0			
32	.4				
34	.2				
36	.1				
38	0.0				

* Galvanometer deflection for free film = 3.62 in.
† Unit of r = 0.1 in. = 2'.03.

CHARACTERISTIC ABSORPTION-CURVES

Characteristic absorption-curves for the type of plate employed were obtained in the laboratory. The time scales, $A = F(\log t)$, where the intensity is constant, and the intensity scales, $A = f(\log I)$, where t is constant, are of the general form shown in Figure 1. The linear portions of the time scales are parallel over a considerable range in I, and those of the intensity scale over a considerable range in t.

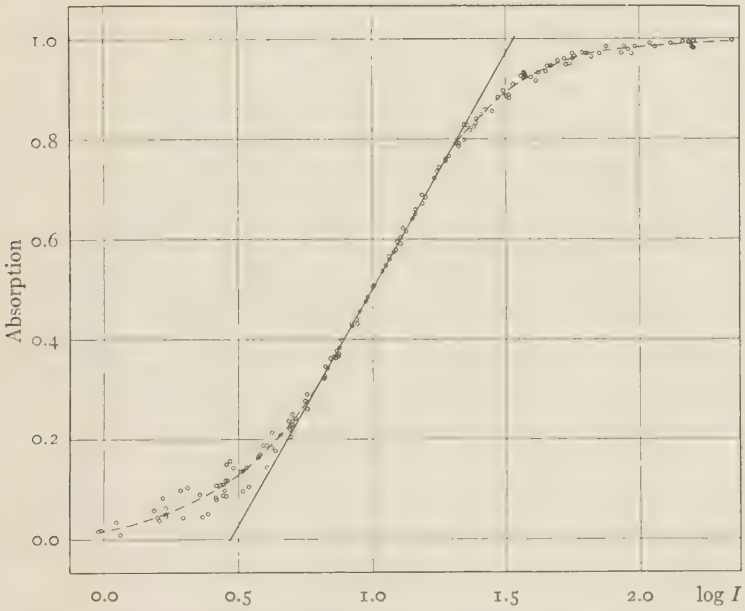

FIG. 1.—Characteristic absorption-curve for Eastman 40 plates exposed to sunlight

Especial attention was paid to the intensity scale since it affords the most direct method of converting a measured A into the corresponding luminosity. The curve in Figure 1 is a composite of twenty individual curves from Eastman 40 plates, exposed to sunlight through a varying-aperture densitometer and fully developed with a hydroquinone (X-ray) developer. Exposures ranged from 8 seconds to 30 minutes, and the transparencies of the films were varied by pre-exposures to simulate the sky fog on the nebular plates. The individual curves are all sensibly parallel, and were combined to form the composite curve by shifting along the axis of log I.

The composite or standard intensity scale is approximately linear from $A = 0.28$ to $A = 0.78$, which covers 50 per cent of the range in galvanometer deflections. Corrections derived from the curve itself readily extend the usable linear relation over a range from $A = 0.10$ to $A = 0.90$. The table of corrections may be further extended, with diminishing accuracy, to the threshold of the plates; but in this region the measures themselves exhibit a considerable scatter, and consistency may be expected only in the general order of quantitative results. On the shoulder of the curve difficulties of another nature were encountered (Eberhard effect, etc.). These were not

FIG. 1*a*.—Transparency-curves for images of N.G.C. 3379

fully investigated, but were avoided by using the shorter exposures for the bright nuclear regions of the nebulae.

The linear portion of the intensity scale is represented by the formula

$$\log I = 1.058A + \text{Constant}. \qquad (1)$$

The corrections used to extend this relation to the beginning of the shoulder and to the toe of the curve are given in Table I. These were derived from the composite curve, and were checked by comparing measured values of A at corresponding distances from the nuclei in the various images of a given nebula. The corrections are not of any high accuracy, but it is believed that they indicate the general order of the deviations down to about $A = 0.02$.

The use of absorption-curves in the present investigations, rather than the conventional density-curves, requires explanation. The microphotometer measures transparencies in terms of galvanometer

deflections, hence the most convenient form of reduction-curve will be that which approximates a straight line over the largest and most reliable range in transparencies. These conditions appear to be met by a relation between intensities of the source and the deflections themselves, used either as transparencies, or, as in the procedure described above, as absorptions. The relation

$$\log I = f(A) \text{ or } f(T) ,$$

as shown in Figure 1, is approximately linear over the middle half of the range in deflections, $A = 0.28$ to $A = 0.78$, where the measures are most reliable. On the toe and the shoulder, which are rather symmetrical, the measures are less precise—on the shoulder, because the deflections themselves are relatively small; on the toe, because the grain of the plate becomes troublesome.

Near the threshold of the plates, corresponding to the toe of the absorption-curve, a linear reduction-curve may be obtained by plotting intensities directly against the deflections. In the form

$$I = f(A) \text{ or } f(T)$$

the data in Figure 1 give a sensibly linear relation from $A = 0.08$ to $A = 0.40$. This method straightens the toe of the absorption-curve at the expense of the shoulder.

The shoulder may be straightened at the expense of the toe by plotting the data in the form

$$\log I = f(\log A) \text{ or } f(\log T) .$$

Since density is defined as $-\log T$, this leads to the usual Hurter and Driffield curve, $\log I = f(D)$. In this form the data in Figure 1 give an approximately linear relation from $A = 0.68$ to $A = 0.98$. The linear range is only 60 per cent of that for the absorption-curve and, moreover, the accidental errors become increasingly troublesome in the upper regions where the galvanometer deflections are very small.

These three forms for the reduction-curve are adapted to different conditions, namely, moderate, low, and high densities, and hence offer a choice to fit particular requirements. For the present investigations, the first of these, $\log I = f(A)$, appears to be the best choice, not only for the reasons stated, but also because of definite incon-

veniences in the other forms. That for low densities, $I=f(A)$, introduces the question of units of luminosity, which is avoided by the use of log I. The density-curves, log $I=f(-\log T)$, appear to be more sensitive in the linear range to the Eberhard or some analogous effect. The latter possibility was tested by comparisons of the reduction-curve derived from a varying-aperture densitometer (Fig. 1) with those from photographic wedges with steep gradients. In the one case we are dealing with isolated patches within any one of which the photographic density is about constant; in the other, the density varies continuously across the negative. It is by no means certain that the development conditions for these two cases may be regarded as equivalent. The tests indicated that the absorption-curves, log $I=f(A)$, were similar over their linear ranges within the errors of observation, but that over the shoulders (the linear region of the density-curves) the curves from the wedges fell slightly but systematically below that from the densitometer. This discrepancy was not investigated further since the necessary reduction in the present study could be made without using the shoulders of the absorption-curves.

As a final test of the efficiency of the absorption-curves as a method of reduction, the wedges were replaced by positive copies from an original negative showing a series of images of a nebula. Transparency-curves of the positives were derived with the microphotometer. Second negatives were then made under the standard conditions, and measures of these negatives were compared with the transparencies of the positives.

Reduction-curves derived from these data agreed with those derived from the wedges, i.e., the absorption-curves agreed with those from the densitometer over the linear range, but over the shoulder they fell systematically below the densitometer-curves. Conversely, by using only the linear region of the reduction-curves previously derived, the transparency distribution in the positives could be reconstructed from the measures of the second negatives with a fair degree of accuracy—say 2 per cent of the central transparency. This last test encourages the belief that the present investigations lead to a fairly reliable representation of luminosity distribution in the images of elliptical nebulae.

REDUCTION OF MEASURES FOR N.G.C. 3379

We may now return to the measures of N.G.C. 3379. The corrections in Table I reduced the values of A for the curves of the various nebular images to quantities proportional to log I over a considerable range in the measured A. The corrected curves were

TABLE III

REDUCTION OF MEASURES OF N.G.C. 3379

r	15m		5m		2m		45s		15s	Combined	
	A	ΔA	A	ΔA	A	ΔA	A	ΔA	A	A	log I
0	.....	.....	.....	.....	0.914	.....	+0.651	0.375	+0.276	+1.634	+1.729
0.5	.....	.....	.....	.....	.886	0.292	.594	.371	.223	1.588	1.680
1	.....	.....	.....	.....	.788	.295	.493	.393	+ .100	1.480	1.566
1.5	.....	.....	.....	.....	.685	.296	.389	0.429	−0.040	1.375	1.451
2	.....	.....	+0.886	0.298	.588	.291	.297	.....	.....	1.274	1.348
3	.....	.....	.721	.308	.413	0.293	+ .120	.....	.....	1.102	1.166
4	.....	.....	.586	.322	.264	.....	−0.057	.....	.....	0.958	1.014
5	+0.846	+0.392	.454	.323	.131	.....	.....	.....	.....	.833	0.881
6	.724	.370	.354	0.335	0.019	.....	.....	.....	.....	.721	.763
7	.628	.378	.250	.....	.....	.....	.....	.....	.....	.627	.663
8	.529	.385	.144	.....	.....	.....	.....	.....	.....	.524	.554
9	.449	.383	.066	.....	.....	.....	.....	.....	.....	.445	.471
10	.387	.370	+ .017	.....	.....	.....	.....	.....	.....	.390	.413
11	.315	0.349	−0.034	.....	.....	.....	.....	.....	.....	.328	.347
12	.267	.....	.....	.....	.....	.....	.....	.....	.....	.267	.282
13	.227	.....	.....	.....	.....	.....	.....	.....	.....	.227	.240
14	.172	.....	.....	.....	.....	.....	.....	.....	.....	.172	.182
15	.144	.....	.....	.....	.....	.....	.....	.....	.....	.144	.152
16	.100	.....	.....	.....	.....	.....	.....	.....	.....	.100	.106
17	.076	.....	.....	.....	.....	.....	.....	.....	.....	.076	.080
18	.042	.....	.....	.....	.....	.....	.....	.....	.....	.042	.044
19	+ .001	.....	.....	.....	.....	.....	.....	.....	.....	+ .001	+ .001
20	− .040	.....	.....	.....	.....	.....	.....	.....	.....	− .040	− .042
22	− .127	.....	.....	.....	.....	.....	.....	.....	.....	− .127	− .134
24	− .213	.....	.....	.....	.....	.....	.....	.....	.....	− .213	− .225
26	− .286	.....	.....	.....	.....	.....	.....	.....	.....	− .286	− .303
28	− .366	.....	.....	.....	.....	.....	.....	.....	.....	− .366	− .387
30	−0.447	.....	.....	.....	.....	.....	.....	.....	.....	−0.447	−0.473

	ΔA		ΔA
15m − 5m	0.375	15m − 5m	0.375
5 − 2	.317	15 − 2	.692
2 −45s	.293	15 −45s	.985
45s −15	0.398	15 −15	1.383

approximately parallel, as was to be expected, since time scales are parallel over a wide range in log I, and were brought into coincidence by displacement along the axis of A by amounts representing the differences in exposure time. The displacements were determined from the overlap of the curves themselves (in practice between corrected $A = 0.0$ to $A = 0.80$), and the entire series was combined into a single absorption-curve representing the image of longest exposure. The reduction for N.G.C. 3379 is shown in Table III.

The relation between displacements, ΔA, and relative exposures, $\log t_0/t$, where t_0 is the longest exposure, furnish a check against the time scale. For N.G.C. 3379 the data in Table III indicate the relation $\Delta A = 0.78 \log t_0/t$. Remeasurement of this plate gave the coefficient 0.785. The average for all the plates of the observed nebulae is about 0.80, which agrees with the slope of the time scales obtained in the laboratory.

LUMINOSITY-CURVE FOR N.G.C. 3379

The final step in the reduction of the measures of N.G.C. 3379 was the conversion of the combined values of A into $\log I$ by means of formula (1). This gave the relation between luminosity, I, and distance from the nucleus, r, which is shown graphically in Figure 2, in three different forms. The curve to the left, 2*a*, represents $\log I = f(r)$. Curve 2*b* corresponds to $\log I = f(\log r)$. A simple inspection indicates that the second curve may be transformed into an approximately linear relation by adding a constant to the successive values of r. The necessary constant was found by trial to be 2.4, which is equivalent to 4".9, and the slope of the straight line thus obtained was so close to 2.0 that the exact integer was accepted and the line so drawn with a straight edge through the points in 2*c*. The relation

$$\log I = 2.62 - 2 \log (r + 2.4)$$

fits the data from near the nucleus to distances at which the luminosities are far down on the toe of the intensity scale, with an accuracy within the probable errors of the observations.

A second set of microphotometer curves from the same negative gave

$$\log I = 2.64 - 2 \log (r + 2.3) .$$

The means of the two sets of measures gave the adopted equation

$$\log I = 2.62 - 2 \log (r + 2.3) .$$

The values of $\log I$ from the two sets of measures show a systematic difference of 0.016 between $\log I = 1.7$ and -0.1, and an average residual of ± 0.018.

INDIVIDUAL LUMINOSITY-CURVES FOR FIFTEEN ELLIPTICAL NEBULAE

The results for N.G.C. 3379 are typical of those found for elliptical nebulae in general, fifteen of which (Table IV) were investigated

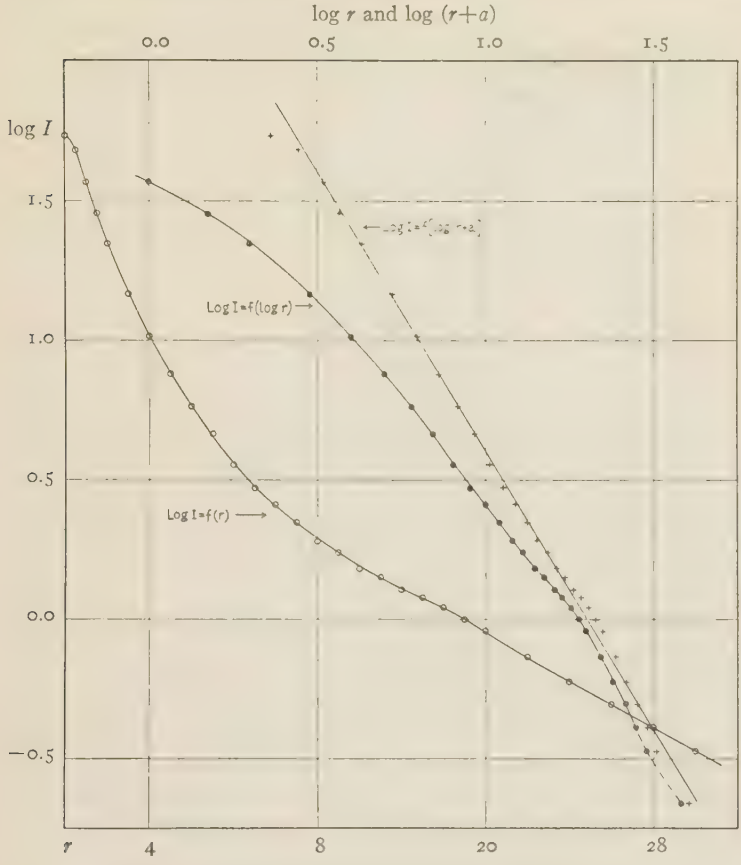

FIG. 2.—Luminosity-curve for the image of N.G.C. 3379

along various diameters, and for the unresolved nuclear regions of at least some of the earlier-type spirals.

The curves were constructed as described for N.G.C. 3379. The four nebulae with sensibly round images, N.G.C. 3379, 4283, 4486, and 4552, were measured along a single diameter, usually that parallel to the equator. For N.G.C. 584, also measured but once, the particular diameter is indicated.

In each object the distribution of luminosity may be represented by a formula of the type

$$\log I = K - 2 \log (r + a) , \tag{2}$$

where a varies from nebula to nebula and, in any elongated nebula, with the diameter along which the luminosities were measured.

Let I_0 be the central luminosity; then $K = \log I_0 a^2$ and formula (2) may be written

$$\log I = \log I_0 - 2 \log \left(\frac{r}{a} + 1 \right) , \tag{3}$$

or

$$I = \frac{I_0}{\left(\frac{r}{a} + 1 \right)^2} . \tag{4}$$

Formula (3) permits a direct comparison of luminosity-curves along various diameters of different nebulae. If $\log I$ is expressed as a function of r/a instead of simply a, the curves are all parallel and are displaced along the axis of $\log I$ by amounts corresponding to differences in $\log I_0$. The curves can then be shifted into coincidence, giving a mean curve for all the nebulae observed, reduced to a standard $\log I_0$.

The constants of the empirical formulae representing the various luminosity-curves, namely, K, a, and $\log I_0$, are listed in Table IV. The third column gives the exposure time of the strongest image in the series measured. The fifth column indicates the quality of the results as judged from the appearance of the plates and the irregularities and discrepancies in the curves for different images in the same series. The other data are self-explanatory.

The actual measures for each nebula are not tabulated, but Table V gives the values of $\log I$ for successive values of r/a, reduced to $\log I_0 = 2.0$ as a standard. These were obtained by adding to each value of $\log I$ measured on any curve the quantity $2.0 - \log I_0$, where I_0 has the value listed in Table IV. These corrections merely shift the curves parallel to themselves along the axis of $\log I$. By reversing the operation the original curves may be derived from Table V, and with the values of a given in Table IV, the measures themselves may be read from the curves for successive values of r.

ACCURACY OF THE MEASURES

Luminosities on the toe of the intensity scale below log $I = 0.0$ become increasingly uncertain, but are included in the hope that mean values for several curves may have some significance. Reference to the standard intensity scale in Figure 1 emphasizes the large scatter among the measures in this region and the consequent

TABLE IV

PARAMETERS FOR LUMINOSITY-CURVES OF INDIVIDUAL NEBULAE

N.G.C.	Type	Exp.	Diam.	Q	a	K	log I_0
221*.....	E2	22^m	Min.	G	2.5	3.14	2.344
			Maj.	G	3.1	3.342	2.359
410.....	E2	60	Min.	G	2.0	2.30	1.698
			Maj.	G	2.6	2.54	1.710
584.....	E4	20	30°†	P	1.7	2.205	1.744
3115*.....	E7	15	Min.	G	1.4	2.21	1.918
			Maj.	G	5.0	3.15	1.752
3379*.....	E0	15	.....	G	2.3	2.62	1.897
4278*.....	E1	15	Min.	G	1.2	2.04	1.880
			Maj.	F	1.8	2.20	1.689
4283.....	E0	15	.....	G	1.0	1.60	1.600
4374.....	E1	15	Min.	F	2.2	2.33	1.645
			Maj.	P	3 0	2.55	1.596
4382.....	E4	15	Min.	P	2.0	2.35	1.748
			Maj.	P	3.6	2.72	1.607
4406*.....	E2	15	Min.	F	2.4	2.40	1.640
			Maj.	F	3.2	2.60	1.590
4472*.....	E1	15	Min.	G	3.3	2.74	1.703
			Maj.	G	4.5	2.90	1.594
4486.....	E0	15	.....	F	4.6	2.66	1.334
4552.....	E0	15	.....	G	1.9	2.40	1.842
4621.....	E5	15	Min.	F	1.5	2.25	1.873
			Maj.	F	2.8	2.67	1.776
4649*.....	E2	15	Min.	G	2.6	2.57	1.740
			Maj.	G	3.6	2.75	1.638

* Mean of two or more plates.

† Inclination of measured diameter to major axis.

uncertainty in the exact delineation of the curve as it approaches the threshold of the plate almost asymptotically to the axis of log I. Very slight errors in the delineation are greatly magnified in the table of corrections which convert the measured values of A into a linear function of log I. Relatively large errors, both systematic and accidental, therefore probably occur among the low values of log I in Table V.

Very high values of log I are subject to uncertainties arising from

the combination of several curves from successively weaker images into a single mean curve. Values of a are sensitive to errors in the upper region of the composite curves. The order of the errors involved may be estimated from remeasures made on eight of the original plates. Systematic differences in log I for log $I > -0.100$ ranged from 0.016 to 0.035, with a mean of 0.025, or 2.5 per cent of the galvanometer deflection for the free film. Average residuals ranged from 0.007 to 0.018.

Measures from duplicate negatives of the same object were made for seven nebulae. Here the systematic differences in log I were much larger, owing to differences in the transparency of the sky, in the silver coats on the mirrors of the telescope, and possibly in the sensitivity of the plates. The maximum systematic difference in log I was 0.160 for two 15-minute exposures of N.G.C. 4472. Average residuals above log $I = -0.100$, however, were only 0.010 and 0.020 for the minor and major diameters, respectively. With one exception the average residuals for all the nebulae lie between 0.012 and 0.025.

TABLE V

LUMINOSITY-CURVES REDUCED TO STANDARD LOG I_0

N.G.C.	r/a									
	0.0	0.25	0.5	0.75	1.0	1.5$_m$	2.0	2.5	3.0	3.5
221 min	1.969	1.846	1.631	1.521	1.381	1.176	1.021	0.896	0.791	0.711
maj	1.911	1.841	1.646	1.521	1.416	1.221	1.066	.941	.831	.731
410 min	1.895	1.812	1.672	1.522	1.382	1.182	1.042	.912	.802	.692
maj	1.909	1.835	1.680	1.510	1.390	1.170	1.030	.900	.800	.700
584	1.794	1.736	1.636	1.496	1.401	1.216	1.066	.946	.846	.736
3115 min	1.700	1.672	1.612	1.532	1.432	1.222	1.072	.937	.827	.707
maj	1.977	1.823	1.628	1.478	1.373	1.208	1.048	.918	.798	.703
3379	1.845	1.793	1.658	1.543	1.408	1.213	1.053	.893	.778	.663
4278 min	1.720	1.690	1.620	1.502	1.382	1.197	1.047	.917	.807	.692
maj	1.833	1.792	1.662	1.512	1.387	1.192	1.042	.912	.792	.682
4283	1.574	1.560	1.525	1.460	1.380	1.215	1.070	.950	.825	.720
4374 min	1.836	1.785	1.655	1.505	1.400	1.185	1.025	.900	.795	.710
maj	1.799	1.764	1.644	1.519	1.394	1.184	1.034	.904	.789	.694
4382 min	1.862	1.802	1.692	1.542	1.412	1.202	1.022	.892	.797	.712
maj	1.963	1.868	1.663	1.503	1.378	1.153	0.973	.838	.743	.663
4406 min	1.954	1.860	1.660	1.490	1.360	1.150	0.990	.880	.770	.680
maj	1.963	1.835	1.635	1.470	1.350	1.160	1.010	.890	.785	.695
4472 min	1.847	1.777	1.647	1.522	1.377	1.177	1.012	.882	.787	.692
maj	1.940	1.856	1.676	1.506	1.391	1.181	1.036	.911	.806	.746
4486	1.851	1.771	1.651	1.541	1.441	1.236	1.076	.936	.816	.701
4552	1.761	1.738	1.648	1.508	1.408	1.228	1.063	.903	.783	.683
4621 min	1.834	1.797	1.657	1.517	1.392	1.192	1.037	.897	.787	.692
maj	1.908	1.844	1.684	1.529	1.414	1.194	0.999	.869	.764	.674
4649 min	1.781	1.760	1.650	1.550	1.445	1.240	1.070	.930	.810	.700
maj	1.820	1.772	1.667	1.532	1.412	1.202	1.042	0.912	0.782	0.682

TABLE V—*Continued*

N.G.C.	r/a									
	4.0	4.5	5	6	7	8	9	10	12	14
221 min	0.626	0.546	0.481	0.351	0.226	+0.111	+0.006	−0.094	−0.264	−0.474
maj	.636	.556	.476	.326	.191	.091	− .009	− .099	− .234	− .354*
410 min	.597	.517	.437	.287	.162	.052	− .078	− .170	.....	.....
maj	.610	.545	.480	.350	.230	+ .110	+ .030	− .130	.....	.....
584	.636	.546	.456	.281	.116	− .004	− .084	− .144	− .244	.....
3115 min	.622	.542	.457	.312	.192	+ .097	+ .012	− .078	− .218	− .338†
maj	.613	.528	.453	.328	.178	.013	− .122	− .277	.....	.....
3379	.578	.503	.428	.308	.208	.123	+ .023	− .067	− .243	− .412
4278 min	.597	.502	.412	.267	.152	.047	− .043	− .108	− .168	− .318
maj	.572	.482	.397	.232	.102	.022	− .058	− .108	− .208	− .288
4283	.610	.505	.420	.225	.165	.085	+ .015	− .050	− .120	− .150
4374 min	.625	.550	.480	.355	.245	.095	− .035	− .135	.....	.....
maj	.624	.564	.509	.394	.279	.184	+ .104	+ .004	.....	.....
4382 min	.647	.582	.522	.412	.307	.202	+ .112	+ .027	− .153	− .323
maj	.593	.528	.478	.383	.308	.223	+ .143	+ .043	− .107	.....
4406 min	.595	.525	.465	.340	.235	.135	+ .050	− .030	− .205	.....
maj	.615	.540	.480	.365	.265	.120	+ .060	− .060	.....	.....
4472 min	.602	.522	.452	.342	.247	.157	+ .067	− .013	− .203	.....
maj	.636	.566	.491	.371	.276	+ .194	+ .111	+ .046	− .139	.....
4486	.591	.486	.376	.195	.076	− .014	.....	.....	.....	.....
4552	.598	.523	.443	.313	.208	+ .108	+ .003	− .107	− .317	.....
4621 min	.612	.532	.467	.327	.212	.112	− .003	− .123	− .333	− .453
maj	.604	.534	.469	.344	.224	.114	− .001	− .104	− .286	− .446
4649 min	.610	.530	.450	.320	.170	.065	− 0.50	− .150	− .370	.....
maj	0.592	0.522	0.457	0.337	0.227	+0.122	+0.032	−0.063	−0.218	−0.328

* Values for $r/a = 16$, 18, and 20 are 0.464, 0.639, and 0.824, respectively.
† Values for $r/a = 16$, 18, and 20 are 0.418, 0.513, and 0.588, respectively.

The exception is N.G.C. 3115, for which the curve along the minor axis derived from the two plates gave perceptibly different slopes, amounting to 0.160 in log I at $r = 19$. The source of this discrepancy was traced to imperfections in the film, affecting two images, on one of the plates. The series of measures thus affected was discarded.

The values of a derived from the seven duplicate plates afforded ten comparisons. The differences averaged about 5 per cent and in no case exceeded 10 per cent. This was rather unexpected, for the determinations of a were made by trial and error and involved a certain amount of compromise and adjustment. In certain cases slightly modified values of a combined with coefficients of log $(r/a + 1)$, differing a little from 2.0, would fit the data as well or possibly better than the adopted values. Since the possible deviations in the coefficient are small and the values clustered closely around 2.0, the exact integer was used in each case and the value of a adjusted to fit. The justification for this rather arbitrary procedure lies in the fact that the deviations are within the range of observational errors and of

the differences between the means of the values in Table V with those computed from formula (3).

MEAN LUMINOSITY-CURVE FOR ELLIPTICAL NEBULAE IN GENERAL

The comparison of the mean luminosity-curve based on the individual curves in Table V with that defined by the standard relation

$$\log I = 2 - 2 \log (r/a + 1)$$

is tabulated in Table VI and is shown graphically in Figure 3.

TABLE VI

MEAN LUMINOSITY-CURVE FOR PROJECTED IMAGES OF ELLIPTICAL NEBULAE

r/a	log I			No.
	Cal.	Obs.	C−O	
0	+2.000	+1.853	+0.147	25
0.25	1.806	1.780	+ .026	25
0.5	1.648	1.647	+ .001	25
0.75	1.514	1.509	+ .005	25
1	1.398	1.396	+ .002	25
1.5	1.204	1.196	+ .008	25
2	1.046	1.039	+ .007	25
2.5	0.912	0.907	+ .005	25
3	.796	.797	− .001	25
3.5	.694	.702	− .008	25
4	.602	.610	− .008	25
4.5	.519	.531	− .012	25
5	.444	.458	− .014	25
6	.310	.322	− .012	25
7	.194	.208	− .014	25
8	+ .092	.104	− .012	25
9	.000	+ .012	− .012	24
10	− .083	− .083	.000	24
12	− .228	− .238	+ .010	18
14	− .352	− .353	+ .001	11
16	− .461	− .441	− .020	2
18	− .558	− .576	+ 018	2
20	−0.644	−0.706	+0.062	2

The large C − O for $r/a = 0.0$ is at least partially explained by the method of measurement. The observed log I_0 represents the average luminosity over the area covered by the slit in the microphotometer, while the calculated value refers to a central point from which the luminosity is assumed to fall rapidly in all directions. The observed

values are thus necessarily smaller than the calculated. Since the area of the slit remains constant, the effect increases with the luminosity gradient, or as a decreases. This is shown graphically in Figure 4 as a relation between a and the observed log I_0 given in Table V. The point $r/a = 0.25$ is similarly affected, although to a less de-

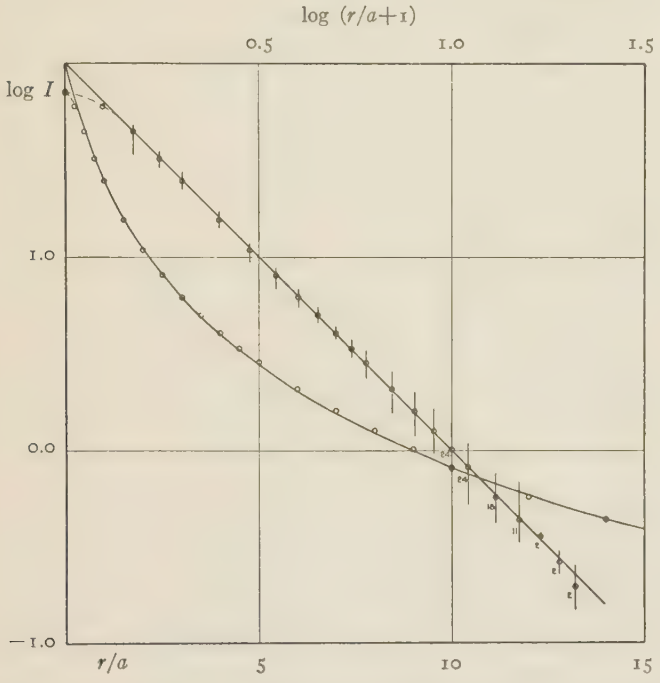

FIG. 3.—Combined luminosity-curve for the images of elliptical nebulae. The vertical lines represent the scatter among the individual curves. The figures indicate the number of individual curves included in the mean. Above log $I = 0.0$ the number for each point is 25.

gree. The influence is especially noticeable where a is small. For N.G.C. 3115 min. ($a = 1.4$), 4278 min. ($a = 1.2$), and 4283 ($a = 1.0$), the values of C−O for $r/a = +0.25$ are +0.134, +0.116, and +0.246, respectively. The rejection of these three residuals reduces the mean C−O for this point from 0.026 to 0.007. The remainder of the data to $r/a = 14$, beyond which the number of curves is too small for precision, shows an average C−O of about 0.0075. The dispersion

in log I is of the order of 0.100 out to $r/a = 5.0$, beyond which the scatter increases, owing probably to the uncertainties in the low values of log I for the fainter nebulae.

The relatively small dispersion in the composite curve suggests that the empirical formula (3) holds out to the limit of measurement. The data for the outer regions are weak, however, even for the brighter nebulae, and must be accepted with caution. Further information on the outer regions has been sought in supplementary measures of such long exposures as were available, and in the correla-

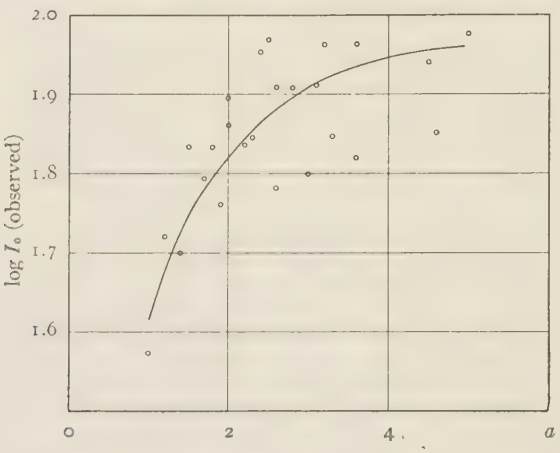

FIG. 4.—Relation between the observed central luminosity and the parameter a

tion of diameters, as measured with the microphotometer, with central luminosities and with exposure times.

SUPPLEMENTARY MEASURES ON LONG EXPOSURES

Exposures ranging from one to two hours on Eastman 40 plates developed with X-ray developer were available for seven of the nebulae given in Table IV. Absorption-curves of these images were recorded, measured, and reduced in the manner previously described, and were combined with the earlier results to obtain luminosity-curves running from the nuclei out to the thresholds of the long exposures. The combined results are given in Table VII with the values of log I for successive values of r/a reduced to a standard log $I_0 = 2.0$.

TABLE VII

LUMINOSITY-CURVES FROM LONG EXPOSURES, REDUCED TO STANDARD LOG I_0

r/a	221		4278		4283	4406	
	Min.	Maj.	Min.	Maj.		Min.	Maj.
4*.....	+0.626	+0.636	+0.613	+0.602	+0.612	+0.598	+0.620
5.....	.481	.476	.448	.425	.430	.462	.508
6.....	.357	.326	.273	.275	.286	.345	.410
8.....	+ .113	+ .095	+ .058	+ .070	+ .090	+ .150	.220
10.....	− .090	− .103	− .082	− .058	− .070	− .010	+ .080
12.....	.267	.275	.212	.172	.185	.160	− .045
14.....	.420	.450	.312	.290	.317	(.260)	.145
16.....	.550	.560	.392	.380	(.386)	(.360)	(.230)
18.....	.680	.675	.477	.475	(.473)	(.455)	(.355)
20.....	.790	.780	.564	(.576)	(.542)	(−0.525)	(−0.470)
22.....	0.905	.845	.662	(.670)	(.589)	.....	.....
24.....	(1.000)	0.920	.762	(.765)	(−0.652)	.....	.....
26.....	(1.100)	(1.000)	(.842)	(−0.905)	.....	.....	.....
28.....	(1.190)	(1.050)	(0.912)	.....	.....	.....	.....
30.....	(−1.280)	(1.150)	(1.012)	.....	.....	.....	.....
32.....	.....	(−1.250)	(−1.098)	.....	.....	.....	.....
	−0.800	−0.800	−0.560	−0.360	−0.170	−0.020	+0.020

r/a	4472		4486	4621		MEAN	
	Min.	Maj.		Min.	Maj.	Obs.	Cal.
4*.....	+0.596	+0.636	+0.570	+0.595	+0.610	+0.609	+0.602
5.....	.451	.500	.405	.445	.470	.458	.444
6.....	.346	.400	.270	.300	.355	.331	.310
8.....	.171	.255	+ .075	+ .135	.165	+ .133	+ .092
10.....	+ .040	.120	− .080	− .022	+ .030	− .020	− .083
12.....	− .045	+ .010	.210	.130	− .090	.148	.228
14.....	.135	− .115	.320	.225	.210	.267	.352
16.....	.235	.260	.420	.320	.315	.367	.461
18.....	.335	(.405)	.525	.410	.430	.475	.558
20.....	(.435)	(.560)	.640	.490	(.550)	.577	.644
22.....	(.550)	(−0.685)	(.795)	.545	(.650)	.684	.723
24.....	(−0.670)	.....	(0.900)	.620	(−0.760)	.783	.796
26.....	.....	.....	(−1.030)	(.685)	.....	.927	.863
28.....	.....	.....	.....	(.745)	.....	0.974	.925
30.....	.....	.....	.....	(.820)	.....	1.065	0.983
32.....	.....	.....	.....	(−0.880)	.....	−1.076	−1.037
	−0.340	−0.210	−0.530	−0.420	−0.280	.....	.....

* Log I for $r/a<4$ may be found in Table V. The quantities at the bottom of each column are the corrections applied to the measured values of log I in order to reduce them to the standard log $I_0=2.0$. Values inclosed in parentheses are from the toe of the characteristic intensity scale (log $I<-0.2$) and are uncertain.

These data were not incorporated in the preceding discussion because the long exposures were not made with this particular end in view and the standard conditions may not always have been strictly maintained. Moreover, the photometric properties of long exposures were not investigated in the laboratory, but were assumed to approximate extrapolations of the relations among the shorter ex-

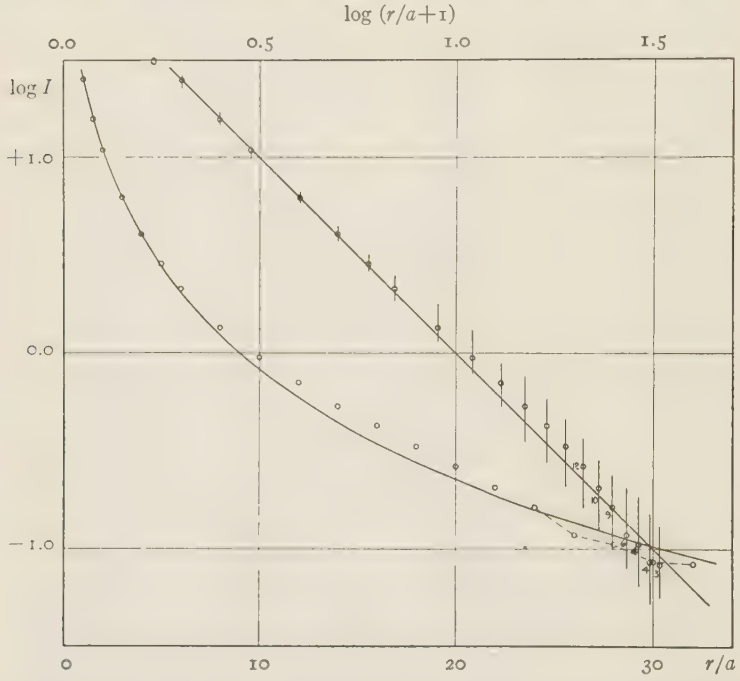

FIG. 5.—Combined luminosity-curve for images of elliptical nebulae derived from long exposures. The vertical lines represent the scatter among the individual curves. The figures indicate the number of individual curves included in the mean. Above log $I = -0.5$ the number for each point is 12.

posures. It was possible, however, to check the time scale from the data themselves, as will be shown in a later paragraph, and this substantially supports the reliability of the results.

In Figure 5, where the means of log I have been plotted against r/a, the data follow the general course of the formula out to points near the limits of the measures. The slight deviations between $r/a = 10$ and 20 appear to be real and may be significant in view of the

purely empirical nature of the formula. Deviations in the opposite direction beyond $r/a = 30$ depend upon a very few uncertain values and probably have less significance.

RELATION BETWEEN DIAMETER AND CENTRAL LUMINOSITY

A second method of testing formula (3) in the outer regions of low luminosity consists in comparing measured diameters of images with diameters computed from $\log I_0$ and the constant threshold value of $\log I$. Diameters measured from the microphotometer curves are rather uncertain, owing to irregularities in the grain of the plates and the almost asymptotic slope of the curve near the threshold; but the errors are largely accidental and may be reduced by multiplying the observations. The value of $\log I$ at the threshold is also uncertain, but in the discussion which follows, this enters as a constant to be determined on the assumption that it does not vary systematically with the exposure time. This assumption may be questionable, but at least it will serve as a first approximation.

If formula (3) holds beyond the limits of the measures, then, at the threshold of a plate,

$$\log I_0 = 2 \log R + \log I_{Th} , \tag{5}$$

where $R = r'/a + 1$, in which r'/a is the semidiameter in units of a, and $\log I_{Th}$ is the threshold value of $\log I$. Relation (5) may be tested by plotting $\log I_0$ against $\log R$ for all the images available.

The observational data are collected in Table VIII. The first group comprises twelve nebulae (twenty luminosity-curves), for which the exposures of the images measured range from 15 minutes to 45 seconds, with additional 15-second exposures for two of the nebulae (four curves), and additional long exposures for six of the nebulae (ten curves). These are followed by data for N.G.C. 410 and 584, and finally in Table VIII*a* for N.G.C. 221, with exposure times differing not only from those of the first group but also among themselves. The significance of the exposure times, which are irrelevant to the testing of formula (5), will be indicated later.

The plot of $\log I_0$ against $\log R$ is shown in Figure 6. The straight line is the relation

$$\log I_0 = 2 \log R - 0.740 , \tag{6}$$

TABLE VIII

SEMIDIAMETERS AND CENTRAL LUMINOSITIES FOR VARIOUS EXPOSURE TIMES

N.G.C.	0.25m		0.75m		2m		5m		15m		Long Exposures		
	log R	log I_o	log R	log I_o	log R	log I_o	log R	log I_o	log R	log I_o	log R	log I_o	log Exp.
3115* min	0.803	0.506	0.911	0.934	1.013	1.220	1.130	1.521	1.307	1.918	.....	.....	.....
maj	.491	.262	.663	.660	0.839	1.008	0.968	1.360	1.100	1.752	.....	.....	.....
3379*	.....	.....	.744	.860	0.934	1.157	1.127	1.489	1.255	1.897	.....	.....	.....
4278* min	.....	.....	.869	.747	1.004	1.097	1.072	1.483	1.283	1.880	1.574	2.560	1.778
maj	.....	.....	.778	.595	0.869	0.927	1.065	1.259	1.220	1.689	1.505	2.360	1.778
4283*	.....	.....	.699	.487	.903	.837	1.114	1.211	1.255	1.600	1.491	2.170	1.778
4374 min	.....	.....	.707	.578	.893	.969	1.004	1.280	1.137	1.645	.....	.....	.....
maj	.....	.....	.727	.563	.865	0.894	1.041	1.217	1.136	1.596	.....	.....	.....
4382 min	.....	.....	.845	.719	.978	1.037	1.114	1.373	1.230	1.748	.....	.....	.....
maj	.....	.....	.637	.558	.817	0.908	0.970	1.210	1.173	1.607	.....	.....	.....
4406* min	.....	.....	.633	.461	.806	.852	.989	1.192	1.196	1.640	1.385	2.020	1.903
maj	.....	.....	.580	.436	.740	.800	0.914	1.154	1.140	1.590	1.405	1 980	1 903
4472* min	.....	.....	.636	.506	.810	.887	1.004	1.258	1.208	1.703	1.447	2.340	2.079
maj	.....	.....	.614	.407	.838	.784	0.954	1.138	1.170	1.594	1 406	2.210	2.079
4486	.....	.....	.478	.400	.691	0.628	.794	0.777	0.987	1.334	1.497	2.530	2.079
4552	.....	.....	.691	.606	.823	1.008	0.946	1.346	1.090	1.742	.....	.....	.....
4621 min	.565	.318	.699	.683	.885	1.093	1.114	1.474	1.230	1.873	1.602	2.420	1.778
maj	0.497	0.173	.624	.570	.751	0.951	0.964	1.312	1.204	1.776	1.438	2.280	1.778
4649* min	.....	.....	.686	.597	.831	.956	.939	1.322	1.149	1.740	.....	.....	.....
maj	.....	.....	0.648	0.566	0.778	0.903	0.854	1.215	1.164	1.638	.....	.....	.....
Mean	(0.589)	(0.320)	.....	.....	.....	.....	.....	.....	.....	.....	(1.475)	(2.287)	.....
	0.524	0.189	0.693	0.597	0.853	0.946	1.004	1.279	1.182	1.698	1.468	2.317	1.893

N.G.C.	0.63m		1.25m		2.5m		5m		10m		20m	
584	0.757	0.590	0.873	0.787	0.873	1.122	0.906	1.403	0.993	1.547	1.144	1.744
	0.7m		2.2m		6.7m		20m		60m			
410 min	.....	.....	0.544	0.430	0.653	0.819	0.903	1.193	1.114	1.698		
maj	0.405	−0.021	0.567	0.377	0.686	0.805	0.877	1.265	1.098	1.710		

which fits the lower end of the plot where formula (3) is known to hold. The constant, −0.740, represents the threshold value of log I and is of the same general order as that estimated from the extra-

TABLE VIII*a*

N.G.C. 221*

Exp.	Min.		Maj.		Mean	
	log R	log I_0	log R	log I_0	log R	log I_0
80^m.....	1.532	2.800	1.602	2.800	1.567	2.800
22.....	1.326	2.344	1.342	2.359	1.334	2.351
11.....	1.260	2.057	1.281	2.144	1.270	2.100
4.5.....	1.176	1.716	1.163	1.819	1.170	1.768
1.83.....	1.057	1.349	1.015	1.407	1.036	1.380
0.5.....	0.823	0.965	0.852	1.001	0.837	0.983
0.15.....	0.602	0.474	0.591	0.512	0.597	0.493

* Mean of two or more plates (asterisk has same meaning in Table VIII).

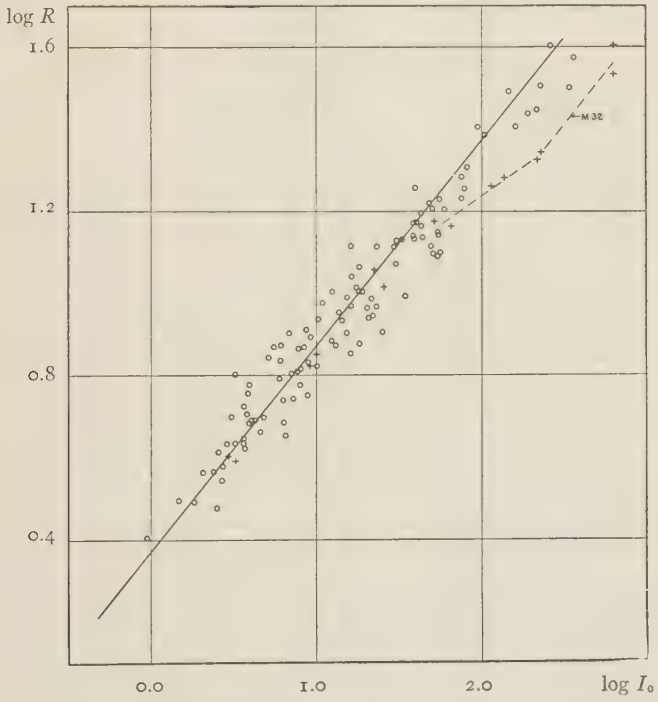

Fig. 6.—Relation between central luminosity and diameter

polation of the intensity scale in Figure 1, namely, $1.058 \times (-0.630) = -0.665$.

In the upper region of the plot most of the points fall below the straight line, a tendency exaggerated by the data for N.G.C. 221 (indicated by crosses), which is superposed on the outer arms of the great spiral, M 31. Its measures may therefore be systematically affected by the luminous background. The marked depression of the points between $\log I_0 = 1.4$ and 1.9 indicates excessive values of $\log I_0$ or deficient values of $\log R$, and hence tends to confirm the observed hump in the corresponding region of the combined luminosity-curve for the long exposures. The remaining high points, however, tend to approach the straight line again rather than to increase the separation. The plot as a whole suggests that formula (3) represents the general trend of the luminosity-curves in the outer regions, but that relatively minor deviations exist which may be significant in the physical interpretation of the curves.

THE SLOPE OF THE TIME SCALES

Results of a similar nature are found in the correlation of diameters with exposure times. The investigation involves, however, the use of the time scales for the plates employed, and, since the necessary data are included in Table VIII, the scales may conveniently be presented at this stage of the discussion and checked against the time scales determined in the laboratory.

The differences between the values of $\log I_0$ for the various images of each nebula represent the displacements of the luminosity-curves due to the different exposure times. They are, in fact, the reduction constants used in combining the various curves of a given nebula. A plot of $\log I_0$ against $\log t$ thus represents the slope of the characteristic time scale of the plates in the form

$$\log I_0 = m_1 \log t + \text{Constant} . \qquad (7)$$

The subscript is used in the coefficient of $\log t$ in order to distinguish it from that in the time scales previously mentioned, where the absorption, A, occurs in place of $\log I$. The relation between the two is, of course, $m_1 = 1.058m$. Since t is expressed in minutes, the con-

stant in formula (7) represents, for a given set of data, the value of log I_0 for an exposure of 1 minute.

In Figure 7, the means of log I_0 for the twenty curves in the first group, representing twelve nebulae, are plotted against log t. The mean of the four values for $t=15$ seconds and the mean of the ten

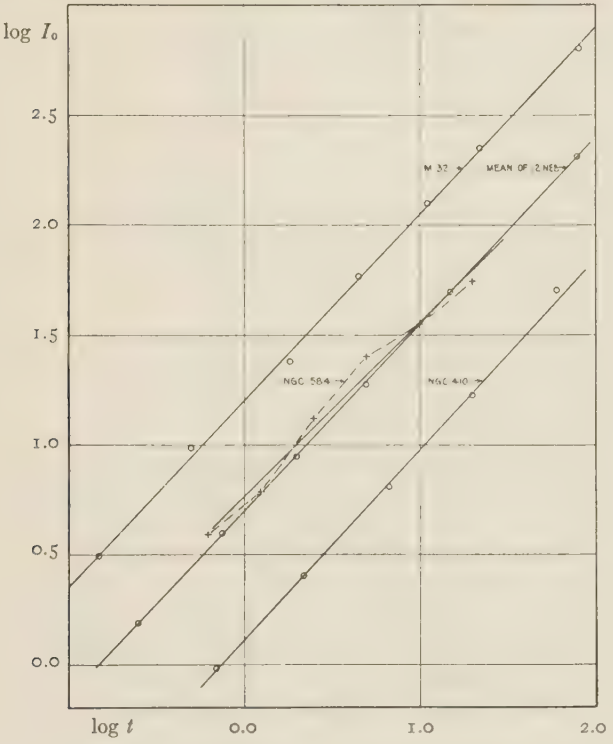

Fig. 7.—Time scales: log $I_0=m_1$ log t+Constant

values for long exposures are corrected by the systematic deviations of these particular curves from the mean curve for the group. The data are well represented by formula (7) with $m_1=0.85$. This corresponds to $m=0.80$, in excellent agreement with the values found in the laboratory. The dispersion among the individual nebulae is satisfactorily small except for a moderate scatter among the points representing the long exposures.

The three plates of N.G.C. 221, with twelve exposures ranging

from 8 seconds to 80 minutes, give the same value, $m_1 = 0.85$. The single plate of N.G.C. 410 gives $m_1 = 0.87$, and the rather poor single series of N.G.C. 584 may be represented by a line with the slope $m_1 = 0.84$. Thus the mean m_1 for all the data, 0.85, agrees with the laboratory value, and the deviations among the individual nebulae are unimportant. This is further evidence of the consistency of the data and the validity of the reductions. It also encourages the hope that the luminosity-curves from the long exposures are not altogether unreliable.

CORRELATION OF DIAMETERS AND EXPOSURE TIMES

After this digression on the time scales, the discussion of the correlation between diameters and exposure times may be resumed. From formulae (5) and (7)

$$2 \log R = m_1 \log t + \text{Constant} , \tag{8}$$

where the constant is the difference between the constants in (7) and (5), that is, between $\log I_0$ for an exposure of 1 minute and the threshold value of $\log I$. The data in Table VIII give a separate correlation-curve for each axis of each nebula. The individual curves may be combined by shifting them along the axis of $\log R$ by amounts representing the differences in $\log I_0$ for a given exposure time. In other words, since diameters are functions of central luminosities, the various nebulae may be reduced to a standard central luminosity, and all the data thus collected in a single homogeneous diagram for the comparison of diameters with exposure times.

This has been done in Figure 8. The standard $\log I_0$, as before, is 2.0 for an exposure of 15 minutes, and hence all values of $\log R$ in Table VIII have been corrected by half the difference $2.0 - \log I_0$ (15 min.) in accordance with formula (5). The comparison of this formula with the observations, shown in Figure 6, indicates that errors introduced by the corrections will be of very minor importance.

The data in Figure 8 are fairly well represented by the straight line

$$2 \log R = 0.85 \log t + 1.73 , \tag{9}$$

which has the slope derived from the time scales. The points for N.G.C. 221, indicated by crosses, show the same systematic discrepancies as in the correlation of log R with log I_0 and may be referred to the same probable source, namely, the luminous background on which the nebula is superposed. Otherwise the most conspicuous discrepancy (the point log $R = 0.845$; log $t = -0.602$) refers to the minor axis of the smallest image of the very elongated nebula

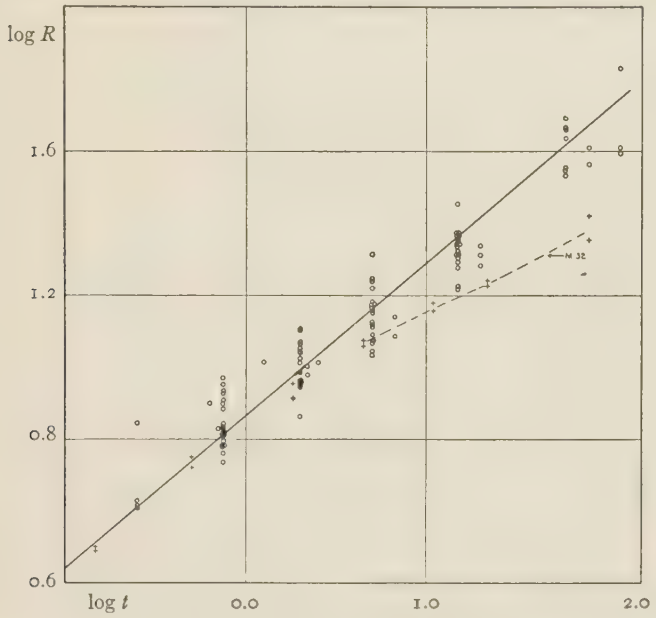

FIG. 8.—Relation between diameter and exposure time

N.G.C. 3115, and hence is entitled to little weight. The slight depression in the region log $t = 1.0$ corresponds to that in Figure 6 and to the hump in the mean luminosity-curve for the long exposures.

The constant in formula (9) is the difference between log I_0 for 1 minute, $2.0 - (0.851 \times 0.176) = 1.00$, and the threshold value of log I. The latter is therefore -0.73, which is in good agreement with the value in formula (7), namely, -0.74.

The three correlations between the three observed quantities, namely, central luminosities, diameters, and exposure times, are not independent. If any two are found to hold, it follows that the third

also must hold. The correlations involving the diameters, and hence referring to the very threshold of the plates, agree with the luminosity-curves for the long exposures and indicate that formula (3) represents the general trend of the luminosity-curves, without serious systematic divergence, out as far as the observations have been carried.

The correlation between diameters and exposure times, moreover, suggests that the boundaries of the nebulae have not been reached even with the longest exposures. Yet elliptical nebulae appear to be rotating bodies, and hence it is reasonable to assume that some sort of boundary actually does exist. The radii, on such an assumption, must be of the order of $r/a = 35$ or greater.

SIGNIFICANCE OF LOG I

Log I in formula (3) represents surface brightness and hence, within reasonable limits, is independent of the size of the microphotometer slit. The unit, log $I = 0.0$, represents a measured absorption of about 0.116, which is well above the threshold of the plates. The unit varies from plate to plate with the exposure time according to the relation expressing the time scale. The numerical value, as recently determined from extra-focal star images under conditions comparable with those of the nebular plates, appears to be of the order of 19.0 pg. mag. per square second of arc for exposures of 1 minute on Eastman 40 plates. The value varies considerably with the condition of the mirrors, the transparency of the sky, and the sensitivity and development of the plates. Since no precise determinations of these variations were made at the time, the mean value will not give accurate results in individual cases. It is hoped, however, that statistical averages based upon the mean value will be of the proper order of magnitude.

The unit of surface brightness corresponds to a threshold value, log $I = -0.7\pm$, of the order of 20.8 pg.mag. per square second of arc, while the surface brightness of the faintest in-focus star images that can be detected on exposures of 1 minute under the same conditions average about 17.5. Much of this discrepancy is due to the greater ease with which large surfaces can be detected, but, as Seares has pointed out, a portion is probably due to the intermittent exposures

of the vibrating focal images as compared with the continuous exposures for the extra-focal surfaces.[1] The subject is further complicated by the minimum linear dimensions possible in photographic images, and hence the type of telescope may play some rôle. The phenomena affect the determination of total luminosities of nebulae in a very evident manner and indicate the necessity of referring such measures to extra-focal star images comparable in size with the nebular images themselves.

Log I_0 represents the central luminosity on the assumption that the luminosity law holds right up to a point center. The assumption cannot be tested directly because of the spreading of photographic images and the finite area of the photometer slit. It may be noted, however, that most of the luminosity-curves follow the formula up to $2''$ from the center. If the formula held to a point center, the values of log I_0 for curves along the minor and the major diameters of any nebula should be about equal. The data in Table IV indicate, however, that the values for the minor diameters are systematically the larger, the difference increasing with the elongation of the images. The one exception is in the mean curves for N.G.C. 221, which represent the combination of curves from seven images, with a consequent uncertainty in the precise values of the log I_0 finally adopted. Even here the difference, 0.014, is negligible. The mean difference for the other eight nebulae is 0.108.

The discrepancy is partially explained by the observed fact that the ellipticities of isophotal contours increase with distance from the nucleus, at least in the more elongated nebulae—a phenomenon

[1] *Mt. Wilson Contr.*, No. 191, p. 14; *Astrophysical Journal*, **52**, 162, 1920. The threshold value of surface brightness given above represents the mean of measures of fifteen extra-focal exposures on ten nights over a period of six months. It is about 2 mag. fainter than the value given by Seares, based on extra-focal exposures on two nights. A re-examination of the two sets of material, in collaboration with Mr. Seares, indicates a mean difference of the order of 10 per cent in the transparencies of the faintest images. Seares adopted for the threshold images readily detected by the eye, while my estimate was based on the faintest that could be seen under the best conditions, with the thermocouple measures as a guide. On the straight-line portion of the intensity scale, this difference of 10 per cent would correspond to a difference of the order of 0.25 mag., but near the threshold the corresponding magnitude difference is enormously magnified by the asymptotic approaches of the absorption-curve to the axis. This alone is sufficient to account for the divergence in the two estimates of the threshold value, although the influence of observing conditions may also be superimposed.

which will be discussed later. The result is that the luminosity-curves along the minor axis are relatively steeper in the inner region than they would be if the nebulae were precisely symmetrical. Near the nuclei, therefore, the curves must flatten out rather suddenly, as though the luminosity law in all elongated nebulae began to operate at the borders of approximately globular nuclei. The plates themselves show some such phenomenon, for the limiting exposures exhibit round images of uniform density of the order of twice the diameters of the faintest star images. The relatively small variation in the appearance of the nucleus from nebula to nebula, however, is partially due to photographic spreading and to the merging of a surface into a point-source image, and its significance is questionable.

SIGNIFICANCE OF THE PARAMETER a AND THE SYMMETRY OF ISOPHOTAL CONTOURS

The parameter a is the distance from the nucleus at which the luminosity falls to one-fourth of I_0. It is a measure of the luminosity gradient and, after a fashion, of the scale on which the nebula is constructed. If the isophotal contours in the image of an elliptical nebula were all of the same ellipticity, a would vary directly with the radius of any given contour, excepting, perhaps, those very near the nucleus. For an Eo nebula, a would be constant for all diameters. For an elongated nebula, the value of a along any diameter making an angle with the major axis would satisfy the relation

$$a_\phi = \frac{a_{\min}}{\sqrt{1 - e^2 \cos^2 \phi}} . \qquad (10)$$

Expressed in terms of r/a, all the isophotal contours would become circles. This relation has been used in correlating diameters with $\log I_0$ and with exposure times.

The assumption that all isophotal contours in a given image are ellipses with the same eccentricity holds as a first approximation, but further investigation suggests slight systematic deviations among the more elongated nebulae, in the sense that the eccentricity increases with distance from the nucleus. The images of elliptical nebulae appear to be projections of figures of revolution orientated at random, and hence, in the Eo images, representing either globular

nebulae or flattened bodies with their axes of revolution orientated in the line of sight, the contours should be strictly circular. The observational data conform with this interpretation.

E7 nebulae lie at the extreme end of the sequence, and their images are the only ones which can definitely be referred to bodies orientated with their axes of revolution perpendicular to the line of

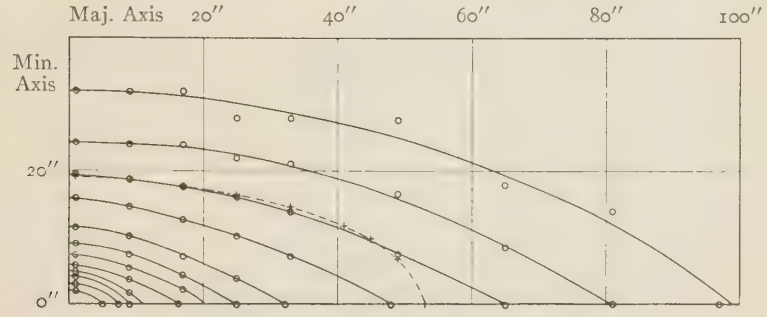

FIG. 9.—Isophotal contours of the image of N.G.C. 3115

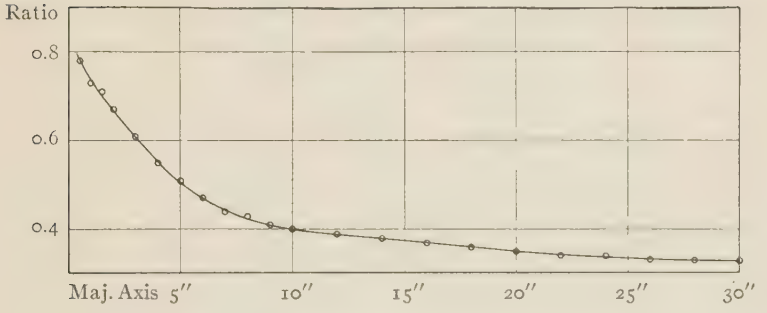

FIG. 10.—Ratios of axes of isophotal contours

sight. Isophotal contours of the type object, N.G.C. 3115 (exposure, 15 min.), have been determined from absorption-curves parallel to the minor axis and cutting the major axis at successive intervals from the nucleus. These contours are shown in Figure 9. They approximate ellipses with the ends drawn out to form the familiar lenticular edge. Although the points very near the nucleus are rather uncertain, the data indicate that the major axis increases faster than the minor, and hence that the outer contours are more elongated than the inner. The reality of this phenomenon is substantiated by com-

paring the luminosity-curves along the two axes of the various images which were combined into the mean curves in Table V. The data are listed in Table IX and are shown graphically in Figure 10. The procedure was as follows. The values of r_{min} were read from the two curves for a given image for values of A corresponding to successive values of r_{maj}. The ratios r_{min}/r_{maj} thus represent the ratio of axes of the successive contours. The results for the various im-

TABLE IX

RATIO OF AXES OF ISOPHOTAL CONTOURS IN IMAGES OF N.G.C. 3115

Major Axis r	Exposure Time					
	15s	45s	2m	5m	15m	Mean
0.5	0.82	0.79	0.75	0.75	0.80	0.78
1	.78	.75	.68	.70	.75	.73
1.5	.79	.73	.70	.68	.63	.71
2	.73	.70	.67	.65	.60	.67
3	.62	.62	.62	.58	.56	.61
4	.58	.56	.56	.54	.54	.55
5	0.54	.51	.53	.51	.48	.51
6	.....	.48	.48	.47	.46	.47
7	.....	.46	.44	.44	.44	.44
8	.....	.44	.43	.42	.42	.43
9	.....	.42	.41	.41	.42	.41
10	.....	0.41	.40	.39	.41	.40
12	.....	.....	.40	.38	.40	.39
14	.....	.....	.39	.37	.39	.38
16	.....	.....	.38	.36	.38	.37
18	.....	.....	.37	.36	.36	.36
20	.....	.....	0.35	.35	.35	.35
22	.....	.....	.....	.34	.35	.34
24	.....	.....	.....	0.34	.34	.34
26	.....	.....	.....	.....	.33	.33
28	.....	.....	.....	.....	.33	.33
30	.....	.....	.....	.....	0.33	0.33

ages agree very well except in the nuclear regions of the longer exposures, where the flatness of the measured absorption-curves introduces uncertainties. The ratios diminish steadily from over 0.7 near the nucleus to about 0.33 in the outer regions. The classification E7 is of course based upon long exposures, and refers to the outer contours.

For images intermediate between Eo and E7 the effect varies with the ellipticity. For E1 and E2, it is inappreciable. Isophotal contours of N.G.C. 221 (E2), for instance, are represented by ellipses

within the small errors of observation, out to luminosities of the order of 1 per cent of the central luminosity. In N.G.C. 4382 (E4) and 4621 (E5), the contours deviate very slightly from ellipses in the direction of lenticular figures, the ratio of axes varying from about 0.70 to 0.63 and from 0.64 to 0.56, respectively. The data for the latter two nebulae are considerably less reliable than those for N.G.C. 221 and 3115, but the phenomena appear to be definite, at least in a qualitative sense. Except for the extremely elongated nebulae, however, the deviations of the contours from symmetrical ellipses are so slight that they may be disregarded in general discussions and rough calculations. The present data are not sufficient to examine the range in luminosity gradients among images of a given ellipticity introduced by the projection factor. The most significant evidence bearing on this question is found in the correlation between total luminosities and major diameters.[1]

By integrating formula (3), the total luminosity along any radius is found to be

$$I_0 a^2 \int_0^r \frac{dr}{(r+a)^2} = I_0 a \left(\frac{\frac{r}{a}}{\frac{r}{a}+1} \right). \qquad (11)$$

This of course represents a strip whose width is the unit in which a is expressed. As r/a increases, the total luminosity approaches the simple product $I_0 a$ as a limit. Out to $r/a = 35$, to which the formula probably holds with fair approximation, the total luminosity is over 97 per cent of this product.

TOTAL LUMINOSITIES OF ELLIPTICAL NEBULAE

The total luminosity of the entire nebula out to the distance r/a is found by integrating successive elliptical rings on the assumption that the isophotal contours are all similar ellipses. For the more elongated images this assumption is only an approximation, but, expressed in stellar magnitudes, the deviations are not very serious. The area of an elementary isophotal ring whose semi-minor axis is r

[1] *Mt. Wilson Contr.*, No. 324; *Astrophysical Journal*, **64**, 321, 1926.

and whose width along the minor axis is dr is, neglecting the second-order differential,

$$\frac{\pi}{\sqrt{1-e^2}}\{(r+dr)^2-r^2\}=\frac{2\pi r dr}{\sqrt{1-e^2}}. \tag{12}$$

The luminosity of the ring is this area multiplied by

$$\frac{I_0}{(r/a_{\min}+1)^2}.$$

Integrating these rings out to the distance r along the minor axis, and remembering that $a_{\min}=a_{\text{maj}}\sqrt{1-e^2}$, we find the total luminosity of the nebula to be

$$\left.\begin{aligned} I_t&=\frac{2\pi I_0}{\sqrt{1-e^2}}\int_0^r \frac{r dr}{\left(\frac{r}{a_{\min}}+1\right)^2}, \\ &=2\pi I_0 a_{\min} a_{\text{maj}}\left\{\log_e\left(\frac{r}{a}+1\right)-\frac{r}{a+1}\right\}. \end{aligned}\right\} \tag{13}$$

The factor within the brackets is independent of the shape of the image and, while the value of a refers formally to the minor axis, that for any radius should lead to approximately the same contour except in the very elongated nebulae. For these the deviations from circularity of the contours, expressed in terms of r/a, introduce an uncertainty as to the proper a to use in the computation, and a similar uncertainty arises in the choice of I_0. More accurate calculations might be based on the assumption of a globular nucleus from the borders of which the luminosity law begins to operate, but for approximate results the mean log I_0 may be used and the deviations from circularity ignored.

The factor within the braces takes care of the exterior regions of the nebula which increasing exposures bring above the threshold of the plate. It depends upon I_0, and both the bracket and I_0 are dependent on the exposure time. The total luminosity derived from a photographic image therefore has little significance except as it is referred to given exposure conditions. The numerical value of the

bracket is unity for $r/a = 5.3\pm$, which corresponds to a mean exposure of the order of 1 minute for the nebulae considered in the present discussion. The total luminosity is then expressed by the simple formula

$$I_t = 2\pi I_0 a_{\min} a_{\text{maj}} .$$

Total magnitudes are derived from the usual formula

$$m_t = m_c - 2.5 \log I_t ,$$

where m_c is the magnitude per square unit of a for the unit of surface brightness, $\log I = 0.0$. The latter, as previously mentioned, appears

TABLE X

PHOTOGRAPHIC MAGNITUDES CALCULATED FROM DISTRIBUTION OF LUMINOSITY

N.G.C.	m_t $r/a=5.3$	r/a 15^m	m_t		HARVARD		HOLETSCHEK‡ (VISUAL)
			15^m	60^m	I*	II†	
221.....	10.29	20	9.49	9.28	.....	8.7	8.85
410.....	13.44	6	13.35	12.92	.....	.....	.....
584.....	12.49	11	12.00	11.77	.....	11.8	10.9
3115.....	11.32	15	10.66	10.43	.....	9.9	9.5
3379.....	11.47	17	10.75	10.53	.....	10.2	9.4
4278.....	12.10	18.5	11.34	11.12	.....	.....	10.8
4283.....	14.02	17	13.30	13.06	.....	.....	12.2
4374.....	11.92	12.7	11.35	11.10	10.8	.....	9.9
4382.....	11.69	15.0	11.03	10.80	10.9	9.7	10.0
4406.....	11.52	13.7	10.91	10.67	10.9	.....	10.0
4472.....	10.97	14.5	10.33	10.09	10.2	9.1	8.85
4486.....	11.38	8.7	11.03	10.74	10.5	9.2	9.7
4552.....	12.27	11.5	11.81	11.50	11.4	.....	9.9
4621.....	11.91	11.5	11.24	11.00	11.3	.....	10.0
4649.....	11.50	13.3	10.91	10.66	10.5	9.8	9.5

* *Harvard College Observatory Circular*, No. 294, 1926.
† *Proceedings of the National Academy of Sciences*, **15**, 564, 1929.
‡ Revised by Hopman; *Astronomische Nachrichten*, **214**, 425, 1921.

to be of the order of 19.0 mag. per square second of arc for an exposure of 1 minute. Since the unit of a is $2''.03$,

$$m_c = 19.0 + 2.5[0.85 \log t - \log (2.03)^2] ,$$
$$= 20.0 \text{ for } t = 15 \text{ min.}$$

Table X gives total photographic magnitudes for the nebulae here discussed. These have been calculated for exposures of 15 minutes and 1 hour. Magnitudes were first calculated for $r/a = 5.3$ and

then corrected for the observed values of r'/a, i.e., of the observed radius, by means of Table XI, which gives the effect of the bracket in formula (13), expressed in magnitudes, as the images grow with increasing exposure time. This effect is not linear for a given nebula and, moreover, for a given range in exposure time it depends on the central luminosity of the nebula.

For use in Table X the means of log I_0 and of r'/a for the two axes corresponding to the 15-minute exposures have been taken from Tables IV and VIII, except for N.G.C. 221, 410, and 584, for which

TABLE XI

CORRECTIONS TO TOTAL MAGNITUDES OF NEBULAE DEPENDING ON DIAMETERS OF THE IMAGES

r/a	Δm_t*	r/a	Δm_t*
1	+1.78	18	−0.75
2	+0.91	20	.80
3	+ .49	22	.845
4	+ .23	24	.885
5	+ .05	26	.92
5.3	.00	28	.95
6	− .09	30	0.98
7	− .20	32	1.005
8	− .29	34	1.03
9	− .37	36	1.05
10	− .43	38	1.075
12	− .54	40	1.095
14	− .62	45	1.14
16	−0.69	50	−1.17

* $\Delta m_t = 2.5 \log_{10} \left\{ \log_e (r/a+1) - \frac{r/a}{r/a+1} \right\}$.

they have been read from curves relating the two quantities with the exposure times. For N.G.C. 584, for which only one luminosity-curve is available, the values of a for the major and minor axes have been computed on the assumption that the ratio of the two corresponds with the ellipticity of the image.

Table X indicates that the calculated luminosities are of the right order of magnitude, but, in view of the unknown variations in m_c and the approximations involved, very little of further value can be expected from the material. Direct measures of the total photographic magnitudes of nebulae are at present in a very unsatisfactory state. Spirals with fairly definite borders offer less difficulty

than the elliptical nebulae, but in both cases extra-focal images must be used unless the scale of the photographs is so small that the nebulae may be treated as point sources. Even then it will be advisable to investigate the manner in which the photometry of surfaces merges into that of focal star images. In the case of all elliptical nebulae and probably also the earlier-type spirals, the results must be referred to definite exposure conditions and perhaps also to definite instruments.

Published data are too limited for serious discussion. The two lists from Harvard,[1] for instance, have only four nebulae in common, and these show an average difference of more than a magnitude (Table X). The problem is under investigation at Mount Wilson, but very few definite results are as yet available. The standard conditions have been set at extra-focal exposures of one hour with the large reflectors, the plates being measured with a thermocouple; the magnitudes are derived from comparisons with Selected Areas. Preliminary results suggest a systematic difference, for elliptical nebulae at least, between the reflectors and the 10-inch Cooke astrographic camera, while the latter and a Tessar I_c ($f=4.5$) with a focal length of about 10 inches appear to give comparable results. The very few nebulae in the Harvard lists for which definite magnitudes are available at Mount Wilson range from 0.5 mag. fainter (N.G.C. 1700) to 1.5 mag. brighter (N.G.C. 7619) than the Harvard values. This illustrates the necessity for careful investigation before a system of photographic magnitudes can be adopted.

DISTRIBUTION OF LUMINOSITY IN ELLIPTICAL NEBULAE

Since formula (3) appears to give a reasonable approximation to the distribution of luminosity in the projected images, it is of considerable interest to examine the corresponding distribution in the nebulae themselves. The absence of conspicuous flattening of luminosity-curves in the central regions suggests that absorption of light is inappreciable. This is in line with the more definite evidence from novae and Cepheids involved in the nuclear region of M 31.[2] Scatter-

[1] *Harvard College Observatory Circular*, No. 294, 1926, and *Proceedings of the National Academy of Sciences*, **15**, 564, 1929. Both lists purport to give photographic magnitudes on the international scale.

[2] *Mt. Wilson Contr.*, No. 376; *Astrophysical Journal*, **69**, 103, 1929.

ing may also be neglected, for plates exposed through a visual color filter show no difference in color between the nuclei and the outer regions of elliptical nebulae. The conditions may be further simplified by considering the case of a globular nebula and assuming, as a first approximation, that the empirical formula holds indefinitely. The problem then becomes analogous to that of determining the distribution of stars in a globular cluster from star counts, as discussed by Plummer, von Zeipel, and many others. The solution of an integral equation leads to the following relation,[1]

$$f(\rho)=-\frac{1}{\pi}\int_{\rho}^{\infty}\frac{F'(r)dr}{\sqrt{r^2-\rho^2}}, \tag{14}$$

where $f(\rho)$ represents the distribution of luminosity in the three-dimensional nebula as a function of distance ρ from the nucleus, and $F(r)$ the observed distribution in the projected image, namely, formula (3) or its equivalent, formula (4). On introducing the derivative of (4), the relation becomes

$$f(\rho)=\frac{2I_0a^2}{\pi}\int_{\rho}^{\infty}\frac{dr}{(r+a)^3\sqrt{r^2-\rho^2}}. \tag{15}$$

This expression can be integrated directly[2] although the procedure is rather clumsy. The three cases in which ρ is less than, equal to, and greater than a must be solved separately. The solutions are

Case I: $\rho=a$

$$f(\rho)=\frac{4I_0}{15\pi a},$$

Case II: $\rho<a$

$$f(\rho)=-\frac{I_0a^2}{\pi(a^2-\rho^2)^2}\left\{3a-\frac{3a^2-(a^2-\rho^2)}{\sqrt{a^2-\rho^2}}\log_e\frac{a+\sqrt{a^2-\rho^2}}{\rho}\right\},$$

Case III: $\rho>a$

$$f(\rho)=-\frac{I_0a^2}{\pi(a^2-\rho^2)^2}\left\{3a-\frac{3a^2-(a^2-\rho^2)}{\sqrt{\rho^2-a^2}}\left(\tan^{-1}\frac{-a}{\sqrt{\rho^2-a^2}}+\frac{\pi}{2}\right)\right\}.$$

[1] Details of the solution will be found in the several articles on the distribution of stars in globular clusters. See, for instance, H. C. Plummer, *Monthly Notices of the Royal Astronomical Society*, **71**, 460, 1911.

[2] Pierce, *A Short Table of Integrals*, Nos. 195, 196, 205, 206.

Let $z_1 = 1 - (\rho/a)^2$ and $z_2 = -z_1 = (\rho/a)^2 - 1$; then, neglecting the constant $I_0/\pi a$, which appears as a coefficient in each case, we find

$$\text{Case I:} \quad f(\rho) = 4/15 ,$$

$$\text{Case II:} \quad f(\rho) = \frac{1}{z_1^2}\left\{\frac{3-z_1}{\sqrt{z_1}} \log_e \frac{1+\sqrt{z_1}}{\sqrt{1-z_1}} - 3\right\}, \tag{16}$$

$$\text{Case III:} \quad f(\rho) = \frac{1}{z_2^2}\left\{\frac{3+z_2}{\sqrt{z_2}}\left(\tan^{-1} - \frac{1}{\sqrt{z_2}} + \frac{\pi}{2}\right) - 3\right\}. \tag{17}$$

The formulae express the distribution of luminosity in the three-dimensional nebula as a function of ρ/a where a is the same quantity

TABLE XII

DISTRIBUTION OF LUMINOSITY IN ELLIPTICAL NEBULAE

ρ/a*	$I = f(\rho/a)$*	log 100 I	ρ/a*	$I = f(\rho/a)$*	log 100 I
0.0	.....	.....	3.5	0.0193	0.286
0.05	4.44	2.647	4	.0142	0.152
.1	3.108	2.493	5	.00790	9.898
.2	1.924	2.284	6	.00491	9.691
.3	1.335	2.126	8	.00227	9.356
.4	0.981	1.992	10	.00123	9.090
.5	.750	1.875	12	.000741	8.870
.6	.588	1.769	15	.000394	8.594
.8	.383	1.583	20	.000173	8.238
1.0	.267	1.426	25	.0000910	7.959
1.2	.194	1.288	30	.0000535	7.728
1.5	.126	1.100	40	.0000230	7.362
2.0	.0697	0.843	50	.0000119	7.076
2.5	.0425	.628	70	.00000442	6.645
3	0.0279	0.446	100	0.00000154	6.187

* ρ/a represents distance from the center of the three-dimensional nebula. The units of both distance and luminosity are arbitrary.

as in formula (3). Table XII gives numerical values of $f(\rho/a)$, which are proportional to the luminosity, for successive values of ρ/a, and Figure 11 shows the luminosity-curve plotted as a relation between log I and log ρ/a.

COMPARISON OF LUMINOSITY DISTRIBUTION IN NEBULAE WITH DENSITY DISTRIBUTION IN AN ISOTHERMAL GAS SPHERE

The complexity of formulae (16) and (17) doubtless arises from the introduction of an empirical formula into an integral equation. The formula, moreover, is assumed to hold from 0 to ∞, although there is reason to suppose that it is not valid for very small values,

say $r/a < 0.25$, and that it cannot be followed indefinitely. The luminosity-curve in Figure 11 can therefore be accepted only as a first approximation for comparison with other curves whose significance is known.

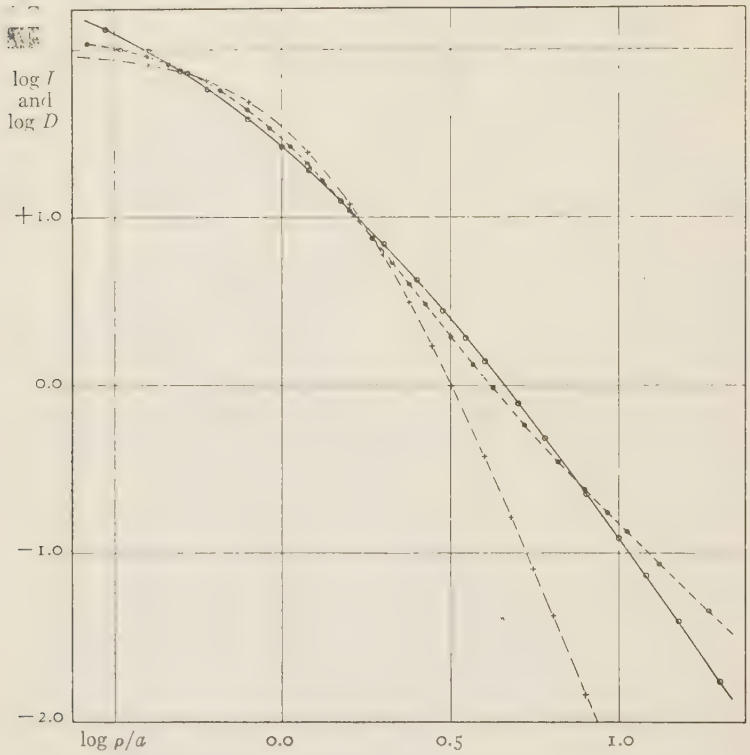

FIG. 11.—Luminosity distribution in globular nebulae (circles) compared with density distribution in an isothermal gas sphere (dots) and with stellar distribution in a globular cluster (crosses).

One such comparison, based on the assumption that distribution of luminosity represents distribution of mass, is with the density distribution in an isothermal gas sphere as computed by Emden in his well-known *Gaskugeln* (Tabelle 14). This also is shown in Figure 11 in the form $\log r_1 = f(\log p_1)$, r_1 and p_1, in Emden's notation, signifying distances from the center and densities, respectively. The curve has been shifted into approximate coincidence with the lumi-

nosity-curve by adding -0.58 to $\log r_1$ and $+2.11$ to $\log p_1$. The third curve in Figure 11 represents the density distribution in an adiabatic gas sphere of class $n=5$, $k=6/5$ (Emden, Tabelle 11), and is included because it approximates in a general way the distribution of stars in a globular cluster, and hence emphasizes the wide difference between these objects and the elliptical nebulae.

The luminosity-curve falls well above both density-curves in the immediate neighborhood of the center, say $\rho/a<0.25$, thus indicating more highly concentrated nuclei in the nebulae. From this point out to $\rho/a=10$ or 11 (isothermal density $=0.001$ central density) the luminosity-curve follows the isothermal density-curve rather closely, but from there outward it deviates systematically from the latter in the general direction of the adiabatic curve. The isothermal sphere extends to infinity and has infinite mass. The nebulae, on the other hand, appear to be rotating bodies, and hence infinite dimensions can scarcely be attributed to them. If we admit the analogy throughout the central region, outside of the nucleus itself, the luminosity-curve would therefore be expected to deviate from the density-curve in the outer regions in the direction actually observed, namely, toward that of finite dimensions, or of the system which Emden calls *isotherm-adiabatische*.

The similarity of the two distribution laws over the central region is confirmed when the isothermal gas sphere is projected on a plane and the projected density distribution is compared with the luminosity distribution actually observed in the nebular images. This comparison evades the assumptions introduced in deriving the luminosity law for the three-dimensional nebula. The projection may be made graphically by constructing density-curves along parallel lines at successive distances from the center and then plotting the areas under these curves against the distances. Since the densities in the extreme outer regions tend to follow the inverse-square law, the areas are finite and may be estimated to approximations sufficient for the present purpose. Results for such a solution are given in Table XIII, although no great accuracy can be assigned to the numerical values. In Figure 12 the projected density-curve is compared with the observed luminosity-curve.

The comparison indicates that the nuclear luminosity is definitely more concentrated than the central density of the gas sphere; that, from about $\rho/a = 0.5$ to 5.0, the two distribution-curves agree fairly well; that beyond 5.0 the luminosity-curve falls increasingly below the density-curve, as would be expected from the finite dimensions of the nebula.

TABLE XIII

PROJECTED DENSITIES IN THE ISOTHERMAL GAS SPHERE

r_1	D	log D	log $(D-30)$
0	3032	3.482	+3.477
0.5	2962	3.472	3.467
1	2729	3.436	3.431
1.5	2430	3.386	3.380
2	2106	3.324	3.317
3	1524	3.183	3.174
4	1103	3.042	3.031
5	832	2.920	2.904
6	649	2.812	2.792
7	522	2.718	2.692
8	430	2.633	2.602
9	366	2.563	2.526
10	318	2.502	2.459
12	254	2.404	2.350
14	210	2.323	2.255
16	179	2.252	2.173
18	157	2.197	2.104
20	140	2.147	2.041
25	111	2.045	1.908
30	92.0	1.964	1.792
40	69.6	1.843	1.598
50	56.5	1.752	1.423
70	41.5	1.618	+1.061
100	30.2	1.480	−0.699
150	21.1	1.324	.....
200	16.3	1.213	.....
300	10.9	1.038	.....
500	6.5	0.814	.....

The order of the discrepancies is indicated when arbitrary boundaries are assigned to the gas sphere out to which Emden's curve is assumed to hold, and the bounded spheres are projected on to a plane. A very good agreement is found when the limit is set at $r_1 = 100\pm$, where the density in the gas sphere is of the order of 0.0002 of the central density and that in the projection about 1 per cent of the projected central density. The projected densities for the bound-

ed sphere are derived with a fair approximation, except near the boundary, by subtracting a constant from the projected densities for the unbounded sphere. For the present purpose the constant has been selected as 30 units, corresponding to the projected density in

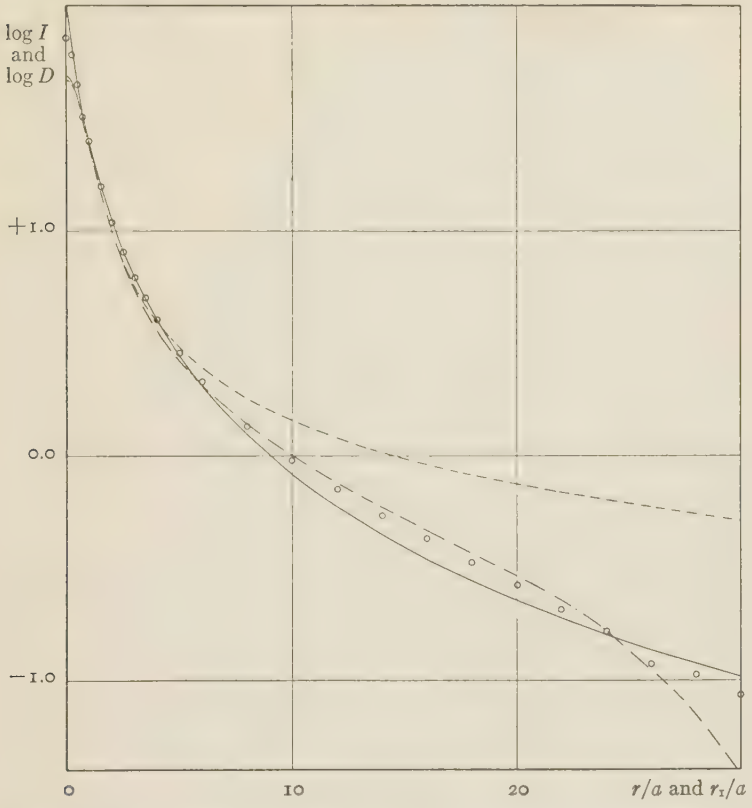

FIG. 12.—Comparison of luminosity distribution in the projected images of elliptical nebulae (full line, formula [3]) with density distribution in the projection of an isothermal gas sphere (dashes) and a bounded gas sphere (dash-dot). The circles represent the measured luminosities on long exposures shown in Fig. 5.

the unbounded sphere at about $r_1 = 101$, and the results of the operation are listed in the fourth column of Table XIII.

These data are represented approximately by a formula similar to (3),

$$\log D = \log D_0 - 2 \log (r_1/a + 1) ,$$

where a is 3.0 and log D_0 is about 3.79, which also holds for the central region of the projection of the unbounded sphere.

Figure 12 gives four curves, representing, respectively, formula (3), the observed luminosity-curve from the long exposures, the density-curve for the projection of the unbounded gaseous sphere, and the density-curve for the projection of the bounded gaseous sphere. The observations fall between the first and last curves, with little choice between them except at the center and in the extreme outer region where the measures have little weight. The deviations of the measures from formula (3) in the interval $r/a = 8$ to 22 represent the hump in the luminosity-curve for long exposures mentioned in a previous paragraph and are in the direction of the bounded gaseous sphere. The latter, moreover, has a radius of the order of $r_1/a = 34 \pm$ which is comparable with the radii observed in the longer exposures of the nebulae. The comparison with the arbitrarily bounded gaseous sphere has no definite physical significance, but it serves to emphasize the similarity between luminosity distribution in the nebulae and density distribution under isothermal conditions, which is partially masked by the infinite dimensions of the complete gaseous sphere.

Further consideration of the problem here raised has no part in the present investigation, which is essentially a presentation of the data of observations. It is hoped that they may furnish an observational basis for the dynamical study of elliptical nebulae.

Carnegie Institution of Washington
Mount Wilson Observatory
February 1930

Contributions from the Mount Wilson Observatory, No. 399
Reprinted from the *Astrophysical Journal*, Vol. LXXI, pp. 285–335, 1930
Printed in the U.S.A.

BEHAVIOR OF BRIGHT LINES IN THE SPECTRA OF SEVERAL LONG-PERIOD VARIABLE STARS

By PAUL W. MERRILL and CORA G. BURWELL

ABSTRACT

The *variables investigated* include ten stars of type Me and three of type Se (see Table I). Numerous spectrograms are listed in Table II.

Intensities of bright lines.—Estimated intensities of *Hδ*, *Hγ*, *Hβ*, *Fe* 4202, *Fe* 4308, and *Mg* 4571 served for the study of the behavior of these lines during the light-cycle. The relative intensities of pairs of lines rather than the intensities of individual lines were employed, thus avoiding serious photometric difficulties. The *intensity ratio* $H\gamma:H\delta$ in Me stars varies with phase in a striking manner. Typical behavior is as follows: At one-fifth of the period before maximum, phase −0.2, the ratio is 1/8; it rises rapidly to 1/2 at −0.05, then remains nearly constant until +0.2, after which it again rises rapidly to 2½ at about +0.4. In Se spectra the ratio has a minimum of 2½ at phase +0.07, with higher values earlier and later. The *intensity ratio* $H\beta:H\gamma$ is not well defined in Me stars because $H\beta$ is seldom observed, and its intensity seems to vary in different cycles. In general, $H\beta$ grows relatively stronger after maximum. In Se spectra $H\beta$ is very intense. The ratio to $H\gamma$ is high at early and late phases, with a minimum after maximum light. The *intensity ratio* λ 4308:λ 4202 behaves as follows in Me spectra: It is about 1/4 at phase +0.2, and increases steadily to 1 at +0.3 and 4 at +0.55. In type Se, λ 4308 is 2½ times as intense as λ 4202 whenever both are visible. In Me spectra the *intensity ratio* λ 4571:λ 4308 has the following typical values: 2/3 at phase +0.15, 1 at +0.30, and 3 at +0.6.

Wave-lengths and identifications of lines.—The mean wave-lengths of fifty-eight bright lines are recorded in Table VIII. Most of these are true emission lines although a few may be maxima in the absorption spectrum. The elements identified include *H*, *Fe* I, *Fe* II (both allowed and forbidden lines), *Mg* I, *Si* I, *Mn* I, *Sr* II?, *In* I?. The forbidden iron lines and an ultra-violet magnesium triplet have not previously been recorded in these spectra. Data on individual stars, including wave-length measurements and the phases at which certain lines appear, are given in Tables V, VI, and VII and in the notes to Table VIII.

Displacements of bright lines.—The apparent velocities from the *blue-violet lines* are given in Table II. Plots showing the variation with phase are given for eleven stars in Figs. 16, 17, and 18. Algebraically decreasing velocity at and shortly after light-maximum, and a flat minimum 30–80 days after light-maximum are typical features. A maximum in the displacement-curve about 30 days before light-maximum is probably also typical. The range in apparent velocity is about 10 km/sec., probably being larger for the stars with the shorter periods. The phenomena appear essentially the same for Me and Se variables. The mean displacement of the *bright Hα line* relative to the blue-violet bright lines is found to be −0.34 A for three stars of type Me and −0.04 A for two of type Se.

Discussion.—Most of the bright lines behave as if they had little *dependence on the photosphere.* In discussing the *effects of band absorption,* the existence of titanium oxide

above the level at which the bright lines are produced is suggested as a working hypothesis to explain the abnormally low intensities of $H\alpha$, $H\beta$, and $H\gamma$ relative to $H\delta$. The fraction of the total band absorption to which the bright lines are subject may be greatest at the first appearance of the lines after minimum and grow less as the phase advances. The bearing of the behavior of the bright lines on *theories of long-period variables* is briefly discussed.

INTRODUCTION

Bright lines are well-known features of the spectra of numerous long-period variable stars, the most conspicuous being the hydrogen lines $H\delta$, $H\gamma$, and sometimes $H\beta$; the iron lines λλ 4202, 4308; and the magnesium line λ 4571. Many instances of variations in intensities of these lines, especially those of hydrogen, have been noted by the Harvard observers.[1] The behavior of the bright lines in the spectrum of *o* Ceti has been studied in detail by Stebbins[2] and by Joy;[3] and one of the present writers has found that approximately the same course of variations is exhibited by several other M-type variables.[4] Observations of the same lines in S-type variables have revealed systematic differences as compared with the Me variables.[5] The principal object of the present paper is a more detailed intercomparison than has heretofore been made of the behavior of the bright lines in several variables.

Photometric data[6] concerning the objects studied are collected in Table I. The next to the last column, $M-m$, gives the interval in days between the minimum and the following maximum of the mean light-curve. The last column gives the fraction obtained by dividing this interval by the period.

The present *Contribution* deals chiefly with the intensities and displacements of the bright lines in the blue-violet region of the spectrum. Outstanding bright lines, other than $H\alpha$, apparently do not occur in the green, yellow, or red. Even $H\alpha$, except in the S-type variables, is much less intense than $H\gamma$ or $H\delta$. This line has been

[1] See *Harvard Annals*, **56**, 209, 1912; *Popular Astronomy*, **36**, 229, 1928; and elsewhere.

[2] *Lick Observatory Bulletins*, **2**, 78, 1903; *Astrophysical Journal*, **18**, 341, 1903.

[3] *Mt. Wilson Contr.*, No. 311; *Astrophysical Journal*, **63**, 281, 1926.

[4] Merrill, *Mt. Wilson Contr.*, No. 200; *Astrophysical Journal*, **53**, 185, 1921; *Mt. Wilson Contr.*, No. 264; *Astrophysical Journal*, **58**, 215, 1923.

[5] Merrill, *Mt. Wilson Contr.*, No. 325; *Astrophysical Journal*, **65**, 23, 1927.

[6] *Harvard Annals*, **79**, 161, 1928.

observed occasionally, however, and a few measurements of its displacement are recorded.

The photographs listed in Table II were obtained with one-prism spectrographs attached to the 100-inch telescope (C series) or the 60-inch telescope (γ series). Most of them were taken with an 18-inch camera; a number taken with a 10-inch camera are indicated by an asterisk, while a few with a 7-inch camera are indicated by a double asterisk. The photometric data were supplied through the

TABLE I

PHOTOMETRIC DATA CONCERNING VARIABLES STUDIED

Star	R.A. 1900	Dec. 1900	Spect.	Max. Mag.	Range in Mags.	Period in Days	$M-m$ in Days	$\frac{M-m}{p}$
T Cassiopeiae	0^h17^m8	$+55°\ 14'$	M8e	8.2	3.7	443	247	0.56
o Ceti	2 14.3	− 3 26	M6e	3.4	5.8	331.6	120	.36
U Orionis	5 49.9	+20 10	M8e	6.0	5.8	372.2	131	.35
R Geminorum	7 1.3	+22 52	Se	7.1	6.1	370	131	.35
R Leonis	9 42.2	+11 54	M8e	5.9	4.2	313	136	.43
S Ursae Majoris	12 39.6	+61 38	Se	7.9	3.6	225.3	110	.49
R Hydrae	13 24.2	−22 46	M7e	4.2	5.3	405	197	.49
W Hydrae	13 43.4	−27 52	M8e	7.1	2.8	385.6	198	.51
R Serpentis	15 46.1	+15 26	M7e	6.9	6.1	357.2	140	.39
R Cygni	19 34.1	+49 58	Se	7.4	6.5	425.5	157	.37
χ Cygni	19 46.7	+32 40	M6pe	5.1	8.2	406.6	167	.41
T Cephei	21 8.2	+68 5	M7e	6.1	4.0	387	211	.54
R Cassiopeiae	23 53.3	+50 50	M7e	7.1	5.8	431.4	167	0.39

kindness of Shapley and Leon Campbell, of the Harvard College Observatory.

The numerical values of the intensities of $H\beta$, $H\gamma$, $H\delta$, $\lambda\lambda$ 4202, 4308, and 4571, given in Table II, are estimates made directly from the plates as viewed in the measuring microscope. The scale was established by assuming that intensity 1 corresponds to a line just strong enough to allow an accurate setting of the micrometer wire. Other intensities represent the observer's attempt to estimate the amount of darkened silver grains in the image in terms of the standard line of intensity 1. Intensities 2–4 correspond to lines best suited to accurate measurement of position. Fractional intensities indicate badly underexposed images; intensities greater than 10, overexposed images. The values given in Table II are the means of several estimates but cannot lay claim to high accuracy.

TABLE II

JOURNAL OF OBSERVATIONS AND DATA CONCERNING BRIGHT LINES

	PLATE	DATE	MAG.	PHASE DAYS	VEL. KM/SEC.	INTENSITIES					
						$H\delta$	4202	4308	$H\gamma$	4571	$H\beta$
					T Cassiopeiae						
C	21	1919 Aug. 29	9.1	−132	−25.9	3	.....	.....	0.5	.....	.....
	25	Aug. 31	9.0	−130	−25.9	2	.....	.....	.....	.....	.....
	48	Sept. 5	8.9	−125	.....	4	.....	.....	0.5	.....	.....
	55	Sept. 7	8.8	−123	−22.0	1	.....	.....	.....	.....	.....
γ	8724	Oct. 3	8.2	− 97	−26.8	1	.....	.....	.....	.....	.....
C	124	Oct. 14	8.1	− 86	−20.8	3	0.6	.....	1	.....	.....
	192	Nov. 9	8.3	− 60	−25.4	4	.9	.....	1	.....	.....
	2350*	1923 July 26	8.4	− 39	−22.5	6	.....	.....	2	.....	.....
	2413*	Aug. 30	7.9	− 4	−26.0	5	.6	.....	2	.....	.....
	2471	Oct. 1	7.8	+ 28	−27.7	2	0.6	.....	2	.....	.....
	2513*	Oct. 27	8.0	+ 54	−23.2	2	1	0.8	2	.....	.....
γ	13163	1925 Jan. 5	7.7	+ 56	−22.3	3	0.9	.4	4	.....	.....
	15949	1928 July 5	8.1	− 35	−26.8	3	.....	.....	0.8	.....	.....
	16053	Aug. 4	7.7	− 5	−28.1	4	.6	.....	2	.....	.....
	16133	Aug. 30	7.6	+ 21	−21.3	4	0.8	.2	3	.....	.....
C	5023	Oct. 4	8.4	+ 56	−22.0	2	1	0.9	2	0.8	0.5
					U Orionis						
C	44	1919 Sept. 4	8.0	+ 75	−32.7	8	0.8	.....	4	.....	.....
	638	1920 Sept. 2	7.0	+ 46	−40.0	10	0.9	.....	7	.....	.....
	671	Sept. 26	8.0	+ 70	−39.3	10	2	.....	8	.....	.....
	727	Oct. 26	8.6	+100	−35.2	8	2	0.8	6	0.9	0.2
	2472	1923 Oct. 1	7.4	+ 44	−33.8	10	0.8	.....	7	.....	.....
	2518	Oct. 28	8.1	+ 71	−33.9	9	1	0.2	5	.....	.....
	2651*	1924 Jan. 23	10.3	+158	−31.1	2	3	4	1	7	0.2
	2704*	Feb. 22	11.0	+188	−23	.....	0.2	0.4	.....	0.9	.....
	3989.5*	1926 Aug. 23	6.7	− 23	.....	2	.....	.....	0.8	.....	.....
	3990*	Aug. 23	6.7	− 23	−29	6	.....	.....	3	.....	.....
γ	14467	Aug. 25	6.6	− 21	−32.7	4	.....	.....	3	.....	.....
C	4015	Sept. 17	5.9	+ 2	−37.2	8	.....	.....	5	.....	1
γ	14532	Sept. 20	5.9	+ 5	−36.9	8	.....	.....	7	.....	1
C	4067	Oct. 22	6.6	+ 37	−39.2	8	0.8	.....	5	.....	0.5
γ	14751	Nov. 27	8.4	+ 73	−43.5	7	1	.4	4	0.5	0.4
C	4481	1927 Oct. 13	6.8	+ 21	−30.3	12	.....	.....	7	.....	.....
	4488*a*	Oct. 14	6.9	+ 22	−32.5	7	.....	.....	6	.....	.....
	4488*b*	Oct. 14	6.9	+ 22	−34.5	7	.....	.....	5	.....	.....
γ	15352	Oct. 19	7.2	+ 27	−36.9	4	.....	.....	2	.....	.....
C	4504*b*	Oct. 28	7.5	+ 36	−37.9	0.5	.....	.....	.....	.....	.....
	4504*c*	Oct. 28	7.5	+ 36	−39.1	2	.....	.....	0.6	.....	.....
	4504*d*	Oct. 28	7.5	+ 36	−37.8	2	.....	.....	0.8	.....	.....
	4538	Nov. 10	7.8	+ 49	−32.4	10	0.6	.....	6	.....	.....
	4611	1928 Jan. 4	8.9	+104	−32.6	6	0.9	.....	4	.....	.....
	4677*	Feb. 10	(9.8)	+141	−31.4	3	1	0.4	3	.....	.....

TABLE II—*Continued*

	Plate	Date	Mag.	Phase Days	Vel. Km/Sec.	Intensities					
						$H\delta$	4202	4308	$H\gamma$	4571	$H\beta$
					R Geminorum						
γ	8727	1919 Oct. 3	7.4	− 23	−57.8	0.4	.....	.....	3	.....	8
C	127	Oct. 14	7.0	− 12	−54.3	2	.....	.....	6	.....	10
	133	Oct. 15	7.0	− 11	−55.5	2	.....	.....	6	.....	12
	144	Oct. 17	7.0	− 9	−56.5	2	.....	.....	7	.....	12
	238	1920 Jan. 9	8.7	+ 75	.....	.....	.....	.....	0.2	.....	0.4
	681	Sept. 28	7.2	− 30	−52.3	.....	.....	.....	2	.....	8
	821	Dec. 27	8.3	+ 60	−59.8	0.4	.....	Tr	4	.....	9
	1339	1921 Sept. 21	8.1	− 50	−57.5	.....	.....	.....	0.4	.....	4
γ	10524	Oct. 10	7.2	− 31	−62.2	0.9	.....	.....	6	.....	14
C	1402	Oct. 13	7.1	− 28	−52.8	.....	.....	.....	(1)	.....	6
	1408	Oct. 14	7.1	− 27	−52.2	.....	.....	.....	?	.....	4
	1456	Nov. 13	7.2	+ 3	−58.7	2	.....	Tr?	8	.....	15
	1501	Dec. 15	7.3	+ 35	−55.2	2	.....	0.4	7	.....	12
	1502	Dec. 15	7.3	+ 35	−54.9	0.2	.....	0.2	2	.....	8
	2003	1922 Nov. 6	6.6	+ 10	−56.0	6	0.4	.....	14	.....	(25)
	2062	1923 Jan. 6	7.6	+ 71	−62.0	1	.....	Tr?	5	.....	9
	2480*	Oct. 3	9.1	− 58	−60.1	.....	.....	.....	1	.....	4
	2515*	Oct. 27	7.8	− 34	.....	.....	.....	.....	2	.....	6
	2519	Oct. 28	7.8	− 33	−52.9	.....	.....	.....	1	.....	7
	2563*	Nov. 27	7.3	− 3	−58.4	.....	.....	.....	2	.....	8
	2701*	1924 Feb. 21	9.2	+ 83	−53.5	.....	.....	0.4	5	.....	12
γ	13098	Nov. 11	6.8	− 9	−63.4	2	.....	.....	9	.....	18
C	3097	Dec. 13	7.0	+ 23	−58.5	6	.4	.7	12	.....	25
	3574*	1925 Oct. 30	6.8	− 20	−57.5	2	.....	.....	9	.....	20
	3623	Dec. 26	7.1	+ 37	−55.5	4	.2	.8	10	.....	24
	3647	1926 Jan. 4	7.2	+ 46	−58.0	2	.....	0.3	7	.....	13
	3671*	Jan. 25	7.7	+ 67	−52.6	4	0.6	1	9	.....	16
	3694*	Feb. 21	9.0	+ 94	−56.0	3	1	2	8	0.6	15
					R Leonis						
C	257	1920 Jan. 16	9.0	− 64	+ 3.1	2	.....	.....	.....	.....	.....
	367	Apr. 8	6.4	+ 19	− 1.6	14	2	.....	10	.....	.....
γ	9147	Apr. 11	6.5	+ 22	− 4.5	14	2	.....	10	.....	.....
	9148	Apr. 11	6.5	+ 22	− 4.9	9	0.8	.....	5	.....	.....
	9173	May 5	7.4	+ 46	− 1.6	14	4	2	13	1	.....
	9201	May 11	7.6	+ 52	− 1.0	13	4	3	14	2	.....
C	446	May 30	8.3	+ 71	+ 1.6	4	3	2	5	2	.....
	818	Dec. 26	5.8	− 15	− 0.3	10	.....	.....	6	.....	.....
	865	1921 Jan. 28	6.2	+ 18	− 1.6	15	1	.....	10	.....	.....
	910	Feb. 25	6.9	+ 46	+ 0.8	15	4	.....	10	.....	.....
	918	Feb. 26	6.9	+ 47	+ 1.0	16	4	1	10	.....	.....
	960	Mar. 26	7.7	+ 75	− 2.0	6	2	1	4	1	.....
	963	Mar. 27	7.7	+ 76	+ 2.6	9	4	2	6	2	.....
	1004	Apr. 28	8.7	+108	+ 1.7	2	4	4	3	5	.....
	1504	Dec. 15	6.0	+ 12	− 5.8	10	1	.....	6	.....	.....
	2016	1922 Dec. 8	7.0	+ 63	+ 2.4	4	0.8	.....	2	.....	.....
	2564*	1923 Nov. 27	9.0	+117	− 0.8	0.8	4	7	2	10	.....

TABLE II—*Continued*

Plate	Date	Mag.	Phase Days	Vel. Km/Sec.	Intensities					
					$H\delta$	4202	4308	$H\gamma$	4571	$H\beta$
R Leonis—*Continued*										
C 2569	1923 Nov. 28	9.0	+118	− 0.3	.....	(0.3)	0.8	.....	1	.....
2594	Dec. 24	9.7	+144	+ 0.9	.....	1	3	.....	5	.....
2952*	1924 Jan. 23	10.2	+174	+ 2	.....	1	3	Tr	6	.....
2798*	May 21	6.9	− 36	+ 3.8	10	.....	.....	2	.....	.....
2802	May 22	6.8	− 35	+ 2.1	3	.....	.....	0.8	.....	.....
γ 14763	1926 Dec. 14	6.1	− 8	+ 0.8	8	.....	.....	4	.....	.....
C 4192	1927 Feb. 18	6.6	+ 58	− 3.6	5	0.8	.....	2	.....	.....
4226*	Apr. 14	8.2	+113	− 1.0	2	4	4	2	4	.....
4267*	May 13	8.8	+142	− 8.2	.....	1	2	.....	3	.....
4273*	May 15	8.8	+144	− 1.6	.....	2	3	.....	4	.....
4593	Dec. 23	6.6	+ 50	− 8.0	10	3	0.9	7	0.6	.....
4612	1928 Jan. 4	7.0	+ 62	− 6.0	8	3	2	8	1	.....
4616*a*	Jan. 5	7.1	+ 63	−12.0	3	0.9	0.4	2	.....	.....
4616*b*	Jan. 5	7.1	+ 63	−12.1	2	Tr	.....	0.9	.....	.....
4678*	Feb. 10	8.3	+ 99	+ 0.7	6	5	6	4	5	.....
4681	Feb. 11	8.3	+100	− 2.7	6	6	7	5	8	.....
4707*	Mar. 16	8.9	+134	+ 9.5	1	4	6	1	10	0.7
4712	Mar. 17	8.9	+135	+ 6.4	0.2	2	3	0.4	5	.....
4745*	Apr. 12	9.7	+161	+11.3	.....	0.6	2	.....	3	.....
4748*	Apr. 14	9.8	+163	− 7.5	.....	5	8	0.9	14	.....
4793*	May 2	10.0	+181	+ 7.7	.....	0.2	1	.....	2	.....
4796*	May 3	10.0	+182	+ 3.0	.....	0.9	2	.....	5	.....
5088*	Nov. 29	7.4	+ 65	+ 3.9	7	2	1	4	1	.....
5098	Dec. 20	8.6	+ 86	+ 0.4	2	1	1	1	2	Tr
5129*	1929 Jan. 24	8.9	+121	+ 2.9	0.6	4	6	0.7	9	.....
5141*	Feb. 28	10.2	+156	+11.6	.....	0.7	2	.....	3	.....
5152*	Mar. 20	10.2	+176	+ 5.4	.....	(0.3)	0.6	.....	1	.....
5172*	Apr. 26	9.7	− 92	.....	.....	.....	.....	.....	.....	.....
5188*	May 22	8.6	− 66	.....	Tr	.....	.....	.....	.....	.....
5191*	May 23	8.6	− 65	+ 7	0.6	.....	.....	.....	.....	.....
5219	June 21	7.0	− 36	+ 5	1	.....	.....	0.5	.....	.....
S Ursae Majoris										
C 369	1920 Apr. 8	8.5	− 37	− 4.2	.....	.....	.....	2	.....	6
373	Apr. 10	8.5	− 35	− 7.2	.....	.....	.....	4	.....	9
γ 9252	June 3	8.2	+ 19	− 6.6	.....	.....	.....	2	.....	5
9848	Dec. 29	8.4	+ 18	−10.1	0.6	.....	.....	3	.....	4
C 866	1921 Jan. 28	8.7	+ 48	− 7.1	.....	.....	Tr	2	.....	4
1169**	July 23	8.1	− 3	−13.4	.8	.....	.....	4	.....	8
1553	1922 Feb. 11	8.5	− 26	+ 4.1	.....	.....	.....	3	.....	7
1626	Mar. 19	7.6	+ 10	− 3.7	.8	.....	.....	5	.....	7
γ 11744**	1923 May 1	8.5	− 42	+ 6.2	.....	.....	.....	4	.....	10
C 2286	June 4	8.0	− 8	− 0.6	0.8	.....	.....	4	.....	10
2340	July 3	8.1	+ 21	− 6.8	2	.....	Tr	6	.....	10
2648	1924 Jan. 22	8.0	− 19	− 5.8	0.8	.....	.....	6	.....	11
2702*	Feb. 21	8.2	+ 11	− 1.1	0.7	.....	.....	5	.....	8
3187*	1925 Mar. 3	8.5	− 55	+ 9.6	.....	.....	.....	4	.....	8

TABLE II—*Continued*

Plate	Date	Mag.	Phase Days	Vel. Km/Sec.	Intensities					
					$H\delta$	4202	4308	$H\gamma$	4571	$H\beta$
R Hydrae										
C 450	1920 May 31	9 0	+241	−17.2	.....	.....	0.4	.....	1	.....
532**	July 8	7.9	−124	−23.7	0.9	.....	.....	.....	.....	.....
γ 9890	1921 Jan. 30	6.7	+ 82	−27.0	0.3	.....	.....	0.5	.....	.....
9891	Jan. 30	6.7	+ 82	−18.2	4	1	0.6	5	0.6	Tr?
C 873	Jan. 30	6 7	+ 82	− 25.0	3	0.8	0.4	5	0.6	.....
911	Feb. 25	7.7	+108	−24.4	2	4	5	8	7	3
964	Mar. 27	8.6	+138	−18.8	.....	2	4	1	6	0.6
1010	Apr. 29	9.3	+171	−20.4	.....	0.6	4	.....	7	Tr
1037	May 26	9.6	+198	−21.2	.....	Tr	1	.....	2	.....
1054**	June 19	(9.9)	+222	− 8.2	.....	.....	0.9	.....	3	.....
1562	1922 Feb. 13	5 6	+ 51	−22.4	6	0.8	.2	5	.....	0.4
γ 11509	1923 Jan. 4	5.6	− 31	19.3	8	.....	.....	4	.....	.....
11513	Jan. 5	5.5	− 30	−20.9	8	.....	.....	4	.....	.....
12517	1924 Feb. 24	5.0	− 23	−22.3	14	.....	.....	10	.....	.....
C 2726	Mar. 24	4 0	+ 6	−15.8	12	0.6	.....	10	.....	3
γ 12583	Apr. 19	4.6	+ 32	−28.1	12	2	.....	12	.....	3
12588	Apr. 20	4.7	+ 33	−23.9	2	.....	.....	2	.....	Tr
12589	Apr. 20	4.7	+ 33	−26.5	2	.....	.....	2	.....	Tr
12667	May 20	5.9	+ 63	−28.2	8	2	0.6	10	0.5	4
12693	June 10	6 2	+ 84	−31.3	7	3	3	10	2?	5
12696	June 11	6.3	+ 85	−30.2	4	1	2	8	3	4
14194	1926 May 17	6.3	− 45	−15.3	9	.....	.....	2	.....	.....
14215	May 26	5.8	− 36	−18.1	10	.....	.....	3	.....	.....
14216	May 27	5.8	− 35	−14.5	11	.....	.....	3	.....	.....
C 3808	May 30	5.7	− 32	−12.1	11	.....	.....	3	.....	.....
3812	June 18	4.8	− 13	−12.4	9	.....	.....	6	.....	.....
3817	June 19	4.8	− 12	−24.9	2	.....	.....	2	.....	.....
3822	June 20	4.8	− 11	−17.6	2	.....	.....	0.8	.....	.....
3823	June 20	4.8	− 11	−12.1	(30)	.....	.....	(18)	.....	.....
γ 14269	June 21	4.7	− 10	−23.2	12	.....	.....	7	.....	Tr
14274	June 22	4.7	− 9	−28.6	9	.....	.....	6	.....	Tr
14275	June 22	4.7	− 9	−28.6	5	.....	.....	3	.....	.....
14276	June 22	4.7	− 9	−26.5	4	.....	.....	3	.....	.....
14277	June 22	4.7	− 9	−30.0	7	.....	.....	5	.....	Tr
C 3902	July 24	4.7	+ 23	−16.7	8	0.6	.....	6	.....	0.6
3903	July 24	4.7	+ 23	−17.0	4	.....	.....	3	.....	.....
3904	July 24	4.7	+ 23	−19.5	3	.....	.....	2	.....	.....
γ 14392	July 27	4.8	+ 26	−29.4	4	.....	.....	3	.....	.....
C 4175*	1927 Jan. 17	8.8	+200	−11.4	.....	0.9	2	.....	3	.....
4193*	Feb. 18	8.9	+232	.....	.....	.....	.....	.....	0.5	.....
4204*	Mar. 17	8.9	+259	.....	.....	.....	.....	.....	?	.....
4228	Apr. 14	8.4	−124	.....	.....	.....	.....	.....	.....	.....
4268*	May 13	6.9	− 95	−17.4	4	.....	.....	.....	.....	.....
4274	May 15	6.8	− 93	−31.9	2	.....	.....	0.2	.....	.....
4278	May 21	6.7	− 87	−18.8	3	.....	.....	0.6	.....	.....
γ 15061	June 18	5.9	− 59	−20.4	6	.....	.....	2	.....	.....
15068	June 19	5.9	− 58	−24.4	6	.....	.....	2	.....	.....
C 4318	June 22	5.8	− 55	−22.1	5	.....	.....	2	.....	.....
4323	June 23	5.8	− 54	−14.9	8	.....	.....	3	.....	.....

TABLE II—*Continued*

Plate	Date	Mag.	Phase Days	Vel. Km/Sec.	Intensities					
					$H\delta$	4202	4308	$H\gamma$	4571	$H\beta$
R Hydrae—*Continued*										
γ 15074	1927 July 6	5.2	− 41	−21.0	4	.....	.....	3	.....	.....
15079	July 7	5.1	− 40	−27.8	3	.....	.....	2	.....	.....
C 4360	July 15	4.9	− 32	−20.1	8	.....	.....	5	.....	0.4
4363	July 16	4.9	− 31	−21.5	7	.....	.....	6	.....	Tr
4364	July 16	4.9	− 31	−20.6	4	.....	.....	3	.....	.....
W Hydrae										
C 931	1921 Feb. 28	(7.3)	− 11	+25.8	8	2	.....	6	.....	.....
970	Mar. 28	(6.5)	+ 17	+23.7	6	2	0.7	7	0.9	.....
1033	May 25	(7)	+ 75	+24.4	0.4	0.8	1	1	2	.....
1057	June 20	(8)	+101	+25.0	.....	1	2	0.6	4	0.7
1664	1922 Apr. 13	(7)	+ 8	+29.0	7	2	.....	5	.....	.....
1701	May 15	(7.2)	+ 40	+27.3	4	2	1	6	1	.2
1744	June 11	(7.5)	+ 67	+39.3	.....	0.2	0.4	0.5	1	.....
1751	June 15	(7.5)	+ 71	+27.9	0.3	.8	1	1	2	.....
2073	1923 Jan. 8	(7)	− 87	+30.8	4	.....	.....	0.8	.....	.....
2703*	1924 Feb. 21	(7.5)	(−64)	+37.3	10	0.8	.....	2	.....	.....
2799*	May 21	(6.5)	(+26)	+30.0	4	2	1	8	1	0.7
2819*	June 13	(6.5)	(+49)	+29.2	2	3	2	4	2	2
2885*	July 18	(7.5)	(+84)	+32.9	.....	0.6	3	1	8	3
R Serpentis										
C 398	1920 May 1	7.6	+ 42	+ 3.1	6	0.4	.....	5	.....	0.3
447	May 30	8.8	+ 71	+ 6.1	6	2	1	6	0.7	.6
454	June 1	8.8	+ 73	+ 3.8	6	1	0.8	6	0.8	.6
533**	July 8	10.7	+110	+ 3.0	5	3	4	4	5	.6
1623	1922 Mar. 18	7.1	+ 15	+ 6.6	8	.....	.....	6	.....	.8
γ 11604	1923 Feb. 5	7.4	− 14	+10.1	4	.....	.....	2	.....	.....
C 2145	Mar. 1	7.2	+ 10	+13.0	8	.....	.....	4	.....	0.4
2219	Apr. 30	8.4	+ 70	+ 3.6	4	.....	.....	2	.....	.....
2727	1924 Mar. 24	7.3	+ 35	+ 8.2	10	0.6	.....	10	.....	2
R Cygni										
C 961	1921 Mar. 26	7.2	+ 31	−49.3	2	.....	.....	6	.....	14
965	Mar. 27	7.3	+ 32	−47.0	2	.....	Tr?	6	.....	15
1007	Apr. 28	8.9	+ 64	−44.8	2	Tr?	0.4	6	.....	14
1038	May 26	9.2	+ 92	−43.7	2	0.2	0.8	6	0.5	15
1055**	June 19	9.7	+116	−44.4	2	2	3	7	2	18
1171**	July 23	10.6	+150	−42.5	0.1	0.8	2	2	2	8
γ 11079	1922 May 17	6.8	+ 4	−49.0	0.8	.....	.....	4	.....	9
11117	June 14	8.0	+ 32	−51.1	2	.....	0.2	6	.....	15
C 1784	July 11	8.9	+ 59	−44.4	2	.....	0.3	6	.....	14
2245	1923 May 5	8.5	− 43	−39.4	Tr	.....	.....	0.9	.....	8

TABLE II—*Continued*

Plate	Date	Mag.	Phase Days	Vel. Km/Sec.	Intensities					
					Hδ	4202	4308	*Hγ*	4571	*Hβ*
R Cygni—*Continued*										
γ 11843....	1923 June 5	6.4	− 12	−53.2	4	.....	.....	9	.....	19
11912....	June 30	6.5	+ 13	−42.6	5	.....	0.8	9	.....	18
C 2411*...	Aug. 30	8.5	+ 74	−48.0	4	1	2	11	.....	20
2474*...	Oct. 2	9.8	+107	−37.1	0.9	1	2	5	2	11
2510*...	Oct. 26	10.3	+131	−41.0	.....	1	3	2	3	7
2886*...	1924 July 18	9.5	− 45	−39.4	0.2	.....	.....	3	.....	7
2918*...	Aug. 9	7.8	− 23	−43.2	0.4	.....	.....	3	.....	9
3019....	Sept. 16	8.2	+ 15	−43.9	2	.....	0.4	5	.....	14
3536*...	1925 Sept. 30	7.4	− 33	−40.8	2	.....	.....	4	.....	12
3572*...	Oct. 30	6.8	− 3	−45.4	2	.....	.....	6	.....	15
χ Cygni										
C 449....	1920 May 30	8.2	− 38	−15.3	8	.....	.....	1	.....	0.6
455....	June 1	8.1	− 36	−17.9	6	.....	.....	1	.....	Tr
γ 9315....	June 30	5.2	− 7	−20.7	14	.....	.....	8	.....	7
C 559....	July 29	5.8	+ 22	−20.6	15	2	0.6	8	.....	7
641....	Sept. 3	6.5	+ 58	−18.8	12	2	2	8	0.9	4
669....	Sept. 26	8.1	+ 81	−18.8	7	2	3	8	2	3
724....	Oct. 26	9.6	+111	−13.0	2	4	5	4	4	2
1204**..	1921 Aug. 13	5.4	− 5	.....	10	.....	.....	2	.....	.....
2362*...	1923 July 27	9.4	−102	−18.8	0.6	.....	.....	.....	.....	.....
2407*...	Aug. 29	7.8	− 69	−10.5	9	.....	.....	0.4	.....	.....
2438....	Sept. 6	7.6	− 61	− 8.5	9	.....	.....	1	.....	.....
2466....	Sept. 30	6.0	− 37	− 6.6	10	.....	.....	4	.....	2
γ 12232....	Oct. 25	4.7	− 12	−17.8	16	.....	.....	9	.....	(8)
C 2561*...	Nov. 26	5.2	+ 20	−15.2	12	0.8	.....	8	.....	(5)
DVI 83....	1926 July 30	11.9	+178	.....	.....	1	3	0.3	3	?
C 4272*...	1927 May 14	7.6	+ 63	−12.8	5	0.8	1	3	0.8	2
γ 14997....	May 17	7.7	+ 66	−20.3	7	2	2	5	1	3
15065....	June 18	9.1	+ 98	−14.2	2	0.8	1	1	0.9	0.2
C 4319....	June 22	9.2	+102	−20.0	6	4	5	5	4	2
4353*...	July 13	10.0	+123	−12.5	2	6	7	3	8	2
4379*...	Aug. 13	11.2	+154	−13.4	.....	2	4	.....	5	.....
4413*...	Sept. 8	12.0	+180	−10.3	.....	2	4	.....	6	.....
4747....	1928 Apr. 13	5.5	− 23	−10.1	8	.....	.....	3	.....	2
γ 15709....	Apr. 15	5.4	− 21	−21.0	6	.....	.....	3	.....	3
15710....	Apr. 15	5.4	− 21	−21.0	8	.....	.....	4	.....	4
C 4757....	Apr. 15	5.4	− 21	− 9.9	6	.....	.....	3	.....	3
4758....	Apr. 15	5.4	− 21	− 8.6	7	.....	.....	4	.....	4
4759....	Apr. 15	5.4	− 21	−11.8	9	.....	.....	5	.....	4
4760....	Apr. 15	5.4	− 21	−11.9	10	.....	.....	5	.....	4
4800*a...	May 3	5.0	− 3	.....	0.9	.....	.....	0.4	.....	Tr
4800*b...	May 3	5.0	− 3	.....	2	.....	.....	1	.....	0.8
4800*c...	May 3	5.0	− 3	.....	7	.....	.....	4	.....	3
4800*d...	May 3	5.0	− 3	.....	10	.....	.....	7	.....	6
4866....	June 28	6.6	+ 53	.....	10	0.8	.....	6	.....	2
γ 15948....	July 5	7.1	+ 60	−14.3	10	1	0.6	6	.....	3

TABLE II—*Continued*

Plate	Date	Mag.	Phase Days	Vel. Km/Sec.	Intensities					
					$H\delta$	4202	4308	$H\gamma$	4571	$H\beta$
χ Cygni—*Continued*										
γ 15950	1928 July 6	7.2	+ 61	−19.6	8	2	1	6	.....	2
16051	Aug. 4	8.7	+ 90	−23.3	1	.....	.....	0.9	.....	.....
16052	Aug. 4	8.7	+ 90	−19.5	5	1	0.8	3	0.4	0.3
C 4958	Aug. 29	9.7	+115	−15.7	2	4	4	3	2	1
5021*	Oct. 4	11.2	+151	− 4.5	0.2	3	6	0.8	4	.....
5058*	Nov. 1	12.2	+179	+ 2.2	.....	1	2	.....	2	.....
R Cassiopeiae										
C 674	1920 Sept. 27	8.6	+ 55	+ 5.7	6	0.2	.....	3	.....	.....
735	Oct. 28	9.2	+ 86	+ 4.8	8	1	.....	3	(0.4)	.....
γ 11504	1923 Jan. 4	7.4	+ 32	+ 5.3	4	.....	.....	1	.....	.....
C 2000	Jan. 8	7.5	+ 36	+12.6	10	0.4	.....	4	.....	.....
2475*	Oct. 2	11.6	−143	.....	.....	.....	.....	.....	.....	.....
γ 14273	1926 June 21	6.1	− 1	+10.5	8	.....	.....	6	.....	.....
14280	June 22	6.1	0	+11.2	14	.....	.....	9	.....	.....
14281	June 22	6.1	0	+ 6.7	3	.....	.....	2	.....	.....
C 3844	June 22	6.1	0	+12.8	6	.....	.....	4	.....	.....
3912	July 25	7.4	+ 33	+11.8	10	1	.....	7	.....	0.4
3913	July 25	7.4	+ 33	+ 5.8	6	0.2	.....	4	.....	.....
γ 14396	July 27	7.4	+ 35	+ 0.9	8	.....	.....	4	.....	.....
C 3994	Aug. 24	8.1	+ 63	+ 6.9	2	.....	.....	1	.....	.....
γ 14465	Aug. 25	8.2	+ 64	+ 6.4	6	.2	.....	4	.....	.....
14505	Sept. 16	8.6	+ 86	+ 3.6	3	0.5	.....	2	.....	.....
C 4013	Sept. 17	8.6	+ 87	+ 3.5	6	2	0.8	5	0.8	.....
4066	Oct. 22	9.4	+122	+ 7.1	6	4	4	5	2	1
4124*	Dec. 11	10.6	+172	+11.0	0.6	2	4	1	5	0.5
4320	1927 June 23	10.1	+ 68	+ 5.0	0.6	.....	.....	.....	.....	.....
4355	July 13	8.7	+ 48	+12.7	2	.....	.....	1	.....	.....
4423	Sept. 10	7.0	+ 11	+10.6	10	.....	.....	6	.....	.....
γ 15273	Sept. 16	7.1	+ 17	+ 3.2	8	.....	.....	4	.....	.....
15278	Sept. 17	7.2	+ 18	+ 5.0	2	.....	.....	0.8	.....	.....
15279	Sept. 17	7.2	+ 18	+ 3.4	2	.....	.....	0.5	.....	.....
C 4537	Nov. 10	8.2	+ 72	+ 7.4	7	0.5	.....	3	.....	.....
4618*	1928 Jan. 6	9.7	+129	+18.6	9	3	2	4	1	.....
5027	Oct. 5	7.4	− 31	+11.6	5	.....	.....	2	.....	.....
5028	Oct. 5	7.4	− 31	+18.1	2	.....	.....	0.6	.....	.....
γ 16239	Oct. 6	7.3	− 30	+12.0	2	.....	.....	0.7	.....	.....
16240	Oct. 6	7.3	− 30	+15.1	7	.....	.....	2	.....	.....

It is not feasible to pass from the apparent intensities in Table II to the actual intensities in the light of the variables, for the reason that length of exposure, seeing, transparency of the air, guiding, slit-width, and other factors cannot be taken into account with sufficient accuracy. The *relative* intensities of two lines in the same

spectral region may, however, be determined within reasonable limits of uncertainty. In this paper, accordingly, attention is given to the intensity ratios of pairs of lines, especially to the variations of such ratios with phase in the light-cycle. The data are suitable for a general comparative survey rather than for an exhaustive investigation of individual stars.

The apparent intensity ratios as estimated from the spectrograms have been used without corrections. Hence it is doubtless true that the data contain systematic errors arising from instrumental and photographic effects, but these errors are probably not extremely large. Moreover, the interest lies not so much in the actual values of the ratios as in their variations with phase, and here systematic errors are not important.

The ratios used in the numerous plots which exhibit the data were not calculated from the figures in Table II, but were estimated directly from the spectrograms. While this was being done, however, the estimated intensities of individual lines were recorded, and the means of these values, rounded off to the nearest integer (except those less than unity), appear in Table II. In some of the figures, material not plotted has been used in determining the position of the ends of the curves. This consists of plates on which only one line of the pair is well seen, but from which a limiting value may be obtained.

For some of the pairs of lines the ratios vary from small fractional values to three or more. In these cases the variations are exhibited better by using logarithms of the ratios rather than the ratios themselves; and to make the plots uniform, logarithms have been used throughout.

THE INTENSITY RATIO $H\gamma:H\delta$

In Figures 1 and 2 the logarithms of the ratio $H\gamma:H\delta$ from individual plates are plotted against the phase counted in days from light-maximum.

o Ceti.—The data for the plot (Fig. 1) were taken largely from Table IX of Joy's paper,[1] supplemented by additional unpub-

[1] *Mt. Wilson Contr.*, No. 311; *Astrophysical Journal*, 63, 281, 1926.

lished estimates which he has been kind enough to make available to us. The spectrograms were taken during the years 1916–1926. The points near maximum and before it lie somewhat higher than

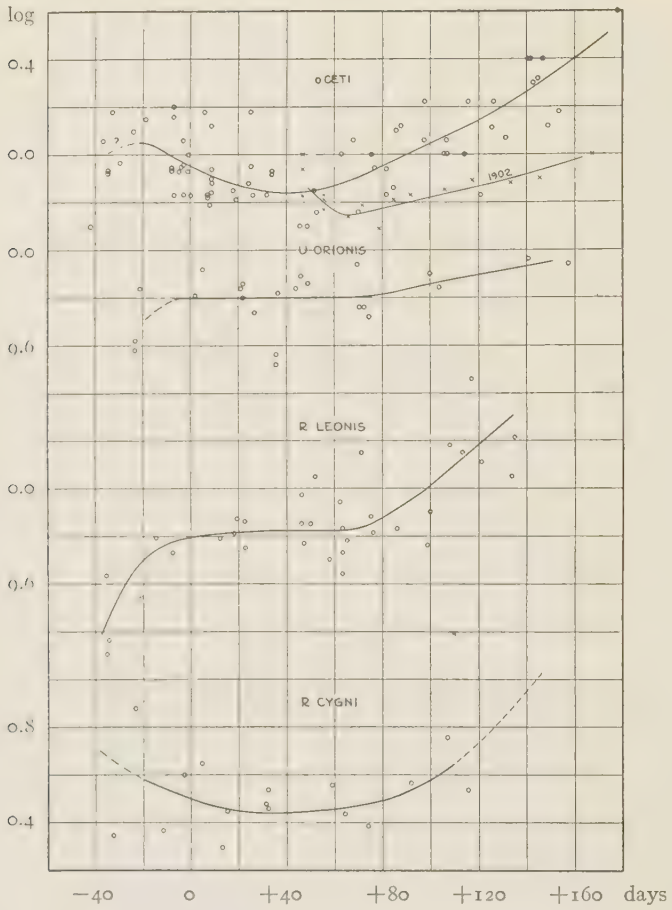

FIG. 1.—Intensity ratio $H\gamma : H\delta$. In the plot for o Ceti, circles represent estimates by Joy, crosses estimates by Stebbins.

for the other Me variables, with considerable scattering. The behavior is thus not quite typical. The beginning of the curve is probably raised by the influence of the bright lines of the companion, but this can scarcely be true at maximum, for at that time the bright

$H\gamma$ and $H\delta$ lines belonging to the spectrum of the variable are overwhelmingly strong compared to these lines in the companion. At the right end of the plot the companion lines again play a part, but

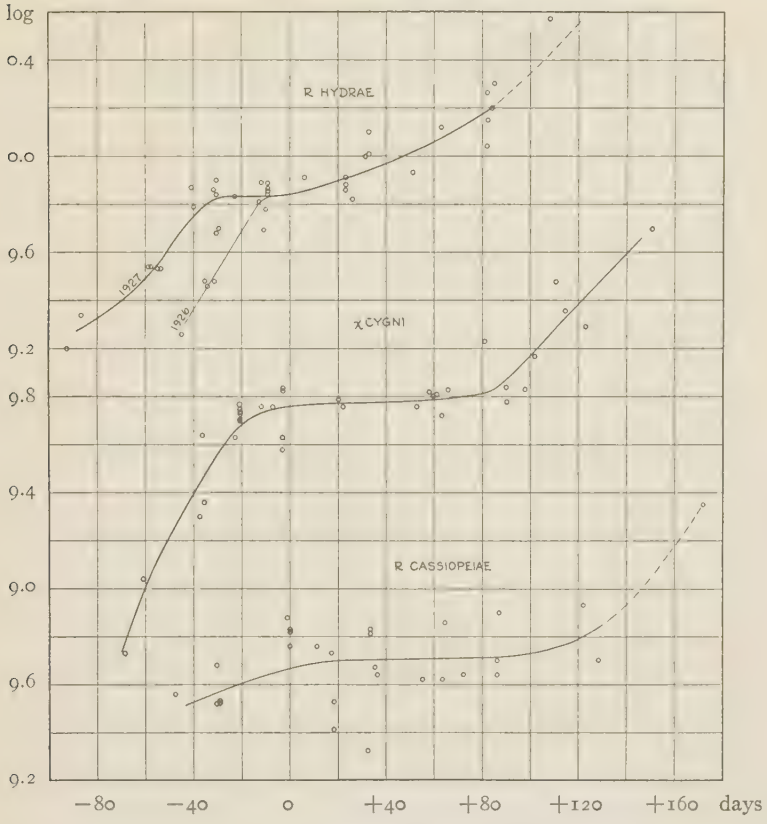

FIG. 2.—Intensity ratio $H\gamma : H\delta$

probably do not here greatly displace the curve, because at this phase the lines have nearly the same ratio in both sources.

Joel Stebbins' observations in 1902[1] are indicated by crosses. At phase +50 days they give the same ratio as Joy's data, but at later phases the ratios are decidedly lower than Joy's. This probably indicates that the scattering of points on the curves may be caused,

[1] *Lick Observatory Bulletins*, **2**, 78, 1903; *Astrophysical Journal*, **18**, 341, 1903.

not only by errors of observation, but by actual differences between individual cycles. Caution should of course be used in comparing intensities on spectrograms obtained with very different instrumental equipment. Joy's tabulated results[1] and those of W. J. S. Lockyer[2] show a slight dependence of the ratio on the magnitude at maximum, the ratio being higher at the brighter maxima. In a complete investigation of these variables it is obvious that the cycles must be studied separately.

U Orionis (Fig. 1).—The bright hydrogen lines are very intense. The number of observations at maximum and before is insufficient to determine the first part of the curve satisfactorily.

R Leonis (Fig. 1).—The form of the curve appears to be that characteristic of emission-line variables having spectra of a late subdivision of class M.

R Cygni (Fig. 1).—Several plates (omitted from the plot) on which $H\delta$ is very weak indicate that the curve rises at both ends, as shown by the dotted portions. For the distribution of the plates on the light-curve see Figure 1, *Contribution* No. 325.[3] The high value of the ratio $H\gamma:H\delta$ at phase -23 is derived from plate C 2918 taken before the low maximum of 1924. The only other plate at this maximum, C 3019, lies near the mean curve. The curve of this S-type star is decidedly different from those of the M-type variables. For a direct comparison see Figure 4.

R Hydrae (Fig. 2).—The observations of 1926 place the first branch of the curve considerably later, i.e., nearer maximum, than do those of 1925. Upon examining the light-curve we find that it had a narrower maximum in 1926 than in 1927, and that the slope immediately preceding maximum was steeper. $H\gamma$ appeared at about the sixth magnitude in both cycles, but the interval between the time of this occurrence and maximum was considerably less in 1926 than in 1927. This suggests that the sequence of the changes of the bright lines may be more closely related to certain features of the rising branch of the light-curve than to the time of maximum.

χ *Cygni* (Fig. 2).—This curve represents an unusually large

[1] *Op. cit.*, Table XIX.

[2] *Monthly Notices of the Royal Astronomical Society*, 84, 563, 1924.

[3] *Astrophysical Journal*, 65, 23, 1927.

change in the ratio, with a well-marked horizontal portion from maximum to phase +80.

R Cassiopeiae (Fig. 2).—The scattering of the observations between phases 0 and +40 may be due largely to errors of observation.

A number of stars in addition to those included in Figures 1 and 2 have reasonably well-determined curves for the ratio $H\gamma:H\delta$. These, with the individual observations omitted, are shown in Figure 3.

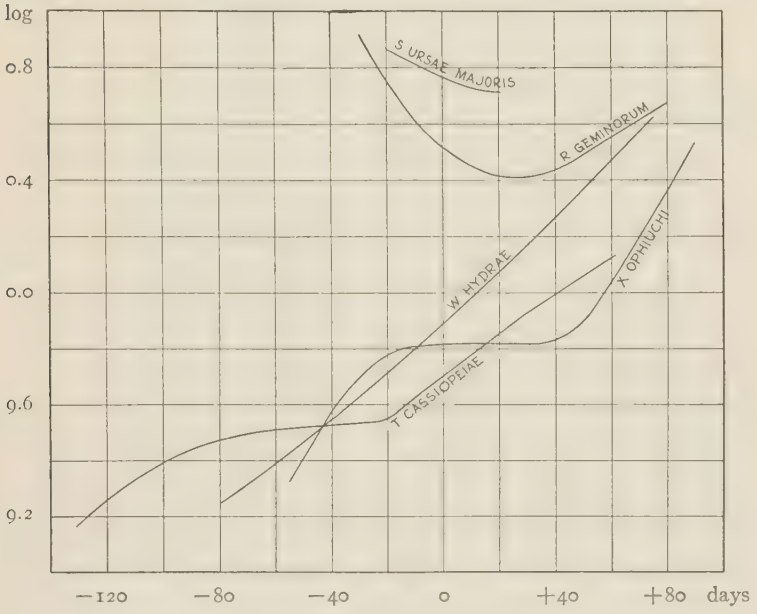

FIG. 3.—Intensity ratio $H\gamma:H\delta$

T Cassiopeiae (Fig. 3).—The flat portion of the curve is short, and the final rise begins at an earlier phase than in most of the Me stars. This may be connected with the unusually long interval from minimum to maximum. The bright hydrogen lines are less intense than in most advanced Me variables. The behavior of these and other bright lines seems to be slightly abnormal.

X Ophiuchi (Fig. 3).—This star is double,[1] but there is no evidence that the companion affects the light emitted by the variable star. The behavior of the ratio $H\gamma:H\delta$ seems to be normal.

[1] *Mt. Wilson Contr.*, No. 261; *Astrophysical Journal*, **57**, 251, 1923.

W Hydrae (Fig. 3).—The flat portion of the curve seems to be missing, the changes being hurried through quickly with no pause after maximum. This may have some connection with the unusually small light-range.

R Geminorum and *S Ursae Majoris* (Fig. 3).—The curves of these S-type stars resemble that of R Cygni (Figs. 1, 4).

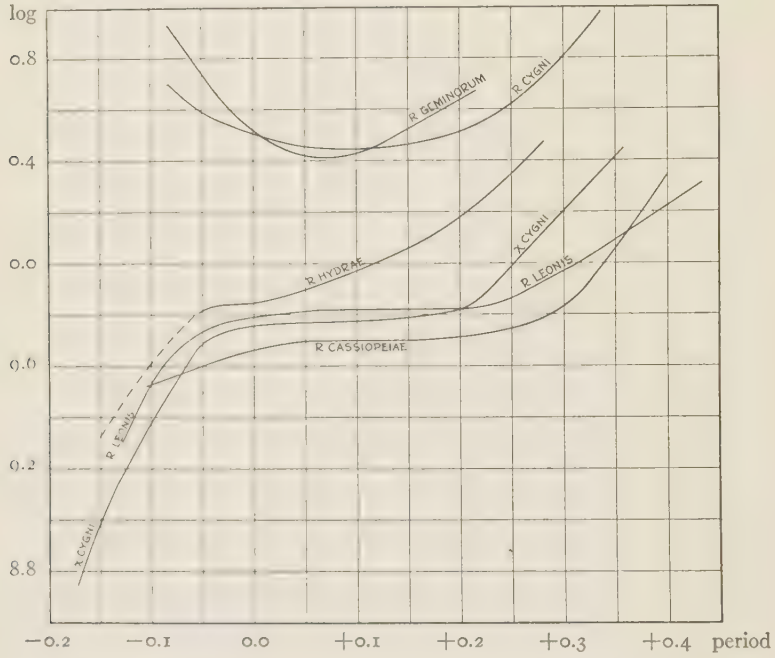

FIG. 4.—Intensity ratio $H\gamma:H\delta$, with phases in fractions of a period

To facilitate comparison, a few of the best-determined curves have been reduced to a common period and plotted together in Figure 4. The phases (abscissae) are here given in fractions of the period instead of days as in the other diagrams. The typical behavior of Me stars may be broadly outlined as follows. At one-fifth of the period before maximum, phase −0.2, the ratio is 1/8;[1] it rises rapidly to 1/2 at −0.05, then remains nearly constant until +0.2, after which it again rises rapidly to $2\frac{1}{2}$ at about +0.4. The behavior in Se stars is very different: The ratio has a minimum of $2\frac{1}{2}$ at phase

[1] The actual ratios are used here instead of logarithms.

+0.07, with considerably higher values both earlier and later. The value of the ratio obtained from a vacuum tube is slightly less than the highest found in Se spectra, but somewhat above the highest in class Me.

In Figure 5 the curves of the Me stars are replotted with the phases counted from minimum light instead of maximum. This procedure seems to bring them into somewhat closer agreement and

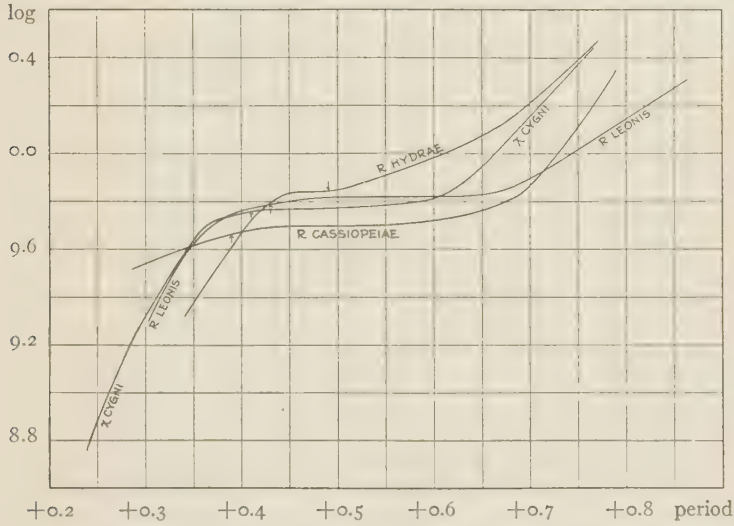

FIG. 5.—Intensity ratio $H\gamma : H\delta$, with phases in fractions of a period from minimum light. Arrows indicate times of maximum light.

suggests that in the periodic behavior of the bright lines, minimum is just as important as maximum; maximum may in fact be a mere incident and not a controlling event.

THE INTENSITY RATIO $H\beta : H\gamma$

In spectra of class Me, bright $H\beta$ is generally much less intense than $H\gamma$ or $H\delta$; in fact, in the later spectral subdivisions it is usually missing. Moreover, its intensity seems to be subject to large variations in different cycles. In general, therefore, the observations are scattering and do not yield well-defined curves for the ratio $H\beta : H\gamma$. In spectra of class Se, $H\beta$ is very intense. Figures 6, 7, and 8, and the following notes give some indication of the behavior of the ratio $H\beta : H\gamma$.

T Cassiopeiae.—One plate, C 5023, at phase +56 shows bright $H\beta$; another, γ 13163, at the same phase does not show it.

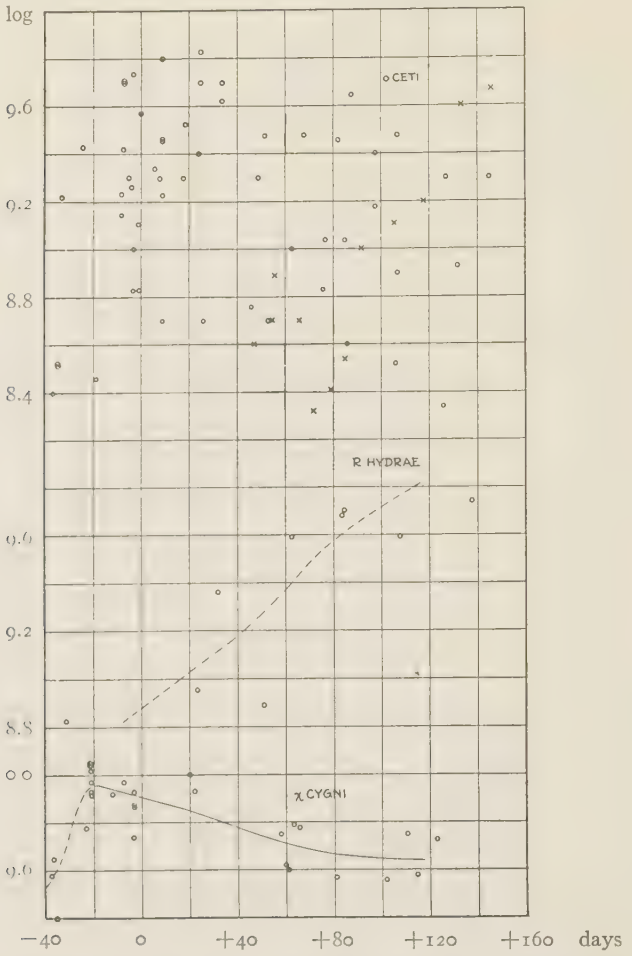

FIG. 6.—Intensity ratio $H\beta:H\gamma$. In the plot for *o* Ceti, circles represent estimates by Joy, crosses estimates by Stebbins.

o Ceti (Fig. 6).—The points are numerous but scatter irregularly over the diagram and do not form a well-defined curve. Joy's tabulation[1] shows a strong dependence on the maximum magnitude at-

[1] *Mt. Wilson Contr.*, No. 311, Table XIX; *Astrophysical Journal*, 63, 281, 1926.

tained at each cycle, $H\beta$ being more intense at the brighter maxima. Stebbins' observations[1] in 1902 indicate a rapid increase in the ratio from phase +60 to +140 days. It is obvious that individual cycles must be studied separately.

R Hydrae (Fig. 6).—The meager material indicates a rapid and continuous increase after maximum.

W Hydrae.—A few observations indicate behavior similar to that of R Hydrae. The rise after maximum may be even more rapid.

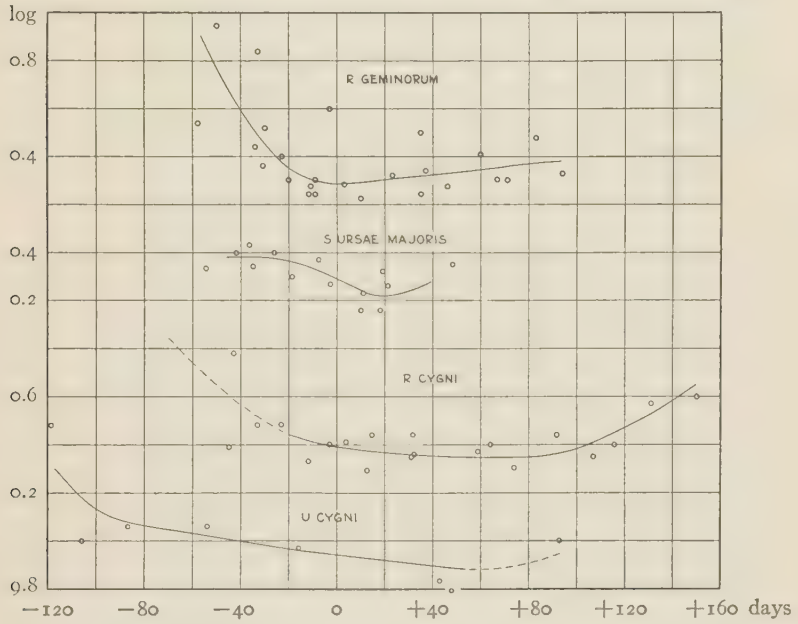

FIG. 7.—Intensity ratio $H\beta:H\gamma$

χ *Cygni* (Fig. 6).—The highest values are near phase −20, with a decrease instead of an increase after maximum. The behavior of the ratio thus more nearly resembles that in S-type spectra than that in class Me. $H\beta$ is, however, relatively weaker throughout in χ Cygni than in R Cygni and R Geminorum (see Fig. 8).

R Cassiopeiae.—$H\beta$ is well marked on only one plate, C 4066, phase +122 days. Traces are seen on two or three other plates taken after maximum.

[1] *Lick Observatory Bulletins*, **2**, 78, 1903; *Astrophysical Journal*, **18**, 341, 1903.

R Geminorum, S Ursae Majoris, R Cygni (Fig. 7).—The curves for these S-type stars are similar and distinctly different from those of class M (excepting χ Cygni). They are high at early and late phases, with a flat minimum after maximum light. The changes are not extremely large.

U Cygni (Fig. 7).—Class R8e, period 461 days: The curve, derived from C. D. Shane's observations,[1] is nearly flat for a consider-

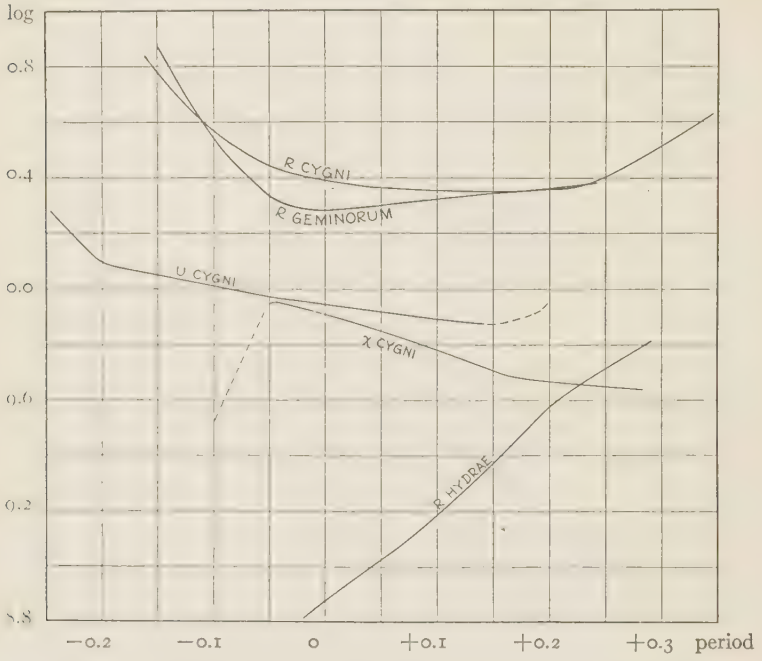

FIG. 8.—Intensity ratio $H\beta$:$H\gamma$, with phases in fractions of a period

able interval before and after maximum. The left end is higher, but at the other end the behavior is uncertain. In general shape, the curve resembles those of class S, but $H\beta$ is relatively less intense.

In Figure 8 several curves, plotted in fractions of the period, are brought together to facilitate comparison.

An experiment with a vacuum tube gave 0.4 for the logarithm of the ratio $H\beta$:$H\gamma$. This is comparable with most of the values for

[1] *Lick Observatory Bulletins*, 10, 79, 1920.

S-type stars but higher than those for U Cygni (R8e) and the stars having titanium oxide bands.

McLaughlin and Petrie have recently made a statistical investigation of the bright hydrogen lines in long-period variables. They have used the intensity ratios $H\gamma:H\delta$ and $H\beta:H\gamma$, as we have done, and have studied their dependence upon spectral type and magnitude relative to minimum light. The brief abstract[1] of their paper at the Forty-first Meeting of the American Astronomical Society, which is the only account of their work available to us, does not indicate that they separated the observations before maximum from those after. Their results are therefore not readily comparable with those in the present *Contribution*, but we do not recognize serious discrepancies in the observational data of the two investigations.

THE INTENSITY RATIO λ 4308:λ 4202

We turn now to consideration of the bright lines at λ 4202 and λ 4308, generally believed to be iron lines. For a discussion of their identification see Joy's paper[2] on *o* Ceti. The periodic changes exhibited by these lines have been previously described.[3] The data concerning the ratio, derived in the same manner as for the hydrogen lines, are represented by Figures 9, 10, 11, and not much description is necessary.

In T Cassiopeiae the presence of λ 4202 long before maximum is an interesting feature probably connected with the large value of $M-m$.

In W Hydrae (Figs. 10 and 11), which has an abnormally small light-range for its period and spectral type, the bright lines λλ 4202, 4308, and 4571 develop more quickly after maximum light than in other Me variables.

The general behavior of the ratio in Me variables is as follows: λ 4308 is first seen at phase +0.1 or +0.2, and is then about one-fourth as intense as λ 4202. Its relative intensity increases at a steady rate, and it becomes equal to λ 4202 at about phase +0.3 and four times as intense at +0.55. The behavior in R Cygni, class

[1] *Popular Astronomy*, **37**, 270, 1929. [2] *Loc. cit.*

[3] *Ibid.*; *Mt. Wilson Contr.*, No. 200; *Astrophysical Journal*, **53**, 185, 1921; *Mt. Wilson Contr.*, No. 325; *Astrophysical Journal*, **65**, 23, 1927.

Se (Figs 9 and 10), is quite different. Whenever both lines are visible in this star, λ 4308 is about two and one-half times as intense as λ 4202. The ratio may have a minimum near phase +0.25. In the

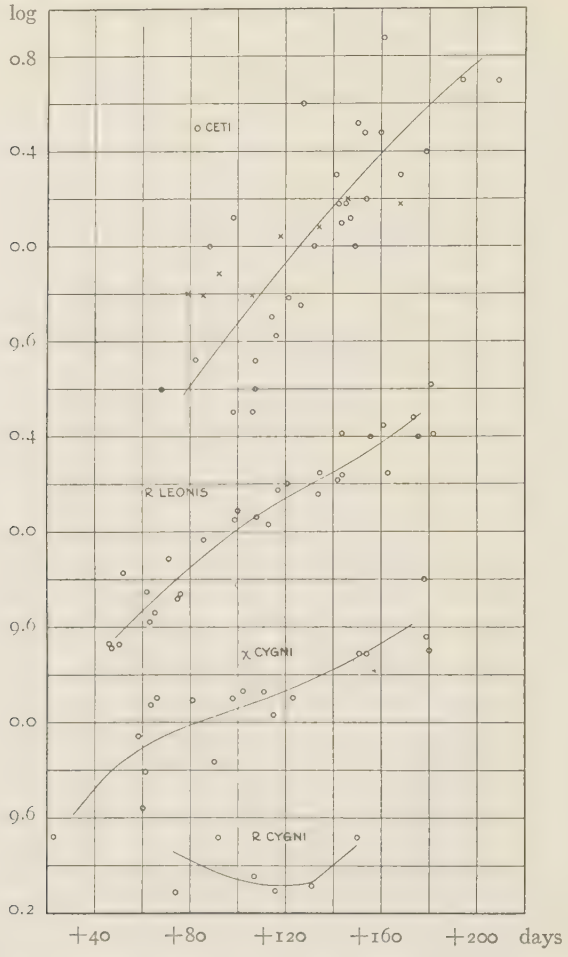

FIG. 9.—Intensity ratio λ 4308:λ 4202. In the plot for o Ceti, circles represent estimates by Joy, crosses estimates by Stebbins.

comparison spectrum (iron arc), λ 4308 appears twice as intense as λ 4202.

It happens in several stars that the lines $H\gamma$, λλ 4202, 4308, become of equal intensity at about the same phase. At this time $H\gamma$

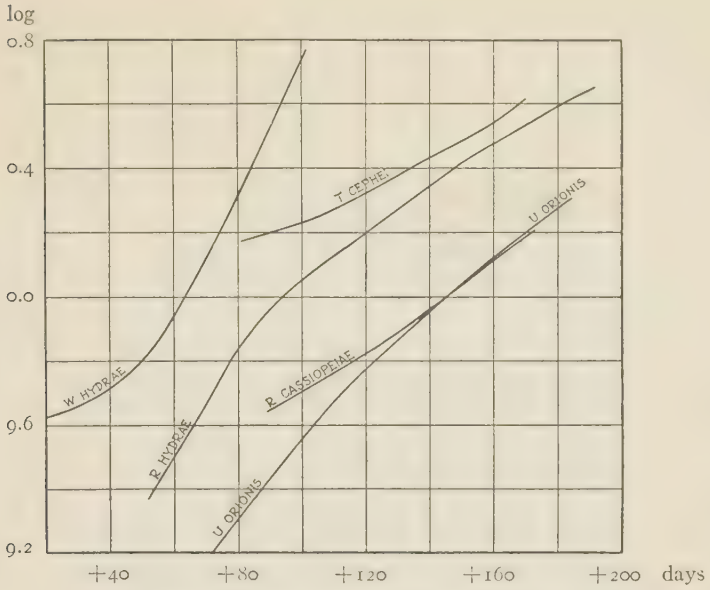

FIG. 10.—Intensity ratio λ 4308:λ 4202

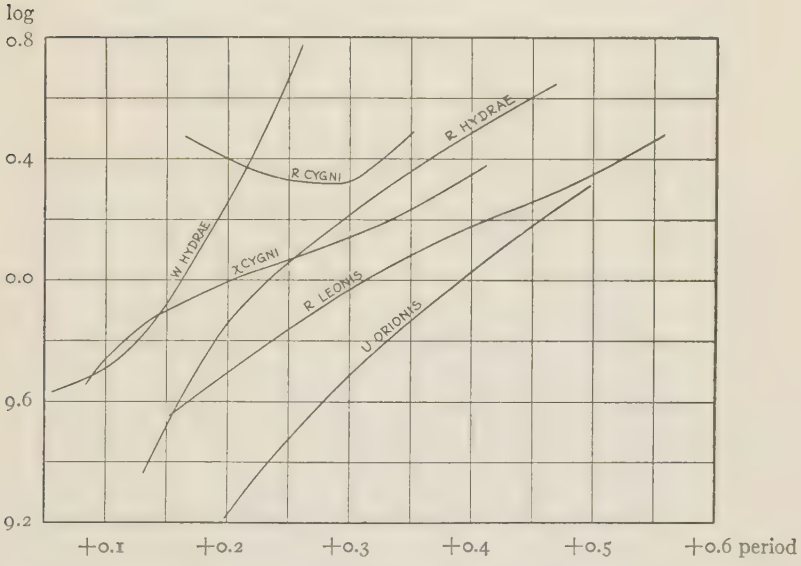

FIG. 11.—Intensity ratio λ 4308:λ 4202, with phases in fractions of a period

is decreasing in intensity with respect to the other two lines, while λ 4202 is decreasing relatively to λ 4308. The approximate mean phases in days and in fractions of the period at which the various lines become equal are shown in Table III.

THE INTENSITY RATIO λ 4571 : λ 4308

The low-temperature magnesium line λ 4571 is the last of the conspicuous bright lines to appear after maximum in each cycle. Toward minimum it frequently becomes the most intense line in the photographic spectrum. The behavior of the ratio λ 4571 : λ 4308 is

TABLE III

PHASES (AFTER MAXIMUM) AT WHICH VARIOUS LINES HAVE EQUAL INTENSITY

STAR	λ 4202 = $H\gamma$		λ 4308 = $H\gamma$		λ 4308 = λ 4202	
	Days	Fraction of Period	Days	Fraction of Period	Days	Fraction of Period
U Orionis	155	0.42	161	0.43	145	0.39
R Leonis	91	.29	93	.30	98	.31
R Hydrae	122	.30	115	.28	94	.23
W Hydrae	87	.23	74	.19	64	.17
X Oph	(95)	(.28)	97	.29	95	.28
χ Cygni	117	.29	107	.26	87	.21
R Cass	142	.33	144	.33	145	0.34
R Cygni	(163)*	(0.38)	133	0.31	†	.....

* Extrapolated.

† λ 4308, whenever visible, is stronger than λ 4202.

displayed in Figures 12, 13, and 14. The changes are not so great as for the other pairs of lines, but λ 4571 tends steadily to become relatively stronger. Typical behavior may be outlined as follows: at phase +0.15, λ 4571 is two-thirds as intense as λ 4308; at +0.25 or 0.30 it is equal to λ 4308; while at +0.6 it is three times as intense.

T Cassiopeiae.—One plate, C 5023, at phase +56 days, shows λ 4571; another, γ 13163, at the same phase does not show it.

U Orionis (Fig. 13).—The intensity of λ 4571 at a given phase varies greatly in different cycles.

W Hydrae (Fig. 13).—The line λ 4571 is typical in behavior, except that it develops more quickly after maximum than in the other variables. This may be connected in some way with the unusually small light-range.

Comparisons of the behavior of a given ratio in different stars are possible by reference to Figures 1–14. In Figure 15 are plotted the curves of the various ratios in R Leonis, χ Cygni, and R Cygni.

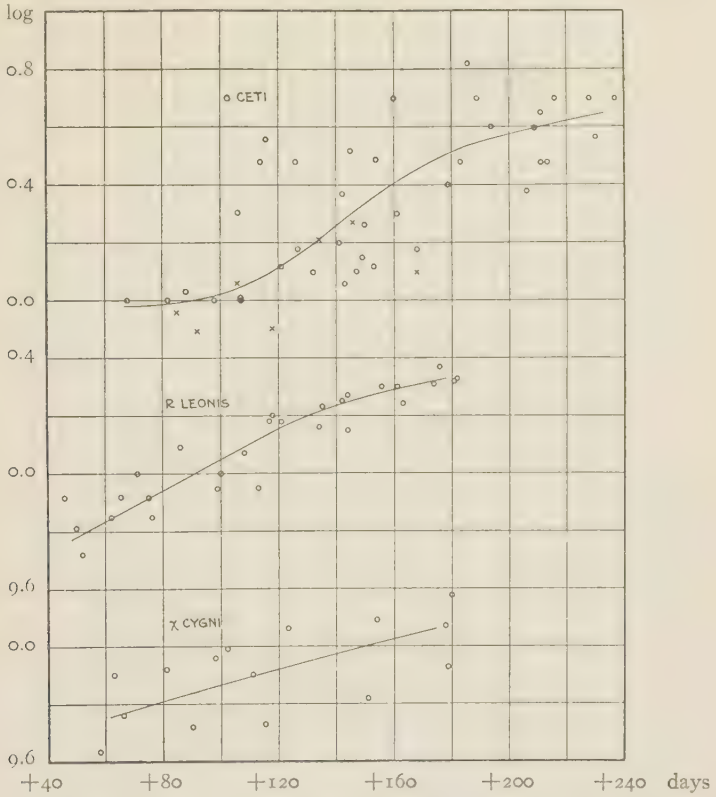

FIG. 12.—Intensity ratio λ 4571 : λ 4308. In the plot for o Ceti, circles represent estimates by Joy, crosses estimates by Stebbins.

WAVE-LENGTHS AND IDENTIFICATIONS OF LINES

In addition to the lines discussed in the preceding pages (namely, $H\beta$, $H\gamma$, $H\delta$, λλ 4202, 4308, 4571), a considerable number of more or less prominent bright lines have been measured on many spectrograms. Most of these have already been observed in the spectra of *o* Ceti[1] and other long-period variables,[2] but the data in

[1] *Op. cit.*, Table VIII.

[2] *Mt. Wilson Contr.*, No. 265; *Astrophysical Journal*, 58, 195, 1923; *Mt. Wilson Contr.*, No. 325; *Astrophysical Journal*, 65, 23, 1927.

Tables V–VIII are more extensive than those previously published.

The mean wave-lengths in twelve stars are recorded in Table V. The wave-lengths measured on each plate were reduced for the

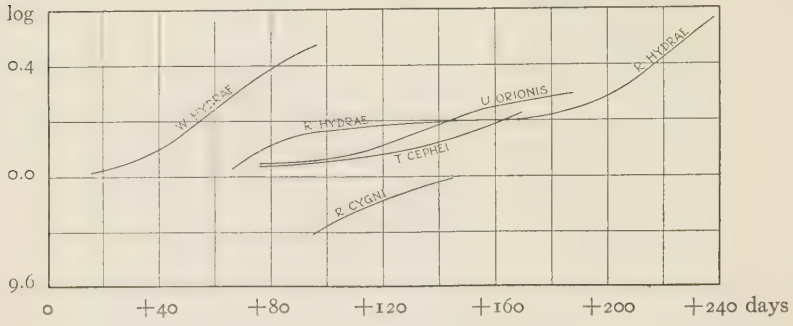

FIG. 13.—Intensity ratio λ 4571 : λ 4308

velocity determined for that plate from a selected list of emission lines given in Table IV. Each column of Table V includes the mean wave-length in international angstroms and the weight of the de-

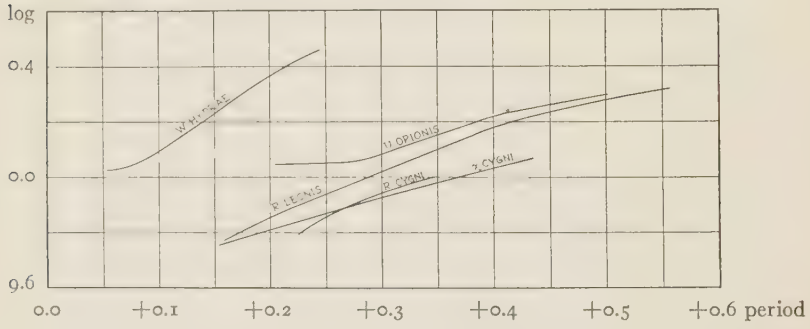

FIG. 14.—Intensity ratio λ 4571 : λ 4308, with phases in fractions of a period

termination. The weight rests on the following system: observations of standard quality, weights 1 and 0.5 for the 18-inch and 10-inch cameras, respectively; poor observations, weights 0.5 and 0.25. In printing, decimals .25 and .75 have been rounded to .2 and .8. To save space the measurements of T Cassiopeiae and the arguments for the whole table have been combined in the first column.

The wave-lengths given without decimals were not measured in T Cassiopeiae.

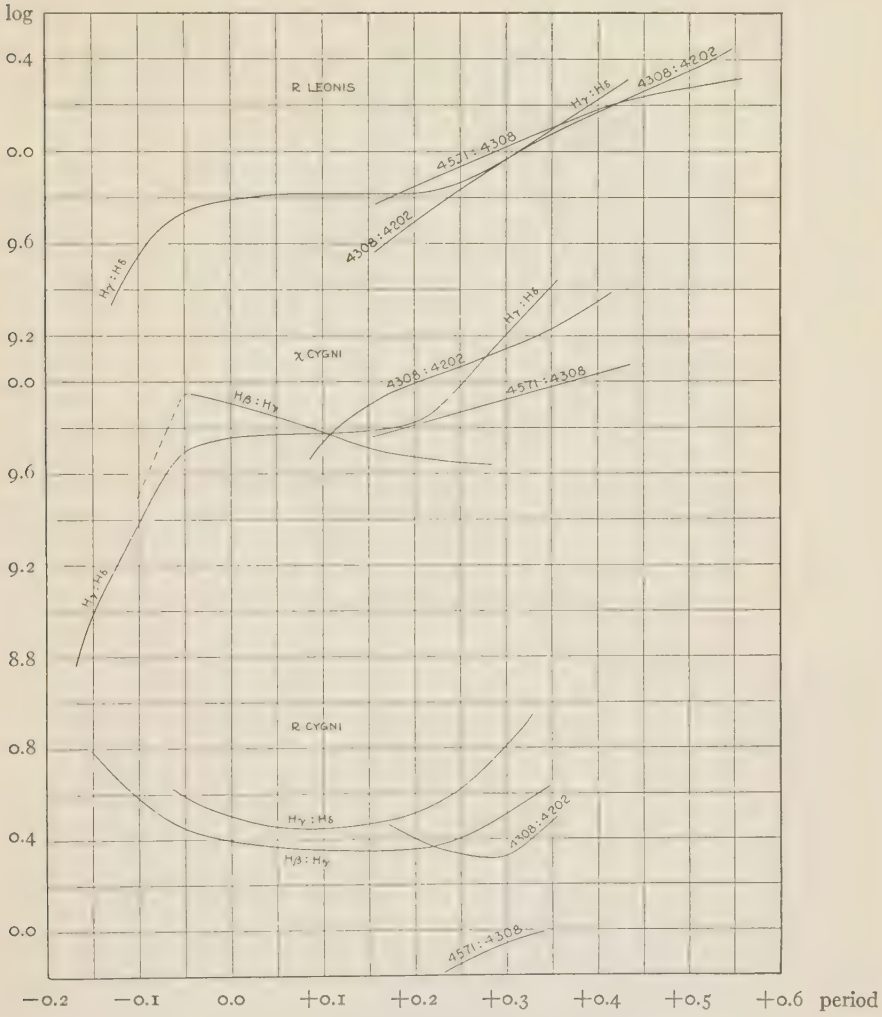

FIG. 15.—Intensity ratios of pairs of lines

T Cassiopeiae.—Lines especially strong before maximum are λλ 3905, 4103, 4511.

U Orionis.—The low-temperature iron line λ 4376 is especially strong on certain plates taken during the declining phase, but its

behavior varies greatly in different cycles. The variation of λ 4571 *Mg* in different cycles has already been noted.

The most interesting plate, perhaps, is C 2651, taken at phase +158 days, magnitude 10.3. The exposure, 4^h56^m, was sufficient to record numerous bright lines whose measured wave-lengths and probable identifications are in Table VI. The representation of iron lines is extraordinary. From the neutral atom, lines in temperature classes I, I A, and II appear, while the ionized atom contributes both normal and forbidden lines. The extreme low-temperature spectrum of neutral iron is well developed. Six of King's "persistent low-temperature lines"[1] lie in the well-observed region in U Orionis.

TABLE IV

EMISSION LINES USED FOR VELOCITY

I.A.	Ident.	I.A.	Ident.
3835.36	*Hη*	4202.03*	*Fe*
3889.05	*Hζ*	4307.91*	*Fe*
3905.51	*Si*	4340.47*	*Hγ*
3970.08	*Hε*	4571.11*	*Mg*
4101.74*	*Hδ*	4861.33	*Hβ*

* Used by Joy in his measurements of *o* Ceti.

Four of these were measured in the stellar spectrum, and there are suggestions of bright lines near the positions of the other two (λλ 4383, 4482). With the exception of λλ 4202, 4308, whose high intensity in these stars is an outstanding problem, λ 4376 is the strongest iron line, as was found by King to be true in the spectrum of the furnace at 1400°.

R Leonis.—Plate C 918, at phase +47, magnitude 6.9, exposure 132 minutes, emulsion Seed 23, is strongly exposed and shows numerous emission lines in the ultra-violet. The continuous spectrum is faint beyond λ 3900. The wave-lengths and intensities, with the probable identifications, are given in Table VII.

The lines of the magnesium triplet near λ 3835 are of low intensity, but their presence is of considerable interest. We are not aware that they have been previously observed in emission in stellar spectra, although it is well known that at a somewhat later phase the

[1] *Mt. Wilson Contr.*, No. 247; *Astrophysical Journal*, 56, 318, 1922.

TABLE V

Collected Wave-Lengths of Bright Lines

T Cas	U Ori	R Leo	R Hya	W Hya	R Ser	χ Cyg	T Cep	R Cas	ο Cet	R Gem	R Cyg
3770	70.62 1	70.67 1	70.69 1			70.47 1			70.58 2		
3797	97.75 1	97.82 1	97.65 1			97.60 1			97.71 2		
3829		29.37 0.5									
3832		32.36 0.5									
3835	35.46 7	35.40 6	35.37 5		35.41 1	35.38 7	35.44 1	35.45 1.5	35.40 16		
3838	38.32 0.5	38.18 0.5									
3852	52.45 0.5	52.62 9				52 66 2		52.64 1.5	52.65 2		
3889 16 2.5	89 13 10	89 08 13	89 08 10		89 09 3	89.11 14 2	89 10 1	89.12 5	89.08 31	89.03 3.5	
3905 54 2	05 50 6	05.57 10.5	05.46 6.5		05.51 1	05.53 13.5	05.63 1	05.52 2.5	05.57 13		
3907		07 51 4							07.58 2		
3938	38.31 1	38.33 6.2				38.30 1		38.34 1.5	38.32 4		
3950	50.00 1	50 01 6.2				49 84 1.5		50.11 1			
3967		67.60 8.8				67.62 2		67.80 1	67.64 St.		
3970	70 07 2	70.08 9.5	70 02 1			70.16 2		69.97 1.5	70.07 11	70.07 1	
3977	77.63 1	77.77 11				77.86 2.5		77.73 1.5	77.9 St.		
4001		01.77 8.5	01.80 1			01.83 7		02.00 2.5	01.8 St.		
4006	06.77 1	06 02 1	06 83 5		06 85 1	06.76 7.5		06.80 2	06.74 9		
4030	30.34 0.5	30.49 10 5	30 53 1		30 70 0 5	30 51 7		30.55 1	30.57 2		
4101.73 11 2	01 73 14	01.72 23.8	01.74 25.5	01.73 7	01.74 6.5	01.70 25.5	01.70 3	01.74 14	01.74 51	01.69 15.5	01.69 13
4103.10 7 5	02 91 7	03.01 12	03 00 11 5	02 99 3	02.79 1	03 05 13		02 96 6	03 00 39		02 96 0.5
4138.75 1	38.51 6	38.69 3	38 06 15		38.50 3	38.64 16		38.02 8	38.60 23	38.53 3.5	38.68 2.5
4151		54 61 1	51 41 1		51 41 1	54 52 10.5				54.52 3	54 60 2
4165	65 87 1		65 82 9		65 76 2	65 78 3		65 96 3	65.84 16		
4178 93 2	78 87 10.5	78 86 13	78 76 14.5		78.67 3	78 79 19.5	78.75 1	78 78 8	78.82 35	79.04 3.5	79 02 3
4202.01 6.5	02.00 11	02 03 28	02.04 10.5	02 01 9 5	02 06 2.5	02 04 14	02.02 3.2	02 02 7	02 02 32	02.01 1	02.01 3.5
4206	06 59 0 5	06 51 3						06.70 1.8	06.70 10		
4215	16.00 1	15 95 8				15 60 4.8		16 08 0.5	16.19 18	15.57 1	15.27 1 5
4233	33.33 6.5	33 24 19.5	33 40 12	33.33 0.5	33.30 2	33.28 14.5	33.59 1	33.36 5	33.33 40	33.35 3.5	
4244	44.06 0.5	44 12 5				44 00 2					
4219 15 1	49 48 0 5	10.23 1.5	10 28 8	49 24 1.2	49.47 1	49 19 6		19 28 3.2	49.34 9	49.16 2 5	
4287	87.45 0.5	87 56 6.8	87.46 1.5			87 44 2		87.84 1.5			
4291	91.62 0.5	91 73 2				91 76 0.5		91.62 2	91.49 10		
4307.91 3.2	07 99 4 5	07.93 20.8	07.95 11	07 99 7.5	07 97 2.5	07.92 14	07.96 3.5	07.91 3	07.94 30	07.83 4.5	07.93 8.5
4340.40 10.5	40.44 14	40.44 26.5	40.45 26	40.43 10.5	40.43 6.5	40.46 25 2	40.47 4	40.45 14.5	40.48 58	40.51 19.5	40.50 15
4359		59.21 3				59.26 0 5					
4372.70 2	72.61 1.5	72.61 12.5	72.70 5	72.66 2	72.58 2	72 59 6.5	72.56 2	72.57 1.5	72.58 12		72.75 1.2
4375	75.88 5.5	75.85 19	75.90 3		75.87 2.5	76.08 2		76.03 4.5	75.93 31	75.94 0.5	75.99 1.5
4413		13.73 1				13.73 0.5					
4416		16 28 1				16.18 1					
4427	27.17 0.5	27.29 5						27.21 1	27.33 11		27.24 1
4461	61.61 0.5	61.50 1						61.62 1.5	61.59 9		61.71 0.5
4511.41 5.2	11.59 3.5	11.44 11	11.36 8	11.38 4 5		11.46 9.5		11 37 5	11.50 13	11.38 8.5	11.42 11.5
4521			21.36 5		21.41 2	21.60 5.5		21.31 2.5	21.40 4	21.44 15	21.48 12
4571.21 1	71.02 5	71.09 20.5	71.04 11	71.09 7	71.01 2.5	71.14 11	71.14 3.5	71.16 3.5	71.14 27	71.29 0.2	71.25 3
4861.34 1	61.29 2	61.40 4	61.34 12	61.40 3.5	61.28 4.5	61.32 21	61.27 1	61.30 1	61.31 26	61.31 15	61.33 12.5

magnesium line λ 4571 becomes very prominent in Me variables. The series relationships are as follows:

λ 3829.36	$^3P_0-{}^3D$	λ 3838.29	$^3P_2-{}^3D$
3832.31	$^3P_1-{}^3D$	4571.11	$^1S_0-{}^3P_1$

λ 4571 cannot be seen in the strong continuous spectrum on plate C 918, and it is weak or absent on C 910, taken the preceding night.

TABLE VI

WAVE-LENGTHS OF BRIGHT LINES IN U ORIONIS
(Plate C 2651; 10-Inch Camera)

STAR		LABORATORY		
I.A.	Int.	I.A.	Ident.	Temp. Class
4030.34*	0	.77	*Mn*	I
4101.60	2	.74	*Hδ*	.....
4178.91	0	.87	*Fe* II	.....
4202.08	3	.03	*Fe*	I
4206.59	1	.70	*Fe*	I A
4216.11	1	.18	*Fe*	I†
4233.27	0	.16	*Fe* II	.....
4244.06	0	3.97	[*Fe* II]‡	.....
4287.45	0.5	.40	[*Fe* II]‡	.....
4291.62	1	.47	*Fe*	I A
4308.11	4	7.91	*Fe*	II
4340.30	1.5	.47	*Hγ*	.....
4372.50	1	.....	?	.....
4375.93	1.5	.93	*Fe*	I†
4427.17	1	.31	*Fe*	I†
4461.61	0.5	.66	*Fe*	I†
4571.22	7	.11	*Mg*	I
4857.04	0	.....	?	.....
4861.31	0.5	.33	*Hβ*	.....

* Poor. Perhaps displaced by a dark line on the red side.
† Persistent low-temperature line.
‡ Forbidden line.

In general, however, this is just about the phase at which λ 4571 begins to be visible. It then strengthens rapidly. The fact that the ultra-violet triplet is not seen at later phases probably indicates that it does not increase in intensity. Unfortunately the observational data are meager, but so far as may be judged, the relative behavior of the ultra-violet lines and λ 4571 is what might be expected from the series relationships. Further observations of the ultra-violet triplet would be of value.

The forbidden lines of ionized iron, measured on one spectrogram

of U Orionis, are regularly seen in R Leonis toward minimum. They are just recognizable at phase +100 days, and thereafter gradually increase in intensity until at phases +160 to +180 they are well marked. They are thus strongest during the few weeks just preceding minimum. The emission of these lines requires the ionization of iron atoms, and their increase in intensity as the star grows cooler is not readily explicable. The paradoxical occurrence of these lines

TABLE VII

WAVE-LENGTHS OF ULTRA-VIOLET BRIGHT LINES IN R LEONIS

(Plate C 918)

STAR		LABORATORY	
I.A.	Int.	I.A.	Ident.
3770.67	2	.63	$H\iota$
3797.82	2.5	.90	$H\theta$
3829.37	0	.36	Mg
3832.36	0.5	.31	Mg
3835.33	4	.39	$H\eta$
3838.18	0.5	.29	Mg
3852.52	3	.....	.....
3889.03	5	.05	$H\zeta$
3905.55	3	.51	Si
3907.41	1.5	.....	.....
3938.33	2	.....	.....
3949.81	2	.....	.....
3967.34	1	.....	.....
3970.06	2	.08	$H\epsilon$
3977.73	2.5	.....	.....

in the same spectrum with the extreme low-temperature lines of neutral iron and λ 4571 of magnesium, as in U Orionis, has been repeatedly observed in R Leonis. The possibility that the ionized iron lines arise in a companion star, as in R Aquarii and *o* Ceti, suggests itself, but is not strongly supported by the observations. Perhaps the forbidden lines occurring just before minimum are in some way connected with the beginning of a new light-cycle.

R Hydrae.—The bright hydrogen lines are very intense in this spectrum. On plate C 3823, phase −11 days, the intensities of the ultra-violet bright lines are as follows:

λ 3905, 4; $H\zeta$, 9; $H\eta$, 5; $H\theta$, 3; $H\iota$, 3− .

$H\iota$ is almost as strong as $H\theta$, but the following line, $H\kappa$, is not seen. Line λ 4511 is visible on a large number of plates from phase −95 to +108 days, but is weak or absent near maximum. Line λ 4521 is weaker, and was measured on only five plates. It is apparently not so much weakened at maximum as λ 4511. We may therefore judge that λ 4521 is a line of higher excitation than λ 4511. Line λ 4373 is especially conspicuous on plate C 911, phase +108 days.

W Hydrae.—Nearly all the phenomena of the bright lines seem to occur at earlier phases than in the other variables. The relatively small light-range may be responsible for this behavior.

χ Cygni.—This variable is of special interest, not only because of its large light-range, but also because the spectrum combines features of classes M and S. A low effective temperature is indicated by the intensity of the titanium bands and of the potassium doublet near λ 4045 and by other lines. The concurrence of the low effective temperature and the class S features leads to the belief that the density is exceptionally low, perhaps the lowest of any well-known star in the sky. Although χ Cygni is fairly bright at maximum (average magnitude, 5.1), the range is so great that it is difficult to obtain spectrograms near minimum (phase about +240 days). The plates taken nearest minimum are at phase +180 and are not strongly exposed. The chief features, however, are well shown. These include the bright lines ordinarily observed at the corresponding phases in other variables (namely, λλ 4202, 4308, 4571) and also the forbidden iron line λ 4244 with traces of other forbidden iron lines which accompany λ 4244 in η Carinae and other stars. On plate DVI 83, taken at phase +178 days, magnitude 11.9, the following bright lines were measured: 4202 *Fe*, 4244 [*Fe* II], (4250) doubtful, 4287 [*Fe* II], 4308 *Fe*, $H\gamma$, 4359 [*Fe* II], (4371) doubtful, 4413 [*Fe* II], 4416 [*Fe* II], 4571 *Mg*, $H\beta$. In spite of the low dispersion, 185 A per millimeter at $H\gamma$, most of the lines stand out clearly from the weak background of continuous spectrum.

o Ceti.—The data are largely from Joy's investigation. The lines used by him for velocity are those starred in Table IV and, in addition, the low-temperature iron lines λλ 4216.18, 4291.47, 4375.93. In the ultra-violet, Joy's values show a systematic deviation from laboratory measurements and from those by one of us in several

variable stars. Accordingly, the following corrections have been applied to Joy's wave-lengths in *o* Ceti:

λ 3770 to λ 3938	−0.12 A
3970	− .09
4006	− .06
4030	− .04
4101	0.00

The figures following Joy's wave-lengths in *o* Ceti in Table V give the number of plates on which each line was measured. A few lines not measured by Joy have wave-lengths from Stebbins' investigation[1] of *o* Ceti; these are marked "St."

The mean wave-lengths of the bright lines, together with their probable identifications, are listed in Table VIII. The values in parentheses refer to maxima in the continuous spectra which may or may not be emission lines. The others are thought to be true emission lines. The agreement between the stellar and laboratory values is reasonably good in most instances. The lines assumed to have their normal values in order to fix the radial velocity are listed in Table IV. Their actual measured values, reduced for the mean velocity, just as in the case of other lines, are used in Tables V, VI, VII, and VIII. Notes on several lines follow Table VIII.

DISPLACEMENTS OF THE BRIGHT LINES

Lines in the blue-violet region.—Previous investigations have shown that near maximum light the bright lines of long-period variables regularly yield apparent velocities algebraically less than those from the absorption lines. In a few stars, observations have indicated systematic changes in the velocities from the bright lines during the time of their appearance in each cycle.[2] The present investigation offers many new data which in general confirm the earlier results.

The measured velocities are found in the sixth column of Table II, and the wave-lengths upon which they depend are listed in

[1] *Lick Observatory Bulletins*, **2**, 78, 1903; *Astrophysical Journal*, **18**, 341, 1903.

[2] *Mt. Wilson Contr.*, No. 264; *Astrophysical Journal*, **58**, 215, 1923; *Mt. Wilson Contr.*, 311; *Astrophysical Journal*, **63**, 281, 1926; *Mt. Wilson Contr.*, No. 382; *Astrophysical Journal*, **69**, 379, 1929.

TABLE VIII

MEAN WAVE-LENGTHS AND IDENTIFICATIONS

Me	Se	Ident.	Me	Se	Ident.
3770.60	.....	.63 *Hι*	(4173.41)	.....	.48 *Fe* II?
3797.71	.....	.90 *Hθ*	4178.81	9.03	8.87 *Fe* II
3829.37	.....	.36 *Mg*	4202.03	.04	.03 *Fe*
3832.36	.....	.31 *Mg*	4206.66	.....	.70 *Fe*
3835.41	.....	.39 *Hη*	4215.....	.4	.52 *Sr* II?
3838.25	.....	.29 *Mg*	4216.11	.....	.19 *Fe*
3852.62	.....	.....	4233.3	.4	.16 *Fe* II
3889.09	.03	.05 *Hζ*	4244.08	.....	3.97 [*Fe* II]
3905.54	.....	.51 *Si*	4249.27	.16	.....
3907.53	.....	.....	4287.56	.....	.40 [*Fe* II]
3938.32	.....	.....	4291.58	.....	.47 *Fe*
3949.99	.....	.....	(4293.05)	(.47)	.....
3967.62	.....	.....	(4304.76)	.....	.....
3970.07	.07	.08 *Hε*	4307.94	.91	.91 *Fe*
3977.77	.....	.....	4340.45	.50	.47 *Hγ*
(3997.69)	.....	.....	4359.21	.....	.34 [*Fe* II]
4001.82	.....	.....	4372.61	.75	.....
4006.78	.....	.....	4375.91	.98	.93 *Fe*
(4010.4)	.....	.....	(4377.84)	(.4)	.....
4030.51	.....	.76 *Mn*	4413.73	.....	.79 [*Fe* II]
(4070.1)	.....	.....	4416.23	.....	.28 [*Fe* II]
4101.73	.69	.74 *Hδ*	4427.30	.24	.31 *Fe*
4103.01	.....	2.95 *Si*	(4458.76)	(.62)	.....
(4119.58)	.....	.....	4461.59	.71	.65 *Fe*
(4122.74)	.....	.....	4511.43	.40	.31 *In*?
4138.62	.59	.43 (*Fe* II calc.)?	4521.44	.46	.....
4154.52	.55	.....	4571.10	.25	.11 *Mg*
4165.83	.....	.....	(4578.83)	.....	.....
(4170.68)	.....	.....	4861.32	.32	.33 *Hβ*

NOTES TO TABLE VIII

3797 *Hθ*.—The wave-length of the stellar line seems to be 0.2 A less than the laboratory value. This discrepancy is probably greater than the error of measurement.

3852.—This is one of the most important unidentified lines. The phases at which it was measured are as follows: U Orionis, 1 plate, +37 days; R Leonis, 10 plates, +46 to +100; χ Cygni, 4 plates, +61 to +123; R Cassiopeiae, 2 plates, +122 to +129. On many plates it is stronger than *Hη* and on a few it is equal to *Hζ*.

3889 *Hζ*.—The wave-length in *Me* spectra is slightly greater than the laboratory value. This was previously indicated by the data in Table II, *Mt. Wilson Contr.*, No. 265; *Astrophysical Journal*, 58, 195, 1923.

3907.—Although of low intensity, this looks like a real emission line.

4001.—This appears to be a real emission line.

4030 *Mn*.—This line first appears as a bright edge on the violet side of the manganese absorption line λ 4030. In R Leonis and χ Cygni its measured wave-length increases from 4030.4 at phase +60 days to 4030.7 at +160. The mean value given in Table VIII is probably smaller than the true wave-length of the line to which it corresponds, and the identification with *Mn* 4030.76 is probably correct in spite of the apparent discrepancy in wave-length.

4101 *Hδ*.—The wave-length in χ Cygni, R Geminorum, and R Cygni is slightly lower than the laboratory value.

4103 *Si*.—Thirteen plates of eight other Me stars give 4103.01. One 7-inch camera plate of R Cygni gives 4102.96.

4119.—Two plates of two other Me stars give 4119.40.

4122.—One plate of W Andromedae gives 4122.85.

4138.—Nine plates of five other Me stars give 4138.64.

4154.—In Me spectra this looks like a maximum in the continuous spectrum and has very seldom been measured. It is more conspicuous in the S-type stars and χ Cygni. It may not be a real emission line.

4165.—Three plates of three other Me stars give 4165.96. This may be a maximum in the continuous spectrum and not a real emission line.

4170.—One plate of R Cancri gives 4170.88.

4173.—U Orionis gives 4173.17 from two plates. Omitting this low value, the mean for the other stars in Table V is 4173.49. Two plates of two other Me stars give 4173.44. Although this line looks like a maximum in the continuous spectrum, it may nevertheless correspond to 4173.48 *Fe* II.

4178.—Nine plates of five other Me stars give 4178.76.

4215.—In χ Cygni and the two S-type stars, the wave-length is approximately that of *Sr* II 4215.52, and decidedly below the low-temperature iron line 4216.19. The value measured in χ Cygni was omitted in taking the mean for the Me stars. In the Me spectra the line generally occurs on the same plates as λ 4376 (clearly a low-temperature iron line) and is probably due largely to neutral iron.

4233.—This line is probably due in part to the iron spark line 4233.16, but the wave-length measured in the variables is apparently modified by other features. It lies in the wing of the broad absorption line *Ca* 4227. In U Orionis, R Leonis, R Hydrae, χ Cygni, R Cassiopeiae, and ο Ceti the measured value is about 4233.43 near maximum and decreases to 4233.15± at later phases. In R Leonis the decrease continues until the wave-length becomes about 4233.0.

4287 [*Fe* II].—Omitting the high value given by R Cassiopeiae, the mean becomes 4287.49.

4340 *Hγ*.—Before maximum the wave-lengths in R Leonis, R Hydrae, W Hydrae, T Cephei, and R Cassiopeiae show a tendency to be a few hundredths higher than the laboratory value, but at later phases they are a few hundredths lower. This effect is not exhibited by T Cassiopeiae or χ Cygni.

4373.—This is an outstanding unidentified line measured at the phases indicated below:

Star	No. Plates	Phase Days
T Cas	2	+ 21 to + 56
U Ori	3	+100 to +158
R Leo	17	+ 46 to +182
R Hya	5	+ 63 to +138
W Hya	3	+ 40 to + 84
R Ser	2	+ 71 to + 73
χ Cyg	8	+ 58 to +180
T Cep	2	+ 77 to +109
R Cas	2	+122 to +172
X Oph	2	+ 87 to + 94

Two plates of X Ophiuchi give 4372.60.

4376 *Fe.*—Six plates of χ Cygni indicate a rapid decrease in wave-length from 4376.35 at phase +65 to 4375.75 at +150, but the observations are of low weight and the effect may be accidental. The mean value for χ Cygni 4376.08 would normally have weight 4, but this was reduced to 2 because of the scattering.

4377.—Most of the measures were made before maximum.

4413 and 4416 [*Fe* II].—These lines were measured as a blend on one plate of R Leonis and four plates of χ Cygni. The mean wave-length is about 4415.16, indicating that the line at λ 4416 is slightly stronger than the other.

4511 *In*?—This is one of the few emission lines to appear before maximum. It has been measured as follows:

Star	No. Plates	Phase Days
T Cas	6	−132 to − 39
U Ori	5	+ 70 to +141
R Leo	12	− 36 to +100
R Hya	9	− 87 to +108
W Hya	5	− 87 to + 17
χ Cyg	10	− 69 to +115
R Cas	6	− 31 to +129

4521.—This line has been observed as follows:

Star	No. Plates	Phase Days
R Hya	6	−45 to + 84
R Ser	2	+10 to + 42
χ Cyg	8	−37 to +102
R Cas	5	−31 to + 33

Two plates of two other stars give 4521.45. The observations indicate that this line requires higher excitation than the neighboring line λ 4511.

4578.—A maximum was measured here on numerous plates of Me variables. It may be part of the band structure.

Table IV. There are indications that the various lines do not at all times give precisely consistent velocities, but the differences are small and have been disregarded in the present study.

The velocities are plotted against phase in the light-cycle in Figures 16, 17, and 18. In most of the stars a definite variation, though of small amplitude, is shown. As in the intensity plots, the scattering of the points at a given phase is caused by errors of observation and by differences between individual cycles.

T Cassiopeiae (Fig. 16).—A straight line at velocity −24.5 km sec. satisfies the observations sufficiently well. This indicates either that the velocity is constant or that it varies through a smaller range than in most of the other stars.

W Hydrae (Fig. 16).—The curve, which is but poorly defined by the meager data, seems to be of the typical form with a flat minimum at +32 days.

R Serpentis (Fig. 16).—The curve is dropping at phase 0, but the observations do not cover a sufficiently long interval to locate the minimum velocity. It probably occurs not earlier than phase +70 days.

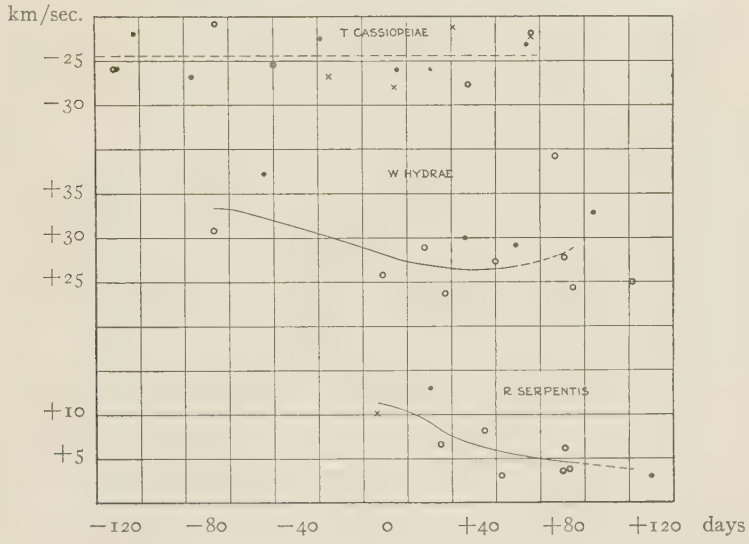

FIG. 16.—Velocities from bright lines. Circles represent observations made with the 100-inch telescope; crosses, observations made with the 60-inch telescope; small disks, observations of less than standard weight.

U Orionis (Fig. 17).—Normal places were formed as follows:

Phase Days	Velocity Km/Sec.	Weight
− 22	−31.5	1.5
+ 16	34.7	6
+ 41	37.1	6.5
+ 72	37.3	4
+102	33.9	2
+162	−28.5	1.5

Weights of 1 and 0.5 were given to observations of standard quality with the 18-inch and 10-inch cameras, respectively, while poor ob-

servations received one-half of these weights. Minimum velocity occurs near phase +55 days.

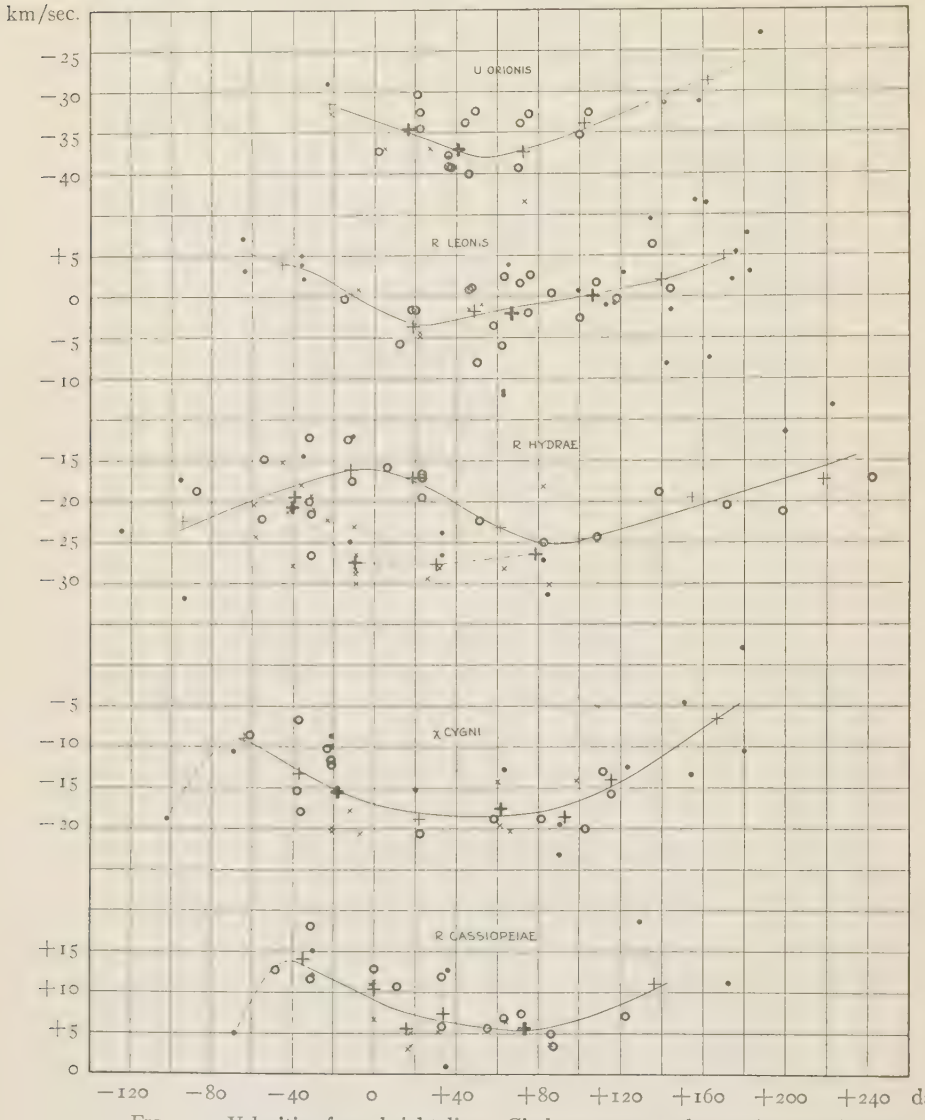

FIG. 17.—Velocities from bright lines. Circles represent observations made with the 100-inch telescope; small crosses, observations made with the 60-inch telescope; small disks, values of less than standard weight. Normal places are represented by large crosses, heavy symbols indicating high weight.

R Leonis (Fig. 17).—Normal places were formed as follows:

Phase Days	Velocity Km/Sec.	Weight
− 45	+3.9	2.25
− 12	+0.2	2
+ 19	−3.7	5
+ 48	−1.8	5
+ 67	−2.0	7.5
+106	0.0	6
+140	+2.0	3.5
+170	+5.0	3.25

Minimum velocity occurs near phase +25 days.

R Hydrae (Fig. 17).—The spectrograph attached to the 60-inch telescope seems to give algebraically lower velocities than that attached to the 100-inch. For this reason the two series have been treated separately. The cause of the systematic difference is not entirely clear. It may be partly an intensity equation and partly an effect of the southern declination. Other observers have found, in general, a negligible systematic difference between results obtained with the two telescopes.

Normal places formed from observations with the 100-inch spectrograph are as follows:

Phase Days	Velocity Km/Sec.	Weight
− 94	−22.5	2
− 39	19.6	6
− 12	16.2	3
+ 19	17.2	4
+ 61	23.3	1.5
+ 99	24.6	1.5
+154	19.6	2
+218	−17.3	2.5

Normal places formed from observations with the 60-inch spectrograph are as follows:

Phase Days	Velocity Km/Sec.	Weight
−40	−20.7	9.5
− 9	27.4	5
+30	27.6	3
+78	−26.4	4

The second normal place differs considerably from one in the other series at nearly the same phase. The five plates in the 60-inch normal place are apparently of good quality, but the four giving the lowest velocities were taken on one evening, and the fifth on the preceding evening. Hence it is barely possible that they are affected by some instrumental error which was especially active at that time.

The normal places from the 100-inch observations give a fairly well-defined curve with a maximum at phase −4 days and a minimum at +87 days. Both maximum and minimum velocity occur at earlier phases than in other stars.

χ Cygni (Fig. 17).—Normal places were formed as follows:

Phase Days	Velocity Km/Sec.	Weight
− 63	− 8.9	1.25
− 37	13.3	3
− 18	15.4	8
+ 21	18.8	1.5
+ 61	17.6	4.5
+ 93	18.6	4
+115	14.0	2.5
+166	− 6.5	2

The velocity-curve has a flat minimum near phase +49 days, and apparently has a maximum at −66 days.

R Cassiopeiae (Fig. 17).—Normal places were formed as follows:

Phase Days	Velocity Km/Sec.	Weight
− 35	+14.0	4
0	10.3	4
+ 16	5.6	4
+ 34	7.4	4
+ 73	5.5	7
+136	+11.0	2

The velocity-curve has a minimum near phase +67 days, and may have a maximum at −41 days.

R Geminorum (Fig. 18).—Three observations before maximum with the 60-inch spectrograph fall considerably lower than the 100-inch observations at the same phase. As these are the only 60-inch observations, it seems best, in view of a possible systematic error,

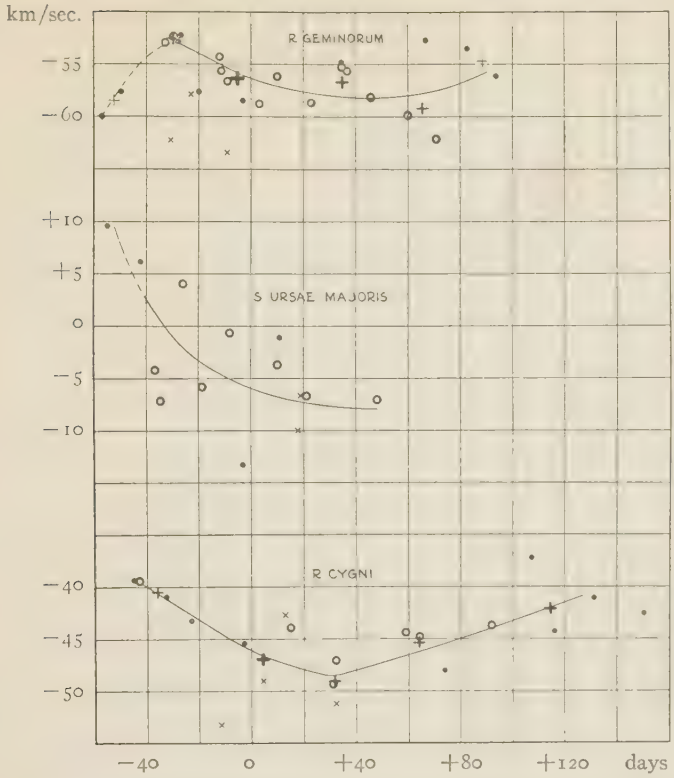

FIG. 18.—Velocities from bright lines. Circles represent observations made with the 100-inch telescope; small crosses, observations made with the 60-inch telescope; small disks, values of less than standard weight. Normal places are represented by large crosses, heavy symbols indicating high weight.

to omit them from consideration and base the curve on the 100-inch spectrograms. From them we find a curve resembling those for the Me stars, with maximum velocity at −30 days, and a flat minimum at about +46. Normal places were formed as follows:

Phase Days	Velocity Km/Sec.	Weight
−53	−58.4	.75
−30	52.6	3
− 5	56.4	5.75
+35	56.6	4.5
+66	59.2	2.5
+88	−54.8	1

S Ursae Majoris (Fig. 18).—The observations are rather scattering but appear to define a velocity-curve which falls more steeply before maximum light and through a larger range than do most of the other curves. This peculiarity may be connected with the relatively short period.

R Cygni (Fig. 18).—Normal places were formed as follows:

Phase Days	Velocity Km/Sec.	Weight
− 36	−40.6	2.25
+ 4	46.9	4.5
+ 32	49.1	3
+ 64	45.3	2.5
+115	−42.1	3

Minimum velocity occurs about 30 days after maximum light.

Two features of the displacement-curve of the bright lines seem definitely established as typical of long-period variables, namely, the algebraically decreasing velocity at and shortly after light-maximum, and the flat minimum from 30 to 80 days after light-maximum. In several stars a maximum in the displacement-curve is indicated about 30 days before light-maximum, and this also is probably typical. The range in displacement is about 10 km/sec., probably being larger for the stars with the shorter periods. The phenomena seem to be essentially the same for Me and Se variables.

The bright Hα line.—Shane's observations of *o* Ceti during the maximum in 1919 indicate that "the hydrogen line *Hα* was displaced 1 A toward the violet with reference to the other hydrogen lines."[1] Joy found this result "to be confirmed, in part at least, by rough measures of the Mount Wilson plates."[2] It was not feasible in the present investigation to give this phenomenon the systematic observation which it deserves. A number of spectrograms were obtained, however, which considerably extend the previous data; these are listed in Table IX.

Most of the plates were taken with the plane-grating spectrograph (G series) having a dispersion of 67 A per millimeter; three

[1] *Lick Observatory Bulletins*, 10, 134, 1922.

[2] *Mt. Wilson Contr.*, No. 311; *Astrophysical Journal*, 63, 302, 1926.

TABLE IX

DISPLACEMENTS OF THE BRIGHT *Hα* LINE

Plate	Date	Mag.	Phase Days	Vel. Km/Sec.	Wt.	Remarks
			o Ceti			
G 47	1925 Jan. 3	3.8	+ 1	+35.0	0.5	
Coudé 37	1926 Oct. 15	3.2	− 4	+25.2	3	
Coudé 40	Oct. 16	3.2	− 3	+33.0	3	
G 198*b*	1928 Aug. 3	3.2	− 18	+30.1	1	
c	Aug. 3	3.2	− 18	+23.2	0.5	Film distorted?
G 207*b*	Sept. 1	3.0	+ 11	+43.8	0.5	Overexposed
c	Sept. 1	3.0	+ 11	+36.8	1	
G 209*a*	Sept. 1	3.0	+ 11	+29.6	1	
b	Sept. 1	3.0	+ 11	+30.5	1	
c	Sept. 1	3.0	+ 11	+26.4	1	
d	Sept. 1	3.0	+ 11	+33.2	1	
G 210	Nov. 30	6.6	+101	+33.6	0.5	Overexposed
G 215*a*	Dec. 1	6.7	+102	+29.3	1	
b	Dec. 1	6.7	+102	+32.2	1	
G 224	1929 Jan. 26	8.7	+158	+35.5	1	
Mean				+30.9	17	
			R Leonis			
G 221	1928 Dec. 1	7.6	+ 67	−16.0	1	
			χ Cygni			
G 186	1928 Aug. 1	8.5	+ 87	−37.8	0.5	Underexposed
G 193	Aug. 2	8.6	+ 88	−28.4	1	
G 246*a*	1929 June 20	5.1	+ 5	−38.4	1	
b	June 20	5.1	+ 5	−31.6	0.5	Underexposed
Mean				−33.8	3	
			R Geminorum			
G 41	1925 Jan. 2	6.3	+ 43	−63.6	1	
G 222	1929 Jan. 25	7.6	+ 37	−59.6	1	
Mean				−61.6	2	
			R Cygni			
γ 10078	1921 Mar. 29	7.4	+ 34	−53.6	1	
R 5	1923 June 2	6.5	− 15	−46.8	1	
R 12	July 1	6.6	+ 14	−38.8	1	
R 14	July 2	6.6	+ 15	−40.6	1	
G 25	1924 Oct. 4	8.5	+ 33	−57.2	1	
G 244	1929 June 20	7.9	+ 21	−50.7	1	
G 245*a*	June 20	7.9	+ 21	−43.4	1	
b	June 20	7.9	+ 21	−49.4	1	
Mean				−47.6	8	

plates of R Cygni, R5, R12, and R14, were taken with a three-prism spectrograph, dispersion at *Hα* 44 A per millimeter; two of *o* Ceti were with the coudé Littrow spectrograph having a 15-foot lens, dispersion at *Hα* 13 A per millimeter;[1] while one of R Cygni, γ 10078, was taken with a one-prism spectrograph and 40-inch camera, dispersion 70 A per millimeter.

TABLE X

MEAN DISPLACEMENT OF *Hα* RELATIVE TO OTHER BRIGHT LINES

Star	Displacement	
o Ceti	−15.9 km/sec.	= −0.35 A
R Leonis	14.8	= .32
χ Cygni	16.5	= .36
R Geminorum	− 3.6	= − .08
R Cygni	0.0	= 0.00

The measured displacements of the bright *Hα* line are given in Table IX. From each of these we have subtracted the value for the same phase read from the curves of the bright lines in the blue-violet region. The mean differences are given in Table X. The average displacement for the three Me stars is −0.34 A, while for the two Se stars it is practically 0.

On the following plates *Hα* is indistinguishable in the continuous spectrum:

Star	Plate	Date	Mag.	Phase Days
R Leonis Minoris	G 63	1925 Apr. 11	(7.0)	+ 9
R Leonis	G 60	Apr. 10	6.1	−17
R Hydrae	G 64	Apr. 11	5.7	−30
	G 69	June 8	5.1	+28
	G 71	June 9	5.2	+29

DISCUSSION

Dependence of spectroscopic features on the photosphere.—The intensities of absorption lines and bands in the spectra of long-period variables appear to change during the light-cycle in a way to be expected if the temperature of the photosphere and the reversing layer

[1] The coudé plates were taken by Messrs. Adams and Joy, to whom we are indebted for permission to use them.

rises and falls in phase with the brightness of the star. In Mc variables, for example, it is well known that the titanium oxide bands and certain lines arising from the lowest atomic levels are less intense near maximum than at other phases. These lines include *Ca* 4227; *Cr* 4254, 4274, 4290; *K* 4044, 4047. In Se variables, *Sr* 4607 behaves in the same way. As far as present data go, the intensities of these features depend upon the magnitude of the variable rather than upon the phase. No systematic differences have been detected between the intensities on the ascending and on the descending branches of the light-curve.

It is important to notice that the foregoing remarks do not apply to the emission lines, for the intensities of these lines seem not to bear a simple relationship to the temperature of the photosphere. This somewhat surprising conclusion is supported by the following phenomena:

1. The intensity ratio $H\gamma:H\delta$, plotted as a function of the light-phase, has a total lack of symmetry with respect to the light-curve.

2. λλ 4202, 4308, 4571, and other lines that are conspicuous during the declining phase are not observable at the corresponding magnitudes *before* maximum.

3. Normal and forbidden lines of ionized iron are present near minimum when the absorption spectrum indicates a relatively low temperature for the reversing layer.

4. Absorption spectra practically identical with those of typical long-period variables, *but without bright lines*, are exhibited by numerous stars, many of which vary irregularly through small ranges. The strongest bright lines are found in the spectra of variables with long periods and large ranges.

5. The displacement-curve of the emission lines does not follow that of the absorption lines.

A few bright lines seem to be more dependent than the others on the brightness of the photosphere. These include λλ 4138, 4178, 4511, 4521.

The only recorded observation of emission bands in stellar spectra is that by Joy[1] of certain anomalous features in the spectrum of o

[1] *Mt. Wilson Contr.*, No. 311; *Astrophysical Journal*, 63, 281, 1926.

Ceti in 1924, which were later identified by Baxandall[1] with aluminum oxide. Curiously enough, these emission bands appeared, not at an abnormally bright maximum, but at an abnormally faint one. This means that the magnitude at which the unusual bands appeared in 1924 was one through which the star regularly passes twice in each cycle. We must therefore assume the existence in 1924 of some influence other than the direct effect of the photosphere at a particular magnitude.

The effects of band absorption.—The important effects of the titanium bands on the spectral energy-curves of Me stars have been discussed by Joy and other writers. The absorption is undoubtedly more generally distributed along the spectrum than might appear at first glance. Even the stronger portions of the continuous spectrum within the region notched by the band heads are probably subject to band absorption. Thus a high-dispersion spectrogram of *o* Ceti clearly shows band lines in the strong continuous spectrum near λ 4615 at a point where the band absorption obviously is relatively weak.[2]

If light pressure on the atoms and molecules of a stellar atmosphere is proportional to the radiant energy absorbed, then titanium oxide must receive far greater upward impulses than any other substance known in M- and S-type stars, and thus may exist at an abnormally high level. The absorption-line spectrum, formed in the reversing layer immediately above the photosphere, would then be subject to modification by the overlying stratum of titanium oxide. This might consist merely of the superposition of the characteristic absorption bands; but if the stratum had sufficient optical thickness, it might be practically opaque in the spectral regions occupied by the bands, shutting off the original photospheric radiations in these regions and substituting for them radiations of the same wavelengths arising in the stratum itself. This would cause the disappearance of the low-level dark lines, or their reduction in intensity if the absorption in the high stratum were not complete.

That something of this sort actually occurs is indicated by the general absence or weakness of atomic lines within the region of the

[1] *Monthly Notices of the Royal Astronomical Society*, 88, 679, 1928.

[2] See Plate Xe *Mt. Wilson Contr.*, No. 311; *Astrophysical Journal*, 63, 281, 1926.

strong bands. This is brought out by a comparison of an advanced M-type spectrum, say M6, with one of type Mo or S. A considerable similarity exists except in the fluted region where the lines are wholly or partially suppressed in M6. The D lines of sodium furnish a striking example of the influence of the bands. These ultimate lines of the neutral sodium atom would be expected to strengthen with decreasing stellar temperature. This appears to hold true except for those stars (the coolest known) with very strong titanium bands; here the sodium lines are scarcely distinguishable with low dispersion, having but a small fraction of the intensity they exhibit in other red stars at somewhat higher temperatures. The ultimate strontium line λ 4607 shows the same phenomenon, although in a somewhat less marked degree, probably because the bands in its region are not so intense as those in the yellow. The same general effect may be observed in the spectrum of a long-period variable at different phases. As the bands increase in intensity after maximum the atomic lines become weak and hazy.

We may now inquire whether the bright lines of Me variables, as well as the continuous spectrum and dark lines, are subject to the absorption of a high stratum of titanium oxide. A more general question is the following: Are the peculiar relative intensities of the bright lines inherent, or are these lines emitted with normal intensities and then modified by absorption?

The hydrogen lines are the most important concerned in this problem. Not only are they very conspicuous, with relative intensities differing widely from those observed in the laboratory, but they undergo surprising systematic changes in each light-cycle, as described on previous pages. Several outstanding facts seem to point toward band absorption as the cause of the low intensities of $H\alpha$, $H\beta$, and $H\gamma$. The first is that no laboratory observation has shown these lines to be of as low intensity compared to $H\delta$ as they are in Me spectra, and no theory of atomic structure offers a plausible explanation of such an abnormality. On the other hand, radical modifications of the laboratory intensities are known only in stars with titanium bands.[1] Moreover, the degree of abnormality seems usually to be approximately proportional to the intensity of the

[1] *Mt. Wilson Contr.*, No. 306; *Astrophysical Journal*, 63, 13, 1926. See Table I.

bands. This is true, not only in a general comparison of one star with another, but also as applied to the various members of the hydrogen series in a given spectrum; that is to say, those lines are most affected which are in the region of the strongest bands.

Now if the hydrogen emission spectrum is subject to modification by the titanium oxide layer, it must be produced at a lower level. Is this physically possible? Ordinarily, emission lines are thought to originate in the outermost portions of stellar atmospheres. In the sun, for example, bright lines are produced by prominences which rise far above the level where absorption lines or bands are formed. Our knowledge of the structure of the atmospheres of giant stars is very incomplete, however, and we must not exclude from consideration far different circumstances in the Me stars. These objects are of enormous size and of extremely low density; their atmospheres, moreover, must be in a continual state of change and readjustment. Anomalous arrangements of various strata which would be impossible in other types of stars might well exist, at least for part of the light-cycle.

The assumption that the abnormally low relative intensities of the first three members of the hydrogen series are caused by the absorption of titanium oxide would seem to have sufficient merit to warrant its use as a tentative working hypothesis,[1] although it is by no means perfectly convincing and may eventually be rejected.

In applying this hypothesis to the data of the present paper we first note that $H\delta$ lies outside the region affected by the bands, that near $H\gamma$ the bands are of moderate intensity, and that near $H\beta$ they are very strong. The effect on $H\gamma$ should therefore always be less pronounced than that on $H\beta$, and this appears to be generally true.[2]

The curves for the ratio $H\gamma$:$H\delta$ begin with a low value (i.e., $H\gamma$ relatively weak), rise rapidly until about the time of maximum, after which they are nearly flat for several weeks, then turn upward

[1] This is not the first time that a hypothesis of this general nature has been introduced to account for irregularities in the Balmer series in Me stars. It has long been considered probable that the bright $H\epsilon$ line is absent because of the absorption of the calcium line H; and Shane has suggested that certain ultra-violet lines are weakened by absorbing vapors of iron and vanadium (*Lick Observatory Bulletins*, 10, 134, 1922).

[2] The strong $H\beta$ line in the spectrum of χ Cygni may furnish an exception. This star is intermediate between classes M and S.

again and approach the normal (laboratory) value before the lines disappear. Whatever the mechanism, we may assume that $H\gamma$ is not at all times subject to the total band absorption but to a fraction of it, which becomes continually smaller as the phase advances, thus explaining a general rise of the curve from left to right. Superposed upon this effect, however, would be that of variations in the total band absorption. It is well known that in the spectra of Me variables the bands have their lowest intensities near maximum light. Thus before maximum the bands are decreasing in intensity and the two effects combine to give a rapid increase in the relative brightness of $H\gamma$. After maximum, as the bands are becoming more intense, the two effects act in opposite directions and thus give the curve a nearly horizontal portion.[1] At a still later phase the hydrogen lines largely escape the effect of the bands, and the curve rises again.[2]

It may be noted that on this hypothesis the observed time of transition from the first steep branch of the curve to the horizontal portion comes a little too early. If, through the whole period of visibility of the hydrogen lines, there were a tendency for them to approach their normal intensities (because of decreasing effective band absorption), we might expect the tangent to the curve at the time of maximum, when the band absorption is momentarily unchanging, to have a slope nearly corresponding to the average rate of change. As a matter of fact, however, the tangent at maximum is nearly horizontal; the tangent parallel to the general upward slope of the curve would occur a few days before maximum. We have then to assume that the reactionary effect of band absorption sets in, not exactly at maximum, but a few days before. It would be interesting if accurate measurements of band intensities should show that the bands begin to strengthen shortly before maximum.

The iron lines λλ 4202, 4308 belong to the same multiplet. Their classifications are

λ 4202	$a^3F_4 - z^3G_4^\circ$
λ 4308	$a^3F_3 - z^3G_4^\circ$

[1] In W Hydrae, whose light-range is unusually small (implying a small change in band intensity), the curve for $H\gamma : H\delta$ seems to lack the pronounced pause after maximum shown by most of the stars with larger ranges.

[2] A non-selective absorption increasing toward the violet may be a partial cause of the relative dimming of $H\delta$ at this phase.

The fact that the lines have a common upper level precludes certain explanations of their changing relative intensities. If the transition probabilities are constant under all circumstances—and this is the common belief—we are apparently forced to call upon changes in the absorption acting on the lines to explain the changing relative intensities shown in Figures 9, 10, and 11. The observed results might be caused by a decrease in the effective titanium band absorption after maximum.

Theory of long-period variables.—It is probable that much more observing and a more detailed organization of the data must precede the formation of a comprehensive theory of long-period variables. The present observations, while extensive, are not sufficiently precise or complete to answer many questions which naturally arise. One of the most evident needs is for a series of spectroscopic observations so frequent and complete that the spectral changes in a number of cycles may be thoroughly studied in their relationship to the details of the light-curve.

The behavior of the bright lines may, however, serve as a guide to certain general features that any finally successful theory must have. One suggestion is that, because of the large size of these stars or the low densities of their atmospheres, or for other reasons, various spectroscopic phenomena are not closely interrelated, but may proceed in partial independence of each other. The temperature of the photosphere, for example, appears not to have immediate control over the appearance and intensity of the bright lines. It seems rather as if the brightening of the photosphere were but one of a number of spectroscopic phenomena set going by a special occurrence at a certain phase. The temperature of the photosphere is probably closely correlated with the observed magnitude of the variable, but it does not dominate all features of the spectrum.

To illustrate the idea, let us postulate a release of energy in a certain level at intervals of time equal to the period of light-variation. These occur presumably just before minimum. The first visible result[1] is the brightening of the continuous spectrum, caused by either an increase in the temperature of the photosphere or a de-

[1] As an interesting speculation, we may ask whether the development of bright enhanced iron lines just before minimum is in some way a precursor of the new cycle.

crease in the absorption to which its light is subject. The aspect of the spectrum does not change materially for a time. A little later, however, there appears the first of a sequence of bright lines which runs throughout the remainder of the cycle while the photospheric spectrum is increasing to a maximum intensity and then fading. These two effects from a common cause apparently proceed with but little interaction. The intensities of the bright lines mark the phase unmistakably, but they seem not to bear a simple relationship to the temperature of the photosphere. The relative intensities of certain lines change in such a way as to suggest that the absorption to which they are subject becomes progressively less as the cycle advances. This may mean that the effective level of emission rises.

Among the lines to develop as the star decreases in brightness, one or two, particularly λ 4571 *Mg*, persist for a time *after minimum*, thus overlapping the new cycle. This indicates that the series of events started by some occurrence near minimum may last longer than a whole period. A similar phenomenon is furnished by the behavior of sun-spots. A given series of spots may remain visible for two or three years after the next cycle begins. This is another instance of periodic disturbances each having a chain of consequences longer than the period.

Carnegie Institution of Washington
Mount Wilson Observatory
February 1930

Contributions from the Mount Wilson Observatory, No. 400
Reprinted from the *Astrophysical Journal*, Vol. LXXI, pp. 351–356, 1930
Printed in the U.S.A.

THE RAYTON SHORT-FOCUS SPECTROGRAPHIC OBJECTIVE

By MILTON L. HUMASON

ABSTRACT

Spectra of very faint stars and nebulae can be observed only with a camera objective of short focus. The California Institute of Technology has a lens of this type, later to be used with the 200-inch telescope, which is an eight-fold enlargement of a microscope objective, with a focal length of 32 mm and an aperture of 50 mm or a focal ratio of $F/0.6$.

Tests made at the 100-inch telescope of the Mount Wilson Observatory show excellent definition and a gain of 50 per cent in speed over the short-focus camera previously used. The spectrograph has a collimator of 24 inches focal length and two light flint prisms. The dispersion at λ 4350 is 418 A per millimeter. Ordinary stellar velocities cannot be measured, since the probable error is of the order of 50–100 km/sec.; but an uncertainty of this amount is not important when large displacements, such as those occurring in the spectra of faint extra-galactic nebulae, are measured.

A single nebula in the Ursa Major cluster has been observed in which the apparent velocity-shift is +11,500 km/sec. The exposure time required was forty-five hours.

The spectra of very faint objects are difficult to obtain on account of the small amount of light made available by even the largest telescopes. The only way in which they can be observed is to use a camera lens of very short focus, which reduces the spectrum to the smallest possible length and width, thereby cutting down the exposure time. Practically the greatest difficulty has been to obtain a short-focus lens which would give good definition.

The California Institute of Technology has procured a lens designed by Dr. W. B. Rayton, of the Bausch and Lomb Optical Company, which is later to be used in connection with the 200-inch telescope. It is an eightfold enlargement of a microscope objective, gives good definition, and has great speed. A technical description by Dr. Rayton will be published elsewhere in this *Journal*.

The Mount Wilson Observatory has tested this lens in a spectrograph mounted at the Cassegrain focus of the 100-inch telescope. The spectrograph includes a collimator of 24 inches focal length, two 60° light flint prisms, and the new Rayton objective, which has a focal length of 32 mm and an aperture of 50 mm or a ratio of $F/0.6$. The consequent reduction from slit to plate is nineteen times, and

makes possible the use of a very wide slit without an appreciable loss of definition or widening of the lines. The instrument shops of the Mount Wilson Observatory are now building a new spectrograph in which this objective will be used. It will have the same optical parts as the one now in use, but the slit will be curved instead of straight, thereby eliminating most of the curvature of the lines, which is quite noticeable with the straight slit now in use. The dispersion is 418 A per millimeter at λ 4350, and the distance between the helium lines λ 3888 and λ 5015 is 2.67 mm. Helium has been used as the source for the comparison spectrum as the number and spacing of the lines in the photographic region have been found satisfactory for the dispersion.

The probable error of measures of line displacement is necessarily large, as large or larger than the ordinary stellar velocity. It is therefore not feasible to use this lens for measurements of stellar velocities, but it can be used successfully for photographing certain classes of very faint stars and nebulae which show very large line displacements and for which an accurate measurement of the displacements in any single object is not expected.

During the few months in which this camera lens has been in use it has been employed almost entirely in observing the faint and very remote extra-galactic nebulae, especially those which occur in clusters and have large apparent radial velocities. It has been found to be an ideal type of spectrograph objective for such objects. A wide slit can be used to great advantage, and although the probable error of the measured displacements amounts to 100 km/sec., the gain in speed is more important than the loss in accuracy. Since the very remote nebulae have apparent radial velocities of 2000 km/sec. or more, a probable error of this order is small as compared with the velocity displacements. The absorption lines or blends observed in the nebulae are more diffuse than in stellar spectra and are few in number. The strongest and most easily recognized are the H and K lines of calcium, which furnish a sure indication of the amount of the displacement and make possible the easy identification of the remaining lines, $H\delta$, the G (λ 4308) band, and $H\gamma$.

The following indicates other investigations for which this lens will be used: The mean velocity from a group of individual stars in

a cluster should give a very good value of the velocity of the cluster as a whole. The spectra of faint Cepheid variables may be studied. An accurate classification of the spectra of faint stars of large proper motion may be made, and, as most of these stars have spectra of late K or M types, a reliable value of the absolute magnitude may be obtained from the spectral classification alone. Photographs of the spectra of novae which occur in the Andromeda nebula and which seldom reach a photographic magnitude brighter than 16.0 at maximum light should be possible and would be very valuable. Spectroscopic records of the minimum phase of galactic novae may also be obtained. The features of the absorption measurable in stellar spectra vary with the type, and the probable error becomes smaller with the use of a narrow slit. The slit width most often used for stellar observations is 0.18 mm, and the probable error of the measurement from a single plate is 50 km/sec. For the nebulae a slit width of 0.20–0.60 mm has been used according to the brightness of the object observed.

In order to give some idea of the speed of the new 1.3-inch camera it may be compared with the one in use just previously. The old camera had a focal length of 3 inches and formed a part of the same spectrograph, having exactly the same optical parts except that only one of the 60° prisms was used. The dispersion was 3.21 mm between λ 3888 and λ 5015, as compared with 2.67 mm for the new camera and two prisms. The reduction from slit to plate was therefore eight times as against nineteen times for the new camera. No direct test of the two instruments has been made, but spectrograms are available of two nebulae in the same cluster, N.G.C. 1270 and 1273, which have approximately the same brightness. N.G.C. 1273 was photographed with the old 3-inch camera and an exposure of twenty hours; N.G.C. 1270 was taken with the new camera and exposed nine hours. The two spectrograms, enlarged fourteen times, are shown in Plate VII. It was difficult to enlarge these spectrograms from their original scale of about 3 mm to one suitable for reproduction, and the illustration does not show all of the added fine detail recorded by the new camera. The negatives show, however, that the spectrogram taken with the new camera is much superior in definition and density to that photographed with the old lens. One of the

striking features of this lens is the lack of coma, which has been a rather persistent difficulty with most other short-focus spectrographic objectives tried at this observatory. A further test of efficiency is the exposure time required to obtain a spectrogram of a star of photographic magnitude 12.0. With fair seeing this is ten minutes for the new camera as against thirty minutes for the 3-inch camera.

The color-curve of the objective is shown in Figure 1, where the points and the full-line curve represent the best focal setting for a given wave-length with a flat plate perpendicular to the optical axis. The crosses and the broken curve represent the best settings for the

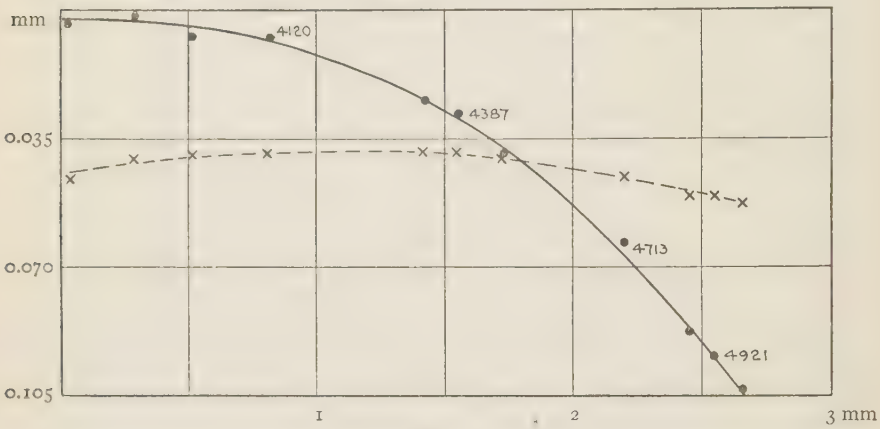

FIG. 1

same wave-lengths with a tilted, curved film. The vertical scale represents the focal settings and the horizontal scale the separation in millimeters of the different wave-lengths, a few of which have been indicated on the plot. The horizontal scale is fourteen times that of the vertical scale. The full-line curve shows the amount of tilt and the curvature which was required in the plate-holder. The tilt has been introduced by displacing the center of curvature of the curved plate in the plate-holder. The broken curve shows that the curvature used was insufficient, but the error is so small that no attempt will be made to correct it.

Eastman portrait films, which are comparable to the Eastman 40 plates in speed and grain, are used at the present time. The size required by the new plate-holder is 1-5/16×5/8 inches.

PLATE VII

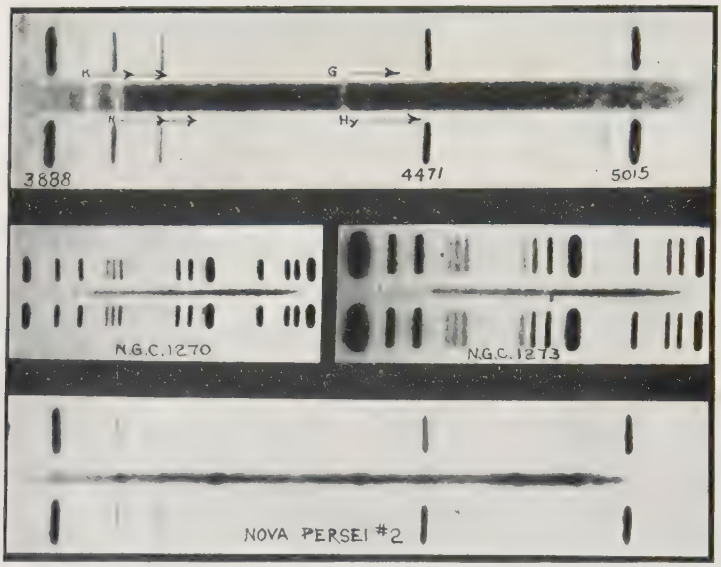

EXAMPLES OF SPECTRA TAKEN WITH RAYTON CAMERA LENS

a) Sky, with Comparison Lines of Helium

b) N.G.C. 1270 and N.G.C. 1273

c) Nova Persei No. 2

The design of the plate-holder was difficult on account of the very small clearance between the film and the lens cell, the focus being only 2 mm back of the rear surface of the lens. A plate-holder of the usual design was tried first, but proved unsatisfactory because the plate-base had to be backed away from the lens until the plate-holder was clamped on and the slide pulled. This arrangement has now been discarded and a plate-holder designed which clamps on to the plate-base, bringing the film into focus without further adjustment. This new plate-holder not only has a slide but carries a curved plate for bending a photographic film, which makes it possible to correct for the tilt and for the color-curve of the lens. The bottom part of the plate-holder carrying the slide consists of three sheets of metal 0.007 inch in thickness, each having a hole 8 mm in diameter. The middle sheet acts as the slide and moves between the outer two, the bottom or outside piece of metal being turned up and soldered to the sides of the plate-holder. When the three openings coincide, the film is exposed, and when the hole in the slide is pushed beyond the holes in the outer pieces, the plate-holder is closed.

When the camera is in focus and the plate-holder in place, a clearance of only 0.1 mm remains between the bottom of the plate-holder and the lens cell. This plate-holder is now in use and has been found very convenient and light-tight.

The spectra reproduced in Plate VII are as follows: At the top is a widened spectrogram of skylight taken with a narrow slit. The calcium lines H and K are seen, the G band, and $H\gamma$. The wave-lengths of three helium lines in the comparison spectrum have also been indicated. The absorption lines in the sky spectrum are the strongest appearing on spectra of very small dispersion, and are those most often measured in the spectra of nebulae. The tips of the arrows to the right show where these lines appear in the spectrum of N.G.C. 4860, a nebula in the Coma Berenices cluster having an apparent radial velocity of +7800 km/sec. Just below the sky spectrum are shown spectra of two nebulae in the Perseus cluster already mentioned, N.G.C. 1270 and N.G.C. 1273. The mean apparent radial velocity of the nebulae in this cluster is +5100 km/sec., and the arrow-tips to the left in the sky spectrum show where the H and K lines appear in these nebulae. A direct photograph showing a small

region of the cluster of spirals in Perseus is seen in Plate VIII. The spectrum at the bottom of Plate VII is of Nova Persei No. 2, photographed in January, 1930, by F. G. Pease with four hours' exposure at the 100-inch telescope. This nova was at maximum in 1901, but was estimated as close to 13.0 when photographed by Pease. It has been included as an illustration of an emission spectrum. The seeing was very poor and the spectrum was widened by moving the star along the slit. Another plate of Nova Persei, not widened and taken during better seeing, was obtained by Pease with an exposure of thirty minutes. The emission lines shown are $H\delta$, $H\gamma$, 4686, and $H\beta$. The two large-scale spectrograms have been enlarged twenty-eight times, and the small-scale spectrograms fourteen times, from the original.

For very faint objects observable only with a small-scale camera the speed of our spectrograph has been doubled by the use of the Rayton lens. It is now possible to observe faint objects which have heretofore seemed hopeless; one of these is a very faint cluster of nebulae in Ursa Major described by W. Baade.[1] This is probably one of the most remote clusters known at present. Baade estimates its distance as one hundred and fifty million light-years, while Hubble from recent data put it at a distance of the order of eighty million light-years. A single observation of one nebula in this cluster has just been made, and the displacement is +11,500 km/sec. The distance obtained from the displacement by the use of Hubble's velocity-distance correlation, in which 500 km/sec. displacement to the red corresponds to a distance of one million parsecs, is of the order of twenty-three million parsecs, or seventy-five million light-years. This is approximately the same as the distance which Hubble obtains from observations of the total brightness of the nebulae involved in the cluster. The exposure time required to photograph the spectrum of this faint object was forty-five hours. Spectroscopic observations with any other short-focus camera would have required an exposure of one hundred hours or more

Carnegie Institution of Washington
Mount Wilson Observatory
May 1930

[1] *Astronomische Nachrichten*, **233**, 65, 1928.

PLATE VIII

Direct Photograph of Region of Cluster of Spirals in Perseus.
Including N.G.C. 1270 and 1273

Contributions from the Mount Wilson Observatory, No. 401
Reprinted from the *Astrophysical Journal*, Vol. LXXI, pp. 336–350, 1930
Printed in the U.S.A.

A SPECTROGRAPHIC STUDY OF U SAGITTAE

By ALFRED H. JOY

ABSTRACT

The spectrographic observations of U Sagittae, which extend from 1921 to 1928, were made with especial reference to the fainter component and the rotation effect.

The period.—A discussion of published photometric observations suggests a variable period with the elements: Min. = 2417130.4111 G.M.T. + 3.3806234E − 0.0057 sin (0°.2E − 34°). But for this study the elements used (Min. = 2424719.9007 G.M.T. + 3.38056E) were derived from the spectrographic observations themselves.

The velocity-curve of the brighter star outside eclipse.—Forty-three spectrograms give the orbit of the principal star. Plates taken during eclipse were excluded. The spectrum, which has poor lines, is B9. The elements found are: $T = 1.5960$ days after minimum, $\omega = 260°$, $e = 0.035$, $\gamma = -15.1$ km/sec., $K = 67.9$ km/sec., and $a \sin i = 3{,}155{,}000$ km.

Observations during totality.—The larger and fainter star alone is visible during totality, which lasts only one hundred minutes. Thirty spectrograms of the companion, taken with low dispersion, were used to determine the slope of the velocity-curve. The spectral type is G2. The mass is one-third that of the primary.

Observations during partial phases for rotation effect.—While the disk of the fainter star encroaches upon that of the brighter star, the velocities are affected by its rotation. With the inclinations and the duration of eclipse indicated by Fetlaar's uniform and darkened solutions, the values of the rotational velocities at the limb are 60 and 62 km/sec., respectively. The radius of the smaller star, corresponding to a velocity of 60 km/sec. at the limb, is 2,790,000 km.

Absolute dimensions and physical properties.—The principal physical dimensions were determined with the aid of Fetlaar's photometric solution. The uniform solution, which is more plausible, gives $a_1 = 3{,}169{,}000$ km; $a_2 = 10{,}457{,}000$ km; $a_1 + a_2 = 13{,}626{,}000$ km; $r_1 = 5.7\odot$; $r_2 = 3.4\odot$; $\rho_1 = 0.011\odot$; $\rho_2 = 0.171\odot$; $M_1 = +1.8$ mag.; $M_2 = -0.4$ mag.; $j_1 = +0.8$ mag.; $j_2 = -2.6$ mag.; $\pi = 0''.003$.

U Sagittae ($19^h14^m.4$, $+19°26'$, 1900; spectrum B9; 6.6–9.4 mag.) is one of the brighter eclipsing stars. It was discovered to be variable by Schwab in 1901, and a large number of photometric observations have been made by Wendell,[1] Luizet,[2] Graff,[3] Maggini,[4] and others. Russell, Fowler, and Borton[5] have given a photometric solution from photographic and visual observations made at the Harvard College Observatory. The extensive series of observations made by Nijland[6]

[1] *Annals of the Harvard College Observatory*, **69**, 82, 1909.

[2] *Astronomische Nachrichten*, **162**, 285, 1903.

[3] *Mitteilungen der Hamburger Sternwarte*, **11**, 44, 1907.

[4] *Astronomische Nachrichten*, **200**, 54, 1915.

[5] *Astrophysical Journal*, **45**, 306, 1917.

[6] *Astronomische Nachrichten*, **176**, 167, 1907; **229**, 353, 1927.

has also been used by Fetlaar[1] for a determination of the elements of the photometric orbit. Hellerich[2] and Bemporad[3] have used their own observations, together with others, for special studies of the period. The spectroscopic orbit of the brighter star was determined by Miss Mary Fowler[4] from spectrograms made with the 30-inch reflector of the Allegheny Observatory.

Spectrographic observations of U Sagittae with the 60-inch and 100-inch reflectors were begun in 1921 for the purpose of studying the secondary star, which could be seen only when the star was faint at the time of total eclipse. It was hoped not only that such observations would reveal the spectral characteristics of the companion, but also that the duration of totality, which amounted to about one hundred minutes, would be sufficient for obtaining spectrograms which would give the slope of the velocity-curve with sufficient accuracy for a determination of the relative masses of the two components of the system. Later it was found necessary, for the sake of having consistent elements, to reobserve the whole velocity-curve. A study of the rotation effect affords a means of checking the absolute dimensions of the stars and gives opportunity for direct observational evidence on the question of darkening at the limb of an early-type star.

I. THE PERIOD

On account of the flat minimum of the light-curve during the time of total eclipse, variable-star observers have found it difficult to estimate the instant of mid-eclipse, yet there is considerable evidence that the period is not constant. Hellerich,[5] from an examination of the observations up to 1922, determined a mean period of 3.3806234 days, which seems to give the best linear representation of all the observations thus far published.

The observations used by Hellerich, together with additional minima by Luyten,[6] Gadomski,[7] and Mergentaler,[8] are listed in

[1] *Bulletin of the Astronomical Institutes of the Netherlands*, **3**, 195, 1926.

[2] *Astronomische Nachrichten*, **216**, 101, 1922; **221**, 29, 1924.

[3] *Contributi del R. Osservatorio Astronomico di Capodimonte*, No. 18, 1921.

[4] *Publications of the Allegheny Observatory*, **3**, 11, 1916. [5] *Loc. cit.*

[6] *Annals of the Leiden Observatory*, **13**, 55, 1922.

[7] *Circulaire de l'Observatoire de Cracovie*, No. 19, 1925.

[8] *Ibid.*, No. 25, 1927.

Table I. Weights have been assigned depending on the number of minima and the completeness with which both branches are cov-

TABLE I

OBSERVED MINIMA

Epoch	G.M.T.	O−C Unit, 0.0001 Day	Wt.	Observer
	J.D.			
− 426	2415690.2760	+105	1	Schwab
368	2415886.3407	− 10	1	Wendell
342	2415974.2438	+ 61	2	Luizet
335	2415997.9080	+ 57	3	Williams
− 333	2416004.6780	+145	1	Yendell
+ 74	2417380.5761	− 11	3	Graff
90	2417434.6649	− 24	4	Nijland
263	2418019.5168	+ 18	8	Nijland
497	2418810.5824	+ 44	3	Nijland
641	2419297.3861	− 46	1	Lehnert
746	2419652.3472	− 89	10	Maggini
757	2419689.5463	+ 33	1	Lacchini
845	2419987.0362	− 16	1	Lazzarino
859	2420034.3646	− 20	1	Lehnert
1198	2421180.4040	+ 61	3	Luyten
1566	2422424.4691	+ 18	3	Bemporad
1826	2423303.4417	+123	1	Hellerich
1831	2423320.3396	+ 71	1	Henz
1918	2423614.4452	− 16	5	Gadomski
+2365	2425125.5800	− 54	1	Mergentaler

ered by the observations. The residuals O−C in ten-thousandths of a day, computed from the elements,

$$\text{Min.} = 2417130.4111 \text{ G.M.T.} + 3.3806234E,$$

are given in the third column.

The observations of Table I may be combined into the normal places of Table II.

TABLE II

NORMALS

Epoch	O−C	Wt.
− 352	+67	8
+ 179	+ 1	15
753	−51	16
1382	+39	6
1892	+16	7
+2365	−54	1

These normals are plotted in Figure 1, where the size of the circles varies inversely with the total weight of the point. The observations are closely represented by a sine-curve with a semi-amplitude of 0.0057 day and a period of 1800 epochs or 6085 days. The resulting elements are

$$\text{Min.} = 2417130.4111 \text{ G.M.T.} + 3.3806234E - 0.0057 \sin (0^{\circ}.2E - 34^{\circ}) .$$

While too much confidence must not be placed in this result, which is based on scattered observations with a wide spread, there can be

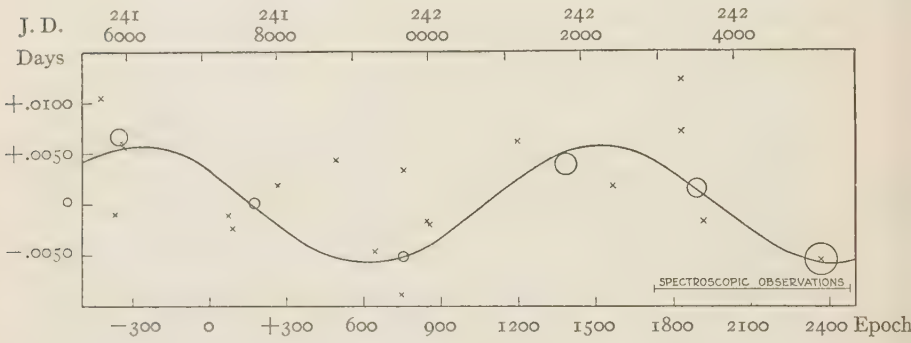

FIG. 1.—Observed minima of U Sagittae. The ordinates are residuals from the elements, Min. = 2417130.4111 + 3.3806234 *E*. The curve is computed from these elements with the addition of the term −0.0057 sin (0°.2 *E* − 34°). The crosses represent the observations of Table I. The circles, with diameters varying inversely with the weight, are the normals of Table II.

no doubt that there is a distinct variation in the time of minimum, which, in the mean at least, is periodic in nature. The accuracy of the observations does not justify the use of second harmonics.

The light-curves thus far determined show little indication of ellipsoidal figures for the stars, which would be expected if the change in period were due to revolution of the line of apsides of the system. Also, the components are rather widely separated for such a revolution in the comparatively short period of less than seventeen years.

If Figure 1 is a correct representation of the change in the time of minimum, the residuals from the linear elements should become increasingly positive from 1928 to 1936, corresponding to a lengthening

period. During the interval of the spectroscopic observations from 1921 to 1928 the period decreased in length.

Since neither the photometric observations nor the spectrographic results from 1921 to 1928 are completely represented by the elements suggested, even with the addition of the sine term, it seemed necessary in the present discussion to determine a period for this interval from the spectroscopic observations alone. The observations during totality are especially adapted to such a purpose. They fall on the steepest part of the velocity-curve, the range is considerable, the lines are numerous and suitable for accurate measurement, and the spectrograms had been taken in several series considerably separated in time. By trial a period was found which would make the sum of the squares of the residuals during totality the least. The results of such a method are much more reliable than those which would have been obtained by including the period in the least-squares solution of the principal star, whose spectrum is much poorer and has only one-third the velocity range of the secondary star.

The period obtained by this method has been used throughout the discussion of the spectrographic data. The elements used are

$$\text{Min.} = 2424719.9007 \text{ G.M.T.} + 3.38056E .$$

II. THE VELOCITY-CURVE OF THE BRIGHTER STAR OUTSIDE ECLIPSE

In order that observations covering the whole of the period might be made on a homogeneous system with the same instruments, spectrograms of the brighter component were taken outside of eclipse. On account of its faintness the spectrum of the secondary component does not appear at this time. These observations may be compared with those used by Miss Fowler[1] at the Allegheny Observatory. Such differences as occur are probably due to the errors of measurement of poor spectra with few lines rather than to any real change in the elements of the orbit.

In Table III are listed the forty-three spectrograms used in the solution of the velocity-curve of the principal star. The measured velocities are given, together with the weights used. Plates taken during partial and total phases are reserved for special treatment of the rotation effect and for the velocity-curve of the secondary star.

[1] *Loc. cit.*

The spectrum of the principal star is B9n. Helium lines are weak and only a few are visible. Measurement of the spectrum is difficult

TABLE III

Observations outside Eclipse

Plate	H.G.M.T.	Phase	Vel.	Wt.	O−C
	J.D. 242+	days	km/sec.		km/sec.
C 4440	5159.6292	0.2557	−40	3	+ 4
γ 15700	5348.9583	0.2734	53	3	− 7
15143	5098.8201	0.2967	45	2	+ 3
C 3978	4750.6361	0.3104	37	2	+13
γ 15715	5365.9945	0.4068	53	2	+ 7
14354	4716.9993	0.4792	91	2	−25
16256	5548.6903	0.5524	66	3	+ 6
C 3982	4750.8791	0.5534	76	2	− 4
γ 15228	5129.6396	0.6911	75	2	+ 5
C 4737	5346.0333	0.7290	77	3	+ 4
γ 15230	5129.7771	0.8286	92	3	− 9
14468	4754.6507	0.9444	81	2	+ 2
15134	5082.7576	1.1370	66	1	+10
15146	5099.6722	1.1488	61	3	+14
14356	4717.6695	1.1494	90	3	−14
14410	4727.8132	1.1514	74	3	+ 2
15135	5082.8514	1.2308	66	3	+ 2
14455	4751.6424	1.3167	73	3	−12
14519	4778.7181	1.3479	72	2	−14
C 4984	5515.7375	1.4052	53	1	− 2
γ 14360	4717.9910	1.4709	34	3	+10
C 3964	4748.6465	1.7013	−26	1	−13
4406	5130.7639	1.8154	+14	1	+12
4961	5492.6423	1.9739	16	3	− 5
γ 10430	2943.7055	1.9794	31	3	+10
15293	5164.7417	1.9876	28	3	+ 5
C 4387	5127.6785	2.1106	14	3	−22
γ 15158	5100.6750	2.1516	34	3	− 5
14361	4718.6813	2.1612	49	2	+10
14422	4728.9160	2.2542	57	3	+12
14459	4752.6479	2.3222	29	3	−19
15162	5100.9000	2.3766	57	3	+ 6
C 4029	4779.8229	2.4527	52	1	− 1
γ 14365	4718.9938	2.4737	63	2	+11
C 4436	5158.5979	2.6050	50	1	− 2
4742	5347.9792	2.6749	59	3	+10
3970	4749.6389	2.6947	61	2	+13
3972	4749.7007	2.7555	29	1	−16
3974	4749.8389	2.8937	36	2	+ 1
4966	5493.6319	2.9635	48	3	+17
γ 15301	5165.7347	2.9806	15	3	−14
15221	5128.6695	3.1016	8	3	−10
C 4941	5483.6368	3.1101	+20	2	+ 4

on account of the width and poor character of the lines, and the resulting velocities show large errors. The plates, usually of the

Eastman 40 emulsion, were taken with one prism and cameras of 18-inch and 10-inch focal length at the 60-inch and 100-inch reflectors. In assigning weights the general character of the spectrum was considered as well as the number of lines and the dispersion employed. The lines usually measured were H; K; $H\delta$; $H\gamma$; $H\beta$; λλ 4026, 4143, 4388, 4471, and 4481.

The total weight of the solution is considerably diminished by the exclusion of observations made during partial phases and the complete absence of the spectrum during totality.

The normal places of the velocity-curve are given in Table IV.

TABLE IV

NORMALS OUTSIDE ECLIPSE

Phase	Vel.	Wt.	O−C
days	km/sec.		km/sec.
0.3013	−45.6	12	+3.4
0.6076	−75.7	12	−0.9
1.0338	−89.6	12	+1.0
1.2330	−71.0	9	−2.5
1.5038	−39.0	8	+0.3
2.0129	+22.2	12	−3.4
2.1925	+46.2	8	+4.6
2.4102	+48.4	10	−3.1
2.7522	+50.1	8	+4.0
3.0325	+22.8	11	−0.4

The orbit is so nearly circular that values of T and ω could not be successfully determined by the usual method of least squares. Accordingly, a method of trial and error was employed for estimating the value of these quantities after the other elements had been determined by assuming a circular orbit. The resulting values are believed to be as accurate as can be expected in view of the nature of the observational material.

The final elements determined, as well as those of Miss Fowler from observations of 1907–1911, are given in Table V.

The difference between the two sets of elements is perhaps not larger than would be expected from such observations. The large change in the value of ω probably indicates that the eccentricity is too small to be determined from such poor data. The probable errors of a single observation of weight unity and an average normal place are 11.1 and 1.9 km/sec., respectively. The value of −15.1 km/sec.

found for γ has been determined entirely from observations of the principal star, but it has considerable additional weight, owing to the fact that the point of crossing of the observed primary and secondary curves has almost exactly this value.

III. THE OBSERVATIONS DURING TOTAL ECLIPSE

At primary minimum the larger star passes centrally or nearly so in front of the smaller. The duration of totality is about one hundred minutes. In this short interval of time it has been found possible, with the 100-inch reflector, to obtain spectrograms which give considerable knowledge of the spectrum and motion of the larger and fainter star. The dispersion employed is necessarily small, about

TABLE V

SPECTROGRAPHIC ELEMENTS OF U SAGITTAE

	Mt. Wilson 1926–1928	Allegheny 1907–1911
P (days)	3.38056	3.380603
T (days after min.)	1.5960	2.998
ω	260°	44°
e	0.035	0.035
γ (km/sec.)	−15.1	−19.13
K (km/sec.)	67.9	66.45
$a \sin i$ (km)	3,155,000	3,090,000

75 A per millimeter, and the exposure times are limited, averaging fifty-two minutes. Thirty spectrograms, as given in Table VI, have been taken which show measurable spectra of the fainter star. Some of these plates were exposed, wholly or in part, immediately before or after totality and give some indication of the presence of the continuous spectrum of the B-type star. Such plates are doubtless less reliable and have been given smaller weight.

The spectral type of the fainter star is gG2. The lines are remarkably good in view of the large rotation effect which must be present. The average number of lines measured is ten per plate.

Figure 2 is a detailed plot of the observations of the secondary star and portions of the two velocity-curves. The diameter of the circles varies inversely as the weight of the observations. There is some indication that the lines of the secondary are seen for a somewhat longer time before minimum than after, although the ap-

pearance of the spectra taken at equal intervals before and after minimum is closely the same.

TABLE VI

OBSERVATIONS OF FAINTER STAR

Plate	H.G.M.T.	Phase	Vel.	Wt.
	J.D. 242+	days	km/sec.	
C 1353	2968.6708	3.2808	−72.6	1
4287	5040.9701	3.2968	41.2	1
1354	2968.6916	3.3016	65.2	1
4827	5395.9354	3.3033	44.9	1
4033	4780.6764	3.3062	43.3	1
4900	5439.8930	3.3136	39.4	1
4288	5040.9938	3.3205	37.4	1
1355	2968.7174	3.3274	47.8	1
4265	5013.9590	3.3302	17.1	2
4299	5047.7715	3.3371	15.2	2
3891	4719.8632	3.3431	26.0	4
3858	4692.8201	3.3445	35.6	4
4034	4780.7181	3.3479	27.2	4
4828	5395.9847	3.3526	29.2	4
4901	5439.9403	3.3608	35.7	2
4300	5047.8000	3.3656	22.0	3
2903	3989.6847	3.3656	13.8	4
4266	5013.9952	3.3664	10.6	3
1273	2941.7132	3.3677	24.0	3
1356	2968.7583	3.3683	20.7	3
3892	4719.9007	0.0000	10.3	4
3859	4692.8618	0.0056	−14.9	3
4902	5439.9820	0.0219	+ 1.6	1
4301	5047.8438	0.0288	−12.2	4
4035	4780.7799	0.0291	+ 2.7	2
3893	4719.9375	0.0368	+12.5	1
2904	3989.7375	0.0378	− 6.6	2
3860	4692.8965	0.0403	− 0.7	3
4302	5047.8812	0.0662	+22.6	1
4991	5517.7826	0.0697	+ 0.9	1

Comparison of the slopes of the two velocity-curves gives the relative values of the velocity range and the ratio of the masses of the two stars. The mass ratio thus found is

$$\frac{m_1}{m_2} = 3.3 .$$

The value of K for the fainter star is $3.3 \times 67.9 = 224.0$ km/sec. The individual masses in terms of the sun are 6.7 for the bright star and 2.0 for the faint.

IV. OBSERVATIONS DURING PARTIAL PHASES: ROTATION EFFECT

During partial phases of the eclipse before and after totality portions of the early-type star are covered by the G-type secondary. The eclipse is nearly central. As the eclipse proceeds, the light reaching the earth from the bright star has a more and more localized ori-

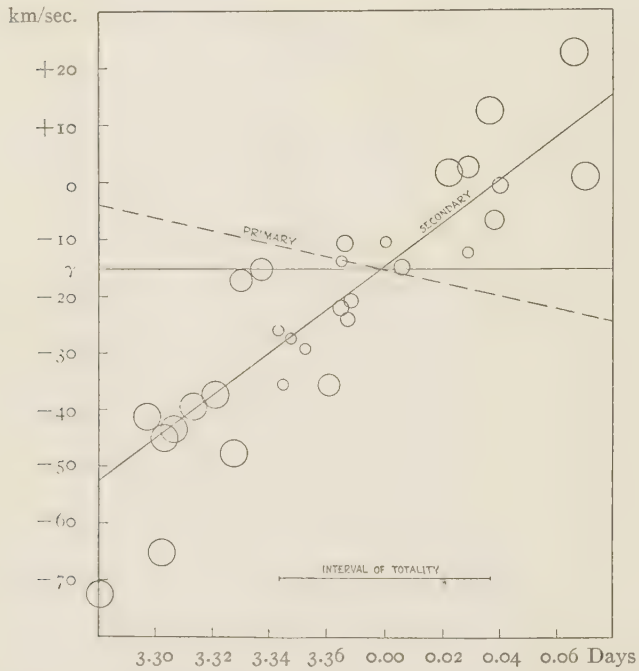

FIG. 2.—Detail of velocity-curves near totality. The size of the circles varies inversely with the weights. Comparison of the two slopes gives the relative masses.

gin toward one limb until it is cut off entirely at the instant of totality. After the total phase has passed, the other limb is first exposed and then the whole disk is gradually uncovered. If the eclipse were exactly central, ideal conditions for observing the rotation effect would prevail, and the maximum effect could actually be observed if the observations could be continued until the instant of totality.

Table VII is a list of the twenty-nine spectrographic observations during partial eclipse.

TABLE VII

OBSERVATIONS OF BRIGHTER STAR DURING PARTIAL ECLIPSE

Plate	H.G.M.T.	Phase	Vel.	Wt.
	J.D. 242+	days	km/sec.	
C 4898	5439.7181	3.1387	+ 8.3	3
4093	4834.6035	3.1443	23.5	1
γ 15222	5128.7181	3.1502	7.1	3
C 4094	4834.6229	3.1637	33.4	1
4825	5395.8208	3.1887	31.0	3
4045	4807.6375	3.2228	21.1	3
γ 15223	5128.7938	3.2259	21.7	3
C 1351	2968.6410	3.2509	21.7	2
1352	2968.6542	3.2641	28.1	1
4032	4780.6389	3.2687	31.1	2
4943	5483.7972	3.2705	24.5	2
4046	4807.6875	3.2728	41.6	1
3856	4692.7611	3.2854	52.6	1
4827	5395.9354	3.3033	35.7	3
4033	4780.6764	3.3062	45.4	1
3857	4692.7833	3.3076	58.1	1
4900	5439.8930	3.3136	43.2	1
4944	5483.8451	3.3184	+29.8	1
4302	5047.8812	0.0662	−56.4	2
4991	5517.7826	0.0697	61.8	2
3861	4692.9264	0.0702	41.2	1
5082	5578.6465	0.0836	62.1	1
3862	4692.9486	0.0924	54.6	2
4303	5047.9104	0.0954	67.7	1
4304	5047.9341	0.1191	47.9	2
γ 15319	5169.6493	0.1341	55.1	3
14349	4716.6834	0.1633	48.8	3
14403	4726.8486	0.1868	53.3	3
C 4440	5159.6292	0.2557	−39.6	3

For U Sagittae, Fetlaar[1] has made both uniform and darkened solutions depending on the long series of visual estimates by Nijland. His results give:

	Uniform	Darkened
Semi-duration of eclipse	0.257 days	0.281 days
Semi-duration of totality	0.037	0.033
Inclination	84°33′	90°

Using these values for the time of eclipse and for the inclination and assuming that the star rotates in the same period as that of its orbital revolution, we may determine the expected velocity corresponding to any given phase for certain values of the rotation at the limb. The four normal points of the observations during partial phases, both

[1] *Loc. cit.*

preceding and following totality, are plotted in Figure 3, the horizontal axis representing the velocity-curve of the brighter star determined from observations outside eclipse. The problem is to determine some mean value of the linear rotational velocity which will most nearly represent the observed normals. While there is perhaps some improvement in the quality of the spectral lines as the eclipse progresses, it is not marked and the spread of the measured velocities

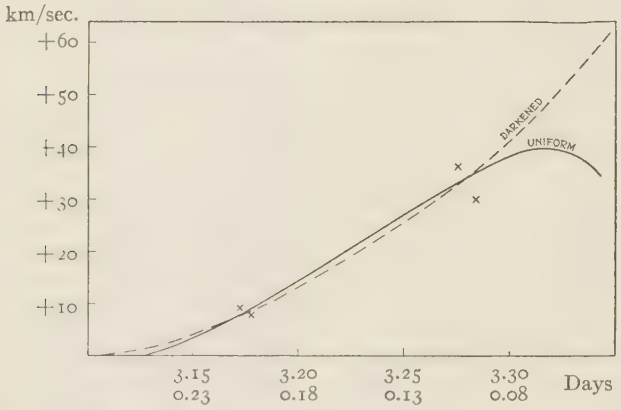

FIG. 3.—Rotation effect using Fetlaar's darkened and uniform solutions. The crosses are observed normal points. The observations after minimum are plotted in reverse direction. The curves represent the computed values.

is still large. The observations preceding minimum have somewhat greater total weight than those following and indicate a higher value of the rotation effect. Perhaps the simplest method of determining the amount of the rotation effect is the graphical solution used by Rossiter[1] in his study of β Lyrae. This method has been followed for both the uniform solution with an inclination of $84^\circ 33'$ and the completely darkened solution with central eclipse. For the darkened solution it was necessary to take into account not only the varying velocity, which increases directly with distance from the axis of rotation, but also the decrease in brightness from the center outward toward the limb in all directions. Following the procedure of Russell and Shapley[2] for darkened stars, we have drawn a disk representing the apparent surface of the brighter star and divided it into areas of

[1] *Astrophysical Journal*, 60, 20, 1924. [2] *Ibid.*, 36, 239, 1912.

equal light-intensity on the assumption that the light is reduced to zero at the limb in accordance with the law

$$J = J_0 \cos i ,$$

where i is the angle between the line of sight and the normal. The projection of the larger and fainter star was then drawn upon the figure as it would appear at certain successive phases of the partial eclipse. The uneclipsed areas of equal luminosity at stated distances from the axis of the star were counted, and the mean velocity of that portion of the star which was visible at the several phases was thus determined by mechanical quadrature for different values

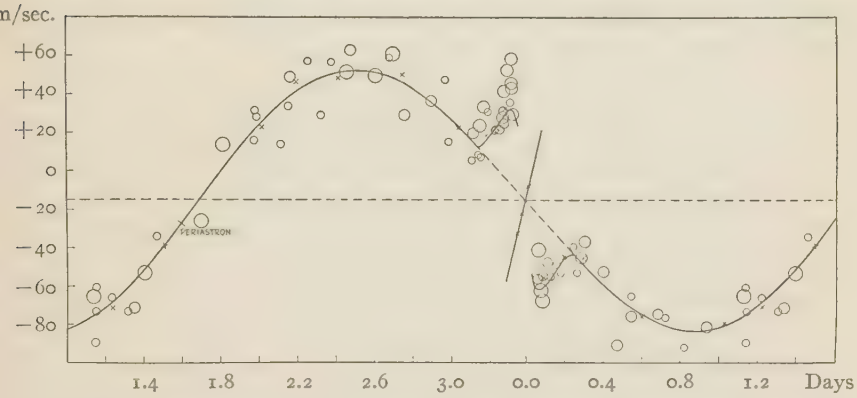

FIG. 4.—Velocity-curve of U Sagittae. Circles are single observations. Crosses are normals. The size of the circles varies inversely with the weight.

of the rotational velocity at the limb. The curves which best fit the weighted normal places are shown in Figure 3. The corresponding mean rotation effects are estimated to be 60 km/sec. for the uniform and 62 km/sec. for the darkened disks.

It is commonly believed that the uniform disk is more probable for stars of B type, and Fetlaar's uniform solution gives better agreement with the photometric observations than the darkened. The spectrographic observations in this case seem utterly inadequate for a decision between the two solutions. Although the forms of the curves are very different near the time of totality, they are much the same for those portions of the curves where the spectra are measurable. The observations of the B-type star cannot be pushed closer to minimum because the G-type star seems to dominate the spectrum

within thirty or forty minutes of totality, when the combined light is fainter than 8.6 mag. and its numerous lines render settings upon the diffuse hydrogen and helium lines of the early-type star uncertain.

The value of 60 km/sec. for the rotational velocity at the limb, which corresponds to the uniform solution, gives 2,790,000 km for the radius of the small, bright star. This result depends chiefly upon the spectrographic data and the period, although the value of the rotation effect also involves the duration of partial and total phases, the inclination of the orbit, and the relative sizes of the two stars as determined by the photometric solution. It agrees reasonably well with the radius computed by combining $a \sin i$ of the spectrographic orbit with the photometric data.

V. ABSOLUTE DIMENSIONS AND PHYSICAL PROPERTIES

Fetlaar's[1] solutions give the inclination of the orbit and the dimensions of the stars in terms of the relative orbit, which are as follows:

	Uniform	Darkened
r_1, radius of large star	0.292	0.280
r_2, radius of small star	.175	.218
cos i	0.095	0.000

By using these results with the spectrographic values of $a \sin i$ (3,155,000 km) and the ratio of the masses (3.3), the absolute dimensions may be determined as follows:

	Uniform		Darkened	
a_1, semi-major axis of primary orbit	3,169,000 km		3,155,000 km	
a_2, semi-major axis of secondary orbit	10,457,000		10,410,000	
a_1+a_2, semi-major axis of relative orbit	13,626,000		13,565,000	
r_1, radius of large star	3,979,000	(5.7⊙)	3,798,000	(5.4⊙)
r_2, radius of small star	2,385,000	(3.4⊙)	2,957,000	(4.2⊙)
ρ_1, density of large star	0.011⊙		0.013⊙	
ρ_2, density of small star	0.171⊙		0.090⊙	
M_1, visual absolute magnitude of large star	+1.8 mag.		+1.9 mag.	
M_2, visual absolute magnitude of small star	−0.4		−0.8	
j_1, surface brightness of large star	+0.8		+0.8	
j_2, surface brightness of small star	−2.6		−2.5	

[1] *Loc. cit.*

The absolute magnitudes are derived from the formula[1]

$$M=\frac{29,500}{T}-5\log r-0.08\,.$$

The temperatures (T) are based on the spectra and taken to be 5200° for the larger star and 12,000° for the smaller. The values of the surface brightness, which are given with reference to the sun ($M\odot=4.85$), depend on the relationship

$$j=5\log r+M-4.85\,.$$

The absolute magnitudes and masses satisfy the mass-luminosity correlation of Eddington very closely. From the absolute and apparent magnitudes ($m=6.7$ and 9.4) the parallax is found to be 0".003. The spectroscopic absolute magnitude of the faint star determined from the recent Mount Wilson reduction-curves is +1.4.

The data from the various sources show satisfactory agreement. Further observations, either spectrographic or photometric, would add to the accuracy of our knowledge of this interesting system; but it seems doubtful whether there would be very great changes in the conclusions presented here. The times of minimum should be observed during the next six years for further confirmation of the change in period.

Much of the computation of the solution for the elements of the orbit and the rotation effect was done by Mr. N. U. Mayall.

Carnegie Institution of Washington
Mount Wilson Observatory
March 1930

[1] Russell, Dugan, and Stewart, *Astronomy*, p. 732, 1927.

Contributions from the Mount Wilson Observatory, No. 402
Reprinted from the *Astrophysical Journal*, Vol. LXXII, pp. 19–40, 1930
Printed in the U.S.A.

UNIVERSITY OF ARIZONA
STEWARD OBSERVATORY
TUCSON, ARIZONA

EVIDENCE FROM BAND SPECTRA OF THE EXISTENCE OF A CARBON ISOTOPE OF MASS 13

By ARTHUR S. KING and RAYMOND T. BIRGE

ABSTRACT

Isotope C^{13}.—Evidence of the existence of this isotope *appeared first in a faint band structure* with head at λ 4744.5, showing on electric-furnace spectrograms in which the Swan (C_2) band λ 4737 was of high intensity. The structure of the latter band being known, the *displacements of the head and 15 component lines* of the faint band *were measured* from corresponding lines of the primary band. An application of the *quantum theory* of band spectra then *showed* that the *band* λ 4744.5 *was due to a molecule* $C^{13}C^{12}$, *the emitter* of λ 4737 being the molecule $C^{12}C^{12}$.

Further experimental work, together with examination of older material, showed that C^{13} *enters into molecules producing isotopic bands* connected with the Swan band λ 4382, the cyanogen bands λ 3883 and λ 3590, and the carbon monoxide bands between λ 1200 and λ 1500.

The *isotopic shift* for the (1,0) band λ 4737 has been *studied in detail* as far as the observational material permitted. The *staggering* of the main band, the presence of *perturbations*, and the *methods of computing* the *vibrational* and *rotational shifts* are discussed. The isotopic shift for this band is found to be about 7.6 A, and the algebraic mean of the differences O−C is −0.0096 A, or 1 part in 800, a difference within the errors of measurement. It follows from this that the *mass ratio* of the two carbon isotopes is *12 to 13, accurate* to about *1 part in 10,000.*

Other isotopic bands.—A faint band structure to the red of the (2,0) band at λ 4382 has a head with an isotopic shift of 12.58 A, agreeing closely with the calculated shift of 12.57 A.

Evidence of a $C^{13}N^{14}$ molecule *is found in the cyanogen band* λ *3883*, where *six faint lines* evidently belong to an isotopic band, their *measured shifts* from corresponding primary lines differing from the calculated by an average amount +0.0057 A. This small discrepancy may be due to an electronic isotope effect. *The (1,0) band of this system,* λ *3590, also shows an isotopic band in the furnace spectrum,* the observed shift from the primary head being 5.3 A, agreeing with the calculated shift of 5.30 A.

These results incidentally furnish quantitative evidence that the *emitters of the Swan and "cyanogen" bands are the C_2 and CN molecules*, respectively.

The *relative abundance* of C^{13} and C^{12}, estimated very roughly from photographic intensities of the bands, *appears to be of the order 1:400.* Such estimates are rendered uncertain, however, by an apparent dependence on the method of excitation. The furnace and other *low-excitation sources, notably N-type stars,* are *very effective in emitting the C^{13} spectrum.* In the *arc,* however, the *only evidence* of C^{13} thus far is the group of lines in the cyanogen band λ 3883, this band being emitted with extraordinary intensity by the arc. *Conditions* in the *three typical sources*—arc, furnace, and star—are discussed with regard to their possible bearing on the excitation of bands in which C^{13} is concerned.

INTRODUCTION

Practically all of our knowledge concerning the isotopes of non-radioactive elements is due to the work of Aston and Dempster, who used some form of mass spectrograph. The most recent list[1]

[1] Report of the German Atomic Weight Committee, *Berichte der Deutschen Chemischen Gesellschaft*, **63B**, 1–24, January, 1930.

of such isotopes gives fifty-seven elements that have been examined for isotopes, of which twenty-three are apparently single, so far as evidence from the mass spectrograph is concerned. Among this list of twenty-three are the two elements, oxygen and carbon, which from their integral atomic weights and other evidence would seem least likely to consist of two or more isotopes.

Under such circumstances, the discovery by Giauque and Johnston[1] of isotopes of oxygen, of mass 17 and 18, is of great significance. The relative abundance of these two new atomic species is very small, compared to the more usual O^{16} species, and this explains the failure of the mass spectrograph to detect them. Thus O^{18} has the same mass as H_2O, except for a slight difference of packing effect,[2] and it is difficult to exclude all moisture from such an apparatus. On the other hand, the spectrum of the O_2 molecule, as employed by Giauque and Johnston, is eminently suitable for the purpose.

The initial application of the quantum theory of band spectra to the matter of isotopes is due independently to Loomis[3] and Kratzer.[4] Later work by Mulliken and others[5] has resulted in the identification in band spectra of a number of isotopes already known from the mass-spectrograph work. This spectroscopic work was of special importance in that it constituted perhaps the most direct and convincing confirmation of the present accepted interpretation of molecular spectra. As a result of it, one can now predict with great confidence just how the spectrum of a molecule containing any atomic species, such as O^{17} or O^{18}, should differ from the spectrum of the molecule containing only the more usual species (here O^{16}) of the same element. Within reasonable limits, the relative scarcity of an atomic species is no bar to its successful identification, for by sufficiently long exposures the new species can be made evident.

[1] *Journal of the American Chemical Society*, **51**, 1436 and 3528, 1929.

[2] At the present time it would appear that the mass of O^{18} is close to 18.000, while that of H_2O is close to 18.014. Hence Aston should be able to distinguish between the two in his precision mass spectrograph, described in 1927 (*Proceedings of the Royal Society*, A, 115, 487, 1927).

[3] *Nature*, **106**, 179, 1920; *Astrophysical Journal*, **52**, 248, 1920.

[4] *Zeitschrift für Physik*, **3**, 460, 1920; **4**, 476, 1921.

[5] See F. W. Loomis, "Molecular Spectra in Gases," *Bulletin of the National Research Council*, **11**, Pt. 3 (No. 57), chap. v, 1926.

Presence of impurities, like H_2O, is irrelevant, since the spectrum of any molecule, such as O_2, is unique. The spectra of molecules containing different atomic species, such as $O^{16}O^{16}$ and $O^{16}O^{18}$, differ, to a first rough approximation, merely in a "shift" of each band to higher or lower frequency, the direction and extent of the shift (vibrational-isotope effect) depending on the masses concerned and on the quantum designation of the particular band. A more extended and correct description of the isotope shift is given later in this paper.

Giauque and Johnston, in their work on the oxygen isotopes, used spectroscopic data obtained by H. D. Babcock for atmospheric lines in the solar spectrum, taken at periods of very low sun when the atmospheric path was of maximum length. These oxygen isotope lines have not yet been detected in laboratory sources.

In the course of investigations by one of the writers on the electric-furnace spectra of metals, spectrograms were occasionally obtained in which high temperature and long exposure caused the Swan spectrum of carbon, from the material of the graphite tube, to appear with high intensity. The origin of this band system has long been in dispute, but recent evidence[1] has pointed rather clearly to the diatomic molecule C_2. The present paper furnishes definite evidence of the correctness of this conclusion.

On the electric-furnace plates just mentioned, a faint band appeared with head at λ 4744.5, the structure being visible until it merged into the head of the strong (1,0) band of the Swan system at λ 4737. Although not accounted for by the analysis of the various series of the λ 4737 band, a physical connection with the latter seemed very probable, borne out by the fact that in spectra of N-type stars, the so-called "carbon stars," the strong band at λ 4737 is accompanied by a fainter one whose position agrees closely with that in the furnace spectrum. This faint band has also figured in the literature, although its band character seems not to have been recognized. Thus Raffety[2] speaks of a well-marked single "line" at λ 4743, associated with the Swan bands, and in Figure 14, Plate XIII, accompanying his article, this line appears clearly, and has

[1] W. E. Pretty, *Proceedings of the Physical Society of London*, **40**, 71, 1928.

[2] *Philosophical Magazine* (6), **32**, 546, 1916.

in fact more the appearance of a band. It appears also in Figure 1, Plate 4, of an article by Johnson[1] on the Swan bands, although it is not mentioned in the article.

Inspired by the discovery of the isotopes of oxygen, the writers examined this faint band at λ 4744 in connection with a possible isotope of carbon. In spite of the faintness of the band, the head and six lines could be recognized and measured. The six corresponding lines in the main band, with head at λ 4737, were obvious, and we therefore had six measurable "shifts." The quantum analysis of the Swan band system was known from the work of Shea,[2] and calculations showed immediately that the λ 4744 band agreed quantitatively (to a fraction of 1 per cent) with the molecule $C^{13}C^{12}$ as an assumed source, the main band being due to $C^{12}C^{12}$. The announcement[3] of this was followed in a few days by another, in which one of the writers[4] showed that certain faint lines found by one of us[5] in electric-furnace spectra, scattered among the component lines of the λ 3883 band of cyanogen, agreed quantitatively with the molecule $C^{13}N^{14}$ as an assumed source, and that a series of subheads, found by Hopfield and Birge[6] in the absorption spectrum of carbon monoxide, agreed with $C^{13}O^{16}$ as an assumed source.

Systematic experimental work was then undertaken, in order to bring out the structure of the band at λ 4744 as fully as possible, to look for evidences of C^{13} in other bands, and to determine if possible the conditions governing the appearance of λ 4744, which in the laboratory occurred only in the spectrum of the furnace. As a result of this work, the λ 4744 band has been obtained in both second- and first-order furnace spectra, taken with the 15-foot concave grating. Its strength in the first order is now sufficient to enable at least fifteen lines to be measured. The corresponding isotope band accompanying the (2,0) band at λ 4382 has been identified, although its position and extreme faintness make accurate measure-

[1] *Philosophical Transactions of the Royal Society of London*, A, **226**, 157, 1927.

[2] *Physical Review*, **30**, 825, 1927.

[3] *Ibid.*, **34**, 376, 1929; *Nature*, **124**, 127, 1929 (dated June 24).

[4] Birge, *Physical Review*, **34**, 379, 1929; *Nature*, **124**, 182, 1929 (dated June 29).

[5] King, *Mt. Wilson Contr.*, No. 194; *Astrophysical Journal*, **53**, 161, 1921.

[6] *Physical Review*, **29**, 922, 1927.

ments very difficult. In cyanogen we have found the $C^{13}N^{14}$ band accompanying the (1,0) band at λ 3590.

Measurements on all of the new bands have been made by each of the writers, and certain preliminary conclusions have been reached and announced.[1] The work already finished is sufficient to establish without question the existence of an isotope of carbon, of mass 13. We are, however, trying to get quantitative measurements of the isotope shift, from which one may obtain an extremely accurate evaluation of the mass ratio and "packing effect" of the two atomic species.[2] We are also investigating the relative intensity of the "isotope" bands, as compared with the main bands. This relative intensity seems, strangely enough, to be a function of excitation conditions. Both of these problems have proved much more difficult than anticipated, and are far from solved at the present time. In regard to the first, it appears necessary to make new measurements, and from these to derive new constants for all the bands under consideration. Such work must necessarily consume a considerable period of time.

The purpose of the present article is then to present, in a semi-quantitative manner, the material bearing on the existence and appearance of the carbon isotope of mass 13. Further details bearing on various aspects of this matter will be published in a series of later articles.

THE $C^{13}C^{12}$ BAND AT λ 4744.5

The (1,0) band of the Swan system is λ 4737, which represents a $^3\Pi - {}^3\Pi$ electronic transition in the $C^{12}C^{12}$ molecule. It corresponds directly to the B band of atmospheric O_2 in the solar spectrum, and is the best available band for observing the C^{13} isotope and for measuring the isotope shift. For this reason special efforts have been made to obtain the $C^{13}C^{12}$ isotope band at λ 4744.5 with as great intensity as possible.

The regular furnace tubes of highly purified Acheson graphite, 19 mm in outside diameter and 12.5-mm bore, the heated portion being 20 cm long, were used in the investigation. As the Swan bands appear in this furnace at about 2400° C and as a high intensity of

[1] *Ibid.*, **35**, 133, 1930 (abstract 3).

[2] See W. F. Giauque, *Nature*, **124**, 265, 1929.

λ 4737 was required, tube temperatures of 2800° to 2900° C were employed for the best results. The use of high-contrast plates gave an improved resolution of the band structure. Details of the isotope band at λ 4744 were brought out best by the first order of the 15-foot concave-grating spectrograph, on account of the negligible strength of the ghosts in this order. Numerous spectrograms were also made in the second order, to obtain superior resolution near the λ 4737 head, but the isotope band was somewhat blurred by a ghost at about λ 4740.

Plate IX is an enlargement of our best first-order spectrogram and shows the heads of the main (1,0) and (2,1) bands, at λ 4737 and λ 4715, respectively, and also the new isotope band at λ 4744.5. The structure just at the λ 4744 head resembles that of the heads of the main Swan bands, although the isotope band as a whole is by no means a copy of its primary. The unresolved head λ 4744.5 has a sharp companion line at λ 4744.63, while on the violet side fifteen band lines are measurable on the best plates before the isotope band merges in the primary head. The identity of the various lines in both the main band and the isotope is shown on the photometric curve *a* of Plate X, which, as in the case of other such curves shown here, was traced with the Zeiss microphotometer in the physics department of the University of California. Curve *a* was made from the first-order spectrogram shown in Plate IX. Curve *b* covers the same region, using a second-order plate. As just noted, some extraneous structure appears in the second-order isotope lines.

Details concerning the fine structure of the Swan bands may be found in the articles by Shea[1] and Johnson.[2] Page 173 of the latter article shows a drawing of the fine structure near the head of λ 4737, and Plate 4 of the same article reproduces photographs of this band, in vacuum tubes and in arc sources. Our own furnace spectrograms correspond to a temperature intermediate between the tube and furnace, but show some striking differences in intensity distribution which will be discussed in later articles. We are here interested only in the general features of the fine structure. Each band consists of *P* and *R* branches only. Each line is itself triple, the spacing being greatest near the origin of the band and diminishing rapidly as the

[1] *Loc. cit.* [2] *Loc. cit.*

PLATE IX

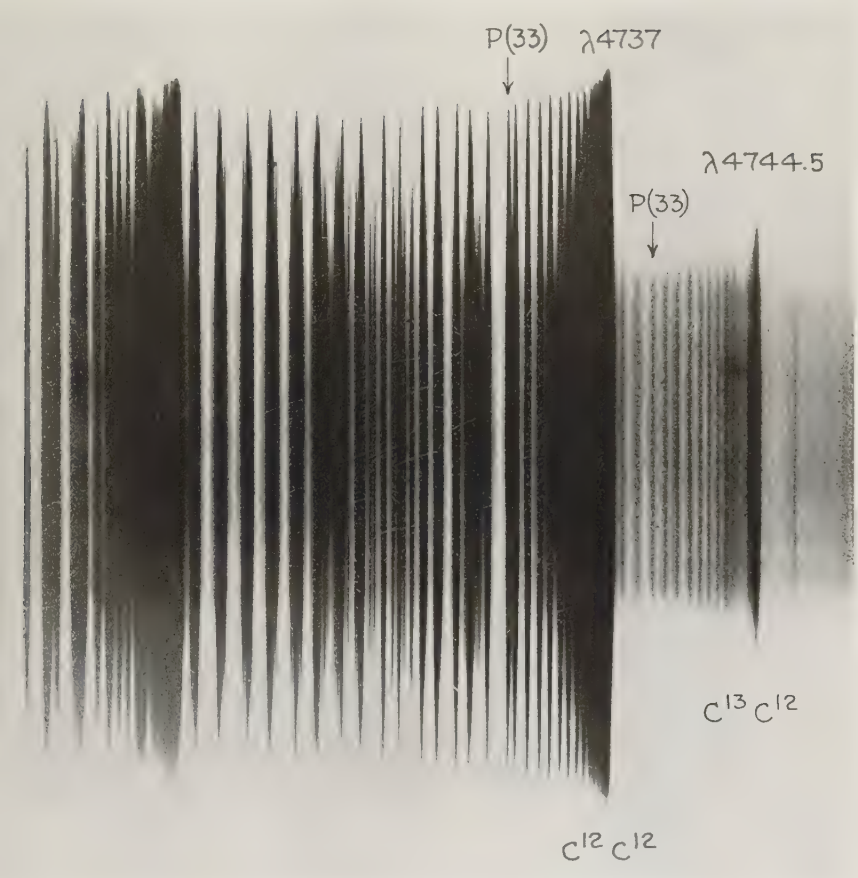

The Carbon Band λ 4737 and Isotope Band λ 4744.5

PLATE X

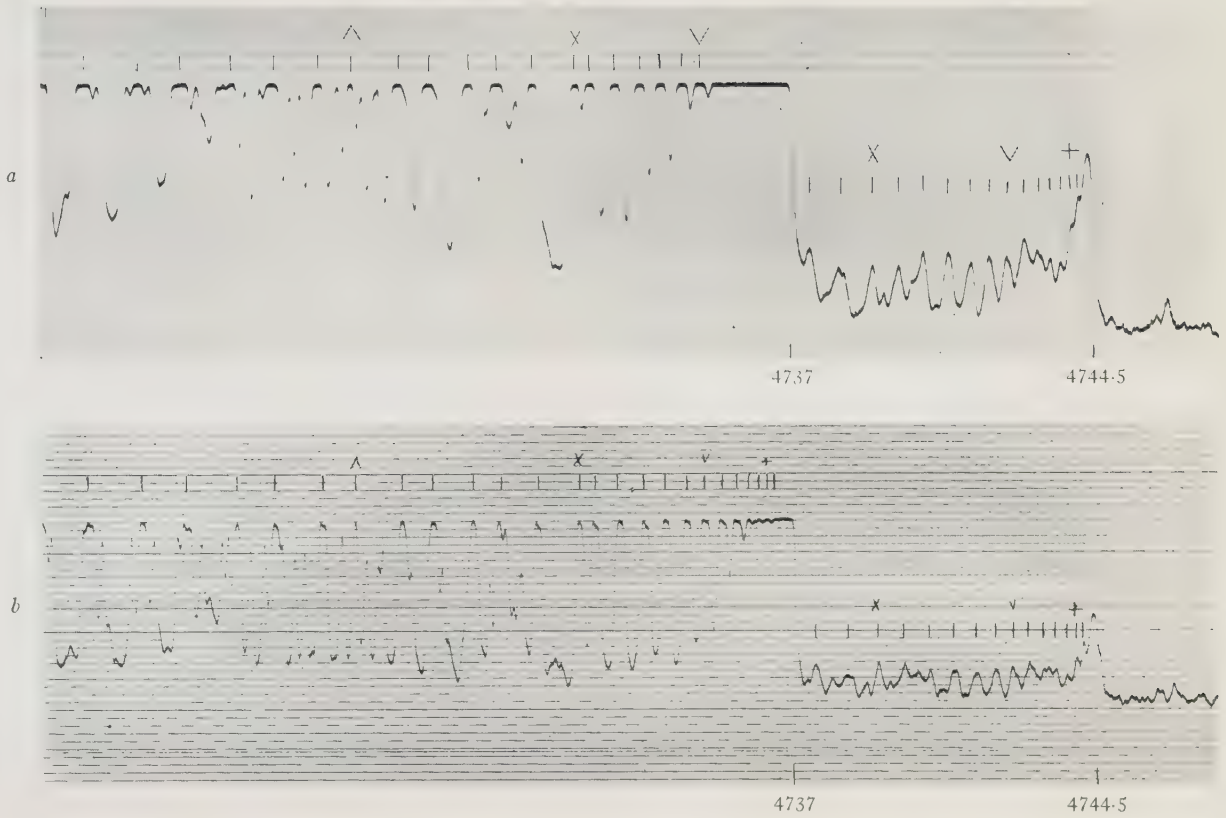

MICROPHOTOMETER CURVES OF THE CARBON BAND λ 4737 AND ITS ISOTOPE λ 4744·5

a) Curve from first-order spectrogram

rotational quantum number J increases.[1] The calculated origin ν_0 of the (1,0) main band is at λ 4730.938 (21,131.56 cm^{-1} in vacuum),[2] while that of the isotope band should be at about λ 4738.72 (21,096.85 cm^{-1} in vacuum). From the origin the P branch runs toward the head, then reverses and returns across the origin. In the spectrograms here used, only the returning P branch appears. Both Johnson and Shea use the same numerical labels for the various triplets composing each branch, and for convenience their labels are retained. Without going into the rather complex details of nomenclature,[3] it may be noted that in a line such as $P(30)$, the number 30 is what Shea assumed the actual rotational quantum number J'' of the lower state to be, for the central line of the three composing a "natural" triplet.[4]

Calculations show that the head of the λ 4737 band occurs at P (17). In the isotope band the first line that can be measured is $P(21)$, and the last is $P(35)$. This gives fifteen lines for measuring the shift, although only the lines $P(25)$ to $P(35)$ have as yet been used. These various lines are indicated in both the main and isotope bands, in Plate X, curves *a* and *b*. Line $P(22)$ is labeled by a plus sign (+), P (27) by a *v*, $P(33)$ by an *x*, and $P(39)$ (main band only) by an inverted *v*. The multiple character of the lines of the main band is shown plainly in curve *b*. The isotope lines appear, however, merely as broad single lines. This is as expected. It is well known that successive triplets in the Swan bands are "staggered" (i.e., alternate lines displaced from a smooth curve), a phenomenon connected with the fact that, theoretically, a $^3\Pi$ level has a sixfold multiplicity. The doubling of each of the three levels is

[1] See Fig. 3, p. 841, of Shea, *loc. cit.*

[2] This is a new calculation and differs very slightly from Shea's value. Johnson's values of ν_0, for the various bands, are incorrect, due to an error in his assignment of J-values. See Shea, *loc. cit.*

[3] We are following, so far as convenient, the new nomenclature proposed by R. S. Mulliken, in an article now in press. See also R. S. Mulliken, *Reviews of Modern Physics*, **2**, 60, 1930.

[4] It is actually the value of $J''+1$, according to the new mechanics, and is also the value of $K''+1$ for all three lines of the triplet. We shall be concerned with the rotational energy change, corresponding to each line, and this is given to the first approximation by $B'(K'+1/2)^2-B''(K''+1/2)^2$. Thus, in calculating the rotational energy change for $P(30)$, one would write $B'(28.5)^2-B''(29.5)^2$.

termed "Λ-type doubling." In a symmetrical molecule, composed of atoms having no nuclear spin moment, like $C^{12}C^{12}$, half of the levels are absent, the remaining levels constituting alternately the upper and lower components of the Λ-type doubling. This produces the staggering of the lines. The isotope molecule, $C^{13}C^{12}$, is, however, not symmetrical and all six levels should occur. The presence of twice as many levels, in an unsymmetrical isotope molecule, has been proved[1] in the case of O_2. Hence each line of the $C^{13}C^{12}$ band is presumably an unresolved sextet, and successive lines should show no staggering.

Another noteworthy difference between the main and isotope bands concerns the location of perturbations. The line $P(33)$ occurs far to the red of its expected position in the main band, but shows no irregularity in the isotope band. Such perturbations are now explained as a "resonance" phenomenon, due to the near-coincidence of a level, or levels, of one electronic state with those of another electronic state.[2] Since all the energy-levels of the isotope molecule $C^{13}C^{12}$ are shifted with respect to those of the primary molecule, and shifted by varying amounts, one should indeed expect perturbations in the isotope molecule, but not at the same value of J. There is no large perturbation in the isotope molecule within the short range covered by the observational data.

As already noted, we have at this time no final quantitative results to report. The following data and discussion will indicate merely in a general way the nature of the evidence. Table I, second column, gives the average of a number of sets of readings for the center of gravity of each triplet in the main band, as well as for the sharp line at the red edge of the head. The third column gives similar data for the isotope band. The absolute scale of wavelengths is based on a direct comparison with iron normals. Because of the great intensity difference between the λ 4737 and λ 4744 bands, they had to be measured on different plates. As a comparison standard, we used the line $P(39)$ at λ 4726.316 in the primary band, since this is sharp and apparently single on all plates. The observed isotope shift is given in the fourth column of Table I,

[1] Giauque and Johnston, *loc. cit.*

[2] See, for instance, G. H. Dieke, *Nature*, **123**, 446, 1929.

and the calculated in the fifth column. The calculated shift was obtained as follows.

The isotope shift[1] is composed of three parts: electronic, vibrational, and rotational. It is to be anticipated that the electronic shift is small (0–0.05 cm^{-1}). This effect can be measured and eliminated only by means of observations on two different bands having a common vibrational state. At present we have usable data only

TABLE I

	λ_{air} $C^{12}C^{12}$	λ_{air} $C^{13}C^{12}$	Obs. Shift	Calc. Shift
			A	A
$P(35)$	4729.913	4737.672	7.759	7.812
$P(34)$	4730.803	4738.430	7.627	7.666
$P(33)$	4731.833	4739.179	7.346	7.353
$P(32)$	4732.210	4739.837	7.627	7.645
$P(31)$	4732.830	4740.452	7.622	7.659
$P(30)$	4733.439	4741.068	7.629	7.618
$P(29)$	4733.954	4741.605	7.651	7.645
$P(28)$	4734.481	4742.072	7.591	7.594
$P(27)$	4734.921	4742.499	7.578	7.601
$P(26)$	4735.352	4742.906	7.554	7.564
$P(25)$	4735.697	4743.278	7.581	7.586
$P(24)$	4735.979	4743.568	7.589	.....
$P(23)$	4736.238	4743.820	7.582	.....
$P(22)$	4736.456	4744.037	7.581	.....
$P(21)$	4736.624	4744.221	7.597	.....
Head	4737.059	4744.628	7.569	7.55

for one band, and therefore cannot evaluate this shift, if present at all. The main portion of the observed shift is vibrational, and the magnitude of a vibrational shift varies roughly with the change in the vibrational quantum number v. For this reason the calculated shift in the (0,0) band is very small,[2] while that in the (2,0) band is nearly double the shift in the (1,0) band. The vibrational shift applies strictly to the origin of a band, and to calculate it one needs the constants giving the origins of the bands of a system as a function of the vibrational quantum numbers v' and v''. For the (0,0) band we have calculated the origin directly from the data given

[1] See R. T. Birge, *Transactions of the Faraday Society*, 25, 718, 1929, for a brief review of the theory, and particularly of the methods used in the present work.

[2] The (0,0) band at λ 5165 is photographically so much fainter than the (1,0) band that the isotope is apparently not detectable with the material now available, regardless of the magnitude of the shift.

by Johnson, the result[1] being 19,377.71 cm^{-1}. With the exception of the origins of the (0,0) and (1,0) bands, we have used the vibrational constants determined by Johnson.[2] Fuller details will be given in later papers.[3]

The finally adopted vibrational constants are

$$\omega_e' = 1792.55 \text{ cm}^{-1} \qquad \omega_e'x_e' = 19.35 \text{ cm}^{-1}$$
$$\omega_e'' = 1641.55 \text{ cm}^{-1} \qquad \omega_e''x_e'' = 11.67 \text{ cm}^{-1}$$

It is known, from the work of Johnson, that the $\omega_v : v$ curve is practically linear, for both upper and lower electronic levels, and the vibrational shift is then given to all desired accuracy by

$$\nu_2 - \nu_1 = (\rho - 1)(\omega_e'u' - \omega_e''u'') - (\rho^2 - 1)(\omega_e'x_e'u'^2 - \omega_e''x_e''u''^2) \; . \qquad (1)$$

In this equation $u = v + 1/2$, and is that number which is zero when the vibrational energy is zero. It may be called the "effective" vibrational quantum number. For the λ 4737 band, $u' = 3/2$, $u'' = 1/2$, and from equation (1), $\nu_2 - \nu_1 = -34.713$ cm^{-1}, with a probable error of about 0.01 cm^{-1}.

For the rotational shift we used the method already proposed by one of us.[4] The rotational constants employed are those given by Shea.[5] These are not complete for the $v' = 1$ state, and for that reason the calculated rotational energy is not in particularly good agreement with the observed value. The method already described gives, however, quite reliable results, even in the case of such discrepancies, and the calculated values are therefore trustworthy so far as these facts are concerned.

The real difficulty in calculating the rotational shift arises from

[1] Shea's value, 19,379.20, is incorrect, due to some arithmetic error.

[2] *Loc. cit.*

[3] As has been noted, we intend to obtain new constants for this system, and hence those now being used are to be considered as provisional. It should be remarked, however, that a change in the constants affects the calculated shifts very slightly. Thus a change of the origin will, in the first approximation, merely redistribute the energy in such a way that a change of 1 cm^{-1} in the actual frequency of the origin will change the calculated shift by only 0.02 cm^{-1}.

[4] Birge, *Transactions of the Faraday Society*, **25**, 718, 1929.

[5] *Loc. cit.*

quite different sources. In the first place, the isotope lines should not be staggered. We have therefore calculated smoothed positions for the lines of the main band (i.e., with the staggering eliminated), and then have calculated theoretical shifts with respect to these smoothed positions. The shifts were then corrected for the observed staggering. The perturbation at $P(33)$ was similarly treated. Hence the values in the fifth column of Table I give the calculated shifts from the observed lines of the main band to a set of lines of the isotope band assumed free from staggering and from perturbations. Now the observed data for the isotope band give no indication of staggering, but in all probability perturbations are present somewhere, and it is now known that a large perturbation at one line affects the positions of all lines in the vicinity.[1] Moreover, new measurements of the main band indicate unmistakably such an effect in the vicinity of $P(33)$, and this has not been taken into consideration in calculating the shifts. In other words, all lines of both the main and the isotope bands are, in all probability, irregular in position in a systematic manner connected with the larger perturbations, and it is very difficult in the calculations to eliminate the effect of such general irregularities. The poor agreement in the case of lines $P(34)$ and $P(35)$ in Table I is undoubtedly due to this cause. Without going into further details concerning this very involved matter, it may be said that, with sufficient experimental material, one should be able to calculate shifts which, taken as a whole, are correct, but which may be quite incorrect for the individual lines. In the present case it has seemed justifiable to use only the nine lines $P(33)$ to $P(25)$, inclusive. Further measurements are needed in order to evaluate properly the shifts for $P(21)$ to $P(24)$.

For the nine lines just cited the algebraic average of the O−C shifts is −0.0096 A. In other words, the observed shift is less than the calculated, on the average, by 1 part in 800. At the present time this discrepancy represents approximately the probable error and so cannot be considered significant. Now it may easily be shown that if the observed vibrational shift (in this case practically the entire shift) differs from the calculated shift by the proportional

[1] See Fig. 6, p. 90, of "Molecular Spectra in Gases," *op. cit.*, for the first known example of this, and F. A. Jenkins, *Physical Review*, **31**, 539 1928, for more recent work.

amount Δ_s, this discrepancy may be removed by changing the mass ratio of the two atoms concerned by

$$\Delta_m = \frac{4\rho_0(\rho_0 - 1)\Delta_s}{1 - 2\rho_0^2}, \qquad (2)$$

where ρ_0 is the square root of the ratio of the assumed reduced masses of the two molecules. This formula is true only for small values of Δ_m and Δ_s. For $C^{12}C^{12}$ and $C^{13}C^{12}$, $\rho_0 = 0.98058$ and $\Delta_m = \Delta_s/12.1$. If, therefore, $\Delta_s = 1/800$, $\Delta_m = 1/9700$. In other words, the mass ratio of the two atoms is to be taken greater than 12:13 by 1 part in 9700. As just noted, this discrepancy is too close to the experimental error to be significant, and we may therefore conclude that the two carbon isotopes have a mass ratio of 12 to 13, accurate to about 1 part in 10,000. This conclusion ignores a possible electronic shift, but such a shift, even if of magnitude 0.04 cm^{-1}, would change the mass ratio only 1 part in 10,000. Work now in progress on the oxygen isotopes, as well as previous line-spectra work, indicates that the electronic shift is not likely to exceed this amount.

The presence or absence of staggering in the isotope band concerns only the relative wave-lengths in this band, and can therefore be determined more easily and accurately than the isotope shift itself. Band series, over a short interval, are given very closely by a parabolic formula, and the second differences are therefore constant. If, however, staggering occurs, the individual second differences are alternately larger and smaller than the average. Such a test has been made on each set of measurements of the λ 4744 band. The results show that in the final average, as well as in the individual sets, there are almost exactly equal numbers of coincidences (second differences larger than the average when so predicted by staggering, etc.) and non-coincidences, and a study of the O−C values, in the case of both coincidences and non-coincidences, was equally conclusive. In other words, a second difference predicted to be larger than the average (on the basis of staggering) was just as likely to be found smaller, and by just as great an amount. It therefore seems safe to conclude that staggering is either entirely absent from the isotope band, or at most is only a small fraction of that found in the main band.

PLATE XI

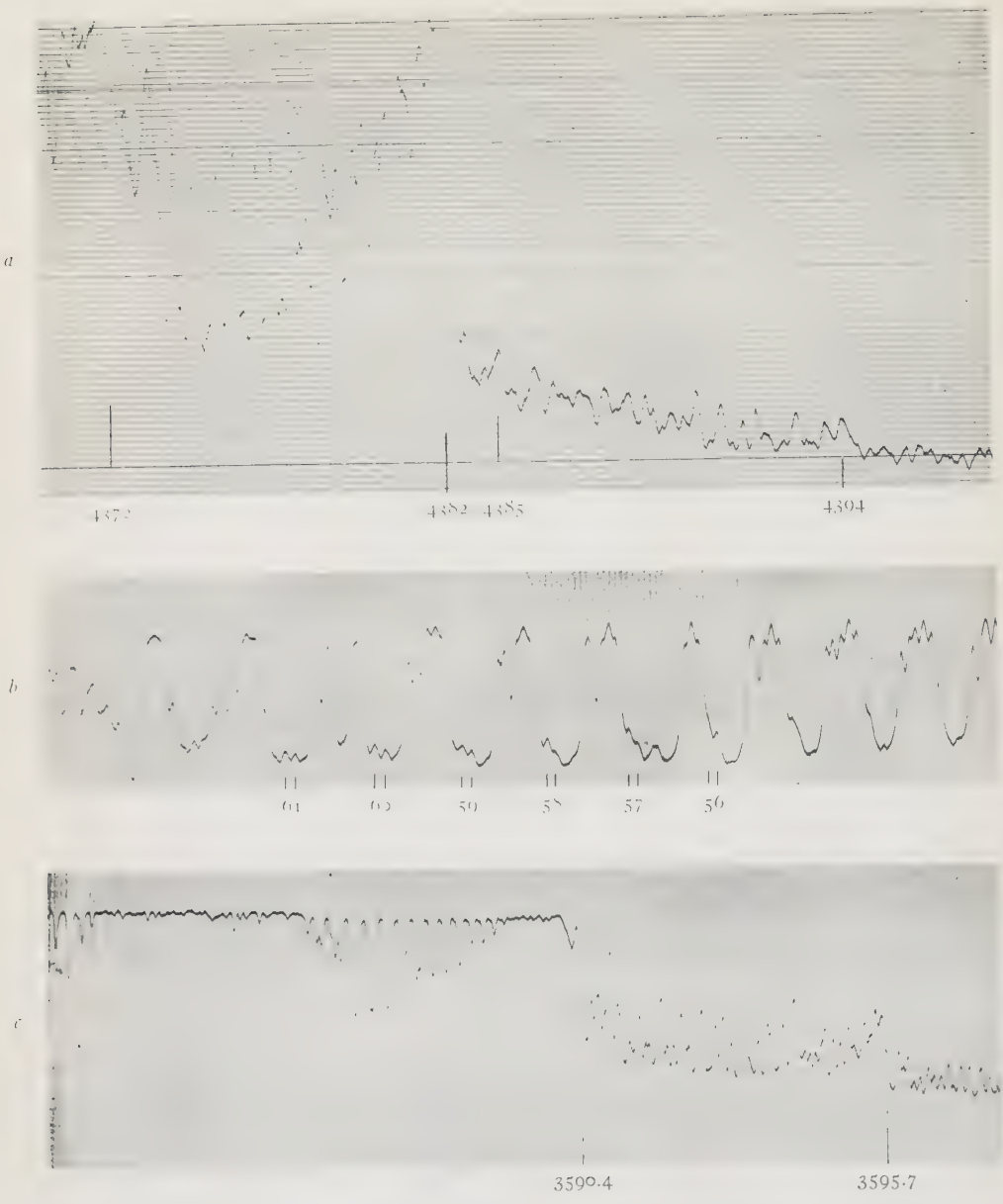

Microphotometer Curves of Carbon and Cyanogen Bands and their Isotopes

a) λ 4382 and isotope λ 4394

b) Structure in cyanogen band λ 3883
Marked lines belong to isotope band

c) λ 3590.4 and isotope λ 3595.7

OTHER NEW BANDS

Considerable work has been done on the remaining new bands, but the quantitative conclusions are less definite than in the case of the λ 4744 band. Plate XI, curve *a*, is a photometric trace showing the (2,0) isotope band at λ 4394.5 and the main band at λ 4382.1. This curve has been made from a first-order spectrogram, with the furnace at a temperature of 3000° C. It has been very difficult to get this band at all, and even on our best plate it differs in intensity so little from the general background that it is not possible to reproduce the spectrogram. In order to bring out the isotope band properly the photometer was made very sensitive—far too sensitive for the main band. The curve shows also the (3,1) head at λ 4372.4. The corresponding isotope head should be at about λ 4385.1, and thus falls to the red of the head of the main (2,0) band. The intensity increases suddenly at this point, and we believe therefore that the isotope band is present, although this is by no means certain as yet. The two main band heads and the two isotope heads are marked on the curve.

Measurements have been made covering the region λ 4394 to λ 4372, but the isotope band is so overrun with lines of the (1,0) band, as is proved by the presence of such lines to the red of λ 4394, that analysis is difficult. Equation (1) gives a calculated vibrational shift of -66.54 cm^{-1} or $+12.812$ A at the origin of the (2,0) band. The distance from the head to the origin is about 33.2 cm^{-1}, and using for the rotational shift the approximate formula $33.2(\rho^2-1)$, one obtains for the total calculated shift at the head -65.27 cm^{-1} or $+12.57$ A. It is difficult to measure the isotope head, since no single sharp line can be seen, but our measurements give, by chance, just 12.58 A as the interval from the strong lines at the head of the main band to what appears to be the corresponding portion of the head of the isotope band. Fifteen other lines, or blends, have been measured in the (2,0) isotope band; but of these only five fall close to predicted positions. It is obvious that practically all of the lines are more or less seriously blended and therefore useless for an accurate test.

In the case of the (0,0) λ 5165 band, the calculated shift at the origin (19,377.71 cm^{-1} or 5159.135 A) is only -1.392 cm$^{-1} = +0.371$

A. At the head it is considerably less, namely, -0.515 cm^{-1} or $+0.137$ A. The isotope head should therefore fall just outside the main head, but so close as to be almost impossible of detection, especially when the necessary intensity of the main band is considered. It seems more likely that isotope lines could be picked up in the region lying just to the red of the head of the (1,1) band at λ 5129, since the calculated shift in this region is about 1.5 A. Unfortunately this is the most difficult region in the entire visible spectrum in which to obtain high photographic intensity.

The C^{13} isotope has, however, been detected in the corresponding region of the (0,0) band of CN (λ 3883), as has already been reported.[1]

TABLE II

K''	Main Band	Calc. Shift	Obs. Shift	O−C
	A	A	A	A
56	3875.342	+0.1317	+0.1350	+0.0033
57	3874.759	.1560	.1634	.0074
58	3874.156	.1810	.1885	.0075
59	3873.534	.2068	.2116	.0048
60	3872.891	.2335	.2451	.0116
61	3872.227	+0.2608	+0.2703	+0.0095

For this work we are using material obtained a number of years ago.[2] As in the case of the Swan bands, the $C^{13}N^{14}$ lines appear in a spectrogram taken with the electric furnace, the temperature being 2700° C. The lines that can be measured with any accuracy consist of six doublets lying in the region λλ 3872–3876. The appearance of the main band in this region is shown on a reproduction[3] of a very similar furnace plate taken at 2500° C. The isotope lines do not appear on that plate. They are shown, however, in curve *b*, Plate XI, of the present article. This curve was made from the 2700° spectrogram, a third-order exposure taken with the 30-foot plane grating of the Mount Wilson Observatory. The six doublets are numbered on curve *b* to correspond with the numbering in the first column of Table II.

[1] Birge, *Physical Review*, **34**, 379, 1929; *Nature*, **124**, 182, 1929.

[2] King, *Mt. Wilson Contr.*, No. 194; *Astrophysical Journal*, **53**, 161, 1921.

[3] *Mt. Wilson Contr.*, No. 194, Pl. XX; *Astrophysical Journal*, **53**, Pl. II (facing p. 162), 1921.

In this case the true values of K'' are used, and the rotational energy change for each doublet is given to the first approximation by $B'(K'+1/2)^2-B''(K''+1/2)^2$. Since the observed doublets belong to the returning P branch, $K'=K''-1$. The second column of Table II gives the mean wave-length of each doublet in the main band. These are smoothed values, based on the data of Uhler and Patterson.[1] Since there are no standard lines on our furnace spectrogram, we have measured only the isotope shift. Each isotope doublet lies just to the red of the corresponding main-band doublet. These main-band doublets are all self-reversed, and so appear as close triplets. They include the well-known perturbation $P(60)$, in which the doublet spacing is 0.22 A, instead of the expected 0.068 A, and in which the center of gravity is at λ 3872.855, or 0.036 A to the violet of its expected position. As in the similar situation in the λ 4737 Swan band, this perturbation does not occur in the isotope band, but its presence in the main band makes it very difficult to calculate a reliable value of the isotope shift. The large values of K'', and hence of the rotational energy, introduce another difficulty, for the higher terms of the rotational energy function are becoming appreciable, and it is necessary to have very accurate values of all the rotational energy constants. In this case we have used constants determined in some unpublished work by R. T. Birge and W. O. Smith. For the vibrational constants we have used Kratzer's values.[2] The third and fourth columns of Table II give the calculated and observed shifts, in angstrom units, with respect to the smoothed wave-lengths of the second column. The O−C values appear in the fifth column and are consistently positive. After excluding the last two lines, which are uncertain because of the perturbation, they average +0.0057 A ($=-0.038$ cm^{-1}). The discrepancy may be due to an electronic shift of this magnitude and sign. The evidence is, however, not yet conclusive.

The wave-lengths of these isotope lines as they occur in the furnace spectrum were determined by one of us in 1921. It is interesting to note, however, that five of the six doublets (not two as stated in ref. 1, p. 14) had been observed, as single lines, by Kayser and

[1] *Astrophysical Journal*, 42, 434, 1915.

[2] *Annalen der Physik*, 71, 72, 1923.

Runge,[1] on arc spectrograms. The isotope $P(60)$ doublet is also definitely present on an extremely heavy arc spectrogram taken by one of us in the third order of the 21-foot grating of the University of Wisconsin. The $P(59)$ and $P(58)$ lines also are probably present, but are too hazy for measurement. The appearance of these CN isotope lines in the arc is important, since, aside from them, no lines involving the isotopes of oxygen, carbon, and nitrogen have as yet been found in the arc. This is discussed later in the paper.

Lines due to $C^{13}N^{14}$ have also been found in the (1,0) band. The head of the main band is at λ 3590.4, and of the isotope band at λ 3595.7. As usual, there is a decided difference between the arc and furnace spectrograms. In the arc a band structure decreasing in intensity toward the red, part of which is probably merged with the λ 3590 head, runs from this head to about λ 3675, beyond which it is obscured by the strengthening series of the λ 3883 band. This structure is due to the "tail" bands of cyanogen.[2] In the furnace it is almost completely suppressed, and in its place appears a faint band at λ 3595.7. The cyanogen spectrum, which in the vacuum furnace arises from the residue of air in the chamber, was strengthened by passing a stream of nitrogen through the furnace tube, with the chamber open to the air. This resulted in partly reversing the cyanogen bands and brought out the structure of the λ 3596 band in emission with satisfactory intensity. This structure is shown in the photometric curve *c* of Plate XI, and also in Plate XII*a*. This latter figure is made up of three exposures. The middle one is the furnace at 2500° C, with nitrogen passing through at atmospheric pressure. Note that the head of the main band, at λ 3590, is self-reversed. This is precisely the state of affairs on the spectrogram in which we found the isotope lines in the (0,0) band. The upper and lower exposures represent the vacuum furnace, at 2800° and 2750° C, respectively. The upper shows the structure of the primary band, while in the lower, more strongly exposed, the isotope is

[1] *Abhandlungen der Preussischen Akademie der Wissenschaften*, 1889. Kayser and Runge's wave-lengths are in the old Rowland system and average 0.16 A greater than Uhler and Patterson's values for the main band lines. Their five isotope lines ($K''=$ 56, 57, 59, 60, and 61) are, respectively, 0.29, 0.215, 0.17, 0.205, and 0.155 A greater than our mean doublet values.

[2] See W. Jevons, *Proceedings of the Royal Society*, A, **112**, 407, 1926, and F. A. Jenkins, *loc. cit.*

PLATE XII

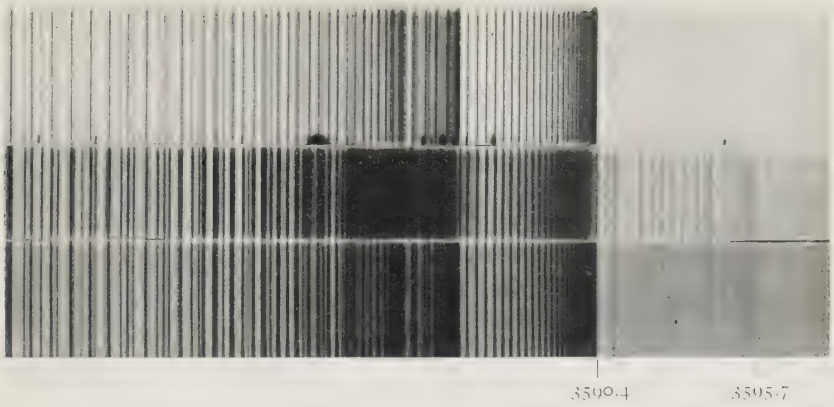

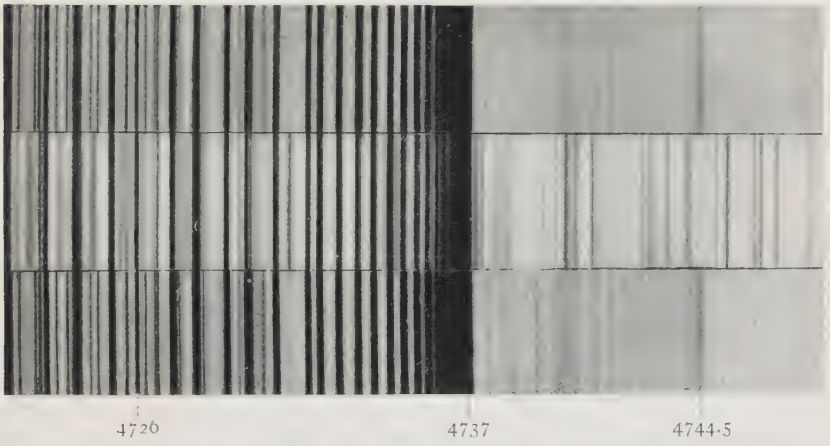

Band Structures with Isotopes

a) Cyanogen band λ 3590 given by nitrogen in furnace (center), compared with vacuum furnace.

b) Furnace spectra of λ 4737 and isotope (above and below), compared with arc spectrum (center).

obviously present, but much blended with other lines, a condition presumably due to the *CN* tail bands. The calculated shift at the origin (27,921.44 cm^{-1}) is -44.54 cm^{-1} ($=5.69$ A). At the head it is about -41.1 $cm^{-1} = +5.30$ A. It has been possible to identify a number of lines in the isotope band, and for these the measured shifts average about 0.025 A (0.19 cm^{-1}) greater than the calculated values. There are, however, no good high-dispersion measurements for this band, and hence no really trustworthy constants.

In view of the more recent discovery[1] of an isotope of nitrogen of mass 15 in the absorption spectrum of nitric oxide, it is important to point out that the observed lines in *CN* cannot be due to a $C^{12}N^{15}$ molecule. For such a molecule the shift would be only 74 per cent of that due to $C^{13}N^{14}$, and the discrepancies in the (0,0) band would therefore run from 0.04 to 0.07 A, as compared with those given in the fifth column of Table II. In the (1,0) band the discrepancies would average 1.4 A. In concluding this discussion of the *CN* isotope bands, it may be pointed out that all of the calculations naturally assume that the main bands are due to the diatomic molecule $C^{12}N^{14}$, and the results verify this assumption. In this particular case, the identity of the carrier had already been established in other ways, but it should not be forgotten that, in general, quantitative proof in regard to this highly controversial matter (identity of carriers of band spectra) is furnished only by means of isotope relations, as was emphasized by Mulliken[2] a number of years ago.

INTENSITY OF ISOTOPE BANDS, AND THE RELATIVE ABUNDANCE OF C^{12} AND C^{13}

The high intensity of the isotope band λ 4744 in the furnace as compared with the arc is a matter of special interest. Spectrograms previously taken of the Swan bands in the arc were examined and other arc exposures taken to decide if the band shows at all. Electrodes for the arc spectra were either commercial carbons or rods of Acheson graphite, the material of the furnace tubes. The appearance of the carbon bands in general is quite different in furnace and arc, as some of the fainter arc series are much strengthened in the furnace. Since in the present case it was necessary to have the λ 4737 band

[1] S. M. Naudé, *Physical Review*, **34**, 1498 (December 1), 1929.

[2] R. S. Mulliken, *ibid.*, **25**, 119, 1925.

in the arc fully as strong as in a furnace showing the isotope, the distinctive *P* series was selected as best representing the strength of the (1,0) band. Experiment showed that the furnace vapor at high temperature is very rich in the emitter of the Swan bands, since a relatively short furnace exposure gives the bands with high intensity and with some of the weaker arc series much strengthened. However, an exposure of the carbon arc ten times as long as that of the furnace at 2900° C gave the main series of the λ 4737 band fully as strong as in the furnace spectrum on the same plate. In fact, the arc spectrum came up first in the developer, indicating greater photographic density of the series of which the λ 4737 head is chiefly composed. The region where the isotope band should fall has some scattered band lines in the arc, apparently belonging to the strong (0,0) band at λ 5165, but the location of the isotope head λ 4744.5 falls in a clear place and the head was distinctly absent from the arc spectrum, as were such of the component isotope lines as should have been undisturbed by blends. Plate XII*b* shows two second-order furnace spectra of λ 4737 and its isotopes, and between them a spectrum of the band in the arc. The upper furnace spectrum has the lines of its main series comparable in strength with those in the arc band, but the isotope is missing from the arc spectrum. The stronger furnace spectrum below shows, by its large scale, that the lines of the isotope band are in general complex, as are those of the primary band.

Arcs in a partial vacuum, at pressures from 1 to 10 cm, also failed to show the head at λ 4744. The experiments with the arc, while not carried far enough to say that this source is quite unable to produce the λ 4744 band, show that the arc radiation is at a decided disadvantage in exciting the $C^{13}C^{12}$ molecule, whereas the furnace, with a long column of vapor giving the Swan spectrum with high intensity, including many of its fainter series, produces the isotope band with comparative ease. That the high temperature of the arc is unfavorable for the isotope radiation is probable, but as yet unproved. The range of furnace temperatures in which the Swan spectrum comes out is not large enough to show whether low temperature favors the isotope at the expense of the main band. At the high furnace temperatures much more carbon vapor is present and all of the phenomena are more pronounced.

Attempts were made to obtain the band at λ 4744 in absorption to test the possibility that a difference in absorption coefficient might explain the relative strength of the isotope band in the tube furnace. On account of the high furnace temperature required to reverse the Swan bands, the λ 4737 head was obtained only faintly in absorption when photographed with a diaphragm in the tube, and the λ 4744 head did not appear. It should have appeared, however, if its strength in absorption were one-fiftieth that of the primary head, or perhaps still fainter.

It has already been noted that certain $C^{13}N^{14}$ lines do appear in the carbon arc, but apparently with much less intensity, compared to the main bands, than in the furnace. It was thought at first that the failure to obtain the isotope bands in the arc was due to the fact that they were lost in the general intense background which develops on an overexposed arc spectrogram. This factor limits the allowed intensity of the main band, but evidently does not explain the great weakness of the isotope lines, as is proved by Plate XII*b*. The λ 4737 Swan band has never been obtained in the arc with the intensity with which the λ 3883 *CN* band can easily be photographed. Hence the failure of the isotope band at λ 4744 to appear in the arc is not inconsistent with the occurrence of $C^{13}N^{14}$ lines in the arc band λ 3883. Rather, the conclusion would be that while C^{13} is present in the arc vapor, its excitation in this source is difficult.

Before considering the possible reasons for this condition of affairs, we shall report a first crude attempt to measure the relative intensity in the furnace of the $C^{12}C^{12}$ and $C^{13}C^{12}$ bands. This was done by using an exposure ratio which gave the λ 4737 and λ 4744 bands with approximately the same intensity, according to a visual estimate. The actual exposure ratio was 100 to 1. We estimate, however, that half of the intensity of λ 4744 is due to the background, giving 200 to 1 as the final estimate. Now if one has two kinds of atoms A and B, with a relative abundance (A to B) of r, and capable of forming with equal facility the molecules AA, AB, and BB, it may easily be shown from elementary statistics that the relative abundance of the three types of molecules will be $r^2 : 2r : 1$. Hence the ratio of AA to AB is $r/2$, which in our case is 200 to 1. Therefore $r = 400$. If, as we have indicated earlier in the paper, the atomic weights of A and B are probably 12 and 13, even, the atomic weight

of the mixture should be 12.0025. This is the best chemical value at the present time.[1] The apparent abundance of C^{13} in the furnace is thus at least not inconsistent with the chemical atomic weight of carbon.

The whole question of relative abundance is, however, rendered uncertain if the strength of the isotope relative to the primary band depends on the excitation conditions. Thus we have found it many times less abundant in the arc than in the furnace. On the other hand, Sanford[2] has pointed out that the λ 4744 band occurs in N-type stars with a relatively high intensity. Menzel[3] has later estimated this relative intensity of λ 4737 to λ 4744 as not over 5 to 1, giving r as not more than 10. In this case a band due to $C^{13}C^{13}$ may be expected to appear, and in fact does so, as discussed by Sanford and Menzel. It has recently been noted by Bobrovnikoff[4] that the λ 4744 $C^{13}C^{12}$ band occurs also in certain comets.[5] The λ 4744 "line" found by Raffety, to which reference has been made,[6] appeared in the Mecker flame spectrum. In Johnson's reproduction,[7] in which it also appears, the source is a vacuum tube. In both these cases the distribution of intensity among the series lines proves that the effective temperature is low, probably only a few hundred degrees Centigrade in the case of the tube. The relative intensity of the λ 4744 and λ 4737 bands in the Mecker flame appears from the reproduction to be about that in our furnace spectrograms. In Johnson's plate λ 4744 seems stronger.

Why the relative intensities of the Swan band λ 4737 and its isotope λ 4744 should vary greatly in different sources is as yet by no means clear, but we may consider the condition as it stands and some of the factors which may influence it.

The relative intensity of the isotope band increases enormously, as just noted, in passing from arc (emission), to furnace (emission) or Mecker flame or vacuum tube (both emission), to star (absorption). The more obvious differences in these sources which might

[1] Birge, *Physical Review Supplement*, 1, 1, 1929; see p. 26.

[2] *Publications of the Astronomical Society of the Pacific*, 41, 271, 1929.

[3] *Ibid.*, 42, 34, 1930. [4] *Ibid.*, p. 117, 1930.

[5] See, for instance, W. H. Wright, *Lick Observatory Bulletin*, 7, 8 (No. 209), 1912: Comet Brooks (1911c).

[6] Raffety, *loc. cit.* [7] *Loc. cit.*

affect this ratio are (1) differences in relative abundance of the atoms C^{12} and C^{13}; (2) excitation differences, probably chiefly in temperature; and (3) the large differences in optical path, which might result in favoring the less abundant isotope.

In the laboratory experiments, the furnace tube and the arc electrodes have been of the same material, Acheson graphite, so that a difference in abundance must result from an easier dissociation in the arc of the $C^{13}C^{12}$ molecule, rather than from the number of each sort of molecule initially present.[1] In the star, a much larger proportion of one kind of atom would be contrary to the hypothesis of the uniformity of matter in the universe—a view which has gained strength since the recent ionization theory has explained many apparent contradictions in stellar spectroscopy.

Considering the possible influence of excitation, we find that the three sources—arc, furnace, and star—decrease in temperature in the same order that the strength of λ 4744 increases. The Mecker flame and the vacuum-tube spectra seem to fit into this same temperature series. This would indicate that lower temperature favors the radiation of the molecule containing C^{13}. The mechanism of this, however, is not obvious. Since the difference between the two atoms rests on the nuclear structure of each, we cannot draw a close analogy to the familiar effects of temperature changes on line spectra, based on electronic transitions. If higher temperature dissociates the heavier molecule more readily, this would result in the change of abundance mentioned in the preceding paragraph; but no definite reason to expect such a dissociation has appeared. While the favorable furnace temperature for the appearance of λ 4744 is higher than the estimated temperature of the absorbing atmosphere of an N-type star, the difference of three or four hundred degrees would not seem large enough to give the greatly increased strength of the isotope band in the star. The temperature range of the furnace does not permit a direct test of the question. The Swan band λ 4737 appears faintly at about 2400° C. At 2600° C enough carbon is

[1] It should be pointed out in this connection that J. L. Hundley, *Physical Review*, **30**, 864, 1927, in the case of lithium, found a different "work function" for the two different atomic species, such that the relative abundance of Li^7/Li^6 decreased with increasing temperature. It does not seem possible, however, that such an effect could account for the magnitude of the differences we have found.

vaporized to allow the isotope band to be photographed, and from this stage to 3000° C both bands strengthen rapidly. No distinct change in relative intensity appears within this range, and above 3000° C the strong continuous ground makes the comparison still more uncertain.

Considering the third possibility, we find the thickness of the optical path in arc, furnace, and stellar atmosphere increasing in the same order as the strength of the isotope band λ 4744 in the three sources. The arc vapor is a few millimeters thick, the heated portion of the furnace tube is 20 cm long, and the reversing layer of the star is of unknown but great thickness. To connect the increasing strength of the isotope band with increase of optical path would mean that the radiation in which C^{12} only is concerned reaches a maximum stage, beyond which increase of the column of vapor is ineffective, while for the less-abundant C^{13}, the longer column of vapor produces an effect more nearly in proportion to the number of molecules present. As in the case of the possible effect of temperature difference, we can only consider difference of optical path as one of the features which may influence the relative strength of these bands.

To summarize briefly, this paper shows that faint band structures appearing in various different regions of the spectrum are accounted for by the presence of a carbon atom of mass 13. The questions which have arisen as to abundance of this isotope and the dependence of its spectrum upon excitation conditions will require much additional evidence.

The calculations incident to this work have been greatly facilitated by an electric computing machine, obtained by Mr. Birge on a grant from the National Research Council, and also by a fund for paying a computer, from the Rumford Committee of the American Academy of Arts and Sciences. Grateful acknowledgment for these grants is hereby made.

Carnegie Institution of Washington
Mount Wilson Observatory

Department of Physics
University of California
June 1930

Contributions from the Mount Wilson Observatory, No. 403
Reprinted from the *Astrophysical Journal*, Vol. LXXII, pp. 41–45, 1930
Printed in the U.S.A.

UNIVERSITY OF ARIZONA
STEWARD OBSERVATORY
TUCSON, ARIZONA

THE SPECTROGRAPHIC ORBIT OF RS CANUM VENATICORUM

By ALFRED H. JOY

ABSTRACT

The orbit of RS Canum Venaticorum is based on 35 spectrograms obtained with the 60- and 100-inch reflectors. Schneller's elements (Min. = J.D. 2423579.344 H.G.M.T. + $4^d.797944E$) were used in the computation of phases. The lines of both components are visible in the spectrograms. Table I gives the observations, velocities, weights, and residuals. The spectrum of the primary star is F4, that of the secondary is dG8. The secondary is best observed at total eclipse, which lasts 3.7 hours. The spectroscopic absolute magnitudes are 3.5 and 4.5, respectively, and the parallax is $0''.010$. The elements of the orbit are: $e = 0.0$ (assumed); $K_1 = 91.6$ km/sec.; $K_2 = 99.0$ km/sec.; $\gamma = -8.9$ km/sec.; $a_1 \sin i = 6{,}040{,}000$ km; $a_2 \sin i = 6{,}530{,}000$ km; $m_1 \sin^3 i = 1.79$; $m_2 \sin^3 i = 1.66$.

The absolute dimensions were determined with the aid of B. W. Sitterly's photometric solution for the inclination and radii of the stars. The fainter star is exceptionally large and massive for its absolute magnitude and spectral type.

The eclipsing variable star RS Canum Venaticorum ($13^h5^m59^s$, $+36°28'$, 1900) was discovered in 1914 by Mme L. Ceraski. The spectral type given in the *Draper Catalogue* is F8. Spectrographic observations were begun at Mount Wilson in 1921 to determine the orbits and the spectrum of the fainter companion. Sitterly's photometric orbit,[1] based on M. Maggini's[2] observations and period, showed that the eclipses are total or annular, and that the surface brightness of the fainter companion is considerably less than that of the principal star. In the following year Sitterly stated in a letter that his observations at Princeton indicated that the double period found by C. Hoffmeister[3] should be used rather than that of 2.338433 days given by Maggini. He suggested the elements Min. = 2422811.666 G.M.T. + $4^d.797851E$, which were the basis of a preliminary solution.[4] Dr. B. W. Sitterly has kindly permitted me to use the complete report of his observations and his computation of the photometric orbit, which will soon appear as a *Contribution from the Princeton University Observatory.*

[1] *Astrophysical Journal*, **53**, 99, 1921.

[2] *Pubblicazioni del R. Osservatorio di Arcetri*, **34**, 64, 1916.

[3] *Astronomische Nachrichten*, **208**, 258, 1919.

[4] *Publications of the Astronomical Society of the Pacific*, **34**, 221, 1922.

In 1927 and 1928 H. Schneller[1] made at Neubabelsberg a series of 139 photographic observations from which he deduced photometric elements.

Since the preliminary solution was published in 1921, further spectrographic observations have been made at the 60- and 100-inch telescopes to strengthen the determination of the orbits and to add to the evidence concerning the spectrum of the fainter star, which is well seen for 3.7 hours during the time of total eclipse.

Thirty-five spectrograms have been measured for velocity as listed in Table I. These were obtained with a single prism and an 18-inch camera except C 1112, 1687, 2301, 2935, 3339, 3664, 3798, 3868, 4663, 5173, and γ 17220 and 17480, which were taken with a 10-inch camera.

Phases were computed from Schneller's elements,

$$\text{Min.} = \text{J.D. } 2423579.344 \text{ H.G.M.T.} + 4^{d}.797944\, E,$$

which are based on all the minima thus far observed. The weights assigned to each plate depend upon the dispersion, the number of

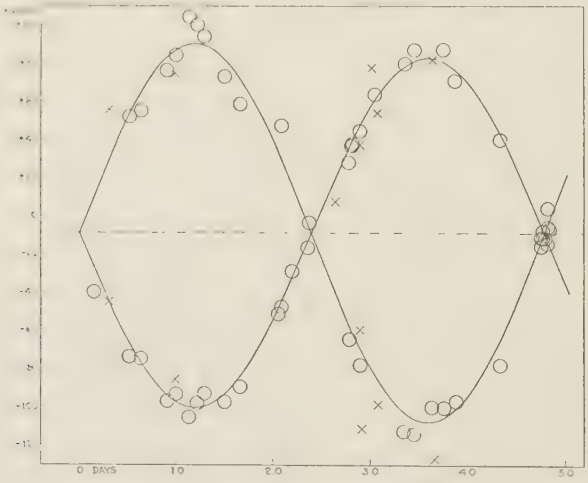

FIG. 1.—Velocity-curve of RS Canum Venaticorum. Crosses are preliminary measures of Victoria spectrograms.

lines measured, and the quality of the spectrum. The observations are plotted in Figure 1.

[1] *Astronomische Nachrichten*, **233**, 365, 1928.

Dr. J. S. Plaskett made eight spectrographic observations of the star at Victoria in 1921 and 1922. His rough preliminary measures of velocity are represented by crosses in the figure. One weak plate

TABLE I

OBSERVATIONS OF RS CANUM VENATICORUM

PLATE	DATE J.D. 242+	PHASE	PRIMARY			SECONDARY	
			Vel.	Wt.	O−C	Vel.	Wt.
			km/sec.		km/sec.	km/sec.	
C 1758	3238.705	0.015	.....	.....	.....	− 5.9	0.5
4663	5277.833	0.017	.....	.....	.....	− 14.1	.5
5181	5752.833	0.020	.....	.....	.....	+ 4.3	.2
5173	5728.851	0.028	.....	.....	.....	− 6.5	.5
γ 17220	6016.840	0.141	− 39.9	.....	.....	.....	.....
10093	2797.785	0.506	73.8	1.0	− 7.9	+ 52.2	.5
10095	2797.903	0.624	74.4	0.5	+ 1.9	+ 55.4	.2
11796	3565.842	0.892	96.9	0.5	− 3.8	+ 76.4	0.5
C 1761	3239.678	0.988	93.1	1.0	+ 3.8	+ 84.2	1.0
3664	4540.055	1.122	105.2	0.5	− 5.3	+104.5	0.2
3864	4693.674	1.206	98.0	.5	+ 2.5	+100.4	.5
3865	4693.747	1.280	92.8	.5	+ 7.3	+ 94.4	.2
2935	4012.651	1.492	97.6	.5	− 3.6	+ 73.2	.5
γ 13413	4276.698	1.652	89.6	.5	− 9.3	+ 58.5	.5
C 1764	3240.736	2.046	51.3	0.5	− 1.9	.....	.....
3364	4334.700	2.079	47.3	1.0	− 0.1	+ 47.5	.5
1803	3269.661	2.184	28.8	1.0	+ 5.2	.....	.....
3868	4694.816	2.349	16.5	0.5	+ 0.1	.....	.....
3339	4315.792	2.363	− 3.5	0.5	+11.0	.....	.....
3286	4277.819	2.774	+ 28.0	1.0	− 5.7	− 64.3	.5
4284	5040.719	2.800	36.6	1.0	+ 1.1	.....	.....
1635	3135.944	2.809	37.7	0.2	− 0.3	.....	.....
γ 13432	4306.722	2.889	44.9	1.0	− 0.4	− 78.0	.5
C 2097	3448.042	3.040	64.0	0.2	+ 4.7	.....	.....
γ 11667	3505.928	3.351	79.9	0.2	+ 2.1	−112.6	.1
C 2197	3534.815	3.450	86.9	1.0	+ 6.1	−114.3	0.5
γ 10063	2776.907	3.618	79.1	1.0	− 3.5	− 99.9	1.0
C 1639	3136.880	3.745	87.2	1.0	+ 6.3	−100.6	0.5
1112	2882.711	3.867	71.0	0.5	− 6.0	− 97.0	.2
γ 10085	2796.806	4.324	+ 40.1	1.0	− 4.2	− 78.0	.5
C 3798	4658.839	4.755	.....	.....	.....	− 15.8	.2
1687	3185.870	4.756	.....	.....	.....	− 11.1	.2
1544	3089.922	4.766	.....	.....	.....	− 8.0	.5
2301	3503.710	4.771	.....	.....	.....	− 11.7	.5
γ 17480	6131.844	4.791	.....	.....	.....	− 11.3	0.5

has been rejected. It will be seen that the Victoria observations confirm the Mount Wilson results for the most part, but for the sake of homogeneity they were not included in the solution.

Because of rotation of the principal star, the velocity from plate γ17220, which was taken during partial eclipse, falls 15 km/sec.

below the curve and has been omitted from the solution. The expected rotation effect at the limb is 17 km/sec.

The spectral type of the more massive and brighter star is F4n. The lines are easily measurable but are not of the best quality.

When the differences of velocity are sufficient, the spectra of both stars appear, but the lines of the secondary are weak and unsatisfactory for accurate measurement. During totality, however, the spectrum of the secondary is easily observed. Nine spectrograms which show the spectrum of the secondary entirely free from interference by the light of the primary star were obtained at this phase. The spectral type is G8, and the usual criteria indicate definitely that it belongs to the dwarf branch.

The spectrographic absolute magnitudes determined with the cooperation of Dr. W. S. Adams are 3.5 for the primary and 4.5 for the secondary. The corresponding apparent visual magnitudes found by Sitterly by comparison with the HP star B.D.$+36^{\circ}2352$ are 8.56 and 9.42, respectively. The parallax from these values is 0″.010.

A velocity-curve drawn through the observations indicates that within the errors of the observations the orbits are circular. Hence, the eccentricity was assumed to be zero. Corrections to the estimated values of γ and K for the primary orbit were determined by least squares. The probable errors given result from this solution. It was not considered worth while to include the observations of the secondary; γ was not derived for the secondary orbit.

The elements thus found are

$P=4^{d}.797944$ (Schneller)	$a_1 \sin i=6{,}040{,}000$ km
$e=0.0$ (assumed)	$a_2 \sin i=6{,}530{,}000$
$K_1=91.6\pm0.10$ km/sec.	$m_1 \sin^3 i=1.79\odot$
$K_2=99.0$	$m_2 \sin^3 i=1.66$
$\gamma=-8.9\pm0.21$	$m_2/m_1=0.93$

The computed curve is shown in Figure 1, and the residuals appear in the sixth column of Table I. Except for some uncertainty in the exact value of i resulting from the various photometric solutions, the masses seem fairly well determined. Both stars are dwarfs with nearly equal masses, approximately 1.7 times that of the sun. The stars do not agree well with Eddington's mass-luminosity curve, which requires an absolute magnitude of $+2.1$ for such a mass.

PLATE XIII

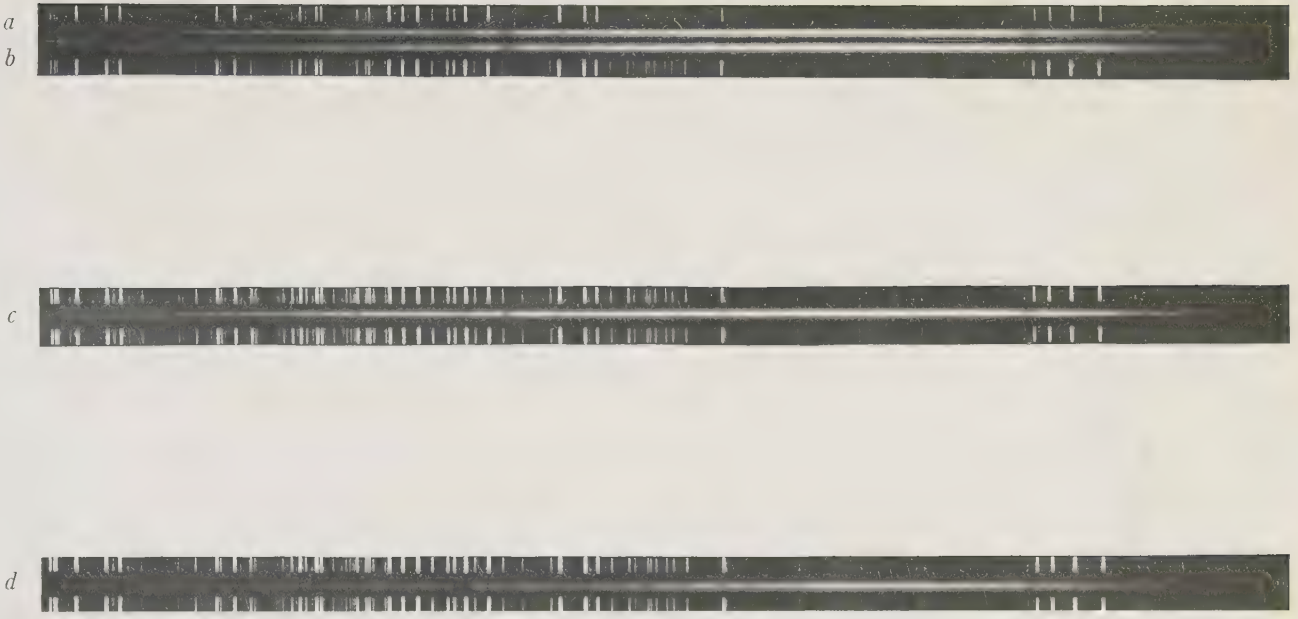

SPECTROGRAMS OF RS CANUM VENATICORUM

a) C1761, double lines, primary displaced to violet
b) C1639, double lines, primary displaced to red
c) C1803, primary star, spectrum F4
d) C1544, secondary star taken during total eclipse, spectrum G8

Using $i = 79°.9$, $r_f = 0.289$, $r_b = 0.087$, from Sitterly's solution II (uniform disk), we have for the absolute dimensions

$a_1 + a_2$, semi-major axis of relative orbit	12,780,000 km
a_1, semi-major axis of primary orbit	6,140,000
a_2, semi-major axis of secondary orbit	6,640,000
r_b, radius of brighter star	1,110,000 (1.6⊙)
r_f, radius of fainter star	3,680,000 (5.3)
m_b, mass of brighter star	1.85⊙
m_f, mass of fainter star	1.71
ρ_b, density of brighter star	0.45⊙
ρ_f, density of fainter star	0.012

The secondary star is certainly peculiar and cannot readily be classified among other stars for which we know the physical characteristics. Its absolute magnitude and spectrum would place it among the dwarfs, but the size and mass are exceptionally large, although not nearly large enough to compare with the normal giants of its spectral class. The density is, correspondingly, intermediate between dwarfs and giants. Its large size is checked by the fact of the long total eclipse during which a distinctly later-type spectrum shows.

The writer wishes to express his appreciation of the kind co-operation of Dr. Plaskett in supplying the valuable independent data of his spectrograms, and of Dr. Sitterly, who has permitted the use of his unpublished results.

Mount Wilson Observatory
Carnegie Institution of Washington
June 1930

Contributions from the Mount Wilson Observatory, No. 404
Reprinted from the *Astrophysical Journal*, Vol. LXXII, pp. 46–68, 1930
Printed in the U.S.A.

UNIVERSITY OF ARIZONA
STEWARD OBSERVATORY
TUCSON, ARIZONA

VARIATIONS IN RADIAL VELOCITY OF THE CEPHEID VARIABLES W GEMINORUM, U AQUILAE, AND DT CYGNI

By ROSCOE F. SANFORD

ABSTRACT

Variation in radial velocity.—Curves of radial velocity for W Geminorum, U Aquilae, and DT Cygni have been derived from Mount Wilson spectrograms and a series for U Aquilae obtained at the Lick Observatory (top curves of Figs. 1, 2, and 3). The semi-amplitudes of variation in velocity are 16.7, 20.8, and 7.5 km/sec., respectively. The velocities of the systems are −0.7, −7.0, and −0.5 km/sec.

Relation of velocity-curves to light-curves.—The velocity-curves of U Aquilae and DT Cygni are mirror images of the light-curves, i.e., maximum velocity coincides with minimum light and minimum velocity with maximum light. For W Geminorum the interval between maximum and minimum velocity is nearly a day less than the mean interval between minimum and maximum light. Since the period derived from the radial velocities shows that maximum velocity coincides in the mean with minimum light, it follows that with this period minimum velocity precedes maximum light by nearly a day.

Superposed minor fluctuations are present in the light-curves of W Geminorum and U Aquilae. Evidence for kindred fluctuations in the velocity-curves is slight for the former and lacking for the latter.

This paper deals with the variations in radial velocity of the three Cepheid variables listed in Table I. With the exception of some

TABLE I

Star	H.D. No.	B.D. No.	α 1900	δ 1900	Harv. Mag.	Sp.
W Geminorum...	46595	+15°1246	$6^h29^m.2$	+15°25′	6.7–7.5	cGo
U Aquilae.....	183344	− 7 4698	19 24.0	− 7 15	6.2–6.9	cF8
DT Cygni.....	201078	+30 4318	21 2.3	+30 47	5.9	F7

early values for U Aquilae, referred to later, all the radial velocities used depend upon spectrograms obtained with one-prism spectrographs attached to the 60- and 100-inch reflecting telescopes at Mount Wilson. Their dispersion is about 37 A per millimeter at $H\gamma$. Plates taken with the 60-inch are designated by γ, and those taken with the 100-inch telescope by C. Most of the wave-lengths of the absorption lines measured are from a list based upon measures of a number of plates of the Cepheid variable T Monocerotis.[1]

[1] *Mt. Wilson Contr.*, No. 340, p. 8; *Astrophysical Journal*, 66, 240, 1927.

The curves of radial velocity have been formally represented by orbital elements by comparing the plot of the velocities with standard curves based on data given by E. S. King.[1] For DT Cygni, which shows little evidence of eccentricity, a simple sine-curve sufficed. The details for each star follow.

W GEMINORUM

E. F. Sawyer's[2] observations in 1895 and 1896 led him to announce the variability of this star in a period of nearly eight days. The light-curve shows definitely that W Geminorum is a Cepheid which oscillates through a range of 0.5 mag. with a median visual magnitude of approximately 7.0. It is therefore bright enough at all times to give spectrograms of good density, with either the 60- or the 100-inch reflector, in reasonably short exposure times. As the number of such Cepheids is small, it seemed worth while to obtain spectra at all phases of the light variation. Observations to determine the variation in radial velocity were begun in 1927. Four spectrograms had already been obtained in 1917–1918, two near maximum light and two near minimum, which showed[3] that the velocities near maximum were approximately 32 km/sec. less than those at minimum, and that the spectrum is that characteristic of Cepheid variation. The Mount Wilson spectral classification is cGo.

Nineteen spectrograms of usable quality were obtained between January, 1927, and March, 1930. The data for all twenty-three spectrograms appear in Table II. The interval of more than ten years between the first four and the remaining observations and the distribution of the latter over three consecutive years should make it possible to derive the period (if constant) with considerable precision from the radial velocities alone. Accordingly, it was decided to use the radial velocities independently of the light observations.

The velocity-curve was judged to be smoothest when the twenty-three velocities were assembled with a period of $7^{d}.91478$. A freehand curve through the plot, compared with typical velocity-curves, gave

[1] *Harvard Annals*, **81**, 231, 1923.

[2] *Astronomical Journal*, **17**, 3, 1896.

[3] Adams, Joy, and Sanford, *Publications of the Astronomical Society of the Pacific*, **36**, 137, 1924.

elements, which, together with the period, were then corrected by the least-squares procedure outlined by Schlesinger.[1]

TABLE II

W Geminorum—Observations of Radial Velocity

Plate No.	Date	G.M.T.	Phase	Vel.	O−C	Wt.
				km/sec.	km/sec.	
γ 6385	1917 Nov. 25	23^h55^m	$7^d.152$	+23.0	+5.4	1.0
6565	1918 Jan. 4	22 31	7.517	+21.4	+3.1	0.5
6595	Jan. 23	19 11	2.632	− 8.9	+0.1	1.0
6673	Jan. 31	18 01	2.668	− 9.9	−1.1	1.0
14793	1927 Jan. 18	19 42	7.666	+17.6	+1.4	0.5
15368	Nov. 2	22 43	2.920	−10.0	−2.3	1.0
15374	Nov. 4	0 10	3.980	− 1.2	+1.8	1.0
C 4527	Nov. 6	22 55	6.928	+11.7	−4.1	1.0
γ 15430	Dec. 6	21 36	5.212	+ 3.4	+0.2	1.0
C 4572	Dec. 7	20 56	6.184	+ 4.1	−5.4	0.5
4606	1928 Jan. 3	19 55	1.480	− 9.3	+4.4	0.5
γ 15610	Mar. 6	15 26	0.969	−16.8	−2.1	0.5
C 4722	Apr. 6	15 07	0.295	− 2.3	+3.9	0.5
γ 16194	Sept. 28	0 30	0.546	−12.7	−0.5	1.0
16283	Nov. 5	23 36	7.846	+16.7	+6.4	1.0
16315	Nov. 22	21 52	1.028	−21.3	−6.6	1.0
16380	Dec. 31	16 55	0.245	− 7.0	−2.7	1.0
16383	Dec. 31	23 02	0.500	− 9.1	+2.4	1.0
C 5153	1929 Mar. 29	15 21	1.110	− 6.1	+8.6	0.5
γ 16503	Mar. 31	16 00	3.317	− 6.6	+0.2	1.0
16506	Apr. 1	16 49	4.171	+ 1.4	+3.5	0.5
17320	1930 Mar. 11	15 27	7.751	+ 7.1	−6.8	0.5
17351	Mar. 19	15 31	7.837	+ 9.1	−1.5	1.0

TABLE III

Elements of W Geminorum

Preliminary		Corrections	Adopted
P = Period	= $7^d.91478$	$+0^d.00065$	$7^d.91543$
K = Semi-amplitude of velocity variation	= 17.9	−1.17	16.7 km/sec.
e = Eccentricity	= 0.55	−0.024	0.53
ω = Angle of periastron	= 70°.0	+2°.31	72°.3
T = Time of periastron passage	= J.D. 2425612.395	+0.064	5612.460
γ = Velocity of the system	= +0.23	−0.93	−0.70 km/sec.

The preliminary elements, corrections, and adopted elements are given in Table III.

The phases and residuals given in Table II were computed with the corrected elements. Some of the residuals are rather large for

[1] *Publications of the Allegheny Observatory*, 1, 33, 1910.

spectrograms as well measurable as these; but attention has already been called[1] to the fact that other Cepheids show a considerable scattering in the radial velocities around maximum light. Most of the large residuals for W Geminorum are near maximum and minimum; further, the representation by orbital elements is only a convenient device which defines the variation in velocity, perhaps to a first approximation only.

The elements show that maximum velocity precedes T, the periastron time, by $0^d.52$, and that minimum velocity follows T by $1^d.00$.

It now becomes of interest to locate the maximum and minimum velocities with reference to light minimum and maximum. The star

TABLE IV

Obs. Light Max. (L max) G.M.T.	L max$-$ L min ($M-m$)	T (Periastron Passage)	L max$-T$	L min$-T$	Authority	Interval
J.D. 2413266.35..	$+2^d.91$	64.39	$+1^d.96$	$-0^d.95$	Luizet*	1895–1905
9029.00..	2.20	26.82	2.18	0.02	Van der Bilt†	1907–1914
2420073.25..	2.00	71.66	1.59	0.41	Dziewulski‡	1912–1915
0682.57..	+2.53	81.15	+1.43	−1.10	Robinson§	1895–1929
Mean.....	+2.41	.....	+1.79	−0.62	.....	.....

* *Astronomische Nachrichten*, **169**, 401, 1905.
† *Journal des observateurs*, **9**, 23, 1926.
‡ *Bulletin de l'Observatoire de Vilno*, No. 4, 1924.
§ *Harvard Bulletins*, No. 872, 13, 1930.

has been observed photometrically by many, but only four have determined epochs of light minima and maxima entitled to considerable weight, either because their own observations are extensive or because their results are based upon several series of observations. The necessary data are in the first two columns of Table IV, which also shows, in the third column, the time of nearest periastron passage. The combination of these three columns gives the results in the fourth and fifth columns, which, in the mean, are L max$-T=+1^d.79$, L min$-T=-0^d.62$.

Since maximum velocity precedes T by $0^d.52$ and minimum follows T by $1^d.00$, the orbital elements represent maximum velocity as coinciding closely on the average with minimum light, while minimum velocity precedes maximum light by $0^d.79$.

[1] *Mt. Wilson Contr.*, No. 340; *Astrophysical Journal*, **66**, 177, 1927.

As they stand, the results for W Geminorum point to a definitely shorter interval between the extremes of radial velocity than between those of light, the one being $1^d.52$ in the mean and the other $2^d.41$ (see Table IV, col. 2). A somewhat shorter period, or one that undergoes a slight secular increase, would reduce the mean difference L max$-T$ from $1^d.79$ to $1^d.00$, or to the interval between T and velocity minimum; but the mean difference $T-L$ min would then no longer accord with $T-$Velocity maximum.

The period required to reduce L max$-T$ to $1^d.00$ is $0^d.00021$ shorter than that adopted in Table III, and is nearly midway between that obtained from the radial velocities and the results of W. Dziewulski and of L. V. Robinson, $7^d.91496$ and $7^d.914995$, respectively, which are based upon the longest intervals of photometric observations.

One way of accounting for the anomaly would be to assume that the representation of the radial velocities by orbital elements places velocity minimum too early, allowance for which would increase the interval between velocity maximum and velocity minimum. The evidence that the velocity-curves of other Cepheids are mirror images of the light-curves rests, however, upon velocity-curves defined by orbital elements. For a strict comparison, therefore, it is necessary to abide by the representation adopted. Whether the period should be that which makes light minimum and velocity maximum coincide, or the reverse, can be decided only by simultaneous observations of light and velocity. Since these are lacking, the period derived from the radial velocities has been retained.

The velocities and the velocity-curve based on the adopted elements are shown at the top of Figure 1. Each velocity is plotted as a circle with a radius of 2.5 km/sec.; those for 1917 are barred. The velocity of the center of mass is represented by the broken horizontal line at the ordinate -0.7 km/sec.

Below, in order from the top, are the light-curves of J. van der Bilt, M. Luizet, Dziewulski, and Robinson. The scales of ordinates at the left and right are in magnitudes and refer to the curves of van der Bilt and Robinson, respectively. The observations of Luizet and Dziewulski are plotted with approximately the same amplitude as the other curves, but bear no relation to either the left- or right-

hand ordinates. All have been arbitrarily placed so that minimum light matches maximum velocity.

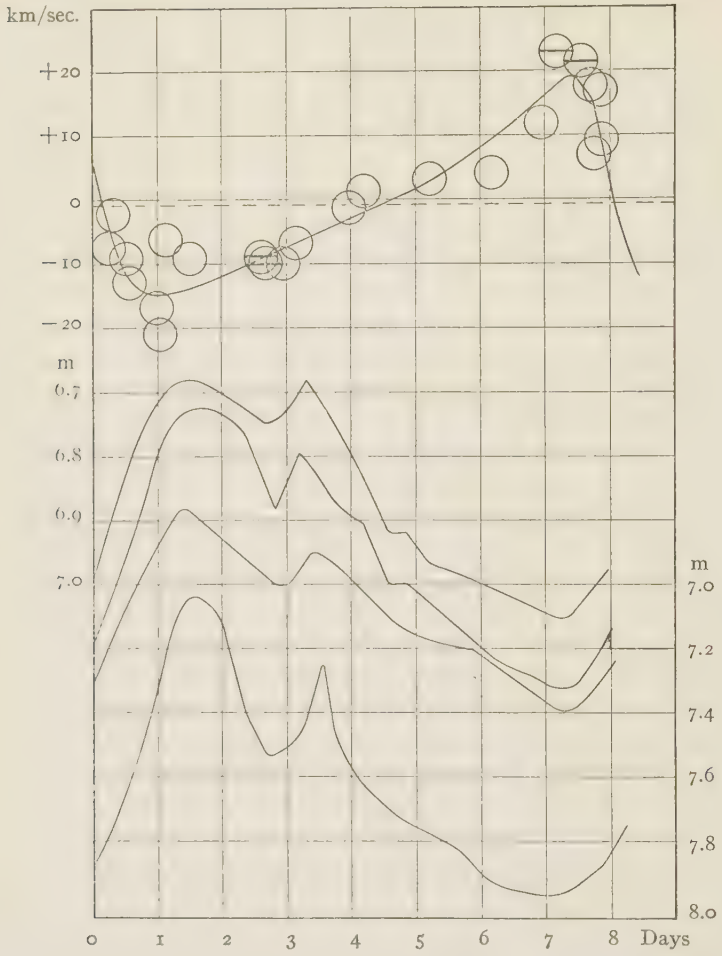

FIG. 1.—Top: Velocity-curve of W Geminorum. Circles represent individual Mount Wilson observations with phases reckoned from periastron. Below this are the light-curves of van der Bilt, Luizet, Dziewulski, and Robinson, respectively. Left- and right-hand ordinates belong to top and bottom light-curves, respectively. Robinson's curve is based on photographic magnitudes, the others on visual estimates.

Dziewulski's and van der Bilt's curves include only their own observations; Luizet's is based upon the data of several observers covering a period of ten years; and Robinson's is constructed from

photographic magnitudes observed during most of the interval since the star has been known to be a variable.

In spite of the diversity of the data, the curves strongly resemble each other in several respects. The values for $M-m$ in Table IV, which average 2^d41, show some spread, but none is as small as the interval between maximum and minimum velocity, 1^d52. A conspicuous common feature is the secondary minimum 1^d4 after light maximum, which is especially marked in Robinson's photographic light-curve. All four curves appear also to have a slight though definite pause or inflexion 3^d4 after light maximum. It should be remarked, however, that E. C. Pickering's[1] light-curve shows a smooth, continuous variation with little evidence of minor fluctuations; but this one determination, excellent though it may be, can scarcely throw doubt upon the reality of features common to the four well-determined curves illustrated in Figure 1. The absence of minor fluctuations from Pickering's curve may perhaps result from the manner of combining observations to form the mean curve.

Although the data for radial velocity are rather meager, it is perhaps worth while to call attention to apparent pauses in the upward trend of the velocities which are roughly in agreement with the two inflections in the light-curves. Many more observations, however, especially during the phase interval from 1^d5 to 2^d5, are needed to settle this point definitely.

U AQUILAE

This variable, discovered by Sawyer[2] in 1886, is a Cepheid with a period of about a week. Luizet[3] discussed the data accumulated between 1886 and 1905 and showed that the maxima could be represented by J.D. $2410170.325+7^d02387E$ (G.M.T.). All the light-curves show a continuous variation with $M-m$ ranging from 1^d98 to 2^d30, the latter being Luizet's values. The range in visual magnitude for his curve is 6.2–6.9.

Sixteen spectrograms of U Aquilae were obtained at Mount Hamilton during 1902–1905. The star was one of the faintest of a number of Cepheids thus observed, and its spectrograms were not

[1] *Harvard Annals*, **46**, 155, 1903.

[2] *Astronomical Journal*, **7**, 22, 1886. [3] *Astronomische Nachrichten*, **171**, 265, 1906.

considered good enough to justify a detailed discussion of the velocity variation. Albrecht[1] noted, however, that the plates showed a range of 25 km/sec., and that the variation appeared to agree with the period of light variation. More will be said later of this series of radial-velocity determinations.

Two spectrograms obtained at Mount Wilson in 1918 showed a range of velocity of about 18 km/sec. A series of observations, be-

TABLE V

U Aquilae—Mount Wilson Observations of Radial Velocity

Plate No.	Date	G.M.T.	Phase	Vel.
				km/sec.
γ 7263	1918 Aug. 25	16^h00^m	$1^d.718$	−14.2
8704	Sept. 12	17 10	5.476	+ 8.8
16630	1929 June 14	20 33	0.491	−21.2
16724	July 18	20 31	6.395	−20.5
16733	July 20	20 20	1.363	−11.8
16817	Aug. 18	16 36	2.071	− 5.0
16822	Aug. 19	15 58	3.086	− 4.9
16831	Aug. 20	18 06	4.175	+ 6.5
16839	Aug. 21	19 13	5.222	+17.3
C 5289	Sept. 10	16 20	4.030	+ 6.1
5294	Sept. 11	15 51	5.009	+14.1
γ 16902	Sept. 12	16 13	6.025	−11.2
16907	Sept. 13	15 7	6.979	−21.8
C 5346	Oct. 20	14 18	1.802	−15.3
5444	1930 May 11	21 33	1.617	−15.8
5449	May 12	23 30	2.698	− 6.9
5453	May 13	23 16	3.688	+ 5.6
γ 17492	June 5	20 57	5.520	+15.0
17495	June 6	21 57	6.562	−20.7
17502	June 7	22 49	0.574	−21.6
17510	June 8	22 20	1.554	−14.9
17514	June 9	23 00	2.581	−11.4

gun in 1929 and continued into 1930, includes twenty spectrograms fairly well distributed in phase. The twenty-two plates and the measured radial velocities are listed in Table V, with phases from maximum light, as computed with Luizet's formula.

The velocities, represented by circles with a radius of 1.5 km/sec., are assembled according to phase at the top of Figure 2. The two observations of 1918 are indicated by barred circles.

Through the kindness of Dr. J. H. Moore the spectrograms obtained at the Lick Observatory were loaned for this discus-

[1] *Publications of the Astronomical Society of the Pacific*, **18**, 142, 1906.

sion, where they have served a very useful purpose in determining phases of the velocity-curve at an epoch more than twenty years earlier than that of the majority of the Mount Wilson observations.

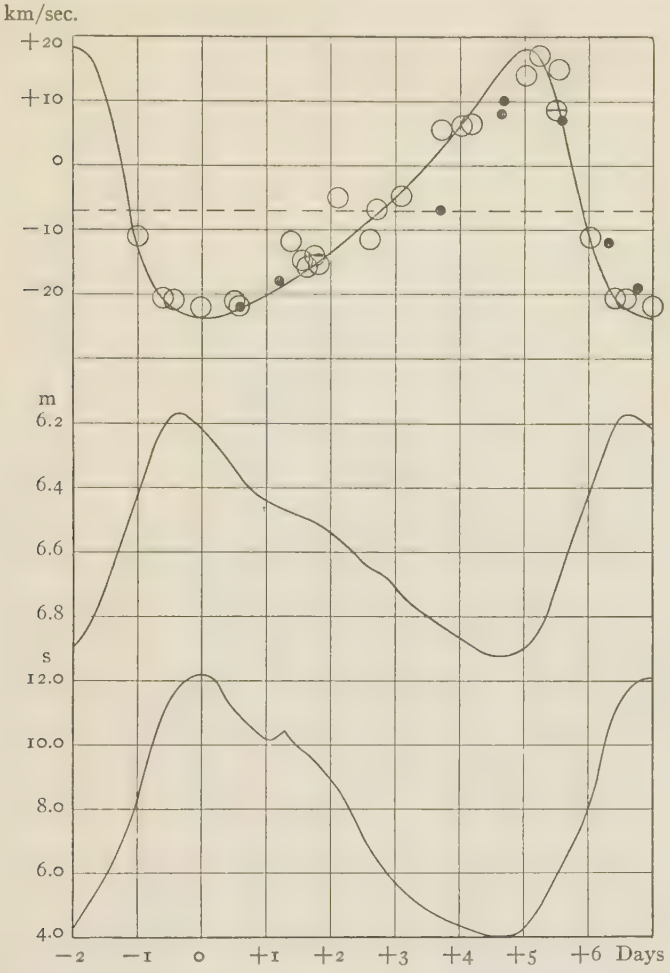

FIG. 2.—Top: Velocity-curve of U Aquilae. Circles represent individual Mount Wilson observations; dots, Lick Observatory normal places. Phases are reckoned from light-maximum. The broken horizontal line represents the velocity of the system. Middle: Pickering's light-curve. Bottom: Luizet's light-curve.

The data for normal places derived from fourteen of the Lick Observatory spectrograms, measured and reduced by the writer, are given in Table VI. The resulting velocities are plotted as solid circles

at the top of Figure 2. Pickering's[1] light-curve appears immediately below with the scale of ordinates in visual magnitudes on the left. Pickering's epoch of maximum light gives a residual of $-0^d.37$ when compared with Luizet's formula. The curve has accordingly been shifted so that its maximum is at phase $-0^d.37$. At the bottom of the figure is Luizet's light-curve with ordinates expressed in "steps."

TABLE VI

U Aquilae—Normal Places from Lick Observatory Radial Velocities

No.	Phase	Vel.	No. of Plates	Dates of Plates
		km/sec.		
I.....	$0^d.564$	−22	3	1904 July 12, 1905 May 17, 1905 Oct. 5
II.....	1.219	−18	2	1902 July 6, 1905 Oct. 20
III.....	3.710	− 7	1	1905 Oct. 15
IV.....	4.644	+ 8	2	1903 Aug. 14, 1905 Oct. 16
V.....	4.686	+10	2	1905 Oct. 9, 16
VI.....	5.588	+ 7	2	1905 May 22, Oct. 17
VII.....	6.296	−12	1	1905 July 11
VIII.....	6.769	−19	1	1905 Oct. 4

The use of Luizet's formula for deriving phases places maximum velocity in close agreement with minimum light and minimum velocity in coincidence with maximum light, and shows that Pickering's light-curve from observations in 1897–1898 agrees well with the data of 1886–1905 upon which Luizet based his curve. The radial velocities from the Lick Observatory spectrograms are also well placed by phases thus computed. Luizet's period must therefore be substantially correct.

TABLE VII

$P = 7^d.02378$
$K = 20.8$ km/sec.
$e = 0.40$
$\omega = 60°$
T = J.D. 2410168.860 (G.M.T.) = Max. light $- 1^d.465$
$\gamma = -7.0$ km/sec.

Comparison of the distribution of the Mount Wilson radial velocities with standard velocity-curves for spectroscopic binaries gave the elements appearing in Table VII, which represent the observations so well that they have not been corrected by the method of least squares. The corresponding velocity-curve is shown in Figure 2. The broken line at −7 km/sec. indicates the velocity of the center of mass.

[1] *Op. cit.*, p. 141, 1903.

The interval between maximum and minimum velocity is almost precisely 2^d. This agrees closely with Pickering's value of $1^d.98$, but is slightly less than the mean of the results by Yendell, Pickering, Chandler, and Luizet,[1] namely, $2^d.19$.

The period of velocity variation for U Aquilae is therefore identical with the period of light variation, and light minimum coincides closely with velocity maximum and light maximum with velocity minimum. The steep part of the velocity-curve may, however, cover a slightly shorter phase interval than the corresponding part of the light-curve.

Both the light-curves illustrated in Figure 2 show some evidence of a pause in the slowly descending branch about a day after maximum. Since no radial velocities are available for the same phase after velocity minimum, the evidence for or against an inflection in the velocity-curve at this point is inconclusive.

The use of a period somewhat shorter than Luizet's would improve the agreement of the Lick and Mount Wilson observations by shifting the latter in Figure 2 to the right with respect to the former, but would still leave something to be desired. Agreement could also be obtained by retaining Luizet's period and assuming that the velocity amplitude in 1902–1905 was less than that at the time the observations at Mount Wilson were made. The 1902–1905 spectrograms were, however, difficult to measure, and it seems best to assume that they are in substantial agreement with the later observations and to conclude for the present that the character of the velocity variation has changed little, if any, during more than twenty years.

DT CYGNI

While observing T Vulpeculae with the photo-electric photometer, J. Stebbins and C. M. Huffer[2] found that one of the comparison stars was itself a variable. This star is known as DT Cygni. Huffer's discussion of their photometric observations obtained in 1925 and 1926 shows that phases computed by

$$\text{Max.} = \text{J.D. } 2424305.651 + 2^d.4993E \text{ (G.M.T.)} \qquad (1)$$

[1] Müller and Hartwig, *Geschichte und Literatur des Lichtwechsels*, **2**, 203, 1920.

[2] *Publications of the Washburn Observatory*, **15**, 132, 1928.

give a very satisfactory light-curve. The variation is continuous and symmetrical, and is well represented by a sine-curve with an amplitude of 0.385 mag.

After these results appeared, it was found that a mean velocity of −6 km/sec. had been published for the star from three spectrograms[1] taken at Mount Wilson in 1913, having individual values ranging between −2 and −9 km/sec.

Huffer's epoch and period placed all three observations within $0^{d}.35$ of light maximum. This raised the question whether the range

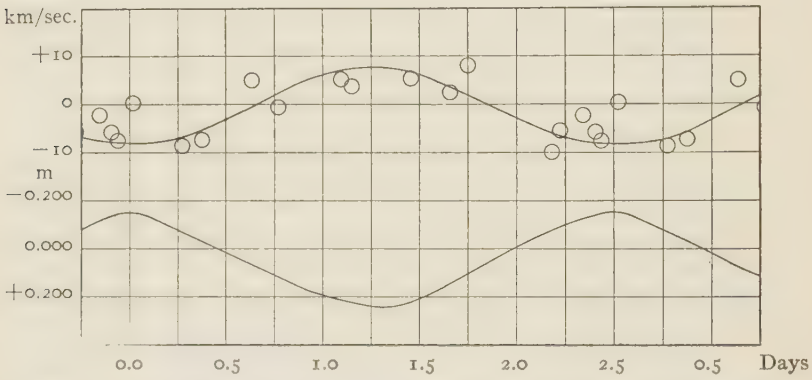

FIG. 3.—Top: Velocity-curve of DT Cygni. Circles represent individual Mount Wilson observations. Velocity of the system is −0.5 km/sec. Phases are reckoned from light-maximum. Bottom: Huffer's light-curve from observations made with the photoelectric cell. Ordinates are magnitude differences between DT Cygni and a comparison star.

in radial velocity might not be greater than that shown by the three plates. A test plate confirmed this suspicion; and, since the light variation is somewhat less than usual for Cepheids, it seemed of interest to obtain enough plates to determine the amplitude of variation and the relationship of the extremes of the light- and velocity-curves. The fifteen satisfactory plates now available are fairly well distributed over all phases of light variation and are sufficient for the present purpose. The data are listed in Table VIII with phases derived with formula (1).

The amplitude is small, and it is to be expected that the unavoidable errors will have a large percentage effect. The distribution of

[1] *Mt. Wilson Contr.*, No. 105, p. 12; *Astrophysical Journal*, 42, 172, 1915.

the velocities when plotted with the phases in Table VIII is shown by the circles at the top of Figure 3. Barred circles represent the three velocities obtained in 1913.

These three early values, especially the first, would perhaps be more consistent with those of 1929–1930 were the period shortened by $0^d.00017$. The improvement, however, would be slight; moreover, for either period, some of the other velocities are more discordant than the early ones. Huffer's period can therefore scarcely be in error by as much as $0^d.0002$.

The radial velocities reach a maximum of +6 km/sec. and a minimum of −9 km/sec. The former falls close to phase 0^d, or maximum

TABLE VIII

RADIAL VELOCITIES OF DT CYGNI

Plate No.	Date	G.M.T.	Phase	Vel.
				km/sec.
γ 2726	1913 Oct. 10	16^h12^m	$2^d.332$	− 2.2
2829	Nov. 7	16 49	0.367	− 7.3
2936	Dec. 7	14 20	0.271	− 8.6
16647	1929 June 18	23 44	1.751	+ 8.0
16725	July 18	21 29	1.664	+ 2.5
16734	July 20	21 2	1.147	+ 3.7
16742	July 21	21 50	2.181	−10.0
16748	July 22	20 30	0.626	+ 5.0
16816	Aug. 18	15 33	2.427	− 7.6
16824	Aug. 19	19 28	1.090	+ 5.1
16835	Aug. 20	22 41	2.224	− 5.5
16901	Sept. 12	15 8	2.416	− 5.9
17023	Oct. 21	15 59	1.463	+ 5.3
17033	Oct. 22	17 13	0.015	+ 0.2
17501	1930 June 7	21 53	0.773	− 0.6

light. No very definite phase for maximum velocity is revealed by the plot, but a sine-curve symmetrical about the mean axis −0.5 km/sec. (velocity of the system) with its minimum at phase 0^d, maximum at phase $1^d.25$, and an amplitude of 15 km/sec. appears to satisfy the observations as well as might be expected. Such a curve has therefore been adopted and is drawn through the plotted velocities.

The results therefore indicate that Huffer's period needs very little, if any, revision, and that the velocity-curve is substantially a mirror image of the light-curve, the relation typical of Cepheid variables.

CARNEGIE INSTITUTION OF WASHINGTON
MOUNT WILSON OBSERVATORY
July 1930

Contributions from the Mount Wilson Observatory, No. 405
Printed in the U.S.A.

UNIVERSITY OF ARIZONA
STEWARD OBSERVATORY
TUCSON, ARIZONA

INVESTIGATIONS ON PROPER MOTION

THIRTEENTH PAPER: THE PROPER MOTION OF N.G.C. 2264

By ADRIAAN VAN MAANEN

ABSTRACT

On two pairs of plates, taken at the 80-foot focus of the 60-inch reflector with an interval of about eleven years, 133 stars were measured for proper motion. The probable errors of the mean μ_α and μ_δ are 0".0027 and 0".0028, respectively.

The mean absolute motion derived for the cluster is: $\mu_\alpha = -0''.0033 \pm 0''.0007$; $\mu_\delta = +0''.0019 \pm 0''.0006$.

About 50 stars are probably members of the cluster.

During the last two years a considerable number of plates have been measured by the writer for proper motion. Among the objects included are six planetary and two spiral nebulae and the open cluster N.G.C. 2264. All the photographs were taken at the Cassegrain focus of the 60-inch reflector (focal length 80 ft.); the intervals between the old and new plates range from eight to fourteen years. The results are very satisfactory. The probable errors for the mean motions derived depend on the interval of time, the number of plates measured, the distribution of the stars over the plate, and the range of magnitudes of the stars measured. The most unfavorable case encountered is that of N.G.C. 2264, where all the stars visible on only two pairs of plates were measured; the range in magnitude is from 4.7 to 15.1, and the field covered is the full size of the 8×10-inch plates, or $24' \times 30'$. But even in this case the probable error of a mean μ_α is only 0".0027 and of a mean μ_δ, 0".0028. On the other hand, as we are dealing with a cluster, we may, to obtain the final motion, combine the values of all stars which are probably members of the group, thereby reducing the probable error to a very small quantity. Accordingly, there is in such a case little reason to measure more than two pairs of plates. In the case of the planetary nebulae, however, we may restrict the measures to stars of a limited range of magnitude, near the nebulae, and thus considerably increase the accuracy. Since we are here dealing with single objects, it seems worth while to measure about four pairs of plates. In the case of the

spiral nebulae the objects, unlike the planetaries, are generally in high galactic latitudes, and the lack of nearby comparison stars has made it desirable to measure as many pairs of plates as were available—nine in all in the case of N.G.C. 4051.

N.G.C. 2264 is a coarse open cluster surrounding 15 S Monocerotis. The 1900 position is $\alpha = 6^h35^m30^s$, $\delta = +9°59'$; the galactic latitude is $+4°$ and the diameter about 30′. Trumpler calls it II3pN,[1] i.e., a detached cluster with little central concentration, composed of less than 50 bright and faint stars, with nebulosity involved in the cluster. Table I gives the necessary data for the plates measured.

Plate 5061 was combined with 2116, 5048 with 2137, Δt being $+4^y.5$ and $-8^y.8$, respectively, or, in the mean, $-2^y.2$; 133 stars

TABLE I

Plate No.	Date	H.A. at End
2116	1919 Jan. 23	12°.5 W
2137	1919 Jan. 25	9.5
5048	1929 Dec. 6	0.7
5061	1930 Jan. 29	17.0

were measured on both pairs of plates in four positions. Of these, 48 were chosen as comparison stars; the brighter and the fainter stars and those which seemed to have a fair chance of being members of the cluster were omitted. The reductions were made for each pair of plates separately, in both right ascension and declination; quadratic terms were used in the reductions, which, as shown before,[2] is necessary when stars more than 8′ or 10′ from the center are used. The results of the measures are collected in Table II, the last two columns of which give the mean annual relative motion in right ascension and declination.

In order to derive the reduction to absolute motion, Oort's[3] value of $0''.0066$ was used for the secular parallax of the comparison stars, which are of about the thirteenth magnitude. While Oort's value is only provisional, its weight has been considerably increased by

[1] *Lick Observatory Bulletins*, **14**, 154 (No. 420), 1930.

[2] *Mt. Wilson Contr.*, No. 167, 1919.

[3] *Publications of the American Astronomical Society*, **5**, 179, 1924.

TABLE II

PROPER MOTIONS OF STARS IN AND NEAR N.G.C. 2264
(Unit of μ is 0".001)

No.	Pg. Mag.*	x	y	μ_{a_1}	μ_{a_2}	μ_{δ_1}	μ_{δ_2}	μ_a	μ_δ
1.....	14.5	−15′.3	−10′.3	− 4	− 3	+ 4	− 3	− 4	0
2.....	14.9	−15.2	− 9.3	+22	− 5	− 1	+ 4	+ 8	+ 2
3.....	14.78	−14.8	+ 5.9	− 1	0	− 2	−11	0	− 6
4.....	14.1	−15.8	+ 8.2	− 4	+ 6	+ 6	− 1	+ 1	+ 2
5.....	13.47	−15.6	+11.1	− 1	− 1	+ 6	+ 7	− 1	+ 6
6.....	11.12	−15.2	+11.9	− 3	+22	+13	+12	+10	+12
7.....	13.33	−13.8	+11.5	+ 4	+ 5	+ 6	+ 5	+ 4	+ 6
8.....	13.57	−12.3	+10.3	+ 4	+11	+ 8	0	+ 8	+ 4
9.....	14.8	−11.1	− 1.6	−27	−12	−19	−15	−20	−17
10.....	14.18	−12.3	− 5.5	− 1	+ 2	+ 3	+ 6	0	+ 4
11.....	14.7	−13.1	− 7.5	− 5	0	− 2	− 1	− 2	− 2
12.....	13.73	−12.0	−12.1	− 2	+ 7	− 2	− 5	+ 2	− 4
13.....	10.58	− 9.0	−11.9	− 9	+ 8	+ 7	+ 1	0	+ 4
14.....	14.9	− 9.7	− 8.2	+29	+ 5	−27	−13	+17	−20
15.....	9.10	− 8.4	− 7.7	− 6	+10	+ 7	+13	+ 2	+10
16.....	7.76	− 7.4	− 4.7	−11	+14	+15	+17	+ 2	+16
17.....	14.8	− 7.1	− 3.6	− 1	+ 1	+15	+12	0	+14
18	14.4	− 8.8	+ 2.6	+ 2	+ 7	−20	−11	+ 4	−16
19.....	14.3	− 8.2	+ 4.8	− 3	+ 1	+11	+ 5	− 1	+ 8
20.....	14.7	− 8.6	+ 6.2	+ 4	− 7	+ 9	+14	− 2	+12
21.....	12.04	−11.0	+10.0	+ 1	+ 6	+14	+12	+ 4	+13
22.....	13.53	−10.8	+11.1	−12	+ 4	− 3	0	− 4	− 2
23.....	14.3	−10.0	+10.8	+ 1	+ 3	+ 2	+ 3	+ 2	+ 2
24.....	14.9	− 9.7	+10.5	+ 4	+ 3	+13	− 2	+ 4	+ 6
25.....	15.0	− 8.8	+11.6	−50	−22	−43	0	−36	−22
26.....	14.8	− 7.0	+ 8.9	− 3	0	− 4	+ 1	− 2	− 2
27.....	13.49	− 6.6	+ 8.1	+ 3	+ 5	+11	+15	+ 4	+13
28.....	15.0	− 5.9	+ 4.0	+11	− 1	− 8	+ 2	+ 5	− 3
29.....	9.98	− 5.1	+ 4.0	− 9	− 1	+ 2	+ 6	− 5	+ 4
30.....	12.19	− 5.2	+ 1.2	− 6	+ 2	+12	+10	− 2	+11
31.....	14.9	− 4.2	+ 1.6	− 4	− 5	+ 8	− 4	− 4	+ 2
32.....	14.38	− 4.2	+ 0.4	− 1	− 3	+ 7	+ 8	− 2	+ 8
33.....	15.0	− 3.8	− 2.7	−14	−11	+ 5	+14	−12	+10
34.....	14.32	− 4.7	− 5.0	+11	− 2	−10	− 8	+ 4	− 9
35.....	11.21	− 5.2	− 6.3	− 4	+ 6	+12	+ 5	+ 1	+ 8
36.....	12.87	− 5.3	− 6.4	− 6	0	+ 3	+ 7	− 3	+ 5
37.....	7.87	− 4.9	− 6.4	−10	+ 9	+ 6	+14	0	+10
38.....	14.9	− 1.6	−10.3	−14	− 9	−17	− 8	−12	−12
39.....	12.77	− 1.8	− 8.9	− 1	+ 3	+ 5	+ 5	+ 1	+ 5
40.....	8.56	− 3.8	− 7.7	− 7	+ 9	+12	+ 7	+ 1	+10
41.....	14.01	− 2.8	− 7.7	+14	+18	+24	+13	+16	+18
42.....	15.0	− 3.4	− 7.1	+ 3	+ 6	+31	−18	+ 4	+ 6
43.....	12.84	− 3.4	− 5.8	− 1	+ 3	+10	+ 6	+ 1	+ 8
44.....	14.79	− 3.3	− 5.3	− 3	+ 7	− 8	− 7	+ 2	− 8
45.....	12.22	− 3.0	− 4.4	+16	+11	− 2	+ 3	+14	0
46.....	14.7	− 2.7	− 4.2	−12	− 5	+ 3	− 2	− 8	0
47.....	14.8	− 2.0	− 4.8	−27	−18	−36	−35	−22	−36
48.....	9.99	− 2.5	− 1.9	− 7	− 6	0	+ 5	− 6	+ 2

* The photographic magnitudes of 88 stars were kindly communicated to me by Dr. Trumpler; for the other stars they were estimated by me from Trumpler's magnitudes. On account of the uncertainty only one decimal is given in these estimated magnitudes.

TABLE II—*Continued*

No.	Pg. Mag.*	x	y	μ_{a_1}	μ_{a_2}	μ_{δ_1}	μ_{δ_2}	μ_a	μ_δ
49.....	8.81	− 1".8	− 1".9	− 9	− 5	+ 4	− 3	− 7	0
50.....	11.41	− 2.2	− 0.4	− 7	− 5	+ 4	+10	− 6	+ 7
51.....	15.1	− 2.2	+ 3.2	−26	+14	− 6	−15	− 6	−10
52.....	8.60	− 1.9	+ 7.9	− 9	− 7	+ 2	+ 1	− 8	+ 2
53.....	15.0	+ 0.1	+ 6.0	0	− 1	+ 8	− 5	0	+ 2
54.....	14.66	+ 0.3	+ 5.1	− 2	0	+ 8	+ 5	− 1	+ 6
55.....	14.66	− 0.3	+ 2.7	− 3	− 1	− 1	+ 4	− 2	+ 2
56.....	13.05	+ 0.1	+ 1.6	+ 1	− 1	+ 3	− 4	0	0
57.....	10.39	+ 1.4	+ 1.0	− 5	0	+ 1	0	− 2	0
58.....	11.4	0.0	+ 0.3	+ 1	− 2	+16	+ 6	0	+11
59.....	13.16	− 0.5	+ .4	+ 2	− 2	+12	+ 6	0	+ 9
60.....	4.70	0.0	.0	+ 5	+23	+29	+ 6	+14	+18
61.....	9.86	+ 0.8	− 0.8	+ 9	−12	+12	0	− 2	+ 6
62.....	8.74	+ 0.8	− 0.9	−15	−10	+ 6	+ 3	−12	+ 4
63.....	9.03	+ 0.3	− 1.4	− 8	0	+ 2	− 1	− 4	0
64.....	13.76	+ 0.8	− 1.9	+ 3	− 1	+ 9	+ 3	+ 1	+ 6
65.....	13.15	+ 1.4	− 1.9	+ 3	0	+ 4	+ 5	+ 2	+ 4
66.....	14.7	+ 0.5	− 2.3	+ 4	− 3	− 9	+ 2	0	− 4
67.....	14.66	+ 1.5	− 3.0	+10	− 3	−19	0	+ 4	−10
68.....	12.77	− 0.4	− 5.1	+ 2	0	+ 9	+ 4	+ 1	+ 6
69.....	14 8	+ 0.8	− 5.3	− 3	− 8	+ 6	− 1	− 6	+ 2
70.....	14.01	+ 1.4	− 5.3	−24	−12	− 7	+ 2	−18	− 2
71.....	12 06	+ 1.1	− 5.8	− 3	+ 2	+ 5	+ 3	0	+ 4
72.....	14.25	− 1.1	− 6.6	− 8	− 2	− 5	− 4	− 5	− 4
73.....	13.65	+ 2.5	− 7.7	+ 1	+ 3	+ 7	+ 9	+ 2	+ 8
74.....	14.0	+ 2.3	− 9.6	+ 2	+ 5	− 1	− 1	+ 4	− 1
75.....	15.0	+ 2.6	−12.5	+ 9	−11	−28	+ 8	− 1	−10
76.....	8 35	+ 5.8	− 9.9	−19	− 2	+18	+ 7	−10	+12
77.....	14 8	+ 5.4	− 8.1	− 7	+ 5	+13	− 1	− 1	+ 6
78.....	14 66	+ 4.1	− 7.0	+ 9	+ 5	− 6	0	+ 7	− 3
79.....	13.03	+ 4.4	− 1.5	+ 8	+ 4	+ 6	+ 4	+ 6	+ 5
80.....	9.80	+ 3.0	− 0.8	−10	− 2	+ 2	0	− 6	+ 1
81.....	9.78	+ 2.8	− 0.7	−17	− 7	+ 4	− 4	−12	0
82.....	13.15	+ 3.7	+ 2.1	+ 1	+ 3	+ 3	+ 5	+ 2	+ 4
83.....	11.60	+ 4.4	+ 3.6	+ 3	+ 4	−33	−40	+ 4	−36
84.....	14.5	+ 5.5	+ 4.9	−19	−22	+15	+ 1	−20	+ 8
85.....	15.1	+ 2.1	+ 4.8	+18	−15	−20	− 5	+ 2	−12
86.....	13.49	+ 2.9	+ 7.0	− 4	−10	+ 2	+ 7	− 7	+ 4
87.....	14.6	+ 3.0	+ 8.6	− 2	+ 4	−19	−10	+ 1	−14
88.....	14.11	+ 3.3	+11.8	+16	+10	+ 4	− 2	+13	+ 1
89.....	12.76	+ 4.7	+12.3	0	+ 2	+ 5	− 5	+ 1	0
90.....	13.68	+ 5.3	+10.5	+ 5	+11	−13	−12	+ 8	−12
91.....	12.84	+ 8.5	+11.2	− 5	− 1	+ 4	+ 2	− 3	+ 3
92.....	12.45	+ 8.8	+ 8.8	−13	− 9	+ 4	+10	−11	+ 7
93.....	14.6	+ 8.1	+ 7.4	− 3	− 4	−26	−21	− 4	−24
94.....	14.12	+ 9.5	+ 4.9	+ 5	+ 1	+15	− 2	+ 3	+ 6
95.....	14.38	+ 8.4	+ 4.2	− 3	−11	−10	+ 5	− 7	− 2
96.....	14.01	+ 8.1	+ 1.6	+22	+23	−14	−21	+22	−18
97.....	12.50	+ 8.0	+ 1.2	+15	+22	+10	+ 4	+18	+ 7
98.....	7.30	+ 7.0	− 2.5	−16	+ 7	+17	− 1	− 4	+ 8
99.....	9.87	+ 8.8	− 2.1	− 8	+ 7	+10	0	0	+ 5
100	9.05	+ 7.7	− 3.8	− 9	− 6	+11	+ 9	− 8	+10
101		+ 7.7	− 3.9	−17	+ 3	+13	−16	− 7	− 2

TABLE II—*Continued*

No.	Pg. Mag.*	x	y	μ_{a_1}	μ_{a_2}	μ_{δ_1}	μ_{δ_2}	μ_a	μ_δ
102.....	14.9	+ 8′.1	− 5′.1	0	− 2	− 2	− 6	− 1	− 4
103.....	10.99	+ 9.6	−10.0	+ 7	− 1	+ 8	0	+ 3	+ 4
104.....	14.9	+11.2	−12.7	+ 6	+ 6	−22	− 4	+ 6	−13
105.....	14.9	+13.6	−11.5	+ 1	− 7	−24	− 2	− 3	−13
106.....	13.96	+12.2	−10.8	− 5	− 7	+ 2	− 2	− 6	0
107.....	11.14	+11.0	−10.1	− 3	− 5	+ 8	− 1	− 4	+ 4
108.....	15.1	+11.0	− 9.5	+ 9	−19	+17	+13	− 5	+15
109.....	15.0	+13.4	− 9.2	+ 2	+10	+ 2	− 9	+ 6	− 4
110.....	14.52	+12.1	− 7.8	+ 2	+ 4	+ 5	0	+ 3	+ 2
111.....	14.91	+11.1	− 7.1	+ 5	− 8	+13	− 3	− 2	+ 5
112.....	9.54	+10.7	− 6.0	−18	− 6	+19	0	−12	+10
113.....	15.1	+12.9	− 6.0	− 6	− 6	+ 3	−15	− 6	− 6
114.....	11.73	+14.2	− 3.6	−45	−34	+ 2	+ 2	−40	+ 2
115.....	14.9	+12.2	− 3.4	− 8	− 7	− 5	+ 6	− 8	0
116.....	14.52	+10.1	− 2.7	+ 5	+11	+ 5	− 4	+ 8	0
117.....	14.25	+12.1	− 1.6	+ 5	+ 7	+11	− 2	+ 6	+ 4
118.....	14.06	+12.9	0.0	− 4	− 7	+17	+ 1	− 6	+ 9
119.....	14.53	+13.8	− 0.1	+ 1	+ 2	+ 7	+ 3	+ 2	+ 5
120.....	14.8	+13.6	+ 0.3	+ 9	+ 5	+ 9	−11	+ 7	− 1
121.....	14.8	+13.3	+ 0.8	−32	− 7	− 1	− 6	−20	− 4
122.....	14.9	+13.3	+ 4.4	−13	+ 2	− 8	+22	− 6	+ 7
123.....	12.51	+13.6	+ 5.1	− 2	+12	+11	− 4	+ 5	+ 4
124.....	14.66	+12.5	+ 5.2	0	0	− 3	−15	0	− 9
125.....	14.12	+13.6	+ 5.9	−14	− 6	− 2	−10	−10	− 6
126.....	14.78	+11.9	+ 6.3	+ 2	− 2	+ 4	− 3	0	0
127.....	12.21	+10.7	+ 6.7	− 7	− 4	+21	+14	− 6	+18
128.....	13.85	+10.0	+ 6.3	−31	−28	+32	+19	−30	+26
129.....	15.00	+11.8	+ 7.8	0	0	−16	−12	0	−14
130.....	9.61	+12.9	+ 8.1	− 9	− 5	+13	+ 5	− 7	+ 9
131.....	9.43	+11.0	+ 8.5	+ 5	+11	− 2	− 5	+ 8	− 4
132.....	12.35	+12.3	+11.1	− 6	− 3	+ 4	− 9	− 4	− 2
133.....	14.9	+13.4	+12.3	0	−29	−29	−30	−14	−30

some recent data on the motions of very faint stars which will be discussed in a subsequent paper, and it is thought to be the best that can be used at present. The resulting corrections are $-0''.0008$ in α and $-0''.0043$ in δ.[1]

In order to derive the motions of the cluster as a whole, 35 stars were chosen from their appearance alone as probable members of the cluster. The central star 15 S Monocerotis was dropped as being too bright for accurate measurement; in addition, one other star, No. 114, was omitted, as it has a considerable motion in right ascension, which excludes it as a probable member of the group.

[1] If the less probable value of the parallactic motion of stars of magnitude 13 suggested by Oort, viz., $0''.0114$ in the direction 6^h, $-60°$, had been used, the reduction from relative to absolute motion would have been $-0''.0011$ in α and $-0''.0105$ in δ.

When plotted according to stellar magnitude the motions of these stars give no indication of a magnitude error in either α or δ. The mean absolute motion of the 33 stars is $\mu_\alpha = -0''.0033 \pm 0''.0007$; $\mu_\delta = +0''.0019 \pm 0''.0006$.

From the probable errors given on page 1 we might have expected the probable error of the motion of the cluster to be $0''.0005$ in each co-ordinate. The difference between the external and internal probable errors is very small and gives considerable confidence in the motions derived.

While the total motion is extremely small, it should be remarked that it is of the order to be expected from Trumpler's parallax of 450 parsecs.

One more point should be mentioned. If we plot the motions in a velocity diagram, we find that of the 98 stars not used for the determination of the motion of the cluster, 28 have motions which fall within a circle with center at the motion of the cluster and a radius twice the probable error of the motions, and 44 in a concentric circle with three times the probable error as radius. As two circles at the same distance from the origin of the proper motions and with the same radii, but located in different quadrants, contain in the mean only $11\frac{1}{2}$ and $29\frac{1}{2}$ stars, the excess of $16\frac{1}{2}$ and $14\frac{1}{2}$ stars, respectively, probably represents additional members of the cluster. Grouping the stars according to magnitude, we find that the excess occurs among stars of magnitudes 11 to 15. For stars of magnitudes 14.50 to 14.99 it is small, while for still fainter stars it becomes negative. We may accordingly conclude with certainty that the cluster contains stars as faint as 14.5 and may have some members as faint as even magnitude 14.5 to 15.0. The total number of group members on the plates may be estimated as nearly 50. While a few of the stars belonging to the cluster may fall outside the region of our plates, their number will be quite small, because if Trumpler's value of $30'$ for the diameter is accepted, our plates cover 90 per cent of the area of the cluster.

Carnegie Institution of Washington
Mount Wilson Observatory
July 1930

Contributions from the Mount Wilson Observatory, No. 406
Printed in the U.S.A.

INVESTIGATIONS ON PROPER MOTION

FOURTEENTH PAPER: THE PROPER MOTIONS OF SIX PLANETARY NEBULAE

By ADRIAAN VAN MAANEN

ABSTRACT

Proper motions were derived for six planetary nebulae from photographs taken at the 80-foot focus of the 60-inch reflector. The mean interval between the old and the new plates is 10.92 years; the probable error of the mean motions is 0″.0010 in α and 0″.0012 in δ. The results for the absolute motions of these six objects range from 0″.004 to 0″.010, the mean being 0″.006. The mean parallax derived from these motions would be about +0″.001, which, compared with the mean rotations found by Campbell and Moore, would yield a mass 180 ⊙, while the absolute magnitude for the central stars would be +3.0.

The values of the trigonometric parallaxes of the planetary nebulae derived by the writer are in general fairly large and for many years have been suspected of being affected by an unexplained systematic error. For this reason it was planned to derive proper motions for some of these objects as soon as possible. For six of them four pairs of plates have now been measured, and, although the observations are being continued, it seems worth while to give the results thus far obtained.

The time interval for all pairs of plates ranges from 8.02 to 12.91 years, with a mean interval of 10.92 years. Since we are dealing with objects of peculiar color, special care was taken to make the difference in hour angle between the old and new plates as small as possible, as a means of avoiding a systematic hour-angle error. Table I gives a summary of the material used.

Table II gives for each field the co-ordinates of the comparison stars, while Table III gives the detailed results for each of the six planetaries. Relative motions for both central and comparison stars are included in order to show the close agreement between the four pairs of plates. The probable error of a mean μ_α is 0″.0010; of a mean μ_δ, 0″.0012. Although the motions in both co-ordinates are very small, there is agreement in sign among all four measures in

TABLE I

N.G.C.	Pg. Mag.	α 1900	δ 1900	Mean Interval in Years	Mean Diff. in H.A.	Red. to Abs. Motion (Unit = 0".001)	
						α	δ
6058.....	13.0	16^h 1^m 0^s	+40°57′	9.77	−2°.7	−3	+1
6543.....	11.3	17 58 32	+66 38	10.72	+0.5	0	+4
6572.....	10.8	18 7 14	+ 6 50	10.00	+0.8	0	−3
6720.....	14.7	18 49 53	+32 54	12.48	−0.4	+2	0
6804.....	13.4	19 26 48	+ 9 1	11.26	−0.7	+2	−3
6905.....	14.5	20 17 56	+19 47	11.50	−0.3	+3	−2
Means..	13.0	.....	.....	10.95	−0.5	.....	.....

TABLE II

Co-ordinates of the Comparison Stars

Star	N.G.C. 6058		N.G.C. 6543		N.G.C. 6572	
	x	y	x	y	x	y
1.....	+4′.8	+5′.4	+1′.9	+5′.4	+2′.3	+3′.3
2.....	+7.1	+1.0	+3.8	+3.6	+2.7	−0.3
3.....	+2.2	−1.0	+7.1	−0.4	+3.4	−1.6
4.....	+0.4	−3.4	+4.0	−1.9	+1.5	−3.7
5.....	+0.8	−7.3	−4.4	−6.9	−2.7	−1.4
6.....	−8.4	0.0	−2.6	−3.6	−5.2	0.0
7.....	−5.2	+0.8	−5.1	−1.1	−1.2	+1.0
8.....	−3.6	+5.8	−2.1	+4.4	−0.1	+2.9
9.....	.....	.....	−1.2	+1.8	.....	.....

Star	N.G.C. 6720		N.G.C. 6804		N.G.C. 6905	
	x	y	x	y	x	y
1.....	+2′.9	+3′.3	+2′.6	+2′.7	+0′.7	+0′.8
2.....	+2.2	+2.2	+2.6	+0.7	+1.1	+1.9
3.....	+1.0	0.0	+1.6	−4.8	+1.0	−0.1
4.....	+1.6	−1.0	+0.8	−1.6	+2.5	−0.8
5.....	+2.7	−2.7	−0.7	−1.0	+0.1	−0.5
6.....	−1.9	−3.8	−3.8	−2.2	−1.2	−2.2
7.....	−4.3	−1.6	−2.6	+1.5	−1.2	−1.6
8.....	−1.0	+0.8	−0.8	+4.8	−1.4	+1.1
9.....	−2.7	+2.9	+0.3	+0.1	−1.8	+2.1

62 per cent of the cases. When the mean value for μ_α or μ_δ is 0".007 or larger, all four measures have the same sign.

TABLE III

Proper Motions of Planetary Nebulae

Object	μ_α					μ_δ				
	1	2	3	4	Mean and P.E.	1	2	3	4	Mean and P.E.
N.G.C. 6058	− 1	+ 4	0	− 2	0″.000±0″.0009	− 3	−10	− 9	0	−0″.006±0″.0016
Comp. star 1	+ 9	+ 5	+ 9	+ 9	+0.008±0.0007	− 4	− 5	0	+ 9	0.000±0.0022
2	− 6	− 8	− 8	− 6	− 7 4	+ 3	+ 2	+ 2	− 6	14
3	−18	−16	−13	−25	− 18 17	+ 2	− 5	− 6	+ 2	− 2 15
4	+32	+34	+33	+47	+ 36 24	− 4	− 2	+ 1	+16	+ 3 31
5	− 8	− 6	−10	−15	− 10 13	+ 3	+ 7	+ 3	−11	0 27
6	+ 7	− 3	+ 5	+ 3	+ 3 15	+ 2	− 5	+ 2	+15	+ 4 28
7	−16	−11	−14	−14	− 14 7	− 6	− 3	− 5	−16	− 8 20
8	0	+ 7	− 1	0	+0.002±0.0013	+ 6	+11	+ 2	− 9	+0.002±0.0029
N.G.C. 6543	− 1	+ 3	+ 2	+ 7	+0.003±0.0011	− 3	+ 3	− 6	+ 4	0.000±0.0016
Comp. star 1	− 1	− 1	+ 5	+ 1	+0.001±0.0010	0	+ 1	+ 1	+ 3	+0.001±0.0004
2	− 2	− 5	− 5	+ 4	− 2 13	− 7	+ 1	− 6	−12	− 6 17
3	− 1	+ 3	+ 4	+ 3	+ 2 8	+15	+ 9	+ 6	+16	+ 12 16
4	+ 1	0	− 6	− 9	− 4 16	−10	−10	+ 5	− 8	− 6 24
5	− 2	+ 1	+ 2	+ 4	+ 1 9	− 2	+ 1	− 1	+ 2	0 8
6	+ 9	+ 3	+ 8	+ 5	+ 6 9	− 1	− 2	− 5	− 6	− 4 8
7	− 7	− 6	− 8	− 4	− 6 6	+13	+ 9	+12	+ 7	+ 10 9
8	+ 6	+ 8	+ 7	+ 4	+ 6 6	+ 5	0	+10	+ 8	+ 6 15
9	− 4	− 4	− 6	− 7	−0.005±0.0005	−12	− 9	−20	−10	−0.013±0.0017
N.G.C. 6572	− 1	− 4	−14	+ 3	−0.004±0.0025	+ 4	0	+13	+11	+0.007±0.0020
Comp. star 1	− 2	0	0	+ 2	0.000±0.0006	− 6	− 6	− 5	− 4	−0.005±0.0003
2	+ 7	+ 7	+13	+ 3	+ 8 14	+15	+17	+13	+ 4	+ 12 19
3	− 6	−10	−15	− 6	− 9 14	− 6	−16	− 7	+ 4	− 6 28
4	+ 2	+ 5	+ 6	+ 2	+ 4 7	− 6	− 1	− 8	− 9	− 6 12
5	− 3	− 3	+ 3	0	− 1 10	+ 4	+11	+13	+ 9	+ 9 13
6	+ 2	+ 1	− 2	− 1	0 6	− 3	−11	−11	− 5	− 8 14
7	− 1	− 2	− 9	+ 6	− 2 21	0	+ 3	+ 6	− 2	+ 2 12
8	0	0	+ 5	− 6	0.000±0.0015	+ 1	+ 3	− 2	+ 3	+0.001±0.0010

TABLE III—*Continued*

Object	μ_α					μ_δ				
	1	2	3	4	Mean and P.E.	1	2	3	4	Mean and P.E.
N.G.C. 6720	+ 2	+ 5	+ 3	+ 5	+0.004±0.0005	+13	+ 6	+ 6	+ 6	+0.008±0.0012
Comp. star 1	+ 1	+ 3	− 4	0	0.000±0.0010	−12	− 9	− 6	− 8	−0.009±0.0009
2	− 7	−13	− 4	− 9	− 8 13	+ 5	0	− 1	+ 1	+ 1 9
3	−11	− 3	− 5	− 9	− 7 12	+ 7	+ 6	+12	+ 5	+ 8 11
4	+12	+ 6	+10	+ 9	+ 9 9	− 3	− 1	0	− 3	− 2 5
5	− 1	+ 5	+ 2	+ 2	+ 2 8	+ 6	+ 6	+ 3	+ 5	+ 5 5
6	0	− 4	− 7	− 4	− 4 10	− 8	− 5	− 7	− 3	− 6 8
7	− 5	− 2	− 1	− 3	− 3 6	+ 1	− 4	+ 2	− 4	− 1 11
8	+10	+ 5	+ 9	+10	+ 8 8	0	− 1	− 6	0	− 2 10
9	+ 1	+ 4	+ 1	+ 2	+0.002±0.0005	+ 4	+ 7	+ 4	+ 6	+0.005±0.0005
N.G.C. 6804	− 7	− 7	− 7	− 9	−0.008±0.0004	− 1	− 2	− 4	− 3	−0.002±0.0005
Comp. star 1	− 3	0	0	− 6	−0.002±0.0010	+ 5	+ 1	− 2	− 1	+0.001±0.0011
2	+ 6	+ 7	+ 3	+ 5	+ 5 6	+ 6	+ 5	+ 5	+ 3	+ 5 4
3	+ 1	− 3	+ 2	− 3	− 1 9	0	− 4	− 6	− 2	− 3 9
4	− 2	+ 4	− 1	+10	+ 3 19	− 6	+ 2	+ 6	+ 1	+ 1 17
5	−10	− 7	−11	− 9	− 9 6	−11	− 5	− 2	− 1	− 5 15
6	+ 1	+ 3	+ 2	0	+ 2 5	+ 6	+ 5	+ 4	+ 2	+ 4 6
7	+ 5	+ 2	+ 7	+ 2	+ 4 8	+ 4	− 1	− 4	− 1	0 11
8	− 1	− 2	− 3	0	− 2 5	− 6	− 2	− 2	0	− 2 9
9	+ 2	− 2	+ 1	0	0.000±0.0006	+ 1	0	+ 2	0	+0.001±0.0003
N.G.C. 6905	− 6	− 5	− 4	− 8	−0.006±0.0008	+ 3	− 2	− 2	+ 2	0.000±0.0009
Comp. star 1	+ 1	+ 3	+ 1	− 2	+0.001±0.0007	− 7	− 7	− 9	−10	−0.008±0.0005
2	−10	− 4	− 8	− 4	− 6 10	0	+ 1	0	− 1	0 3
3	+ 6	0	− 2	+ 6	+ 2 14	+ 5	+ 4	+ 6	+ 7	+ 6 5
4	0	+ 1	+ 5	+ 1	+ 2 8	+ 3	0	+ 2	+ 2	+ 2 4
5	+ 4	+ 2	+ 3	+ 1	+ 2 5	− 2	0	− 1	0	− 1 3
6	− 3	− 1	− 5	− 2	− 3 6	0	+ 2	0	0	0 4
7	− 3	− 1	− 1	− 2	− 2 3	− 1	− 3	− 2	0	− 2 5
8	− 1	0	+ 2	+ 1	0 5	− 2	− 1	0	− 2	− 1 3
9	+ 6	0	+ 3	+ 1	+0.002±0.0009	+ 5	+ 3	+ 3	+ 4	+0.004±0.0003

It is clear that the motions thus derived deserve a great deal of confidence. This is not surprising if we keep in mind the large focal length of the instrument used, the interval in time between the old and the new plates, and the closeness of the comparison stars to the central stars in the nebulae, which in the mean have a galactic latitude of only 19°. In fact, only two comparison stars are more than 8′ from the central star (8′.2 and 8′.4), while the mean distance is only 3′.8. All the motions given are relative to the mean motion of the comparison stars. Using as in the preceding *Contribution* a parallactic motion of 0″.0066 in the direction 6^h,−30°, we find for the corrections necessary to change the relative into absolute motions the values given in the last column of Table I.

Of the 52 comparison stars 39, or no less than 75 per cent, have an absolute total motion of 0″.010 or less. In the case of the Pleiades[1] the corresponding number was only 38 per cent, while the theoretical number is 83 per cent.

The results for the total absolute motions of the six planetary nebulae range from 0″.004 to 0″.010, the mean being 0″.006.

The mean of the parallaxes of these same objects formerly derived by the writer[2] is +0″.0085, but doubt about these parallaxes has been felt for some time. By combining the radial velocities of the nebulae, amounting to about 30 km/sec., with the proper motions here derived, we would find a mean parallax of only +0″.001. We may also derive a parallax by assuming that the nuclei of the planetaries are normal O-type or Wolf-Rayet stars, in which case their absolute magnitudes would be somewhere between −2 and −4 and their parallaxes accordingly a little less than +0″.0001. The uncertainty as to the real parallax is emphasized if for each of these three values we compare the corresponding absolute magnitudes and the masses of the planetaries calculated with the aid of the rotations found by Campbell and Moore.[3] Accepting their mean result, $V = 5.3$ km/sec. at a distance of 5″.7 from the center, Russell, Dugan,

[1] *Mt. Wilson Contr.*, No. 167, 1919.

[2] *Ibid.*, No. 356, p. 12, 1928.

[3] *Publications of the Lick Observatory*, **13**, 176, 1918.

and Stewart[1] give the formula for the derivation of the mass: $m = 0.18/\pi$. For the three values of the parallax given above we have:

$\pi = +0''.0085$	gives $M = +7.6$	$m = 22\odot$
$\pi = +0.001$	$+3.0$	180
$\pi = +0.00085$	-2.4	2200

The mass generally accepted for the O-type stars is about $16\odot$, which agrees well with the first value. Yet the proper motions and the parallax derived from them are undoubtedly more reliable than the trigonometric parallax. Neither of the values derived from trigonometric parallaxes or from the proper motion, however, agrees well with the absolute magnitude generally accepted for the early-type stars.

Carnegie Institution of Washington
Mount Wilson Observatory
July 1930

[1] *Astronomy*, **2**, 835, 1927.

Contributions from the Mount Wilson Observatory, No. 407
Printed in the U.S.A.

INVESTIGATIONS ON PROPER MOTION

FIFTEENTH PAPER: THE PROPER MOTION OF THE SPIRAL NEBULA N.G.C. 4051

By ADRIAAN VAN MAANEN

ABSTRACT

From nine pairs of photographs taken at the 80-foot focus of the 60-inch reflector, with a mean interval of 10.77 years, the absolute motion of the spiral nebula N.G.C. 4051 was found to be $\mu_a = -0''.003 \pm 0''.0008$, $\mu_\delta = +0''.015 \pm 0''.0011$, $\mu_T = 0''.014$. An investigation into various possible sources of error was made, including a magnitude error, an hour-angle error, and an error depending on the quadratic terms. None of these seems to have influenced the result materially.

The motion is practically at right angles to the Milky Way and cannot therefore be explained by a rotation of that system. It is also difficult to explain it by the motion of the stellar system or by a motion of the comparison stars used.

By comparing the motion found with the radial velocity, a parallax of $0''.000073$ was derived, giving -2.7 as the absolute magnitude of the nucleus, which has a spectrum of the planetary-nebula type.

About a dozen years ago several papers were published on the proper motions of nebulae; these results derived by Wirtz, Curtis, Lundmark, and van Maanen were based partly on an intercomparison of old and new micrometer observations and partly on measures of photographic plates taken principally with the Crossley reflector of the Lick Observatory and the Mount Wilson 60-inch reflector. In both cases the plates were obtained at the primary focus (focal length 18 and 25 ft., respectively); and it must be borne in mind that the original photographs were not taken with the view of making accurate measurements on them.

Soon after it became evident that parallaxes could be determined with great accuracy from photographs made at the Cassegrain focus of the Mount Wilson 60-inch reflector (focal length 80 ft.), many nebulae, including several spirals, were put on the parallax program. It soon appeared from all sources of information, however, that the parallaxes of the spiral nebulae are too small to be measured successfully by the trigonometric method; nevertheless it seemed worth while to duplicate some of the older plates after an interval of several years in order to derive their proper motions.

One object well suited to this purpose is N.G.C. 4051 ($\alpha = 11^h58^m0^s$, $\delta = +45°5'$, 1900). According to Curtis,[1] it is "a fine, rather bright spiral $4' \times 2'$ in p.a. 122°. Very bright stellar nucleus. There are numerous almost stellar condensations. It is a two-branched spiral, and each branch is bifid." While an exposure of 40 minutes at the Newtonian focus of the 100-inch telescope confirms its spiral structure, plates taken at the Cassegrain focus of the 60-inch with exposures of 15 to 20 minutes show only the nucleus, which appears so much like the comparison stars that it seems almost

TABLE I

Plate No.	Date of Exposure	Interval	Δt
$4899_1 - 1781_1$	1929.28 − 1918.34	10.94	−0.7
$4899_2 - 1781_2$	1929.28 − 1918.34	10.94	−2.5
$4918_1 - 1767_1$	1929.35 − 1918.34	11.01	+2.7
$4918_2 - 1768_1$	1929.35 − 1918.34	11.01	−1.0
$4951 - 1768_2$	1929.42 − 1918.34	11.08	+4.7
$5090_2 - 2582$	1930.26 − 1920.12	10.14	+0.2
$5081_1 - 2654_1$	1930.25 − 1920.32	9.93	−0.7
$5081_2 - 1767_2$	1930.25 − 1918.34	11.91	−1.0
$5090_1 - 2654_2$	1930.26 − 1920.32	9.94	−2.0
Mean		10.77	0.0

impossible that any influence originating in the character of the image should vitiate the measures.

In 1929, five pairs of exposures, each with approximately eleven years' interval, were measured with the new stereocomparator in four positions, with east, west, north, and south in the direction of the increasing readings of the micrometer screw. The result derived from these five pairs for the motion of N.G.C. 4051 was $\mu_\alpha = +0''.005 \pm 0''.0007$; $\mu_\delta = +0''.017 \pm 0''.0016$. The old plates were all taken in 1918, the new in 1929. To avoid any influence arising from the fact that all the plates were obtained during only two seasons, four more exposures were made in 1930 and compared with three exposures taken in 1920 and one in 1918. Table I shows the data for the nine pairs of plates, the last column giving the differences in hour angle between new and old plates.

Table II gives the full details of these measures, both for the

[1] *Lick Observatory Publications*, 13, 28, 1918.

nebula and for the seven comparison stars. The co-ordinates of the stars relative to the nebula are in Table III.

TABLE II

Object	Plate Pair 1	2	3	4	5	6	7	8	9	Mean P.M.	P.E.
	μ_α										
N.G.C. 4051...	+ 1	+ 4	+ 7	+ 6	+ 4	+ 5	− 2	+ 8	− 2	+0″.003	±0″.0008
Star 1.....	− 5	− 1	+ 5	+ 1	+ 2	− 3	+ 8	0	+ 1	+0.001	±0.0009
2.....	+ 4	+ 3	− 4	+ 3	+ 3	0	− 6	− 1	0	0	8
3.....	0	− 4	− 3	− 4	− 5	+ 2	− 6	0	− 1	− 2	6
4.....	+ 3	+ 7	+ 5	+ 1	+ 3	+ 1	+ 6	+ 3	+ 3	+ 4	5
5.....	− 8	− 4	− 5	0	+ 1	− 1	+ 2	+ 1	− 5	− 2	8
6.....	− 5	−13	− 6	− 2	− 4	− 5	−10	− 6	− 4	− 6	7
7.....	+10	+13	+ 7	+ 1	+ 2	+ 6	+ 4	+ 5	+ 5	+0.006	±0.0008
	μ_δ										
N.G.C. 4051...	+16	+ 9	+20	+21	+21	+16	+19	+19	+ 8	+0.017	±0.0011
Star 1.....	+22	+14	+12	+14	+ 9	+19	+15	+15	+20	+0.016	±0.0009
2.....	−18	− 3	−10	−11	− 9	−13	− 9	−10	−15	− 11	10
3.....	− 3	−10	− 6	− 6	− 5	− 5	− 4	− 8	− 7	− 6	5
4.....	+ 7	+ 3	0	+ 1	− 4	+ 4	0	+ 7	0	+ 2	8
5.....	− 8	0	+16	+15	+26	+ 8	+ 6	+ 5	+19	+ 10	23
6.....	+ 2	+ 2	− 7	− 4	− 7	− 6	+ 1	− 7	− 3	− 3	9
7.....	− 2	− 6	− 7	− 9	−11	− 4	− 9	0	−13	−0.007	±0.0005

TABLE III

Co-ordinates of the Comparison Stars

Star	x	y
1.....	+0′.7	+3′.8
2.....	+2.5	+1.2
3.....	+5.1	−0.1
4.....	+4.5	−8.6
5.....	−2.2	−0.7
6.....	−4.8	−0.8
7.....	−6.9	+3.6

The final relative motion of N.G.C. 4051,

$$\mu_\alpha = +0''.003 \pm 0''.0008,\ \mu_\delta = +0''.017 \pm 0''.0011,$$

is in good agreement with the result derived from the five exposures mentioned before.

As this motion is rather large, considerable care has been taken to investigate several sources of error which might have influenced the results.

a) MAGNITUDE ERROR

On all the plates measured the nucleus of the nebula is somewhat fainter than star 3 and brighter than star 6. Table IV gives the results of the measures in 0″.001 as unit arranged according to the brightness of the comparison stars. Apparently there is no trace of a magnitude error.

TABLE IV

>4051	μ_α	μ_δ	N.G.C. 4051		<4051	μ_α	μ_δ
5.....	−2	+10	.....	.....	6	−6	− 3
7.....	+6	− 7	.....	.....	4	+4	+ 2
3.....	−2	− 6	.....	.....	1	+1	+16
					2	0	−11
Mean.....	+1	− 1	+3	+17	.....	0	+ 1

b) HOUR-ANGLE ERROR

The difference in hour angle of each pair is quite small; for the three pairs where Δt is positive we have $\mu_\alpha = +0''.0054 \pm 0''.0006$, $\mu_\delta = +0''.0190 \pm 0''.0010$; for those where Δt is negative, $\mu_\alpha = +0''.0025 \pm 0''.0012$, $\mu_\delta = +0''.0153 \pm 0''.0015$. Since the mean Δt is exactly zero, the final result, $\mu_\alpha = +0''.003$, $\mu_\delta = +0''.017$, seems to need no correction for this possible source of error.

c) QUADRATIC TERMS

We may further suppose that the values derived need a correction due to a neglect of quadratic terms in the reductions. As the distances of the seven comparison stars are 3′.9, 2′.8, 5′.1, 9′.7, 2′.3, 4′.9, and 7′.8, respectively, or in the mean 5′.2, no large errors can be expected. A solution including the quadratic terms based on only seven comparison stars becomes rather uncertain. Sixteen comparison stars were accordingly measured on the last three pairs of plates, which were then reduced both with seven stars and no quadratic terms, and with sixteen stars and quadratic terms. These solu-

tions give $\mu_a = +0''.001 \pm 0''.0022$, $\mu_\delta = +0''.015 \pm 0''.0024$, and $\mu_a = -0''.003 \pm 0''.0018$, $\mu_\delta = +0''.013 \pm 0''.0024$, respectively, for N.G.C. 4051. These values are consistent within the range of the probable errors, whence it may be concluded that neglect of the quadratic terms has not seriously influenced the results. Accordingly we may accept as the motion of the nebula relative to the seven (or sixteen) comparison stars, $\mu_a = +0''.003$, $\mu_\delta = +0''.017$.

The absolute motion of the nebula has been derived with the value for the parallactic motion of the thirteenth-magnitude stars used in the two preceding *Contributions*. The corrections are $-0''.006$ in μ_a and $-0''.002$ in μ_δ; the absolute motion is therefore $\mu_a = -0''.003$, $\mu_\delta = +0''.015$. If a larger parallactic motion should be thought necessary, since we are dealing with stars at high galactic latitude ($\beta = +70°$), these values would be changed somewhat, but the τ-component of the motion is $0''.014$, and this of course is independent of the parallactic motion, as long as we retain $A = 6^h$, $D = -30°$ for the antapex of the sun's motion.

The small chance, pointed out by Oort,[1] that the parallactic motion of the thirteenth-magnitude stars is $0''.0114$ toward the antapex 6^h, $-60°$, is contradicted by evidence afforded by the proper motions of some still fainter stars, which will be discussed in a subsequent paper; but allowance for even this motion would not materially change the absolute motion of N.G.C. 4051, but would give $\mu_a = -0''.003$, $\mu_\delta = +0''.010$. With all these possible sources of error taken into consideration, the best result for the absolute motion seems to be:

$$\mu_a = -0''.003,\ \mu_\delta = +0''.015,\ \mu_\tau = 0''.014.$$

This motion is practically at right angles to the Milky Way and cannot therefore be explained by the rotation of that system.

Taking the result at its face value, we may suppose that the nebula is moving with respect to the system of stars on which all proper motions are based. Such a motion may be due to the nebula, or to the stellar system, or to both. The much smaller relative motion found in the case of Messier 51, discussed in the following *Contribu-*

[1] *Publications of the American Astronomical Society*, **5**, 179, 1924.

tion, excludes the probability that most of the motion is due to the stellar system. Another possibility is that the comparison stars in the field of N.G.C. 4051 have in the mean an exceptional group motion, which is not shared by the stars in other fields; this would require that practically all the stars in a region 24′ by 30′ (16 out of the 20 stars on the plates were measured) form a kind of cluster with hardly any stars which are not members of this local group. The chances that this should be the case are very small.

If, then, we accept the motion of the nebula as real, an approximate idea of the parallax of N.G.C. 4051 may be obtained by comparing this motion with its radial velocity, 650 km/sec. The result is $\pi = 0''.000073$. As the nucleus is of about the thirteenth magnitude, its absolute magnitude would be about -2.7. Its spectrum has been photographed on several occasions by Humason; it is of the planetary-nebula type, with the nebulium and hydrogen lines and λ 4686 bright.

If, on the other hand, we apply Hubble's results to N.G.C. 4051, we should have to admit a distance about one hundred times greater than that corresponding to the foregoing parallax, and the motion derived here would then represent a velocity of the order of 65,000 km/sec., a quantity which is difficult to accept.

Carnegie Institution of Washington
Mount Wilson Observatory
July 1930

Contributions from the Mount Wilson Observatory, No. 408
Printed in the U.S.A.

INVESTIGATIONS ON PROPER MOTION

SIXTEENTH PAPER: THE PROPER MOTION OF MESSIER 51, N.G.C. 5194

By ADRIAAN VAN MAANEN

ABSTRACT

From five pairs of photographs, taken at the 80-foot focus of the 60-inch reflector, with a mean interval of 13.02 years, the absolute motion of Messier 51 was found: $\mu_\alpha = -0''.0015 \pm 0''.0010$, $\mu_\delta = +0''.006 \pm 0''.0011$. This is only 40 per cent of the motion found for N.G.C. 4051. Since the nebulae are separated by only 16° in the sky their motions cannot be explained by a motion of the stellar system, but must belong to the nebulae themselves.

In the case of Messier 51, the well-known spiral in Canes Venatici ($\alpha = 13^h25^m42^s$, $\delta = +47°43'$ 1900), H. D. Curtis mentions the nucleus as "sharp stellar," but on plates taken at the Cassegrain focus

TABLE I

Plate No.	Date of Exposure	Interval	t
4914 −1380	1929.34−1917.37	11.97	+1°.5
4919 − 832	1929.35−1916.20	13.15	−2.7
4920 − 954	1929.35−1916.40	12.95	−0.7
5105$_1$− 953	1930.31−1916.40	13.91	+1.2
5105$_2$−1299	1930.31−1917.20	13.11	+2.7
Mean		13.02	+0.4

of the 60-inch reflector it appears as a round disk about 3″ in diameter. The nucleus can be measured without difficulty, but not with the same feeling of certainty as in the case of N.G.C. 4051.

The data for the five pairs of plates measured are given in Table I.

The measures were started with eight comparison stars, but from the first pair of plates it was evident that one of the stars has a considerable proper motion in right ascension and should not be used for comparison purposes. If this star is left out, another must also be omitted in order to maintain a proper distribution of the comparison stars around the nucleus. Since six comparison stars is a rather small group, it was decided to use as many stars as could be

well measured on all the plates, consistent with a good distribution over the field. Eleven stars satisfy these requirements. (The star with large motion was measured, but not used for the derivation of the plate constants; it is given at the bottom of Table II under *a*). In order to strengthen the reductions for N.G.C. 5195, the companion nebula 4′.4 NE from N.G.C. 5194, the eleven stars were chosen somewhat farther away from the center than usual. The distribution is such as to allow the use of quadratic terms in the reductions. During measurement it was found that the settings on the companion were rather difficult because this object is quite elongated. Not much faith should be put in the motion derived for it.

The results of the measures are collected in Table II. Table III gives the co-ordinates of the comparison stars with respect to the nucleus.

For completeness, motions were also derived with only the first six comparison stars and three plate constants. These results are $\mu_\alpha = +0''.003 \pm 0''.0010$, $\mu_\delta = +0''.008 \pm 0''.0011$. As in the case of N.G.C. 4051, the results of both methods agree within the range of the probable errors. Except that six is a rather small number of comparison stars, there is no reason why the first solution should be preferred. The mean of the two solutions is therefore accepted as the final relative motion: $\mu_\alpha = +0''.003^5$, $\mu_\delta = +0''.007$.

The reduction from relative to absolute motion corresponding to a parallactic motion of $0''.0066$ toward the antapex 6^h, $-30°$, requires corrections of $-0''.005$ and $-0''.001$ in right ascension and declination, respectively, leaving as the final motion of the nebula $\mu_\alpha = -0''.001^5$, $\mu_\delta = +0''.006$.

For completeness, the absolute motion which results from the use of a parallactic motion of $0''.0114$ toward 6^h, $-60°$, is also given. The corrections for this case are $-0''.004^5$ in α and $-0''.005$ in δ, with a final motion of $\mu_\alpha = -0''.001$, $\mu_\delta = +0''.002$.

Although the motion is in about the same direction as that found for N.G.C. 4051, its amount is only 40 per cent; as the nebulae are separated only 16° in the sky, both should have practically the same relative motion, if the motion is due to the motion of the stellar system.

One or more early exposures are also available for about ten other

TABLE II

Object	Plate Pair 1	2	3	4	5	Mean P.M.	P.E.
				μ_α			
N.G.C. 5194.....	+ 4	+ 1	+ 9	+ 4	+ 2	+0.″004	±0.″0009
5195.....	+11	−12	+ 2	+11	0	+0.002	±0.0029
Star 1.....	+ 7	+ 1	+ 1	0	0	+0.002	±0.0009
2.....	+ 1	+ 7	0	+ 7	+ 6	+ 4	13
3.....	+ 1	−10	− 7	−18	−10	− 9	21
4.....	+ 2	− 2	− 2	− 6	− 9	− 3	13
5.....	+ 8	+17	+ 8	+15	+14	+ 12	13
6.....	−21	− 7	− 1	+ 1	+ 3	− 5	29
7.....	+ 1	− 2	+ 1	+ 1	− 1	0	4
8.....	+ 3	+ 3	+ 5	+ 4	+ 2	+ 3	4
9.....	− 4	− 7	− 3	− 4	− 3	− 4	5
10.....	+ 5	− 2	− 2	0	− 2	0	9
11.....	− 3	0	− 1	− 1	0	− 1	4
a.....	−63	−79	−75	−70	−73	−0.072	±0.0018
				μ_δ			
N.G.C. 5194.....	+ 4	+11	+10	+ 2	+ 3	+0.006	±0.0013
5195.....	−10	+ 6	−11	+ 3	− 9	−0.004	±0.0024
Star 1.....	+ 1	− 1	+ 2	− 1	− 4	−0.001	±0.0007
2.....	+ 4	+ 2	0	+ 7	+ 8	+ 4	10
3.....	0	−12	− 5	− 7	−16	− 8	19
4.....	+20	+22	+13	+11	+ 6	+ 14	20
5.....	− 7	− 3	−11	−10	−14	− 9	13
6.....	−18	−12	− 2	+ 3	+13	− 3	37
7.....	+ 1	+ 2	0	− 2	+ 4	+ 1	7
8.....	+ 3	+ 4	+ 5	+ 6	+ 1	+ 4	6
9.....	− 7	− 6	− 6	− 8	+ 1	− 5	11
10.....	+ 5	+ 2	+ 3	0	− 1	+ 2	7
11.....	− 1	+ 1	− 2	0	+ 2	0	5
a.....	+13	+19	+13	+ 7	+11	+0.013	±0.0013

TABLE III

Star	x	y	Star	x	y
1.....	+7.′0	+4.′9	7.....	−8.′2	− 2.′2
2.....	+2.5	−6.5	8.....	+2.7	− 9.5
3.....	−1.5	−2.5	9.....	+5.8	− 9.3
4.....	−1.1	−1.0	10.....	−4.4	+ 9.6
5.....	−1.9	+0.3	11.....	+6.7	+11.2
6.....	−2.3	+1.9	*a*.....	−6.6	+ 2.7

spirals and these will be duplicated as soon as possible. For only two, however, is the number of old plates large enough to permit the derivation of proper motions with the same accuracy as for N.G.C. 4051 and 5194.

On the other hand, a considerable number of exposures has been made since 1925 at the Newtonian focus of the 100-inch reflector on spirals which are noted by Curtis as having stellar or almost stellar nuclei. In several cases, such as N.G.C. 200, 3596, and 4790, the nuclei on these plates look exactly like stars, and in others, such as N.G.C. 691 and 2775, they will be fairly easy to measure. Several years must of course elapse before this material can be successfully utilized for the determination of proper motions.

In connection with the star *a*, which has a large motion more or less in the direction of the parallactic drift, it may be recalled that two considerably fainter stars (too faint to be measured on the 80-ft.-focus plates) were found earlier by the writer[1] in this same region, which have motions about double the amount and also roughly in the direction of the antapex of the sun's motion.

Carnegie Institution of Washington
Mount Wilson Observatory
July 1930

[1] *Mt. Wilson Contr.*, No. 213; *Astrophysical Journal*, **54**, 237, 1921.

Contributions from the Mount Wilson Observatory, No. 409
Reprinted from the *Astrophysical Journal*, Vol. LXXII, pp. 98–110, 1930.
Printed in the U.S.A.

UNIVERSITY OF ARIZONA
STEWARD OBSERVATORY
TUCSON, ARIZONA

NOTES ON THE SPECTRA OF TEN BRIGHT-LINE STARS OF CLASSES B AND A

By PAUL W. MERRILL

ABSTRACT

Among the stars whose spectra have been found at Mount Wilson to exhibit bright hydrogen lines are a number with peculiarities of special interest. Ten of these are here briefly described.

Peculiarities of special interest have been found at Mount Wilson in the spectra of more than twenty bright-line stars of early type. Descriptions of the following have already been published: H.D. 45910;[1] H.D. 51480;[2] DM. −27°11944;[2] H.D. 53179, Z Canis Majoris;[3] B.D.+14°3887;[3] H.D. 169515, RY Scuti;[4] H.D. 163181;[5] H.D. 45677;[6] H.D. 207757, B.D.+11°4673.[7] A few others are being extensively observed and are reserved for future detailed discussion. For the ten remaining stars, for each of which there are two to thirteen spectrograms, it does not appear feasible to obtain long series of observations in the near future. These are briefly described in the present *Contribution*.

These ten stars (Table I) are among those in whose spectra bright hydrogen lines have been detected at Mount Wilson from objective-prism spectrograms of the *Hα* line. Data concerning all but the last, H.D. 218393, which has not previously been announced as having bright lines, will be found in *Contribution* No. 294.[8]

[1] *Publications of the Astronomical Society of the Pacific*, **35**, 303, 1923. See also Plaskett, *ibid.*, p. 145, 1923.

[2] *Mt. Wilson Contr.*, No. 295; *Astrophysical Journal*, **61**, 418, 1925.

[3] *Mt. Wilson Contr.*, No. 334; *Astrophysical Journal*, **65**, 286, 1927.

[4] *Mt. Wilson Contr.*, No. 349; *Astrophysical Journal*, **67**, 179, 1928.

[5] Humason and Nicholson, *Mt. Wilson Contr.*, No. 353; *Astrophysical Journal*, **67**, 341, 1928.

[6] *Mt. Wilson Contr.*, No. 355; *Astrophysical Journal*, **67**, 405, 1928.

[7] *Mt. Wilson Contr.*, No. 381; *Astrophysical Journal*, **69**, 330, 1929.

[8] *Astrophysical Journal*, **61**, 389, 1925.

The plates designated by C in Tables II–XII were taken with a one-prism spectrograph attached to the 100-inch telescope; those by γ, with a similar spectrograph attached to the 60-inch telescope. An 18-inch camera was employed in both instruments, giving a dispersion at $H\gamma$ of about 35 A per millimeter. Unless otherwise

TABLE I

LIST OF STARS

H.D.	R.A. 1900	DEC. 1900	MAG.	SPECTRUM	
				H.D.	Mt. W.
29866.....	4^h37^m3	+40°36′	6.1	B5	B4ev
45995.....	6 25.6	+11 9	5.8	Bo	B2ev
160095.....	17 32.9	−33 29	8.7	B8	B8ev
163296.....	17 50.3	−21 56	6.6	Ao	A2ev
169454.....	18 19.6	−14 2	6.8	Bo	Boe
172694.....	18 36.5	−15 57	8.3	B3	Bep
180398.....	19 11.3	+12 56	7.7	B9	B(3)e
183143.....	19 23.0	+18 6	6.9	B	B9sea
195407.....	20 26.0	+36 39	7.7	B5	B(3)e
218393.....	23 2.6	+49 40	6.8	A5p	var

TABLE II

SPECTROGRAMS OF H.D. 29866

Plate	Date	Remarks
C 838.....	1920 Dec. 30	
C 855.....	1921 Jan. 5	
γ 11374.....	1922 Oct. 7	
C 2106.....	1923 Feb. 5	Region from $H\beta$ to $H\alpha$
γ 13216.....	1925 Jan. 13	
γ 13265.....	Mar. 1	
γ 14466.....	1926 Aug. 25	
γ 14760.....	Dec. 14	

noted, the spectrograms are of the usual blue-violet region. The G plates are of the yellow and red regions; these were made with a plane-grating spectrograph attached to the 100-inch telescope, and have a dispersion of 66 A per millimeter.

H.D. 29866

This spectrum is not particularly noteworthy except for small changes in the bright components of the hydrogen lines, described in the following notes.

On plates C 838 and C 855, $H\beta$, $H\gamma$, and $H\delta$ are broad, diffuse absorption lines with ill-defined edges. $H\beta$ is weak, as if partly filled with emission. Its width is about 16 A. The helium lines are weak and diffuse. *Mg* 4481 is weaker than *He* 4471. γ 11374 is a rather poor plate but shows no certain change. $H\alpha$ is a well-marked emission line on plate C 2106; $H\beta$ is about the same as on previous plates. Plates γ 13216 and γ 13265 exhibit small but decided changes in $H\beta$ and $H\gamma$; weak emission features appear within these

TABLE III

SPECTROGRAMS OF H.D. 45995

PLATE	DATE	$H\beta$, INTENSITY RATIO Er:Ev	RAD. VEL.	DISPLACEMENT Ev	
				$H\gamma$	$H\beta$
			km/sec.	km/sec.	km/sec.
C 728	1920 Oct. 26	1.0	+11	−84	.....
γ 11382	1922 Oct. 8	0.1	.....	31	−35
γ 11433	Nov. 5	0.0	.....	61	27
γ 11515	1923 Jan. 6	0.0	.....	59	27
γ 12154	Sept. 29	0.2	.....	83	65
γ 12502	1924 Feb. 19	0.3	31	77	64
γ 12509	Feb. 21	0.7	(13)	73	91
γ 12997	Oct. 8	0.6	51	96	73
γ 13138	Dec. 14	0.8	12	.....	−89
γ 13332	1925 Mar. 15	0.8	+17	−76	.....
Mean	.....	.....	+23	.....	.....
	Faint companion				
C 840	1920 Dec. 30	Under-exposed	.....	.....	.....
C 3544	1925 Oct. 1	.....	+ 6	.....	.....

broad, dark lines. The violet emission component, *Ev*, is stronger than the red component, *Er*. The separation of the bright components is 4 or 5 A. On γ 14466, *Ev* and *Er* have nearly equal intensities. The spectrum appears much the same on γ 14760 as on the preceding plate, but the emission components are weaker.

H.D. 45995

This star is a double, β G.C. 3427: position angle 3°.8, distance 16″.3, magnitudes 6.0–8.2.

$H\beta$ consists of a weak, ill-defined absorption line on which are superposed two emission components of moderate intensity. On

certain plates these are run together; on others, distinctly separated. The average measured separation is 3.4 A. The violet component, *Ev*, remains of approximately constant intensity, while the other, *Er*, is decidedly variable. On the first plate and the last two, the components are of nearly equal intensity, but on several plates taken in 1922 and 1923 *Er* is weak or invisible. Table III gives estimates of the relative intensities. These suggest a period somewhat longer than five years.

$H\gamma$ resembles $H\beta$ except that the emission components are extremely weak. The average separation is 3.4 A, the same as at $H\beta$. *Er* is of variable intensity as in $H\beta$. The displacements of the violet emission components of $H\beta$ and $H\gamma$ are given in Table III. The displacements are smallest when the red component is very weak, apparently indicating a motion of *Ev* toward the center of the line. At $H\beta$ the effect might arise from a systematic error of measurement when both components are visible, but at $H\gamma$ the components are probably too weak and too well separated to produce such an error. The accuracy of the measurements is low, and small differences between various plates are without meaning.

The helium absorption lines are weak and diffuse and are thus unsuited for accurate measurement. It is therefore difficult to determine the radial velocity. The values given in Table III depend largely on the assumption that the central minima of the hydrogen lines occupy the normal positions of these lines. In several cases the helium lines give approximately the same velocities, but the measurements are scattering. K, measured on two plates, gives +18 km/sec.

The companion star is of type Ao. The mean velocity from six lines is +6 km/sec. The agreement of individual lines is poor.

Plaskett obtained seven spectrograms[1] of the brighter star (B.D.+11°1204) between October 28, 1922, and March 20, 1923, which showed "fuzzy absorption lines of helium and hydrogen with narrow sharp emission at $H\beta$ and $H\gamma$." This is in agreement with the Mount Wilson observations, for at that time the second emission component of $H\beta$ and $H\gamma$, *Er*, was invisible.

[1] *Publications of the Dominion Astrophysical Observatory*, **2**, 306, 1924.

H.D. 160095

On the first plate, $H\gamma$ is a strong, well-defined absorption line with a faint bright edge on the violet side. The measured distance between the centers of the bright and dark components is 2.14 A. $H\beta$ is somewhat similar except that the bright part is stronger and the absorption line much weaker. The measured distance between bright and dark components is 2.91 A. Weak absorption is probably present on the violet side of the bright portion of $H\beta$. This is not clearly seen at $H\gamma$. The principal dark components of $H\beta$ and $H\gamma$ agree in giving an apparent radial velocity of +25 km/sec. Seven dark lines of ionized iron give +35 km/sec., while *He* 4471 and *Mg* 4481 give a much larger value (see Table IV). λ 4481 is a broad

TABLE IV

SPECTROGRAMS OF H.D. 160095

PLATE	DATE	DISPLACEMENTS OF ABSORPTION LINES IN KM/SEC.			
		H	*Fe*	*He* 4471	*Mg* 4481
C 1776.....	1922 July 9	+25	+35	+110	+111
C 5246.....	1929 July 19	− 6	.....	.....	.....

line, but fairly well defined and measurable with reasonable accuracy; λ 4471 is weaker and more difficult to measure. The explanation of the decided difference between the displacements of these lines and those of iron and hydrogen is not obvious.

The second plate is underexposed, and $H\beta$ is the only line well shown. The absorption component is sharply defined and stronger than on the first plate, while the emission component is scarcely visible. The spectrum is weak toward the violet from λ 4400. $H\gamma$ can be seen, however, and is essentially an absorption line with no visible bright portion. Lines of iron, helium, and magnesium are not clearly seen and are probably weaker than on the other plate. This star may belong to that small group of Be stars which have α Cygni lines of variable intensity.

The difference in the measured displacements of the dark hydrogen lines on the two plates probably represents a real change in the position of these lines. The shift toward the violet exhibited by the

second plate as compared to the first is accompanied by the disappearance of the bright edge. This suggests that an underlying bright line serves as the background for an absorption line whose position varies. The phenomenon may be similar to that displayed by the long-period binary H.D. 33232, whose spectral variations will be described in a future *Contribution*.

H.D. 163296

On most plates $H\gamma$ is a wide dark line, which has, however, a narrow minimum measurable with fair accuracy. This minimum

TABLE V

SPECTROGRAMS OF H.D. 163296

PLATE	DATE	DISPLACEMENTS OF ABSORPTION LINES IN KM/SEC.				
		$H\gamma$	$H\beta$	*Mg* 4481	*Fe* and *Ti*	
C 1184	1921 July 26	− 91	−144	− 1	?	1*
C 2275	1923 May 28	−200	−209	+ 5	?	4
C 2287†	June 14	.....	.....	.....	.....	.....
γ 12581	1924 Apr. 18	(−100)	− 99	−21	−20	5
γ 12668	May 20	− 36	− 77	−15	12	5
Hilger 25	1925 May 17	.....	.....	.....	.....	.....
γ 15059	1927 June 17	−150	−178	+ 2	9	3
γ 15947	1928 July 5	+ 13	+ 12	+ 5	?	3
C 5193	1929 May 23	− 46	−119	− 2	− 7	3
Mean	.....	.....	.....	− 4	−12	.....

* Number of lines. † Red region.

usually lies toward the violet from the center of the line; in fact, on several plates $H\gamma$ might be described as a narrow dark line having a broad indefinite wing extending toward longer wave-lengths. $H\beta$ is similar to $H\gamma$, except that within the wing on the red side of the minimum is a portion which tends to be bright. The structure of $H\gamma$ and $H\beta$ is variable. Table V gives the measured displacements of the narrow minima; these vary through a large range and suggest a period somewhat less than four years. Plate C 2287, although underexposed, shows $H\alpha$ to be bright.

Mg 4481 is a well-marked dark line, rather wide but with fairly definite edges. On several plates it appears to have hazy bright borders. Its displacement (Table V) is probably constant within the error of measurement. A few enhanced lines of iron and titanium

are faintly seen. They yield nearly the same displacement as the magnesium line. Thus we have variable hydrogen lines accompanying metallic lines which exhibit little or no change.

Plate Hilger 25 was taken with a small ultra-violet spectrograph. It shows the unsymmetrical structure of $H\gamma$ and $H\delta$. $H\epsilon$, $H\zeta$, $H\eta$, and K are strong dark lines, probably of normal strength for class A2.

H.D. 169454

$H\beta$ consists of a dark line having a bright border on its red edge. $H\alpha$ is similar except that the bright portion is much more intense.

TABLE VI

SPECTROGRAMS OF H.D. 169454

PLATE	DATE	DISPLACEMENTS OF ABSORPTION LINES IN KM/SEC.					
		$H\gamma$	$H\beta$	He	O II	N II	Si III
γ 10413..	1921 Aug. 23	(−138)	−142	(+ 9) 3*	+10 7*	.....	+ 3 3*
C 1259..	Aug. 25	110	138	+20 4	+20 20	.....	+19 3
γ 10984..	1922 Apr. 13	(38)	142	− 5 3	+10 7	.....	+ 3 3
γ 10988..	Apr. 14	59	139	−21 5	− 2 8	.....	.....
γ 11075..	May 16	(80)	157	(+18) 3	+ 5 17	.....	(−23) 3
C 2195..	1923 Apr. 7	.....	133	+19 3	+20 7	.....	+22 3
γ 11911..	June 30	(60)	178	.....	− 7 17	.....	(+12) 3
C 2749..	1924 Apr. 17	(58)	139	−33 2	0 7	.....	− 8 3
γ 12698..	June 11	62	126	−14 5	− 2 16	.....	− 7 3
γ 12974..	Sept. 17	.....	126	(−31) 4	− 6 5	.....	−27 3
γ 14487..	1926 Aug. 29	− 53	−134	(+11) 4	+11 11	.....	− 9 3
G 360..	1930 Apr. 16	.....	.....	.....	.....	.....	.....
G 379..	Apr. 19	.....	.....	.....	.....	.....	.....
Mean..	.....	− 72	−141	− 4	+ 5	(+13)	− 1

* Number of lines.

TABLE VII

MEAN DISPLACEMENTS OF HYDROGEN LINES IN KM/SEC.

	$H\gamma$	$H\beta$	$H\alpha$
Emission.....	.....	+ 63	+ 47
Absorption....	−72	−141	−159
Em−Abs.....	.....	+204 (3.3 A)	+206 (4.5 A)

$H\gamma$ appears wholly dark, but is displaced toward the violet, probably by a rudimentary bright line on the red side. The measured displacements of the effective centers of the dark portions of $H\beta$ and $H\gamma$ are found in Table VI. Additional data are given in Table VII.

Both bright and dark components of the Balmer lines are evidently displaced from the normal positions. The dark lines grow relatively stronger in passing from $H\alpha$ to $H\gamma$ and their centers show smaller displacements. The bright line, on the other hand, gives at $H\alpha$ a smaller displacement than at $H\beta$, presumably because the relative intensity of the absorption is less.

The spectrum is notable for the prominence of the lines of *O* II. About twenty are measurable on the best plates, while several, including λλ 4254, 4317, 4319, 4345, 4349, 4366, 4414, 4416, 4639, 4642, and 4650, are conspicuous. The lines of *Si* III also are strong. The spectrum resembles that of χ^2 Orionis, but the *N* II lines are less intense and the *O* II lines slightly more intense.

The measured displacements of the lines of several elements are in Table VI. The lines, while of fair quality for measurement, are not particularly sharp, and the results for individual lines are rather scattering. The radial velocity derived from the lines of *He*, *O* II, and *Si* III is about zero. A few *N* II lines give +13 km/sec., which may agree within error of measurement. The line *Mg* 4481 is weak and the measures unreliable; the mean displacement from six plates is −28 km/sec.

Measurements of the $H\alpha$ line on the grating plates G 360, 379 are in Table VII. The dark helium lines 5876 (D_3) and 6678 are considerably displaced toward the violet. D_3 may have some emission on the red edge. The following lines are probably present: *Al* III 5696.47, 5732.65; *Si* III 5739.62; *N* II 5941.67. There is an unidentified line near λ 5780. The sodium lines D_1 and D_2 are strong and well defined. They give a mean displacement of −7 km/sec., corresponding to a residual velocity (after subtraction of the solar motion) of +7 km/sec., and are probably detached.

This spectrum has several interesting features which would probably repay more detailed study.

H.D. 172694

$H\beta$ and $H\gamma$ are sharply defined absorption lines with emission on the violet edge. Weak emission on the red edge of $H\beta$ may vary in intensity. Changes have not been noted in other features of the spectrum. The helium lines, wholly dark, are strong and well de-

fined. λ 4549 *Fe* is a narrow, weak, dark line. Its presence causes confusion as to the spectral classification. The mean displacements of the principal lines measured are as follows: $H\gamma$, +40 km/sec.; λ 4471 *He*, +57; λ 4549 *Fe*, +58; $H\beta$, +58. The agreement of the last three is very close, although the individual values have considerable spread. The systematic relative displacement of $H\gamma$ does

TABLE VIII

SPECTROGRAMS OF H.D. 172694

Plate	Date	Rad. Vel.
		km/sec.
γ 10358	1921 Aug. 14	+49
γ 11922	1922 July 3	62
γ 12692	1924 May 25	54
C 3347	1925 June 15	+60
Mean		+56.1

not have an obvious explanation. Measurements of $H\gamma$ were given half-weight in computing the apparent radial velocities in Table VIII. If these results correspond to the actual radial motion, then the residual velocity, +70 km/sec., is abnormally high for a B-type star.

H.D. 180398

TABLE IX

SPECTROGRAMS OF H.D. 180398

Plate	Date
C 1319	1921 Sept. 18
C 2890	1924 July 19
C 4417	1927 Sept. 9

$H\gamma$, $H\delta$, and $H\epsilon$ are broad, ill-defined absorption lines. $H\beta$ is complex with weak emission superposed on a hazy, dark line. The emission is most distinct on the first plate; on the second it is very weak but clearly double; while on the last plate its presence is doubtful. The helium lines, wholly dark, are faint and diffuse.

An objective-prism plate taken September 5, 1921, shows the bright $H\alpha$ line much more distinctly than others taken July 6 and 28, 1927.

The bright lines probably decreased in intensity from 1921 to 1927.

H.D. 183143

On the Mount Wilson spectrograms the dark hydrogen, helium, and silicon lines are generally strong and narrow; *Hβ*, however, is abnormally weak, and on plate C 4482 scarcely visible, probably

TABLE X

SPECTROGRAMS OF H.D. 183143

Plate	Date	Rad. Vel.	Remarks
		km/sec.	
C 1320.....	1921 Sept. 18	+12.3	
C 1932.....	1922 Oct. 7	.....	Red region
C 1940.....	Oct. 8	.....	Red region
γ 11389.....	Oct. 10	14.4	
C 2420.....	1923 Sept. 1	.....	Red region
γ 12821.....	1924 July 21	13.4	
C 4482.....	1927 Oct. 14	6.8	
C 4848.....	1928 June 18	.....	Includes red region
G 366.....	1930 Apr. 17	14.1	
G 375.....	Apr. 18	+16.1	
Mean....	.....	+12.8	.....

because the absorption is nearly balanced by emission. *Hα* is a bright line of low intensity. λ 4471 and λ 4481 form a pair of unusually well-defined lines. The spectrum must have been quite different on the plates used for the Harvard classification, as the *Henry Draper Catalogue* states: "The spectrum appears to be nearly continuous."

On the grating plates *Hα* is seen in emission. The following lines are dark: *He* 5876, 6678; *Si* II 6347, 6371; *Na* 5890, 5896, together with several unidentified lines of which the following are the most important: 5780, 5796, 5944, 6283, 6613. The first of these is near the silicon line 5780.38, but this line is of low intensity in the laboratory and has been ascribed by Fowler[1] to the spectrum of the neutral atom; hence its identification with the stellar line is improbable. Several atmospheric lines are known near λ 6283, but these do not seem sufficiently intense or in quite the right positions to account for the line in the spectrum of H.D. 183143. The identifi-

[1] *Philosophical Transactions of the Royal Society*, A, **225**, 41, 1926.

cations of these lines will be further studied when additional data become available.

The radial velocity exhibits no large variation from its mean value +12.8 km/sec. The largest residual is given by plate C 4482, but this does not clearly exceed errors of measurement. As far as present data go, therefore, we may consider the velocity constant.

The sodium lines, which are strong and well defined, give a mean velocity of +3.4 km/sec. The correction for solar motion is +18.4 km/sec., giving a residual velocity of +21.8, which is high for detached lines. The lines are abnormally strong for the spectral type of the star, however, and may be blends of stellar and detached lines. The H and K lines of calcium are also strong. Their displacement, measured on plate C 4482, is −11 km/sec., but this determination unfortunately has low weight. These lines require further observation.

This star is abnormally red for one of class B9. Viewed on the reflecting slit of the spectrograph, it has an orange tinge like a K-type star. Miss Burwell has carefully compared its spectrum with others of various types on several objective-prism plates taken with the 10-inch telescope from 1920 to 1927. She finds that the ratio of the intensity of red light to that of the blue-violet light is very nearly the same as for the spectra of Ko stars. The color-curve, however, does not appear quite identical with that of a Ko star, but may be slightly higher in the green and the ultra-violet. The color index determined on July 3 and 4, 1930, by Dr. B. W. Sitterly with the 10-inch telescope is +1.3 (international system). This is approximately the value for a giant G7 star.[1]

Several features of this spectrum are very interesting and merit further investigation.

H.D. 195407

$H\beta$ is a bright line with a narrow central minimum. At $H\gamma$ the bright portions are fainter than at $H\beta$, and the dark center is stronger; it would more naturally be described as an absorption line with bright borders. At $H\delta$ the bright borders are not seen. On the first plate the bright portions of $H\beta$ and $H\gamma$ are stronger and the dark centers weaker than on the 1924 plates, among which slight varia-

[1] Seares, *Mt. Wilson Contr.*, No. 226; *Astrophysical Journal*, 55, 165, 1922.

tions probably occur. The behavior may be somewhat similar to that of ϕ Persei. The average separation of the bright components of $H\gamma$ is 3.1 A, of $H\beta$ 4.0 A. The spectral type is not well defined and may vary.

TABLE XI

SPECTROGRAMS OF H.D. 195407

Plate	Date	Rad. Vel.
		km/sec.
C 1327	1921 Sept. 19	−68
γ 12596	1924 Apr. 21	82
γ 12688	May 24	(Underexposed)
γ 12726	June 15	82
C 3072	Nov. 8	−66
Mean		−74

The radial velocities depend largely on the hydrogen lines, but the lines of helium and iron, although very weak and seldom measured, appear to yield approximately the same results. The residual velocity, −57 km/sec., is high for a B-type star. Detached H and K, measured on plate C 3072, give the velocity −15 km/sec., corresponding to the small residual velocity +2 km/sec.

H.D. 218393

Hα was suspected to be bright on an objective-prism spectrogram taken with the 10-inch telescope on November 18, 1920, by Mr. Milton Humason.

The following remark occurs in the *Henry Draper Catalogue:* "The lines are very narrow, and the intensities resemble those in the spectrum of α Cygni, H.D. 197345."

On the Mount Wilson spectrograms the hydrogen lines are variable in structure and intensity. *Hγ* is chiefly a dark line, but on a few plates it has a distinctly bright edge toward the red. *Hβ* consists of a broad, hazy, dark line with a double bright line of moderate intensity centrally superposed. The relative intensities of the two bright components change considerably. Their average separation is 3.92 A. On the grating plates G 21 and G 273, *Hα* is a very intense emission line with a narrow, nearly central, reversal.

The similarity to α Cygni noted by Miss Cannon is exhibited by

certain Mount Wilson plates, particularly γ 11288 and γ 13157, more strongly than by others. On these plates the α Cygni lines are conspicuous, while on γ 12988 they are but faintly visible.

The measured displacements of the absorption lines of various elements are given in Table XII. Most of the lines are not sharply defined, and the accuracy of measurement is not great. The helium velocities depend largely on λ 4471. *Si* II lines at λ 4128 and λ 4131, measured on four plates, give a mean displacement of +61 km/sec. Three *Ti* II lines on plate γ 13157 give +72 km/sec.; one line on

TABLE XII

SPECTROGRAMS OF H.D. 218393

PLATE	DATE	DISPLACEMENTS IN KM/SEC.			
		H	*He*	*Mg* 4481	*Fe* II
γ 11288	1922 Sept. 1	(+22)	−74	+66	+51
γ 11312	Sept. 27	−13	+ 1	+25	+38
γ 11961	1923 July 25	−18	+21	+11	.....
γ 12965	1924 Sept. 15	− 3	− 5	+26	+27
G 21	Oct. 3	.....	.....	.....	.....
γ 12988	Oct. 7	−26	−34	+15	−32
γ 13095	Nov. 11	−11	−32	−56	−27
γ 13157	1925 Jan. 4	+21	−62	+54	+71
C 3348	June 15	−29	−44	+ 3	(−33)
G 273	1929 Oct. 10	.....	.....	.....	.....

plate C 3348 gives −40. In general the results appear scattering and difficult to interpret. Rather large errors of measurement are doubtless present, but the more outstanding discrepancies must be due to actual changes in the effective displacements of the lines. Comparison of the data of Table XII with the intensities of the α Cygni lines suggests that when these lines are strong they have large positive displacements, while the helium lines have negative displacements.

The very strong K line, measured on plate C 3348, gives a displacement of −20 km/sec. The strong D lines on the grating plates give a mean displacement of −27 km/sec. These lines may or may not be detached. We hope to make later a more complete investigation of several features of this spectrum.

CARNEGIE INSTITUTION OF WASHINGTON
MOUNT WILSON OBSERVATORY
June 1930

Contributions from the Mount Wilson Observatory, No. 410
Reprinted from the *Astrophysical Journal*, Vol. LXXII, pp. 111–116, 1930
Printed in the U.S.A.

UNIVERSITY OF ARIZONA
STEWARD OBSERVATORY
TUCSON, ARIZONA

A METHOD FOR DETERMINING THE DISTRIBUTION OF STELLAR ABSOLUTE MAGNITUDES FROM THE DISTRIBUTIONS OF PARALLACTIC MOTIONS AND RADIAL VELOCITIES

By GUSTAF STRÖMBERG

ABSTRACT

The paper outlines a method for deriving the distribution of absolute magnitudes within a group of stars from the distributions of the reduced v-components of proper motions and of the radial velocities. The method is similar to that developed in *Contribution* No. 395, which was based on the distribution of τ-components.

Mount Wilson Contribution No. 395[1] outlines a method for determining the distribution of stellar absolute magnitudes from the distributions of reduced τ-components and radial velocities. A similar method has now been developed for the parallactic motions and is described in the following pages.

The proper motion of a star projected on a great circle passing through the star and the antapex, counted positive toward the antapex, is the parallactic motion or the v-component of the proper motion. It is expressed in seconds of arc per year and may be regarded as the sum of two angular velocities: a component due to the reflection of the sun's motion relative to the group of stars studied and the component of the peculiar velocity in the direction of the antapex. If the distance R to the star is known, we can convert the angular motion into a linear velocity. The relation

$$kRv = V_0 \sin \lambda + \epsilon \qquad (1)$$

then holds. In this equation v is the v-component, V_0 the sun's velocity relative to the group—which is numerically the same as the group motion relative to the sun; λ is the angular distance from the sun's apex, ϵ the linear peculiar tangential velocity in the direction of the v-component, and k a constant depending on the units

[1] *Astrophysical Journal*, **71**, 163, 1930.

employed. If R is expressed in parsecs and the linear velocities in km/sec.,

$$k = 4.738 \text{ km year/sec.} \tag{2}$$

The absolute magnitude M, the apparent magnitude m, and the distance R are connected by the relation

$$M = m + 5 - 5 \log R , \tag{3}$$

where M is defined as the apparent magnitude at a distance of 10 parsecs. Eliminating R between equations (1) and (3), we find

$$10 k v 10^{0.2(m-M)} = V_0 \sin \lambda + \epsilon = \mu_1 . \tag{4}$$

In this equation v, m, and λ are known for the individual stars. From the radial velocities we can determine the group motion V_0 and the distribution of peculiar radial velocities V', which, under certain conditions, are statistically comparable with the velocities ϵ.

Before proceeding farther we must consider existing correlations. There is a strong correlation between v and μ_1, between M and ϵ (correlation between absolute magnitude and average velocity), between V_0 and ϵ (correlation between solar motion and velocity dispersion due to the asymmetry in the velocity distribution), and between ϵ and λ (since the peculiar velocity of a star is a function of the direction of motion), besides indirect correlations arising from those just mentioned.

If the stars are so numerous that within the spectral range studied they may be subdivided according to M—by means of a criterion which need not be accurate—and also according to $\sin \lambda$, we may simply take the logarithms of both sides of equation (4) and, writing

$$\left.\begin{aligned} x &= \log v + 0.2m = \log v' , \\ y &= \log \mu_1 - \log k - 1 , \\ M' &= 0.2M , \end{aligned}\right\} \tag{5}$$

obtain the fundamental equation

$$x = M' + y , \tag{6}$$

where M' and y may be regarded as independent since the range in M is limited.

These formulae are very similar to those used in *Contribution* No. 395, but there are some important differences. One is that the distributions of positive and negative v and μ_I, respectively, are not similar, as are those of positive and negative τ and V', respectively. The number of negative values of v and μ_I is, of course, in general smaller than the number of positive values. But a positive or negative value of v must correspond to a positive or negative value, respectively, of μ_I, whatever the distance or absolute magnitude of the star.

We might discuss the positive and negative values separately, but usually the number of stars in the group studied is too small for a separate analysis of the negative values. Instead, positive and negative values have been grouped together, which means that all have been regarded as positive. This is permissible since the numerical change in μ_I with change in M is the same for positive and negative parallactic motions. The distributions used are therefore superpositions of the distributions of positive and negative parallactic motions.

In limiting ourselves to the two zones for which sin λ has the same value, we must also limit the radial velocities used to determine the distribution of ϵ to two corresponding zones. The direction of the tangential linear velocity ϵ in equation (4) is the same as that of the peculiar radial velocity V' for a star situated 90° from the proper-motion star and on the same great circle, apex—star—antapex. Hence, deriving the distribution of y, we use the distribution of radial velocities for stars in two zones, one of which has an angular distance from the apex of λ plus or minus 90°, according as λ is smaller or larger than 90°, while the other is at the same distance from the antapex.

When the distribution of ϵ has been found, we can easily derive numerically the distribution of $\log |V_0 \sin \lambda + \epsilon|$ and of y, the vertical bars here and in the following indicating that the signs are disregarded. The method for combining several independent distributions is given in *Contribution* No. 395.

In most cases, however, the stars are not numerous enough for a subdivision according to both M and sin λ. We then combine stars of different values of sin λ; but since λ is known for each star, we can

reduce the dispersion in x by dividing with sin λ. We thus find from equation (4)

$$\frac{10kv10^{0.2m}10^{-0.2M}}{\sin\lambda}=V_0+\frac{\epsilon}{\sin\lambda}=\mu_2\,. \tag{7}$$

It is clear that small values of sin λ cannot be used; sin $\lambda>0.5$, that is, $30^\circ<\lambda<120^\circ$, has been found to be a practical limit. This excludes stars around the apex and antapex, but the areas involved are together only 13 per cent of the whole sky.

Taking the logarithms of both sides of equation (7) and introducing the new variables,

$$\left.\begin{aligned} x&=\log|v|+0.2m-\log\sin\lambda\,,\\ y&=\log|\mu_2|-\log k-1\,,\\ M'&=0.2M\,,\end{aligned}\right\} \tag{8}$$

we have as before

$$x=M'+y\,. \tag{9}$$

The method for determining the distribution of y depends on whether or not there is an appreciable correlation between ϵ and sin λ. The distribution of $\epsilon/\sin\lambda$ is statistically equivalent to that of $V'/\cos\lambda_1$, where λ_1 is the distance of a radial-velocity star from the apex, the signs of V' and of cos λ_1 being disregarded. We have here also to exclude stars for which cos λ is small; and if we limit ourselves to stars for which cos λ_1 is numerically larger than 0.5, we utilize only half of the sky. A somewhat smaller limit is thus advisable.

If the correlation between ϵ and sin λ is inappreciable, we may derive separately the distribution of $\epsilon=V'$ and of sin λ; and to find the distribution of y we combine numerically the two probabilities and use the value of V_0 for the particular range in absolute magnitude.

The correlation between $|\epsilon|$ and sin λ for the proper-motion stars is the same as that between $|V'|$ and $|\cos\lambda|$ for the radial-velocity stars. A glance at the scatter diagram will often tell if any appreciable correlation exists.

If no correlation between $|V'|$ and $|\cos\lambda|$ exists, we may simply

form the distribution of V' from all the radial-velocity stars within the spectral range, and also derive the group motion V_0 and the average radial velocity θ for different groups of absolute magnitude. The combined distribution of V' can then be adjusted to conform to the different values of θ by assuming that the corrections to the distribution of V' are the same as those of a normal error distribution when the dispersion is varied.

The following formula is easily derived:

$$\frac{dF(\epsilon)}{F(\epsilon)} = \left(\frac{\epsilon^2}{\sigma^2} - 1\right)\frac{d\sigma}{\sigma}, \tag{10}$$

where σ is the dispersion in the error function.

Complete equivalence between the distributions of V' and ϵ is difficult to realize, in particular when the stars have a strong galactic concentration. If this concentration is very great, the equivalence may be good as far as motion parallel to the galaxy is concerned; but we cannot directly determine the distribution of radial velocities which would correspond to angular motions perpendicular to the galactic circle, since the number of stars at the pole of the galaxy is insufficient for this purpose.

The method for finding the logarithmic distribution for very small values of the variables is given in *Contribution* No. 395 for the case of a distribution which is constant in the neighborhood of zero. In the present case the distribution is not constant near zero, but it can be shown that the formula given also holds for a linear variation in the neighborhood of zero values. For any variable z we therefore assume

$$F(z)dz = k(a_0 + a_1 z)dz \quad (-\delta < z < \delta). \tag{11}$$

Denote the number of z-values numerically less than δ by n, and we find

$$k = \frac{n}{2a_0\delta}.$$

Thus

$$F(z)dz = \frac{n}{2\delta}\left(1 + \frac{a_1}{a_0} z\right)dz.$$

Integration between $-z$ and $+z$, z being numerically less than δ, gives

$$\int_{-z}^{+z} F(z)dz = \frac{nz}{\delta}.$$

Regarding now all z's as positive and defining a new variable y by the equation

$$y = \log |z| + a_2,$$

we find the relation

$$\int_{-\infty}^{y} F(y)dy = \frac{n}{\delta} 10^{y-a_2}, \tag{12}$$

which is valid for $y < \log \delta + a_2$.

The derivation of the distribution of M' is made in exactly the same way as for the τ-components. An approximate distribution of M' is assumed and combined with the distribution of y to form an expected distribution of x. From the differences between the observed and expected distribution of x, corrections to $F(M')$ are derived by a least-squares solution. The process is repeated until a satisfactory reproduction of $F(x)dx$ is obtained.

Carnegie Institution of Washington
Mount Wilson Observatory
July 1930

Contributions from the Mount Wilson Observatory, No. 411
Reprinted from the *Astrophysical Journal*, Vol. LXXII, pp. 117–126, 1930
Printed in the U.S.A.

THE DISTRIBUTION OF ABSOLUTE MAGNITUDES AMONG M STARS BRIGHTER THAN THE SIXTH APPARENT MAGNITUDE AS DETERMINED FROM PARALLACTIC AND PECULIAR VELOCITIES

By GUSTAF STRÖMBERG

ABSTRACT

1. The distribution of absolute magnitudes among M stars brighter than the sixth apparent magnitude has been determined from the distributions of parallactic and peculiar reduced proper motions and the distribution of radial velocities. The methods used are described in *Mount Wilson Contributions* Nos. 395 and 410. The number of proper-motion stars used is 247, and of radial-velocity stars 292.

2. The distribution of absolute magnitudes shows two distinct groups: supergiants with a maximum frequency at absolute magnitude −4.5 and ordinary giants around magnitude zero. The groups are separated by a clear gap around absolute magnitude −3.0. The relative proportions of stars in the two groups are 9 and 91 per cent, respectively.

3. Numerical values are given which will enable one to compute the mean absolute magnitude from the mean apparent magnitude and the mean of the logarithms of the τ- or v-components.

Mount Wilson Contribution No. 395[1] describes a method for determining the distribution of absolute magnitudes from the distribution of angular and linear peculiar velocities. In *Contribution* No. 396[2] the method was applied to the K and M stars brighter than the sixth apparent magnitude. *Contribution* No. 410[3] gives a similar method for the parallactic motions. This method, however, is somewhat more complicated, since both angular and linear parallactic motions depend on the position of the star and the computation is affected by the existence of several correlations. The method for parallactic motions has also been applied to the M stars brighter than the sixth apparent magnitude, and the results of an analysis of both the parallactic and the peculiar motions are given in this paper.

All stars in the *H.D. Catalogue* classified as M type and brighter than the sixth apparent magnitude were included in the study. To these were added some stars classified as M type by the Mount

[1] *Astrophysical Journal*, **71**, 163, 1930.

[2] *Ibid.*, p. 175, 1930.

[3] *Ibid.*, **72**, 111, 1930.

Wilson observers. The list of radial velocities includes some stars down to the seventh apparent magnitude, but since these stars were not selected on the basis of large proper motion, their radial velocities can still be regarded as representative for the group studied, particularly since the effect of absolute magnitude is separately determined.

The proper motions were taken from Boss's *Catalogue*. H. Raymond's[1] corrections to the proper motions in declination have been applied. The v- and τ-components were computed from the equations

$$\left.\begin{aligned} v &= \gamma_1\mu_1+\gamma_2\mu_2 , \\ \tau &= \gamma_1\mu_2-\gamma_2\mu_1 , \\ \gamma_1 &= \frac{A}{\sqrt{A^2+B^2}} ; \qquad \gamma_2 = \frac{B}{\sqrt{A^2+B^2}} , \\ A &= x_0 \sin\alpha - y_0 \cos\alpha , \\ B &= x_0 \cos\alpha \sin\delta + y_0 \sin\alpha \sin\delta - z_0 \cos\delta . \end{aligned}\right\} \qquad (1)$$

The proper motions in right ascension (great circle projection) and declination are here denoted by μ_1 and μ_2, respectively; x_0 and y_0 are proportional to the components of the solar motion in the equatorial system of co-ordinates. A constant apex of $\alpha = 270°$, $\delta = +30°$ is assumed throughout. That this apex may not be the best obtainable for the stars studied and may vary for the different absolute magnitudes, is of no importance as long as we use the same apex for both proper motions and radial velocities. The number of proper-motion stars used was 247; and for each of these the quantity $x_1 = \log|\tau| + 0.2m$ was computed, in which the vertical bars indicate that the signs are disregarded. After rejecting the stars within 30° of the apex and the antapex, 210 stars remained, for which the quantity $x_2 = \log|v| + 0.2m - \log\sin\lambda$ was derived, λ being the angular distance from the apex. The distributions of x_1 and x_2 were then derived, the interval used being 0.1. All values of x_1 and x_2 less than -1.7 were combined in one group and then redistributed according to the method described in *Contributions* Nos. 395 and 410. Apart from their effect on the smallest values of τ and v, the accidental errors have an entirely negligible influence on the distributions.

[1] *Astronomical Journal*, 36, 129, 1926.

The radial-velocity stars used were 292 in number. For 250 of these, spectroscopic absolute magnitudes were available. The stars were collected in four groups according to the spectroscopic absolute magnitude. Table I shows the group motion V_0 and the average residual velocity θ. The increase in group motion with absolute magnitude is noticeable, but not large, as is also the increase in θ with M, although the supergiants seem to have abnormally large peculiar velocities.

The next step was to find if any correlation exists between ϵ (linear peculiar tangential motion) and sin λ. This correlation is the same as that between $|V'|$ (peculiar radial velocity without regard to sign) and $|\cos \lambda|$. A scatter diagram for the latter quantities showed no appreciable correlation; in fact, the value of θ for $|\cos \lambda| > 0.5$ is 17.8 km/sec., and for $|\cos \lambda| < 0.5$, θ is 17.6 km/sec. It was

TABLE I

M Spec.	No.	V_0	θ
		km/sec.	km/sec.
$\leqq -0.6$	41	20.1	17.4
−0.5 to −0.3	41	21.0	16.3
− .2 to 0.0	102	23.3	17.6
+0.1 to +0.6	66	23.2	20.6

therefore possible to derive the distribution of $y = \log |V_0 + \epsilon' \sin \lambda| - 1.6756$ from the distributions of ϵ and of sin λ. Estimates of absolute magnitude based on spectroscopic determinations and reduced total proper motion were made for each star, and appropriate values of V_0 were used to derive the peculiar radial velocities V'. The combined distribution of V' for all the M stars together was determined. Small corrections to this distribution based on the values for θ in Table I were then derived to represent the velocity distribution for the different absolute-magnitude groups. Four distributions of V' were thus found which were supposed to be identical with those for ϵ. Finally, the distributions of y were derived by combining the probabilities of ϵ with those of sin λ, with the aid of appropriate values of V_0 for the four groups of absolute magnitude.

The second and fifth columns of Table II give the results for the observed distributions of x_1 and x_2, respectively, reduced to a total

TABLE II

x	$F(x_1)dx$		O−C	$F(x_2)dx$		O−C
	Obs. Dist.	Comp. Dist.		Obs. Dist.	Comp. Dist.	
−4.0	0	0.1	− 0.1	0	0.0	0.0
−3.9	0	0.2	− 0.2	0	0.0	0.0
−3.8	0	0.2	− 0.2	0	0.1	− 0.1
−3.7	1	0.3	+ 0.7	1	0.1	+ 0.9
−3.6	0	0.3	− 0.3	0	0.1	− 0.1
−3.5	0	0.3	− 0.3	0	0.1	− 0.1
−3.4	0	0.3	− 0.3	0	0.3	− 0.3
−3.3	0	0.3	− 0.3	1	0.3	+ 0.7
−3.2	1	0.5	+ 0.5	0	0.4	− 0.4
−3.1	0	0.8	− 0.8	0	0.5	− 0.5
−3.0	1	1.0	0.0	1	0.5	+ 0.5
−2.9	1	1.0	0.0	1	0.5	+ 0.5
−2.8	1	1.3	− 0.3	1	0.8	+ 0.2
−2.7	1	1.8	− 0.8	1	1.1	− 0.1
−2.6	1	2.2	− 1.2	2	1.3	+ 0.7
−2.5	2	2.7	− 0.7	2	1.6	+ 0.4
−2.4	2	3.5	− 1.5	2	2.0	0.0
−2.3	3	4.5	− 1.5	3	2.3	+ 0.7
−2.2	4	5.5	− 1.5	4	3.1	+ 0.9
−2.1	4	6.9	− 2.9	5	3.8	+ 1.2
−2.0	6	8.5	− 2.5	6	4.8	+ 1.2
−1.9	8	10.5	− 2.5	8	6.0	+ 2.0
−1.8	9	12.9	− 3.9	10	7.6	+ 2.4
−1.7	16	16.2	− 0.2	29	10.0	+19.0
−1.6	32	20.3	+11.7	2	13.1	−11.1
−1.5	26	25.0	+ 1.0	21	16.6	+ 4.4
−1.4	14	30.1	−16.1	21	20.3	+ 0.7
−1.3	43	35.6	+ 7.4	31	24.6	+ 6.4
−1.2	37	41.1	− 4.1	19	29.5	−10.5
−1.1	61	46.5	+14.5	40	35.1	+ 4.9
−1.0	39	52.0	−13.0	43	40.8	+ 2.2
−0.9	87	58.5	+28.5	36	45.4	− 9.4
−0.8	69	67.6	+ 1.4	50	51.2	− 1.2
−0.7	117	76.4	+40.6	48	60.1	−12.1
−0.6	77	82.4	− 5.4	52	69.9	−17.9
−0.5	43	84.5	−41.5	79	79.6	− 0.6
−0.4	79	80.0	− 1.0	95	87.1	+ 7.9
−0.3	79	69.3	+ 9.7	79	88.1	− 9.1
−0.2	49	55.6	− 6.6	74	81.7	− 7.7
−0.1	37	41.6	− 4.6	95	70.8	+24.2
0.0	34	26.7	+ 7.3	43	57.1	−14.1
+0.1	8	14.8	− 6.8	67	40.5	+26.5
+0.2	4	6.5	− 2.5	19	23.7	− 4.7
+0.3	0	2.4	− 2.4	9	11.3	− 2.3
+0.4	4	0.9	+ 3.1	0	4.3	− 4.3
+0.5	0	0.2	− 0.2	0	1.4	− 1.4
+0.6	0	0.1	− 0.1	0	0.4	− 0.4
+0.7	0	0.0	0.0	0	0.1	− 0.1
+0.8						

of 1000 stars. No smoothing has been done except, of course, below the limit -1.7. The computed distributions of x_1 and x_2 are given in the third and sixth columns, respectively. These were derived from the last approximation for the distribution of absolute magnitude, which appears in Table IV, combined with the distribution of

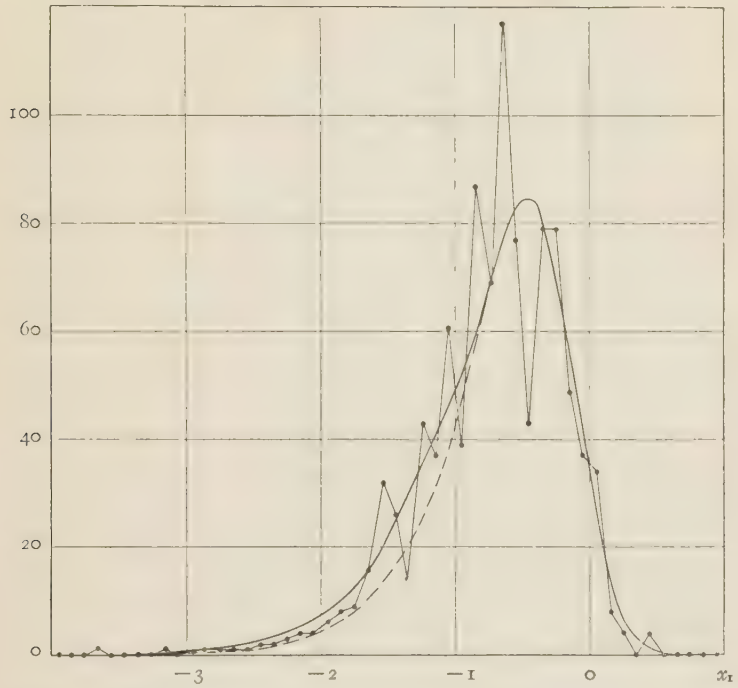

FIG. 1.—Distribution of $x_1 = \log \tau + 0.2m$ for stars of spectral type M. The dots joined by straight lines represent observed numbers within intervals $dx = 0.1$. For $x < -1.7$ the dots are not independent observations, but indicate the probable extension of the distribution-curve. The smooth full-drawn curve is computed from the distributions of absolute magnitudes and peculiar velocities. The dotted curve shows the distribution when the supergiants are excluded.

y in Table III. The fourth and the last columns of Table II show the difference between observed and computed distributions. The computed distribution-curves are shown in Figures 1 and 2 as continuous curves, observed values being indicated by dots connected by straight lines.

Table III shows the distribution of $y_1 = \log |V'| - 1.6756$ and

of $y_2 = \log |V_0 + \epsilon/\sin \lambda| - 1.6756$. These distributions have been smoothed graphically and are reduced to a total of 1000 stars. The absolute magnitudes at which the transition from one distribution to the next occurs are given at the top between the columns.

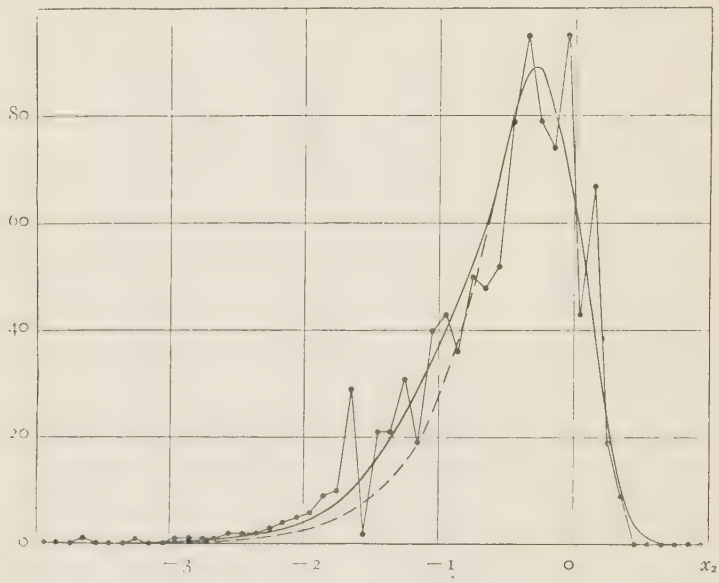

FIG. 2.—Distribution of $x_2 = \log v + 0.2m - \log \sin \lambda$ for stars of spectral type M. Similar to Fig. 1, but the computed curve is based on a combination of group motions and peculiar velocities.

At the bottom of Table III are given the mean values of y_1 and y_2 for the different absolute magnitude groups. These may be used for computing mean absolute magnitudes when the mean of the logarithms of the τ- or v-components is given. The following formulae then hold:

$$M = 5 \overline{\log \tau} + \bar{m} - 5\, \bar{y}_1$$
$$M = 5 \overline{\log v} + \bar{m} - 5 \overline{\log \sin \lambda} - 5\, \bar{y}_2$$

The formulae for parallactic motions can be used only if the stars are well distributed over the sky, since this assumption is involved in the derivation of y_2.

TABLE III

y	$F(y_1)dy$				$F(y_2)dy$			
	−3.0	−1.2	−0.2		−3.0	−1.2	−0.2	
−3.6	1	1	1	1	0	0	0	0
−3.5	0	0	0	0	0	0	0	0
−3.4	0	0	0	0	0	0	0	0
−3.3	0	0	0	0	0	0	0	0
−3.2	0	1	0	0	0	1	1	1
−3.1	1	0	1	1	1	0	0	0
−3.0	0	0	0	0	0	0	0	0
−2.9	1	1	1	0	0	1	1	1
−2.8	1	1	1	1	1	0	0	0
−2.7	1	1	1	1	0	0	0	1
−2.6	1	1	1	1	1	1	1	1
−2.5	1	1	1	1	1	1	1	1
−2.4	2	2	2	2	1	1	1	1
−2.3	2	3	2	2	1	1	1	1
−2.2	3	3	3	2	2	2	2	2
−2.1	4	4	4	3	2	2	2	2
−2.0	5	5	5	4	2	2	3	3
−1.9	6	6	6	5	3	3	3	3
−1.8	7	8	7	6	4	4	4	4
−1.7	9	10	9	8	5	5	5	5
−1.6	12	12	11	10	6	6	7	7
−1.5	15	15	15	13	8	8	9	8
−1.4	19	19	18	15	9	10	11	10
−1.3	23	25	23	20	12	12	14	13
−1.2	29	31	29	25	15	16	17	17
−1.1	36	39	36	31	19	20	22	21
−1.0	44	48	45	38	24	25	27	26
−0.9	53	56	55	47	31	31	33	33
−0.8	63	67	65	57	39	41	40	40
−0.7	76	80	76	67	57	60	49	50
−0.6	93	92	93	82	76	71	62	59
−0.5	106	109	106	98	91	82	77	72
−0.4	111	112	111	109	103	102	93	86
−0.3	108	101	105	110	111	118	110	97
−0.2	86	79	83	100	117	121	117	107
−0.1	51	45	50	75	116	111	113	110
0.0	19	14	20	38	76	86	90	104
+0.1	7	5	10	21	44	38	54	70
+0.2	3	2	2	3	16	13	21	30
+0.3	1	1	1	2	5	4	6	10
+0.4	0	0	1	1	1	1	2	3
+0.5	0	0	0	0	0	0	1	1
+0.6								
$\bar{y}$	−0.618	−0.643	−0.617	−0.547	−0.402	−0.407	−0.396	−0.374

TABLE IV

M	$F(M)dM$	M	$F(M)dM$	M	$F(M)dM$
−5.6	1	−3.0	0	−0.4	79
−5.4	4	−2.8	0	−0.2	80
−5.2	8	−2.6	0	0.0	79
−5.0	11	−2.4	2	+0.2	73
−4.8	13	−2.2	8	+0.4	62
−4.6	14	−2.0	18	+0.6	40
−4.4	14	−1.8	32	+0.8	22
−4.2	13	−1.6	44	+1.0	14
−4.0	10	−1.4	53	+1.2	8
−3.8	4	−1.2	63	+1.4	4
−3.6	0	−1.0	72	+1.6	1
−3.4	0	−0.8	76	+1.8	
−3.2	0	−0.6	78		
−3.0		−0.4			

For values of τ or υ smaller than a certain limit δ (e.g., $\delta = 0''.01$), the observed values should be replaced by means based on a uniform or linear distribution around zero values. Russell[1] has proved that for a uniform distribution we can then replace each of the small values by $\delta : e$, where e is the base of the natural logarithms. It is easily shown that the same formula holds for a linear distribution in the neighborhood of zero values, when all numbers are regarded as positive.

Table IV gives the final distribution of absolute magnitudes. This distribution was found by a simultaneous least-squares solution from equations of condition based on both τ- and υ-components. The differences $M_2' - M_1'$, $M_3' - M_2'$ were taken equal to 0.4; that is, the interval in M was 2 mag. Four solutions with a shift of 0.1 in x and y were made simultaneously, with the result that the determination of $F(M)dM$ gave values for an interval of 0.5 mag. A curve drawn through the points representing the calculated frequencies is shown in Figure 3, and the final distribution with an interval of 0.2 mag. was derived from this curve.

The distribution of absolute magnitudes shown in Table IV and Figure 3 is of great interest. It indicates a clear division into two groups: supergiants with a mean absolute magnitude of −4.5 and ordinary giants with a mean absolute magnitude of about zero. The

[1] *Publications of the Astronomical Society of the Pacific*, **32**, 243, 1920.

relative proportion of stars in the two groups is 9 and 91 per cent, respectively. The groups are separated by a clear gap extending from -2.5 to -3.5 mag.

A comparison of the new absolute-magnitude curve with that derived from the τ-components alone and published in *Contribution* No. 396[1] shows a marked difference. The earlier curve of absolute magnitude has two maxima, one at -1.6 and the other at -0.1 mag. The reason for this discrepancy is immediately seen from Fig-

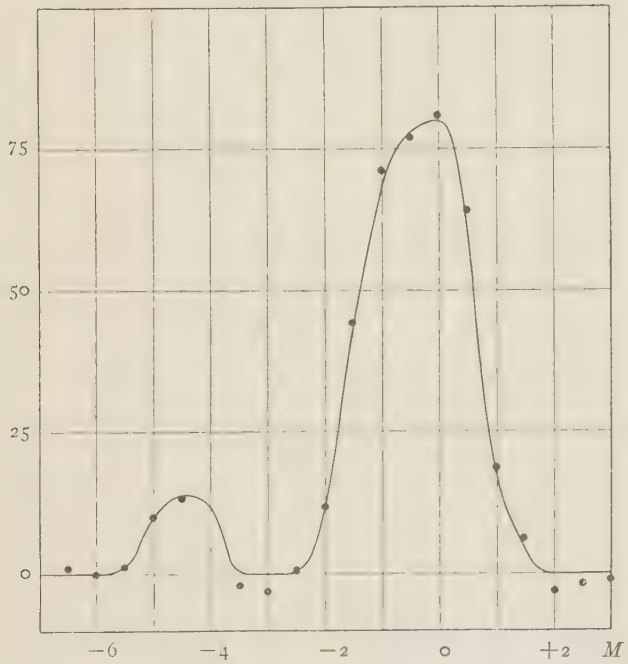

FIG. 3.—Distribution of absolute magnitudes for stars of spectral class M. The points are computed from the distribution of reduced τ- and v-components. Note the two frequency maxima.

ures 1 and 2 of the present paper. The observed distribution of reduced τ-components in Figure 1 shows a large drop at $x = -0.65$ to $x = -0.45$ and a subsequent rise to a new maximum at $x = -0.3$. These two maxima in $F(x)dx$ are responsible for the two maxima in

[1] *Astrophysical Journal*, **71**, 175, 1930.

$F(M)dM$. No such maxima appear in the distribution of the v-components, consequently they cannot be due to a minimum in the absolute-magnitude curve at -0.9 mag.

The reproduction of the distribution-curves of the τ- and v-components is, of course, not so good as that of the τ-components alone in the preceding study. The computed curve now lies above the observed distribution of τ-components for $x < -1.7$, and below the observed distribution of v-components in the same region. It is to be noted that the observed values of $F(x)dx$ for $x < -1.7$ are not independent of one another as are the values of $x > -1.7$.

In order to see more easily the effect of the supergiants on the distribution of τ- and v-components, I have indicated by a dotted smooth curve in Figures 1 and 2 the values of $F(x)dx$ after the supergiants have been subtracted.

The present results are in good agreement with the spectroscopic absolute magnitudes, except that the gap separating the supergiants from the giants does not show in the spectroscopic data. I have shown[1] that the accidental error in the spectroscopic absolute magnitudes for the supergiant M stars is much larger than for the ordinary giants, and the extra dispersion may well obliterate the gap in the luminosity-curve. The present value for the absolute magnitude of the supergiants is somewhat brighter than that given for the spectroscopically determined supergiants, but the difference is quite within the uncertainties of both determinations. It is quite possible that the true value of the average radial velocity θ for the supergiants is somewhat smaller than the adopted value of 17.4 km/sec. If so, the true mean absolute magnitude for these stars may be as much as half a magnitude fainter than the value -4.5 here given.

Carnegie Institution of Washington
Mount Wilson Observatory
July 1930

[1] *Mt. Wilson Contr.*, No. 327; *Astrophysical Journal*, 65, 108, 1927.

Contributions from the Mount Wilson Observatory, No. 412
Printed in the U.S.A.

ARIZONA

INVESTIGATIONS ON PROPER MOTION

SEVENTEENTH PAPER: PROPER MOTIONS OF SOME VERY FAINT STARS

By ADRIAAN VAN MAANEN AND HOWARD C. WILLIS

ABSTRACT

Proper motions of faint stars.—Forty-two of the Selected Areas, including about 60,000 stars, were examined with the blink arrangement of the stereocomparator on plates taken at an interval of about eighteen years; 122 stars ranging in magnitude from 6.68 to 20 were found to have proper motions between 0″.041 and 0″.925. The percentage of stars having a considerable motion increases from 0.07 for galactic regions to 1.02 for high galactic latitudes. The amount of the mean motion for the fainter stars decreases with magnitude, but seems to be independent of the galactic latitude. Three methods were used to determine the antapex of the motions; the mean result is $A = 6^h43^m$; $D = -28°$. The mean parallaxes were derived from the peculiar motions for different groups of magnitude and proper motion. For the stars in question the mean parallax seems to depend very little on the magnitude, but is strongly correlated with the amount of motion.

The antapex and the mean parallaxes were also derived for the fainter stars of large motion found by Ross and by Wolf. Results from these stars corroborate those from the Mount Wilson material.

During the earlier years of the activities with the 60-inch reflector (1909–1912) Messrs. Fath and Babcock made a series of photographs of Kapteyn's Selected Areas, Nos. 1–139, extending from the North Pole down to 15° southern declination. The plates were taken at the Newtonian focus ($f = 25$ ft.) on Lumière Σ plates with exposures of one hour, and formed part of the material used for the *Mount Wilson Catalogue.*

At my request several of these regions have recently been rephotographed, partly by Messrs. Duncan and Hoge, but mostly by Mr. Christie. The new exposures of one hour were made on Eastman 40 plates, and, in general, show about as many stars as the older plates. On the average, stars of the eighteenth to nineteenth magnitude can be seen, while occasionally still fainter objects are found. The 42 regions for which new plates are now available have been investigated with the blink arrangement of the stereocomparator for the detection of stars showing considerable proper motion. The motions found range from $\mu = 0''.041$ to $0''.925$ per year.

Because it is difficult to discover small displacements both for the

brighter stars, which are badly overexposed, and for stars more than 15′ from the center, which show considerable coma, it is probable that some stars with motions between 0″.040 and 0″.100 have not been included; but we think that practically all having motions larger than 0″.100 were found.

When a star showed a decided displacement, the faint stars in the neighborhood were superposed as accurately as possible and the displacements of the star in question were measured in both right ascension and declination.

The magnitudes were kindly furnished by Miss Joyner. For stars appearing in the *Mount Wilson Catalogue*,[1] the magnitudes were taken from this source. For stars not in this catalogue, but given in *Harvard Annals* 101, the magnitudes published there were used after reduction to the international scale.[2] In five cases the corrections had to be extrapolated from the published values; the magnitude is then marked by an asterisk in Table III.

For the stars which do not appear in either of these sources, estimates were made by Miss Joyner. In the tables these stars are marked "anonymous," and their magnitudes, which may be in error as much as half a magnitude, are given to one decimal only.

The data for the different fields investigated have been collected in Table I. The number of stars in the sixth column was computed as follows: The areas measured for the *Mount Wilson Catalogue* were circular with a diameter of 23′; the areas examined for proper motions cover 2270 square minutes, or about five times as much. Since, however, the number of stars falls off rapidly with increasing distance from the center, it was estimated that about two and one-half times as many stars were "blinked" in each region as are given in the *Catalogue*. Among the 60,000 stars examined, only 122, or 1 in 500, were found to have an appreciable proper motion. The percentage of proper-motion stars, however, increases rapidly with increasing galactic latitude, as may be seen from Table II.

The detailed results for the 122 stars are collected in Table III. The third column gives the identification, either in the *Mount Wilson*

[1] *Publications of the Carnegie Institution of Washington*, No. 402, 1930.

[2] Seares, Joyner, and Richmond, *Mt. Wilson Contr.*, No. 289, Table III; *Astrophysical Journal*, 61, 303, 1925.

TABLE I

Selected Area	Central Star	α 1875	δ 1875	β	No. Stars Examined	No. P.M. Stars	Interval between Plates
							Years
23	+44° 790	$3^h36^m51^s$	+44° 57′.5	− 8°	1840	4	16.98
25	44 1275	5 35 34	+44 46.8	+ 8	1980	1	18.01
44	29 85	0 22 47	+30 2.6	−32	560	3	17.06
45	29 256	1 24 45	+29 58.8	−32	540	0	18.67
47	29 566	3 21 7	+29 56.4	−21	210	0	18.67
54	30 2024	10 22 43	+30 9.0	+59	220	0	19.18
57	30 2371	13 2 39	+30 3.2	+84	240	1	20.00
59	29 2622	15 0 52	+29 55.0	+60	370	1	19.96
60	30 2735	15 55 10	+29 59.3	+48	335	2	18.09
61	30 2925	16 57 52	+29 59.9	+34	750	3	16.25
62	30 3096	17 54 16	+30 3.5	+23	1815	3	16.88
63	29 3460	18 59 12	+29 59.0	+10	4320	1	16.89
64	29 3857	19 56 32	+29 52.4	− 1	7300	7	18.01
65	29 4292	20 58 13	+29 59.7	−12	4200	0	16.98
66	29 4566	21 57 14	+30 0.9	−21	1500	3	16.88
68	15 30	0 10 7	+15 8.5	−47	365	5	16.97
69	14 204	1 14 1	+15 2.4	−47	330	2	16.96
70	14 383	2 14 57	+14 56.8	−42	270	9	16.96
75	15 1544	7 13 31	+15 7.8	+13	1300	2	18.84
77	14 2057	9 9 15	+14 39.2	+39	290	2	20.91
82	15 2695	14 13 28	+15 30.7	+66	230	1	19.88
83	14 2850	15 7 56	+14 55.0	+54	330	7	18.98
84	15 2972	16 11 2	+15 6.2	+40	470	4	17.26
85	15 3141	17 9 45	+15 3.3	+27	1240	4	17.86
86	15 3419	18 10 37	+15 1.9	+15	3980	2	16.89
87	14 3849	19 10 7	+15 0.3	+ 1	4170	2	16.96
88	14 4240	20 9 48	+15 3.4	−12	5800	3	16.95
89	14 4556	21 7 0	+15 4.5	−23	1650	2	16.95
90	14 4768	22 11 34	+15 5.9	−34	750	4	16.95
91	14 4967	23 11 54	+14 55.2	−43	530	0	16.89
92	+ 0 142	0 48 37	+ 0 6.8	−62	240	1	16.98
102	− 0 2389	10 49 1	− 0 8.8	+52	390	8	18.21
103	+ 0 2858	11 48 37	+ 0 8.4	+61	270	5	19.26
104	+ 0 2975	12 36 42	+ 0 8.8	+63	290	7	20.95
107	+ 0 3387	15 32 38	+ 0 6.0	+41	520	4	19.92
108	− 0 3148	16 30 57	− 0 9.4	+29	1140	2	18.61
109	− 0 3352	17 38 26	− 0 4.7	+14	3000	1	18.61
110	+ 0 3995	18 35 54	+ 0 2.2	+ 2	370	4	18.09
111	+ 0 4265	19 31 58	+ 0 3.8	−11	4440	1	17.05
113	− 0 4251	21 36 3	− 0 7.3	−38	740	5	17.05
114	+ 0 4911	22 36 0	+ 0 7.1	−48	420	1	17.04
115	+ 0 5039	23 36 51	+ 0 12.7	−58	380	5	16.73
Totals and mean					60,085	122	17.93

TABLE II

Galactic Latitude	Stars Investigated	Number of μ Stars	Per Cent	Number of Fields
0°–19°	42,700	28	0.07	12
20–39	11,185	31	0.28	12
≧40	6,200	63	1.02	18

TABLE III

PROPER MOTIONS OF 122 FAINT STARS

Current No.	Sel. Area	No. in Cat.	Mag.	α 1875	δ 1875	x	y	μ_α	μ_δ	μ
1.....	23	H 658	12.90	$3^h37^m59^s$	+45° 8′.0	+12′.1	+10′.5	+0″.125	−0″.336	0″.359
2.....	23	Anon.	17.3±	3 35 53	45 4.0	−10.2	+ 6.5	+ .454	− .158	.481
3.....	23	130	16.96	3 36 34	44 52.6	− 3.0	− 4.9	+ .083	− .123	.148
4.....	23	H 231	16.09	3 35 50	44 45.8	−10.7	−11.7	− .005	− .208	.208
5.....	25	Anon.	18.0±	5 34 26	44 26.4	−12.1	−20.4	− .025	+ .199	.200
6.....	44	67*s*	16.67	0 23 10	29 55.5	+ 5.0	− 7.1	− .029	− .078	.083
7.....	44	38*s*	17.29	0 22 31	30 13.5	− 3.5	+10.9	.000	− .064	.064
8.....	44	H 334	15.50	0 22 45	30 16.8	− 0.4	+14.2	+ .146	− .029	.149
9.....	57	Anon.	17.5±	13 4 25	30 0.9	+23.1	− 2.3	− .096	− .044	.106
10.....	59	H 210	14.06	15 1 55	29 41.7	+13.6	−13.3	− .363	.000	.363
11.....	60	104	12.18	15 55 32	29 53.5	+ 4.7	− 5.8	− .143	+ .069	.159
12.....	60	49	17.36	15 54 55	29 55.0	− 3.3	− 4.3	− .035	− .058	.068
13.....	61	84	17.75	16 57 53	29 59.6	+ 0.3	− 0.3	− .021	− .056	.060
14.....	61	142	15.55	16 58 18	29 52.3	+ 5.7	− 7.6	− .056	− .113	.126
15.....	61	45*s*	16.92	16 57.42	30 9.3	− 2.2	+ 9.4	− .041	− .046	.062
16.....	62	428*c*	17.8±	17 53 39	29 57.2	− 7.9	− 6.3	+ .015	− .084	.085
17.....	62	H 794	12.70	17 53 13	30 8.7	−13.6	+ 5.2	+ .128	+ .010	.128
18.....	62	H 1206	11.30	17 55 57	30 19.2	+22.0	+15.7	− .035	+ .168	.172
19.....	63	267*c*	17.30	18 58 56	30 1.6	− 3.5	+ 2.6	+ .054	− .074	.092
20.....	64	H 1921	15.76	19 57 40	30 6.7	+14.8	+14.3	+ .009	− .093	.093
21.....	64	H 1475	13.42	19 57 38	29 59.7	+14.3	+ 7.3	− .069	− .058	.090
22.....	64	791	16.12	19 56 27	29 49.5	− 1.1	− 2.9	+ .037	+ .109	.115
23.....	64	H 379	15.59	19 57 25	29 39.8	+11.5	−12.6	− .032	− .060	.068
24.....	64	Anon.	16.5±	19 58 21	29 31.4	+23.6	−21.0	+ .759	− .528	.925
25.....	64	HD 190360	6.68	19 58 33	29 33.1	+26.1	−19.3	+ .759	− .528	.925
26.....	64	H 668	13.31	19 55 42	29 46.9	−10.8	− 5.5	− .023	− .044	.050
27.....	66	H 316	12.76	21 55 53	29 47.3	−17.6	−13.6	+ .074	+ .045	.087
28.....	66	H 348	12.60	21 56 35	29 43.8	− 8.5	−17.1	+ .119	+ .094	.152
29.....	66	H 549	12.44	21 56 15	29 58.9	−12.8	− 2.0	+ .045	+ .049	.067
30.....	68	50	15.92	0 9 53	+15 13.5	− 3.4	+ 5.0	+0.216	+0.162	0.270

31	68	83	14.66	$0^h10^m\ 9^s$	$+15°\ 1'.3$	$+\ 0'.6$	$-\ 7'.2$	$+0''.088$	$+0''.064$	$0''.109$
32	68	H 179	10.59	0 8 55	15 6.6	−17.4	− 1.9	+ .133	+ .069	.150
33	68	Anon.	15.0±	0 10 17	14 56.5	+ 2.3	−12.0	− .049	+ .020	.053
34	68	Anon.	15.7±	0 9 6	15 12.6	−14.8	+ 4.1	+ .182	− .172	.250
35	69	70	18.44	1 14 1	15 5.6	0.0	+ 3.2	+ .049	− .005	.049
36	69	Anon.	15.7±	1 13 15	14 58.4	−11.2	− 4.0	+ .207	− .010	.207
37	70	55	12.13	2 14 56	14 53.2	− 0.2	− 3.6	+ .148	− .034	.152
38	70	95	13.35	2 15 43	14 57.0	+11.1	+ 0.2	+ .148	− .118	.189
39	70	H 118	15.36	2 14 52	14 39.2	− 1.3	−17.6	+ .098	− .039	.105
40	70	H 176	10.80	2 16 27	14 50.6	+21.7	− 6.2	+ .064	+ .231	.240
41	70	H 178	10.21	2 16 29	14 50.7	+22.2	− 6.1	+ .064	+ .231	.240
42	70	H 204	14.23	2 13 29	14 57.8	−21.4	+ 1.0	+ .172	− .153	.230
43	70	H 228	13.82	2 15 45	14 56.6	+11.6	− 0.2	− .059	− .005	.059
44	70	H 284	13.61	2 15 22	15 9.6	+ 6.0	+12.8	+ .398	− .079	.406
45	70	Anon.	18.5±	2 15 16	14 42.1	+ 4.5	−14.7	+ .108	− .084	.137
46	75	Anon.	18.5±	7 13 40	15 26.3	+ 2.1	+18.5	− .066	− .066	.093
47	75	Anon.	17.0±	7 12 34	15 22.2	−13.7	+14.4	− .075	− .075	.106
48	77	21	16.24	9 9 4	14 46.0	− 2.8	+ 6.8	+ .072	− .267	.277
49	77	44	8.66	9 9 15	14 39.2	0.0	0.0	+ .052	− .289	.294
50	82	140	17.61	14 14 11	15 25.4	+10.2	− 5.3	− .034	+ .038	.051
51	83	H 268	14.96	15 6 21	14 52.1	−23.1	− 2.9	− .123	+ .020	.125
52	83	H 225	16.24	15 8 39	14 37.1	+10.3	−17.9	− .070	+ .037	.079
53	83	Anon.	18.5±	15 9 33	14 41.9	+23.5	−13.1	− .110	− .174	.206
54	83	Anon.	17.5±	15 6 30	14 48.9	−20.7	− 6.1	+ .022	− .062	.066
55	83	Anon.	16.5±	15 6 42	14 39.6	−17.9	−15.4	+ .035	− .068	.077
56	83	Anon.	17.0±	15 6 57	14 53.3	−14.3	− 1.7	− .136	− .042	.142
57	83	125	16.16	15 8 39	14 51.3	+10.4	− 3.7	− .048	− .068	.083
58	84	91	17.65	16 10 46	15 7.0	− 3.8	+ 0.8	− .048	− .034	.059
59	84	Anon.	15.6±	16 10 6	15 3.1	−13.4	− 3.1	+ .029	− .116	.119
60	84	Anon.	16.5±	16 9 29	14 55.3	−22.4	−10.9	− .135	+ .106	.172
61	84	Anon.	19.0±	16 10 3	15 10.9	−14.4	+ 4.7	− .116	− .019	.118
62	85	55	17.52	17 9 25	15 10.6	− 4.8	+ 7.3	+ .033	− .121	.125
63	85	50	17.42	17 9 24	15 10.3	− 5.1	+ 7.0	+ .035	− .093	.099
64	85	91	16.81	17 9 32	15 7.9	− 3.2	+ 4.6	+ .054	+ .070	.088
65	85	129	12.08	17 9 43	15 8.4	− 0.5	+ 5.1	− .133	+ .047	.141
66	86	Anon.	20.0±	18 12 8	+15 20.2	+22.0	+18.3	−0.054	+0.084	0.100

TABLE III—*Continued*

Current No.	Sel. Area	No. in Cat.	Mag.	α 1875	δ 1875	x	y	μ_α	μ_δ	μ
67.....	86	Anon.	18.0±	18h 10m58s	+14°50'.9	+ 5'.0	−11'.0	−0s.035	+0".198	0".201
68.....	87	H 633	15.13	19 11 9	+15 1.7	+15.1	+ 1.4	− .079	− .044	.090
69.....	87	Anon.	18.7±	19 11 5	+14 57.3	+14.0	− 3.0	− .049	− .093	.105
70.....	88	1036	11.38	20 9 55	+14 58.7	+ 1.7	− 4.7	+ .015	− .182	.183
71.....	88	Anon.	15.3±	20 11 14	+15 3.6	+20.9	+ 0.2	+ .079	− .005	.079
72.....	88	Anon.	18.3±	20 11 15	+15 3.6	+21.0	+ 0.2	+ .118	− .005	.118
73.....	89	H 672	16.33	21 8 38	+15 1.3	+23.7	− 3.2	+ .113	+ .108	.156
74.....	89	Anon.	16.3±	21 7 8	+15 17.9	+ 2.0	+13.4	− .059	− .221	.229
75.....	90	Anon.	18.7±	22 12 11	+15 11.7	+ 8.9	+ 5.8	− .049	− .074	.089
76.....	90	H 166	14.60	22 11 14	+14 44.2	− 4.7	−21.7	+ .236	− .044	.240
77.....	90	H 492	15.59	22 10 30	+15 13.9	−15.5	+ 8.0	+ .093	− .089	.129
78.....	90	H 528	15.47	22 11 50	+15 19.1	+ 3.9	+13.2	− .020	− .143	.144
79.....	92	98	11.74	0 48 47	+ 0 15.6	+ 2.6	+ 8.8	− .260	− .172	.312
80.....	102	41	11.05	10 48 42	− 0 8.4	− 4.7	+ 0.4	− .249	+ .018	.250
81.....	102	67	17.43	10 48 58	− 0 15.4	− 0.8	− 6.6	− .064	− .041	.077
82.....	102	Anon.	19.5±	10 49 4	− 0 26.7	+ 0.7	−17.9	+ .053	+ .050	.073
83.....	102	Anon.	19.0±	10 49.48	+ 0 5.0	+11.8	+13.8	+ .023	+ .055	.060
84.....	102	Anon.	18.5±	10 49 51	+ 0 4.1	+12.4	+12.9	− .066	+ .014	.067
85.....	102	H 679	10.65*	10 50 33	− 0 10.8	+23.1	− 2.0	+ .140	− .137	.196
86.....	102	H 680	12.18*	10 50 35	− 0 11.0	+23.5	− 2.2	+ .105	− .137	.173
87.....	102	H 739	11.81*	10 47 48	+ 0 7.8	−18.3	+16.6	− .114	+ .046	.123
88.....	103	42	17.64	11 48 18	+ 0 12.6	− 4.6	+ 4.2	+ .052	+ .037	.064
89.....	103	39	17.28	11 48 18	+ 0 12.5	− 4.8	+ 4.1	+ .052	+ .037	.064
90.....	103	22	17.36	11 48 8	+ 0 11.7	− 7.2	+ 3.3	+ .013	− .091	.092
91.....	103	70	15.97	11 48 36	+ 0 10.6	− 0.2	+ 2.2	− .065	− .121	.137
92.....	103	Anon.	18.0±	11 48 27	+ 0 23.7	− 2.4	+15.3	− .117	+ .065	.134
93.....	104	H 419	15.51	12 35 4	+ 0 14.5	−24.5	+ 5.7	+ .068	+ .048	.083
94.....	104	H 551	16.60	12 36 10	+ 0 20.3	− 8.1	+11.5	− .028	− .030	.041
95.....	104	H 559	15.65	12 36 23	+ 0 23.3	− 4.7	+14.5	+ .111	− .127	.169
96.....	104	39	17.08	12 36 39	+ 0 9.5	− 0.7	+ 0.7	− .068	+ .060	.091
97.....	104	40	14.00	12 36 40	+ 0 12.8	− 0.6	+ 4.0	− .127	+ .014	.128
98.....	104	H 568	16.85	12 37 0	+ 0 24.1	+ 4.5	+15.3	−0.100	−0.056	0.115

99.....	104	H 369	16.50	$12^h37^m37^s$	+ 0° 3'.7	+13'.6	− 5'.1	−0".070	+0".024	0".074
100.....	107	17	13.19	15 32 5	+ 0 10.8	− 8.2	+ 4.8	+ .167	− .268	.316
101.....	107	99	8.07	15 32 38	+ 0 6.0	0.0	0.0	− .220	− .230	.318
102.....	107	H 684	9.05	15 30 54	+ 0 15.0	−26.1	+ 9.0	− .042	− .113	.121
103.....	107	Anon.	18.0±	15 31 46	+ 0 22.3	−13.0	+16.3	− .046	− .138	.146
104.....	108	H 1492	16.50*	16 30 50	+ 0 8.5	− 1.6	+17.9	+ .049	− .049	.069
105.....	108	H 733	16.50*	16 29 55	− 0 12.4	−15.4	− 3.0	+ .038	− .116	.122
106.....	109	Anon.	16.0±	17 37 4	+ 0 1.2	−20.4	+ 5.9	− .009	− .063	.064
107.....	110	H 470	16.27	18 34 55	+ 0 18.8	−14.9	+16.6	.000	− .125	.125
108.....	110	H 406	16.61	18 34 58	+ 0 16.1	−14.0	+13.9	.000	− .138	.138
109.....	110	H 409	11.57	18 35 13	+ 0 13.8	−10.3	+11.6	− .023	− .161	.163
110.....	110	7	13.13	18 35 27	− 0 1.7	− 6.7	− 3.9	− .069	− .171	.184
111.....	111	Anon.	17.4±	19 31 56	− 0 10.2	− 0.6	−14.0	− .015	− .122	.123
112.....	113	43	17.38	21 35 55	− 0 11.4	− 2.1	− 4.1	− .186	− .411	.451
113.....	113	116	13.41	21 36 26	− 0 5.9	+ 5.9	+ 1.4	+ .064	− .010	.065
114.....	113	H 397	15.39	21 36 37	+ 0 2.9	+ 8.4	+10.2	+ .083	− .113	.140
115.....	113	H 468	15.82	21 35 6	+ 0 7.8	−14.2	+15.1	− .068	− .044	.081
116.....	113	Anon.	18.3±	21 36 43	+ 0 2.4	+ 9.9	+ 9.7	+ .157	+ .005	.157
117.....	114	Anon.	17.2*	22 37 8	− 0 6.9	+17.1	−14.0	+ .113	+ .044	.121
118.....	115	92	17.57	23 37 11	+ 0 7.1	+ 4.9	− 5.6	+ .050	− .155	.163
119.....	115	27	16.50	23 36 30	+ 0 14.3	− 5.3	+ 1.6	− .040	− .324	.326
120.....	115	115	13.37	23 37 31	+ 0 13.1	+10.0	+ 0.4	+ .095	+ .030	.100
121.....	115	H 201	16.20	23 36 36	− 0 2.3	− 3.7	−15.0	+ .145	+ .040	.150
122.....	115	Anon.	18.2±	23 37 22	+ 0 27.8	+ 7.8	+15.1	−0.100	−0.020	0.102

In the third column *s* indicates the number in the supplementary list of the *Mount Wilson Catalogue.*

In the third column *c* indicates the faint companion.

For star 25 the magnitude was taken from the *Henry Draper Catalogue;* both this star and No. 24 are on the edge of the plate and the motion is therefore uncertain.

* The correction for the reduction of the Harvard magnitude to the Mount Wilson scale is extrapolated.

Catalogue or in *Harvard Annals* 101; in the latter case an "H" precedes the number. For some purposes it is easier to use right ascension and declination, while for others rectangular co-ordinates are preferable; both systems are accordingly included in the table. The

TABLE IV

DISTRIBUTION OF PROPER MOTION ACCORDING TO MAGNITUDE

Mag.	n	$\bar{\mu}$	Mag.	n	$\bar{\mu}$
<10.00	4	0".414	6–10	8	0".310
10.00–10.99	4	0.206			
11.00–11.99	6	0.200			
12.00–12.99	9	.158	11–13	24	0.170
13.00–13.99	9	0.162			
14.00–14.99	6	0.199			
15.00–15.99	19	.131	14–16	48	0.139
16.00–16.99	23	0.130			
17.00–17.99	23	0.124			
18.00–18.99	14	.129	17–20	41	0.122
>19.00	4	0.088			

last three columns give the proper motions in right ascension and declination and the total motion.

As might be expected a priori, the brighter stars show in the mean a larger proper motion than the fainter stars. This is best seen from

TABLE V

DISTRIBUTION OF PROPER MOTION ACCORDING TO GALACTIC LATITUDE

Lat.	0°–9°	10°–19°	20°–29°	30°–39°	40°–49°	50°–59°	>60°
$\bar{\mu}$	0".208	0".116	0".123	0".154	0".169	0".132	0".126
n	17	10	14	17	27	20	16
$\bar{\mu}$	0.164	0.116	0.123	0.145	0.165	0.132	0.126
n	16	10	14	16	25	20	16

the summary given in Table IV. For this and for the following discussion, star No. 24, a faint companion of No. 25, has been omitted.

Investigating the relation between size of proper motion and galactic latitude, we find a surprising lack of correlation, as indicated in Table V. The last two lines in the table are the results after omitting

the four stars brighter than the tenth magnitude. The values are a little smoother, owing particularly to the omission of the very large motion of star No. 25 (6.68 mag.). The mean motion of the 121 stars is 0".151; that of the 117 faint stars, 0".142. The deviations of the figures from these means are quite small, if we keep in mind the limited amount of material available.

A result of considerable interest which was derived from the present material is the position of the antapex of the motions of these faint stars. For this purpose the stars were divided into three groups, including magnitudes 11–13, 14–16, 17–20, and containing 24, 48, and 41 stars, respectively. Three methods were used:

a) *Herschel's method.*—When plotted on a sphere, the proper motions, if produced along great circles, would all cross in the antapex, provided the motions were due only to parallactic motion and not to peculiar motions as well. Since random peculiar motions are also present, it is evident that the great circles will not cross in a point; it is, however, fairly easy to determine the point of preferential crossing.

b) *Bessel's method.*—For each star the pole of the proper motion is computed and plotted on a sphere; the great circle best fitting these poles has as its poles the apex and antapex of the proper motions; the apex and antapex may be distinguished by noting the direction of the motions. The deviations of the individual poles corresponding to five to eight trial positions of the antapex were found, and from the run of these deviations a fair estimate of the position of the antapex could be made.

c) *Airy's method.*—Indicating the parallactic motion by p, the right ascension and the declination of the antapex by A and D, and the components of the vector directed toward the antapex by X, Y, and Z, we have

$$p \cos A \cos D = X; \quad p \sin A \cos D = Y; \quad p \sin D = Z . \qquad (1)$$

Further, we have

$$\left.\begin{aligned} -X \sin \alpha + Y \cos \alpha &= \mu_\alpha , \\ -X \cos \alpha \sin \delta - Y \sin \alpha \sin \delta + Z \cos \delta &= \mu_\delta . \end{aligned}\right\} \qquad (2)$$

Each star furnishes a set of equations of form (2). These may be solved for all the stars by least squares, and from the resulting values of X, Y, and Z, we may then derive A and D by

$$\tan A = \frac{Y}{X}\,; \quad \tan D = \frac{Z}{\sqrt{X^2+Y^2}}\,. \tag{3}$$

In this method a star with a very large motion has an undue influence on the results. Stars were accordingly omitted when the deviations found by substituting the quantities X, Y, and Z in equations (2) were larger than five times the probable error. Only

TABLE VI

CO-ORDINATES OF THE ANTAPEX

Mag.	a	b	c	Mean
11–13.....	$\begin{cases} A = 7^h0^m \\ D = -10^\circ \end{cases}$	6^h20^m -24°	7^h4^m -33°	$6^h48^m \pm 11^m$ $-22^\circ \pm 4^\circ.4$
14–16.....	$\begin{cases} A = 7^h20^m \\ D = -34^\circ \end{cases}$	6^h13^m -18°	7^h4^m -39°	$6^h52^m \pm 13^m$ $-30^\circ \pm 4^\circ.1$
$\geqq 17$.....	$\begin{cases} A = 6^h0^m \\ D = -30^\circ \end{cases}$	6^h27^m -18°	7^h0^m -41°	$6^h29^m \pm 12^m$ $-30^\circ + 4^\circ.4$

in the case of the faintest stars were exclusions necessary. Numbers 2 and 112 were omitted and a new solution made.

Table VI gives the results obtained by the three methods. These are very interesting because of indications in the past that the declination of the antapex for the fainter stars is farther south than -30°. Of course in this connection it should be kept in mind that we are here dealing with only the nearer of the faint stars; but it is also safe to say that we are concerned with the faster moving of these stars, and for the fast-moving stars a lower declination of the antapex has been noticed before.

We may also derive the mean parallaxes for the stars discussed above. The best results will be obtained from the τ-components, as it is easier to estimate the peculiar radial velocities of these stars than the amount of the solar motion. From a comparison with the peculiar radial velocities of brighter stars having large proper motion,

we may accept 50 km/sec. as a fair estimate for the mean peculiar radial velocity. From $\overline{\pi} = 4.74\overline{\tau}/\overline{V}$ we then obtain $\overline{\pi} = 0.0948\,\overline{\tau}$. The results are collected in Table VII. The last three lines have little significance, as the number of stars involved is too small. From the stars with $\mu < 0''.300$ it seems to follow that the mean parallaxes are more closely correlated with proper motion than with magnitude.

TABLE VII

MEAN PARALLAXES

Mag.	Mean Mag.	Mean μ	Mean π	π Comp.	n
	Stars with $\mu < 0''.100$				
11–13.....	13.19	0".070	0".0049	0".0045	6
14–16.....	16.06	.075	.0045	.0045	17
17–20.....	17.86	0.073	0.0045	0.0041	20
	Stars with $\mu = 0''.100$–$0''.299$				
11–13.....	12.20	0.162	0.0095	0.0095	14
14–16.....	15.76	.163	.0090	.0087	29
17–20.....	18.04	0.137	0.0055	0.0071	19
	Stars with $\mu = 0''.300$–499				
11–13.....	12.86	0.348	0.0201	0.0179	4
14–16.....	15.28	.344	.0178	.0169	2
17–20.....	17.34	0.466	0.0356	0.0208	2

This statement is corroborated if we treat the material analytically. Each of the nine groups furnishes an equation of condition of the form of Kapteyn's well-known equation:

$$\log \overline{\pi} = a + b\overline{m} + c \log \overline{\mu} ,$$

where $\overline{m}$ is the mean magnitude and $\overline{\mu}$ the mean proper motion of the stars in the group. Using weights proportional to the number of stars included, we derive by a least-squares solution

$$a = -1.207 \pm 0.133 ,$$
$$b = -0.011 \pm 0.008 ,$$
$$c = +0.862 \pm 0.080 .$$

The factor b, correlating the mean parallax and the mean magnitude, is very much smaller than in Kapteyn's general formula; Russell,[1] for instance, gives $b = -0.0713$. Substituting these constants in the equations of condition, we derive the values given in the fifth column of Table VII. It therefore seems safe to combine the results for the eight stars having $\mu \geqq 0''.300$. We then obtain

$$\bar{\mu} = 0''.377 , \quad \bar{\tau} = 0''.247 , \quad \bar{\pi} = 0''.0234 ,$$

corresponding to a value -3.2 for the difference between absolute and apparent magnitudes. While of course nothing can be said of the individual parallaxes, the discovery, in the present list, of exceptionally faint stars, say of absolute magnitude $+18$ or $+20$, does not look very promising.

TABLE VIII

DETERMINATION OF THE ANTAPEX OF THE FAINTER ROSS STARS

Method a	$A = 7^h10^m$	$D = -30°$
b	7 4	20
c	7 52	−36
Mean	$A = 7^h22^m \pm 10^m$	$D = -29° \pm 3°.1$

To check the foregoing result for the position of the antapex of the fainter stars of considerable proper motion, the proper motions of faint stars published by Ross[2] and by Wolf[3] have also been utilized to determine the co-ordinates of the antapex. From Ross's material we selected the stars of the fourteenth magnitude or fainter, 86 in number, of which two, Nos. 419 and 476, were omitted from the discussion as being companions of much brighter stars. The motions of these stars range from $0''.10$ to $3''.30$. In using Airy's method it was necessary to omit No. 578, for which the deviation surpassed five times the probable error of the solution. The results are given in Table VIII.

The same methods were also applied to the stars in Wolf's cata-

[1] Russell, Dugan, Stewart, *Astronomy*, 2, 667, 1926.

[2] *Astronomical Journal*, 40, 38, 1930.

[3] *Veröffentlichungen der Sternwarte zu Heidelberg*, 7, 195, 1919.

logue of 1053 stars having large proper motion.[1] As Wolf's magnitudes are too bright, at least for the stars of magnitude 11–15, it was decided in this case to use stars for which his values range from 13 to 16, in order to make the material comparable with that of Ross and with the middle group of magnitudes among the Mount Wilson stars. This gives 203 stars, of which, however, Nos. 191, 611, 884, 886, and 977 have been omitted as probable companions of much brighter stars. As there are 36 stars whose motions are $\geqq 0''.50$ annually, the material was subdivided into two groups: 162

TABLE IX

DETERMINATION OF THE ANTAPEX OF THE FAINTER WOLF STARS

Stars with $\mu < 0''.50$		
Method *a*	$A = 6^h17^m$	$D = -40°$
b	7 0	35
c	7 8	−36
Mean	$A = 6^h48^m \pm 11^m$	$D = -37° \pm 1°.0$
Stars with $\mu \geqq 0''.50$		
Method *a*	$A = 6^h40^m$	$D = -36°$
b	5 0	25
c	8 34	−52
Mean	$A = 6^h45^m \pm 41^m$	$D = -38° \pm 5°.2$

stars with $\mu < 0''.50$ and 36 with $\mu \geqq 0''.50$, from which, however, Nos. 359 and 489 were excluded in using Airy's method. The results from the three methods are collected in Table IX. For convenience, the mean results from the three different groups of data are collected in Table X. Apparently there is no indication of a value for the declination of the antapex larger than $-30°$ to $-35°$.

Comstock[2] was the first to raise the question of a change in the declination of the antapex with decreasing magnitude, although he prefers to call it a progression in galactic longitude rather than in declination; for stars of magnitude 8.6 he found $D = -58°$; for magnitude 11.1, $D = -71°$. Much work on this problem has been done in recent years; and in *Monthly Notices*, 90, 460, 1930, Smart gives a

[1] *Ibid.* [2] *Astronomical Journal*, 28, 54, 1913.

résumé of the different articles published on the subject. The results for the declination of the antapex range from $-29°$ to $-46°$. Most of the material is based on the system of Boss's *Preliminary General Catalogue*. It is now generally accepted that Boss's proper motions in declination need a correction, although the amount of this correction differs as determined by various astronomers. The important fact, however, is that all corrections applied effect a considerable change in the antapex, which amounts to as much as 16°,[1] and all in

TABLE X

DETERMINATION OF THE ANTAPEX; SUMMARY

Authority	Mag.	*A*	*D*	*n*
van Maanen and Willis	11–13	6^h48^m	$-22°$	24
	14–16	6 52	30	48
	≦17	6 29	−30	41
Ross	14–15	7 22	−29	84
Wolf $\mu<0''.50$	14–16*	6 48	−37	162
Wolf $\mu\geqq 0''.50$	14–16*	6 45	−38	36

* Magnitudes given by Wolf corrected by +1.00.

the same direction, viz., a shift of the antapex to the north. Comstock's motions are also based on the *Preliminary General Catalogue* and his results in consequence require a correction in the same direction. Moreover, we must keep in mind that while his material when published was of the highest accuracy then attained, it has now been surpassed both in quantity and in quality. His results, therefore, have less weight than some of the more recent determinations. This becomes evident if we compare the distribution of his values with that given in *Groningen Publications* No. 30, which deals with the number of stars between definite limits of proper motion and is based on all the material available at that time (1920). Comstock divides his material into stars brighter and fainter than the tenth magnitude. The distribution of his motions is given in Table XI, together with the numbers to be expected on the basis of the Groningen researches. As due care has been taken of the different percentages of stars in different galactic latitudes, the numbers are strictly comparable.

[1] Kovalenko, *ibid.*, **37**, 149, 1927.

It is clear from Table XI that Comstock's proper motions have too few small motions. This also appears from a comparison of Comstock's results with those of Lee. For mean magnitude 11.8 Comstock finds mean $\mu = 0''.0265$; Lee, $0''.0182$. The discrepancy is undoubtedly due to a larger probable error in the motions than was expected by Comstock. One of us[1] has called attention to the fact that large probable errors result in a deficiency of stars having the smaller motions. From a rediscussion of Nechville's motions by Smart and Green[2] it seems that this, too, affects the positions of the antapex and again in the same direction as the systematic error in

TABLE XI

COMPARISON OF COMSTOCK'S RESULTS WITH *Groningen Publication* No. 30

LIMITS OF μ	STARS BRIGHTER THAN 10		STARS FAINTER THAN 10	
	Comstock	*Gron.* 30	Comstock	*Gron.* 30
$0''.000$–$0''.020$	72	125.5	78	153.3
.020– .040	77^5	62.1	85^5	43.1
.040– .060	42^5	23.6	36	16.0
.060– .080	29	11.9	11^5	7.3
.080– .100	9	6.9	8	3.2
.100– .150	11	8.4	7	3.5
.150– .200	2^5	3.2	1	1.1
0.200–0.300	0^5	2.4	1	0.5
Totals	244	244	228	228

Boss's motions. The total correction required by Comstock's value of D may be estimated at 20°, which brings his result into fair agreement with all the material known at present. Taking all results into account, we find no reason to expect a declination of the antapex differing much from $-30°$ to $-35°$, except for the stars of extremely high velocity (70 km/sec. or more).

Finally, the mean parallaxes were derived from the τ-components of the proper motions for both Ross's and Wolf's stars. The results are collected in Table XII and in combined form are given in Table XIII.

The last column but one of Table XIII gives mean parallaxes

[1] van Maanen, *Mt. Wilson Contr.*, No. 167, p. 12, 1919.

[2] *Monthly Notices of the Royal Astronomical Society*, **89**, 147, 1928.

computed with the constants derived on page 11. The agreement with those derived from the τ-components is quite satisfactory. It

TABLE XII

MEAN PARALLAXES OF THE STARS OF ROSS AND WOLF

Limits of μ	Mean Mag.	Mean μ	Mean π	n	
0".10–0".29	14.19	0".207	0".0075	27	Ross
0.30–0.49	14.30	0.395	0.0246	30	
0.50–0.99	14.44	0.667	0.0338	24	
≧ 1".00	14.33	1.910	0.1014	3	
<0".10	14.29*	0.075	0.0036	13	Wolf
0.10–0".29	14.51*	0.195	0.0101	99	
0.30–0.49	14.60*	0.375	0.0164	50	
0.50–0.99	14.61*	0.661	0.0365	27	
≧ 1".00	14.33*	1.951	0.0525	9	

* Magnitudes given by Wolf corrected by +1.00.

TABLE XIII

COMBINED RESULTS FOR THE STARS OF ROSS AND WOLF

Limits of μ	Mean Mag.	Mean μ	Mean π	π Comp.	n
<0".10	14.29	0".075	0".0036	0".0046	13
0".10–0.29	14.44	0.198	0.0096	0.0107	126
0.30–0.49	14.49	0.383	0.0195	0.0188	80
0.50–0.99	14.53	0.664	0.0352	0.0302	51
≧ 1".00	14.33	1.941	0.0647	0.0766	12

should be kept in mind, however, that both sets of parallaxes are based on the value of 50 km/sec. for $\overline{V}$. If for any reason it becomes necessary to use a different value, the results for π will change in inverse proportion.

CARNEGIE INSTITUTION OF WASHINGTON
MOUNT WILSON OBSERVATORY
September 1930

Contributions from the Mount Wilson Observatory, No. 413
Reprinted from the *Astrophysical Journal*, Vol. LXXII, pp. 256–266, 1930
Printed in the U.S.A.

STEWARD OBSERVATORY TUCSON, ARIZ.

MULTIPLET INTENSITIES IN THE SOLAR SPECTRUM

By R. VAN DER R. WOOLLEY

ABSTRACT

The *widths of the lines in a titanium multiplet in the solar spectrum* have been measured and *compared with the theoretical intensities* given by the quantum theory, which are in agreement with the observations of laboratory emission spectra. There is a *marked divergence in the solar spectrum*, the weaker lines appearing relatively stronger. Further, a *survey of all* the *lines* in the *solar spectrum* in the *region* λλ 4500–4600 was made. When the lines are grouped together according to Rowland intensity, the square of the mean width, which gives the number of atoms concerned in the formation of the line, shows a similar marked divergence from the values found by Adams and Russell, who calibrated the Rowland intensities on the basis of theoretical multiplet intensities. *Multiplet intensities in the solar spectrum differ widely from intensities in emission spectra, the weaker lines being relatively stronger in the solar spectrum.*

Using the 150-foot solar tower and 75-foot spectrograph, the writer has made a photometric survey of the lines in a small region in the solar spectrum from λ 4500 to λ 4600. The work is preliminary and supplements the projected Mount Wilson survey of the solar spectrum. The method of standardizing the photographic plates is different from that used by St. John in his investigation of selected multiplets, and utilizes apparatus designed by Dunham, which is equivalent to a step wedge placed in front of a spectrograph. The procedure adopted was to cut a plate in half. One half was exposed to the solar spectrum and the other in the standardizing spectrograph, both halves being developed together. The contours of the absorption lines were then measured with a microphotometer.

All but the strongest lines are, however, very narrow. Hence, on account of the finite resolving power of the original spectrograph and also of the microphotometer, the contour so determined is necessarily only approximate. The limitations of the method and various corrections have frequently been discussed elsewhere, and some experimenters are devoting themselves to increasing the accuracy of the method; but a great deal of information, particularly about the stronger lines, can be obtained with the methods at present

available. In particular, the widths of the lines, in thousandths of an angstrom, taken at some definite point (e.g., where the intensity has fallen to nine-tenths that of the continuous background), can be determined for the stronger lines. These widths have been used by A. Unsöld to determine the "number of atoms above 1 sq.cm of the photosphere." Milne has attached a definite meaning to this phrase,[1] namely, the number of atoms above a certain optical depth which depends on the intensity, expressed as a fraction of the intensity of the continuous background, at which the width is measured.

The immediate application of the present set of observations is to examine the calibration of Rowland's scale of intensities by Russell and Adams, and to test the underlying assumption that the intensities of lines in a multiplet are proportional to the corresponding intensities in laboratory emission spectra. The present observations give the important result that there is considerable divergence, the weaker lines being relatively much stronger in the solar spectrum than in emission spectra. This result has been suspected by St. John and others for some time.

Individual observations of the width of a line are subject to considerable uncertainty. The chief sources of error and methods of combating them are set out later, but whether a homogeneous set of observations contains systematic errors or not, the relative widths of the lines have a definite meaning, namely, that the squares of the relative widths at some definite point are proportional to the number of atoms above a certain optical depth, systematic errors introducing an uncertainty into the precise value of this depth. Hence the relative intensities in a multiplet may be taken from a homogeneous set of observations (i.e., observations derived from the same plate) with considerably more confidence than can be attached to any individual observation. The same remark holds for statistical observations on the Rowland intensities.

This expected result is borne out by some sets of observations given in Table II. Details of the standardizing apparatus are indicated by Figures 1 and 2. The apparatus was constructed by Dr. Dunham and used by him in his stellar work. The design fol-

[1] *Monthly Notices of the Royal Astronomical Society*, **89**, 3, 1928.

lows the work of G. Hansen[1] and R. Frerichs.[2] Light from an iron arc *A* falls on a system *B* consisting of two sheets of ground glass and a condensing lens, after which it falls on a "raster" *C*. The raster is a brass plate from which a number of horizontal strips

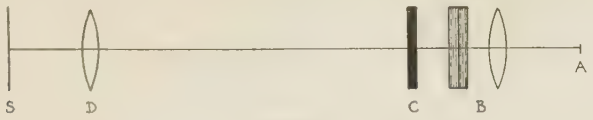

FIG. 1

have been cut. A different fraction of the space so formed is blocked in again with black paper in each strip, so that each presents a different open area and passes a different amount of light from the arc. Owing to the ground glass, the illumination of the raster is uniform, and the amount of light passed by each strip is proportional to the open area.

A cylindric lens *D* focuses the strips vertically but not horizontally on the slit *S* of a spectrograph, the images being uniform horizontal strips whose intensities are in known ratio. The slit is left open about a millimeter. The images of the lines are therefore wide, and the spectrograph records for each a definite pattern broken up into a number of patches corresponding to the strips on the raster.

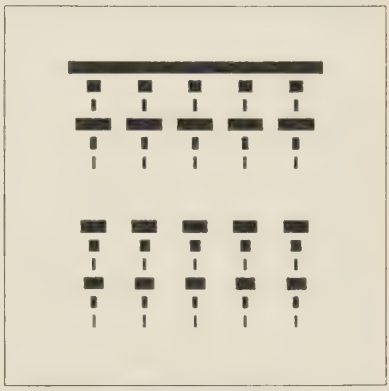

FIG. 2.—The raster *C* in Fig. 1. The relative areas of the open spaces are, from top to bottom: 100, 25, 5.6; 70, 11.6, 3.1; 49.4, 18.5, 4.4; 35.7, 8.7, 2.0.

The standardizing curve can be made in any wave-length in the iron arc by measuring the photographic densities of these patches. A very wide range of photographic densities may be used by a judicious choice of arc lines different in intensity but close together in wave-length.

A typical curve is shown in Figure 3.

[1] *Zeitschrift für Physik*, **29**, 356, 1924. [2] *Ibid.*, **31**, 305, 1925.

Using Eastman 33 plates, developed four minutes at 65° F in Kodak formula D61*a* developer (half-strength), I have found no distinct variation in the curves for the same plate over a range of wave-lengths from λ 4400 to λ 4700; probably this is true from λ 4200 to λ 4900. Provisionally it seems safe to suppose that two plates with the same emulsion number exposed and developed under similar circumstances have the same curve; but this has not been tested thoroughly, and it is better in any case to determine the curve again for each plate used.

The errors to be expected in this type of observation fall into two classes, photographic and instrumental. Photographic errors are due to (1) errors in standardizing, (2) the presence of chemical fog, and (3) the Eberhard effect. With regard to (1), there should be no difficulty in obtaining a reliable curve if such precautions are observed as making the time of the standardizing exposure equal to the exposure time on the solar spectrum. With regard to (2), it is necessary to have a very clean plate. Washing must be very thorough and the time of development chosen carefully. A fogged plate is useless. With regard to (3), with the very large dispersion used, there should not be much trouble, especially as the observations have been made in different orders and the plates developed with different developers. I have, however, developed some plates with ferrous oxalate, which gives no Eberhard effect, but with which it is difficult to get clear plates. Good results have been obtained by washing very thoroughly after developing and then fixing in an acid hardening bath (Kodak formula F 1).

The instrumental errors are due to finite theoretical resolving power, imperfect focus, the presence of scattered light, ghosts, and lens reflections.

Two gratings have been tested in the present series of observations, one ruled by Michelson and one ruled very recently by Jacomini at the Mount Wilson Observatory. The latter is a much faster grating but does not give as good resolution on absorption lines, although the theoretical resolving power of the two gratings is about the same. The Michelson grating has therefore been used for the observations, but the comparison reminds us to what an extent we are relying on the performance of the grating.

OBSERVATIONAL ERRORS

The general method of checking the observational errors has been to examine the line λ 4554 of Ba^+ in detail, with the conditions varied as much as possible. The observations on this line are given in Table I. The width $\lambda - \lambda_0$ of the line is given in thousandths of an angstrom at three points where r, the ratio of the intensity inside the line to that of the continuous background just outside the line, has the values $\frac{9}{10}$, $\frac{3}{4}$, and $\frac{6}{10}$. The central intensity is also given, as a percentage of the intensity of the continuous background.

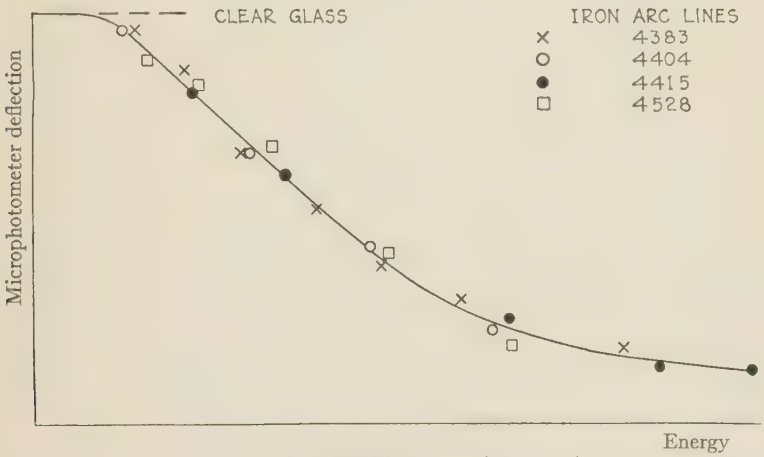

FIG. 3.—Standardizing curve (Plate 263)

With the scale used in making the microphotometer tracings, 1 mm corresponds to about 0.01 A in width, and the slope of λ 4554 is such that an error of 1 mm in fixing the position of the ordinate $r = \frac{9}{10}$ introduces an error of about 2 mm (20 units in Table I) in the width of the line. Owing to various irregularities, it is sometimes difficult to fix the position of the continuous background within half a millimeter, and, owing to plate grain, the curve traced by the photometer may have an effective width of a millimeter.

The series of readings in Table I fixes the limitation of the method at about 0.01 A for any individual observation.

To test how much of the error is systematic and how much accidental, the three weaker lines given in Table II were observed re-

peatedly. These are good, clean lines, free from blends. The measured widths are given for each spectrogram. The values in parentheses are corrected widths corresponding to a width of 100 for

TABLE I

(Unit for $\lambda-\lambda_0=0.001$ A)

Plate	Grating	Order	$\lambda-\lambda_0$			Central Intensity (Per Cent)	Developer
			$r=\frac{9}{10}$	$\frac{3}{4}$	$\frac{6}{10}$		
W 194...	Michelson	2	150	85	70	30	D61*a*
301...	Michelson	3	A 154	97	70	31	X-ray
			B 154	102	78	29	X-ray
317...	Michelson	3	165	104	77	26	Oxalate
313...	Michelson	2	162	108	83	33	Oxalate
332...	Michelson	2	160	101	82	26	Borax D76
324...	Michelson	3	165	116	80	20	Borax D76
350...	Michelson	2	160	108	83	25	Oxalate
264...	Mt. Wilson	2	152	83	50	50	D61*a*

NOTES TO TABLE I

W 301.—The two spectra A and B were taken on the same plate. The slit on the 75-ft. spectrograph is several inches long, and only a small section is used to make the actual spectrum, which is admitted through a screen near the plate. In B, only the section of the slit actually used was exposed to sunlight; in A, all was uncovered, thus increasing about threefold the amount of light scattered by the grating. As indicated above, the effect on the observations is negligible.

W 350.—Standardized by a different method (rotating sector).

W 264.—Results obtained with the Mount Wilson grating are given for comparison.

TABLE II

Line	4533.25	4534.78	4545.96
Element	*Ti*	*Ti*	*Cr*
Rowland intensity	4	4	3
	$r=\frac{9}{10}$		
W 194	96 (64)	87 (58)	80 (53)
W 301	101 (65)	95 (62)	77 (51)
W 313	104 (64)	100 (62)	90 (55)
W 350	101 (63)	97 (61)	90 (56)
	$r=\frac{3}{4}$		
W 194	61 (72)	50 (59)	47 (55)
W 301	65 (64)	66 (65)	52 (51)
W 313	64 (59)	71 (66)	60 (55)
W 350	61 (56)	61 (56)	61 (56)

λ 4554 taken from the same plates. A comparison of the measured and corrected widths shows that the errors are about one-half systematic and one-half accidental. We therefore eliminate part, at least, of the systematic errors when we consider relative widths.

OBSERVATIONS ON A MULTIPLET

The best multiplet[1] occurring in the spectral region examined in the present series of measures is titanium $a^5F - y^5F^\circ$. In this multiplet no less than eight lines occur free from serious blending in the solar spectrum. For photometry a line must be free from other lines, and it is very difficult to find in the solar spectrum multiplets giving many lines of sufficient intensity (i.e., having a Rowland

TABLE III

Line	Rowland Intensity	Observed Values of log N*					Theoretical log N
		W 194	W 301	W 313	W 350	Mean	
4512.74.....	3	−0.25	.....	−0.23	.....	−0.24	−0.95
4518.03.....	3	.21	.....	.18	.....	.20	0.80
4527.32.....	3	.25	.....	.13	−0.10	.16	1.00
4533.25.....	4	.00	0.00	.00	.00	.00	0.00
4534.78.....	4	.10	− .06	.03	.04	.06	0.19
4535.58.....	3	.28	.16	.23	.18	.21	0.40
4536.06†.....	2	.21	.34	.08	.08	.18	0.70
4544.70†.....	3	−0.10	−0.17	−0.07	−0.10	−0.11	−1.00

* Where no value is recorded, the line does not occur on the plate concerned.

† 4536 and 4544 are slightly blended.

number greater than or equal to 1) and sufficiently clear of other lines.

The relative widths in a homogeneous set of readings were taken at $r = \frac{9}{10}$. The square of these widths is proportional to N, the number of atoms above a certain optical depth. The observed values of log N thus found are given in Table III. They may be compared with theoretical values given by the quantum theory,[2] which are in general agreement with observations of laboratory emission spectra. The divergence between the observed and theoretical values is very marked, the weaker lines appearing relatively much stronger in the solar spectrum.

[1] Russell, *Mt. Wilson Contr.*, No. 345; *Astrophysical Journal*, **66**, 347, 1927.

[2] Russell, *Proceedings of the National Academy of Sciences*, **11**, 314, 322, 1925.

TABLE IV

Line	Rowland Intensity	Element	$\lambda-\lambda_0$		
			$r=\frac{9}{10}$	$r=\frac{3}{4}$	$r=\frac{6}{10}$
4501.28	5	*Ti*$^+$	150	70	59
4502.23	2	*Mn*	75	30	*t*
4508.29	4	*Fe*	90	50	28
4511.90	1	*Cr*	50	*t*	.....
4512.75	3	*Ti*	72	37	17
4515.34	3	*Fe*$^+$	90	45	25
4517.54	3	*Fe*	85	38	15
4518.03	3	*Ti*	75	40	25
4520.23	3	*Fe*$^+$	70	40	26
4522.81	2	*Ti*	70	35	24
4523.41	1	*Fe*	40	.....	.....
4525.15	5	*Fe*	120	60	40
4526.93	3	*Ca*	83	48	26
4527.33	3	*Ti*	72	42	30
4531.16	5	*Fe*	104	70	48
4531.63	2	*Fe*	75	30	.....
4533.25	4	*Ti*	96	61	37
4533.97	6	***Ti***$^+$ *Co**	120	71	55
4534.17	1	*Fe*$^+$	70	26	.....
4534.79	4	*Ti*	87	50	35
4535.58	3	*Ti*	70	45	35
4536.06	2	*Ti*	75	42	30
4540.51	2	*Cr*	75	38	*t*
4540.71	2	*Cr*	72	35	*t*
4541.52	2	*Cr* ***Fe***$^+$	80	35	10
4544.02	1	*Ti*$^+$	55	20	.....
4544.70	3	*Ti*	85	40	30
4545.15	1	*Ti*$^+$	60	20	.....
4545.98	3	*Cr*	80	47	28
4548.77	2	*Ti*	60	40	30
4550.78	2	*Fe*	70	35	15
4554.04	8	*Ba*$^+$	150	85	70
4554.46	1	*Fe*	50	.....	.....
4554.99	2	*Cr*$^+$	70	10	.....
4555.49	3	*Ti*	63	35	14
4555.89	3	*Fe*$^+$	75	40	30
4556.14	4	*Fe*	105	60	36
4558.65	3	*Cr*$^+$	90	45	21
4560.10	2	*Fe*	50	20	.....
4563.77	4	*Ti*$^+$	150	70	45
4566.53	1	*Fe*	50	*t*	.....
4566.87	1	*Fe*	48	.....	.....
4568.77	1	*Fe*	70?	*t*	.....
4571.10	5	*Mg*	87	60	40
4571.98	5	*Ti*$^+$	120	75	50
4574.22	1	*Fe*	43	.....	.....
4574.73	2	*Fe*	60	30	*t*
4576.34	2	*Fe*$^+$	75	35	.....
4578.56	3	*Ca*	85	45	22
4580.06	3	*Cr*	80	49	25

* Bold-face type indicates the dominating element in a blend.

TABLE IV—*Continued*

Line	Rowland Intensity	Element	$\lambda-\lambda_0$		
			$r=\frac{9}{10}$	$r=\frac{3}{4}$	$r=\frac{6}{10}$
4580.42	1	*V*	70	*t*	.....
4582.83	1	*Fe*+	60	26	.....
4583.84	4	*Fe*+	140?	70	35
4584.73	1	*Fe*	35?	.....	.....
4584.83	2	*Fe*	35	28	.....
4585.88	4	*Ca*	105?	70	47
4586.38	1	*V*	50	*t*	.....
4587.14	2	*Fe*	60	20	.....
4588.21	3	*Cr*+	85	35	14
4589.95	3	*Ti*+	95	50	23
4591.40	2	*Cr*	65	35	12
4592.06	1	*Cr*+	60	*t*	.....
4592.53	2	*Ni*	80	40	10
4592.66	4	*Fe*	90	50	40
4594.13	2	*N V*	60	*t*	.....
4595.37	2	*Fe*	70	33	*t*
4596.07	2	*Fe*	70	30	.....
4596.42	1	*Cr*+	42	.....	.....
4598.13	3	*Fe*	77	45	20
4598.84	2	*Fe*?	57	28	.....
4599.37	2	*N*	50	25	.....
4599.76	3	*Cr*	70	40	26
4602.01	3	*Fe*	60	35	10
4602.95	6	*Fe*	90	63	36

OBSERVATIONS IN THE INTERVAL λλ 4500–4600

These observations, given in Table IV, are a homogeneous set, that is to say, they are taken from the same plate (W 194) and reduced with the same standardization curve. The wave-length, Rowland intensity, and element are given, followed by the width $\lambda-\lambda_0$ at $r=\frac{9}{10}$, $\frac{3}{4}$, and $\frac{6}{10}$. All the identified lines of Rowland intensity 1 or greater in the range λλ 4500 4600 are given, except those too badly blended to be measurable.

THE ADAMS-RUSSELL CALIBRATION OF ROWLAND'S SCALE

In the region observed, λλ 4500–4600, there are 17 lines of Rowland intensity 1, 21 lines of intensity 2, 20 lines of intensity 3, and 8 of intensity 4. Taking the measures of plate W 194 at $r=\frac{9}{10}$, we find the arithmetic mean widths of the lines grouped according to their Rowland numbers to be as shown in the second column of Table V. The square of the relative width gives the number N. The resulting observed values of log N in the second column of

Table V are to be compared with the values given by Adams and Russell,[1] which appear in the last column.

The divergence between the two series is, of course, an illustration of the general phenomenon of the difference in relative multiplet

TABLE V

Rowland Intensity	Mean Width	log N	
		Observed	Adams and Russell
1	0.053	0.00	0.00
2	.067	.20	0.54
3	.078	.34	1.06
4	0.106	0.60	1.59

intensities between absorption and emission spectra, since Adams and Russell derived their values of N by using the assumption that the absorption lines have the same relative strengths as the lines in laboratory emission spectra.

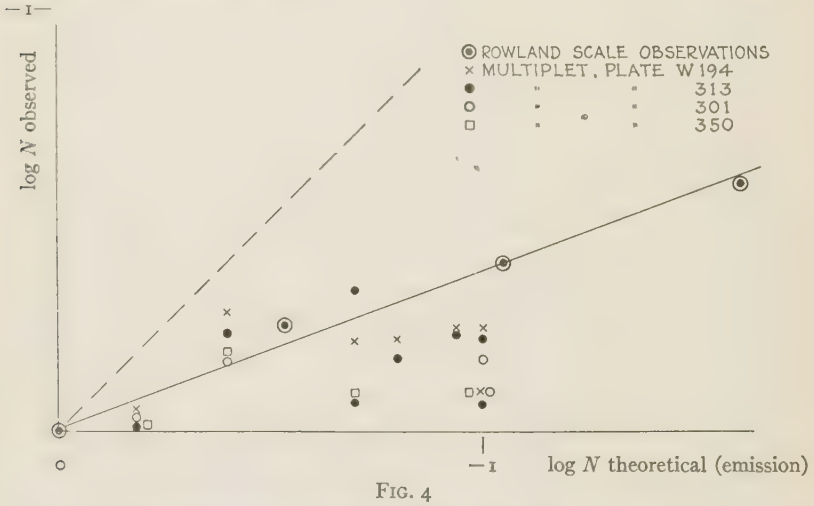

FIG. 4

This result seems to be established by the present series of observations beyond the limits of possible observational error. The values are shown graphically in Figure 4, the values of $-\log N$ as ob-

[1] *Mt. Wilson Contr.*, No. 358; *Astrophysical Journal*, **68**, 1, 1928. To be distinguished carefully from their analysis of stellar spectra (*Mt. Wilson Contr.*, No. 359; *Astrophysica Journal*, **68**, 9, 1928).

served in this series being plotted vertically against the theoretical (or emission) values of $-\log N$, which are entered horizontally. The points all fall unmistakably below the broken line representing equality between the two values.

The observed values of $-\log N$ for the Rowland intensities are plotted vertically (the o being shifted to give $\log N = 0$ for $R = 4$) against the values of Adams and Russell. The slope of the line joining them is roughly the same as that for the individual multiplet, as one would expect. The weaker multiplet lines show some divergence from the Adams-Russell line, which may be a real characteristic of the multiplet or may be due to the greater difficulty of measuring weaker lines.

It should be noted that the above divergence between theory and observation assumes the correctness of Unsöld's formula for the atomic scattering coefficient and the Unsöld-Milne theory of the formation of absorption lines. The present observational results may, alternatively, be regarded as a failure of Unsöld's theory. On this view, the multiplet intensities are normal and the Adams-Russell calibration is correct; but Unsöld's method deduces the wrong number of atoms from the relative widths of the lines.

It is a pleasure to record my gratitude to the Director of the Mount Wilson Observatory, to the staff generally, and to Dr. Dunham especially, for apparatus, help, and advice. My best thanks are due to Miss Ware for assistance in preparing the photometric curves. I am indebted to the Commonwealth Fund for the Fellowship which has made it possible for me to work at Mount Wilson.

Carnegie Institution of Washington
Mount Wilson Observatory
August 1930

Contributions from the Mount Wilson Observatory, No. 414
Reprinted from the *Astrophysical Journal*, Vol. LXXII, pp. 221–255, 1930
Printed in the U.S.A.

STEWARD OBSERVATORY

TEMPERATURE CLASSIFICATION OF THE SPECTRA OF EUROPIUM, GADOLINIUM, TERBIUM, DYSPROSIUM, AND HOLMIUM, λ 3850 TO λ 4700

By ARTHUR S. KING

ABSTRACT

Spectra of europium, gadolinium, terbium, dysprosium, and holmium, as given by *electric furnace, arc, and spark*, have been examined in the range λ 3850 to λ 4700 with regard to the segregation of *neutral* and *enhanced* lines, *temperature classification*, the occurrence of *hyperfine structure*, and other distinctive features. The total of 2277 lines listed is made up of 219 lines of europium, 627 of gadolinium, 733 of terbium, 534 of dysprosium, and 164 of holmium.

Measurements of wave-length were made for 666 lines. These are in part new lines prominent in the furnace but faint in the arc spectrum, partly known lines for which improved measurements could be obtained, and partly close doublets previously measured as single lines.

The spectra of *gadolinium*, *terbium*, and *dysprosium* are especially rich in *neutral lines* which are relatively strong in the furnace. *Europium* and *dysprosium* show *low-temperature lines* which have high intensity and are easily reversible, a type which is unusual in the spectra of the rare earths.

Lines having *hyperfine structure* are numerous in the spectra of *europium*, *terbium*, and *holmium*. The patterns of hyperfine holmium lines resemble those of praseodymium. The present material, taken in connection with data at hand for other rare earths, shows that hyperfine structure occurs regularly in the spectra of rare earths of *odd atomic number*, as far as their spectra have been observed with reference to this phenomenon, while for even-numbered rare earths the spectrum lines are uniformly without hyperfine structure.

The treatment of material in this paper is similar to that for the spectra of cerium and praseodymium,[1] the chief object being the temperature classification of the lines of both the neutral and the ionized atoms by means of a comparison of furnace spectra at several temperatures with the spectra of the arc and spark. Preliminary to this classification, it was necessary to distinguish between lines of the neutral and of the ionized spectra, and throughout the entire investigation attention has been paid to special features which may aid in an analysis of the spectra when these have been examined through a greater range of wave-length.

The spectral region examined is the most useful for comparison with celestial spectra, and, on account of the mingling of neutral

[1] *Mt. Wilson Contr.*, No. 368; *Astrophysical Journal*, **68**, 194, 1928.

and ionized lines in about equal proportions, shows best the characteristics of the spectra concerned. For the rare-earth spectra thus far studied, ionized lines are relatively numerous in the violet, and at shorter wave-lengths make up almost the whole spectrum, while in the blue-green and farther to the red the neutral lines predominate.

Between λ 3850 and λ 4700, as for cerium and praseodymium, the ionized lines are strong in the arc spectrum, and normally exposed spectrograms of arc and spark thus appear much alike. The furnace spectrum has a very different appearance, being made up of the neutral lines, often inconspicuous in the arc, while the ionized lines which persist in the furnace are faint as compared with their arc intensities. A mixture of caesium with the element studied has been used in the furnace for all five of the elements. The large supply of free electrons obtained by reason of the low-ionization potential of caesium produces a recombination of the ionized rare-earth atoms and thus suppresses the ionized lines at temperatures for which many of them show distinctly when the rare earth is vaporized alone. The spectral characteristics of the individual elements will be considered later in the paper.

EXPERIMENTAL METHOD

The second order of the 15-foot concave grating was used, giving a dispersion of 1.86 A per millimeter. For the classification of the lines the carbon-tube furnace was operated in vacuum at temperatures of approximately 2000°, 2300°, and 2600°–2800° C for the low, medium, and high stages, respectively.

The samples of rare earths used were oxides, prepared by G. Urbain, of Paris, and obtained by the writer from Professor G. Eberhard, of Potsdam. The impurities present in some of the samples were chiefly other members of the group of five under investigation, and an intercomparison of spectra usually indicated clearly the source of the impurity lines.

All these elements belong to the scarcer group of rare earths, and to conserve the material the oxide was usually placed in a graphite combustion boat located midway in the furnace tube. This tended to avoid explosive expulsion of the oxide at the first heating. For

the arc and spark, the oxide was either held in the lower electrode of carbon or graphite, or, when the elimination of the carbon spectrum was desirable, mixed with silver filings in a bored-out silver electrode.

MEASUREMENTS OF WAVE-LENGTH

Most of the existing wave-length tables for these elements leave much to be desired. The scarcity of the substances has resulted in measurements by only a few observers, for the most part before modern standards of wave-length were established. In the present work 666 lines were measured, chiefly in the furnace spectrum from iron standards or from good lines of titanium or vanadium given by impurities in the graphite tube. Part of these wave-lengths are for the stronger known lines, both neutral and enhanced, for which good three-place values could be obtained on account of their sharpness in the present spectrograms. Others are for neutral lines distinct in the furnace spectrum, though faint in the arc and not previously measured. A third group consists of close doublets, measured by former observers as single lines but clearly resolved on my plates. Such a pair often consists of a neutral and an ionized line, and these were measured in either the furnace or the arc spectrum, or in both, to obtain the best value for each component. Measurement of hyperfine lines was usually deferred until plates of higher dispersion had become available, since the components are often graduated in intensity, as well as in spacing, and a single wave-length for such a pattern is of limited value. Some of these wave-lengths, as well as those of some faint single lines, are given to only one decimal place.

The writer was assisted in the work of measurement and in making up the tables by Miss Brayton, of the Computing Division.

HYPERFINE STRUCTURE

In studying the spectra of lanthanum[1] and praseodymium[2] it was noted that a large proportion of the lines of these elements are complex. Such lines of lanthanum form close patterns of at least three components, while the praseodymium patterns are wider and, when resolved, show regularly six components. For some of these the spac-

[1] *Mt. Wilson Contr.*, No. 326; *Astrophysical Journal*, 65, 86, 1927.

[2] *Loc. cit.*

ing increases toward shorter, and for others toward longer waves. The structure of praseodymium lines was examined further under high dispersion by the writer, and then more extensively by H. E. White[1] and by Gibbs and Gartlein.[2]

The fact that lanthanum and praseodymium have odd atomic numbers, while the even-numbered elements, cerium, neodymium, and samarium, were found by the writer to show no complex lines beyond occasional doublets, suggested that the frequent occurrence of hyperfine lines might be a characteristic of the odd-numbered rare earths. This is fully borne out by the present investigation, in which complex lines were found to be numerous in the spectra of europium (63), terbium (65), and holmium (67), while the lines of gadolinium (64) and dysprosium (66) show no complexity. With the exception of illinium (61), we have data concerning hyperfine structure for elements 57–67 inclusive; and, as an extension of the evidence, it may be added that my preliminary spectrograms of erbium (68) show no hyperfine lines, while a letter from Dr. Meggers states that the lines of lutecium (71) have hyperfine structure and those of ytterbium (70) are sharp. Complex line structure thus seems to be general for the odd-numbered rare earths. Although data are lacking for the spectra of illinium (61) and thulium (69), both may be expected to contain hyperfine lines.

Hyperfine structure, according to modern theory,[3] arises from the influence of nuclear spin on the outer part of the atom. The components of complex lines can then be expected to result from the slight changes of energy-level due to the magnetic moment of the nucleus. A consequence of the present observations would be that in the rare-earth atoms of odd atomic number the interaction between the nuclear moment and the outer electrons is much more pronounced than for the general run of elements, which only occasionally exhibit hyperfine structure. The hyperfine patterns of holmium and praseodymium are comparable in size and similar in appearance to those of bismuth, the element for which this phenomenon has been most carefully studied.

[1] *Physical Review*, **34**, 1397, 1929.

[2] Unpublished.

[3] Pauling and Goudsmit, *Structure of Line Spectra*, 1930.

EXPLANATION OF THE TABLES

In Tables I to V the first column gives wave-lengths on the international system. The sources of these, when taken from lists already available, are noted in the descriptions of the several spectra. An asterisk (*) refers to a note at the end of the table, and a dagger (†) indicates that the line was measured during this investigation.

The second and third columns give intensities for the arc and high-temperature furnace, respectively. The addition of *R* or *r* indicates complete or partial self-reversal. A minus sign after intensity 1 means that the line is very faint on the arc spectrogram examined, which was of such general intensity as not to show serious overexposure of the stronger lines. The intensities at medium and low temperature, which were required for the classification, are omitted in order to condense the tables. The relative intensities of the lines at these lower temperatures are indicated in some degree by the class designations in the last column. Thus the more decided low-temperature lines are in class I, and those strengthening more rapidly with rising temperature in class II. Lines of class III are faint or absent at low temperature, but strong at the medium stage, while lines of class IV appear only at high temperature and those of class V only in the arc.

For the spectra of europium, terbium, and holmium, Arabic numbers denoting the probable number of hyperfine components making up the given line are placed after the class numbers. The addition of *v* or *r* to the number indicating hyperfine structure means that the pattern in question has wider spacing of the violet or of the red components.

TABLE I

TEMPERATURE CLASSIFICATION OF EUROPIUM LINES

λ (I.A.)	Intensities		Class, No. Comps.	λ (I.A.)	Intensities		Class, No. Comps.
	Arc	Fur.			Arc	Fur.	
3884.76.....	50	8	III, 3	3988.22.....	3	.....	V E, 3
3891.46.....	1	.....	V, 2	3988.55.....	1	.....	V E, 2
3893.40.....	4	?	IV ?, 4	3992.36.....	2	.....	V
3896.84.....	6	2	IV, 2	3993.91.....	1	.....	V E
3897.80.....	10	3	IV, 2	3996.00.....	2	.....	V E
3898.80.....	12	4	IV, 2	4000.72.....	3	2	IV, 2
3900.15.....	8	.....	V E, 3	4000.80.....	2	1	IV, 2
3900.50.....	6	.....	V E, 2	4003.74.....	2	.....	V E
3901.70.....	1	.....	V, 2	4010.42.....	4	2	IV, 2
3903.18.....	8	2	IV, 2	4011.71.....	25	1?	V E
3907.113*†..	300*R*	30	III E, 4	4012.83.....	3	.....	V E
3909.89.....	3	.....	V, 2	4014.39.....	4	2	IV, 2
3910.13.....	2	.....	V, 2	4014.66.....	2	1	IV, 2
3914.14.....	4	.....	V, 2	4016.72.....	10	6	III, 2
3915.24.....	3	.....	V E, 2	4017.63.....	15	.....	V E, 2
3915.62.....	6	2	IV, 2	4025.97.....	2	.....	V, 2
3915.98.....	20	4	III, 2	4026.62.....	6	1?	IV ?, 2
3916.80.....	4	2	IV, 2	4028.64.....	{2	1	IV
3917.30.....	30	5	III, 3		{5	2	IV, 2
3917.68.....	4	.....	V, 2	4030.04.....	20	8	III, 2
3918.48.....	8	4	IV, 2	4036.11.....	12	6	IV, 4
3919.12.....	6	.....	V E, 2	4039.20.....	30	12	III, 2
3927.46.....	2	1?	IV ?	4040.48.....	15	5	III, 3
3928.92.....	6	.....	V, 2	4042.05.....	4	.....	V E, 2
3929.88.....	4	.....	V, 2	4058.49.....	2	.....	V, 2
3930.425*†..	15?	2?	III E	4059.47.....	6	.....	V E, 2
3930.504†...	300*R*	50	III E, 3	4062.23.....	3	.....	V E, 2
3935.88.....	2	.....	V E	4065.48.....	4	2	IV
3936.64.....	3	1?	IV, 2	4066.05*....	2?	.....	V E
3941.55.....	3	.....	V E, 2	4069.02*....	4	1	IV, 3
3942.21.....	6	.....	V, 2	4071.25.....	8	4	III, 2
3942.35.....	4	1?	IV ?	4078.23.....	7	3	III, 2
3943.10.....	12	.....	V E, 2	4085.36*....	15	1	IV E, 2
3949.57.....	10	3	III, 4	4087.83.....	5	.....	V E
3955.73.....	20	5	III, 4	4096.84.....	8	.....	V E, 2
3957.91.....	4	.....	V E, 2	4102.72.....	3	2	IV
3961.15.....	4	2	IV, 3	4103.87*....	2	?	IV, 2
3963.63.....	4	2	IV, 2	4106.87.....	15	6	III, 2
3964.48.....	6	4	IV, 4	4112.08.....	{12	.....	V E, 2
3964.92.....	20	2	IV E, 2		{6	.....	V E, 3
3967.12.....	5	5	III, 3	4116.97.....	1	.....	IV
3969.23.....	8	2?	IV E, 2	4119.35*....	12	.....	V E, 3
3971.899*†..	20?	3?	III E	4127.30.....	15	6	III, 2
3971.989†...	400*R*	60	III E, 3	4129.639*†..	25?	4?	III E
3976.87.....	3	1	IV, 2	4129.734†...	500*R*	80	III E, 3
3978.45.....	20	3	III, 3	4136.62.....	2	.....	V E, 2
3979.08.....	4	.....	V E, 3	4137.11*....	10?	5	III, 2
3979.62.....	3	.....	V E, 2	4141.03.....	5	.....	V E, 2
3985.35.....	2	1	IV, 2	4141.73.....	7	.....	V E, 2
3986.64.....	15	{3	IV, 2	4145.26.....	2	.....	V E, 2
		{1		4145.97.....	2	.....	V E, 2

TABLE I—*Continued*

λ (I.A.)	Intensities		Class, No. Comps.	λ (I.A.)	Intensities		Class, No. Comps.
	Arc	Fur.			Arc	Fur.	
4151.56.....	6	.....	V E, 2	4352.20.....	2	.....	V E, 2
4157.81*....	20	?	IV, 2	4354.82.....	20	4	III
4172.81.....	10	.....	V E, 3	4355.10.....	30	.....	V E
4175.22.....	3	.....	V E, 2	4357.71.....	1	.....	V E
4176.66.....	2	2	III, 2	4360.04.....	1	.....	V, 2
4182.28*....	20	?	III, 2	4361.57.....	1	.....	V E
4194.46.....	2	2	IV, 2	4368.43.....	1	.....	V E, 3
4195.40.....	3	.....	V E, 2	4369.46.....	6	.....	V E, 3
4202.05.....	5	.....	V E, 2	4370.43.....	8	3	III, 2
4202.65.....	8	4	III, 3	4372.22.....	1	.....	V E
4204.909*†..	30?	5?	III E	4375.14.....	1	.....	V E
4205.046†...	600*R*	100	III E, 3	4383.02.....	15	.....	V E, 2
4209.09.....	4	2	III, 3	4387.85.....	20	10	III, 2
4220.71.....	3	2	IV, 2	4391.35.....	3	.....	V E, 3
4221.10.....	1	.....	V E	4397.73.....	1	.....	V E
4222.33.....	5	3	IV, 2	4399.34.....	1	.....	V, 2
4224.30.....	3	.....	V	4405.28.....	3	1	IV, 2
4229.34.....	3	.....	V E, 2	4407.07.....	2	.....	V E, 2
4232.48.....	5	.....	V E, 2	4413.55*....	2	1	IV, 3
4234.13.....	2	.....	V E	4417.25.....	8	4	III, 3
4235.14.....	2	.....	V, 2	4419.65.....	1	.....	V E, 2
4237.52.....	4	.....	V E, 2	4426.41.....	1	.....	V E, 2
4238.72.....	2	.....	V E, 2	4429.76.....	1	.....	V E
4244.79.....	10	6	III, 2	4434.81.....	8	.....	V E
4247.07.....	3	.....	V E, 3	4435.473†...	20?	10	III E
4249.49.....	3	.....	V, 4	4435.602†...	400*r*	80	III E, 3
4253.85.....	2	.....	V E	4464.94.....	10	.....	V E
4255.27.....	2	1	IV, 2	4471.99.....	3	2	IV, 2
4258.13.....	4	3	IV, 3	4477.26.....	2	.....	V, 2
4269.48.....	1	.....	V, 2	4485.17.....	6	.....	V E, 2
4270.52.....	2	.....	V E	4488.30.....	2	.....	V E, 2
4276.16.....	3	.....	V E, 2	4516.55.....	2	.....	V, 3
4281.90.....	1	.....	V E	4517.36.....	1	.....	V
4284.70.....	2	1?	IV, 3	4522.602*†..	200*r*	50	III E, 4
4287.45.....	1	.....	V	4526.69.....	6	3	III, 2
4288.60.....	1	.....	V E, 2	4535.59*....	15	8?	III, 2
4292.96.....	2	.....	V, 3	4539.29.....	2	.....	V E, 2
4293.92.....	2	.....	V E	4586.46*....	3	.....	V, 3
4295.43.....	1	.....	V E	4593.993†...	500*R*	200*R*	II
4298.73*....	30	4?	III	4597.35*....	5	2	IV, 3
4300.84.....	1	.....	V E	4616.53.....	3	?	IV, 3
4317.67.....	1	.....	V E	4625.32.....	6	3?	III, 2
4322.58.....	6	4	III, 3	4627.122†...	300*R*	150*R*	II
4329.38.....	20	8	III, 3	4641.40.....	1	.....	V
4330.00*....	20	?	III?, 2	4644.25.....	4	.....	V
4330.62.....	15	.....	V E	4650.47.....	6	2?	IV, 2
4331.20.....	8	4	III, 2	4651.56.....	1	.....	V
4334.16.....	1	.....	V	4656.70.....	8	3	III, 2
4334.74.....	1	.....	V E	4658.60.....	4	?	IV, 2
4337.67.....	25	8	III, 2	4660.35.....	10	3?	III, 2
4343.26.....	4	2	IV, 2	4661.865†...	250*R*	100*R*	II
4345.91.....	12	5	III, 2	4665.07.....	3	.....	V, 2
4349.78.....	1	.....	V, 3	4671.20.....	2	1?	IV, 2
4351.28.....	1	.....	V E	4675.46.....	1	?	IV, 2

NOTES TO TABLE I

λ	
3907.113	Line measured is unresolved triplet; faint fourth component to violet not measurable
3930.425	Not fully resolved from strong triplet
3971.899	Not fully resolved from strong triplet
4066.05	Blend *Gd* I
4069.02	Violet component stronger
4085.36	Red component shows in furnace
4103.87	Furnace line probably *Ho*
4119.35	Components partially resolved
4129.639	Not fully resolved from strong triplet
4137.11	Blend *Gd* II in arc
4157.81	Blend *Gd* I in furnace
4182.28	Furnace line largely *C*
4204.909	Not fully resolved from strong triplet
4298.73	Close to *Ti* in furnace
4330.00	Blend *V* in furnace
4413.55	Components partially resolved
4522.602	Line measured is unresolved triplet; faint line to violet not measurabl
4535.59	Blend *Ti* in furnace
4586.46	Very diffuse
4597.35	Shaded to violet

TABLE II

Temperature Classification of Gadolinium Lines

λ (I.A.)	Intensities		Class	λ (I.A.)	Intensities		Class
	Arc	Fur.			Arc	Fur.	
3836.90.....	100	2?	IV E	3935.393†...	40	30	II
3839.63.....	60	1	IV E	3938.13.....	8	.....	V E
3840.264†...	6	5	II	3938.98.....	12	.....	V E
3842.20.....	80	1	IV E	3941.802†...	40	25	II
3843.275†...	40	10	I	3942.643†...	60	30	I
3844.58.....	125	2	IV E	3943.244†...	30	20	II
3850.69.....	150	?	IV E	3943.631†...	30	20	III
3851.00.....	200	4	III E	3945.548*†..	150	100	I
3852.50.....	150	?	IV E	3945.753†...	2	8	III A
3855.57.....	20	.....	V E	3947.05.....	6	6	IV
3863.05.....	10	.....	V E	3949.23.....	8	.....	V E
3866.989†...	30	15?	I	3952.01.....	40	1	V E
3867.62†....	8	6?	II	3953.372†...	80	40	I
3874.476†...	8	6	II	3957.69.....	150	2	IV E
3875.33.....	10	.....	V E	3958.681†...	8	30	III A
3884.71.....	4	.....	V E	3959.437†...	30	.....	V E
3887.16.....	10	.....	V E	3959.526†...	50	.....	V E
3887.739†...	8	15	III A	3960.113†...	15	30	III A
3888.94.....	12	5	III	3962.12.....	6	.....	V E
3890.415†...	8	10	IV	3963.66.....	15	.....	V E
3890.88.....	4	.....	V E	3964.97*†...	1	1	IV
3892.75.....	4	4	IV	3965.03*†...	3	4	III
3894.72.....	200	6	IV E	3966.279†...	60	60	II
3895.25.....	20	.....	V E	3966.84.....	4	.....	V E
3895.791†...	40	.....	V E	3968.34.....	15	.....	V E
3895.960†...	4	8	IV A	3969.004†...	60	50	I
3896.45.....	4	.....	V E	3969.28.....	40	.....	V E
3897.323†...	8	8	IV	3970.199†...	4	5	IV
3898.46.....	4	.....	V E	3971.09.....	20	.....	V E
3902.42.....	150	4	IV E	3971.77.....	40	1	V E
3902.718†...	30	25	II	3972.20.....	8	.....	V E
3904.293†...	20	25	II	3972.713†...	30	40	I
3905.653†...	30	25	II	3974.06.....	40	1	IV E
3907.12.....	6	5	IV	3974.241†...	2	.....	V E
3908.149†...	2	.....	V E	3974.819†...	30	40	II
3909.25.....	4	4	IV	3975.13.....	8	.....	V E
3909.945†...	6	8	III			2	IV
3910.23.....	2	.....	V E	3979.346*†..	60	80	II A
3911.66.....	4	5	IV	3979.759†...	2	2	IV
3912.76.....	8	10	IV	3980.14.....	2	2	IV
3913.79.....	6	.....	V E	3983.04.....	15	.....	V E
3916.58.....	300	3	IV E	3984.82.....	2	6	III A
3916.672†...	10	12	IV	3985.67.....	2	1	IV
3918.07.....	15	.....	V E	3987.24.....	60	2	IV E
3918.26.....	15	.....	V E	3987.840†...	50	50	II
3923.249†...	30	1	IV E	3989.27.....	8	.....	V E
3923.333†...	8	.....	V E	3991.70.....	2	.....	V E
3924.23.....	2	1	IV	3992.696†...	20	40	II A
3926.688†...	12	15	IV	3993.26.....	20	1	IV E
3932.95.....	15	.....	V E	3994.19.....	40	1	IV E
3934.790*†..	200	50	I	3996.34.....	40	.....	V E

TABLE II—*Continued*

λ (I.A.)	Intensities		Class	λ (I.A.)	Intensities		Class
	Arc	Fur.			Arc	Fur.	
3997.78.....	20	.....	V E	4049.197†...	15	40	III A
4000.16.....	4	10	IV A	4049.44.....	150	1	IV E
4001.20.....	30	tr	IV E	4049.548†...	4	8	III A
4001.63.....	2	2	IV	4049.90.....	200	2	IV E
4001.95.....	4	.....	V E	4050.373*†..	10	20	III A
4003.37.....	4	6	IV	4051.62.....	2	6	IV
4003.85.....	6	.....	V E	4053.31.....	100	.....	V E
4004.93.....	20	.....	V E	4053.643†...	200	150	I
4006.975†...	6	30	III A	4054.731†...	80	75	I
4008.339†...	25	50	II A	4056.04.....	2	.....	V E
4008.91*....	30	?	V E	4058.222†...	250	200	I
4009.21.....	8	.....	V E	4059.39.....	6	.....	V E
4013.430†...	6	8	III	4059.876†...	40	50	III
4013.83.....	20	.....	V E	4060.933†...	1	3	III A
4013.92.....	8	.....	V E	4061.163†...	4	20	III A
4015.21.....	6	6	III	4061.30.....	10	.....	V E
4015.592†...	6	10	III	4061.85.....	4	8	III A
4017.255†...	10	8	III	4062.61.....	50	.....	V E
4017.720†...	20	12	III	4063.45.....	150	1	IV E
4019.739†...	12	40	II A	4065.63.....	2	.....	V E ?
4020.42.....	2	1	IV	4066.11.....	10	20	III A
4021.91.....	2	2	IV	4068.358†...	15	30	III A
4022.33.....	15	.....	V E	4068.77.....	10	20	III A
4023.154†...	80	100	I	4070.292†...	40	1	IV E
4023.355†...	60	100	I	4070.396†...	20	1	IV E
4023.76.....	2	3	IV	4073.21.....	40	1	IV E
4027.613†...	12	50	III A	4073.78.....	200	2	IV E
4028.155†...	40	50	III	4075.47.....	4	.....	V E
4030.881†...	30	50	III	4078.47.....	150	2	IV E
4032.11.....	2	3	IV	4078.705†...	300	200	I
4033.493†...	30	50	III	4080.534†...	15	30	II A
4034.05.....	2	1	IV	4080.78.....	4	3	IV
4034.38.....	2	4	III A	4083.710†...	30	50	III
4035.396†...	20	60	II A	4083.95.....	2	.....	V E
4036.842†...	15	40	III A	4084.35.....	2	1	IV
4037.34.....	200	2	IV E	4084.71.....	4	.....	V E
4037.90.....	125	1	IV E	4085.60.....	200	3	IV E
4038.28.....	2	3	IV	4087.330†...	2	8	III A
4039.50.....	10	.....	V E	4087.71.....	20	.....	V E
4039.67.....	15	.....	V E	4087.847†...	2	10	III A
4042.50.....	2	2	IV	4088.81.....	2	.....	V E
4042.77.....	4	.....	V E	4090.418†...	40	30	I
4043.712†...	15	40	III A	4090.747†...	2	3	III
4044.030†...	4	20	III A	4091.754†...	4	8	III A
4045.013†...	60	100	I	4091.966†...	2	3	III
4045.11.....	12	.....	V E	4092.718*†..	100	80?	I
4045.862*†..	?	30	III	4093.723†...	15	30	III A
4046.84.....	15	.....	V E	4094.48.....	30	1	IV E
4047.087†...	12	40	III A	4098.04.....	4	.....	V E
4047.81.....	8	.....	V E	4098.64.....	300	4	IV E
4048.59.....	8	.....	V E	4098.90.....	80	1	IV E
4048.82.....	4	8	III A	4100.269†...	60	50	I

TABLE II—*Continued*

λ (I.A.)	Intensities		Class	λ (I.A.)	Intensities		Class
	Arc	Fur.			Arc	Fur.	
4104.99.....	8	12	III	4188.77†....	2	1	IV
4105.79.....	2	.....	V E	4189.10†....	2	1	IV
4108.42.....	6	.....	V E	4190.16.....	6	10	III
4109.493†...	2	10	III A	4190.779†...	200	200	I
4110.432†...	6	.....	V E	4191.06.....	200	2	IV E
4110.609†...	20	.....	V E	4191.628†...	125	100	I
4111.251†...	2	3	III A	4193.14.....	6	.....	V E
4111.45.....	60	.....	V E	4197.06.....	15	.....	V E
4111.74.....	12	.....	V E	4197.68.....	80	1	IV E
4112.93.....	6	8	III	4200.28.....	2	2	IV
4113.78.....	2	.....	V E	4202.49.....	8	.....	V E
4115.37.....	8	.....	V E	4204.839†...	100	1	V E
4119.199†...	6	4	III	4206.76.....	2	3	III
4119.380†...	12	.....	V E	4208.064†...	6	6	III
4121.05.....	2	2	III	4212.01.....	200	2	IV E
4123.00.....	2	.....	V E	4214.97.....	150	?	IV E
4123.40.....	2	1	IV	4216.49.....	2	2	IV
4123.59†....	2	4	III A	4217.15.....	100	1	IV E
4125.76.....	4	5	IV	4222.580†...	2	4	III A
4127.3†.....	2	4	IV A	4222.98.....	4	.....	V E
4127.68.....	4	.....	V E	4224.22.....	4	10	III A
4129.2†.....	2	3	IV	4225.028†...	20	50	II A
4130.35.....	300	3	V E	4225.156†...	15	.....	V E
4131.48.....	40	.....	V E	4225.264†...	4	3	III
4132.28.....	200	2	IV E	4225.846†...	300	300r	I
4134.169†...	100	100	I	4227.14.....	20	.....	V E
4137.09.....	50	.....	V E	4229.77.....	15	.....	V E
4138.020†...	2	5	III A	4232.46.....	4	.....	V E
4140.450†...	12	.....	V E	4232.941†...	4	3	IV
4140.567†...	2	3	III	4235.03.....	2	.....	V E
4141.00.....	2	.....	V E	4235.890†...	8	.....	V E
4144.240†...	6	8	III	4238.77.....	80	1	V E
4148.864*†..	20	40	II A	4240.67.....	2	6	III A
4149.475†...	8	10	III	4241.30.....	8	.....	V E
4150.61.....	2	.....	V E	4243.85.....	15	.....	V E
4151.59.....	2	.....	V E	4245.353†...	12	25	III A
4153.53.....	12	.....	V E	4246.52.....	15	.....	V E
4154.86.....	20	.....	V E	4250.281†...	4	10	III A
4157.781†...	15	50	II A	4251.76*....	300	6	IV E
4158.469†...	2	2	III	4253.36.....	150	1	IV E
4162.72.....	60	.....	V E	4253.62.....	150	.....	V E
4163.111*†..	30	15	III	4254.03.....	4	8	III A
4167.157†...	6	.....	V E	4255.44.....	4	.....	V
4167.271†...	12	30	II A	4255.54.....	4	.....	V
4170.11*....	10	.....	V E	4260.123†...	125	100	II
4171.72.....	8	8	III	4262.094*†..	250	40	{III V E
4173.56.....	10	.....	V E				
4175.539†...	200	150	I	4266.234†...	2	4	III A
4182.76.....	4	8	III A	4266.601†...	125	100	II
4183.65†....	2	2	IV	4267.010†...	80	80	II
4184.25.....	300	3	IV E	4268.73.....	30	.....	V E
4188.06.....	10	.....	V E	4270.26.....	6	10	III

TABLE II—*Continued*

λ (I.A.)	Intensities		Class	λ (I.A.)	Intensities		Class
	Arc	Fur.			Arc	Fur.	
4270.80.....	2	4	III A	4336.50.....	2	2	IV
4273.25.....	4	8	III A	4336.71.....	2	2	IV
4274.167†...	40	60	II	4337.504*†..	15	20	III
4278.20.....	2	.....	V E	4340.25.....	2	2	IV
4280.50.....	200	5	IV E	4340.47*....	2	1	IV
4282.78.....	4	.....	V E	4341.9†.....	2	2	IV
4284.953†...	4	8	III A	4341.24.....	150	2	IV E
4285.483†...	2	5	III A	4342.18.....	300	3	IV E
4285.822†...	100	40	III	4344.34.....	20	.....	V E
4286.127†...	100	60	II	4344.45.....	4	.....	V E
4289.91.....	8	.....	V E	4346.460†...	400	250	I
4290.065†...	6	10	III	4346.624†...	200	150	I
4292.76.....	2	.....	V E	4347.25.....	40	.....	V E
4294.76.....	2	2	IV	4353.74.....	8	3	III
4296.04.....	150	2	IV E	4354.02.....	4	.....	V E
4296.30.....	40	.....	V E	4357.80.....	2	8	III A
4296.509†...	2	3	IV	4359.14.....	4	.....	V E
4296.90.....	6	15	III A	4359.61.....	2	.....	V E
4297.15.....	40	.....	V E	4360.12.....	2	3	IV
4298.39.....	2	.....	V E	4360.90.....	40	1	IV E
4299.301†...	80	40	III	4364.13.....	2	.....	V E
4303.46.....	2	.....	V E	4366.51.....	2	5	IV A
4304.90.....	30	.....	V E	4368.53.....	2	1	IV
4306.348†...	200	150	I	4369.161†...	20	20	III
4308.24.....	6	.....	V E	4369.77.....	80	3	IV E
4308.392†...	2	3	III	4370.183†...	30	50	III
4309.295†...	60	50	III	4372.01.....	2	1	IV
4309.93.....	2	1	IV	4373.831†...	300	150	I
4310.95.....	30	.....	V E	4374.24.....	4	.....	V E
4313.851†...	200	200	I	4374.986†...	4	4	IV
4314.409†...	80	60	III	4376.083†...	8	20	III A
4316.05.....	150	1	IV E	4378.53.....	30	30	III
4316.23.....	20	.....	V E	4379.52.....	2	1	IV
4320.521†...	80	60	III	4380.63.....	20	.....	V E
4321.111†...	60	.....	V E	4382.04.....	15	.....	V E
4321.202†...	100	100	II	4383.16.....	30	.....	V E
4322.012†...	2	5	III A	4386.18.....	6	3	IV
4322.18.....	20	1	IV E	4387.15.....	6	3	IV
4323.60*....	4	3	IV	4387.63.....	100	2	IV E
4324.04.....	20	1	IV E	4388.98.....	2	.....	V E
4324.57.....	4	.....	V E	4389.893†...	30	20	III
4325.568†...	30	.....	V E	4390.003†...	10	?	?
4325.691†...	200	200	I	4390.95.....	80	1	IV E
4326.29.....	4	.....	V E	4391.45.....	15	.....	V E
4327.106*†..	250	200	I	4391.652†...	2	3	IV
4328.943†...	12	25	III A	4392.063†...	100	50	III
4329.585†...	60	50	III	4392.77.....	2	1	IV
4330.27.....	2	.....	V E	4394.71.....	4	.....	V E
4330.58.....	100	2	IV E	4397.388†...	2	3	IV
4331.385†...	40	40	III	4397.50*....	60	.....	V E
4333.20.....	6	4	III	4400.17.....	4	.....	V E
4335.27.....	2	.....	V E	4400.765†...	15	20	III

TABLE II—*Continued*

λ (I.A.)	Intensities		Class	λ (I.A.)	Intensities		Class
	Arc	Fur.			Arc	Fur.	
4401.849†...	300	150	I	4465.78.....	6	12	III A
4403.129†...	100	40	III	4466.547†\	125	?	V E
4403.224†...	8	4	IV	4466.604†/..		15	III
4406.68*....	60	?	IV E	4467.088†...	150	40	III
4407.19.....	2	3	IV	4467.17.....	20	.....	V E
4408.25*....	80	?	IV E	4468.18.....	2	.....	V E
4409.264†...	40	30	III	4470.45.....	2	1	IV
4411.160†...	150	80	I	4471.28.....	60	1	V E
4413.44*....	4	4	III	4473.282†...	20	40	II A
4414.162†...	200	60	III	4474.131†...	150	40	III
4414.741†...	200	100	I	4475.08.....	2	2	IV
4415.029†...	6	10	III	4476.144†...	300	150	I
4415.42.....	10	5	IV	4478.79.....	80	1	IV E
4415.63.....	2	6	III A	4479.834†...	2	3	III
4415.97.....	2	2	IV	4481.06.....	100	2	IV E
4419.03.....	150	2	IV E	4483.32.....	80	1	IV E
4420.64.....	2	1	IV	4484.49.....	2	.....	V E
4421.21.....	30	.....	V E	4484.710†...	30	15	III
4422.409†...	300	150	I	4485.484†...	8	30	II A
4424.09.....	4	.....	V E	4486.34.....	12	.....	V E
4425.01.....	15	10	III	4486.908†...	125	100	II
4426.13.....	12	.....	V E	4488.44.....	12	.....	V E
4427.58.....	10	.....	V E	4488.57.....	8	12	III
4428.93.....	2	6	III A	4489.77.....	2	3	III
4430.631†...	300	150	I	4491.27.....	2	6	III
4431.769†...	15	20	III	4492.03.....	2	2	IV
4433.65.....	8	.....	V E	4494.84.....	4	.....	V E
4436.103*†..	20	30?	III?	4496.61.....	8	12	III
4436.226†...	40	1	IV E	4497.133†...	150	100	I
4437.84*....	6	?	IV ?	4497.33.....	40	15	III
4438.143†...	4	.....	V E	4497.55.....	2	1	IV
4438.262†...	60	3	IV E	4498.26.....	60	1	IV E
4438.463†...	4	4	IV	4499.89.....	2	6	III A
4444.95.....	4	4	IV	4500.65.....	2	.....	V E
4445.53.....	2	1	IV	4500.89.....	2	.....	V E
4446.46.....	30	1	IV E	4501.49.....	2	2	IV
4447.34.....	2	1	IV	4502.30.....	2	4	III A
4448.13.....	2	8	IV A	4503.17.....	8	5	III
4449.01.....	4	3	IV	4503.803†...	8	30	II A
4449.36.....	6	4	IV	4504.96.....	4	10	III A
4449.95.....	2	.....	V E	4506.226†...	200	125	I
4452.71.....	8	12	IV	4506.337†...	60	1	IV E
4453.92.....	6	.....	V E	4506.933†...	8	.....	V E
4454.71.....	4	3	III	4507.065†...	4	8	III A
4456.67.....	2	1	IV	4507.66.....	12	10	III
4458.35.....	2	1	IV	4508.03.....	2	1	IV
	2	1	IV	4508.986†...	10	8	III
4461.079†...	2	1	IV	4509.079†...	6	.....	V E
4461.35.....	6	10	III	4510.38*....	4	.....	V E
4462.78.....	20	12	III	4512.43.....	2	5	III A
4463.23.....	12	.....	V E	4513.80.....	4	8	III A
4464.745†...	80	25	III	4514.504†...	40	.....	V E

TABLE II—*Continued*

λ (I.A.)	Intensities		Class	λ (I.A.)	Intensities		Class
	Arc	Fur.			Arc	Fur.	
4516.980†...	10	6	III	4582.49.....	40	.....	V E
4517.075†...	2	.....	V E	4583.083†...	125	80	III
4518.76.....	2	6	III A	4583.37.....	2	.....	V E
4519.661†...	200	150	I	4584.27.....	8	15	III A
4520.069†...	15	.....	V E	4585.16.....	2	2	IV
4520.77.....	2	4	IV A	4586.07.....	4	3	IV
4521.291†...	12	.....	V E	4586.97.....	25	15	III
4521.919†...	15	.....	V E	4588.72.....	2	.....	V E
4522.43.....	2	2	IV	4589.54.....	2	8	IV A
4522.82*....	80	{20	III	4590.00.....	2	1	IV
		{ ?	V E	4594.28.....	2	1	IV
4523.848†...	2	.....	V E	4595.37.....	4	6	III
4524.09.....	15	15	III	4596.98.....	60	1	IV E
4524.33.....	2	.....	V E	4597.91*....	100	4	IV E
4526.01.....	2	4	IV A	4598.897†...	100	80	III
4531.12.....	6	12	III A	4601.03.....	100	1	IV E
4531.79.....	10	15	III	4602.932†...	40	60	II
4533.49.....	6	5	IV	4606.06.....	8	2	IV
4534.74*....	2	?	?	4606.64.....	2	.....	V E
4536.96.....	15	15	III	4608.00.....	4	.....	V E
4537.820†...	200	150	I	4608.583†...	8	30	III A
4539.18.....	2	2	IV	4611.04.....	4	2	IV
4540.01.....	20	.....	V E	4611.60.....	2	1	IV
4541.22.....	2	1	IV	4614.498†...	150	100	III
4542.034†...	125	100	II	4619.14.....	10	5	III
4542.72.....	8	15	III A	4622.187†...	2	4	III A
4543.60.....	2	4	IV A	4622.311†...	4	7	III
4544.23.....	8	20	III A	4624.427†...	20	40	III A
4545.11.....	1	3	IV A	4627.62.....	6	.....	V E
4548.011†...	80	50	III	4630.50.....	6	4	III
4549.47.....	2	6	III A	4636.649†...	100	80	III
4550.15.....	1	3	III A	4637.27.....	4	8	III A
4550.95.....	15	.....	V E	4638.61.....	4	1	IV
4551.45.....	2	.....	V E	4638.98.....	15	.....	V E
4554.98.....	6	.....	V E	4640.04.....	15	10	III
4558.07.....	40	1	IV E	4640.543†...	4	20	III A
4559.61.....	2	1	IV	4641.30.....	4	3	IV
4561.05*....	8	6	IV	4645.98.....	20	8	III
4563.40.....	2	.....	V E	4646.33.....	6	.....	V E
4563.71.....	2	1	IV	4647.650†...	30	50	II
4564.57.....	4	5	IV	4648.585†...	8	3	III
4570.838†...	2	4	IV	4648.704†...	10	6	III
4570.94.....	2	.....	V E	4652.32.....	10	4	III
4572.210†...	8	25	III A	4653.543†...	80	60	III
4572.42.....	2	6	III A	4654.765†...	4	20	III A
4573.811†...	40	80	II A	4654.98.....	10	.....	V E
4575.912†...	60	60	III	4658.60.....	6	40	II A
4579.593†...	60	40	III	4659.84.....	2	10	III A
4581.05.....	15	.....	V E	4664.24.....	4	.....	V E
4581.294†...	100	100	II	4666.45.....	4	.....	V E
4582.332†...	2	6	III A	4668.23*....	2	?	IV ?
4582.37.....	20	.....	V E	4670.84*....	15	8	III

TABLE II—*Continued*

λ (I.A.	Intensities		Class	λ (I.A.)	Intensities		Class
	Arc	Fur.			Arc	Fur.	
4676.98.....	4	.....	V E	4679.16.....	40	10	III
4677.63.....	6	30	II A	4680.04.....	40	20	II
4678.24.....	6	3?	IV	4680.62.....	4	3	III

NOTES TO TABLE II

λ	
3934.790	Double, red component is *Gd* II; λ for neutral line in furnace
3945.548	May be double
3964.97 3965.03	Not fully resolved
3979.346	Double
4008.91	Blend *Ti* in furnace
4045.862	Blend *Fe* in arc; measured in furnace without *Fe*
4050.373	Faint *Gd* I to violet
4092.718	Furnace line partly *V;* λ measured in arc
4148.864	Faint neutral line on violet side
4163.111	Strong in spark, indicating blend with *Gd* II line; arc line measures 4163.084
4170.11	Probably double
4251.76	May be blend with *Gd* I
4262.094	Close blend; violet component is *Gd* I
4323.60	Double
4327.106	Close doublet in arc; red component is *Gd* II
4337.504	Strong in spark; probably blend *Gd* II
4340.47	Probably blend *Gd* II
4397.50	Faint *Gd* I line to violet
4406.68	Blend *V* in furnace
4408.25	Blend *V* in furnace
4413.44	Double; red component is *Gd* II
4436.103	Furnace line may be partly *V*
4437.84	Blend *V* in furnace
4510.38	Double
4522.82	Close blend *Gd* I and *Gd* II; furnace line measured λ 4522.795
4534.74	Furnace line chiefly *Ti*
4561.05	Arc line probably double
4597.91	Probably blend *Gd* I and *Gd* II
4668.23	Furnace line in carbon band
4670.84	May be double

TABLE III

TEMPERATURE CLASSIFICATION OF TERBIUM LINES

λ (I.A.)	Intensities		Class, No. Comps.	λ (I.A.)	Intensities		Class, No. Comps.
	Arc	Fur.			Arc	Fur.	
3837.18.....	5	3	III	3897.25.....	4	5	III
3841.77.....	5	.....	V E, 4	3897.39.....	4	.....	V E, 2
3842.49.....	40	.....	V E, 6	3897.852† }	15	{3	III
3845.61.....	10	.....	V E, 4	3897.925† }		{6	III
3847.88*....	8	?	III ?	3898.734†...	4	6	III
3848.75.....	100	6	IV E, 6	3899.19.....	200	6	IV E, 3
3849.59.....	4	2	III	3899.54.....	15	.....	V E
3851.86.....	5	.....	V E	3900.40.....	2	.....	V E
3854.04*....	2	?	III ?	3900.72.....	4	5	III, 2
3855.38.....	10	15	II	3901.35.....	50	50	II
3855.58*....	10	?	V E, 4	3901.60.....	6	.....	V E
3866.54.....	6	6	III	3901.98.....	15	.....	V E, 4
3868.90.....	4	.....	V E	3902.35.....	10	.....	V E
3869.75.....	15	.....	V E, 3	3903.11.....	3	5	III
3872.10*....	2	—?	V ?	3904.186†...	4	6	III
3873.00.....	10	12	III	3904.65.....	1	.....	V
3873.78.....	8	.....	V E	3905.61.....	10	8	III
3874.18.....	200	10	IV E, 6	3905.83.....	2	5	III A
3874.73*....	5	4?	III ?, 2	3906.53.....	4	.....	V E, 3
3875.21.....	20	.....	V E, 4	3907.65.....	3	.....	V E
3876.13.....	8	8	III	3907.79.....	3	.....	V E
3876.47*....	3	?	III ?	3907.912†...	5	10	III A
3876.67.....	8	6	III	3908.076†...	20	30	II
3877.56*....	6	?	IV ?	3908.66.....	4	1	III
3878.21*....	10	.....	V E ?	3909.150†...	15	12	III
3879.99*....	4	4	III ?	3909.54.....	15	5	III
3880.35*....	4	?	III ?	3910.13.....	4	.....	V E
3881.29*....	8	8	III ?	3910.40.....	5	5	III
3881.75*....	4	.....	V E ?	3910.57.....	2	.....	V E
3885.12†....	8	10	III	3910.85.....	5	8	III
3886.01.....	3	.....	V E	3912.25.....	5	10	III A
3886.70†....	3	5	III	3912.78.....	5	.....	V E
3886.83.....	20	.....	V E, 4	3913.45.....	8	{6	III
3887.29†....	2	8	III A			{2	III
3887.49.....	4	.....	V E	3913.79*....	2	1	III
3887.67.....	25	.....	V E, 4	3914.59.....	5	8	III
3887.88†....	10	8	III	3914.73.....	2	2	III
3888.21.....	30	25	III, 3	3915.45.....	30	100	III A, 2
3889.85.....	10	.....	V E, 3	3916.64.....	4	8	III A
3890.95.....	5	1	III	3916.94.....	4	4	III
3891.76.....	2	3	III	3917.32.....	6	6	III
3893.35.....	15	.....	V E	3918.82.....	8	.....	V E
3893.70.....	5	4	III	3919.00.....	6	8	III
3894.63.....	20	20	III	3919.54.....	40	1	IV E, 3
3895.065†...	4	5	III	3920.72.....	10	.....	V E, 2
3895.376†...	3	2	III	3920.962†...	1	4	III A
3895.478†...	1	2	III A	3921.264†...	4	8	III A
3895.969†...	3	5	III	3921.76.....	3	4	III, 2
3896.04.....	25	.....	V E	3922.09.....	20	.....	V E, 2
3896.488†...	4	8	III A	3922.74.....	50	.....	V E
3896.60.....	25	.....	V E, 2	3923.33.....	6	.....	V E

TABLE III—*Continued*

λ (I.A.)	Intensities		Class, No. Comps.	λ (I.A.)	Intensities		Class, No. Comps.
	Arc	Fur.			Arc	Fur.	
3924.40.....	4	.....	V E	3957.368†...	12	20	II
3924.81.....	10	.....	V E	3957.97.....	40	.....	V E, 4
3925.45.....	150	.....	V E, 3	3958.35.....	60	.....	V E, 6
3926.09.....	1	.....	V E	3958.62.....	8	3	III
3927.15.....	4	.....	V E, 3	3960.10.....	6	.....	V E
3927.35.....	2	1	III	3960.308†...	5	10	III A
3928.99.....	3	5	III	3960.69.....	8	8	III
3929.42.....	2	2	III	3962.634†...	10	15	III
3929.75.....	5	2	III	3965.120†...	15	10	III
3929.88.....	10	12	III	3965.95.....	15	.....	V E
3930.76.....	8	.....	V E, 4	3966.283†...	12	8	III
3932.366†...	12	20	III	3967.21.....	15	1	IV, 3
3932.55.....	3	3	III	3967.672†...	20	10	III
3933.469†...	6	3	III	3969.90.....	5	6	III
3933.905†...	4	5	III	3970.19.....	30	.....	V E, 4
3934.40.....	10	4	III	3971.790†...	30	20	III
3935.25.....	50	1	IV E, 3	3972.05.....	20	.....	V E
3937.15.....	5	5	III	3972.93.....	4	.....	V E
3937.636†...	15	20	III	3974.30.....	15	.....	V E, 3
3938.04.....	4	8	III A	3974.70.....	12	10	III
3938.16.....	3	.....	V E	3976.86.....	250	15	IV E, 6
3939.60.....	200	4	IV E, 6	3977.760†...	2	5	III A
3940.10.....	2	.....	V E	3980.28.....	3	.....	V E
3941.16.....	15	.....	V E	3981.15.....	20	.....	V E, 3
3941.35.....	4	.....	V E	3981.92.....	150	.....	V E, 4
3942.20.....	15	.....	V E	3983.85.....	15	.....	V E
3942.94.....	6	10	III	3984.04.....	15	.....	V E
3943.66.....	8	15?	III A	3984.84.....	6	.....	V E
3944.20.....	6	4	III	3985.08.....	{5	.....	V E
3946.87.....	150	3	IV E, 4		{5	5	III
3947.25.....	5	3	III	3986.34.....	15	.....	V E
3947.51.....	2	1	III	3986.940†...	3	8	III A
3948.35.....	20	.....	V E, 2	3987.69.....	8	20	III A
3949.39.....	4	1	III	3989.50.....	6	20	III A
3949.51.....	6	.....	V E	3990.22.....	4	4	III
3949.88.....	4	.....	V E	3990.63.....	25	12	III, 2
3950.147†...	15	15	II	3991.59.....	{4	3	III
3950.445†...	15	10	III		{4	5	III
3950.76.....	4	.....	V E	3992.20.....	2	.....	V E
3951.71.....	3	.....	V E	3993.54.....	10	3	III
3951.889†...	8	15	III A	3995.15.....	8	15	III A
3952.047†...	8	6	III	3995.80.....	6	.....	V E, 2
3952.60.....	2	1	III, 2	3996.68.....	2	.....	V E
3953.00.....	3	3	III	3998.41.....	15	.....	V E
3954.040†...	10	6	III	3998.887†...	5	20	III A
3954.131†...	5	8	III	3999.41.....	25	.....	V E
3954.51.....	1	2	III A	4000.01.....	10	.....	V E
3954.77.....	1	.....	V E	4001.279†...	15	20	III
3955.05.....	2	2	III	4002.20.....	50	.....	V E, 6
3955.65.....	3	2	III	4002.60.....	100	2	IV E, 4
3955.80.....	2	1	III, 2	4003.78.....	15	.....	V E
3956.16.....	8	.....	V E	4003.91.....	10	.....	V E

TABLE III—*Continued*

λ (I.A.)	Intensities		Class, No. Comps.	λ (I.A.)	Intensities		Class, No. Comps.
	Arc	Fur.			Arc	Fur.	
4004.52.....	8	.....	V E	4041.537†...	3	8	III A
4004.618†...	5	8	III	4041.846†...	4	8	III A
4005.55.....	200	4	IV E, 4	4042.36.....	6	.....	V E
4005.97.....	8	.....	V E	4045.35.....	5	10	III A
4007.73.....	2	5	III A	4047.18.....	6	15	III A
4009.193†...	10	10	III	4048.80.....	6	{3	III A
4009.54.....	12	.....	V E			{2	III A
4010.064†...	15	15	II	4051.52.....	4	.....	V E, 2
4010.644†...	2	3	III	4051.87.....	30	.....	V E
4010.741†...	6	8	II	4052.43.....	4	.....	V E, 2
4010.869†...	8	10	II	4052.87.....	20	.....	V E, 3
4012.46.....	4	.....	V E	4053.35.....	3	8	III A
4012.84.....	40	1	IV E, 4	4054.03.....	10	15	III A
4013.276*†..	25	20	III	4054.14.....	25	15	III A
4015.52.....	15	.....	V E, 6	4055.34.....	8	8	III, 3
4015.625†...	4	10	III A	4056.10.....	2	2	III
4015.94.....	8	.....	V E, 3	4057.06.....	4	.....	V E
4016.04.....	2	.....	V E	4059.47.....	4	.....	V E
4016.34.....	12	.....	V E, 6	4060.39.....	40	30	II
4016.86.....	4	4	III, 2	4060.86.....	40	.....	V E, 6
4017.85.....	4	.....	V E	4061.58.....	60	60	II
4018.48.....	8	5	III	4062.20.....	4	8	III A
4019.14.....	20	.....	V E, 4	4062.80.....	10	.....	V E, 3
4020.47.....	30	.....	V E	4063.95.....	15	.....	V E, 2
4020.734†...	4	6	III	4066.21.....	30	.....	V E, 4
4021.13.....	4	.....	V E, 2	4067.35.....	4	15	III A
4022.870†...	10	12	III	4069.30.....	1	.....	V E
4023.716†...	10	20	III A	4070.13.....	10	10	III
4024.10.....	30	.....	V E, 6	4070.58.....	10	.....	V E, 4
4024.703†...	5	10	III A	4070.70.....	5	4	III
4024.781†...	10	15	II	4071.21.....	10	15	III
4025.146†...	4	10	III A	4072.35.....	4	.....	V E, 3
4025.74.....	10	.....	V E, 3	4072.71.....	10	15	III
4026.39.....	3	1	III	4073.96.....	10	20	III A
4028.28.....	15	.....	V E	4074.19.....	8	8	III
4028.59.....	6	6	III	4075.22.....	{20	.....	V E, 4
4029.25.....	2	5	III A		{15	20	III
4031.65.....	50	.....	V E, 4	4075.90.....	2	.....	V E
4032.282†...	60	40	II	4079.15.....	2	5	III A
4032.625†...	8	20	III A	4081.24.....	30	60	II A, 4
4032.705†...	5	15	III A	4082.23.....	4	.....	V E
4033.05.....	200	6	IV E, 4	4082.79.....	15	15	III
4036.219†...	12	10	III	4083.20.....	15	15	III
4036.45.....	6	.....	V E	4084.25.....	12	20	III, 2
4038.864†...	10	15	III	4084.83.....	10	15	III
4039.20.....	3	.....	V E	4086.60.....	20	50	II A
4039.482†...	10	15	III	4088.65.....	4	8	III A
4039.724†...	1	3	III A	4089.34.....	{10?	15	III
4040.100†...	6	10	III		{15?	.....	V E, 3
4040.43.....	6	.....	V E, 2	4089.50.....	6	.....	V E
4040.677†...	3	10	III A	4090.14.....	2	2	III
4040.938†...	2	5	III A	4091.32†....	4	8	III A

TABLE III—*Continued*

λ (I.A.)	Intensities		Class, No. Comps.	λ (I.A.)	Intensities		Class, No. Comps.
	Arc	Fur.			Arc	Fur.	
4091.42†	4	4	III	4133.51	2	4	III A
4092.19	20	60	II A	4135.37	20	30	III, 3
4093.37	2	1	III	4136.45	4	5	III
4094.05	8	8	III	4139.06	10	30	III A
4094.45	5	.....	V E,3	4139.35	3	1	IV
	15	40	II A	4139.78	20	60	III A
4095.93	10	10	III	4140.75	10	.....	V E, 4
4096.38	2	2	III	4141.55	30	60	III A
4099.44	10	.....	V E	4142.45	6	12	III A
4097.85	6	.....	V E	4143.24	8	12	III
4098.15	4	.....	V E	4143.51†	40	40	II
4099.47	15	.....	V E, 4	4143.63†	20	20	III
4100.94	8	8	III	4144.47	100	6	IV E, 4
4101.65	15	20	III, 3	4146.91†	15	40	III A
4102.54	15	.....	V E,3	4149.16	6	.....	V E
4103.21†	5	8	III	4150.87	4	10	III A
4103.37†	15	15	III	4152.24	5	15	III A
4103.49†	6	10	III	4153.49	5	1	III
4103.91	20	.....	V E, 3	4153.84	3	2	III
4105.37	25	50	II A	4154.64	5	5	III
4106.35	4	6	III	4155.40	4	6	III
4107.77	4	8	III A	4156.28	8	5	III, 2
4108.40	3	6	III A	4158.28	6	.....	V E
4109.08	1	1	III	4158.54	30	50	II
4110.09	2	6	III A	4159.19	3	2	III
4110.86	4	4	III	4160.01	1	2	III A
4111.00	2	2	III	4161.35	5	8	III
4112.53	30	40	III	4162.99	3	2	III
4112.88	15	20	III	4167.12	4	8	III A
4114.15	20	.....	V E, 6	4169.11	10	15	III
4115.34	20	.....	V E, 6	4169.30	20	30	III
4117.22	10	15	III	4169.90	6	10	III
4118.426†	8	12	III	4170.46	10	25	III A
4119.987†	20	30	II	4171.04	20	5	III
4120.43†	3	6	III A	4171.78	12	15	III
4120.51	15	.....	V E	4172.55	15	2	III
4121.04	5	12	III A, 2	4172.83	10	50	III A
4122.49	8	10	III	4173.44	10	2	III
4123.80	5	.....	V E, 2	4175.05	4	15	III A
4124.25	2	3	III	4175.86	8	15	III A
4125.25	15	.....	V E, 6	4178.97	15	.....	V E, 4
4125.38	4	2	III	4180.40	10	40	III A
4126.72	10	8	III	4180.88	15	2	III, 3
4126.93	4	3	III	4184.66	2	4	III A
4127.29	4	4	III	4185.44	2	1	III
	10	.....	V E	4185.89	5	15	III A
4128.72	3	2	III	4186.24	15	10	III
4129.40	3	1	III	4187.16	25	60	II A, 2
4130.15	20	25	III	4188.12	15	40	III A
4131.11	8	4	III	4188.53	8	.....	V E
4132.51	6	15	III A	4189.30	3	15	III A
4132.84	8	8	III	4190.43	2	3	III

TABLE III—*Continued*

λ (I.A.)	Intensities		Class, No. Comps.	λ (I.A.)	Intensities		Class, No. Comps.
	Arc	Fur.			Arc	Fur.	
4191.06.....	20	15	II	4266.34.....	50	80	II
4193.34.....	5	10	III A	4269.34.....	6	30	III A, 2
4194.02.....	5	5	III	4269.72.....	25	40	III
4196.74.....	15	25	III	4270.74.....	3	2	III
4198.45.....	5	15	III A	4273.19.....	3	.....	V E
4198.99†....	5	10	III A	4275.23†....	20	20	III
4199.07†....	3	10	III A	4275.39†....	5	8	III
4201.00*....	30	2	III V E	4276.14.....	2	.....	V E
				4276.75.....	15	.....	V E, 6
4203.74.....	40	60	II	4277.78†....	6	8	III
4206.49.....	25	20	II	4278.54.....	200	.....	V E, 6
4207.54.....	8	20	III A	4281.31.....	4	6	III
4208.70.....	5	5	III	4285.12.....	25	.....	V E
4211.13.....	3	5	III	4285.74.....	5	.....	V E
4213.50.....	20	50	III A	4286.89.....	8	.....	V E, 2
	30	.....	V E, 4	4287.10.....	8	15	III A
4214.42.....	15	.....	V E	4287.31.....	4	.....	V E
4216.69.....	2	8	III A	4289.70.....	20	40	III A
4218.85.....	8	15	III A	4291.39.....	2	4	III A
4219.19.....	20	30	III A	4292.63.....	2	.....	V E
4220.12.....	6	.....	V E, 2	4293.14.....	6	8	III, 2
4222.71.....	15	10	III	4294.34.....	5	.....	V E, 2
4223.34.....	12	.....	V E	4295.34.....	15	30	III A
4224.29.....	25	30	II	4296.34.....	10	4	III A
4224.85.....	4	.....	V E, 2	4298.36.....	30	60	II A
4226.45.....	60	.....	V E, 6*r*	4299.89.....	15	15	III
4230.60.....	4	6	III, 2	4302.95.....	12	10	III
4231.34.....	5	20	III	4303.99.....	10	8	III
4231.89.....	20	40	III	4304.24.....	4	3	III, 2
4232.20.....	20	.....	V E	4307.19*....	15	80?	II A
4232.84.....	25	20	III	4308.68.....	25	.....	V E, 6
4235.35.....	30	60	III A, 2	4310.44.....	20	30	III
4239.29.....	15	40	III A	4310.65*....	3	3	III
4239.91.....	8	30	III A	4310.99.....	8	.....	V E
4240.14.....	15	.....	V E, 6*v*	4311.29.....	5	10	III A
4242.27.....	8	6	III	4311.58.....	15	20	III
4242.57.....	12	.....	V E	4312.09.....	8	.....	V E
4245.19.....	10	20	III A	4313.25.....	15	20	III
4246.60.....	20	60	III A	4313.41.....	10	12	III
4248.59.....	4	.....	V E	4315.74.....	6	8	III
4251.34.....	15	15	III	4318.84.....	200	200	I
4252.66.....	5	12	III A	4320.27.....	12	30	III A
4254.02.....	4	12	III A	4321.50.....	4	3	III
4255.24.....	25	80	III A, 2	4322.23.....	50	50	III
4256.10.....	8	20	III A	4322.87.....	15	15	III
4258.24.....	30	60	III A	4323.65.....	15	.....	V E, 4
4259.94.....	5	20	III A	4324.09.....	8	20	III A
4261.84.....	6	10	III	4325.50.....	10	60	III A
4263.56†....	6	15	III A	4325.82.....	60	4	IV E, 4
4263.69†....	15	25	III A	4326.48.....	200	200	I
4264.73†....	6	20	III A	4328.08.....	1	.....	V E
4264.98.....	6	20	III A, 2	4328.94.....	10	20	III A

TABLE III—*Continued*

λ (I.A.)	Intensities		Class, No. Comps.	λ (I.A.)	Intensities		Class, No. Comps.
	Arc	Fur.			Arc	Fur.	
4329.40.....	4	5	III	4384.06.....	5	.....	V E
4329.56.....	8	5	III	4385.69.....	12	10	III
4330.34.....	8	4	III, 2	4386.09.....	10	.....	V E
4330.83.....	2	10	III A	4387.43.....	2	15	III A
4330.94.....	3	12	III A	4388.25.....	15	20	III
4332.13.....	50	50	III	4389.04.....	3	.....	V E, 2
4333.73.....	8	20	III A	4389.94.....	4	2	III
4334.69.....	12	20	III	4390.93*....	25	30	III, 2
4335.74.....	2	.....	V E	4392.23.....	8	8	III
4335.89.....	6	8	II, 2	4392.96.....	3	2	III, 2
4336.52.....	60	80	II	4394.04.....	5	15	III A
4337.64.....	40	50	III	4394.92.....	3	.....	V E
4338.47.....	150	150	I	4396.58.....	10	8	III
4339.61.....	8	15	III A, 2	4398.61.....	2	4	III A
4339.88.....	4	5	III	4400.52*....	2	2 ?	III ?
4340.63.....	100	150	I	4401.54.....	10	.....	V E, 2
4340.99.....	10	15	II	4403.20.....	10	10	III
4342.5*†....	30	.....	V E, 6	4405.41.....	8	.....	V E, 4
4342.526*†..	8?	8	III	4409.51.....	20	.....	V E, 6*v*
4342.595*†..	20	20	III	4411.93.....	2	3	III, 2
4343.29.....	1	2	III A	4412.83.....	2	1	III
4343.85.....	3	3	III, 2	4413.63.....	4	6	III
4344.20.....	3	.....	V E, 2	4416.28.....	20	.....	V E, 4
4348.34.....	3	.....	V E	4420.19.....	15	100	III A
4349.60.....	8	8	III	4423.11.....	40	200	II A
4350.74.....	6	10	III	4427.391†...	4	12	III A
4351.57.....	8	.....	V E, 4	4428.33.....	2	4	III A
4353.19.....	50	.....	V E, 4	4430.13.....	2	.....	V E
4356.08.....	20	20	III	4430.740†...	3	6	III A
4356.83.....	100	100	I	4432.164†...	3	6	III A
4357.48.....	10	30	III A	4432.722†...	12	40	II A
4358.42.....	3	2	III	4434.48.....	10	.....	V E, 2
4360.17.....	20	30	III	4436.13*....	20	100 ?	III A
4360.66.....	3	6	III A	4437.65†....	2	2	III
4362.47.....	5	10	III A	4438.98.....	10	.....	V E
4363.94.....	1	1	III	4439.39†....	8	10	III
4366.01.....	3	.....	V E	4441.27.....	6	.....	V E, 4
4367.32.....	25	2	III	4441.49.....	5	8	III
4370.33.....	4	1	III	4448.04.....	30	20	III, 4
4370.93.....	3	.....	V E	4449.23.....	3	10	III A
4372.07.....	20	50	II A	4449.5†.....	8	4	IV, 4
4372.34.....	2	1	III	4450.11.....	2	.....	V E
4372.50.....	4	.....	V E	4451.63.....	12	15	III
4372.63.....	2	.....	V E	4452.82.....	30	15	III, 6
4374.46.....	4	10	III A	4458.45.....	2	.....	V E
4374.83.....	2	10	III A, 2	4459.38.....	8	.....	V E
4375.36.....	3	2	III	4461.23.....	8	4	III, 4
4375.62.....	3	.....	V E	4462.18.....	10	.....	V E, 4
4376.44.....	5	.....	V E, 2	4465.69.....	2	6	III A
4378.73.....	4	.....	V E, 4	4467.69.....	10	50	III A
4381.32.....	8	25	III A	4469.13.....	8	30	III A
4382.45.....	20	40	III A, 2	4469.68.....	8	.....	V E, 4

TABLE III—*Continued*

λ (I.A.)	Intensities		Class, No. Comps.	λ (I.A.)	Intensities		Class, No. Comps.
	Arc	Fur.			Arc	Fur.	
4471.72.....	5	.....	V E	4541.24.....	1	4	III A
4472.84.....	3	.....	V E	4542.4*†.....	4	.....	V E, 4
4473.67.....	4	20	III A	4544.233†...	1	3	IV A
4476.429†...	2	20	III A	4547.682†...	1	6	III A
4480.04.....	2	.....	V E	4549.07.....	10	6	IV, 4
4481.03.....	10	.....	V E	4549.138*†..	5	10	III A
4485.67.....	4	10	III A	4549.70.....	8	.....	V E, 4
4488.16.....	12	100	III A, 2	4550.450†...	12	40	III A, 2
4489.76.....	3	.....	V E	4556.42.....	20	4	III, 4
4490.63.....	8	.....	V E, 4	4556.92.....	8	.....	V E, 4
4491.02.....	10	20	III A	4556.962*†..	5	20	III A
4491.78.....	2	2	III, 4	4557.230†...	4	10	III A
4493.07.....	100	200	II A	4557.29.....	2	.....	V E
4495.03.....	2	.....	V E, 2	4557.635†...	6	10	III
4496.93.....	1	1	III	4560.775†...	3	20	III A
4498.96.....	1	.....	V E	4562.25.....	8	.....	V E, 2
4499.47.....	2	1	III	4563.68.....	20	.....	V E, 2
4501.26.....	2	.....	V E	4564.83.....	4	.....	V E, 2
4501.73.....	3	15	III A	4567.72.....	6	.....	V E, 6
4503.58.....	2	.....	V E	4568.523†...	6	8	III
4504.59.....	3	8	III A	4569.29.....	2	.....	V E, 2
4507.97.....	2	4	III A	4571.42.....	1	.....	V E
4508.67.....	1	2	III A	4571.83.....	2	2	III
4509.03.....	15	.....	V E, 4	4573.18.....	8	.....	V E
4511.53.....	20	20	III, 4	4573.895†...	4	8	III A
4512.97.....	8	.....	V E, 2	4575.42.....	2	.....	V E
4513.639†...	1	8	III A	4578.62.....	30	.....	V E, 4
4514.308†...	8	.....	V E	4581.42.....	12	40	III A
4515.87.....	6	.....	V E, 4	4582.57.....	6	.....	V E
4516.145†...	1	3	III A	4584.82.....	6	.....	V E
4516.532†...	1	12	III A	4587.710†...	6	8	III, 4
4518.214†...	2	1	III	4591.56.....	8	.....	V E
4520.09.....	4	.....	V E	4592.4†.....	4	3	III, 2
4521.839†...	2	3	III	4593.943†...	2	10	III A
4524.133†...	3	1	IV	4599.607†...	2	15	III A, 2
4524.333†...	4	15	III A	4600.162†...	6	15	III A
4524.99.....	8	.....	V E, 4	4604.08.....	3	.....	V E
4525.946†...	2	6	III A	4611.92.....	2	5	III A, 2
4526.449†...	1	3	III A	4617.27.....	3	2	III
4527.180†...	1	5	III A	4620.88.....	2	1	III
4528.323†...	1	4	III A	4621.97.....	1	3	III A
4530.658†...	2	8	III A, 2	4626.32.....	6	.....	V E, 4
4531.83.....	6	.....	V E, 4	4626.91.....	15	.....	V E
4532.920†...	2	8	III A	4627.52.....	2	1	III
4534.13.....	5	1	III	4631.038†...	2	8	III A
4534.290†...	1	3	III A	4632.02.....	8	10	III, 4
4536.93.....	8	.....	V E, 4	4636.61.....	8	10	III, 4
4537.15.....	8	20	III A	4637.00.....	3	.....	V E, 2
4537.23.....	8	10	III	4638.516†...	4	8	III A
4538.74.....	2	.....	V E	4640.98.....	15	.....	V E
4540.23.....	4	.....	V E	4641.97.....	30	.....	V E, 2
4540.58.....	3	.....	V E, 4	4645.26*....	50	.....	V E, 6r

TABLE III—*Continued*

λ (I.A.)	Intensities		Class, No. Comps.	λ (I.A.)	Intensities		Class, No. Comps.
	Arc	Fur.			Arc	Fur.	
4648.30.....	2	1	III	4658.67.....	3	4	III
4651.07.....	1	.....	V E	4662.78.....	10	30	III A
4651.58.....	2	5	III A	4676.86.....	10	40	III A, 4
4658.35.....	4	10	III A, 4				

NOTES TO TABLE III

λ	
3847.88 to 3881.75	Starred lines uncertain on account of λ 3883 *CN* band
3913.79	Blend *Tb* I (to violet) and *Tb* II
4013.276	Blend complex *Tb* II line
4201.00	Close blend *Tb* I and *Tb* II
4307.19	Furnace line partly *V*
4310.65	Blend *Tb* II in arc
4342.5 4342.526 4342.595	Difficult blend
4390.93	Blend in arc with *Gd* II
4400.52	Blend *V* in furnace
4436.13	Blend *V* and *Gd* I
4542.4	Components partially resolved
4549.138	Blend in arc with λ 4549.07
4556.962	Blend in arc with λ 4556.92
4645.26	Components partially resolved

TABLE IV

TEMPERATURE CLASSIFICATION OF DYSPROSIUM LINES

λ (I.A.)	INTENSITIES		CLASS	λ (I.A.)	INTENSITIES		CLASS
	Arc	Fur.			Arc	Fur.	
3836.49.....	60	5?	III E	3903.332†...	3	4	III
3838.67.....	5	.....	V E	3904.089†...	1	4	III A
3840.91.....	10	5?	II	3904.14.....	8	.....	V E
3841.313†...	40	3	IV E	3905.56.....	2	.....	V E
3842.015†...	20	2?	III	3910.108†...	1	5	III A
3844.30.....	6	3	II	3910.51.....	1	.....	V E
3846.351†...	15	.....	V E	3911.677†...	1	4	III A
3846.99.....	8	6	II	3912.544†...	2	4	III A
3848.36.....	2	3	III	3912.85.....	3	.....	V E
3849.399†...	15	.....	V E	3913.628†...	4	8	III A
3850.049†...	5	.....	V E	3913.95.....	6	.....	V E
3850.449†...	4	.....	V E	3914.869†...	25	1	V E
3850.527†...	5	.....	V E	3915.599†...	25	1	V E
3853.040†...	50	3	IV E	3917.294†...	8	8	III
3854.90.....	4	.....	V E	3917.372†...	6	6	III
3855.60.....	5	.....	V E	3918.53.....	4	.....	V E
3858.08.....	5	.....	V E	3919.145†...	2	6	III A
3858.39.....	15	8?	II	3920.122†...	1	3	III A
3862.66.....	5	3	III	3920.84.....	1	3	III A
3863.20.....	4	.....	V E	3923.300†...	3	.....	V E
3865.45.....	8	.....	V E	3923.390†...	10	.....	V E
3866.590†...	20	.....	V E	3924.415†...	1	3	III A
3867.83.....	5	.....	V E	3924.46.....	2	.....	V E
3868.464†...	25	2?	IV E	3927.866†...	4	4	III
3868.817†...	50	12?	II	3929.33.....	5	.....	V E
3869.10.....	3	.....	V E	3930.153†...	15	10	III
3869.439†...	10	.....	V E	3931.297†...	8	.....	V E
3869.871†...	25	?	V E	3931.533†...	150	5	IV E
3871.642†...	10	.....	V E	3932.231†...	10	.....	V E
3872.14.....	300	?	IV E	3932.97.....	5	.....	V E
3873.989†...	40	?	IV E	3934.17.....	8	.....	V E
3875.15.....	4	.....	V E	3936.03.....	4	.....	V E
3877.94.....	2	.....	V E	3936.29.....	4	.....	V E
3879.05*....	20	.....	V E	3936.708†...	10	8	III
3881.995†...	12	.....	V E	3937.165†...	4	4	III
3883.05.....	4	.....	V E	3937.990†...	3	5	III
3887.52.....	8	1	IV	3938.1†.....	4	.....	V E
3888.40.....	6	.....	V E	3938.209†...	5	5	III
3888.99.....	12	2	IV	3939.23.....	1	3	IV A
3891.85.....	3	.....	V E	3939.793†...	1	5	IV A
3891.982†...	6	5	III	3942.050†...	4	.....	V E
3892.87*....	12	8?	II?	3942.527†...	25	1	V E
3893.390†...	1	6	III A	3944.688†...	600	15	III E
3894.533†...	2	6	III A	3946.939†...	10	.....	V E
3895.35.....	15	.....	V E	3950.395†...	20	.....	V E
3896.18.....	1	6	III A	3953.515†...	1	6	III A
3896.656†...	2	6	III A	3954.559†...	12	.....	V E
3898.540†...	300	20	IV E	3957.797†...	30	1	V E
3899.15.....	6	{4	III	3958.004†...	2	4	III A
		{6	III	3959.35.....	3	.....	V E
3902.39.....	2	.....	V E	3961.810†...	1	5	III A

TABLE IV—*Continued*

λ (I.A.)	Intensities		Class	λ (I.A.)	Intensities		Class
	Arc	Fur.			Arc	Fur.	
3962.601†...	8	8	III	4020.88.....	4	.....	V E
3963.80.....	3	.....	V E	4020.897†...	1	4	III A
3964.70.....	2	.....	V E	4023.722†...	8	15	III A
3966.362†...	3	6	III A	4024.437†...	12	.....	V E
3967.517†...	10	8	III	4024.906†...	6	6	III
3968.393†...	1000	20	III E	4025.205†...	1	4	III A
3969.233†...	3	5	III	4025.605*†..	?	4	III A
3971.214*†..	3	6	III A	4025.75.....	3	.....	V E
3972.414†...	2	5	III A	4027.787†...	15	.....	V E
3973.879†...	5	6	III	4028.325†...	8	.....	V E
3976.965†...	1	4	III A	4028.418†...	12	8	II
3978.556†...	150	5	IV E	4031.081†...	2	4	III A
3979.477†...	8	.....	V E	4032.480†...	30	.....	V E
3981.372†...	3	6	III A	4032.847†...	4	4	III
3981.930†...	75	2	V E	4033.588†...	1	4	III A
3983.659†...	100	5	IV E	4033.666†...	10	.....	V E
3984.221†...	60	1	V E	4036.335†...	15	1	V E
3984.70.....	2	.....	V E	4037.628†...	1	4	III A
3985.360†...	1	4	III A	4038.528†...	8	.....	V E
3986.05.....	2	4	III A	4038.719†...	1	4	IIIA
3987.06.....	3	.....	V E	4038.834†...	4	6	III
3988.886†...	2	5	III A	4041.989†...	10	.....	V E
3990.35.....	2	.....	V E	4043.046†...	1	3	III A
3991.328†...	30	.....	V E	4045.281†...	2	5	III A
3991.89.....	2	.....	V E	4045.977†...	400	300*R*	II
3993.575†...	4	4	III	4047.740†...	2	4	III A
3993.857†...	1	3	III A	4048.942†...	4	4	III
3994.535†...	1	6	III A	4049.374†...	3	3	II
3995.993†...	1	6	III A	4050.581†...	150	3	IV E
3996.694†...	200	4	IV E	4052.40.....	1	3	III A
3996.926†...	1	4	III A	4055.013†...	3	5	III
3998.10.....	2	.....	V E	4055.13.....	30	.....	V E
3998.940†...	1	5	III A	4057.40.....	2	.....	V E
4000.454†...	600	10	III E	4060.58.....	4	.....	V E
4000.588†...	1	3	III A	4061.054†...	1	3	III A
4001.524†...	1	3	III A	4065.15.....	1	2	III A
4004.48.....	2	3	III	4065.400†...	2	5	III A
4005.840†...	12	6	III	4066.70.....	1	4	III A
4006.071†...	10	6	III	4067.968†...	1	4	III A
4007.137†...	2	4	III A	4071.032†...	2	4	III A
4007.77.....	3	.....	V E	4072.65.....	3	.....	V E
4010.08.....	3	.....	V E	4073.110†...	200	10	IV E
4011.295†...	20	.....	V E	4074.02.....	3	.....	V E
4011.820†...	1	3	III A	4077.35.....	1	3	IV A
4012.523†...	1	4	III A	4077.974†...	600	20	III E
4013.826†...	15	40*r*	II A	4079.27.....	2	5	III A
4014.094†...	1	4	III A	4079.595†...	2	5	III A
4014.713†...	25	1	V E	4083.109†...	2	6	III A
4015.18.....	4	.....	V E	4083.74.....	1	4	III A
4017.055†...	1	4	III A	4085.140†...	6	10	III A
4019.40.....	1	.....	V E	4085.344†...	12	8	III
4019.55.....	1	.....	V E	4087.22.....	8	.....	V E

TABLE IV—*Continued*

λ (I.A.)	Intensities		Class	λ (I.A.)	Intensities		Class
	Arc	Fur.			Arc	Fur.	
4087.388†...	2	6	III A	4154.22.....	2	.....	V E
4089.511†...	1	5	III A	4154.27†....	1—	4	III A
4090.399†...	1—	3	III A	4154.54.....	1—	4	III A
4091.53.....	6	.....	V E	4156.39.....	1—	3	III A
4091.77.....	4	.....	V E	4156.98.....	1	6	III A
4093.647†...	1	5	III A	4157.86.....	1	.....	V E
4095.251†...	1—	3	III A	4158.04.....	1	5	III A
4096.109†...	8	15	III A	4159.34.....	3	6	III A
4096.639†...	1	5	III A	4160.24.....	1	3	III A
4099.886†...	2	4	II A	4162.25.....	1	4	III A
4101.43.....	1	4	III A	4164.74.....	1—	4	III A
4101.850†...	1—	3	III A	4166.23.....	1	3	III A
4101.95.....	2	.....	V E	4167.40.....	2	.....	V E
4103.312†...	500	15	IV E	4167.966†...	200	100*R*	II
4103.878*†..	30	6	III	4169.07.....	1	5	III A
4105.032*†..	?	5	III A	4169.241†...	2	.....	V E
4105.05.....	8	.....	V E	4170.34.....	1—	5	III A
4105.814†...	1	3	III A	4170.55.....	1	4	IV A
4106.39.....	3	.....	V E	4171.925†...	4	8	III A
4106.70.....	2	.....	V E	4171.992†...	6	8	III
4107.45.....	2	.....	V E	4176.64.....	1	3	III A
4111.346†...	150	8	IV E	4176.81.....	1	3	III A
4113.05.....	2	8	III A	4177.754†...	2	3	III
4114.09.....	1	.....	V E	4178.072†...	5	4	III
4114.69.....	1	6	IV A	4181.25.....	2	5	III A
4119.33.....	8	.....	V E	4182.42.....	2	.....	V E
4120.66.....	1	4	III A	4183.611†...	6	10 ?	III
4124.626†...	30	1	V E	4183.726†...	30	30*r*	II
4126.14.....	4	15*r*	II A	4186.810†...	600	300*R*	II
4128.241†...	20	1	IV E	4189.4†.....	2	4	III A
4129.13.....	8	15*r*	III A	4190.90.....	10	8	III
4129.425†...	100	3	IV E	4191.627†...	80	50*R*	II
4130.42.....	6	12*r*	II A	4194.827†...	500	200*R*	II
4131.04.....	6	.....	V E	4195.22*....	6	?	III
4132.85.....	3	.....	V E	4197.93.....	25	15	II
4133.38.....	8	.....	V E	4201.01.....	2	5	III A
4133.86.....	10	6	III	4201.314†...	20	15	III
4134.14.....	8	4	III	4201.372†...	10	.....	V E
4134.75.....	2	3	III	4202.245†...	30	20*r*	II
4136.94.....	1	1	IV	4203.99.....	1	4	III A
4138.54.....	3	6	III A	4205.03.....	8	10	III
4139.56.....	3	6	III A	4206.544*†..	25	6	IV E
4141.395†...	1	6	III A	4207.68.....	5	6	III
4141.514†...	20	2	IV E	4211.20.....	15	30*r*	II A
4143.100†...	300	5	IV E	4211.719†...	1200	600*R*	II
4145.59.....	1	.....	V E	4213.182†...	60	50*R*	II
4146.069†...	40	30*r*	II	4214.38.....	4	12	III A
4148.00.....	1	4	III	4215.166†...	125	100*R*	II
4149.84.....	1	4	III	4216.96.....	1	4	III A
4152.43.....	1	.....	V E	4218.091†...	200	150*R*	II
4153.11.....	3	4	III	4218.58.....	5	.....	V E
4153.36.....	1	5	III A	4221.104†...	250	200*R*	II

TABLE IV—*Continued*

λ (I.A.)	Intensities		Class	λ (I.A.)	Intensities		Class
	Arc	Fur.			Arc	Fur.	
4222.21.....	20	15	III	4277.76†....	1—	3	III A
4224.68.....	2	4	III A	4279.78†....	2	8	III A
4225.153†...	150	100*R*	II	4282.11†....	1—	3	III A
4232.02.....	30	15	II	4283.31†....	1—	5	III A
4234.14.....	1	4	III A	4283.63†....	1—	5	III A
4234.83.....	2	4	III A	4284.28†....	1—	3	III A
4236.27†....	1	4	III A	4288.01†....	1—	3	III A
4236.59†....	1—	4	III A	4288.3†.....	1—	2	III A
4237.54.....	2	.....	V E	4288.71†....	1—	3	III A
4237.95†....	1—	3	III A	4290.44.....	2	8	III A
4238.04.....	1	.....	V E	4291.0†.....	1—	3	III A
4238.44.....	2	.....	V E	4291.93*†...	8	15	III A
4239.87†....	40	30*r*	II	4294.45†....	1—	2	III A
4240.69†....	1—	2	III A	4294.936†...	10	.....	V E
4241.83†....	1—	5	III A	4295.038†...	25	7	III
4242.73†....	1—	4	III A	4296.34†....	1—	3	III A
4243.00†....	1	4	III A	4297.76†....	1—	3	III A
4243.45†....	2	10	III A	4298.7†.....	1—	3	III A
4244.79.....	1	.....	V E	4298.90†....	1	5	III A
4245.92.....	30	20	III	4300.41.....	1	.....	V E
4247.36.....	8	.....	V E	4300.6†.....	1—	4	III A
4248.44.....	2	.....	V E	4300.76.....	1	.....	V E
4248.91†....	1—	2	III A	4302.35†....	1—	2	III A
4250.35†....	1	3	III A	4302.57.....	4	.... ..	V E
4250.46†....	1	5	III A	4302.72.....	2	.....	V E
4251.33†....	1	8	III A	4306.77†....	1—	3	III
4251.73†....	2	6	III A	4308.344†...	2	5	III A
4252.11†....	1—	3	III A	4308.623†...	100	7	IV E
4254.92†....	1—	3	III A	4311.93†....	1	4	III A
4255.97.....	1	.....	V E	4312.429†...	1—	4	III A
4256.204†...	3	.....	V E	4313.886†...	2	.....	V E
4256.323†...	15	3	IV E	4313.929†...	1—	6	III A
4257.72.....	1	.....	V E	4315.60†....	1—	4	III A
4257.78†....	1—	10	III A	4318.355†...	1—	4	III A
4258.14†....	4	10	III A	4318.985†...	1—	4	III A
4258.51†....	1—	5	III A	4322.19.....	1	.....	V E
4258.56†....	8	10	III	4322.363†...	1	4	III A
4259.76†....	1—	3	III A	4322.55.....	2	.....	V E
4259.82†....	1	3	III A	4323.794*†..	1	5	III A
4260.71†....	1—	2	III A	4325.14.....	10	.....	V E
4264.82†....	1—	2	III A	4326.39.....	2	4	III A
4265.83.....	1	.....	V E	4328.69†....	1—	2	III A
4266.00†....	1—	4	III A	4328.90.....	5	.....	V E
4267.92†....	1	3	IV A	4329.89.....	1	.....	V E
4268.31†....	2	10	III A	4334.07†....	1—	3	III A
4269.60†....	3	8	III A	4334.37†....	1—	6	III A
4273.03†....	1—	4	III A	4336.01.....	1—	6	III A
4273.14.....	2	.....	V E	4339.68.....	8	.....	V E
4275.00.....	1	6	III A	4346.3.....	1	.....	V E
4275.45†....	1	3	III A	4347.72†....	4	8	III A
4275.96†....	1—	3	III A	4356.13†....	1—	6	III A
4276.74.....	10	15	III A	4356.77†....	1—	3	III A

TABLE IV—*Continued*

λ (I.A.)	Intensities		Class	λ (I.A.)	Intensities		Class
	Arc	Fur.			Arc	Fur.	
4358.47†....	12	2	IV E	4506.96.....	1	2	IV A
4361.39.....	2	.....	V E	4508.11.....	1—	3	IV A
4364.06.....	2	.....	V E	4513.60.....	1—	12	III A
4364.28.....	5	.....	V E	4516.94*....	3	5	III
4365.62†....	1—	4	III A	4518.53.....	3	.....	V E
4366.73.....	5	12	III A	4519.79.....	2	.....	V E
4368.26†....	1—	2	III A	4522.68.....	1—	4	III A
4369.55.....	1—	6	III A	4525.10.....	1	3	IV A
4374.24†....	20	3	IV E	4526.09.....	1	3	IV A
4374.80.....	20	2	IV E	4527.74.....	6	.....	V E
4375.33.....	6	.....	V E	4531.59.....	1	8	II A
4380.23.....	2	.....	V E	4538.74.....	5	.....	V E
4380.48†....	1—	5	III A	4539.14.....	1—	6	IV A
4384.30.....	2	.....	V E	4541.69.....	4	.....	V E
4385.29.....	2	.....	V E	4545.35.....	1	.....	V E
4389.79†....	1	3	IV A	4546.48.....	1—	2	IV A
4390.32†....	1—	2	III A	4546.82.....	1—	3	III A
4390.94†....	1—	5	III A	4550.90.....	2	.....	V E
4393.28†....	1—	3	III A	4553.15.....	1—	8	III A
4394.98.....	6	.....	V E	4555.02.....	1—	4	III A
4397.51†....	1—	4	III A	4555.23.....	1	8	III A
4399.73†....	1—	4	III A	4556.48.....	1	.....	V E
4400.10.....	1	.....	V E	4557.36.....	1—	4	III A
4403.98†....	1—	4	III A	4559.62.....	1—	3	III A
4408.05.....	2	.....	V E	4565.098†...	8	20*r*	II A
4409.384†...	40	5	IV E	4565.95†....	1—	5	III A
4409.93†....	1—	2	III A	4566.22.....	1—	3	IV A
4411.37.....	1	3	IV A	4567.06.....	1	8	III A
4411.69†....	1—	3	III A	4568.42.....	1—	3	III A
4414.20†....	1—	3	III A	4573.83.....	2	.....	V E
4421.69.....	1	.....	V E	4576.61.....	2	.....	V E
4426.87.....	1	3	IV A	4577.777†...	30	40*R*	II
4431.00.....	3	.....	V E	4585.73.....	1—	5	III A
4435.78.....	1	.....	V E	4585.99.....	1—	4	III A
4436.65.....	1	.....	V E	4586.18.....	1—	3	III A
4444.61.....	6	12	III A	4586.64.....	1	1	IV
4448.23.....	2	.....	V E	4587.93.....	5	.....	V E
4449.16.....	2	.....	V E	4589.078†...	1	12	III A
4449.702†...	60	7	IV E	4589.367†...	150	150*R*	II
4454.334†...	1—	4	III A	4590.55.....	1	3	III A
4455.49.....	4	.....	V E	4591.6†.....	1—	3	III A
4467.88.....	2	.....	V E	4591.73.....	1	.....	V E
4468.16*....	8	3	IV E	4595.13.....	1	.....	V E
4480.68.....	2	10	III A	4599.84.....	1—	6	IV A
4482.33.....	1	2	IV A	4606.04.....	1	4	III A
4484.37.....	2	10	III A	4612.27.....	100	80	II
4487.85.....	1—	2	III A	4613.83.....	1	5	IV A
4492.14.....	1—	5	III A	4614.82.....	1	6	IV A
4496.41.....	1	2	IV A	4617.25.....	4	.....	V E
4499.26.....	1	2	III A	4620.02.....	10	.....	V E
4503.26.....	5	.....	V E	4622.34.....	1	.....	V E
4503.38†....	1—	4	III A	4622.78†....	1—	4	III A

TABLE IV—*Continued*

λ (I.A.)	Intensities		Class	λ (I.A.)	Intensities		Class
	Arc	Fur.			Arc	Fur.	
4624.10.....	1	5	IV A	4650.17.....	1	12	III A
4627.45.....	1—	8	III A	4651.54.....	2	.....	V E
4628.07.....	1	.....	V E	4662.20.....	1	3	III A
4631.51.....	1	8	III A	4662.76.....	1	4	III A
4634.78.....	1—	3	IV A	4664.68.....	5	1	IV E
4635.32.....	1	6	III A	4673.62.....	2	.....	V E
4638.52.....	1	.....	V E	4675.81.....	2	2	IV
4641.1†.....	1—	4	III A	4681.01.....	1	5	III A
4643.49.....	1	4	III A				

NOTES TO TABLE IV

λ	
3879.05	Double
3892.87	Blend *V* in furnace
3971.214	Blend *Dy* II in arc
4025.605	Blend in arc with λ 4025.75
4103.882	Blend in furnace with *Ho* λ 4103.84
4105.032	Blend in arc with λ 4105.05
4195.22	Difficult; close to preceding line
4206.544	Probably blend with *Dy* I
4291.93	Double
4323.794	Blend in arc with faint *Dy* II
4468.16	Probably blend with *Dy* I
4516.94	Blend in arc with *Dy* II

TABLE V

TEMPERATURE CLASSIFICATION OF HOLMIUM LINES

λ (I.A.)	Intensities		Class, No. Comps.	λ (I.A.)	Intensities		Class, No. Comps.
	Arc	Fur.			Arc	Fur.	
3837.45.....	15	.....	V E, 6	3975.88.....	3	4	III
3842.05.....	4	.....	V E, 4	3976.86.....	6	6	III, 2
3843.86.....	8	.....	V E, 2	3977.05.....	3	.....	V E, 4
3846.68.....	10	.....	V E, 4	3985.80.....	6	.....	V E, 6
3851.4†.....	4	.....	V E, 4	3986.5*†.....	5	.....	V E
3854.08.....	20	.....	V E, 6	3987.55.....	3	.....	V E ?, 2
3856.98.....	8	.....	V E, 6	3990.35.....	1	.....	V E
3861.7*†....	40	?	V E, 6	3991.85.....	1	.....	V E
3874.11.....	2	.....	V E, 4	3992.55.....	4	6	III, 6
3874.70.....	6	.....	V E, 4	3998.28.....	40	20	II, 4
3886.4†.....	6	.....	V E, 6	3999.56.....	6	8	III, 2
3888.95.....	40	8	IV E, 6	4000.62.....	4 ?	2	III
3890.42.....	5	8	III	4002.70.....	3	.....	V E, 6
3891.02.....	200	40	IV E, 6*v*	4003.36.....	4	6	III, 2
3892.70.....	2	6	III A	4014.18.....	2	.....	V E, 2
3892.95.....	6	12	III A	4016.00.....	2	4	III A, 2
3893.10.....	4	.....	V E, 6	4020.51.....	1	2	III A
3893.54.....	5	.....	V E, 6	4022.86.....	2	.....	V E, 6*r*
3895.53.....	4	.....	V E	4023.93.....	4	.....	V E, 6*r*
3896.24.....	4	2	III	4025.39.....	3	4	III
3896.6†.....	5	3	III	4027.20.....	5	6	III, 2
3896.75.....	5	.....	V E, 4	4028.85.....	4	3	III, 2
3897.27.....	4	.....	V E, 6	4031.75.....	4	15	II A, 4
3900.79.....	1	2	III A, 2	4036.10.....	2	4	III A, 4
3901.15.....	1	1	III, 2	4040.84*....	150	100*R*	I, 2
3901.53.....	1	1	III	4045.43.....	200	40	IV E, 4
3902.24.....	4	.....	V E ?, 6	4048.79.....	2	.....	V E, 4
3904.45.....	4	4	III	4052.45.....	1	1	III
3905.78.....	30	4	IV E, 6	4053.92*....	400	300*R*	I, 2
3906.26.....	3	.....	V E	4054.49.....	3	3	IV
3909.56.....	2	10	III A, 4	4057.55.....	2	3	III, 2
3910.30.....	1	1	III	4061.02*....	1	3	III A
3911.80.....	3	6	III A, 2	4065.10.....	10	1	IV E
3912.44.....	4	2	III	4067.04.....	2	.....	V E?, 2
3913.96.....	3	.....	V E	4067.8†.....	2	.....	V E?, 6*v*
3919.45.....	6	6	III	4068.05.....	6	10	III, 2
3923.37.....	5	.....	V E	4087.35.....	4	5	III
3936.51.....	10	.....	V E, 6	4087.65*....	4	6	II, 2
3937.00.....	2	4	III A	4100.2†.....	4	4	III, 4
3938.84.....	2	6	III A, 4	4100.59.....	1	.....	V E
3940.55.....	12	.....	V E, 6*v*	4101.09.....	40	30	I, 2
3949.00.....	1	1	III	4103.84*....	400	300*R*	I, 2
3950.50*....	8?	6	III, 2	4104.30.....	2	2	III
3955.05.....	4	1	III, 2	4105.85.....	2	4	III A
3955.74.....	15	20	I, 2	4106.50.....	4	4	III
3957.39.....	1	3	III A, 2	4106.6†.....	2	.....	V E, 4
3959.68.....	6	8	III, 2	4107.36.....	1	3	III A
3963.27.....	1	1	III	4108.63.....	100	60*r*	II
3972.60.....	2	.....	V, 4	4111.99.....	4	6	III
3973.05.....	1	4	III A	4116.63.....	3	3	III
3973.59.....	1	4	III A	4120.20.....	50	30	II

TABLE V—*Continued*

λ (I.A.)	Intensities		Class, No. Comps.	λ (I.A.)	Intensities		Class, No. Comps.
	Arc	Fur.			Arc	Fur.	
4125.65.....	20	30	III	4348.34.....	1	1	III
4127.16*....	150	60	II, 2	4350.73.....	40	40	I
4134.56*....	5	5 ?	III?, 2	4363.93*....	2	?	IV ?, 4
4136.24.....	40	30	II	4364.18.....	3	.....	V E
4142.19.....	2	3	III, 2	4369.17.....	1	4	III A, 2
4148.97.....	3	3	III, 2	4373.33.....	1	3	III A
4150.8†.....	2	6	III A, 6	4384.94.....	3	.....	V, 6
4151.14.....	4	6	II	4390.53.....	2	4	III A, 2
4152.54*\	30	6	IV, 6*r*	4400.54*....	1	?	?, 2
4152.75*/...		3	IV, 6*v*	4403.27.....	3	8	III A, 2
4160.0†.....	3	6	IV A, 4	4420.54.....	2	.....	V E
4163.03.....	100	8*or*	I	4455.59*....	5	.....	V, 4
4172.23.....	2	4	III A, 2	4477.63.....	3	1	III
4173.23*....	50	4*or*	I	4497.7†.....	2	25	III A, 6
4194.34.....	30	60	I, 6	4510.81.....	2	2	III, 4
4223.47.....	4	5	III	4512.54.....	1	.....	V
4229.49.....	6	2	IV, 2	4526.14.....	2	1	III, 2
4234.79.....	2	2	III	4531.28.....	2	2	III, 4
4243.76.....	3	6	III A	4534.58.....	4	12	III A, 4
4254.43.....	100	100	I, 6	4562.52.....	6	15	III A, 6
4264.07.....	15	4*or*	I A	4572.43.....	2	.....	V, 4
4266.04.....	5	20	III A, 2	4606.62*....	1	5	III A
4273.63.....	1	.....	V, 2	4608.0†.....	2	.....	V, 4
4284.54.....	1	3	III A, 2	4609.52.....	6	.....	V, 6
4290.17.....	1	.....	V E	4613.37.....	4	12	III A, 4
4301.09.....	2	.....	V, 4	4618.84.....	2	2	III, 4
4311.04.....	2	4	III A, 2	4628.22.....	2	10	III A, 4
4326.39.....	2	2	III	4629.10.....	6	.....	V E
4328.99.....	3	.....	V	4640.61.....	2	.....	V
4330.64.....	2	?	IV ?, 4	4641.7†.....	1	12	III A, 6
4337.13.....	4	.....	V E	4661.33*....	4	?	III

NOTES TO TABLE V

λ	
3861.7	Blend head of *CN* band
3950.50	Blend *Y* in arc
3986.5	Probably two complex lines together
4040.84	Reversal is for red component, which is complex
4053.92	May have four close components
4061.02	May be impurity
4087.65	Red component shows at low temperature
4103.84	Resembles λ 4053.92
4127.16	Red component stronger in furnace
4134.56	Blend *V* in furnace
4152.54\ 4152.75/	Apparently a blend of two six-component lines, with components oppositely graduated
4173.23	Blends in furnace with foreign line
4363.93	Disturbed by band
4400.54	Blend *V* in furnace
4455.59	Given by Kayser as welsium
4606.62	May be impurity
4661.33	Disturbed by band

DISCUSSION

Europium.—Table I contains 219 lines, of which 133 belong to the neutral and 86 to the ionized atom. Each of these main divisions contains two groups of very different type, one group responding to low and the other only to high excitation, with a lack, in this portion of the spectrum, of lines of intermediate character. Hyperfine structure prevails for a large proportion of the lines, the patterns being narrow and seldom sufficiently resolved to permit more than a rough estimate, from the appearance of the line, of the probable number of components. That hyperfine structure, rather than the widening due to high excitation, is responsible for the soft and diffuse appearance of many lines in the arc spectrum is indicated by the failure of these lines to sharpen when barely visible in the furnace spectrum, where excitation widening should disappear.

The lines of low excitation in the ionized spectrum have intensities seldom found in rare-earth spectra. These are λλ 3907.1, 3930.5, 3971.9, 4129.7, 4205.0, 4435.6, 4522.6. The line λ 3819.6, outside the range here studied, belongs to the group. In structure each line consists of an unresolved triplet, with a fourth line, usually separated in the furnace spectrum, on the violet side. The complex line reverses strongly in the arc, the single line to the violet making this side of the reversal stronger. The ionized character of these lines was clearly shown by their almost complete extinction when caesium was added in the furnace; but with europium alone the lines are strong in the furnace, and with long exposure show at temperatures as low as 2000° C. This behavior places them in class III E. The other enhanced lines in this region are of very different type. These were selected by comparison of arc and spark spectra and require high excitation, belonging usually to class V E.

The neutral lines of europium present a similar contrast between groups. Three low-temperature lines occur at λλ 4593.993, 4627.122, 4661.865. These reverse widely in the arc and at the higher furnace temperatures. At low temperatures they widen strongly while the vapor is plentiful, after the manner of "flame" lines, but the strong sharp line which persists at low vapor density in each case indicates an absence of hyperfine structure. Aside from these three, the neutral lines in this region are weak in the furnace and appear faint-

PLATE XIV

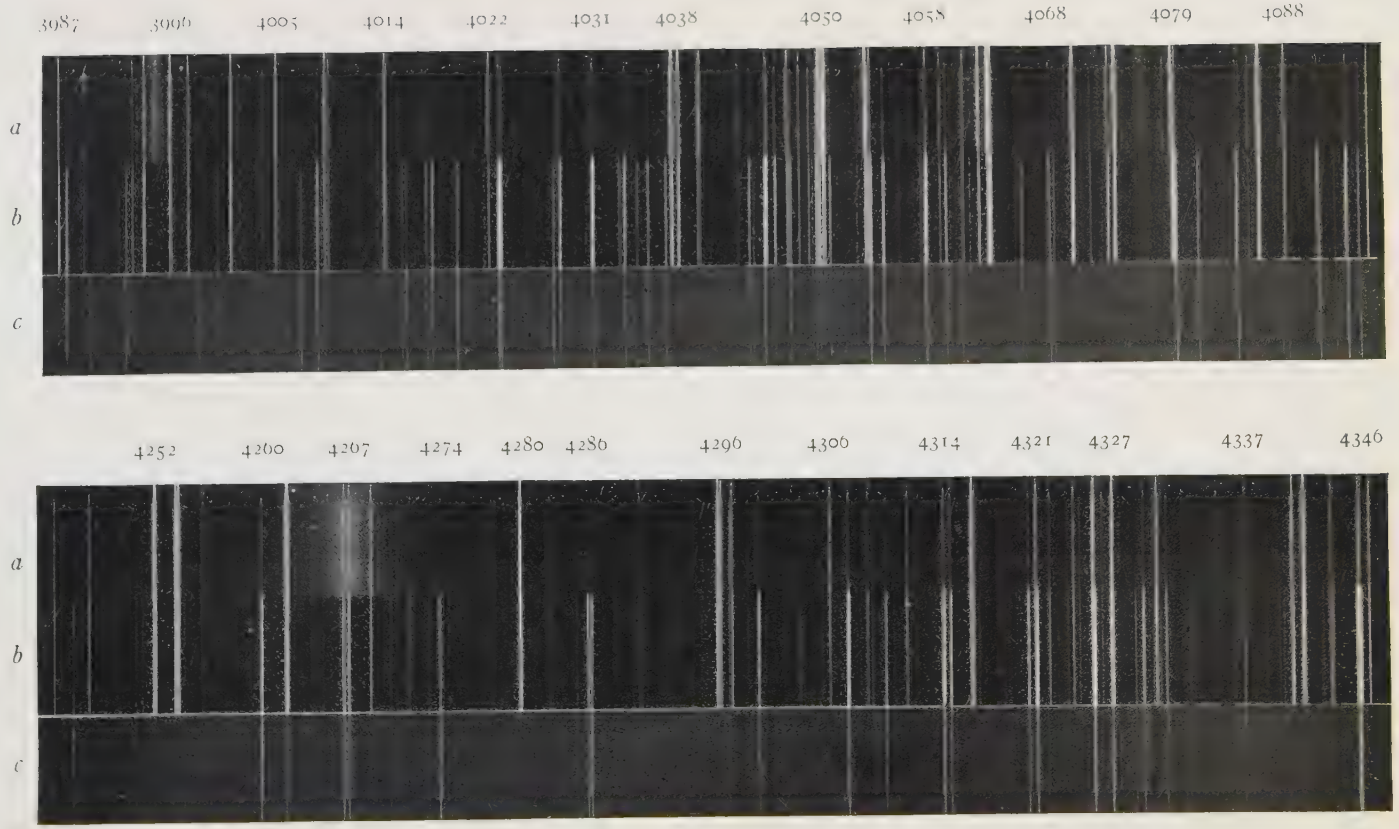

SPECTRUM OF GADOLINIUM

a) Spark spectrum
b) Arc spectrum

ly at high temperature, though some of the strongest can be seen at temperatures as low as 2300° C.

The wave-lengths in Table I are for the most part by Eder.[1] The lines belonging to the strong groups discussed above have been measured by the writer in the furnace spectrum, where superior definition of the components of the complex ionized lines was obtained in spectrograms taken at moderate temperature. Standards were furnished by lines of titanium and vanadium given by the graphite tube.

Gadolinium.—Table II contains 627 lines, of which 365 are neutral, while 262 belong to the ionized atom. The wave-lengths are for the most part the international values of Eder,[2] but are supplemented by 236 wave-lengths measured on the writer's spectrograms. The spectrum is typical of the even-numbered rare earths, its lines being sharp and reversing with difficulty. The lines of class I are visible at 2000° C, and the low-temperature spectrum is well developed at 2100°. Between this and the spectrum at 2300° there is a decided contrast, owing to the development of class III lines. The stronger ionized lines show at 2600°, but were fully suppressed at this temperature by the addition of caesium chloride. Spectra of the spark, arc, and high-temperature furnace are reproduced in Plate XIV, which illustrates the slight difference between the arc and spark spectra in this region, other than the usual weakening in the spark of the neutral lines forming the furnace spectrum.

Terbium.—The region under examination is very rich in lines, 733 being of sufficient strength to be listed in Table III. The wave-lengths are for the most part converted from those of Exner and Haschek,[3] but some are from Eder[4] and from Eberhard,[5] and 128 lines, a part of them new, have been measured by the writer. The numbers of neutral and ionized lines are 482 and 251, respectively. The furnace spectrograms showed a small number of class I lines, of which several are grouped near λ 4300; but the very rapid development at medium temperature places a large proportion of the furnace lines in class III.

[1] *Sitzungsberichte der Akademie der Wissenschaften in Wien*, IIa, **126**, 473, 1917.
[2] *Ibid.*, **125**, 1467, 1916. [3] *Loc. cit.* [4] *Op. cit.*, **131**, 199, 1922.
[5] *Zeitschrift für wissenschaftliche Photographie*, **4**, 137, 1906.

Hyperfine structure, while not a conspicuous feature of this spectrum, is present in a considerable number of lines (see final column of Table III). The patterns are in general narrow. The lines given as having two components may be more complex, and occasional patterns of six components, with partial resolutions, are found.

Dysprosium.—The wave-lengths in Table IV, which contains 534 lines, are for the most part those of Eder,[1] who also lists the converted values of Exner and Haschek[2] and of Eberhard.[3] These are supplemented by 274 wave-lengths obtained from the writer's plates, chiefly for lines which can be measured to advantage in the furnace spectrum. A large proportion of the neutral dysprosium lines appear at about 2200° and are often very faint in the arc. Their absence at the lowest temperature used places them as a rule in class III or III A. Many other lines belonging in class IV A show distinctly in the high-temperature furnace spectrum and must be measured when a complete listing of neutral lines is undertaken. The region under examination contains also a very distinctive group of low-temperature lines, of which the first is λ 4045.977, and the others are near λ 4200. These are distinct and sharp at 2000°, reverse widely in the high-temperature furnace, and are strong in the arc. They are typical class II lines, none of the dysprosium lines in this region being assigned to class I. As Eder has noted, these class II lines are the only ones which show marked widening. Most of the dysprosium lines remain sharp for different excitations, and no evidence of hyperfine structure has appeared.

The ionized lines of dysprosium are easily excited, some appearing in the furnace at temperatures as low as 2200°. An arc spectrum of moderate exposure is made up of the ionized and a few of the stronger neutral lines, the furnace or a very strong arc exposure being required to bring up the lines forming the greater part of the neutral spectrum. The arc intensity of these is often so low as to be given as 1− in the table.

Holmium.—The holmium spectrum in this region presents many features of interest. The study is difficult on account of the impure material which the writer and apparently all previous workers have had to use and the unsatisfactory state of the wave-lengths for this

[1] *Op. cit.*, **127**, 1, 1918. [2] *Loc. cit.*

[3] *Publikationen des Astrophysikalischen Observatoriums zu Potsdam*, **20**, 60, 1909.

spectrum. Table V contains 164 lines, whose identification with holmium was in nearly all cases clear. The wave-lengths are for the most part those of Exner and Haschek, converted to the international system. Dysprosium lines, which occur very generally in Exner and Haschek's holmium list, were eliminated by means of my material for dysprosium.

Hyperfine structure with wide patterns is very common for both neutral and enhanced lines of holmium, 58 of the lines having either four or six components. Lines given as having four components may be really six-component lines with close patterns. The lines of another large group are distinctly double. A few of the six-component lines[1] were partially resolved, the structure being similar to that of praseodymium[2] in that the spacing of components is graduated, with the larger interval in some cases to the violet, in others to the red. Wide patterns of holmium lines are not confined to lines of high excitation as are those of praseodymium. While the stronger ionized lines in this region are always highly complex, and the strongest neutral lines, a group between λ 4050 and λ 4200, are single or at most double, a number of low-temperature neutral lines having wide patterns are found. Of these the class I line λ 4254.43 is strong in the arc and at all furnace temperatures, but others, of which λ 4497.7 and λ 4262.52 are typical, are faint in the arc, but strong at high and medium furnace temperatures.

The neutral spectrum contains the prominent lines of classes I and II, photographed at about 2000°, and, in addition, a large number of class III lines which are often relatively faint in the arc. The latter lines are usually at least double and in the blue region show many good examples of hyperfine structure.

The ionized lines, usually complex, become less frequent near λ 4000, some of them having considerable intensity in the high-temperature furnace, as well as in the arc. Their ionized character was readily shown, however, by their disappearance when a mixture with caesium was used in the furnace.

Carnegie Institution of Washington
Mount Wilson Observatory
August 1930

[1] Some of these having the best resolution appear as if they may have eight components.

[2] *Loc. cit.*

Contributions from the Mount Wilson Observatory, No. 415
Reprinted from the *Astrophysical Journal*, Vol. LXXII, pp. 311–342, 1930
Printed in the U.S.A.

HARVARD OBSERVATORY

MAGNITUDES OF SOUTHERN COMPARISON STARS FOR EROS

By F. H. SEARES, B. W. SITTERLY, and MARY C. JOYNER

ABSTRACT

Magnitudes, photographic and *photovisual*, have been determined for *300 southern comparison stars for Eros* (Table IV, mag. 7–10) and *74 bright extra stars* (Table V, mag. 5–7.) Scales and zero points were established by polar comparisons and strengthened by connecting plates. Screen exposures give added weight to the brighter Eros stars and provide data for the extra stars.

Mean color index and spectrum.—The mean color index for Ao stars (Harvard spectra) is −0.14 mag. Colors for F, G, and K stars are less than those found by King, Parkhurst, and Seares (Table XI). The presence of dwarfs may account for part but not all of the differences.

Comparison with Yerkes measures.—One hundred and twelve of the stars have been observed by Ross and Zug. Agreement in *zero points* is *good*, but *scale divergence is appreciable* for both photographic and photovisual magnitudes (Table VII). A large accidental difference $MW - Y = \pm 0.19$ for photographic magnitudes was traced to a progressive change in zero points. Two independent series of MW polar comparisons are accordant (Table IX), while comparisons of color indices for stars of the same spectral type in different fields indicate that the discordance is to be apportioned between MW and Y in the ratio of 3 to 7 (Table X). This assumes the types to be free from error.

Comparisons with Harvard magnitudes.—Provisional formulae for reduction to the international system (Tables XII, XIII) were derived for visual measures by Pickering, Wendell, and Bailey in *H.A.* **14, 24, 44, 45, 46, 70,** and **74**. The color coefficient varies with the observer, instrument, and apparent magnitude of the star. Comparisons with magnitudes in the *Draper Catalogue* which were derived from *Durchmusterung* catalogues—the *SDM*, *CD*, *CPD* (Table XV)—show no scale divergence and only small zero-point differences, in striking contrast with the 34 per cent divergence found by Ross and Zug for the *BD*.

1. THE OBSERVATIONS

The International Commission on Solar Parallax asked the Commission on Stellar Magnitudes to provide for the determination of the magnitudes and colors of the comparison stars[1] of Eros for the opposition of 1930–1931. Dr. F. E. Ross and Mr. R. S. Zug of the Yerkes Observatory consented to undertake the measurement of the northern stars and to extend their observations as far south as observing conditions would permit; the limit actually reached by them[2] is −17°. The stars south of the Equator have been observed with the 10-inch Cooke triplet at Mount Wilson.

[1] Kopff, *Astronomische Nachrichten*, **224**, 387; **226**, 33, 1925.

[2] *Astronomische Nachrichten*, **239**, 289, 1930.

The Mount Wilson photographs, all taken by Sitterly, consist of three series:

A. Polar comparisons, 15 photographic and 15 photovisual (Table I); 2 exposures on the field, 2 on the pole, arranged in a symmetrical order. The spacing of the centers is such that each plate includes about half the stars shown on each of the adjacent plates.

B. Centers and exposures as in A, with a wire-gauze screen absorbing 3.01 mag. in front of the objective.

TABLE I

FIELDS AND PHOTOGRAPHS FOR SERIES A AND B

FIELD	α 1930	δ 1930	SERIES A		SERIES B	
			Pg.	Pv.	Pg.	Pv.
1.....	10^h24^m2	$-2°36'$	April 19	April 19	April 19	April 19
2.....	21.7	5 6	18	March 29	20	25
3.....	17.7	8 14	March 26	26	24*	22*
4.....	13.5	11 2	April 18	April 18	22	22
5.....	8.8	13 51	17	17	20	20
6.....	4.7	16 46	25	1	22	22
7.....	9 56.7	18 58	1	25	20	20
8.....	51.6	22 8	25	March 27	March 27	March 27
9.....	45.5	24 16	25	26	25	April 20
10.....	34.9	26 38	March 24	24	24	March 24
11.....	46.0	25 24	25	25	25	April 19
12.....	57.1	24 46	27	27	27	March 28
13.....	10 9.7	23 54	26	26	26	26
14.....	21.3	23 4	April 22	29	28	28
15.....	31.4	-22 23	March 29	29	24	24

* Additional Pg. and Pv. plates were obtained on April 25.

C. Connecting plates, 13 photographic and 13 photovisual (Table II); centered on points midway between the centers for A and B; one exposure with screen, one without. Field 10, at the point where the motion of Eros changes from retrograde to direct, is connected by a single plate with both fields 9 and 11.

The screen exposures strengthen the determination of magnitudes for the brighter comparison stars and extend the investigation to still brighter objects (extra stars) not included in the list for Eros. Several plates of the pole, each with and without screen, determine the screen constant.

Exposures for photographic magnitudes were 2^m on Eastman 40 plates, with the aperture reduced to 6.5 inches to sharpen the images near the edge of the plate (4×5 in.); for photovisual magnitudes,

4^m with the full aperture on Cramer Iso Presto plates through a yellow filter (MW1).

With few exceptions each star occurs on at least two polar comparison plates of series A and two connecting plates of series C. In the region of fields 9, 10, and 11, additional exposures are available, and throughout the list many of the brighter stars are recorded by both screened and unscreened exposures. Finally, the extra stars measured on the screen exposures of C have an independent scale and zero-point determination in the polar comparisons of series B.

TABLE II

PHOTOGRAPHS FOR SERIES C

Fields	Pg.	Pv.	Fields	Pg.	Pv.
1,2	March 28	March 24	8,9	April 1	April 1
2,3	26	26	9,10,11	March 25	March 25
3,4	April 1	April 1	11,12	28	April 17
4,5	17	18	12,13	29	March 29
5,6	March 28	March 28	13,14	April 1	April 1
6,7	April 25	April 19	14,15	March 24	March 24
7,8	1	1			

2. PROVISIONAL REDUCTIONS

The plates were measured (series A and C by Sitterly, B by Miss Joyner) with a low-power microscope provided with a scale of star images placed at the common focus of eyepiece and objective. Scales *a* and *b* were used for series A and C: *a* with large images to the right for the first measurement, *b* with large images to the left for the second. Series B was measured twice with scale *b*, in the direct and the reversed position. For series A and B the order of measurement of polar and field images was inverted for the second series of settings. The adopted scale readings are the means of four estimates, two on each of two images for each star.

Scale readings were transformed into magnitudes by means of the international standards,[1] reduced to the color system of the 10-inch refractor by the formulae[2]

$$Pg_{10} = Pg - 0.19C, \qquad Pv_{10} = Pv\,,$$

[1] *Transactions of the International Astronomical Union*, 1, 71, 1922.

[2] *Seares and Humason, Mt. Wilson Contr.*, No. 234; *Astrophysical Journal*, 56, 84, 1922.

where *Pg*, *Pv*, and the color index *C* refer to the international system (the same as that of the 60-inch reflector). Stars 5–17, 2r–9r, 2s, 4s, and 6s were used for series A. For B, 4 and 11 were also required. Both scale and zero point adopted for the results of this paper depend on the adopted magnitudes of these stars.

The magnitudes of field stars on the polar comparison plates were found by plotting polar magnitudes against scale readings and using the resulting curve as a relation applicable to the field stars on the same plate. Corrections for differential atmospheric extinction between field and pole were obtained from Table XII, page xxxvi, *Mount Wilson Catalogue*.[1] Distance corrections had to be determined from the observations; for the provisional reduction they were neglected.

The provisional magnitudes of field stars from the A plates were used to reduce the plates of series C, each of which gave two curves, derived by plotting scale readings against provisional magnitudes for the two fields covered by the plate. Were it not for instrumental and observational errors, these curves would be identical. As it is, accidental, and especially plate and zero-point, errors affect the curves, and their differences may be used to determine the errors.

Since each curve depends on a separate determination of the zero point, the mean ordinate difference of the curves includes the zero-point errors and should show an accidental distribution of algebraic signs from plate to plate. The ordinate differences actually found from plate pairs 1, 2; 2, 3; 3, 4; etc., of the photographic series, taken in the order field 1 – field 2, field 2 – field 3, etc., down to field 10, were all positive and equal to about 0.4 mag. For fields 10 to 15 the differences were less conspicuous but still systematic. The corresponding differences from the photovisual plates were much smaller and relatively unimportant.

3. PLATE CORRECTIONS

Since the centers of the fields connected by a C plate are in opposite halves of the plate, these large systematic differences in the curves indicated an unusual plate error affecting the Eastman 40 negatives, positive in one half of the plate and negative in the other

[1] *Publications of the Carnegie Institution of Washington*, No. 402, 1930.

half. The cause seems to be an error in the centering of the lenses of the Cooke triplet which seriously affects the photographic rays but has little influence on the light transmitted by the yellow filter.

The determination of the corrections which harmonize the results was greatly facilitated by a manuscript copy of the Yerkes magnitudes kindly supplied by Dr. Ross. Differences $Y-MW$ were formed for each of the hundred-odd stars common to the two series of observations for each of the Mount Wilson plates on which it occurred. These differences were grouped according to magnitude and entered on diagrams at points corresponding to the positions of the stars on the plates. Since the Yerkes magnitudes had been corrected for plate errors, the difference between the value of $Y-MW$ for any point on the plate and its value at the center is the correction to be applied to the Mount Wilson magnitude.

Provisional corrections were thus found for a zone 2° wide, extending across the plate along the path of Eros. These were strengthened and extended to other parts of the plate with the aid of the Mount Wilson measures. Let m_1 and m_2 be the uncorrected magnitudes of the same field star obtained from two polar comparisons. In the absence of other errors, the value of m_1-m_2 will be the difference in the plate errors for the images from which m_1 and m_2 were obtained. If both images are within the region for which provisional corrections are known, m_1-m_2 may be used to revise these corrections; if only one image is within this region, the difference leads to the correction for the outside point. Actually both m_1 and m_2 are affected by zero-point and ordinary accidental errors; but with abundant material the zero-point errors become accidental and only the mean error for the entire series of polar comparisons enters into the final smoothed corrections.

Since the correction depends on the size of the image as well as its position on the plate, separate tables were prepared for the magnitude limits <8, 8–9, 9–10, and >10 for both photographic and photovisual results. The corrections are all asymmetrical with respect to the center, especially so for mag. 8–10 on the plates of the photographic series, for which the corrections range from about $+0.5$ to -0.3 mag. in opposite halves of the plate. The change with brightness near the tenth magnitude is rapid, particularly in the

northern half of the field, and failure to use the exact value of the correction may have introduced a slight discontinuity into the scale of the adopted photographic magnitudes at this point. A similar irregularity may also affect stars near the eighth magnitude, where the transition from one group to the next is not well determined. The corrections to the photovisual results are smaller than those required by the photographic magnitudes, show less asymmetry with respect to the center of the plate, and present some resemblance to what might normally be expected in the way of a distance correction.

4. COLOR COEFFICIENT FOR 10-INCH COOKE TRIPLET

After the correction tables were completed, all the results from the A plates were revised as a preliminary to re-reduction of series C. Before proceeding with C, however, the plots of polar magnitudes used in forming the reduction-curves for series A were examined for evidence bearing on the color coefficient of the 10-inch Cooke triplet. Any error in referring the international standards to the color system of this instrument must show as a systematic difference between the plotted points for red and blue stars in respect to their deviations from the adopted reduction-curve. The mean of these deviations from all the curves was formed for each standard star for both photographic and photovisual results and compared with the aid of the relation

$$x + Cy = \Delta ,$$

where Δ is the mean deviation and C the color index, and where, further, y is a correction to the color coefficient, 0.19, originally used to refer the standards to the system of the 10-inch telescope, and x a correction to the magnitudes necessitated by the fact that any error in the coefficient used affects the zero point. Incidentally, x also takes care of any systematic error in the position of the curves with respect to the plotted points.

Least-squares solutions gave

x	y	
+0.03 mag	−0.036	(Photographic)
+0.01	−0.026	(Photovisual)

The second value of y is unreliable and has been disregarded; the other corrections were adopted. The revised color coefficient of the

10-inch triplet for photographic magnitudes is therefore 0.19 − 0.036 = 0.154.

For the present, however, the values of x alone need be considered. These were applied to the magnitudes of the field stars as read from

TABLE III

CLOSING ERRORS AND ZERO-POINT CORRECTIONS

(Unit = 0.01 mag.)

FIELD	SERIES A AND C				SERIES B				SERIES C − SERIES B	
	Pg.		Pv.		Pg.		Pv.			
	φ	Corr.	φ	Corr.	φ	Corr.	φ	Corr.	Pg.	Pv.
1	.....	(+21)	.....	0	.....	+18	.....	+ 9	− 1	+ 3
	(−24)	.....	+ 2	.....	−37 (5)	.....	−18 (5)	.....	.....	.....
2	.....	− 3	.....	+ 2	.....	−19	.....	− 9	+15	+12
	− 3	.....	− 3	.....	−12 (1)	.....	−19 (1)	.....	.....	.....
3	.....	− 6	.....	− 1	.....	0	.....	0	0	+ 4
	+ 2	.....	− 4	.....	.....	.....	.....	.....	.....	.....
4	.....	− 4	.....	− 5	.....	+ 6	.....	− 3	−13	− 5
	+ 6	.....	−10	.....	−13 (4)	.....	+ 6 (5)	.....	.....	.....
5	.....	+ 2	.....	−15	.....	− 7	.....	+ 3	+ 2	−17
	+ 4	.....	+14	.....	−32 (2)	.....	−38 (1)	.....	.....	.....
6	.....	+ 6	.....	− 1	.....	+11	.....	− 2	−12	− 9
	+ 3	.....	0	.....	−23 (5)	.....	+ 3 (4)	.....	.....	.....
7	.....	+ 9	.....	− 1	.....	−12	.....	+ 1	− 2	+ 7
	− 8	.....	− 5	.....	.....	.....	.....	.....	.....	.....
8	.....	+ 1	.....	− 6	.....	− 6	.....	+15	− 9	− 8
	+ 5	.....	0	.....	+ 9 (4)	.....	− 6 (2)	.....	.....	.....
9	.....	+ 6	.....	− 6	.....	+ 3	.....	+ 9	0	− 4
	− 7	.....	+12	.....	− 4 (1)	.....	0 (2)	.....	.....	.....
10	.....	− 1	.....	+ 6	.....	− 1	.....	+ 9	+ 1	− 3
	0	.....	+ 1	.....	+ 9 (4)	.....	−17 (4)	.....	.....	.....
11	.....	− 1	.....	+ 7	.....	+ 8	.....	− 8	+ 2	+ 2
	+ 8	.....	− 1	.....	+ 2 (5)	.....	0 (5)	.....	.....	.....
12	.....	+ 7	.....	+ 6	.....	+10	.....	− 8	− 5	+ 3
	−11	.....	− 2	.....	−12 (4)	.....	− 2 (4)	.....	.....	.....
13	.....	− 4	.....	+ 4	.....	− 2	.....	−10	− 5	− 4
	− 2	.....	+ 1	.....	−10 (5)	.....	+ 3 (5)	.....	.....	.....
14	.....	− 6	.....	+ 5	.....	−12	.....	− 7	+ 2	− 8
	− 5	.....	− 2	.....	− 5 (2)	.....	+31 (1)	.....	.....	.....
15	.....	−11	.....	+ 3	.....	0	.....	0	− 7	+ 8
Sums	+28	+31	+30	+33	.....	+56	.....	+46	+22	+39
	−36	−36	−27	−35	.....	−59	.....	−47	−54	−58
Means	.....	0	.....	0	.....	0	.....	0	− 2	− 1

the reduction-curves of the polar comparison photographs, which were then corrected for plate error and used for the final reduction of series C.

5. ZERO-POINT ADJUSTMENT

The mean differences in the ordinates of the reduction-curves for the C plates were again formed, with the results (unit = 0.01 mag.) shown under the heading ϕ in the second and fourth columns of Table III. The order, as before, is field 1 − field 2, etc., and the numbers themselves, approximately at least, are differences in the zero points for successive fields as determined by the polar comparisons of series A. The comparison for field 1 is clearly defective; but otherwise what in the photographic series first appeared as a persistent positive difference of 0.4 mag. is now reduced to a few hundredths, with a satisfactory alternation of signs. The distribution of signs is not quite accidental, but except for the discordant field 1, the sums of positive and negative differences are in good balance.

Since for measures free from all error ϕ should be zero, the values in Table III may be regarded as closing errors in the equations of condition

$$z_2 - z_1 = 0; \qquad z_3 - z_2 = 0, \text{ etc.},$$

and used to determine corrections to the zero points z_1, z_2, z_3, etc., which will satisfy these conditions. The formulae for the corrections[1] are

$$\begin{aligned} v_1 &= \quad +k_1 \qquad \ldots, \\ v_2 &= -k_1 + k_2 \qquad v_{14} = -k_{13} + k_{14}, \\ v_3 &= -k_2 + k_3 \qquad v_{15} = -k_{14}, \end{aligned}$$

where the 14 correlates k are defined by

$$\begin{aligned} +2k_1 - k_2 + \phi_1 &= 0, \\ -k_1 + 2k_2 - k_3 + \phi_2 &= 0, \\ \cdots\cdots\cdots\cdots\cdots & \\ -k_{12} + 2k_{13} - k_{14} + \phi_{13} &= 0, \\ -k_{13} + 2k_{14} \quad + \phi_{14} &= 0, \end{aligned}$$

[1] *Mt. Wilson Catalogue*, p. xxiii, 1930.

in which the ϕ's have the successive values entered in Table III. The solution is given by

$$15k_{14}+\Sigma n\phi_n=0\,,$$

$$k_1+k_{14}+\Sigma\phi_n\ =0\,,$$

$$v_{15}=-k_{14},\ v_{14}=v_{15}-\phi_{14},\ \ldots\ .\ v_1=v_2-\phi_1\,,$$

with $v_1=+k_1$ and $\Sigma v_n=0$ as check formulae.

The results are in the third and fifth columns of Table III. The difference ϕ_1 in the second column was disregarded in calculating the corrections. This in effect rejects the zero point given by the photographic polar comparison for field 1. The correction used for this field, +21, reduces the magnitudes to the zero point of field 2.

The adopted corrections were applied to all magnitudes which depend on the polar comparison for the field in question. Thus the correction for field 3, −6, was applied to the results from the A plate for this field, to those from the second reduction-curve for the C plate 2,3, and to those from the first curve for C plate 3,4.

6. MEAN MAGNITUDES FOR COMPARISON STARS

To the results thus collected were added those from the screen images of the comparison stars in so far as they appear on the C plates. These images were treated exactly as the others, except that 3.01, the reduction constant of the screen, was subtracted from the magnitudes read from the curves. The mean of all the results for each star represents the final magnitude, photographic or photovisual, referred to the color system of the 10-inch Cooke triplet.

In forming means the results from a single plate were in general given unit weight. The two or three values obtained from the C plates for each star were combined, since the same mean scale reading was used for both. Results from screen images, however, were treated as independent measures of unit weight.

The mean magnitudes have still to be referred to the international color system. Since the small coefficient found in section 4 has been disregarded, the correction for photovisual results is zero; and since

$$Pg_{10}=Pg-0.154C\,,$$

where C is the color index referred to the international system, the reduction formula for photographic results is

$$Pg = Pg_{10} + 0.182 C_{10} ,$$

where C_{10} is the color index observed with the 10-inch triplet. Final results, all on the international system, are given in Table IV. Spectral types from the *Draper Catalogue* or from *Harvard Bulletin* No. 871 appear in the last column.

7. RESULTS FOR BRIGHT STARS

The 74 bright extra stars measured on the plates of series C were treated in the same way as the comparison stars for Eros. The reduction constant 3.01 mag., used to reduce the screen images, although based on recent data, is practically the same as the value (3.02) found in an earlier investigation.[1] The present result is derived from two polar plates, each with a screen and a full-aperture exposure, and from magnitudes for screened and unscreened images read from the reduction-curves for series C. The separate values are

	Const.	Wt.
N.P. 1930, July 7, Pl. I	3.00 mag.	2
N.P. 1930, July 7, Pl. II	3.01	1
Series C, pg. curves	3.02	3
Series C, pv. curves	3.00	1
Mean	3.01	

The magnitudes of the bright stars derived from series C were supplemented by values from the entirely independent polar comparisons of series B. The number of images on these plates is much less than in the case of A, the reduction-curves are less clearly defined, and the precision lower. A partial check on the zero points, similar to that used for series A and C, is shown in Table III. For series B, however, the values of ϕ are the means of the differences in the individual magnitudes for the same star derived from overlapping polar comparisons, the number of stars in each mean being indicated by the figures in parentheses. Values of ϕ based on 4 or 5 stars are usually satisfactory and are the basis for the zero-point

[1] Seares and Humason, *loc. cit.*

TABLE IV

MAGNITUDES OF COMPARISON STARS FOR EROS

Kopff No.	Pg. Mag.	Pv. Mag.	C.I.	No. Plates	*HD* Sp.
420	11.22	10.10	1.12	2,2	Ko
421	10.24	10.00	0.24	2,2	A
422	9.98	8.96	1.02	2,2	G_5
423	9.54	9.50	0.04	2,2	A_5
424	9.07	7.29	1.78	2,3	K_5
425	9.02	7.78	1.24	3,2	Ko
426	9.23	7.42	1.81	3,3	K_2
427	9.20	8.94	0.26	4,3	F_2
428	9.85	8.79	1.06	4,4	Ko
429	9.04	8.47	0.57	4,4	G_5
430	10.04	9.64	0.40	5,4	F8
431	10.60	10.20	0.40	3,3	F_5
432	11.07	9.63	1.44	4,4	K_5
433	11.68	10.29	1.39	4,4	M
434	9.76	9.67	0.09	5,4	F_2
435	8.77	8.68	0.09	4,4	Ao
436	10.93	10.65	0.28	3,2	F8?
437	8.82	8.52	0.30	5,4	F8
438	11.06	10.17	0.89	4,3	K_2
439	8.00	8.06	−0.06	5,5	B_9
440	10.84	9.99	0.85	5,4	Ko
441	10.51	10.23	0.28	4,5	G_5
442	10.32	9.94	0.38	4,4	F_5
443	10.68	9.73	0.95	3,3	.....
444	9.53	9.71	−0.18	5,5	A_7
445	10.13	9.35	0.78	5,5	Ko
446	9.09	8.76	0.33	5,5	F8
447	8.67	7.36	1.31	4,3	Ko
448	8.66	8.33	0.33	5,5	F_5
449	9.75	9.02	0.73	5,5	K_5
450	10.79	10.47	0.32	6,5	.....
451	9.47	8.69	0.78	6,6	Ko
452	10.11	9.35	0.76	6,6	Ko
453	10.18	9.15	1.03	6,6	G_5
454	9.04	8.07	0.97	5,5	Ko
455	10.88	10.03	0.85	3,3	.....
456	8.99	8.56	0.43	5,6	Go
457	10.93	9.46	1.47	3,3	K_5
458	10.79	9.40	1.39	6,6	Mo
459	9.89	9.05	0.84	6,6	Ko
460	9.68	9.54	0.14	5,4	F_5
461	10.06	9.30	0.76	8,7	Ko
462	9.07	8.30	0.77	7,7	Ko
463	10.47	9.13	1.34	3,3	K_2
464	9.21	8.45	0.76	7,7	Ko

TABLE IV—*Continued*

Kopff No.	Pg. Mag.	Pv. Mag.	C.I.	No. Plates	*HD* Sp.
465.....	10.32	9.27	1.05	6,5	K
466.....	10.43	9.15	1.28	4,3	K5
467.....	10.01	9.57	0.44	3,3	F8
468.....	10.76	9.83	0.93	7,7	G5
469.....	9.57	8.71	0.86	7,6	K2
470.....	9.63	8.29	1.34	6,7	K2
471.....	8.95	9.42	−0.47	8,8	B8
472.....	11.56	10.51	1.05	6,5	K5
473.....	8.71	8.73	−0.02	3,3	A5
474.....	8.46	8.44	0.02	5,4	Fo
475.....	8.74	9.00	−0.26	6,6	Ao
476.....	9.93	9.28	0.65	4,5	G5
477.....	9.81	9.46	0.35	6,5	Ko
478.....	10.02	9.90	0.12	6,6	Go
479.....	10.75	10.34	0.41	7,7	Go
480.....	9.24	9.07	0.17	7,7	F5
481.....	8.69	7.97	0.72	8,7	G5
482.....	10.10	9.93	0.17	3,3	A2
483.....	9.68	9.29	0.39	3,3	Go
484.....	9.61	9.22	0.39	3,3	G5
485.....	9.73	8.43	1.30	5,5	K5
486.....	9.65	8.35	1.30	7,7	K5
487.....	9.95	9.49	0.46	4,3	G5
488.....	9.89	8.90	0.99	3,3	G5
489.....	9.22	8.06	1.16	6,6	K2
490.....	9.17	8.59	0.58	4,3	G5
491.....	8.79	8.51	0.28	6,5	Go
492.....	10.33	9.98	0.35	6,6	F5
493.....	10.33	10.00	0.33	4,3	G
494.....	10.25	9.17	1.08	3,3	Ko
495.....	9.95	9.17	0.78	3,4	G5
496.....	10.76	9.21	1.55	4,4	K5
497.....	8.92	7.93	0.99	3,3	Ko
498.....	10.10	9.97	0.13	8,8	F5
499.....	8.56	8.04	0.52	11,8	Go
500.....	9.60	9.69	−0.09	7,6	Fo
501.....	9.96	9.50	0.46	3,3	Ko
502.....	8.64	8.36	0.28	8,7	F8
503.....	10.61	9.64	0.97	4,3	Ko
504.....	11.61	10.36	1.25	4,3	.....
505.....	10.10	9.78	0.32	3,3	F8
506.....	10.40	9.97	0.43	7,7	Go
507.....	9.98	9.28	0.70	8,7	Ko
508.....	10.16	9.30	0.86	4,4	Ko
509.....	10.15	9.65	0.50	3,3	F8

TABLE IV—*Continued*

Kopff No.	Pg. Mag.	Pv. Mag.	C.I.	No. Plates	*HD* Sp.
510	10.72	9.18	1.54	3,3	K7
511	8.43	8.11	0.32	11,7	F5
512	9.18	9.30	−0.12	7,7	Fo
513	10.88	10.62	0.26	4,2	.....
514	9.57	9.30	0.27	3,4	F8
515	10.14	9.68	0.46	3,3	Fo
516	10.94	10.05	0.89	6,6	K5
517	9.20	9.22	−0.02	7,6	Fo
518	8.50	8.67	−0.17	4,3	Ao
519	10.42	10.18	0.24	4,3	F2
520	11.62	10.51	1.11	5,3	.....
521	9.03	8.94	0.09	3,3	A5
522	9.26	9.30	−0.04	4,3	A2
523	8.85	8.60	0.25	3,3	Ao
524	10.24	9.53	0.71	5,5	Ko
525	9.44	9.20	0.24	3,3	F5
526	8.83	8.89	−0.06	7,6	Fo
527	10.34	10.23	0.11	4,3	Fo
528	9.17	7.54	1.63	3,3	K2
529	10.48	9.16	1.32	4,4	K5
530	10.64	9.67	0.97	4,4	K5
531	8.13	7.93	0.20	4,3	Ao
532	10.78	9.50	1.28	3,3	K2
533	10.40	9.45	0.95	6,6	K2
534	10.51	9.52	0.99	4,3	Ko
534c	10.69	10.29	0.40	4,3	.....
535	10.53	9.50	1.03	4,4	K2
536	9.64	9.60	0.04	4,4	A2
537	9.76	9.55	0.21	3,3	G5
538	10.67	9.95	0.72	4,3	Ko
539	10.01	9.61	0.40	3,3	F5
540	10.69	8.94	1.75	3,3	Mo
541	9.58	9.05	0.53	3,3	G5
542	10.50	9.71	0.79	4,4	.....
543	10.36	9.58	0.78	6,5	F8
544	9.71	8.85	0.86	4,3	Ko
545	10.35	9.32	1.03	5,5	Ko
546	10.00	9.23	0.77	3,3	Ko
547	11.01	9.72	1.29	5,5	K5
548	8.54	7.72	0.82	4,3	G5
549	10.79	10.03	0.76	3,3	F5
550	12.20	10.31	1.89	5,3	F2
551	10.83	9.01	1.82	4,3	M2
552	10.44	10.37	0.07	5,4	F8
553	9.59	9.34	0.25	5,4	F8

TABLE IV—*Continued*

Kopff No.	Pg. Mag.	Pv. Mag.	C.I.	No. Plates	*HD* Sp.
554	8.08	8.14	−0.06	5,4	A0
555	9.49	9.25	0.24	3,3	F8
556	8.10	7.65	0.45	7,4	F5
557	9.02	9.04	−0.02	7,4	F0
558	9.88	9.51	0.37	3,3	G0
559	10.96	9.28	1.68	3,3	K7
560	8.40	7.99	0.41	4,3	F0
561	9.39	8.34	1.05	5,4	K5
562	9.83	9.57	0.26	4,4	G0
563	11.14	9.20	1.94	3,3	M1
564	10.30	9.89	0.41	4,4	F5
565	10.54	9.37	1.17	3,3	K5
566	8.96	7.86	1.10	4,4	K0
567	10.10	9.40	0.70	4,4	K2
568	8.24	7.37	0.87	4,3	G5
569	12.02	10.40	1.62	3,2	.....
570	8.75	8.23	0.52	5,4	G5
571	9.41	8.05	1.36	5,4	Ma
572	9.21	9.26	−0.05	4,4	A5
573	11.68	10.29	1.39	4,4	K0
574	9.27	9.29	−0.02	3,3	A2
575	10.06	9.89	0.17	3,3	F5
576	10.49	9.67	0.82	3,3	K5
577	8.89	8.57	0.32	4,3	F0
578	9.72	10.03	−0.31	4,4	A0
579	9.67	8.37	1.30	3,3	K2
580	9.90	10.23	−0.33	4,4	A0
581	8.84	8.58	0.26	4,4	F8
582	9.52	8.85	0.67	3,3	K2
583	9.32	7.83	1.49	4,3	Ma
584	10.59	10.32	0.27	4,3	F8
585	9.25	8.93	0.32	3,3	F8
586	8.58	8.58	0.00	3,2	F0
587	10.10	9.34	0.76	3,3	G5
588	9.43	9.10	0.33	3,3	K0
589	10.39	9.82	0.57	4,5	G5
590	9.00	8.88	0.12	3,3	F0
591	10.64	10.36	0.28	4,5	G0
592	9.91	9.70	0.21	2,2	F5
593	10.03	9.47	0.56	4,4	K0
594	9.78	9.92	−0.14	3,3	F5
595	9.83	8.99	0.84	3,3	G5
596	10.64	9.97	0.67	4,4	K0
597	9.15	9.14	0.01	4,4	F0
598	9.68	9.76	−0.08	3,3	F0

TABLE IV—*Continued*

Kopff No.	Pg. Mag.	Pv. Mag.	C.I.	No. Plates	*HD* Sp.
599.....	9.91	9.69	0.22	4,4	F2
600.....	10.38	8.96	1.42	3,3	Ma
601.....	10.23	9.98	0.25	3,3	F8
602.....	11.21	10.50	0.71	4,1	G
603.....	7.88	7.84	0.04	5,3	Fo
604.....	10.03	10.07	−0.04	4,4	F2
605.....	10.72	9.96	0.76	3,3	K2
606.....	11.04	10.08	0.96	3,3	K5
607.....	9.98	9.80	0.18	4,4	G5
608.....	10.43	9.59	0.84	3,3	K2
609.....	8.63	8.88	−0.25	4,4	A5
610.....	8.03	7.08	0.95	5,4	G5
611.....	8.68	8.53	0.15	3,2	F5
612.....	9.12	8.22	0.90	3,4	Ko
613.....	9.32	8.48	0.84	3,3	K5
614.....	10.37	9.97	0.40	5,5	Go
615.....	10.42	9.53	0.89	3,3	Ko
616.....	8.38	7.35	1.03	5,7	Ko
617.....	9.97	10.01	−0.04	5,3	A5
618.....	9.91	9.59	0.32	3,3	Go
619.....	9.47	9.60	−0.13	4,4	F8
620.....	8.34	8.29	0.05	6,5	A3
621.....	9.70	9.35	0.35	4,4	G5
622.....	9.62	8.69	0.93	3,3	Ko
623.....	9.75	9.53	0.22	4,4	Go
624.....	9.02	8.94	0.08	3,2	F8
625.....	9.72	8.70	1.02	3,3	K5
626.....	8.09	8.43	−0.34	4,3	A2
627.....	8.88	9.27	−0.39	4,4	F2
628.....	8.68	8.55	0.13	6,5	F5
629.....	10.15	10.00	0.15	3,3	F8
630.....	9.36	8.82	0.54	3,3	K2
631.....	9.31	9.14	0.17	3,3	Fo
632.....	8.54	7.75	0.79	6,5	Ko
633.....	9.67	9.41	0.26	4,4	F8
634.....	9.65	9.54	0.11	4,5	A5
635.....	8.21	8.06	0.15	6,6	A2
636.....	10.20	9.23	0.97	4,3	K5
637.....	9.82	9.22	0.60	3,3	Ko
638.....	9.49	8.62	0.87	3,3	Ko
639.....	8.12	6.62	1.50	6,6	K2
640.....	10.38	10.38	0.00	4,4	Ao
641.....	10.77	10.44	0.33	4,2	Fo
642.....	7.60	7.68	−0.08	6,3	A5
643.....	9.68	8.94	0.74	3,3	Ko

TABLE IV—*Continued*

Kopff No.	Pg. Mag.	Pv. Mag.	C.I.	No. Plates	*HD* Sp.
644	9.40	9.14	0.26	4,3	F5
645	10.29	9.96	0.33	3,3	Go
646	10.56	9.34	1.22	4,4	Ko
647	10.58	9.35	1.23	3,3	K5
648	9.21	8.60	0.61	3,3	Ko
649	10.00	9.09	0.91	3,3	Mo
650	9.42	8.76	0.66	4,4	Ko
651	9.91	9.14	0.77	4,4	Ko
652	10.13	10.09	0.04	4,4	F2
653	9.74	9.18	0.56	5,4	G
654	11.10	10.17	0.93	3,3	K2
655	9.52	9.31	0.21	3,3	G5
656	9.97	9.80	0.17	5,5	F8
657	9.16	9.02	0.14	2,2	F8
658	8.34	7.04	1.30	2,1	G5
659	9.58	8.82	0.76	4,4	K2
660	10.49	9.39	1.10	5,5	K5
661	8.18	7.14	1.04	5,5	Ko
662	8.91	7.94	0.97	5,4	K5
663	9.85	9.01	0.84	5,5	K2
664	7.56	7.73	−0.17	1,1	Ao
665	10.16	10.16	0.00	5,5	Go
666	9.39	9.26	0.13	1,1	Go
667	9.35	8.52	0.83	3,3	K2
668	11.10	9.78	1.32	1,1	K
669	10.36	9.53	0.83	3,3	K5
670	10.34	9.42	0.92	3,3	Ko
671	10.83	10.49	0.34	5,4	Go
672	8.72	7.68	1.04	7,5	Ko
673	10.03	9.84	0.19	1,1	F8
674	9.29	8.24	1.05	3,3	K2
675	9.75	9.53	0.22	2,1	F8
675c	10.88	.....	.....	2,-	.....
676	9.70	9.57	0.13	4,4	Go
677	10.53	9.70	0.83	4,4	K5
679	10.44	9.48	0.96	1,1	Go
680	9.29	8.34	0.95	2,2	K2
681	9.31	9.12	0.19	3,3	F5
684	9.99	8.48	1.51	3,3	K5
685	9.30	9.02	0.28	4,4	G5
686	8.48	8.28	0.20	3,2	F2
688	9.81	9.47	0.34	3,3	Go
689	9.75	8.05	1.70	4,5	Ma
690	9.05	8.85	0.20	4,3	F5
693	9.09	9.11	−0.02	4,4	A5

TABLE IV—*Continued*

Kopff No.	Pg. Mag.	Pv. Mag.	C.I.	No. Plates	*HD* Sp.
693c	10.65	10.38	0.27	4,1	.....
696	9.67	8.15	1.52	4,5	K5
697	8.70	8.36	0.34	3,3	Go
698	9.96	9.46	0.50	4,3	F8
699	10.02	9.56	0.46	1,1	F5
703	9.27	7.86	1.41	1,1	K2
706	9.74	9.65	0.09	3,3	F5
714	9.04	8.26	0.78	2,2	Ko
716	10.00	9.04	0.96	4,4	Ko
717	10.11	9.73	0.38	1,1	F5
720	9.12	8.92	0.20	1,1	G5
726	9.80	9.78	0.02	4,4	F2
727	9.44	9.11	0.33	4,4	G5
728	8.94	8.31	0.63	4,3	Ko
737	8.78	8.98	−0.20	1,1	F8
749	9.14	8.95	0.19	3,3	F5
752	9.62	8.37	1.25	3,3	K5
757	9.86	9.67	0.19	3,3	F8
769	8.37	7.63	0.74	4,4	Ko
774	9.13	9.17	−0.04	3,3	A3
782	10.05	8.99	1.06	3,2	K2
785	9.21	9.02	0.19	3,2	A2
788	10.90	10.64	0.26	3,2	.....
796	10.06	9.22	0.84	2,2	Ko
798	10.34	9.56	0.78	2,2	G5
813	10.05	9.34	0.71	2,2	Ko
818	9.18	8.93	0.25	2,2	F8
819	7.86	7.22	0.64	3,3	Ko
820	9.61	9.00	0.61	2,2	Go
821	9.29	8.82	0.47	2,2	G5

corrections in the seventh and ninth columns of the table. The corrections for fields 8 to 14 were found by the adjustment formulae of section 5; the others by distributing the better-determined differences equally between the two fields from which they were derived.

Further evidence on the internal agreement is shown by the differences in the last two columns of Table III, which represent the deviation of each B plate from the mean magnitudes for the extra stars found from series C. Since these magnitudes from series C depend on from two to four polar comparisons of series A, the differences in question are largely zero-point errors in the plates of series B. Their average is ±0.06 mag., about that normally to be expected

from single polar comparisons; the uncertainty arising from the small number of images on the B plates has been offset by the corrections applied to the zero points.

The value of these corrections is shown by their effect on the differences. Of the 30 values in the last two columns of Table III, 18 are smaller, 6 larger, and 6 the same as would have been obtained without adjustment for series B. As for the adjustment of series A and C, 17 differences are smaller, 11 larger, and 2 unchanged. The improvement for the photographic magnitudes is marked, 11 differences being smaller and only 4 increased.

The distribution of algebraic signs in the last two columns of Table III excludes the possibility of any large progression in the zero-point differences for series B and C; the general systematic means $(C-B)$ for photographic and photovisual results are, respectively, -0.02 and -0.01 mag.

The mean magnitudes for the bright extra stars derived from both series B and C are given in Table V, which is similar to Table IV.

The average probable error of a magnitude from a single plate, including scale and zero-point errors, is

	Pg.	Pv.
Comparison stars.....	±0.096	±0.081
Extra stars.....	±0.093	±0.090

These mean values were calculated from

$$\text{P.E.} = \frac{0.845\Sigma v}{\sqrt{n(n-1)}} \qquad (n = 2, 3, \ldots .),$$

where Σv is the mean of the sums of residuals without regard to sign for all stars for which the number of residuals n is the same. The agreement for different values of n is excellent.

8. COMPARISON WITH THE MAGNITUDES OF ROSS AND ZUG

The satisfactory internal agreement shown by the preceding discussion becomes much less reassuring when the magnitudes in Table IV are compared with those of Ross and Zug. The differences for 112 stars occurring in both series of measures are given in Table VI. The large discordance for No. 569 seems to arise from a wrong identi-

TABLE V

MAGNITUDES OF BRIGHT EXTRA STARS

HD No.	Pg. Mag.	Pv. Mag.	C.I.	No. Plates	*HD* Sp.
83261.....	6.84	6.85	−0.01	4,2	F2
83332.....	6.87	5.83	1.04	5,3	Ko
83953.....	5.08	4.57	0.51	4,3	B2p
84117.....	5.54	4.82	0.72	4,4	Go
84367.....	5.29	4.88	0.41	3,3	F5p
84458.....	7.25	7.27	−0.02	5,4	Fo
84709.....	7.33	7.15	0.18	5,5	F2
85043.....	7.02	6.69	0.33	8,6	Fo
85725.....	6.86	6.38	0.48	6,3	F8
85859.....	6.06	4.75	1.31	6,5	Ko
86266.....	6.35	6.47	−0.12	6,5	A2
86463.....	6.75	6.99	−0.24	7,6	A2
86612.....	5.98	6.32	−0.34	7,7	B5
87019.....	7.71	6.97	0.74	6,4	G5
87318.....	6.65	6.76	−0.11	5,4	Ao
87427.....	6.07	5.86	0.21	4,4	Fo
87793.....	7.52	7.25	0.27	7,5	F8
87870.....	8.62	7.00	1.62	5,2	Ma
88806.....	7.98	6.38	1.60	6,4	Ma
89828.....	6.32	6.49	−0.17	4,4	Ao
89816.....	6.42	6.53	−0.11	4,4	A3
90027.....	6.48	6.94	−0.46	4,5	B9
90197.....	7.36	7.23	0.13	6,6	Go
90955.....	6.95	7.49	−0.54	5,5	Ao
90954.....	7.24	7.17	0.07	5,5	Fo
91398.....	6.79	7.10	−0.31	2,2	B9
91550.....	6.60	5.28	1.32	2,2	K2
91706.....	6.55	5.84	0.71	2,2	F5
91975.....	8.63	6.82	1.81	3,2	K5
92098.....	8.32	7.21	1.11	3,3	Ko
84412.....	7.89	7.12	0.77	3,3	G5
84669.....	8.69	7.09	1.60	2,2	Ko
85905.....	5.98	6.33	−0.35	4,4	A2
87810.....	7.25	6.58	0.67	1,1	F2
87130.....	7.11	6.70	0.41	4,3	Ao
86626.....	8.05	6.71	1.34	4,3	K2
85951.....	6.45	4.81	1.64	2,3	Ma
87344.....	6.02	6.37	−0.35	3,3	Ao
87330.....	6.81	7.40	−0.59	3,3	Ao
86030.....	8.43	7.14	1.29	2,2	Ma
87768.....	6.77	6.89	−0.12	4,5	Fo
87808.....	7.03	5.52	1.51	5,4	K2
88359.....	8.72	7.22	1.50	5,3	Ko
86371.....	6.57	6.88	−0.31	3,1	Fo
88346.....	8.74	7.20	1.54	3,3	K2

TABLE V—*Continued*

HD No.	Pg. Mag.	Pv. Mag.	C.I.	No. Plates	*HD* Sp.
88025.....	5.94	6.29	−0.35	3,3	Ao
88549.....	6.81	7.18	−0.37	3,3	Ao
89746.....	6.57	6.52	0.05	2,3	A2
89351.....	7.88	7.08	0.80	5,6	G5
88108.....	8.74	7.11	1.63	5,4	Ma
87096.....	7.34	6.97	0.37	3,3	F8
87504.....	4.47	4.53	−0.06	1,2	B8
88215.....	5.76	5.20	0.56	2,3	Fo
89455.....	6.16	6.03	0.13	3,3	Fo
88284.....	4.71	3.71	1.00	1,3	Ko
88182.....	6.23	6.40	−0.17	3,3	A2
89033.....	6.85	6.12	0.73	3,3	Ko
89945.....	8.63	7.14	1.49	3,2	Ma
89565.....	6.34	6.34	0.00	3,3	F2
88195.....	5.6	6.0	−0.4	2,1	Ao
88333.....	6.74	5.69	1.05	1,2	Ko
89254.....	5.51	5.36	0.15	3,3	Fo
88372.....	5.9	6.4	−0.5	2,2	Ao
90362.....	6.91	5.52	1.39	3,4	K5
90430.....	6.65	6.96	−0.31	3,4	Ao
91318.....	7.41	6.81	0.60	3,3	Ko
89669.....	6.59	6.91	−0.32	4,4	A2
89490.....	6.90	6.33	0.57	4,3	Ko
90485.....	7.37	6.42	0.95	4,3	Ko
90044.....	5.72	5.94	−0.22	3,3	B9
91638.....	6.86	6.69	0.17	3,3	F8
90763.....	5.95	6.03	−0.08	3,3	Ao
90057.....	8.11	6.31	1.80	4,3	K5
90882.....	5.44	5.22	0.22	2,2	B9

fication. The star in Kopff's list is B.D.−15°2990. The presence of the brighter star B.D.−15°2989, 7′ and 5ˢ Np No. 569, possibly affords an explanation of the Yerkes magnitudes.

Scale divergence and accidental error.—Grouped according to magnitude and reduced to mean values, both with and without regard to algebraic sign, the differences of Table VI give the results in the second and third and the sixth and seventh columns, respectively, of Table VII. The run in the systematic differences represents the divergence in the scales of the Mount Wilson and Yerkes magnitudes, which is appreciable for both photographic and photovisual results. The means for all magnitudes together, −0.03 and 0.00

TABLE VI

COMPARISON WITH THE MAGNITUDES OF ROSS AND ZUG

(Unit = 0.01 mag.)

KOPFF NO.	*MW − Y*		KOPFF NO.	*MW − Y*	
	Pg.	Pv.		Pg.	Pv.
522	+ 47	+21	610	+ 9	+16
531	+ 49	+12	611	+ 5	+20
532	+ 35	− 2	613	− 4	+17
534	+ 33	+ 6	615	−15	− 7
538	+ 18	−17	617	− 4	+13
540	+ 33	+17	618	−16	−10
541	+ 27	0	619	−14	− 5
542	+ 23	+15	621	−21	+ 3
548	+ 37	+10	622	− 2	+ 2
549	+ 36	−23	623	−14	+ 5
551	+ 22	0	624	+ 8	+30
554	+ 28	+13	625	−18	+21
555	+ 26	+25	626	−30	+ 7
559	− 2	−16	627	−24	+22
560	+ 31	+ 1	629	−16	+ 1
562	+ 38	+13	630	− 9	+17
563	+ 17	− 4	631	−11	−12
564	+ 3	−26	633	−30	− 9
565	+ 15	0	636	−35	+15
566	+ 9	+ 4	637	−11	− 2
568	+ 52	+ 7	638	− 8	+12
569	(+143)	(−40)	639	− 4	− 5
571	+ 10	+12	641	0	− 6
574	+ 32	+ 8	642	−14	+ 8
575	+ 27	−10	643	−24	−16
576	− 4	+ 2	645	−22	−22
577	+ 15	+ 9	647	−17	−12
579	− 13	+ 2	648	−35	− 6
581	+ 13	+10	649	−25	− 9
583	+ 7	+21	650	−19	+ 8
585	+ 29	+10	651	−13	−15
586	− 9	+12	652	− 7	+22
587	+ 3	− 2	654	−42	− 8
588	− 10	+27	655	−33	− 1
590	+ 3	+ 1	657	−25	−10
592	− 15	+ 4	658	+19	− 8
594	− 13	+10	659	−44	+12
595	− 3	+15	661	−14	−23
598	− 15	+15	662	−12	+ 3
599	+ 4	−25	664	− 7	−20
600	− 13	+ 4	666	−10	+11
601	+ 21	−10	667	−48	− 1
602	+ 3	− 9	668	+21	−11
603	+ 7	+10	669	−12	−27
605	− 10	−12	670	−20	−10
606	− 45	−11	673	−14	+ 4
608	− 12	−14	674	−33	−11
609	− 39	+16	675	−21	−11

TABLE VI—*Continued*

Kopff No.	*MW−Y*		Kopff No.	*MW−Y*	
	Pg.	Pv.		Pg.	Pv.
677.....	−13	−36	697.....	−18	−13
679.....	+18	+ 5	699.....	+23	− 4
680.....	−34	− 7	703.....	−10	− 6
681.....	+ 6	− 5	706.....	−19	+11
684.....	−22	−26	714.....	− 9	− 6
686.....	− 1	+ 7	717.....	+17	+ 5
688.....	−27	−13	720.....	−11	+ 7
690.....	− 6	−16	737.....	−39	+ 3

mag., respectively, are the zero-point differences for the two series of observations.

The photographic magnitudes have all been reduced to the international color system, and, in fact, their differences show no dependence on color. Ross and Zug have assumed that their photovisual magnitudes are also on this system. Relative to the Mount Wilson values, they indicate, however, a small but definite color coefficient:

$$MW - Y = -0.06C\ .$$

Had the doubtful color correction found in section 4 for the Mount Wilson photovisual magnitudes been applied, the color difference $MW - Y$ would have been larger still. The difference has been disregarded in the remaining comparisons.

The third and seventh columns of Table VII, which include accidental as well as systematic errors, indicate the accordance between Mount Wilson and Yerkes for individual stars. The average of ± 0.11 mag. for the photovisual series is acceptable; but ± 0.19 for the photographic magnitudes is very unsatisfactory.

Table VI shows that this large value originates in a zero-point difference which changes with the position of the stars along the path of Eros. The fields involved, in the order of star numbers, are 7 to 1 of Table I, covering an interval of about 30^m in R.A. and 17° in Dec.

Agreement for Mount Wilson plates.—In searching for the cause of the difference, the first question concerns the agreement of results

for the same star from different Mount Wilson plates. Table VIII gives data for four stars showing large positive and negative differences, but otherwise selected at random. The magnitudes read from the curves include the extinction correction, but both plate and zero-point corrections are given in detail. Bracketed magnitudes depend on the same image on a connecting plate, reduced with different polar comparisons, and are therefore united to obtain a value of unit weight. The last pair for star 531 is from screen images, and allowance must be made for the screen constant of 3.01 mag.

TABLE VII

SUMMARY FOR $MW-V$

PHOTOGRAPHIC				PHOTOVISUAL			
Yerkes Mag.	Syst. Diff.	Aver. Diff.	No. Stars	Yerkes Mag.	Syst. Diff.	Aver. Diff.	No. Stars
7.5– 8.0.....	+18	±24	7	<7.5.....	− 3	±12	5
8.0– 8.5.....	+ 5	19	7	7.5– 8.0.....	+ 5	10	11
8.5– 9.0.....	+12	17	11	8.0– 8.5.....	+ 6	11	14
9.0– 9.5.....	− 5	17	19	8.5– 9.0.....	+ 8	12	18
9.5–10.0.....	−14	20	26	9.0– 9.5.....	+ 1	9	27
10.0–10.5.....	+ 1	20	23	9.5–10.0.....	− 2	10	25
10.5–11.0.....	− 7	15	15	>10.0.....	−16	±16	11
>11.0.....	−28	±30	3				
Means and totals.....	− 3	±19	111	Means and totals.....	0	±11	111

The reduction for color transfers the results to the international color scale.

The zero points depend directly on the polar comparisons of series A for the fields listed in the first column of Table VIII; for example, Nos. 9, 10, and 11 in the case of star 522. In fact, all the comparisons are involved through the adjustment process, which assigns to each field a correction depending on all the observed zero points. The agreement is such that something more than the ordinary accidental error affecting polar comparisons is required to explain the large deviations from the Yerkes results. The plate corrections are large, but not in general strongly systematic for a given star; the accordance which they bring into the results is good testimony of their general validity.

Test of zero points by series B.—A further test is afforded by the independent polar comparisons of series B, which have been used only for the extra stars of Table V and do not enter into the results for the Eros stars. The agreement of these comparisons, field by field, with the mean results from series A and C has already been

TABLE VIII

DETAILED RESULTS FOR INDIVIDUAL STARS

Field	Curve	Pl. Corr.	Z. Pt. Adj.	Mag.	v	Field	Curve	Pl. Corr.	Z. Pt. Adj.	Mag.	v
Kopff 522						Kopff 659					
9.....	8.75	+34	+9	9.18	+ 9	13.....	9.20	+31	−6	9.45	+ 1
10.....	9.33	−12	+6	9.27	0	12,13.....	8.90	+43	−4	9.29	+18
9,10.....	9.19	+17	+9	9.45	−15		9.00	+34	−6	9.28	
	9.16	+16	+6	9.38		14.....	9.80	−22	−3	9.55	− 9
10,11.....	9.52	−42	+6	9.16	+ 5	13,14.....	9.59	+ 2	−6	9.55	−10
	9.59	−34	+2	9.27			9.54	+ 5	−3	9.56	
Mean				9.27						9.46	
Red. for color				−0.01						+ 0.12	
MW pg. mag				9.26						9.58	
Yerkes mag				8.79						10.02	
MW − *Y*				+0.47						− 0.44	
Kopff 531						Kopff 667					
10.....	8.23	+ 8	+6	8.37	−27	14.....	8.86	+30	− 3	9.13	+ 9
11.....	8.36	−30	+2	8.08	+ 2	15.....	9.16	− 5	+21	9.32	−10
10,11.....	8.00	−13	+6	7.93	+10	14,15.....	9.08	+17	− 3	9.22	0
	8.17	−13	+2	8.06			8.82	+18	+21	9.21	
(10,11)s...	11.09	− 9	+6	8.05	+15						
	10.92	− 9	+2	7.84							
Mean				8.10						9.22	
Red. for color				+0.03						+ 0.13	
MW pg. mag				8.13						9.35	
Yerkes mag				7.64						9.83	
MW − *Y*				+0.49						− 0.48	

given in the last two columns of Table III. For the present test, however, it is necessary to know the relation of the Yerkes magnitudes to the results obtained from individual plates of series A.

The mean values of $A - Y$ for each A plate are given in the second and sixth columns of Table IX. These means reproduce the systematic progression shown by the results in Table VI in a form which admits a comparison with similar differences referred to series B. Since the zero points for series C are the same as for A, the differences in the last two columns of Table III have the form $A - B$, and as

such are transferred to the fourth and eighth columns of Table IX. Combined with the corresponding values of $A-Y$, they give the desired values of $B-Y$. These show that when referred to the zero points of series B, the Mount Wilson magnitudes, especially the photographic series, diverge from the Yerkes measures in substantially the same way as when referred to series A. The mean discordance for the photographic magnitudes, which is the more serious of the two, is

$A-Y$	$B-Y$	
+0.22	+0.25	(Fields 5, 6, 7)
−0.16	−0.21	(Fields 1, 2, 3)

TABLE IX

AGREEMENT OF YERKES MAGNITUDES WITH INDIVIDUAL POLAR COMPARISONS OF SERIES A AND SERIES B

(Unit=0.01 mag.)

FIELD	PG.				PV.			
	$A-Y$	No. Stars	$A-B$	$B-Y$	$A-Y$	No. Stars	$A-B$	$B-Y$
7	+25	5	− 2	+27	−4	1	+ 7	−11
6	+31	23	−12	+43	+5	23	− 9	+14
5	+14	33	+ 2	+12	+4	32	−17	+21
4	− 6	28	−13	+ 7	+7	27	− 5	+12
3	−17	30	0	−17	+2	29	+ 4	− 2
2	−18	28	+15	−33	−6	28	+12	−18
1	−13	28	− 1	−12	−7	28	+ 3	−10

The general agreement of the A and B series does not necessarily mean that the large relative error for the two groups of fields is to be attributed wholly to the Yerkes magnitudes. Although the photographs for the two series of Mount Wilson comparisons were usually made on different nights, peculiar sky conditions may have introduced similar errors into each. Among other causes, sky illumination from lights in the valley to the southwest of Mount Wilson is a possible source of systematic error; but in the present case the fields were all observed at so nearly the same altitude as to make a relative error of 0.4 mag. wholly inadmissible.

Color indices in different fields for stars of same spectral type.—An indication as to the location of the error may be found by comparing the color indices for the two groups of fields with the spectral types

of the stars. The differences in the Mount Wilson and Yerkes color indices have the form

$$C - C_1 = (Pg - Pg_1) - (Pv - Pv_1) \qquad \text{(Fields 5, 6, 7)},$$
$$C' - C_1' = (Pg' - Pg_1') - (Pv' - Pv_1') \qquad \text{(Fields 1, 2, 3)}.$$

The values of the first of the parentheses in these formulae are +0.22 and −0.16, respectively. The corresponding photovisual differences from the sixth column of Table IX are +0.05 and −0.04. Hence

$$(C - C') - (C_1 - C_1') = \Delta C = +0.29 \text{ mag.}$$

The two differences in the left-hand member of this relation, which must be satisfied by the color indices of stars of the same spectral type, indicate the apportionment of error between the Mount Wilson and Yerkes magnitudes.

The results are collected in Table X, which gives for the two groups of fields and the two series of observations the mean color indices corresponding to the spectral types in the first column. The values of ΔC in the last column agree well and show that the effect of accidental errors is unimportant. The mean ΔC is less than the 0.29 found from the individual polar comparisons because it depends on color indices derived from the final magnitudes. Since these include the zero-point determination for the transition field No. 4, the discordance is partly smoothed out (see Table IX).

The values of ΔC check the consistency of the results, but the feature of present interest is their origin. The sequences of differences in the sixth and twelfth columns, and more particularly their mean values, +0.07 and −0.17 mag., indicate that 0.3 of the discordance originates in the Mount Wilson measures and 0.7 in the Yerkes results.

This conclusion depends on a comparison of observed colors for different groups of stars which supposedly have the same color. Errors of classification, lack of discrimination between giants and dwarfs, and dispersion in color for the same type all tend to invalidate the supposition. The single M-type star in the second group of fields, for example, if retained, would seriously modify the distribution of error. Its color index is 1.0 mag.; but no M star, either giant

or dwarf, as far as we know, has so small a color index. The spectral type doubtless is in error. For the other spectral groups the number of stars is generally sufficient to eliminate most of the accidental errors of classification. Systematic differences between the two groups of fields may, however, affect the result. Comparison of the frequencies of spectral types for these groups with those for several other groups of stars selected from Tables IV and V shows a general agreement, with a maximum at Ko in all cases except for fields 5, 6, 7, for which it occurs at G7. The frequency-curve for this group would agree better with the others if 0.3 of an interval could be added to the spectral types for most of the stars. If this difference in frequencies is real, the results in Table X require no change;

TABLE X

COMPARISON OF COLORS FOR STARS OF SAME SPECTRAL TYPE

HD Sp.	Mount Wilson						Yerkes						ΔC
	C	No.	C'	No.	$C-C'$	Wt.	C_1	No.	C_1'	No.	C_1-C_1'	Wt.	
A2	+0.08	5	−0.12	2	+0.20	1	−0.19	4	−0.10	2	−0.09	1	+0.29
F4	0.30	10	+ .16	14	+ .14	6	+0.14	10	+0.26	14	− .12	6	.26
G3	0.50	7	.53	8	− .03	4	0.34	5	0.60	8	− .26	3	.23
K2	1.01	10	.96	23	+ .05	7	0.89	8	1.08	23	− .19	6	.24
M	+1.67	6	+0.91	1	(+0.76)	0	+1.58	6	1.07	1	(+0.51)	0	+0.25
Weighted mean					+0.07						−0.17		+0.25

but if it represents an error in classification, the values of C and C_1 should be decreased by about 0.1 mag. This would improve the agreement for the Mount Wilson color indices, but make that for the Yerkes values less satisfactory.

9. RELATION BETWEEN COLOR INDEX AND SPECTRAL TYPE

Table XI gives the mean color index for each spectral type based on all the stars in Tables IV and V for which spectra are available.

The large positive color index for the single B2 star (H.D. 83953, Table V) seems to be real; but in view of the discordances shown in Table VIII confirmation is required. The star is I Hydrae. The *HD* remarks: "The line $H\beta$ is a narrow, bright line superposed on a hazy, dark band. Other lines are dark." Merrill classifies it as B2e and finds it to be a normal object of its kind. A short-focus camera plate of the region by Hubble gives no indication of surrounding nebulosity.

The general relation between color and spectrum expressed by Table XI is essentially the same as that found by Ross and Zug. The Mount Wilson color indices are systematically a few hundredths smaller than the Yerkes values, as might be expected from the relation between zero points shown in Table VII. The most noteworthy features of these results, however, are, first, that both series of measures show a color index of about −0.15 mag. for Ao stars, whereas the value for the polar region is zero; and, second, that both depart widely from the accordant relations between color and spec-

TABLE XI

MEAN COLOR INDEX AND SPECTRUM

Sp.	C	No. Stars	Sp.	C	No. Stars	Sp.	C	No. Stars
B2p	+0.51	1	A5	−0.02	9	G5	+0.63	33
B5	− .34	1	A7	− .18	1	Ko	+0.89	66
B8	− .26	2	Fo	+ .10	26	K2	+1.11	29
B9	− .19	5	F2	+ .11	13	K5	+1.21	31
Ao	− .14	21	F5	+ .29	27	K7	+1.61	2
A2	− .08	13	F8	+ .26	33	M	+1.53	16
A3	−0.03	3	Go	+0.37	27	Total	.....	359

trum found by King, Parkhurst, and Seares. Some of this last difference is doubtless to be accounted for by the presence of dwarfs among the fainter comparison stars for Eros, but this cannot wholly explain the divergence. These questions will be discussed in a later *Contribution*.

10. COMPARISONS WITH HARVARD MAGNITUDES

Intercomparison of the various Harvard catalogues has shown that they differ appreciably in scale and in color equation.[1] The general catalogues, *HA* **50, 54,** and especially the *Draper Catalogue*, which is a compilation from other volumes of the *Harvard Annals*, are therefore not homogeneous, and at present it is impossible to say what correction should be applied to any given star to reduce it to the international system. To utilize fully this rich observational

[1] See, for example, *Harvard Annals*, **64**; Müller and Kempf, *Publikationen des Astrophysikalischen Observatoriums zu Potsdam*, **17**, 1907; Zinner, *Veröffentlichungen der Remeis-Sternwarte zu Bamberg*, **2**, 65, 1926; Seares, *Mt. Wilson Contr.*, No. 288; *Astrophysical Journal*, **61**, 284, 1925.

material it will be necessary to discuss the original magnitudes, reduce them to the international system, and then recombine them into mean catalogue values. The photovisual magnitudes in Tables IV and V permit a few comparisons of this sort—not enough for final conclusions, but sufficient to show the importance of the corrections.

The differences $MW-H$ thus found for different Harvard sources were grouped according to Harvard magnitude and plotted against MW color indices. Graphical solutions then gave the linear expressions collected in Tables XII and XIII. These relate to measures made by Pickering, Wendell, and Bailey with the 2-inch, 4-inch, and 12-inch meridian photometers. A few observations by Searle were also found in *HA* **14**, but they indicate little more than the presence of a considerable color equation. The absence of a color coefficient does not mean that the coefficient is zero, but merely that the data do not permit a satisfactory determination.

In any one of the groups of relations in Tables XII and XIII the sequence of first terms represents the scale divergence after the Harvard measures have been freed from color in accordance with the coefficients of the second terms. For the first two groups the color coefficients of Pickering and Wendell are approximately the same, and mean values are used in Table XI; but this cannot be done for the first terms. For these Pickering's values are given, with values of $P-W$ following in parentheses. For results in *HA* **14**, the mean zero-point difference $P-W$ is -0.17; for *HA* **24**, $+0.14$.

The significant features of the comparisons are: (1) the progression in the scale difference shown by all the measures of Pickering and Wendell and the size of the color coefficient affecting their results; (2) the increase in the color coefficient with magnitude and the systematic differences between the coefficients for the three photometers; (3) the difference in the scale corrections for Bailey and Pickering and the relative freedom of Bailey's measures from the influence of color.

It is not suggested that the results in Tables XII and XIII are final or that they are applicable to all portions of the catalogues involved. The data on which they are based are far too slender for that. The characteristic features are revealed so clearly, however,

TABLE XII

COMPARISONS WITH DIFFERENT HARVARD CATALOGUES ($MW-H$)

Harv. Vis. Mag.	2-Inch M.P.		4-Inch M.P.						12-Inch M.P.	
	HA 14, *P* and *W*	No. Obs.	*HA* 24, 1, 4, *P* and *W*	No. Obs.	*HA* 44, *P*	No. Obs.	*HA* 45, *P*	No. Stars*	*HA* 70, 74, *P*	No. Stars*
3.9	−0.16(+0.13)	6	.....	....	−0.13	3	−0.12	1	.....	.....
4–5	+ .10(− .17)	16	−0.30(+0.15)	9	− .25	7	− .08−0.10C	3	.....	.....
5–6	+ .20(− .20)−0.32C	33	+ .04(+ .16)−0.15C	26	− .04−0.23C	33	+ .07− .20C	5	.....	.....
6–7	+0.30(−0.25)−0.46C	28	+ .10(+ .14)− .38C	37	+0.07−0.35C	39	+ .11− .27C	33	.....	.....
7–8	.....	....	+ .15 −0.40C	7	.....	....	+0.25−0.33C	26	−0.10	1
8–9	.....	....	+0.25(+0.13)	16	.....	....	.....	.....	+0.20−0.30C	16

TABLE XIII

COMPARISON WITH BAILEY ($MW-B$)

Harv. Vis. Mag.	4-Inch M.P.			
	HA 44, *B*	No. Obs.	*HA* 46, *B*	No. Stars*
3.8	−0.06	3	−0.05	1
4–5	− .18	1	− .19	2
5–6	− .10−0.10C	10	− .12+0.00C	9
6–7	0.00−0.10C	17	−0.16	3

The number of observations is roughly three times the number of stars.

as to indicate that reliable formulae for reduction to a homogeneous system may be obtained with comparatively little effort.

The diversity in the corrections shown in Tables XII and XIII lessens the importance of any comparison with the mean Harvard magnitudes given in the *Draper Catalogue*. The general agreement with a similar comparison made some years ago for the stars of the Polar Sequence[1] is, nevertheless, of interest.

The results, after a slight smoothing, are as given in the third column of Table XIV. The comparison with the polar sequence is in the following column. The divergence in the color coefficients probably arises from differences in instruments and observers con-

TABLE XIV

COMPARISON WITH MEAN HARVARD VISUAL SCALE

Harv. Vis. Mag.	No. Stars	*MW−H* Present Results	*MW−H* Polar Sequence	Differences
3.8.....	1	−0.05−(0.10)C	−0.08−0.09C	−0.03+0.01C
4–5.....	3	− .10−(.13)C	− .07− .10C	+ .03+ .03C
5–6.....	13	− .01− .17 C	− .04− .12C	− .03+ .05C
6–7.....	42	+ .08− .21 C	+ .02− .13C	− .06+ .08C
7–8.....	28	+ .17− .26 C	+ .10− .14C	− .07+ .12C
8–9.....	12	+0.25− 0.36 C	+0.19−0.15C	−0.06+0.21C

cerned in the two groups of Harvard magnitudes. The scale difference, which is mainly in the zero point and amounts to about 0.05 mag., may also arise partly from this source.

Magnitudes given in the *Draper Catalogue* to a single decimal are from the *Durchmusterung* catalogues, reduced to the *HD* system by the application of mean corrections. The catalogues involved are the *SDM*, the *CD*, and the *CPD*, the last only for stars south of −16° declination. Comparisons with these catalogues are given in Table XV. *HD* magnitudes printed in italics have not been used.

For none of the three catalogues is there any certain evidence of a progression in the values of *MW−H*. As far as the present data go, the only difference is in the zero points, for which the means are +0.01, +0.11, and +0.12 mag., respectively. The parallelism of scales is in surprising contrast to the 34 per cent divergence found

[1] Seares, *Mt. Wilson Contr.*, No. 288, Table II; *Astrophysical Journal*, 41, 284, 1925.

by Ross and Zug[1] in a similar comparison of visual magnitudes. Nearly all their stars, however, are from the northern *Durchmusterung* (with Harvard corrections); and the discrepancy between their results and ours apparently represents a real difference in the magnitude systems for the northern and southern catalogues.

TABLE XV

COMPARISON WITH *DM* MAGNITUDES REDUCED TO *HD* SYSTEM

HARV. MAG.	*MW−H(SDM)*			*MW−H(CD)*			*MW−H(CPD)*		
	S.D.	A.D.	No.	S.D.	A.D.	No.	S.D.	A.D.	No.
7.5– 7.9	−0.15	±0.22	6	.....	.....	.....	.....	.....	.....
8.0– 8.4	− .02	.35	13	+0.22	±0.40	9	+0.20	±0.20	7
8.5– 8.9	− .05	.26	45	+ .04	.32	17	+ .05	.18	20
9.0– 9.4	+ .11	.28	49	+ .15	.27	17	+ .14	.23	37
9.5– 9.9	−0.07	±0.12	9	+0.02	±0.10	5	+ .18	.29	32
10.0–10.4	.....	.....	.....	.....	.....	.....	−0.03	±0.17	14
Means and sums	+0.01	±0.27	122	+0.11	±0.30	48	+0.12	±0.23	110

The approximate character of the *Durchmusterung* magnitudes means a large scatter in the values of $MW-H$ for individual stars, and it is therefore difficult to speak definitely of the influence of color. The *CD* and *CPD* show nothing; the representation of the *SDM* differences would be somewhat improved by adopting a color coefficient of 0.2 to 0.4, but the correlation is uncertain and the results of Table XV are preferred for the present.

CARNEGIE INSTITUTION OF WASHINGTON
MOUNT WILSON OBSERVATORY
November 1930

[1] *Loc. cit.*

Contributions from the Mount Wilson Observatory, No. 416
Reprinted from the *Astrophysical Journal*, Vol. LXXIII, pp. 13–25, 1931
Printed in the U.S.A.

STEWARD OBSERVATORY

TEMPERATURE CLASSIFICATION OF THE STRONGER LINES OF COLUMBIUM, WITH PRELIMINARY NOTES ON THEIR HYPERFINE STRUCTURE

By ARTHUR S. KING

ABSTRACT

The paper gives the temperature class, the ionization, and a preliminary discussion of the hyperfine structure of 646 of the stronger lines of columbium between λ 3100 and λ 6900. The results were obtained by comparing electric-furnace spectra at temperatures of about 2500° and 2900° C with the spectra of the arc and spark. Approximately 200 lines appear in the furnace spectrum, but many neutral and all of the ionized lines require higher excitation. Much variation in response to excitation was found for lines in both groups.

Of special interest is the large proportion of columbium lines having hyperfine structure. Of the lines listed, about 40 per cent are evidently complex. The patterns, for the most part unresolved, appear to consist usually of two, four, or six components, with some still more complex. As the wave-length increases, the spacing of hyperfine patterns becomes in general wider. Lines of complex structure occur in all temperature classes.

The data presented in this paper cover the stronger lines emitted by the columbium arc from λ 3100 to λ 6900. Of these, the proportion appearing in the electric-furnace spectrum is smaller than for other elements which have been studied, probably in large measure because of the high vaporization-point of the metal. The lines of the ionized atom, selected by a comparison of arc and spark spectra, are beyond the reach of the furnace excitation, and only those which attain considerable strength in the arc are included in the present discussion. These and the neutral lines of sufficient strength to be expected in the furnace spectrum were selected from a very large preliminary list. All lines below intensity 8 were omitted.

To the difficulty arising from the faintness of the furnace spectrum is added that caused by the masking of many columbium lines by the carbon bands (from the graphite tube), which are strong at temperatures required for the vaporization of the metal. The results give, however, the behavior of the more sensitive lines in both the ionized and neutral spectra, the degree of excitation required for the latter being indicated by the furnace intensities.

EXPERIMENTAL METHOD

The spectrograms were made with the 15-foot concave-grating spectrograph, the second-order spectrum (scale, 1 mm = 1.86 A) being used to the violet of λ 5400. The graphite tube of the vacuum furnace was charged with powdered columbium and heated, for the high-temperature stage, to 2800° or 2900° C. Another series of furnace spectrograms made at 2400°–2500° was used to determine the persistence of the furnace lines.

In addition, a large collection of arc and spark spectrograms was made, to serve for the selection of ionized lines and for measurement of the columbium wave-lengths from iron standards. The electrodes used to obtain these spectra were of highly purified columbium procured from Dr. C. W. Balke, of the Fansteel Products Company, by Dr. W. F. Meggers, of the Bureau of Standards, and kindly loaned to the writer.

EXPLANATION OF THE TABLE

The wave-lengths in the first column of Table I are on the international system, converted from the values of Exner and Haschek,[1] with some wave-lengths, usually of close doublets, measured by the writer. The second column gives the estimated arc intensities, none of which is less than 8. Partial reversal, observed for a few arc lines, is indicated by *r*. The furnace intensities in the third column are for the high-temperature stage, 2800°–2900° C. The frequent question marks in this column indicate uncertainties arising from blends with foreign lines, usually those of the carbon bands. The temperature classes in the final column are based on the strength of the lines in the arc, in the high-temperature furnace, and in the furnace at about 2400° C, data for the last not being entered in the table. Lines of the ionized spectrum, none of which appears in the furnace, are placed in class V E. An asterisk (*) after a wave-length refers to a note at the end of the table.

The probable number of hyperfine components, when the line is evidently not single, is indicated by an Arabic numeral following the class number. The significance of these component-numbers is given in the discussion of this feature of the spectrum.

[1] *Spektren der Elemente*, **2**, 1911.

TABLE I

Temperature Classification of Columbium Lines

λ	Intensities		Class No. Comps.	λ	Intensities		Class No. Comps.
	Arc	Fur.			Arc	Fur.	
3094.21	300†	.....	V E, 6	3264.59	50	2	IV
3096.50	10	.....	V	3267.05	12	.....	V
3099.20	15	.....	V E	3270.44	20	1	IV, 2
3111.47	20	.....	V	3270.76	25	2	IV
3116.34	10	.....	V	3271.98*	10	.....	V
3122.66	10	.....	V	3272.07*	30	4	IV
3127.53	30	.....	V E, 4	3277.65	50	4	IV
3130.81	200†	.....	V E, 4	3279.24	8	.....	V E, 4
3133.01	10	.....	V	3283.45	15	.....	V E, 2
3136.97	8	.....	V	3285.66	80	6	IV
3145.40	50†	.....	V E	3287.59	60	3	IV
3151.86	30	2	IV	3287.91	50	.....	V
3163.39	150†	.....	V E, 2	3291.91*	8	.....	V
3172.54	8	.....	V	3292.00*	12	.....	V E
3175.80*	10	.....	V E, 3	3296.03*	80	6	IV
	8	.....	V E	3299.62	30	1	IV
3180.29	40†	.....	V E	3304.86	15	.....	V
3186.54	10	.....	V, 2	3308.05	40	2	IV
3187.46	40	3	IV	3310.45	20	1	IV
3189.24	10	.....	V E, 4	3311.37	8	.....	V
3191.10	100	.....	V E, 6	3312.61	150	10	IV
3191.44	15	.....	V E	3315.20	50	.....	V
3194.97	150†	.....	V E	3318.96	60	4	IV, 2
3200.52	10	1	IV	3319.25*	25	.....	V E
3206.32	60†	.....	V E				V
3210.16	10	.....	V	3319.57	15	.....	V E
3215.24	8	.....	V	3326.61*	60	1	IV
3215.59	80†	.....	V E, 4	3329.37	30	.....	V, 2
3217.27	30	.....	V	3332.16	30	1	IV
3217.83	20	.....	V	3335.40	10	.....	V, 4
3220.91	8	.....	V	3336.31	10	.....	V
3221.13	12	.....	V	3341.58	10	.....	V E
3223.32	10	.....	V E	3341.95	300	30	III
3225.46	200†	.....	V E, 6	3343.68	150	20	III
3229.55	20	.....	V E	3346.92	15	.....	V
3236.44	80†	.....	V E, 2	3349.04	200	25	III
3238.06	8	.....	V E, 6	3349.51*	20	.....	V, 4
3246.77	15	.....	V	3352.27	10	.....	V
3247.47	12	.....	V E, 2	3352.59	8	.....	V, 2
3248.94	10	.....	V E	3353.52	12	.....	V E
3249.50	50	4	IV	3354.69	100	4	III
3251.55	8	.....	V	3355.41	8	.....	V
3251.66	30	1	IV	3357.02	30	.....	V
3254.03	60†	.....	V E, 3	3358.39	300	25	III
3260.13	20	.....	V	3365.58	20	.....	V E
3260.56	20	.....	V E, 4	3366.98	80	1	IV
3261.89	15	.....	V, 2	3367.38	20	.....	V
3263.36	10	.....	V E	3369.21*	10	.....	V E, 2

* See notes at end of table.

† Reversed in spark.

TABLE I—*Continued*

λ	Intensities		Class No. Comps.	λ	Intensities		Class No. Comps.
	Arc	Fur.			Arc	Fur.	
3371.33	60	2	IV	3456.52	10	.....	V
3372.12	10	.....	V	3457.79	10	.....	V
3372.58	8	.....	V E, 4	3458.94	10	.....	V
3374.92	100	2	IV	3459.68	20	.....	V, 2
3376.33	10	.....	IV	3462.64	15	.....	V
3376.73	12	.....	IV, 2	3463.03	8	.....	V
3380.06	20	.....	V	3463.68*	8	.....	V
3380.45	40	4	III	3463.80*	25	.....	V, 4
3383.75	8	.....	V, 2	3465.85*	50	2?	IV
3384.66	10	.....	V	3467.46	8	.....	V, 2
3385.66	8	.....	V	3469.43	15	.....	V
3386.24	20	.....	V E	3473.06	20	.....	V, 4
3387.68	10	.....	V	3475.61	8	.....	V
3387.79	15	.....	V	3478.70	40	.....	V, 2
3390.64	20	.....	V, 4	3478.81	8	.....	V E, 2
3392.34	150	6	IV, 2	3479.55	20	.....	V E
3395.94	50	2	IV	3481.06	10	.....	V
3398.24	12	.....	V, 2	3484.05	12	.....	V E, 2
3399.41	30	1	IV, 2	3489.07	10	.....	V E
3399.71	15	.....	V E, 2	3491.05	50	1	IV, 2
3399.97	8	.....	V	3491.48	10	.....	V
3403.02	10	.....	V, 4	3497.78*	40	2?	IV
3403.73	10	.....	V	3498.61	40	4	IV
3405.39	60	.....	V, 2		30	.....	V
3406.11	40	.....	V	3503.18	15	.....	V
3406.60	10	.....	V	3507.94	80	8	III
3408.35	60	4	IV	3510.26*	15	.....	V E, 2
3408.67	30	.....	V E	3511.16	15	.....	V, 2
3409.16	20	.....	V E	3515.40	15	.....	V E, 2
3409.89	12	.....	V	3516.84	15	.....	V
3412.90	30	.....	V E	3518.16	8	.....	V
3414.03	15	.....	V	3520.05	40	2	IV
3415.96	15	.....	V, 4	3520.71	12	.....	V
3417.86	10	.....	V	3525.22	20	.....	V, 4
3420.62	10	.....	V E	3533.65	60	4	IV
3423.76	40	1	IV	3535.29	500	20	III, 2
3425.44	30	.....	V E, 2	3537.51	200	15?	III
3425.85	20	.....	V, 4	3537.65	10	.....	V E
3426.56	25	.....	V E, 2	3539.62	10	.....	V
3427.47	60	4	IV	3540.99	30	.....	V E
3428.77	10	.....	V, 4	3542.97	10	.....	V
3429.06	20	.....	V	3543.91*	10	.....	V
3431.97	8	.....	V	3544.01*	60	?	IV?
3432.42	15	.....	V, 4	3544.65	50	2	IV
3432.72	20	.....	V E	3548.11	10	.....	V E?
3433.11*	15	.....	V	3550.44	50	?	IV?
3436.96*	8	.....	V, 2	3554.52*	40	?	IV?, 2
3439.91	15	.....	V E	3554.65*	80	6	III
3440.62	40	.....	V E	3559.11	8	.....	V
3442.65	10	.....	V	3563.49*	100	3	IV
3445.65	20	.....	V, 4	3563.60*	80	2	IV
3452.35	15	.....	V, 4	3568.75	12	.....	V

TABLE I—*Continued*

λ	Intensities		Class No. Comps.	λ	Intensities		Class No. Comps.
	Arc	Fur.			Arc	Fur.	
3569.46.....	50	.....	V	3717.51.....	12	.....	V, 2
3575.86.....	200	8	III	3725.21.....	8	.....	V, 4
3577.71.....	40	.....	V	3726.26.....	250	20	III
3580.28.....	500r	30?	III?	3738.47.....	20	.....	V
3584.96.....	100	?	IV?	3739.86.....	300r	30	III
3589.09.....	100	?	IV?	3740.73*.....	10	.....	V E
3589.35.....	80	.....	V, 4	3740.84*.....	50	3	III
3593.96.....	80	6	III	3741.83.....	20	2	IV, 2
3599.27.....	10	.....	V, 2	3742.46.....	200r	20	III
3599.62.....	15	.....	V	3744.04.....	20	2	IV, 2
3602.56.....	60	4	III	3746.95.....	10	.....	V
3615.47.....	12	.....	V, 4	3748.56.....	15	.....	V
3617.67.....	8	.....	V	3753.20.....	30	1	IV
3618.40.....	8	.....	V	3755.77.....	15	.....	V, 2
3618.86.....	10	.....	V	3759.59.....	200r	15	III
3619.46.....	30	.....	V E	3763.48.....	50	4	III
3619.68.....	10	.....	V E, 2	3764.10.....	15	.....	V
3621.01.....	30	.....	V	3765.08.....	25	.....	V, 2
3625.15.....	8	.....	V	3766.15*.....	20	.....	V, 2
3625.70.....	8	.....	V	3769.16.....	15	.....	V
3633.71.....	15	.....	V	3770.89*.....	10	.....	V
3636.95.....	15	.....	V, 4	3771.85.....	30	.....	V
3637.52.....	20	.....	V	3775.46.....	10	.....	V
3637.84*.....	25	.....	V, 4	3781.07.....	60	5	III
3638.75.....	15	.....	V, 2	3786.21.....	8	.....	V
3639.30.....	40	.....	V, 4	3787.12.....	150	3?	IV?
3640.65.....	30	.....	V	3790.16.....	200r	10	III
3644.91.....	15	.....	V	3791.29.....	300r	15	III
3649.84.....	80	3	III	3795.56.....	15	.....	V
3650.77.....	30	.....	V, 4	3796.46*.....	10	.....	V, 4
3651.17.....	50	.....	V E	3798.15.....	300r	10	III, 2
3659.59.....	15	.....	V E, 2	3800.96.....	20	.....	V, 2
3660.37.....	100	2	IV, 2	3801.27*.....	10	.....	V
3664.71.....	80	10	III	3802.99.....	400r	2?	IV?
3668.61.....	15	.....	V	3803.92.....	100	2?	IV?
3669.01.....	40	.....	V	3804.75.....	40	.....	V E, 2
3674.77*.....	50	.....	V, 6	3806.17.....	10	.....	V
3687.95.....	15	.....	V E, 6	3810.50.....	80	.....	V, 6
3693.36.....	15	.....	V	3811.03.....	60	4?	III?
3694.66.....	10	.....	V, 2	3815.47.....	60	?	IV?, 2
3697.39.....	15	.....	V	3818.83.....	15	.....	V E
3697.86.....	200	20	III	3819.18.....	20	.....	V, 2
3703.16*.....	8	.....	V E, 4	3824.87.....	100	2?	IV?
3703.90.....	8	.....	V, 2	3831.85.....	12	.....	V E
3704.15*.....	15	.....	V E, 4	3835.17.....	30	?	IV?
3709.43*.....	20	.....	V	3836.47.....	10	.....	V
3711.36.....	50	.....	V, 2	3842.70.....	8	.....	V
3713.07.....	400r	30	III	3845.96.....	30	.....	V
3713.79*.....	15	.....	V	3858.93.....	40	?	V?
3716.19*.....	10	.....	V, 4	3862.93*.....	10	.....	V, 4
3717.02.....	{20	.....	V, 2	3863.38.....	40	?	V?, 2
	{20	.....	V E	3867.91.....	30	?	V?, 4

TABLE I—*Continued*

λ	Intensities		Class No. Comps.	λ	Intensities		Class No. Comps.
	Arc	Fur.			Arc	Fur.	
3871.19*.....	8	.....	V, 4	4001.12.....	8	.....	V, 4
3875.78.....	10	.....	V	4008.27.....	20	.....	V
3876.95.....	8	.....	V, 2	4009.69	20	.....	V
3877.52.....	50	.....	V, 2	4013.26.....	20	.....	V
3878.84*.....	40	?	V?	4017.51.....	10	.....	V
3878.95*.....	15	?	V	4023.14.....	8	.....	V
3883.14*.....	100	?	V?	4027.30.....	8	.....	V
3885.45.....	100	3	IV, 2	4027.95.....	8	.....	V, 2
3885.73.....	100	1	IV	4032.57.....	200	10	IV, 2
3886.08.....	20	.....	V	4033.19.....	50	.....	V
3891.37.....	60	2	IV	4039.07.....	12	.....	V, 2
3893.75.....	30	3	IV	4039.54.....	60	.....	V, 6
3894.09.....	40	1	IV	4044.10.....	20	.....	V, 2
3895.91.....	10	.....	V	4044.71.....	10	.....	V
3898.56.....	8	.....	V	4049.75.....	12	1?	IV?
3899.24.....	8	.....	V, 4	4051.53.....	20	.....	V
3904.18.....	15	.....	V, 2	4058.99.....	2000	100	III, 6
3906.91.....	8	.....	V	4059.50.....	30	.....	V
3908.98.....	30	2	IV	4060.82.....	30	1?	IV?, 2
3914.73.....	150	3	IV	4067.17.....	12	.....	V
3919.00.....	8	.....	V	4068.26.....	20	.....	V, 4
3919.15.....	8	.....	V, 2	4070.98.....	10	.....	V
3920.24.....	100	1	IV, 4	4079.73.....	1000	50	III, 4
3922.32*.....	10	.....	V	4084.19.....	8	.....	V
3925.00.....	40	.....	V, 2	4084.87.....	40	1	IV
3929.31.....	30	1	IV, 2	4090.16.....	10	2	III
3934.16.....	10	.....	V, 6	4099.10.....	20	1	IV, 2
3934.42.....	15	.....	V	4100.40.....	80	3	IV, 2
3935.45.....	8	.....	V, 4	4100.99.....	600	30	III, 2
3936.46.....	8	.....	V	4112.15.....	10	.....	V, 4
3937.54.....	150	4	IV, 2	4113.95.....	20	.....	V
3937.99.....	15	.....	V	4116.91.....	40	5	III, 2
3941.31.....	30	.....	V, 2	4122.81.....	8	.....	V
3943.69.....	60	4	IV, 2	4123.86.....	400	15	III
3947.50.....	10	.....	V, 2	4125.24.....	8	.....	V, 4
3955.66.....	15	.....	V	4129.45.....	100	4	IV, 4
3959.36.....	8	.....	V, 2	4129.97.....	125	.....	V, 4
3961.02.....	8	.....	V, 6	4134.63.....	20	1	IV
3965.70.....	40	1	IV	4137.15.....	200	8	III, 2
3966.14*.....	30	.....	V	4139.43.....	100	3	IV, 2
3966.29*.....	200	.....	V E	4139.74.....	300	10	IV, 6
3970.70.....	8	.....	V	4143.22.....	60	1	IV, 2
3971.93.....	20	.....	V	4147.19.....	10	?	IV?, 2
	15	.....	V	4150.17.....	100	.....	V
3972.54.....	30	.....	V, 2	4152.06.....	10	.....	V, 2
3976.64.....	10	.....	V, 2	4152.65.....	600	20	III, 4
3977.95.....	12	.....	V, 4	4158.02.....	10	.....	V
3978.76.....	10	.....	V	4163.48.....	50	.....	V
3979.38.....	8	.....	V	4163.64.....	400	10	III
3980.53.....	60	1	IV, 4	4164.65.....	400	10	III
3991.68.....	10	.....	V, 4	4168.14.....	200	10	IV, 4
3999.17.....	40	.....	V	4169.58.....	20	.....	V, 2

TABLE I—*Continued*

λ	Intensities		Class No. Comps.	λ	Intensities		Class No. Comps.
	Arc	Fur.			Arc	Fur.	
4184.44	60	2	IV, 2	4342.83	15	.....	V
4186.08	8	.....	V	4348.64	15	.....	V, 6
4190.67	15	.....	V, 2	4349.03	15	.....	V
4190.93	100	2	IV, 6	4351.64	40	?	IV?
4192.07	60	2	IV, 4	4359.81	12	.....	V, 6
4195.13	60	2?	IV?	4368.46	30	1?	IV?, 2
4195.65	10	.....	V	4377.96	10	.....	V, 2
4198.46	8	.....	V, 4	4388.37	15	.....	V
	30	1	IV	4392.74	15	.....	V
4201.54	40	.....	V	4410.24	50	3	IV
4205.34	100	4	IV, 2	4411.53	8	.....	V
4208.13	15	.....	V	4419.45	40	2	IV
4212.03	8	.....	V	4419.84	8	.....	V
4212.51	8	.....	V, 2	4420.45	8	.....	V
4214.75	50	.....	V, 6	4420.64	20	.....	V, 4
4217.98	125	4	IV, 4	4426.67	15	.....	V, 2
4229.15	60	.....	V, 6	4429.45	10	.....	V, 2
4229.82	20	.....	V	4437.25	50	.....	V, 6
4230.32	10	.....	V	4441.82	8	.....	V, 4
4231.95	20	1	IV	4446.21	8	.....	V, 2
4242.64	8	.....	V, 4	4447.24	80	4	IV
4246.28	10	.....	V, 2	4456.81	30	3	IV
4249.46	12	1	IV	4457.41	30	?	IV?, 2
4253.05	30	.....	V, 6	4458.10	8	.....	V
4253.74	20	.....	V, 4	4460.19	8	.....	V, 4
4254.75	20	.....	V	4460.45	10	.....	V, 2
4255.51	40	.....	V, 4	4464.15	10	2	IV
4261.72	15	.....	V, 6	4469.73	20	1	IV, 2
4262.15	100	6	IV	4471.33	20	.....	V, 4
4266.06	30	1	IV	4472.56	20	2	IV, 4
4268.66	8	.....	V	4499.84	10	.....	V, 2
4270.71	20	.....	V, 6	4503.07	40	5	III
4277.47	15	.....	V	4508.44	10	.....	V
4280.64	25	.....	V, 2	4511.12	10	.....	V, 2
4286.20	10	.....	V	4523.45	150	10	III, 2
4286.99	50	4	IV	4524.14	10	.....	V
4289.47	25	.....	V	4546.83	100	15	III
4291.26	20	.....	V, 2	4553.84	15	.....	V
4292.04	15	.....	V, 4	4564.56	50	.....	V
4292.55	25	.....	V, 6	4573.13	200	10	III, 2
4295.55	10	.....	V	4574.85	10	.....	V, 4
4296.24	12	.....	V, 4	4581.68	80	.....	V, 2
4299.65	100	.....	V	4582.29	10	.....	V
4301.19	100	.....	V	4600.22	20	.....	V
4309.57	10	.....	V	4606.79	300	15?	III, 4
4311.33*	30	.....	V, 2	4616.13	40	.....	V, 2
4312.45	15	.....	V	4630.13	100	2?	IV?
4326.38	40	.....	V, 6	4648.93	100	?	IV?, 2
4327.42	10	.....	V, 2	4649.25	20	.....	V, 6
4328.44	8	.....	V, 4	4663.82	100	2?	IV?
4329.75	8	.....	V, 4	4666.21	50	?	IV?
4331.44	50	.....	V	4667.20	30	.....	V

TABLE I—*Continued*

λ	Intensities		Class No. Comps.	λ	Intensities		Class No. Comps.
	Arc	Fur.			Arc	Fur.	
4672.08.....	200	?	V?, 6	5193.04.....	30	.....	V, 4
4675.36.....	150	?	V?, 4	5195.84.....	25	6	IV
4678.43.....	{6 / 8}	.....	V, 2	5203.18.....	8	.....	V
4685.11.....	50	?	V?	5219.09.....	10	.....	V, 6
4694.46.....	8	.....	V, 4	5225.14.....	8	.....	V
4695.42.....	15	.....	V, 6	5232.83.....	25	.....	V
4697.43.....	20	.....	V, 2	5251.65.....	15	.....	V, 6
4706.11.....	40	.....	V, 6	5253.93.....	15	.....	V
4708.23.....	60	?	IV?, 2	5271.53.....	60	5	IV, 2
4713.45.....	30	.....	V, 2	5276.13*.....	30	.....	V, 6
4733.43.....	15	.....	V, 2	5318.61.....	50	20	III
4733.85.....	30	.....	V, 6	5319.47.....	8	.....	V, 2
4743.82.....	8	.....	V	5334.85.....	15	1	IV, 4
4744.61.....	20	.....	V	5340.80.....	10	.....	V
4749.60*.....	60	.....	V, 6	5344.20.....	200	40?	III, 4
4766.81*.....	10	.....	V, 4	5350.78.....	100	15	III, 2
4809.32.....	12	.....	V, 2	5381.33.....	10	5?	III?
4810.57*.....	30	.....	V, 6	5411.25.....	8	.....	V
4816.33.....	50	2	IV, 4	5422.43.....	20	2	IV
4829.25.....	15	.....	V	5431.28.....	12	.....	V, 2
4833.34.....	30	5?	III?	5437.30.....	80	8	III
4838.02.....	8	.....	V, 6	5481.01.....	10	.....	V
4845.15.....	10	.....	V	5504.61.....	20	8?	III, 2
4848.27*.....	60	.....	V, 6	5512.84.....	12	.....	V, 6
4868.98.....	12	.....	V	5523.59.....	30	?	IV?
4890.75.....	20	1	IV	5551.39.....	80	.....	V
4900.78.....	10	5	III	5562.98.....	8	.....	V
4904.53.....	15	2	IV	5576.13.....	12	.....	V, 4
4910.92.....	15	3	IV, 2	5578.28.....	10	.....	V
4928.06.....	8	?	IV?	5586.97.....	40	2	IV
4965.35.....	20	.....	V, 6	5603.51.....	30	.....	V
4967.81.....	20	2	IV, 6	5629.17.....	40	.....	V
4973.13.....	15	.....	V	5642.10.....	100	4	III
4988.98.....	40	3	IV, 6	5664.68.....	150	8	III
4997.85.....	8	.....	V, 2	5665.59.....	100	3	III
5000.94.....	10	.....	V, 4	5671.06*.....	40	.....	V, 6
5017.73.....	40	?	IV?, 2	5671.88.....	40	2	IV
5026.35.....	15	.....	V, 2	5706.49.....	40	2?	IV?
5039.05.....	40	3	IV, 2	5716.38.....	30	.....	V
5058.01.....	30	?	IV?	5729.18.....	100	10	III
5065.24.....	20	?	IV?	5751.44.....	30	.....	V
5078.94.....	200	15	IV	5760.37.....	80	1	IV
5095.31.....	80	?	IV?, 2	5765.00.....	30	.....	V
5100.16.....	20	2	IV, 2	5776.08*.....	12	.....	V, 6
5120.31.....	20	?	V?	5787.54.....	80	8	III
5134.73.....	40	?	IV?, 2	5794.27.....	15	.....	V
5160.34.....	60	?	IV?	5804.06.....	15	.....	V, 2
5164.36.....	30	?	IV?, 6	5819.49*.....	80	—?	V?
5180.32.....	60	8	IV	5834.93.....	30	.....	V
5186.97.....	15	4	IV	5838.69.....	60	3	IV, 4
5189.17.....	30	6	IV	5842.54.....	25	.....	V, 2
				5846.14.....	8	.....	V, 6

TABLE I—*Continued*

λ	Intensities		Class No. Comps.	λ	Intensities		Class No. Comps.
	Arc	Fur.			Arc	Fur.	
5866.54.....	100	?	IV?	6164.32.....	10	.....	V
5874.76.....	30	.....	V, 4	6213.00.....	8	.....	V
5877.81.....	20	.....	V	6221.92.....	20	.....	V
5893.50.....	15	.....	V, 2	6251.80.....	15	.....	V, 6
5900.64.....	150	.....	V, 6	6430.51.....	100	.....	V, 6
5903.89.....	12	.....	V, 6	6433.29.....	30	.....	V, 2
5928.21.....	8	.....	V, 6	6544.70.....	60	.....	V, 4
5934.21.....	10	.....	V, 6	6660.76*.....	150	.....	V, 6
5957.77.....	10	.....	V	6677.36.....	80	.....	V, 6
5983.28.....	100	10?	IV?	6701.25.....	10	.....	V
5986.17.....	20	.....	V	6723.66.....	30	.....	V, 2
5998.03*.....	20	.....	V, 6	6739.95.....	10	.....	V, 2
6029.78.....	12	.....	V	6828.16.....	20	.....	V, 2
6031.88.....	8	.....	V	6876.51.....	10	.....	V
6045.54.....	20	.....	V	6908.16.....	10	.....	V
6148.11.....	8	.....	V, 2	6918.46.....	10	.....	V

NOTES TO TABLE

3175.80 Violet triplet resolved in arc

3271.98, 3272.07 } Measured by writer

3291.91, 3292.00 } Measured by writer

3299.62 *Cb* II line to violet

3319.25 Blend *Cb* II, *Cb* I

3326.61 *Cb* II line to violet

3349.51 Measured by writer

3369.21 *Cb* II line to red

3433.11 Faint line to red

3436.96 *Cb* II line to violet

3463.68, 3463.80 } Measured by writer

3465.85 Blend strong *Fe* line

3497.78 Blend strong *Fe* line

3510.26 May be blend with *Cb* I line given in Meggers' multiplet

3543.91, 3544.01 } Measured by writer

3554.52, 3554.65 } Measured by writer

3563.49, 3563.60 } Measured by writer

3637.84 *Cb* II line on red edge

3674.77 Probably pair of complex lines

3703.16 Slightly enhanced

NOTES TO TABLE—*Continued*

3704.15	Slightly enhanced
3709.43	Six-component *Cb* II line to violet
3713.79	*Cb* II line to violet
3716.19	Blend *Cb* II (violet), *Cb* I
3740.73, 3740.84	Measured by writer
3766.15	Measured by writer
3770.89	*Cb* II line to violet
3796.46	Equal strength in arc and spark
3801.27	Measured by writer
3862.93	Measured by writer; *Cb* II line at λ 3863.05
3871.19	Measured by writer
3878.84, 3878.95	Measured by writer
3883.14	Measured by writer
3922.32	Faint line to violet
3966.14, 3966.29	Measured by writer; λ 3966.29 slightly enhanced
4311.33	Faint line to red
4749.60	Components partially resolved
4766.81	Blend *Cb* I, *Cb* II
4810.57	Components partially resolved
4848.27	Components partially resolved
5276.13	Components partially resolved
5671.06	Components partially resolved
5776.08	Measured by writer
5819.49	Very faint if present
5998.03	Very wide pattern
6660.76	Very wide pattern; probably more than six components

FEATURES OF THE *Cb* I SPECTRUM

Five hundred and seventy-eight of the 646 lines given in Table I belong to the neutral spectrum; 172 of these appear in the furnace spectrum with sufficient clearness to be assigned intensities; 33 others, very strong in the arc, are masked by foreign lines, usually belonging to carbon bands, and their presence is questioned in the furnace column. In general, the stronger neutral lines of the arc appear in the furnace, but an excitation considerably higher is evidently needed to bring out the complete neutral spectrum. The intensities of lines appearing at the low-temperature stage were estimated and used in the assignment of lines to temperature classes. These intensities were usually about one-third of those of the high-temperature stage, and to save space have been omitted from the table.

Certain outstanding groups appear, the lines of which are very strong in the arc, but show also in the furnace with considerable strength, and usually go into class III. Because of the absence of reversed lines and of the difficulty in producing the furnace spectrum, no lines are placed in the low-temperature classes I or II. Many lines obtained only at the highest temperature are placed in class IV. Among the numerous neutral lines in class V are some which are very strong in the arc but fail to appear in the furnace. A large proportion, however, being of moderate arc intensity, are scarcely to be expected in the furnace, by reason of the high excitation required for the columbium lines. This consideration rendered it useless to include the fainter lines of the arc spectrum.

A beginning in the analysis of the neutral lines was made in 1924 by Meggers,[1] who found three multiplets, and later Meggers and Kiess[2] gave two more, as well as several multiplets of *Cb* II. Almost all of the 56 lines of these neutral multiplets appear in the furnace spectrum, and half of them show at the lower furnace temperature. All are to the violet of λ 4218. In one of these multiplets are found the three ultimate lines of A. de Gramont[3]—λλ 4059, 4080, and 4101—which are the strongest lines, both of the arc and furnace spectra, in the region examined.

FEATURES OF THE *Cb* II SPECTRUM

The arc and spark spectra of columbium were photographed during this investigation as far as λ 2650. The ionized spectrum is very rich in the ultra-violet, many of its lines being strong enough in the arc above λ 3100 to be included in Table I. Some of these, though beyond the reach of the furnace, evidently are from low levels of the ionized atom, as they reverse widely in a strong spark. Many of the weaker *Cb* II lines are as yet unmeasured. To the red of λ 3500 the ionized lines become more scattered, and the spectrum above λ 4100 is chiefly made up of neutral lines. Some spark lines, usually of hazy structure, have not appeared in the arc spectrograms and may belong to the doubly ionized spectrum. Considerable variety

[1] *Journal of the Washington Academy of Sciences*, **14**, 442, 1924.

[2] *Journal of the Optical Society of America*, **12**, 417, 1926.

[3] *Comptes rendus*, **171**, 1106, 1920.

in the relative intensities in arc and spark appears among the ionized lines, and much may be learned as to the relative energy-levels of *Cb* II lines from a comparison of arc and spark spectra.

HYPERFINE STRUCTURE

A conspicuous feature of the columbium spectrum is that a large proportion of the lines are by no means sharp, but show, even under low excitation, the definite spreading which characterizes hyperfine structure. Only preliminary data on the extent and character of this phenomenon are now available, as a proper examination will require apparatus of high resolution. The figures after the class numbers in the table indicate, for lines clearly complex, the probable number of hyperfine components according to the present spectrograms. The components of the columbium patterns are so densely spaced, however, that these figures, for the most part 2, 4, or 6, are useful mainly as an indication of the relative widths of the patterns, since resolution, even of the wider-spaced components, was obtained for only a few lines. Of the 646 lines in Table I, 268 show clear evidence of hyperfine structure, and 57 of these have widths indicating at least six components in each case. For the few patterns showing partial resolution, the spacing of components is graduated, with the wider intervals on the violet side. These resemble the patterns of praseodymium,[1] except that some of the latter are graduated in the opposite direction.

Both neutral and ionized lines of columbium show hyperfine structure, and in neither group is its presence confined to lines requiring high excitation. An interesting instance of variation in structure among lines in the same multiplet is shown by the ultimate lines mentioned above—λλ 4059, 4080, 4101. The widths of their patterns, apparently of six, four, and two unresolved components, respectively, remain unchanged at the lowest furnace temperature.

Toward the red the average width of the columbium patterns increases. In the violet, complex lines have their components closely spaced, the total width of a six-component pattern being less than 0.2 A. In the green the greatest line-widths are about 0.33 A and

[1] King, *Mt. Wilson Contr.*, No. 368; *Astrophysical Journal*, **68**, 194, 1928; H. E. White, *Physical Review*, **34**, 1397, 1929.

comparable with those of praseodymium in this region; while in the red, widths near 0.5 A are found, although the first-order spectrograms show little resolution. The widest line observed in the spectrum is λ 6660.76, with a total width of about 0.75 A.

To resolve the columbium patterns will require an examination with the higher orders of the 75-foot spectrograph on Mount Wilson. Some preliminary spectrograms, made with a plane grating of insufficient size, gave partial resolution of a few of the wider patterns and showed the instrumental requirements for a detailed study. Several of these very wide lines showed in each case three components distinctly resolved, and these three made up less than half the total width of the line. Since the remainder of the pattern should consist of at least five closely spaced components, the wider lines of this element may be expected, if sufficient resolution is attained, to show eight or more components.

Carnegie Institution of Washington
Mount Wilson Observatory
October 1930

Contributions from the Mount Wilson Observatory, No. 417
Reprinted from the *Astrophysical Journal*, Vol. LXXIII, pp. 1–12, 1931
Printed in the U.S.A.

STEWARD OBSERVATORY

POSITIONS, ORBIT, AND MASS OF PLUTO

By SETH B. NICHOLSON and NICHOLAS U. MAYALL

ABSTRACT

Positions and orbit of Pluto.—Positions of Pluto were obtained from photographs taken by M. L. Humason in 1919 with the 10-inch Cooke triplet and from photographs made with the 60- and 100-inch reflectors in 1930.

Orbital elements were computed which include the perturbations of the four major planets. The resulting period is 247.6968 years, which corresponds to a mean distance of 39.45743 astronomical units. The time of perihelion passage is 1989 Nov. 6.98 U.T., and the eccentricity 0.24852.

Determination of the mass of Pluto.—The perturbations of Pluto on Neptune were used to determine the mass. A least-squares solution of twenty-two observation equations with the mass of Pluto and the corrections to four of the elements of Newcomb's orbit of Neptune as unknowns gave 0.94 ± 0.25 times the mass of the earth as the mass of Pluto.

I. POSITIONS AND ORBIT OF PLUTO

As soon as it was announced that a trans-Neptunian object had been discovered by Tombaugh at the Lowell Observatory, the records of photographs taken at the Mount Wilson Observatory were examined to see whether any prediscovery positions could be obtained. The only photographs which could show images of the newly discovered object were four of a series begun in December, 1919, by M. L. Humason in a search for trans-Neptunian planets.

This search was stimulated by an article by W. H. Pickering which had just appeared in *Harvard Annals*, 82, in which he reviewed the previous investigations concerning the existence of a trans-Neptunian planet and gave a new solution of the problem, including the observed deviations of Neptune from its predicted positions. The search covered the position predicted in this paper and also those given by W. H. Pickering in 1909[1] and by Percival Lowell in 1915.[2] The 10-inch Cooke triplet was used with exposures of 2 hours, which

[1] *Harvard Annals*, 61, 162, 1909.

[2] *Memoirs of the Lowell Observatory*, 1, No. 1, 1915.

showed stars down to about the seventeenth magnitude. The plates were 35.5×43 cm (14×17 in.), with a scale of 2 cm to the degree, thus covering a region 18° in declination by 1^h28^m in right ascension. Three fields were photographed, centered on the ecliptic in right ascension 5^h38^m, 6^h34^m, and 7^h46^m, respectively, and at least three exposures were made on each field during December, 1919, and January, 1920. These plates were very carefully searched with an improvised blink comparator in a zone 3° wide along the ecliptic, and, although many asteroids and a few variable stars were found, no trans-Neptunian planet was discovered. The search was then extended, but less exhaustively, to a zone about 10° wide, with no success. The search was continued the following year with exposures of 15 minutes at the 60-inch reflector, which covered a region along the ecliptic 1°.6 wide and 7° long, centered on the predicted positions. If the planet discovered at the Lowell Observatory had been within a degree and a half of the ecliptic in 1920, it almost certainly would have been found at that time.

The preliminary orbits of Pluto gave the position of the orbit plane with considerable accuracy and indicated that in 1921 the planet was not in the region covered by the 60-inch plates, but was within the field of four of the plates taken with the 10-inch triplet in 1919. The search on these plates was then limited to a narrow region along the orbit plane, but it was not until the region to be examined was still further limited by better orbits that images of the planet were at last found on June 7, 1930. Two ephemerides were used, one by E. C. Bower and F. L. Whipple, which had been received by letter, and one by A. C. D. Crommelin.[1] The latter made use of an observation by Delporte[2] from a plate taken in 1927.

Four plates of the series taken by Humason showed images of Pluto: two on December 27, 1919, the others on December 28 and 29, respectively. The estimated photographic magnitude of the planet was 15. The positions of Pluto were measured on these plates with reference to six stars, the co-ordinates of which were obtained

[1] *Circulaire du Bureau Central Astronomique de l'Union Astronomique Internationale*, No. 282, 1930.

[2] *Astronomische Nachrichten*, **238**, 314, 1930.

from the *Catalogue* of the Astronomische Gesellschaft. The mean of these four positions was telegraphed to the Harvard College Observatory.[1]

From the close agreement of the computed and observed positions it was evident that small differential corrections to the orbits on which the ephemerides used in the search were based would suffice to represent the 1919 observations exactly. The observations then available for improving the orbit were those just determined for 1919, the single position by Delporte for 1927, and those made in 1930 since the planet's discovery. It soon became apparent that the declination of the position by Delporte was in error by about 20″, and this observation was therefore discarded. Many observations of the planet had been made between the time of the announcement of its discovery and the end of May, but we decided to base our computations of the orbit on the observations made at Mount Wilson in March and May, 1930, the discovery position made in January, 1930, at the Lowell Observatory, and the 1919 Mount Wilson positions. The following orbit, which best represented these observations, was reported to the Harvard Observatory.[2]

$T = 1988$ June 5.5 U.T.	$q = 29.6$
$\omega = 111°46'$	$e = 0.2575$
$\Omega = 109\ 22$	$P = 251.80$ years
$i = 17\ 9$	

Soon after the planet's position in 1919 became known, F. E. Ross at the Yerkes Observatory found images of it on plates taken by E. E. Barnard in 1921 and by himself in 1927.[3] Between the observation of 1921 and the mean of those of 1919 there was an apparent discrepancy amounting to about 14″ in α. The 1919 plates were therefore remeasured with the aid of six faint comparison stars from the Paris zone of the *Astrographic Catalogue*. The images of the planet were almost central in right ascension on the 1919 plates, but were nearly 4° south of the centers of these plates. The eccentric coma of

[1] *Harvard Announcement Card*, No. 133, 1930.

[2] *Ibid.*, No. 134, 1930.

[3] *Astronomische Nachrichten*, **239**, 118, 1930.

the overexposed images of the A.G. stars might therefore have produced an error in measures of the declination, but should have had no effect on the measures in right ascension. The error due to coma should be nearly eliminated from the positions referred to the fainter stars of the *Astrographic Catalogue*. The new measures gave corrections to the original positions of $+0^{s}.06$ in α and $-2''.6$ in δ.

Soon after the 1927 observation by Delporte was shown to be in error, corrections to it were published,[1] amounting to $+0^{s}.26$ in α and $-15''.5$ in δ.

The preliminary orbit was next corrected by using these additional observations and the remeasured positions for 1919 and 1927. In the preliminary orbit the mass of the sun alone was used, and the center of the sun was taken as the origin of co-ordinates. The perturbations by the four major planets were therefore computed in rectangular co-ordinates and taken into account in correcting the orbit. Table I gives the corrections which must be applied to the equatorial co-ordinates of Pluto (equator and equinox of 1930.0) derived from an orbit osculating at January 7.0, 1930, to obtain the true co-ordinates. In the meantime, some additional observations had been made at Mount Wilson after Pluto had passed conjunction with the sun, and these were also included in the final calculation of the heliocentric orbit.

It is possible, however, to derive an elliptic orbit which by itself will represent the motion of Pluto more accurately than the heliocentric orbit unless the perturbations are accurately taken into account. This may be done by transferring the origin to the center of mass of the solar system and changing the Gaussian constant k to 0.01721363, which includes the total mass of the system. The motion of Pluto referred to this center is almost exactly elliptic, which explains why the barycentric orbit thus obtained is sufficient to describe the motion with high approximation without the inclusion of perturbations. Geocentric positions computed with the heliocentric elements and perturbations are, however, more accurate than those computed with the barycentric elements alone.

[1] *Ibid.*

TABLE I

PERTURBATIONS BY THE FOUR MAJOR PLANETS

(Unit = 0.00001)

Date U.T.	In x	In y	In z
1919 Mar. 6.0	−2668	+1101	+530
1919 Sept. 2.0	2705	1011	493
1920 Feb. 29.0	2723	892	443
1920 Aug. 27.0	2716	751	383
1921 Feb. 23.0	2678	594	315
1921 Aug. 22.0	2607	429	243
1922 Feb. 18.0	2503	261	168
1922 Aug. 17.0	2366	+ 98	96
1923 Feb. 13.0	2198	− 54	+ 27
1923 Aug. 12.0	2003	187	− 34
1924 Feb. 8.0	1785	297	86
1924 Aug. 6.0	1553	380	127
1925 Feb. 2.0	1312	433	155
1925 Aug. 1.0	1072	453	170
1926 Jan. 28.0	841	444	171
1926 July 27.0	628	406	160
1927 Jan. 23.0	441	347	139
1927 July 22.0	286	273	111
1928 Jan. 18.0	167	194	79
1928 July 16.0	83	118	49
1929 Jan. 12.0	31	56	23
1929 July 11.0	6	15	6
1930 Jan. 7.0	0	0	0
1930 July 6.0	4	16	8
1931 Jan. 2.0	− 9	− 61	− 26

The elements for the two methods of describing the motion are:

	Heliocentric Elements with Mass of Sun	Barycentric Elements with Mass of Solar System	
T	1989 Oct. 2.03 U.T.	1989 Nov. 6.98 U.T.	
ω	113°01′41″.3	113°52′50″.6	1930.0
Ω	109 21 39.4	109 21 43.7	1930.0
i	17 06 58.4	17 08 38.1	1930.0
a	39.60038	39.45743	
e	0.2460861	0.2485200	
P	249.2097 years	247.6968 years	
μ	14″.23833	14″.32530	
q	29.85528	29.65147	
k	0.01720210	0.01721363	

Constants for the Equator 1930.0

$x = r[9.982578] \sin (313°12′55″.1 + v)$ $\quad$ $x = r[9.982520] \sin (314°04′18″.8 + v)$

$y = r[9.980816] \sin (228\ 15\ 17.7 + v)$ $\quad$ $y = r[9.980843] \sin (229\ 06\ 58.1 + v)$

$z = r[9.604295] \sin (182\ 03\ 08.0 + v)$ $\quad$ $z = r[9.604461] \sin (182\ 50\ 47.8 + v)$

Co-ordinates computed by the barycentric elements, which refer to the center of mass of the solar system, may be used to obtain geocentric positions by combining them with co-ordinates of the earth referred to the same origin. Co-ordinates computed with the heliocentric elements must have added to them the perturbations from Table I in order to obtain the true heliocentric co-ordinates. Both sets of elements give the same geocentric position on January 7.0, 1930, and the difference in representation for other dates may be seen from Table II. This table shows the residuals for the various observations used in the computations which correspond to the pre-

TABLE II

REPRESENTATION OF OBSERVATIONS BY DIFFERENT ORBITS

Date U.T.	Preliminary Orbit		Preliminary Orbit + Perturbations		Heliocentric Orbit + Perturbations		Barycentric Orbit	
	$\Delta\alpha$	$\Delta\delta$	$\Delta\alpha$	$\Delta\delta$	$\Delta\alpha$	$\Delta\delta$	$\Delta\alpha$	$\Delta\delta$
1919 Dec. 29.0667*	+ 0".8,	−2".6	−131".4,	−3".0	+1".1,	+0".5	+2".6,	+0".5
1921 Jan. 29.0896.	+14.4,	−2.1	.....		−3.4,	−1.0	−2.8,	−1.2
1927 Jan. 6.2500.	+10.1,	+1.4	.....		−2.7,	−3.7	−2.9,	−3.7
1927 Jan. 27.8942.	+13.8,	+5.6	−13.6,	+8.2	+2.6,	+1.9	+2.4,	+1.9
1930 Jan. 23.2274.	0.0,	−2.9	0.0,	−2.9	−0.3,	−3.5	−0.3,	−3.5
1930 Mar. 23.1733*	− 0.1,	−0.3	− 0.1,	−0.3	+0.3,	−0.3	+0.3,	−0.3
1930 May 27.1927*	− 0.2,	+0.3	− 0.1,	+0.3	−0.6,	+0.3	−0.6,	+0.3
1930 Oct. 1.0945*	.....		.....		+0.1,	+0.3	+0.1,	+0.2

* Normal place.

liminary orbit, to the preliminary orbit with perturbations applied, to the corrected heliocentric orbit with perturbations included, and to the barycentric orbit.

Table III gives the individual observations used in the computations and their residuals obtained from the heliocentric elements by including the perturbations given in Table I. All the Mount Wilson observations in 1930 were derived from photographs taken with the 60-inch reflector, except those of May 27 and June 1, which were taken with the 100-inch reflector.

As shown in Table II, the preliminary orbit indicated a discrepancy of about 14″ between the position of 1921 and that of 1919. The corrected orbit represents all the observations of 1919 and 1921 within the errors of measurement inherent in plates of such small scale. It is evident, therefore, that the apparent discrepancy was

due to the perturbations of the major planets, and not to errors of observation.

No ephemeris has been computed from the final elements given here, since they differ so little from those derived by Bower and Whipple[1] that the ephemeris computed by them is entirely sufficient. After these elements were obtained, an observation from a plate taken in 1914 was published by Wolf.[2] The representation of this

TABLE III

OBSERVATIONS AND THEIR REPRESENTATION BY HELIOCENTRIC ORBIT WITH PERTURBATIONS INCLUDED

Date U.T.	α(1930.0)	δ(1930.0)	Observer	$\Delta\alpha$	$\Delta\delta$
1919 Dec. 28.1861..	$6^h29^m08^s.53$	$+19°21'47''.0$	Humason	$+2''.5$	$+0''.1$
1919 Dec. 28.2861..	6 29 07.68	19 21 49.0	Humason	-2.5	$+1.4$
1919 Dec. 29.4285..	6 29 02.13	19 21 56.8	Humason	$+3.1$	$+1.2$
1919 Dec. 30.3660..	6 28 57.14	19 22 01.5	Humason	$+1.2$	-0.7
1921 Jan. 29.0896..	6 31 22.14	19 43 13.8	Barnard	-3.4	-1.0
1927 Jan. 6.2500..	7 04 03.17	21 13 03.1	Ross	-2.7	-3.7
1927 Jan. 27.8942..	7 02 10.69	21 17 29.3	Delporte	$+2.6$	$+1.9$
1930 Jan. 23.2274..	7 18 56.37	21 57 40.1	Tombaugh	-0.3	-3.5
1930 Feb. 23.1944..	7 16 36.39	22 04 06.8	Tombaugh	-1.1	-1.2
1930 Mar. 23.1733..	7 15 33.83	22 07 55.4	Mayall	$+0.4$	-0.1
1930 Mar. 24.1458..	7 15 33.02	22 08 00.7	Mayall	$+0.2$	-0.2
1930 Mar. 28.1497..	7 15 30.80	22 08 20.7	Mayall	$+0.4$	-0.5
1930 Apr. 22.1602..	7 15 54.82	22 09 18.2	Mayall	-0.6	$+0.5$
1930 May 22.1719..	7 17 43.42	22 07 56.2	Mayall	-0.9	$+0.3$
1930 May 27.1927..	7 18 08.72	22 07 27.8	Pease	-0.5	-0.3
1930 June 1.1809..	7 18 35.51	22 06 58.1	van Maanen	-0.3	$+1.0$
1930 Oct. 1.4906..	7 29 57.22	21 51 43.3	Mayall	$+0.4$	$+0.4$
1930 Oct. 2.4984..	7 29 59.35	$+21$ 51 42.3	Nicholson	-0.2	$+0.2$

observation by the barycentric elements is $\Delta\alpha = +9''.9$, $\Delta\delta = +0''.8$. The residuals from the orbit of Bower and Whipple are $\Delta\alpha = -112''.5$, $\Delta\delta = -25''.2$.[3] These indicate the order of the corrections due to perturbations which should be applied to their search ephemeris.

II. DETERMINATION OF THE MASS OF PLUTO

The mass of Pluto may be determined from its perturbations on Neptune and Uranus. A recent paper by J. Jackson[4] on "The Orbit

[1] *Lick Observatory Bulletin*, **15**, 35 (No. 427), 1930.

[2] *Nature*, **126**, 485, 1930. [3] *Harvard Announcement Card*, No. 142, 1930.

[4] *Monthly Notices of the Royal Astronomical Society*, **90**, 728, 1930.

of Neptune" gives a summary of the differences between the observed longitudes of that planet and those computed from Newcomb's elements. With this convenient summary available a solution for the mass of Pluto from its perturbations on Neptune was readily made. Normal equations were formed from the twenty-two observation equations which Jackson used, with the mass of Pluto added as a fifth unknown. These equations then read

$$\Delta\lambda = a + \beta t + \gamma \cos g + \delta \sin g + m p_\lambda ,$$

where t is the time in centuries from 1870.0, g the mean anomaly of Neptune, m the mass of Pluto in units of the earth's mass, and p_λ the perturbation in λ which Pluto would have produced on Neptune if its mass were unity. The origin of time for both t and p_λ was chosen as 1870.0, since that was near the middle of the series of observations on which Newcomb's orbit of Neptune was based. The values of p_λ are given in Table IV. Corresponding values for p_β, the perturbation in β, are also included in Table IV. The magnitude of the perturbations in latitude at the present time is such that their inclusion might have improved the determination of the mass of Pluto, but since no homogeneous series of observations of the latitude of Neptune was immediately available, they were not used.

A least-squares solution of the twenty-two observation equations, with equal weights, gave

$$m = 0.94 \pm 0.25$$

$$a = -0''.72 \qquad \gamma = +0''.63$$

$$\beta = -0''.18 \qquad \delta = -0''.25$$

Since the observation equation for 1795 is based on two prediscovery positions by Lalande, while the others are the means of several observations made during four-year intervals, there seems to be sufficient reason for assigning less weight to the equation depending on Lalande's observations.

A second solution was therefore made, with zero weight assigned to the doubtful equation.

The solution of the normal equations based on the remaining 21 observation equations is nearly indeterminate. Values of m ranging

from 0 to 1.5, with values of the other four unknowns to correspond, represent the observation equations almost equally well. The residual for the mean of Lalande's observations is $-6''.2$ with $m=0$, $0''.0$ with $m=0.9$, and $+3''.5$ with $m=1.5$.

The solution for the mass of Pluto from observations of the longitude of Neptune depends, therefore, on the observations of Lalande and indicates that if the mass of Pluto is less than 0.6 or greater than 1.3, Lalande's observations are in error by more than $2''$, or else the

TABLE IV

PERTURBATIONS OF PLUTO ON NEPTUNE
ASSUMED MASS OF PLUTO = 1.0 EARTH

Date	p_λ	p_β	Date	p_λ	p_β
1796	−0".82	−0".02	1864	+0".01	0".00
1800	− .69	+ .09	1868	.00	.00
1804	− .57	+ .16	1872	.00	.00
1808	− .45	+ .19	1876	+ .01	.00
1812	− .34	+ .18	1880	+ .03	.00
1816	− .24	+ .16	1884	+ .05	+ .01
1820	− .14	+ .11	1888	+ .07	+ .03
1824	− .07	+ .06	1892	+ .08	+ .04
1828	− .01	+ .01	1896	+ .05	+ .04
1832	+ .04	− .04	1900	− .02	+ .01
1836	+ .06	− .06	1904	− .15	− .08
1840	+ .08	− .07	1908	− .33	− .20
1844	+ .08	− .07	1912	− .58	− .35
1848	+ .08	− .07	1916	−0.90	− .54
1852	+ .06	− .06	1920	−1.23	− .77
1856	+ .04	− .04	1924	−1.57	−0.96
1860	+0.02	−0.01	1928	−1.93	−1.09

residuals of the other observations are larger than those given by this solution. Such a dependence on the early observations in problems of this sort is to be expected, according to E. W. Brown.[1]

The corrections to Newcomb's orbit of Neptune obtained from all twenty-two equations are appreciably smaller than those derived by Jackson on the assumption of no unknown perturbing masses. The residuals of each observation equation given by Newcomb's orbit, by the solution which includes Lalande's observations, and by Jackson's orbit of Neptune are given in Table V. The third column of the table gives the corrections due to the mass factor, which are obtained by multiplying p_λ from Table IV by 0.94.

[1] *Proceedings of the National Academy of Sciences*, **16**, 364, 1930.

In his paper Jackson says:

It may be worth pointing out that the existence of a disturbing body would be shown by the residuals running through two complete cycles in the interval covered by the observations. When we analyse the residuals in longitude to correct the elements we really have four disposable constants, and the natural effect of attempting to fit the observed and computed longitudes (if a disturb-

TABLE V

RESIDUALS IN LONGITUDE FOR NEPTUNE

Date	O−C Newcomb	Corr. for Pluto	O−C Jackson	O−C All Equations	Fourth Col.− Fifth Col.
1795.....	−2".05	−0".80	−0".12	−0".01	−0".11
1848.....	−0.27	+ .08	+ .27	− .09	+ .36
1852.....	+ .26	+ .06	+ .61	+ .39	+ .22
1856.....	+ .07	+ .04	+ .27	+ .15	+ .12
1860.....	− .52	+ .02	− .45	− .46	+ .01
1864.....	− .37	+ .01	− .41	− .32	− .09
1868.....	+ .12	.00	.00	+ .16	− .16
1872.....	− .30	.00	− .46	− .26	− .20
1876.....	+ .20	+ .01	+ .04	+ .25	− .21
1880.....	+ .32	+ .03	+ .19	+ .39	− .20
1884.....	− .36	+ .05	− .40	− .26	− .14
1888.....	− .30	+ .07	− .23	− .17	− .06
1892.....	+ .25	+ .08	+ .48	+ .45	+ .03
1896.....	− .28	+ .05	+ .14	+ .04	+ .10
1900.....	− .75	− .02	− .11	− .28	+ .17
1904.....	−0.72	− .14	+ .18	− .02	+ .20
1908.....	−1.03	− .31	+ .16	− .05	+ .21
1912.....	−1.28	− .55	+ .20	+ .06	+ .14
1916.....	−1.71	−0.85	+ .09	+ .03	+ .06
1920.....	−2.29	−1.16	− .16	− .13	− .03
1924.....	−2.59	−1.48	− .14	.00	− .14
1928.....	−2.92	−1.81	−0.14	+0.10	−0.24
[vv].....	.....	.....	1.80	1.22	.....

ing body is present) is to make the residuals vanish four times in the interval covered by the observations. This is very clearly shown in the residuals Leverrier found after making the best fit for Uranus, and the fact that a similar series of residuals is not found in the case of Neptune indicates that the effect of such outside bodies as may exist does not exceed the error of observation.[1]

In order to exhibit this effect the residuals from Jackson's orbit are plotted in the upper part of Figure 1. The continuous curve is the difference between Jackson's corrections to Newcomb's residuals and the corrections including a mass factor of 0.94 for Pluto. These

[1] *Ibid.*

differences are given in the sixth column of Table V and may be obtained by subtracting the fifth column from the fourth. They may be thought of as a smooth curve drawn through Jackson's residuals, which are comparable with the residuals of Uranus found by Leverrier before the effect of Neptune was taken into account. These residuals of Uranus, which are also given in Jackson's paper, have a maximum range of 31″ compared with the range of 0″.60 found in the smoothed curve for Neptune. The probable error of the mean

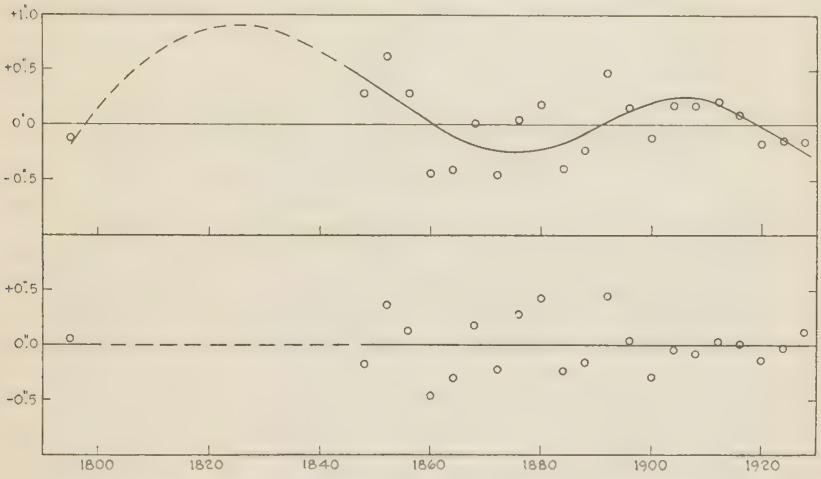

FIG. 1.—The residuals of Neptune in longitude. Above, those derived by Jackson with no perturbing masses assumed; below, those remaining after correction for perturbations by Pluto based on a mass of 0.94 (earth = 1).

of the observations of Neptune combined in four-year intervals, as used in these solutions, is ±0″.18. The residuals of Neptune when a mass of 0.94 for Pluto is introduced are given in the fifth column of Table V and are plotted in the lower part of Figure 1.

The mass of Pluto can be determined more accurately when its perturbations on Neptune have reached a maximum and when the perturbations in latitude are considered. Although the maximum perturbations by Pluto on Uranus are smaller than those produced on Neptune, they may yield a more reliable value of Pluto's mass because at the present time Uranus has been observed at more conjunctions with Pluto than has Neptune. The photographic magni-

tude of Pluto has been estimated as 15 to 16 by various observers. A single comparison with the North Polar Sequence made with the 60-inch reflector gave 15.5. Preliminary observations with a yellow color-screen indicate that the color-index is at least one magnitude. The visual magnitude, therefore, probably lies between 14.0 and 14.5. If Pluto has a density equal to that of the earth and if it reflects like the moon, a visual magnitude of 14.0 would correspond to a mass two-thirds that of the earth; for a magnitude of 14.5 the mass would be one-third that of the earth. If the mass of Pluto is more than two-thirds that of the earth, the density must be higher or the albedo lower than any yet determined in the solar system. Although Pluto may differ radically from other planets in these respects, a consideration of its magnitude favors the lower limit of the mass derived here. Until further evidence becomes available, it may be accepted as probable that the mass of Pluto is of the order of two-thirds that of the earth.

NOTE.—While the preceding article was in press, a paper by F. Zagar[1] was received. His results for the orbit of Pluto, after taking into account the perturbations of the four major planets, are in substantial agreement with those given here.

CARNEGIE INSTITUTION OF WASHINGTON
MOUNT WILSON OBSERVATORY
November 1930

[1] *Astronomische Nachrichten*, **240**, 335, 1930.

Contributions from the Mount Wilson Observatory, No. 418
Reprinted from the *Astrophysical Journal*, Vol. LXXIII, pp. 40–53, 1931
Printed in the U.S.A.

SMITHSONIAN OBSERVATORY

THE DISTRIBUTION OF ABSOLUTE MAGNITUDES AMONG K STARS BRIGHTER THAN THE SIXTH APPARENT MAGNITUDE AS DETERMINED FROM PARALLACTIC AND PECULIAR VELOCITIES

By GUSTAF STRÖMBERG

ABSTRACT

1. The distribution of absolute magnitudes among stars of spectral types K0–K2 and K3–K9 and brighter than apparent magnitude 6.0 has been determined from the distributions of parallactic and peculiar reduced proper motions and of radial velocities by methods described in *Mount Wilson Contributions* Nos. 395 and 410 (Table V). The number of proper-motion stars in the two groups is 1058 and 375, respectively; of radial-velocity stars, 849 and 348.

2. The distribution of absolute magnitudes for spectral types K0–K2 shows four distinct maxima: *bright giants* at −2.5, *normal giants* at +0.3, *faint giants* at +2.7, and *dwarfs* at +6.1. The relative proportions of stars in the four groups are 13.9, 78.3, 6.5, and 1.3 per cent.

For the interval K3–K9 the distribution shows three distinct maxima: *supergiants* at −4.5, *normal giants* at −0.1, and *dwarfs* at +6.7, the relative proportions of stars being 7.1, 90.5, and 2.4 per cent, respectively.

3. The distributions of reduced angular parallactic and peculiar motions and of the corresponding linear motions are given in Tables II–IV. Values are also given for the computation of the mean absolute magnitude for a group of stars from the mean apparent magnitude and the mean of the logarithms of the τ- or v-components.

The methods for determining the distribution of absolute magnitudes from peculiar and parallactic motions outlined in *Mount Wilson Contributions* Nos. 395[1] and 410[2] have been applied to stars of spectral type K brighter than the sixth apparent magnitude, with the results given in this paper.

All stars in the *Draper Catalogue* classified as K and brighter than the sixth apparent magnitude were included. To these were added stars classified as K by the Mount Wilson observers, but not given as K in the *HD*, where they appear mostly as G5 or Ma stars. The stars were divided into two groups including spectral types K0–K2 and K3–K9, respectively.

The apparent magnitudes were taken from the *HD*. In the case of doubles the apparent magnitude of the brighter star was used as given in the *HD*, or was derived from the difference in brightness

[1] *Astrophysical Journal*, 71, 163, 1930. [2] *Ibid.*, 72, 111, 1930.

between the components. Certain double stars whose combined apparent magnitude is brighter than six, but none of whose components attains this brightness, were thus excluded.

The proper motions have been taken from Boss's *Catalogue*. Raymond's corrections have been applied to the proper motions in declination.

The total number of stars in the two groups is 1058 and 375, respectively. Since certain stars are classed differently in the *HD* and by the Mount Wilson observers, the groups overlap each other partly and also, to a small extent, the group of M stars studied in *Contribution* No. 411.[1] Thus, a star classified as K5 in the *HD* and as K2 at Mount Wilson appears in both groups of K stars. It should also be noted that a very large group of stars is classified uniformly as Ko in the *HD*, whereas a great number of these stars are classified at Mount Wilson as G8 or G9. The present results for the early K stars are thus to a large extent representative for stars of types G8–K2 on the Mount Wilson scale.

From the two spectral groups were first subtracted, respectively, 14 and 9 stars having very large reduced proper motions. All of these stars have well-determined trigonometric parallaxes, and their absolute magnitudes are thus known individually with fair accuracy. Further, 153 and 63 stars whose angular distances from the apex or antapex are less than 30° were omitted from the two groups in analyzing the parallactic motions.

Among the K stars brighter than the seventh magnitude are 849 and 348 stars, respectively, for which spectrographically determined absolute magnitudes M_s and radial velocities V are available. Many of these are unpublished and were kindly put at my disposal by Dr. Adams. The group motions for these stars, computed for groups arranged according to absolute magnitude, are given in Table I.

The distribution of the peculiar radial velocities V' was derived for each absolute-magnitude group separately and combined with the distribution of $\sin \lambda$. The distribution of $\log |V_o + (\epsilon/\sin \lambda)|$ was then determined and smoothed graphically. This computation was based on the assumption that the distribution of the linear peculiar tangential velocities ϵ is identical with that of the peculiar radial

[1] *Astrophysical Journal*, 72, 117, 1930.

velocities V' and that there is no correlation between $|\epsilon|$ and $\sin\lambda$. Similarly, the distribution of $\log|V'| = \log|\epsilon|$ was determined for each group separately. The distributions of $y_1 = \log|V'| - 1.6756$ and $y_2 = \log|V_0 + (\epsilon/\sin\lambda)| - 1.6756$, reduced to a total of 1000 stars, are shown in Tables II and III. The values of the absolute magnitudes at which the transition from one distribution to the next is supposed to occur are given at the head of the table between the columns. The distribution for the dwarfs, being based on only a few stars, is very uncertain and has not been used for determining the absolute magnitudes. The mean values of y_1 and y_2 for the different groups of

TABLE I

K0–K2			K3–K9		
M_S	No.	V_0	M_S	No.	V_0
		km/sec.			km/sec.
<-1.0.....	27	19.4	<-1.0.....	40	22.7
-0.9 to 0.0	268	22.3	-0.9 to -0.5...	54	13.6
$+0.1$ to $+0.8$....	474	21.2	-0.4 to -0.1...	99	19.6
$+0.9$ to $+2.6$....	52	21.0	0.0 to $+0.3$...	93	26.7
			$+0.4$ to $+1.0$...	51	35.1

absolute magnitude are given at the bottom of Tables II and III. These numbers are analogous to the values given for the M stars in *Contribution* No. 411,[1] and may be used to derive mean absolute magnitudes by means of the formulae

$$\bar{M} = 5\,\overline{\log|\tau|} + \bar{m} - 5\,\bar{y}_1$$
$$\bar{M} = 5\,\overline{\log|v|} + \bar{m} - 5\,\overline{\log\sin\lambda} - 5\,\bar{y}_2\,.$$

The second formula can be used only when the stars are well distributed over the sky.

The distributions of $x_1 = \log|\tau| + 0.2m$ and $x_2 = \log|v| + 0.2m - \log\sin\lambda$ are given in Table IV. For values of x_1 and x_2 less than -1.7 the frequencies are determined by the methods outlined in *Contributions* Nos. 395 and 410; otherwise no smoothing has been done. The observed and computed distributions are given under the headings "O" and "C," respectively.

[1] *Ibid.*

TABLE II

K0–K2

y	$F(y_1)dy$					$F(y_2)dy$				
	−1.0	0.0	+2.0	+4.5		−1.0	0.0	+2.0	+4.5	
−3.6	1	0	0	0	1	0	0	0	0	0
3.5	0	1	0	0	0	0	0	0	0	0
3.4	0	0	1	1	0	1	0	0	0	0
3.3	1	0	0	0	0	0	0	1	1	0
3.2	0	0	0	0	1	0	1	0	0	1
3.1	1	1	0	0	0	0	0	0	0	0
3.0	1	0	1	1	1	0	0	0	0	0
2.9	1	1	1	0	1	0	0	0	0	0
2.8	1	1	1	1	1	1	0	1	1	0
2.7	2	1	1	1	1	1	1	0	0	1
2.6	2	1	1	1	2	1	0	1	1	0
2.5	3	2	1	1	2	1	1	1	1	1
2.4	4	2	2	1	3	1	1	1	1	1
2.3	5	3	2	2	3	2	1	1	1	1
2.2	6	4	3	3	4	2	1	1	1	1
2.1	7	4	3	3	5	3	1	2	2	1
2.0	9	5	5	4	7	4	2	2	2	2
1.9	10	7	6	5	8	5	2	3	3	2
1.8	14	9	8	6	11	6	3	4	4	3
1.7	18	11	9	8	13	7	4	5	5	4
1.6	21	14	12	10	17	9	5	6	6	5
1.5	24	17	15	12	22	11	6	7	7	6
1.4	27	20	18	15	25	14	7	9	9	8
1.3	31	24	22	19	30	17	9	12	12	10
1.2	36	29	27	23	36	20	13	15	15	13
1.1	41	35	39	29	43	24	17	18	19	17
1.0	48	46	51	37	51	27	23	21	22	25
0.9	55	59	62	46	63	32	32	26	28	38
0.8	66	74	70	59	75	40	41	34	35	58
0.7	90	85	78	82	82	49	52	45	44	82
0.6	122	97	85	100	85	70	72	62	58	101
0.5	134	101	91	102	85	106	91	84	76	113
0.4	134	97	93	101	84	133	115	107	97	114
0.3	36	86	91	94	82	134	120	120	111	112
0.2	22	70	80	77	72	114	116	120	114	95
−0.1	13	46	57	60	55	76	98	105	108	77
0.0	8	27	38	42	27	40	80	84	86	54
+0.1	4	14	22	32	2	22	48	56	64	36
0.2	2	5	4	18	0	14	22	29	36	16
0.3	0	1	0	4	0	8	10	12	20	2
0.4	0	0	0	0	0	4	4	4	8	0
0.5	0	0	0	0	0	1	1	1	2	0
+0.6										
$\bar{y}$..	−0.787	−0.647	−0.611	−0.544	−0.704	−0.476	−0.371	−0.362	−0.346	−0.441

TABLE III

K3–K9

y	$F(y_1)dy$						$F(y_2)dy$					
	−1.0	−0.4	0.0	+0.4	+4		−1.0	−0.4	0.0	+0.4	+4	
−4.0	1	0	0	0	0	0	0	0	0	0	0	0
3.9	0	0	0	0	0	0	0	0	0	0	0	0
3.8	0	0	0	0	0	0	0	0	0	0	0	0
3.7	0	1	0	0	0	0	0	0	0	0	0	0
3.6	1	0	1	0	0	0	0	0	0	0	0	0
3.5	0	0	0	1	1	0	0	0	0	0	0	0
3.4	0	0	0	0	0	0	0	1	0	0	0	0
3.3	1	0	0	0	0	1	1	0	0	0	0	0
3.2	1	1	0	0	0	0	0	0	1	0	1	0
3.1	1	0	1	0	1	0	0	0	0	1	0	0
3.0	1	1	0	1	0	0	0	0	0	0	0	0
2.9	2	1	0	0	0	0	0	0	0	0	0	0
2.8	2	1	1	0	1	1	1	1	1	0	1	1
2.7	2	1	1	1	1	0	0	0	0	1	0	0
2.6	3	1	1	1	1	0	1	1	1	0	0	0
2.5	4	2	1	1	1	1	1	1	1	0	1	0
2.4	5	2	2	1	2	1	1	1	1	1	1	1
2.3	6	3	2	2	2	1	1	1	1	1	1	0
2.2	8	3	2	2	2	1	1	1	1	1	1	0
2.1	10	4	3	2	3	2	1	1	2	1	1	1
2.0	12	6	4	3	4	2	2	2	2	2	2	1
1.9	15	7	5	4	5	2	2	2	3	2	2	1
1.8	19	9	6	5	6	3	3	3	4	3	3	1
1.7	22	11	8	6	8	4	4	4	5	3	4	2
1.6	27	14	10	8	10	5	5	5	6	4	5	2
1.5	34	17	12	11	12	6	6	6	7	5	6	3
−1.4	40	22	15	16	14	8	7	8	9	6	7	3

−1.3													4
1.2	47	27	19	25	16	10	8	10	12	8	9		5
1.1	54	35	23	35	20	12	10	16	15	10	12		6
1.0	60	50	31	44	25	15	12	25	21	13	15		8
0.9	67	64	36	51	33	19	14	41	27	17	22		10
0.8	73	77	42	59	42	23	18	58	35	22	29		13
0.7	77	88	56	65	56	31	23	66	43	35	35		17
0.6	77	95	70	71	69	36	31	82	53	64	43		22
0.5	73	98	88	80	82	42	54	91	66	86	55		35
0.4	67	97	112	83	92	56	92	99	80	96	70		64
0.3	59	85	120	89	97	70	185	103	92	100	89		86
0.2	44	70	120	92	98	88	227	106	103	101	98		96
−0.1	32	55	105	91	93	112	124	103	112	101	102		100
0.0	23	33	69	78	80	120	70	80	116	100	103		101
+0.1	15	17	25	45	56	120	48	46	92	97	101		101
0.2	9	2	8	18	36	105	26	26	50	70	80		100
0.3	4	0	1	7	17	69	13	8	26	34	52		97
0.4	2	0	0	2	8	25	6	2	10	10	28		70
0.5	0	0	0	0	4	8	2	0	2	4	13		34
0.6	0	0	0	0	2	1	0	0	0	1	6		10
0.7	0	0	0	0	0	0	0	0	0	0	2		4
0.8	0	0	0	0	0	0	0	0	0	0	0		1
+0.9													
$\bar{y}_{..}$	−0.904	−0.720	−0.558	−0.568	−0.497	−0.258	−0.367	−0.482	−0.384	−0.333	−0.291		−0.033

TABLE IV

x	K0–K2						K3–K9					
	$F(x_1)dx$			$F(x_2)dx$			$F(x_1)dx$			$F(x_2)dx$		
	O	C	O−C	O	C	O−C	O	C	O−C	O	C	O−C
−4.3							0	0.1	− 0.1			
4.2							0	0.1	− 0.1			
4.1							0	0.1	− 0.1			
4.0	0	0.1	− 0.1				0	0.1	− 0.1			
3.9	0	0.1	− 0.1				0	0.2	− 0.2			
3.8	1	0.1	+ 0.9				1	0.3	+ 0.7	0	0.0	0.0
3.7	0	0.1	− 0.1				0	0.3	− 0.3	1	0.1	+ 0.9
3.6	0	0.2	− 0.2				0	0.4	− 0.4	0	0.1	− 0.1
3.5	0	0.2	− 0.2	0	0.1	− 0.1	0	0.5	− 0.5	0	0.1	− 0.1
3.4	0	0.3	− 0.3	1	0.1	+ 0.9	1	0.7	+ 0.3	0	0.2	− 0.2
3.3	1	0.4	+ 0.6	0	0.2	− 0.2	0	0.8	− 0.8	0	0.2	− 0.2
3.2	0	0.5	− 0.5	0	0.3	− 0.3	0	1.0	− 1.0	1	0.2	+ 0.8
3.1	1	0.6	+ 0.4	0	0.3	− 0.3	1	1.3	− 0.3	0	0.4	− 0.4
3.0	1	0.8	+ 0.2	1	0.4	+ 0.6	1	1.5	− 0.5	1	0.4	+ 0.6
2.9	1	1.3	− 0.3	0	0.4	− 0.4	1	1.9	− 0.9	1	0.5	+ 0.5
2.8	1	1.5	− 0.5	0	0.5	− 0.5	1	2.3	− 1.3	1	0.6	+ 0.4
2.7	1	1.7	− 0.7	1	0.7	+ 0.3	2	2.9	− 0.9	1	0.8	+ 0.2
2.6	2	2.0	0.0	1	0.9	+ 0.1	2	3.7	− 1.7	1	0.9	+ 0.1
2.5	2	2.4	− 0.4	1	1.3	− 0.3	2	4.6	− 2.6	2	1.0	+ 1.0
2.4	3	3.0	0.0	1	1.5	− 0.5	3	5.6	− 2.6	2	1.2	+ 0.8
2.3	4	4.0	0.0	1	1.7	− 0.7	4	6.8	− 2.8	3	1.5	+ 1.5
2.2	5	4.8	+ 0.2	2	2.0	0.0	5	8.3	− 3.3	4	1.9	+ 2.1
2.1	6	5.8	+ 0.2	3	2.5	+ 0.5	6	10.0	− 4.0	5	2.4	+ 2.6
2.0	7	6.9	+ 0.1	3	3.3	− 0.3	8	11.9	− 3.9	6	3.0	+ 3.0
1.9	9	8.8	+ 0.2	4	4.0	0.0	10	14.1	− 4.1	7	3.9	+ 3.1
1.8	12	10.6	+ 1.4	5	5.1	− 0.1	12	16.7	− 4.7	9	4.9	+ 4.1
1.7	9	12.8	− 3.8	2	6.4	− 4.4	24	19.4	+ 4.6	3	6.1	− 3.1
1.6	18	15.3	+ 2.7	11	7.8	+ 3.2	45	22.2	+22.8	16	7.9	+ 8.1
−1.5	15	18.7	− 3.7	8	9.3	− 1.3	25	25.4	− 0.4	6	11.2	− 5.2

| | | |

The distributions of x_1 and x_2 are shown graphically in Figures 1–4, the observed values, as points joined by straight lines; the values computed from the distribution of absolute magnitudes and linear velocities, by continuous curves. The dotted curves represent the distributions when only the normal giants are included in the distribution of absolute magnitudes.

The distributions of absolute magnitudes for the two spectral groups are given in Table V and illustrated in Figures 5 and 6, the total number of stars being reduced to 1000. The distribution of absolute magnitudes among the stars of types K0–K2 shows four distinct maxima in accordance with the result obtained in *Contribution* No. 396.[1] The number of stars in this spectral interval is so large that separate solutions from the τ- and v-components could be made with fair accuracy; these are distinguished by plus signs and crosses in Figure 5. The absolute magnitudes of the dwarfs are those determined from the trigonometric parallaxes. The existence of the separate maxima is indicated by both the parallactic and the peculiar velocities. The relative proportion of stars in the four groups is 13.9, 78.3, 6.5, and 1.3 per cent; their mean absolute magnitudes are -2.5, $+0.3$, $+2.7$, and $+6.1$ mag., respectively.

The stars of types K3–K9 show frequency maxima at absolute magnitudes -4.5, -0.1, and $+6.7$, the percentage in each group being 7.1, 90.5, and 2.4, respectively.

The four groups among the early K stars were designated in *Contribution* No. 396[1] by the terms "supergiants," "ordinary giants," "subgiants," and "dwarfs." In that investigation, based exclusively on peculiar motions, the supergiants of the early K stars were of about the same brightness as those of late K type. The distribution of the brightest absolute magnitudes determined from parallactic motions has considerably higher weight than that based on peculiar motions. Further, the high galactic concentration of the supergiants introduces a systematic error into the absolute magnitudes derived from τ-components. These components are more or less perpendicular to the galactic circle, and the corresponding linear motion, on the basis of an ellipsoidal velocity distribution, averages less than that derived directly from the radial velocities. The absolute magnitudes

[1] *Astrophysical Journal*, **71**, 175, 1930.

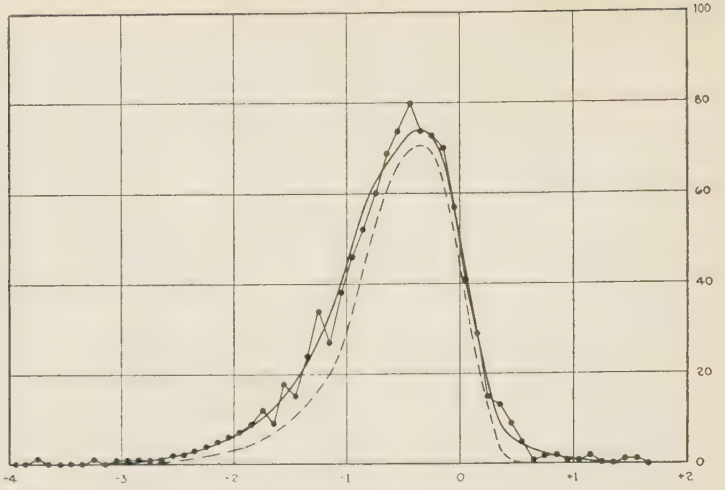

FIG. 1.—Distribution of $x_1 = \log \tau + 0.2\ m$ for stars of spectral types K0 to K2. The dots represent observed numbers within intervals $dx = 0.1$. The smooth curve is computed from the distributions of absolute magnitudes and peculiar radial velocities. The dotted curve shows the distribution when only the normal giants are included. For $x < -1.7$ the dots do not indicate independent observations, but show the probable extension of the distribution-curve.

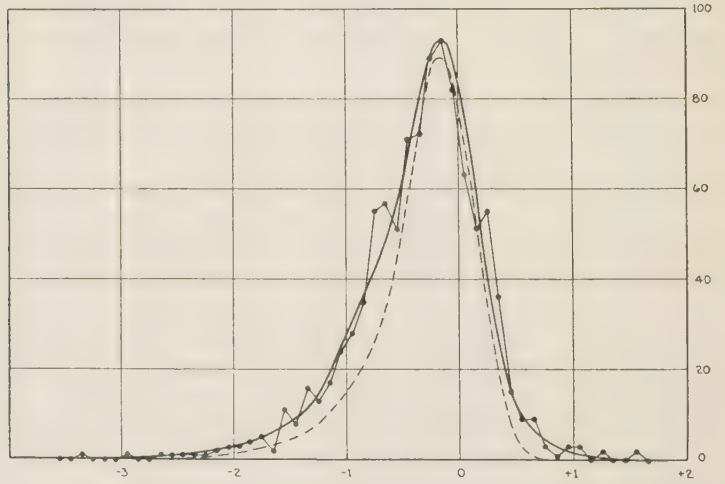

FIG. 2.—Distribution of $x_2 = \log v + 0.2\ m - \log \sin \lambda$ for stars of spectral types K0 to K2. Similar to Fig. 1, but the computed curve is based on a combination of group motion and peculiar radial velocities.

for the supergiants determined from τ-components are therefore systematically too faint. This explains why the present analysis makes the supergiants of late K type considerably brighter than did

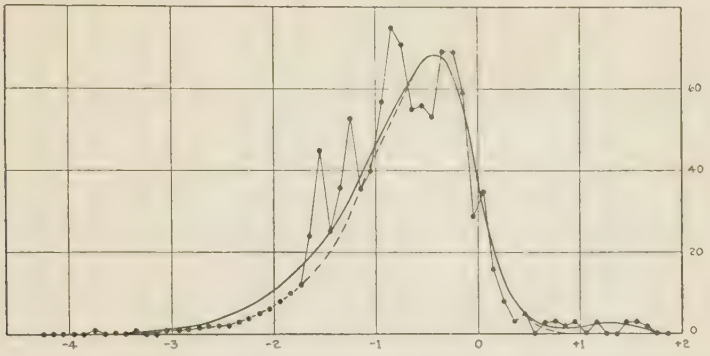

FIG. 3.—Distribution of $x_1 = \log \tau + 0.2\ m$ for stars of spectral types K3 to K9. Otherwise similar to Fig. 1.

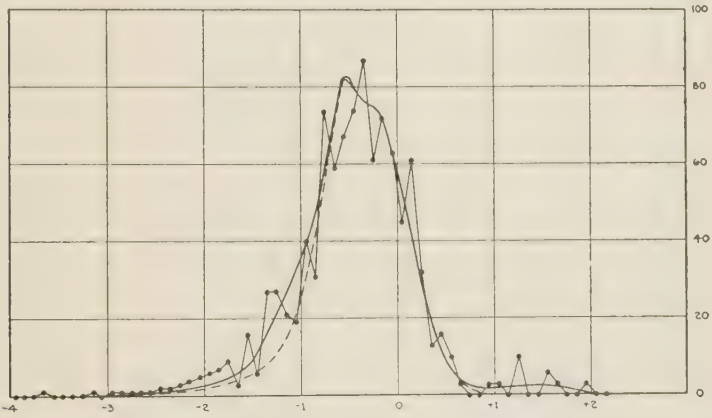

FIG. 4.—Distribution of $x_2 = \log v + 0.2\ m - \log \sin \lambda$ for stars of spectral types K3 to K9. Otherwise similar to Fig. 2.

the former investigation based on τ-components alone. It also explains certain systematic differences between the observed and computed values of the distribution $F(x_1)dx$ and $F(x_2)dx$ found for stars of types M and late K.

The present results indicate that the supergiants of late K type have about the same visual absolute magnitude as that found for

the supergiant M stars in *Contribution* No. 411.[1] It is thus quite possible that the group with a mean absolute magnitude -2.5 present among the early K stars is not an extension of the group of super-

TABLE V

$F(M)dM$

M	K0–K2	K3–K9	M	K0–K2	K3–K9
−5.8	0	1	+1.0	13	20
5.6	0	3	1.2	11	16
5.4	0	4	1.4	9	14
5.2	0	6	1.6	8	11
5.0	0	7	1.8	7	9
4.8	0	7	2.0	7	6
4.6	0	8	2.2	7	4
4.4	2	7	2.4	8	3
4.2	3	7	2.6	9	2
4.0	5	6	2.8	9	1
3.8	6	6	3.0	8	0
3.6	8	5	3.2	6	0
3.4	9	4	3.4	3	0
3.2	11	4	3.6	1	0
3.0	12	5	3.8	0	0
2.8	13	7	4.0	0	0
2.6	13	9	4.2	0	0
2.4	13	12	4.4	0	0
2.2	12	15	4.6	0	0
2.0	11	18	4.8	0	0
1.8	9	21	5.0	0	0
1.6	7	25	5.2	1	0
1.4	5	30	5.4	1	1
1.2	5	36	5.6	2	1
1.0	7	47	5.8	2	1
0.8	16	64	6.0	2	2
0.6	32	78	6.2	2	3
0.4	67	93	6.4	2	3
−0.2	100	98	6.6	1	4
0.0	135	87	6.8	0	3
+0.2	137	64	7.0	0	3
0.4	132	48	7.2	0	2
0.6	83	33	7.4	0	1
0.8	28	25	7.6	0	0
+1.0			+7.8		

giants of absolute magnitude -4.5 among the late K and the M stars. The probability that the groups are of different nature is strengthened by the fact that, although stars having *c*-characteristics, which are really the same as the pseudo-Cepheids, exist among both the late K and the G stars and are about absolute magnitude

[1] *Astrophysical Journal*, **72**, 117, 1930.

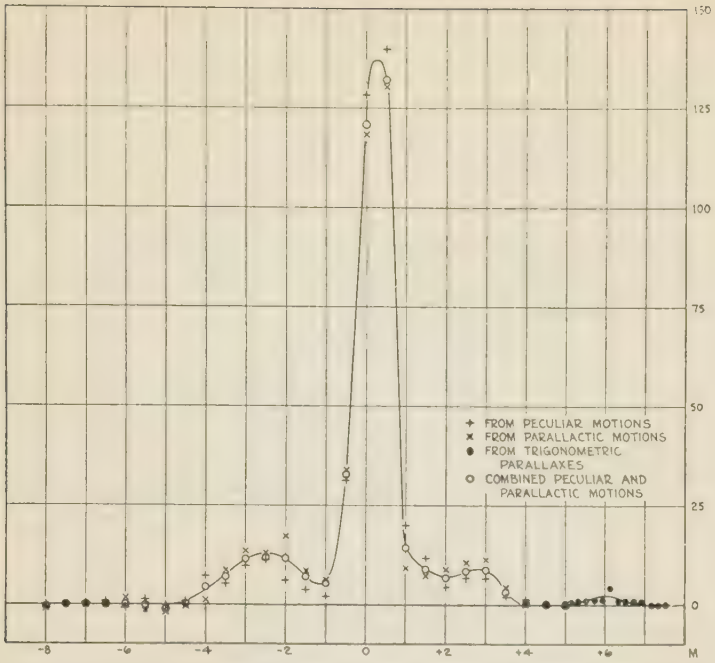

FIG. 5.—Distribution of absolute magnitudes for stars of spectral types K0 to K2 brighter than the sixth apparent magnitude.

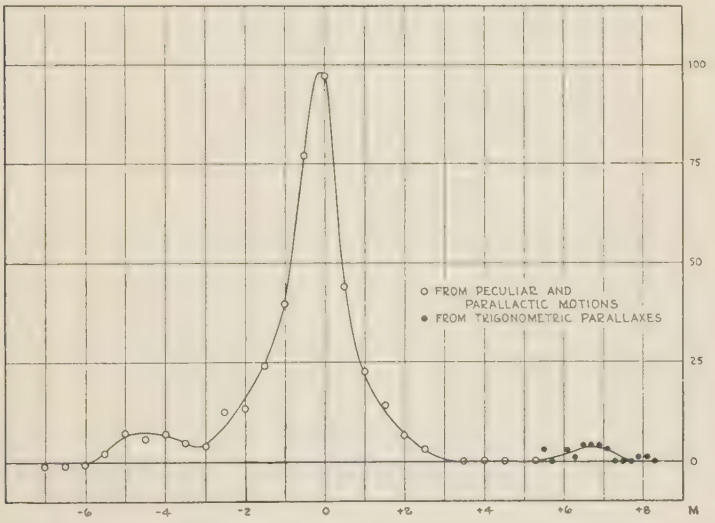

FIG. 6.—Distribution of absolute magnitudes for stars of spectral types K3 to K9 brighter than the sixth apparent magnitude.

-4, only one or two of them are found among the numerous stars in the spectral interval K0–K2. If future investigation identifies the pseudo-Cepheids with the supergiants found by the statistical investigations, we shall have no right to use the term "supergiants" for the group of early K stars of a mean absolute magnitude -2.5. The name *bright giants* may be adopted provisionally. In conformity with this new notation the name *faint giants* may replace the name subgiants, the latter name having also the disadvantage, when abbreviated, of being difficult to distinguish from the term supergiants. Also the term *normal giants*, which has been used in the summary, will in future investigations be used to designate the large group of stars of type G to M and of absolute magnitude about zero.

A similar study of F and G stars will appear in a future *Contribution*.

Carnegie Institution of Washington
Mount Wilson Observatory
November 1930

Contributions from the Mount Wilson Observatory, No. 419
Reprinted from the *Astrophysical Journal*, Vol. LXXIII, pp. 77–93, 1931
Printed in the U.S.A.

PHOTOMETRIC AND SPECTROGRAPHIC ORBITS OF TT AURIGAE

By ALFRED H. JOY and BANCROFT W. SITTERLY

ABSTRACT

Photometric observations of the eclipsing star TT Aurigae were made with the *polarizing photometer* at Princeton in 1910–1911 and 1915. The variable was compared with B.D.+39°1191. The *spectrographic* observations were made at Mount Wilson, 1917–1930.

The photometric observations and period.—Table I gives the 693 photometric observations of the difference in magnitude between the variable and the comparison star, together with the weights assigned. The period used was determined from the observed minima. The elements are

Min. = J.D. 2419065.9041 H.G.M.T. + $1^d.332732E$.

The photometric orbit.—The *light-curve* is of the *β Lyrae type. Ellipsoidal stars and a reflection effect* are indicated, but the evidence is against darkening at the limb. Because the duration of secondary eclipse is less than that of primary eclipse, the circular uniform elements can be slightly improved by introducing an orbital eccentricity of 0.09 with perihelion at secondary minimum. The primary eclipse is annular: $i = 88°.4$; $k = 0.90$; $r_1 = 0.36$; $r_2 = 0.32$; $b_1 = 0.31$; $b_2 = 0.27$; $V z/\sin^2 i = 0.54$; $L_1 = 0.66$; $L_2 = 0.34$; $J_1/J_2 = 1.56$; $2s = 0.05$.

The spectrographic observations and orbit.—The data for 32 spectrograms are listed in Table IV. The type of the bright star is B3 with poor lines. The spectrum of the fainter star seems to be similar. The lines of interstellar calcium are strong and give a mean velocity of +4.3 km/sec. The elements are: $e = 0.0$; $\gamma = +10.2$ km/sec.; $K_1 = 196.8$ km/sec.; $K_2 = 246.1$ km/sec.; $a_1 \sin i = 3{,}600{,}000$ km; $a_2 \sin i = 4{,}500{,}000$ km; $m_1 \sin^3 i = 6.7$ ⊙; $m_2 \sin^3 i = 5.3$ ⊙.

Absolute dimensions.—Photometric and spectrographic results were combined to find the absolute dimensions: $a_1 + a_2 = 8{,}100{,}000$ km; $r_1 = 4.5$ ⊙; $r_2 = 4.0$ ⊙; $b_1 = 3.7$ ⊙; $b_2 = 3.3$ ⊙; $m_1 = 6.7$ ⊙; $m_2 = 5.3$ ⊙; $\rho_1 = 0.11$ ⊙; $\rho_2 = 0.12$ ⊙; $M_1 = -1.2$ mag.; $M_2 = -0.9$ mag.; $\pi = 0.001$.

TT Aurigae ($5^h2^m.8$, +39°27′, 1900; 8.0–9.4 mag.) is an eclipsing star of early type. Miss Leavitt in 1907 found it to be variable. The variation was confirmed by S. Enebo[1] and by W. Münch,[2] who suspected that the curve outside eclipse was rounded like that of β Lyrae; but they failed to note the difference in depth of alternate minima which necessitated doubling the period. In 1910–1911 Joy made the observations presented in this paper. At the time these revealed the character of the light-curve, but the results have not heretofore been published.

[1] *Astronomische Nachrichten*, **180**, 63, 1909.

[2] *Ibid.*, **182**, 125, 1909.

J. Balanowsky[1] made a series of 175 observations with the Zöllner photometer at Pulkowa in 1911–1913 from which he deduced orbital elements and the relative dimensions of the stars. Extensive photographic observations have been carried out by C. Martin and H. C. Plummer (1914–1916)[2] and by F. C. Jordan (1914–1916 and 1922).[3] A number of observations have been reported by A. A. Nijland (1917–1920),[4] but the individual estimates have not been published.

I. THE PHOTOMETRIC OBSERVATIONS

The photometric observations (Table I) were obtained at Princeton with the sliding-prism photometer attached to the 23-inch refractor. The instrument and methods employed are the same as those used by R. S. Dugan in his well-known work on eclipsing stars. Six hundred and ninety-three sets of sixteen readings each were made, TT Aurigae being compared with the neighboring star B.D.+39°1191 by bringing the stars side by side and reducing them to apparent equality by rotating the nicol prism. Since the comparison star (8.02 mag.)[5] is somewhat brighter than the variable at its brightest, all the magnitude differences have the same sign. According to the *Draper Catalogue* the comparison star, like the variable, is of spectral type B5. Their colors seem to be very closely alike.

The phases given in Table I were computed from the elements

$$\text{Min.} = \text{J.D. } 2419065.9041 \text{ H.G.M.T.} + 1^{d}.332732E\,,$$

which were determined from a least-squares solution based on the times of twelve minima indicated by these observations.

II. THE PHOTOMETRIC ORBIT

The final photometric orbit and elements have been computed by Sitterly, although some preliminary solutions had previously been made by H. N. Russell and Joy. The observations given in Table I

[1] *Mitteilungen der Nikolai-Hauptsternwarte zu Pulkowa*, **5**, 123, 1913.

[2] *Monthly Notices of the Royal Astronomical Society*, **76**, 395, 1916.

[3] *Publications of the Allegheny Observatory*, **7**, 177, 1929.

[4] *Astronomische Nachrichten*, **211**, 358, 1920.

[5] *Annals of the Harvard College Observatory*, **63**, 156, 1913.

TABLE I

PHOTOMETRIC OBSERVATIONS OF TT AURIGAE

H.G.M.T.	Phase	$a-v$	Wt.	H.G.M T.	Phase	$a-v$	Wt.
	Days	Mag.			Days	Mag.	
J.D. 241+				8974.7819	0.8363	0.46	3
8961.7021	1.0838	0.33	2	8974.7937	.8482	.42	3
8961.7111	1.0928	.35	2	8974.8049	.8593	.33	3
8961.7306	1.1123	.48	2	8974.8514	.9058	.38	3
8961.7465	1.1282	.48	3	8974.8597	.9141	.37	4
8961.7708	1.1525	.42	3	8974.8701	.9245	.27	4
8961.7833	1.1650	.43	3	8974.8806	.9350	.35	3
8961.8000	1.1817	.51	3	8974.8910	.9454	.34	3
8961.8125	1.1942	.53	3	8974.9049	.9593	.26	1
8962.7188	0.7678	.55	2	8975.6604	.3821	.35	4
8962.7299	.7789	.56	3	8975.6674	.3891	.35	5
8962.7424	.7914	.50	2	8975.6750	.3967	.36	5
8962.7528	.8018	.36	3	8975.6819	.4036	.36	5
8962.7667	.8157	.43	3	8975.6896	.4113	.29	5
8962.7778	.8268	.39	3	8975.6965	.4182	.32	5
8962.7889	.8379	.44	3	8975.7257	.4474	.38	5
8962.8021	.8511	.46	3	8975.7347	.4564	.35	5
8962.8118	.8608	0.47	3	8975.7424	.4641	.42	5
8968.6208	.0061	1.41	3	8975.7500	.4717	.42	5
8968.6333	.0186	1.48	2	8975.7611	.4828	.39	5
8968.6458	.0311	1.15	3	8975.7681	.4898	.41	5
8968.6563	.0416	0.94	3	8975.8056	.5273	.51	5
8968.6674	.0527	1.06	3	8975.8125	.5342	.41	5
8968.6889	.0742	0.87	2	8975.8389	.5606	.39	5
8968.6979	.0832	.83	3	8975.8465	.5682	.48	5
8968.7090	.0943	.69	3	8975.8535	.5752	.56	5
8970.7458	.7984	.69	0	8975.8611	.5828	.49	5
8970.7639	.8165	.56	2	8975.8806	.6023	.54	5
8970.7972	.8498	.49	2	8975.8882	.6099	.57	5
8970.8444	.8970	.39	3	8975.8965	.6182	.59	5
8970.8549	.9075	.35	3	8975.9090	.6307	.76	5
8970.8729	.9255	.46	2	8975.9160	.6377	.69	4
8970.8910	.9436	.40	3	8975.9278	.6495	.71	4
8970.9049	.9575	.55	3	8975.9347	.6564	.70	4
8970.9264	.9790	.37	3	8975.9417	.6634	.82	3
8970.9347	.9873	.44	3	8976.6729	.0619	.86	2
8970.9458	.9984	0.37	2	8976.6785	.0675	.86	4
8974.6264	.6808	1.04	2	8976.6861	.0751	.75	5
8974.6340	.6884	0.92	3	8976.6917	.0807	.67	5
8974.6424	.6968	.88	3	8976.6972	.0862	.63	5
8974.6493	.7037	.79	3	8976.7028	.0918	.75	5
8974.6576	.7120	.70	3	8976.7215	.1105	.55	5
8974.6681	.7225	.64	3	8976.7285	.1175	.56	5
8974.6958	.7502	.56	3	8976.7347	.1237	.52	5
8974.7028	.7572	.49	3	8976.7417	.1307	.57	5
8974.7104	.7648	.39	3	8976.7479	.1369	.59	5
8974.7167	.7711	.51	3	8976.7535	.1425	.43	4
8974.7250	.7794	.42	2	8976.7819	.1709	.31	4
8974.7326	.7870	.47	3	8976.7882	.1772	.48	5
8974.7590	.8134	.44	3	8976.7944	.1834	.44	5
8974.7667	.8211	.51	3	8976.8139	.2029	.45	5
8974.7736	0.8280	0.44	3	8976.8243	0.2133	0.41	5

TABLE I—*Continued*

H.G.M.T.	Phase	$a-v$	Wt.	H.G.M.T.	Phase	$a-v$	Wt.
	Days	Mag.			Days	Mag.	
8976.8333	0.2223	0.32	5	8982.8354	0.8934	0.42	5
8976.8514	.2404	.36	5	8982.8542	.9122	.31	5
8976.8611	.2501	.43	4	8982.8646	.9226	.44	5
8976.8729	.2619	.32	4	8982.8736	.9316	.28	4
8976.8826	.2716	.38	4	8982.8799	.9379	.32	4
8976.8931	.2821	.30	4	8982.8910	.9490	.36	4
8976.9014	.2904	.33	4	8982.9007	.9587	.38	4
8977.6021	.9911	.38	4	8982.9090	.9670	.36	4
8977.6076	0.9966	.39	4	8982.9153	.9733	.38	4
8977.6132	1.0022	.36	4	8982.9278	.9858	.58	3
8977.6194	1.0084	.32	4	8982.9347	.9927	.41	3
8977.6264	1.0154	.38	4	8982.9410	0.9990	0.26	1
8977.6326	1.0216	.38	4	8984.5708	1.2961	1.02	4
8977.6458	1.0348	.34	4	8984.5778	1.3031	1.15	4
8977.6507	1.0397	.39	4	8984.5854	1.3107	1.17	4
8977.6569	1.0459	.47	4	8984.5917	1.3170	1.23	4
8977.6632	1.0522	.43	4	8984.5972	1.3225	1.31	4
8977.6715	1.0605	.41	4	8984.6021	1.3274	1.31	4
8977.6771	1.0661	.36	4	8984.6111	0.0037	1.42	4
8977.7000	1.0890	.36	4	8984.6174	.0100	1.37	4
8977.7069	1.0959	.42	4	8984.6215	.0141	1.32	4
8977.7160	1.1050	.42	4	8984.6264	.0190	1.28	4
8977.7229	1.1119	.39	4	8984.6313	.0239	1.27	4
8977.7313	1.1203	.33	4	8984.6368	0.0294	1.20	4
8977.7389	1.1279	.36	4	8996.5722	1.3029	1.14	4
8982.5764	0.5344	.80	3	8996.5778	1.3085	1.26	4
8982.5840	.6420	.91	4	8996.5840	1.3147	1.29	4
8982.5889	.6469	.84	4	8996.5896	1.3203	1.30	4
8982.5938	.6518	.97	4	8996.5958	1.3265	1.49	4
8982.5993	.6573	.95	4	8996.6014	1.3321	1.37	4
8982.6049	.6629	.95	4	9003.6847	0.4190	0.45	5
8982.6167	.6747	.97	5	9003.6944	.4287	.31	4
8982.6264	.6844	.90	5	9003.7042	.4385	.28	1
8982.6319	.6899	.85	5	9003.7139	.4482	.32	3
8982.6375	.6955	.73	5	9003.7236	.4579	.30	2
8982.6438	.7018	.80	5	9003.7674	.5017	.43	3
8982.6486	.7066	.73	5	9003.7819	.5162	.39	4
8982.6681	.7261	.55	5	9003.7972	.5315	.52	3
8982.6743	.7323	.65	5	9003.8111	0.5454	0.45	3
8982.6806	.7386	.62	5	9008.5694	1.3055	1.14	4
8982.6861	.7441	.61	5	9008.5750	1.3111	1.18	4
8982.6917	.7497	.56	5	9008.5799	1.3160	1.26	4
8982.6972	.7552	.61	5	9008.5847	1.3208	1.31	4
8982.7201	.7781	.53	5	9008.5903	1.3264	1.34	4
8982.7257	.7837	.51	5	9008.5958	1.3319	1.39	4
8982.7326	.7906	.45	5	9008.6097	0.0131	1.39	4
8982.7389	.7969	.49	5	9008.6160	.0194	1.23	4
8982.7486	.8066	.41	5	9008.6222	.0256	1.29	4
8982.7570	.8150	.47	5	9008.6292	.0326	1.20	4
8982.7688	.8268	.39	5	9008.6347	.0381	1.10	4
8982.7757	.8337	.49	5	9008.6396	.0430	1.05	3
8982.8125	.8705	.41	5	9008.6590	.0624	0.97	4
8982.8208	.8788	.39	5	9008.6653	.0687	.88	4
8982.8285	0.8865	0.33	5	9008.6729	0.0763	0.70	3

TABLE I—*Continued*

H.G.M.T.	Phase	$a-v$	Wt.	H.G.M.T.	Phase	$a-v$	Wt.
	Days	Mag.			Days	Mag.	
9008.6785	0.0819	0.67	4	9015.8861	0.6259	0.68	4
9008.6847	.0881	.74	3	9015.8938	.6336	.80	4
9008.6903	.0937	.62	3	9015.9097	.6495	.84	4
9009.5674	.9708	.32	4	9015.9188	.6586	.80	4
9009.5729	.9763	.34	4	9015.9271	.6669	.83	4
9009.5778	.9812	.43	5	9015.9375	.6773	.87	4
9009.5833	.9867	.39	5	9015.9431	.6829	.81	4
9009.5889	.9923	.36	5	9015.9500	.6898	.80	3
9009.5944	0.9978	.38	5	9046.6972	.7842	.49	4
9009.6125	1.0159	.38	4	9046.7090	.7960	.48	4
9009.6181	1.0215	.38	4	9046.7160	.8030	.44	4
9009.6236	1.0270	.35	4	9046.7292	.8162	.47	4
9009.6285	1.0319	.37	4	9046.7368	.8238	.42	4
9009.6333	1.0367	.28	2	9046.7438	.8308	.48	4
9013.5792	0.9844	.39	3	9046.7792	.8662	.39	4
9013.5875	.9927	.40	3	9046.7861	.8731	.42	4
9013.5931	0.9983	.32	3	9046.7986	.8856	.34	4
9013.5986	1.0038	.37	3	9046.8056	.8926	.41	4
9013.6069	1.0121	.40	3	9046.8194	.9064	.27	3
9013.6139	1.0191	.34	3	9046.8257	.9127	.41	3
9014.6347	0.7072	.75	4	9047.5049	.2592	.40	4
9014.6410	.7135	.72	4	9047.5111	.2654	.37	4
9014.6465	.7190	.67	4	9047.5181	.2724	.47	4
9014.6528	.7253	.62	4	9047.5243	.2786	.43	4
9014.6597	.7322	.57	4	9047.5319	.2862	.43	4
9014.6674	.7399	.64	4	9047.5382	.2925	.40	4
9014.6729	.7454	.61	4	9047.5597	.3140	.41	4
9014.6799	.7524	.54	4	9047.5053	.3196	.41	4
9014.6861	.7586	.62	4	9047.5694	.3237	.49	2
9014.6944	.7669	.62	4	9047.5833	.3376	.45	2
9014.6986	.7711	.48	4	9047.5889	.3432	.48	2
9014.7042	.7767	.55	4	9047.5931	.3474	.41	2
9014.7556	.8281	.35	3	9047.6819	.4362	.48	3
9014.7722	.8447	.45	4	9047.6889	.4432	.37	3
9014.7792	.8517	.52	4	9047.7111	.4654	.38	3
9014.7896	.8621	.49	4	9047.7167	.4710	.42	3
9014.7986	.8711	.38	4	9047.7243	.4786	.40	3
9014.8063	.8788	.44	4	9047.7306	0.4849	0.38	3
9014.8326	.9051	.49	4	9052.5500	1.3061	1.24	3
9014.8417	.9142	.49	4	9052.5563	1.3124	1.21	3
9014.8528	.9253	.41	4	9052.5611	1.3172	1.38	3
9014.8590	.9315	.41	4	9052.5660	1.3221	1.35	3
9014.8667	.9392	.41	4	9052.5722	1.3283	1.44	3
9014.8736	.9461	.34	4	9052.6868	0.1102	0.72	4
9014.8896	.9621	.38	4	9052.6938	.1172	.57	4
9014.8965	.9690	.39	4	9052.7007	.1241	.49	3
9014.9035	.9760	.33	4	9052.7083	.1317	.43	3
9014.9132	.9857	.22	3	9052.7292	.1526	.48	4
9014.9208	0.9933	.29	3	9052.7354	.1588	.44	4
9014.9292	1.0017	.29	3	9052.7444	.1678	.37	3
9015.8514	0.5912	.54	4	9052.7507	.1741	.46	4
9015.8590	.5988	.60	4	9052.7570	.1804	.52	3
9015.8681	.6079	.69	4	9052.7632	.1866	.37	3
9015.8792	0.6190	0.78	4	9052.7688	0.1922	0.50	3

TABLE I—*Continued*

H.G.M.T.	Phase	$a-v$	Wt.	H.G.M.T.	Phase	$a-v$	Wt.
	Days	Mag.			Days	Mag.	
9052.7813	0.2047	0.48	3	9060.4688	1.2286	0.53	3
9053.4771	.9005	.45	4	9060.4757	1.2355	.55	3
9053.4847	.9081	.53	4	9060.4840	1.2438	.62	3
9053.4910	.9144	.49	3	9060.4903	1.2501	.59	3
9053.4972	.9206	.53	3	9060.4979	1.2577	.65	3
9053.5035	.9269	.51	4	9060.5035	1.2633	.74	3
9053.5111	.9345	.50	4	9060.5181	1.2779	0.96	3
9053.5340	.9574	.31	3	9060.5236	1.2834	1.02	3
9053.5403	.9637	.36	3	9060.5313	1.2911	1.08	3
9053.5472	.9706	.30	3	9060.5382	1.2980	1.22	3
9053.5542	.9776	.30	3	9060.5444	1.3042	1.20	3
9053.5597	.9831	.36	3	9060.5514	1.3112	1.29	3
9053.5660	.9894	.42	3	9060.6132	0.0403	1.06	4
9053.5743	0.9977	.39	3	9060.6201	.0472	0.96	4
9053.5806	1.0040	.46	2	9060.6299	.0570	1.01	4
9053.6326	1.0560	.40	2	9060.6368	.0639	0.90	4
9053.6403	1.0637	.35	2	9060.6431	.0702	.89	4
9053.6486	1.0720	.30	2	9060.6486	.0757	.90	3
9053.6618	1.0852	.43	3	9060.6688	.0959	.67	5
9053.6688	1.0922	.46	3	9060.6743	.1014	.61	5
9053.6750	1.0984	.45	3	9060.6806	.1077	.72	5
9053.6882	1.1116	.43	3	9060.6861	.1132	.70	5
9053.6944	1.1178	.56	2	9060.6931	.1202	.60	5
9053.7007	1.1241	.42	2	9060.7014	.1285	.53	5
9054.5118	0.6025	.76	3	9060.7236	.1507	.42	4
9054.5188	.6095	.80	3	9060.7306	.1577	.49	4
9054.5278	.6185	.89	3	9060.7389	.1660	.46	4
9054.5340	.6247	.77	3	9060.7458	.1729	.42	4
9054.5403	.6310	.87	3	9060.7556	.1827	.45	4
9054.5458	.6365	0.91	3	9060.7639	0.1910	.51	4
9054.5556	.6463	1.00	4	9061.5854	1.0125	.49	5
9054.5604	.6511	0.90	4	9061.5917	1.0188	.40	5
9054.5674	.6581	1.00	4	9061.5979	1.0250	.39	5
9054.5743	.6650	1.01	4	9061.6042	1.0313	.38	5
9054.6111	.7018	0.81	4	9061.6097	1.0368	.40	5
9054.6174	.7081	.79	4	9061.6153	1.0424	.44	5
9054.6361	.7268	.65	4	9061.6292	1.0563	.55	1
9054.6444	.7351	.52	4	9061.6340	1.0611	.43	5
9054.6507	.7414	.52	4	9061.6389	1.0660	.41	5
9054.6569	.7476	.59	4	9061.6451	1.0722	.44	5
9054.6653	.7560	.50	4	9061.6500	1.0771	.34	5
9054.6722	.7629	.51	4	9061.6576	1.0847	.43	5
9054.6951	.7858	.43	4	9061.6840	1.1111	.48	4
9054.7007	.7914	.48	4	9061.6896	1.1167	.48	4
9054.7083	.7990	.56	4	9061.6951	1.1222	.55	4
9054.7146	.8053	.54	3	9061.7021	1.1292	.44	4
9054.7208	.8115	.50	4	9061.7076	1.1347	.54	4
9054.7271	.8178	.51	4	9061.7139	1.1410	.52	4
9054.7597	.8504	.39	4	9061.7361	1.1632	.55	4
9054.7653	.8560	.41	4	9061.7417	1.1688	.58	4
9054.7708	.8615	.43	4	9061.7479	1.1750	.52	4
9054.7826	.8733	.44	4	9061.7535	1.1806	.48	4
9054.7889	.8796	.45	4	9061.7639	1.1910	.66	4
9054.7938	0.8845	0.49	4	9061.7694	1.1965	0.58	4

TABLE I—*Continued*

H.G.M.T.	Phase	$a-v$	Wt.	H.G.M.T.	Phase	$a-v$	Wt.
	Days	Mag.			Days	Mag.	
9061.7764	1.2035	0.58	4	9067.5458	0.3090	0.36	3
9061.7847	1.2118	.69	3	9067.5514	.3146	.34	3
9061.7903	1.2174	.70	3	9067.5569	.3201	.41	2
9061.7965	1.2236	.56	3	9067.6347	.3979	.44	5
9062.5528	0.6472	.87	3	9067.6403	.4035	.44	4
9062.5583	.6527	.83	3	9067.6465	.4097	.45	4
9062.5632	.6576	.88	3	9067.6528	.4160	.39	4
9062.5681	.6625	.85	3	9067.6583	.4215	.36	4
9062.5729	.6673	.86	3	9067.6903	.4535	.42	4
9062.5785	.6729	.98	3	9067.6958	.4590	.35	4
9062.6076	.7020	.85	4	9067.7014	.4646	.44	4
9062.6139	.7083	.72	4	9067.7097	.4729	.48	5
9062.6188	.7132	.69	4	9067.7153	.4785	.50	5
9062.6243	.7187	.58	4	9067.7208	.4840	.53	5
9062.6333	.7277	.73	4	9067.7340	.4972	.49	5
9062.6389	.7333	.68	4	9067.7403	.5035	.49	5
9062.6632	0.7576	.59	2	9067.7486	.5118	.51	5
9065.6174	1.0460	.39	3	9067.7570	.5202	.45	5
9065.6229	1.0515	.43	2	9067.7625	.5257	.51	5
9065.6292	1.0578	.39	4	9067.7694	.5326	.53	5
9065.6347	1.0633	.45	4	9067.7799	.5431	.53	5
9065.6500	1.0786	.47	4	9067.7889	.5521	.44	5
9065.6556	1.0842	.40	4	9067.7931	.5563	.47	4
9065.6604	1.0890	.42	4	9067.8049	.5681	.50	3
9065.6667	1.0953	.49	4	9067.8146	.5778	.58	3
9065.6736	1.1022	.50	4	9067.8215	.5847	.53	2
9065.6799	1.1085	.46	4	9070.6979	.7956	.45	4
9065.6924	1.1210	.46	4	9070.7028	.8005	.48	4
9065.6972	1.1258	.49	4	9070.7104	.8081	.48	4
9065.7035	1.1321	.50	4	9070.7194	.8171	.47	4
9065.7111	1.1397	.48	4	9070.7257	.8234	.47	4
9065.7160	1.1446	.51	4	9070.7361	.8338	.49	4
9065.7208	1.1494	.52	4	9070.7472	.8449	.42	5
9065.7299	1.1585	.46	4	9070.7528	.8505	.41	5
9065.7347	1.1633	.51	5	9070.7611	.8588	.39	5
9065.7396	1.1682	.51	5	9070.7660	.8637	.38	5
9065.7444	1.1730	.54	5	9070.7806	.8783	.40	5
9065.7493	1.1779	.52	5	9070.7861	.8838	.44	5
9065.7549	1.1835	.58	5	9078.4694	.5707	.51	3
9065.7681	1.1967	.54	4	9078.4750	.5763	.58	3
9065.7736	1.2022	.49	4	9078.4806	.5819	.58	3
9065.7826	1.2112	.58	3	9078.5174	.6187	.73	3
9065.7882	1.2168	.58	3	9078.5229	.6242	.74	3
9065.7944	1.2230	.51	3	9078.5285	0.6298	.73	3
9065.7993	1.2279	.55	3	9084.4736	1.2440	.64	3
9067.4611	0.2243	.46	5	9084.4806	1.2510	.73	3
9067.4667	.2299	.44	5	9084.4875	1.2579	.71	3
9067.4715	.2347	.42	5	9084.4958	1.2662	.80	3
9067.4764	.2396	.42	5	9084.5021	1.2725	0.95	3
9067.4819	.2451	.42	5	9084.5090	1.2794	1.00	3
9067.5194	.2826	.41	5	9084.5326	1.3030	1.14	4
9067.5250	.2882	.55	3	9084.5444	1.3148	1.29	5
9067.5306	.2938	.38	3	9084.5500	1.3204	1.35	5
9067.5375	0.3007	0.41	3	9084.5556	1.3260	1.53	5

TABLE I—*Continued*

H.G.M.T.	Phase	$o-v$	Wt.	H.G.M.T.	Phase	$o-v$	Wt.
	Days	Mag.			Days	Mag.	
9084.5611	1.3313	1.55	5	9096.6444	0.0876	0.63	5
9084.5674	0.0051	1.43	5	9096.6590	.1022	.64	5
9084.5792	.0169	1.36	5	9096.6646	.1078	.62	5
9084.5854	.0231	1.29	5	9096.6708	.1140	.66	5
9084.5951	.0328	1.27	5	9096.6764	.1196	.58	5
9084.6007	.0384	1.10	5	9096.6868	.1300	.59	5
9084.6083	.0460	1.07	5	9096.6931	.1363	.57	5
9084.6146	.0523	1.00	5	9098.5056	.6161	.81	4
9084.6417	.0794	0.90	4	9098.5118	.6223	.78	4
9084.6479	.0856	.70	4	9098.5438	.6543	.94	4
9084.6542	.0919	.73	4	9098.5500	.6605	0.99	4
9084.6611	.0988	.66	4	9098.5569	.6674	1.05	4
9084.6674	.1051	.65	4	9098.5632	.6737	0.96	4
9084.6736	.1113	.59	4	9098.5757	.6862	.92	4
9090.5285	.6353	.77	4	9098.5813	.6918	.86	4
9090.5368	.6436	.74	5	9098.5868	.6973	.81	3
9090.5431	.6499	.91	5	9098.6118	.7223	.70	3
9090.5521	.6589	.93	5	9098.6181	.7286	.68	3
9090.5583	.6651	.97	5	9098.6243	.7348	.69	3
9090.5639	.6707	.99	4	9098.6479	.7584	.61	3
9090.5792	0.6860	.92	3	9098.6535	.7640	.59	3
9092.5069	1.2810	0.95	4	9098.6597	.7702	.61	4
9092.5132	1.2873	1.03	4	9098.6757	.7862	.59	4
9092.5181	1.2922	1.09	4	9098.6826	.7931	.61	3
9092.5229	1.2970	1.06	4	9098.6917	0.8022	0.59	4
9092.5340	1.3081	1.25	5	9100.5333	1.3111	1.30	5
9092.5389	1.3130	1.31	5	9100.5396	1.3174	1.42	5
9092.5465	1.3206	1.46	5	9100.5472	1.3250	1.46	5
9092.5521	1.3262	1.51	5	9100.5542	1.3320	1.48	5
9092.5576	1.3317	1.50	5	9100.5590	0.0040	1.47	5
9092.5632	0.0046	1.50	5	9100.5653	.0103	1.38	5
9092.5729	.0143	1.36	4	9100.5771	.0221	1.32	4
9092.5785	.0199	1.32	4	9100.5833	.0283	1.26	4
9092.5847	.0261	1.18	4	9100.5896	.0346	1.18	4
9092.6167	.0581	0.95	4	9100.6181	.0631	0.96	4
9092.6222	.0636	.85	4	9100.6257	.0707	.78	3
9092.6278	0.0692	.76	5	9100.6444	0.0894	0.71	3
9096.5056	1.2815	0.90	5	9112.5278	1.3109	1.33	4
9096.5118	1.2877	1.00	5	9112.5333	1.3164	1.34	4
9096.5181	1.2940	1.00	5	9112.5444	1.3275	1.44	4
9096.5264	1.3023	1.21	5	9112.5507	0.0011	1.42	4
9096.5326	1.3085	1.28	5	9112.5569	.0073	1.46	4
9096.5396	1.3155	1.33	5	9112.5625	.0129	1.46	4
9096.5500	1.3259	1.44	5	9112.5736	.0240	1.27	4
9096.5556	1.3315	1.42	5	9112.5792	.0296	1.15	4
9096.5611	0.0043	1.49	5	9112.5840	.0344	1.21	4
9096.5674	.0106	1.40	5	9112.5965	.0469	1.01	4
9096.5771	.0203	1.35	5	9112.6028	.0532	1.00	4
9096.5840	.0272	1.20	5	9112.6097	0.0601	1.00	3
9096.5979	.0411	1.14	5	9116.5222	1.3071	1.25	5
9096.6035	.0467	1.12	5	9116.5292	1.3141	1.42	5
9096.6118	.0550	0.96	5	9116.5382	1.3231	1.49	5
9096.6181	.0613	.94	5	9116.5451	1.3300	1.51	5
9096.6389	0.0821	0.81	5	9116.5507	1.3356	1.49	5

TABLE I—*Continued*

H.G.M.T.	Phase	$a-v$	Wt.	H.G.M.T.	Phase	$a-v$	Wt.
	Days	Mag.			Days	Mag.	
9116.5569	0.0091	1.40	5	0502.5694	1.3129	1.10	.....
9120.5104	1.2971	1.10	5	0502.5785	1.3220	1.34	.....
9120.5181	1.3048	1.27	5	0502.5868	1.3303	1.34	.....
9120.5257	1.3124	1.25	5	0502.5944	0.0052	1.28	.....
9120.5333	1.3200	1.36	5	0502.6056	.0164	1.38	.....
9120.5417	1.3284	1.45	5	0502.6132	0.0240	0.88	.....
9120.5486	0.0026	1.47	5	0506.5132	1.2585	.77	.....
9120.5604	.0144	1.33	5	0506.5229	1.2682	.75	.....
9120.5674	.0214	1.35	5	0506.5319	1.2772	.87	.....
9120.5806	.0346	1.13	5	0506.5396	1.2849	0.93	.....
9120.5896	.0436	1.10	5	0506.5618	1.3071	1.14	.....
9120.5979	.0519	0.97	5	0506.5785	1.3238	1.35	.....
9120.6063	0.0603	.89	5	0506.5903	0.0029	1.43	.....
J.D. 242+				0506.5965	.0091	1.28	.....
0502.4826	1.2261	.76	.....	0506.6090	.0216	1.16	.....
0502.4910	1.2345	.70	.....	0506.6146	0.0272	1.21	.....
0502.4958	1.2393	.42	.....	0507.8660	1.2786	0.82	.....
0502.5014	1.2449	.54	.....	0507.8736	1.2862	0.97	.....
0502.5118	1.2553	.63	.....	0507.8806	1.2932	1.00	.....
0502.5236	1.2671	.90	.....	0507.8882	1.3008	1.05	.....
0502.5424	1.2859	.82	.....	0507.9000	1.3126	1.23	.....
0502.5500	1.2935	.94	.....	0507.9062	1.3188	1.36	.....
0502.5590	1.3025	0.90	.....	0507.9146	1.3272	1.31	.....
0502.5653	1.3088	1.06	.....	0507.9222	0.0021	1.36	.....

were combined into the eighty-two normals of Table II by forming weighted means for eight consecutive observations after arranging the differences $a-v$ in order of phase. The observations of 1915 have not been used in the solution because they are few in number and greatly separated in time from the others.

The resulting light-curve (Fig. 1) shows a primary eclipse of depth 1.09 mag. and duration about 8^h, and a secondary eclipse of depth 0.57 mag. and apparently slightly shorter duration. The curve between eclipses has the pronounced arch of the β Lyrae type, indicating decidedly ellipsoidal stars. Near secondary it appears a little higher than near primary minimum, possibly the result of a reflection effect of radiation from the brighter star upon the adjacent side of the fainter.

In accordance with Russell's method, which was used for the solution, the differences in magnitude were reduced to intensities l, unit value for which was assumed to correspond to 1 when $a-v=0.360$

TABLE II

WEIGHTED NORMALS OF LIGHT-CURVE

Phase	$a-v$	O−C	O−C′	Phase	$a-v$	O−C	O−C′
Days	Mag.	Mag.	Mag.	Days	Mag.	Mag.	Mag.
0.0011	1.464	+0.020	+0.018	0.7586	0.555	−0.003	+0.029
.0080	1.402	+ .006	+ .004	.7716	.532	+ .019	+ .047
.0148	1.326	+ .003	.000	.7843	.489	− .003	+ .020
.0213	1.272	+ .017	+ .019	.7946	.488	+ .015	+ .031
.0289	1.206	+ .036	+ .037	.8052	.482	+ .024	+ .030
.0370	1.085	+ .003	+ .002	.8161	.475	+ .031	+ .032
.0466	1.024	+ .029	+ .025	.8275	.440	+ .002	+ .002
.0566	0.947	+ .038	+ .030	.8441	.429	+ .001	+ .002
.0642	.859	+ .011	+ .002	.8562	.427	+ .005	+ .005
.0758	.773	+ .004	− .006	.8709	.408	− .004	− .004
.0844	.707	− .008	− .020	.8845	.408	− .002	− .002
.0976	.658	+ .010	− .004	.9043	.402	+ .005	+ .003
.1097	.621	+ .025	+ .010	.9168	.425	+ .033	+ .033
.1229	.548	.000	− .010	.9316	.399	+ .012	+ .012
.1464	.491	− .002	− .004	.9508	.373	− .009	− .009
.1736	.432	− .035	− .035	.9679	.352	− .028	− .028
.2040	.432	− .012	− .012	.9798	.385	+ .005	+ .005
.2412	.403	− .014	− .014	.9888	.385	+ .006	+ .006
.2754	.413	+ .015	+ .015	0.9967	.356	− .025	− .025
.3004	.381	− .006	− .006	1.0106	.397	+ .013	+ .013
.3638	.393	+ .013	+ .013	1.0248	.365	− .020	− .020
.4078	.390	− .001	− .001	1.0417	.414	+ .021	+ .021
.4370	.376	− .027	− .027	1.0577	.405	+ .003	+ .003
.4608	.391	− .025	− .025	1.0763	.403	− .006	− .006
.4808	.454	+ .025	+ .025	1.0912	.435	+ .013	+ .013
.5145	.479	+ .031	+ .033	1.1081	.455	+ .021	+ .021
.5462	.463	− .036	− .012	1.1215	.441	− .002	− .002
.5746	.539	− .038	− .005	1.1407	.496	+ .044	+ .044
.6018	.652	− .018	+ .005	1.1684	.523	+ .041	+ .041
.6184	.731	− .010	+ .003	1.1871	.549	+ .042	+ .038
.6307	.785	− .020	− .020	1.2133	.593	+ .017	+ .002
.6439	.845	− .011	− .025	1.2433	.627	− .086	− .097
.6518	.899	+ .010	− .019	1.2733	0.915	− .015	− .022
.6591	.922	+ .011	− .029	1.2899	1.045	− .031	− .032
.6682	.941	+ .031	− .009	1.3003	1.185	− .003	− .002
.6833	.885	+ .031	+ .017	1.3059	1.240	− .013	− .011
.6958	.812	+ .013	+ .015	1.3101	1.304	+ .006	+ .005
.7076	.711	− .034	− .023	1.3146	1.328	− .018	− .022
.7218	.655	− .031	− .009	1.3196	1.377	− .023	− .025
.7330	.610	− .032	− .006	1.3242	1.438	+ .003	+ .001
0.7469	0.575	−0.020	+0.012	1.3288	1.460	+0.012	+0.011

mag. The light-intensities outside the eclipses were then plotted and represented by the expression

$$l = a - s\cos\theta - \tfrac{1}{2} z\cos^2\theta\,,$$

where a is the maximum intensity, $2s$ the difference in intensity of the two sides of the fainter star, θ the phase angle, and $z = \epsilon^2 \sin^2 i$,

ϵ being the eccentricity of the ellipsoidal stars. Approximate values of the constants were found to be

$$a=0.980, \qquad s=0.026, \qquad \tfrac{1}{2}z=0.140\,.$$

A correction by least squares gave

$$a=0.9808, \qquad s=0.0247, \qquad \tfrac{1}{2}z=0.1434\,,$$

which reduced the sum of the squares of the residuals from 119 to

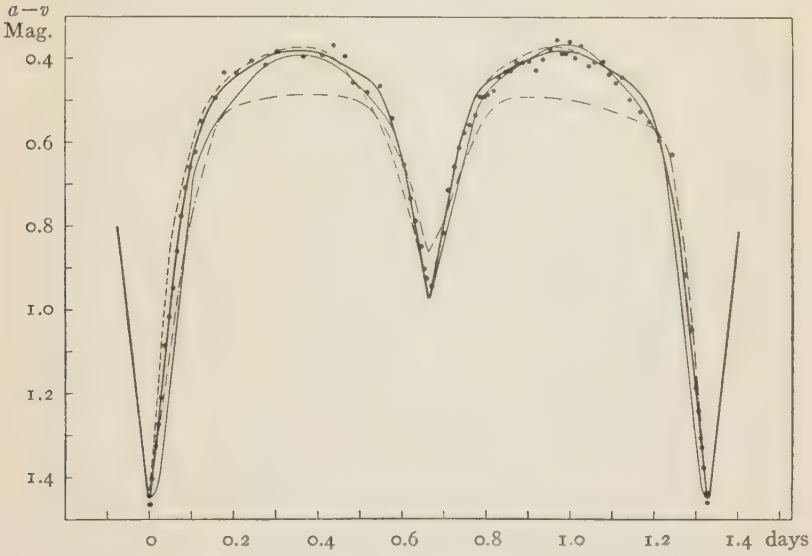

FIG. 1.—Photometric observations and light-curves of TT Aurigae. The dots are the Princeton observations by Joy. The heavy curve is computed from the uniform elliptical solution derived in this investigation. The light line represents the photographic observations of Martin and Plummer; the dot-and-dash curve, Jordan's photographic observations; and the dash curve, Balanowsky's observations with the Zöllner photometer. These curves have been shifted so that the primary minima coincide with that observed at Princeton.

101. The intensities of all the normals were then rectified by the formula

$$l'=\frac{l+0.025(1+\cos\theta)+0.143\,l\cos^2\theta}{0.981+0.025}\,,$$

which reduced the intensity at maximum of the rectified curve to 1.

The rectified eclipse-curves are different in shape, the secondary being distinctly steeper and narrower than the primary, except near the top. It was thought that darkening at the limbs of the stars might account for this; but in the first solution the difference was ignored, only the shape of the primary (which is better defined than the secondary) and the two depths being taken into account. The resulting elements I appear in Table III, and the residuals O−C are given in Table II. They might be varied in the direction of

TABLE III

PHOTOMETRIC ORBITAL ELEMENTS

	I Uniform Circular	II Uniform Elliptical	Balanowsky
e, orbital eccentricity	0.00	0.09	0.048
ω, longitude of periastron	.....	270°	262°.3
i, inclination	87°.1	88°.4	88°.3
k, ratio of radii	0.90	0.90	0.84
r_1, longer radius, large star	.38	.36	.307
r_2, longer radius, small star	.34	.32	.244
b_1, shorter radius, large star*	.32	.31	.258
b_2, shorter radius, small star*	.29	.27	.205
b/r, ellipticity of stars	.84	.86	.840
L_1, light of large star	.68	.66	.734
L_2, light of small star	0.32	0.34	0.266
J_1/J_2, ratio of mean surface brightness	1.68	1.56	1.95
$2s$, difference in intensity of two sides of fainter star	0.05	0.05	.....
Primary eclipse	Partial, α_0= 0.975, small star in front	Grazing, annular	Annular

* Disregarding polar flattening (*Contributions from Princeton University Observatory*, No. 3, 116, 1915).

closer equality of diameters and a slightly smaller inclination by favoring the curve of the secondary minimum at the expense of that of the primary, but the possible changes would be small. A second solution, attempting to account for the discrepancy in shape by introducing darkening at the limb, was unsuccessful; no set of elements could be found which came near to reproducing the curve forms of both minima.

It was therefore decided to introduce eccentricity into the orbit. The secondary minimum is midway between primary minima, but the observations indicate that it is of shorter duration. Hence, periastron must occur at the time of secondary minimum. The spectro-

scopic observations are not inconsistent with a small eccentricity with the line of apsides perpendicular to the line of nodes, but on account of the quality of the spectrum it appears impossible to determine the amount of the eccentricity from these observations. A few approximations show that except at the shoulders of the curve, which are poorly defined anyway, an orbital eccentricity around 0.09, with periastron at secondary (270° long.), would give a much better fit for secondary minimum than the circular elements, and an equally good fit for primary minimum. The adopted solution gave elements II in Table III and the residuals O−C′ of Table II. For the whole series of observations the probable error of a normal place (eight observations) is 0.015 mag. and that of a single observation of average weight (3.9) is 0.043 mag. These values are of the same order as have been found by Dugan and others who have used the Princeton photometer and similar methods of solution.

It is instructive to compare these elements with those of Balanowsky (also in Table III). His smaller orbital eccentricity was obtained not from the width of his secondary minimum, but from the maximal and minimal points of his observed curve, reflection effect being neglected; but his secondary minimum, though not very definite in shape, is perceptibly narrower than his primary. His observed ranges of variation are very close to those of Joy, but his minima are a little narrower and he used a larger value of z, thus obtaining smaller rectified ranges and smaller and more unequal stars. The observed strength of the lines of the secondary star in the spectrograms favors the results found here. However, the general resemblance of the two solutions from entirely independent sources is satisfactory. The shape of primary minimum and the depths fix k, r, and i fairly definitely. Darkened elements are less satisfactory and are not given.

Unfortunately, the two published photographic curves are at variance with the visual curves and with each other, as is apparent from Figure 1. Martin and Plummer's primary minimum is steep with a flat bottom, while Jordan's is narrower, more pointed, and asymmetrical. Joy, Balanowsky, and Martin and Plummer agree fairly well on the form of the curve outside eclipse and on the depths

of minima; but Jordan's curve outside eclipse is much flatter than the others, and his secondary minimum 25 per cent shallower.

III. SPECTROGRAPHIC OBSERVATIONS AND ORBIT

From 1917 to 1930 thirty-two spectrograms of TT Aurigae were obtained by Joy at Mount Wilson as listed in Table IV. The spectral type of the brighter star is B3. The lines are so wide and indefinite that it is nearly impossible to measure them with any accuracy. The rotational effect from limb to limb is 340 km/sec. The spectrum of the companion is clearly present at the time of maximum separation of the lines and is about one-half as strong as that of the primary. It seems to be similar in type to that of the principal star. Spectrogram C 5392 was exposed during primary eclipse especially to show the spectrum of the fainter star, but no difference in type could be detected when the spectra of the two stars were compared. The eclipse, however, is not total. Since only 80 per cent of the brighter star is covered at maximum of eclipse, its light may mask that of the smaller star to some extent.

The H and K lines of both components are faint, but are visible under the best conditions. They have been measured on nine of the plates.

The lines of interstellar calcium are present in fair strength and can be accurately measured on plates correctly exposed. Velocities from these lines, reduced to the sun, and their weights are given in the last two columns of Table IV. The weighted mean velocity for the interstellar calcium lines measured on eighteen plates is +4.3 km/sec., which is approximately the value, with reversed sign, of the solar motion (7.0 km/sec.) in that direction.

The measures are plotted in Figure 2. The smaller circles represent the primary and the larger the secondary. The velocities of stationary H and K are represented by crosses. The curve is drawn on the basis of a circular orbit.

No attempt was made to distribute the observations over the whole of the velocity-curve but rather to confine them to times of maximum in order to determine the range and masses of the com-

TABLE IV

SPECTROGRAPHIC OBSERVATIONS

PLATE	J.D. 242+	PHASE	VELOCITY			INTERSTELLAR CALCIUM	
			Primary	Secondary	Wt.	H and K	Wt.
		Days	km/sec.	km/sec.		km/sec.	
C 5392.....	6018.774	0.007	.....	+ 5	1	+16.1	2
γ 5543.....	1267.658	.081	−114	+112	1	.....	.....
C 3092.....	4123.854	.232	−188	+181	1	+ 9.5	4
γ 6523.....	1595.754	.324	−183	+245	2	−11.1	1
7657.....	1944.931	.325	−184	+218	1	.....	.....
C 274.....	2360.743	.326	−169	+245	1	.....	.....
3709.....	4571.750	.330	−176	+215	1	+11.2	2
γ 6439.....	1567.772	.330	−170	+226	3	−14.4	2
6726.....	1655.736	.334	−154	+256	2	.....	.....
C 177.....	2268.797	.338	−187	+277	2	+ 5.0	3
3660.....	4539.774	.340	.....	.....	.....	+12.4	2
685.....	2597.993	.349	−174	+303	1	+12.8	2
2576.....	3770.823	.375	−224	+253	1	+ 4.1	2
3038.....	4068.022	.375	−168	+282	1	+15.1	1
885.....	2740.642	.396	−249	+240	1	.....	.....
γ 5577.....	1270.658	.415	−228	+246	1	.....	.....
C 4533.....	5192.892	.419	−207	+305	2	− 4.3	3
325.....	2395.719	.650	+ 1	.....	3	.....	.....
607.....	2561.010	.683	+ 40	.....	1	.....	.....
γ 6431.....	1566.794	.685	+ 11	.....	2	+13.8	3
C 4509.....	5183.837	.693	0	.....	3	.....	.....
2572.....	3769.825	.710	+ 21	.....	1	−18.0	1
3070.....	4097.878	.911	+214	−208	2	+ 8.9	4
4099.....	4834.953	.985	+195	−208	1	.....	.....
168.....	2266.785	.991	+160	−225	1	.....	.....
1633.....	3135.728	.993	+204	−221	2	.....	.....
675.....	2595.973	0.994	+218	−239	1	.....	.....
4595.....	5246.792	1.009	+227	−265	3	− 2.0	3
5398.....	6019.793	1.026	+182	−252	3	+ 9.8	4
227.....	2330.806	1.041	+225	−252	2	.....	.....
2617.....	3800.819	1.051	+175	−280	1	−17.0	2
942.....	2766.661	1.093	+183	−210	1	− 1.1	2

ponents. After weighting and combining the observations, the elements

$e=$ 0.0 (assumed)	$a_1 \sin i = 3{,}600{,}000$ km
$\gamma=$ +10.2 km/sec.	$a_2 \sin i = 4{,}500{,}000$
$K_1=$ 196.8	$m_1 \sin^3 i = 6.7\ \odot$
$K_2=$ 246.1	$m_2 \sin^3 i = 5.3$

were found. The probable error of a single observation is very large, as might be expected from the character of the spectrum.

IV. ABSOLUTE DIMENSIONS

The photometric and spectroscopic results may be combined to obtain the absolute dimensions of the system. The primary eclipse is produced when the smaller star, which is also less massive and of lower surface brightness, passes in front of the larger, more mas-

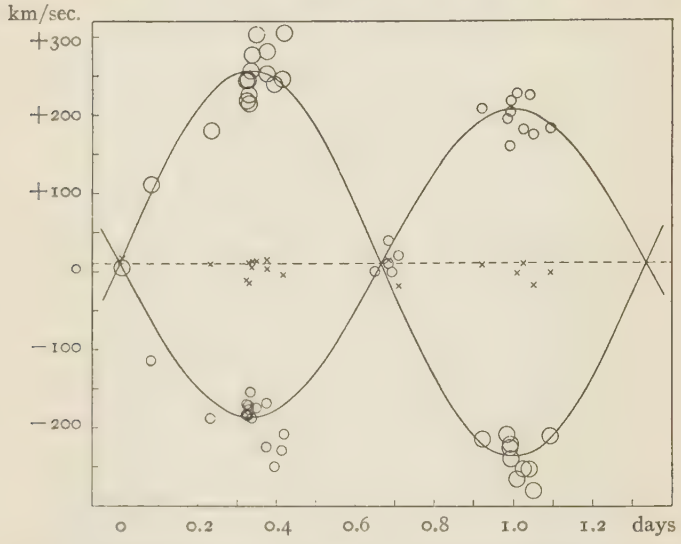

FIG. 2.—Velocity-curve of TT Aurigae. The small and large circles represent the observations of the primary and secondary, respectively. The crosses give the radial velocities of interstellar calcium relative to the sun.

sive star. The following values for the circular elements are thus determined:

a_1, semi-major axis of primary orbit	3,600,000 km
a_2, semi-major axis of secondary orbit	4,500,000
a_1+a_2, semi-major axis of relative orbit	8,100,000
r_1, longer radius of large star	3,100,000 (4.5 ⊙)
r_2, longer radius of small star	2,800,000 (4.0)
b_1, shorter radius of large star	2,600,000 (3.7)
b_2, shorter radius of small star	2,300,000 (3.3)
m_1, mass of large star	6.7 ⊙
m_2, mass of faint star	5.3
ρ_1, density of large star	0.11 ⊙
ρ_2, density of faint star	0.12
M_1, absolute magnitude of large star	−1.2 mag.
M_2, absolute magnitude of small star	−0.9
π, parallax	0".001

The absolute magnitudes are derived from the formula

$$M = \frac{29{,}500}{T} - 5 \log r - 0.08 .$$

The temperatures are taken to be 15,000°. If the temperature of the fainter star were assumed to be 12,000° instead of 15,000°, its absolute magnitude would become −0.4, which would satisfy the light ratio of the two stars found in the photometric solution. The parallax is determined for the brighter star by using the absolute magnitude (−1.2) and apparent magnitude (8.9). An absolute trigonometric parallax of −0″.003 has been found at the Yerkes Observatory.[1]

The stars are quite normal in every way. The masses and luminosities are in fair agreement with Eddington's mass-luminosity relationship.

Our thanks are especially due to Professor Russell and Professor Dugan of Princeton University, through whose interest and encouragement this investigation was begun and finally brought to completion.

Carnegie Institution of Washington
Mount Wilson Observatory
August 1930

[1] *Astronomical Journal*, **37**, 44, 1926.

END OF VOLUME XVIII

INDEX TO VOLUME XVIII

Nos. 391 to 419

AUTHORS

PAGE

BIRGE, RAYMOND T. *See* King, Arthur S.

BURWELL, CORA G. *See* Merrill, Paul W.

HALE, GEORGE E.—The Spectrohelioscope and Its Work: Part II. The Motions of the Hydrogen Flocculi near Sun-Spots 55

HUBBLE, EDWIN.—Distribution of Luminosity in Elliptical Nebulae . 131

HUMASON, MILTON L.—The Rayton Short-Focus Spectrographic Objective 229

JOY, ALFRED H.—
The Spectrographic Orbit of RS Canum Venaticorum 273
A Spectrographic Study of U Sagittae 235

JOY, ALFRED H., AND BANCROFT W. SITTERLY—Photometric and Spectrographic Orbits of TT Aurigae 481

JOYNER, MARY C. *See* Seares, F. H.

KING, ARTHUR S.—
Temperature Classification of the Spectra of Europium, Gadolinium, Terbium, Dysprosium, and Holmium, λ 3850 to λ 4700 . . . 373
Temperature Classification of the Stronger Lines of Columbium, with Preliminary Notes on Their Hyperfine Structure 441

KING, ARTHUR S., AND RAYMOND T. BIRGE—Evidence from Band Spectra of the Existence of a Carbon Isotope of Mass 13 251

MAYALL, NICHOLAS U. *See* Nicholson, Seth B.

MERRILL, PAUL W.—Notes on the Spectra of Ten Bright-Line Stars of Classes B and A 315

MERRILL, PAUL W., AND CORA G. BURWELL—Behavior of Bright Lines in the Spectra of Several Long-Period Variable Stars 177

NICHOLSON, SETH B., AND NICHOLAS U. MAYALL—Positions, Orbit, and Mass of Pluto 455

NICHOLSON, SETH B. *See* Pettit, Edison

PETTIT, EDISON, AND SETH B. NICHOLSON—
Lunar Radiation and Temperatures 21
Spectral Energy-Curve of Sun-Spots 121

PAGE

SANFORD, ROSCOE F.—
On the Radial Velocity of R Lyrae 85
Variations in Radial Velocity of the Cepheid Variables W Geminorum, U Aquilae, and DT Cygni 279

SEARES, F. H., AND B. W. SITTERLY AND MARY C. JOYNER—Magnitudes of Southern Comparison Stars for Eros 409

SITTERLY, BANCROFT W. *See* Joy, Alfred H.; Seares, F. H.

STRÖMBERG, GUSTAF—
The Distribution of Absolute Magnitudes among K and M Stars Brighter than the Sixth Apparent Magnitude as Determined from Peculiar Velocities 105
The Distribution of Absolute Magnitudes among K Stars Brighter than the Sixth Apparent Magnitude as Determined from Parallactic and Peculiar Velocities 467
The Distribution of Absolute Magnitudes among M Stars Brighter than the Sixth Apparent Magnitude as Determined from Parallactic and Peculiar Velocities 335
A Method for Determining the Distribution of Stellar Absolute Magnitudes from the Distributions of Angular and Linear Peculiar Velocities 93
A Method for Determining the Distribution of Stellar Absolute Magnitudes from the Distributions of Parallactic Motions and Radial Velocities 329

VAN MAANEN, ADRIAAN—
Investigations on Proper Motion. Thirteenth Paper: The Proper Motion of N.G.C. 2264 293
Investigations on Proper Motion. Fourteenth Paper: The Proper Motions of Six Planetary Nebulae 299
Investigations on Proper Motion. Fifteenth Paper: The Proper Motion of the Spiral Nebula N.G.C. 4051 305
Investigations on Proper Motion. Sixteenth Paper: The Proper Motion of Messier 51, N.G.C. 5194 311
The Photographic Determination of Stellar Parallaxes with the 60-Inch and 100-Inch Reflectors. Eleventh Series 1

VAN MAANEN, ADRIAAN, and HOWARD C. WILLIS—Investigations on Proper Motion. Seventeenth Paper: Proper Motions of Some Very Faint Stars 345

WILLIS, HOWARD C. *See* van Maanen, Adriaan

WOOLEY, R. VAN DER R.—Multiplet Intensities in the Solar Spectrum . 361

SUBJECTS

Absolute magnitudes, distribution among K and M stars, 105, 335, 467
———, stellar, method for determining distribution, 93, 329
Band spectra, evidence for existence of carbon isotope of mass 13, 251
Bright-line stars, of classes B and A, spectra, 315
Bright lines, behavior in spectra of long-period variable stars, 177
Carbon isotope of mass 13, 251
Cepheid variables. *See* Stars, Cepheid variable
Clusters, open, proper motion of N.G.C. 2264; 293
Columbium, spectrum, temperature classification, 441
Dysprosium, spectrum, temperature classification, 373
Energy-curve, spectral, of sun-spots, 121
Eros, magnitudes of southern comparison stars, 409
Europium, spectrum, temperature classification, 373
Flocculi, hydrogen, motions near sun-spots, 55
Gadolinium, spectrum, temperature classification, 373
Holmium, spectrum, temperature classification, 373
Hydrogen flocculi, motions near sun-spots, 55
Isotope, carbon, of mass 13, 251
Luminosity, distribution in elliptical nebulae, 131
Magnitudes, absolute, distribution among K and M stars, 105, 335, 467
———, of southern comparison stars for Eros, 409
———, stellar absolute, method for determining distribution, 93, 329
Moon, radiation and temperatures, 21
Motion, proper, of Messier 51, N.G.C. 5194; 311
———, ———, of N.G.C. 2264; 293
———, ———, of six planetary nebulae, 299
———, ———, of spiral nebula N.G.C. 4051; 305
———, ———, of very faint stars, 345
Multiplet intensities, in solar spectrum, 361
Nebulae, elliptical, distribution of luminosity, 131
———, planetary, proper motions of N.G.C. 6058, 6543, 6572, 6720, 6804, 6905; 299
———, spiral, proper motion of Messier 51, N.G.C. 5194; 311
———, ———, proper motion of N.G.C. 4051; 305
Objective, short-focus spectrographic, 229
Orbit, spectrographic, of RS Canum Venaticorum, 273
Parallactic motions, distribution, used to determine distribution of stellar absolute magnitudes, 329
Parallaxes, stellar, photographic determination with the 60- and 100-inch reflectors, 1
Pluto, positions, orbit, mass, 455
Radial velocities, distribution, used to determine distribution of stellar absolute magnitudes, 329

Radial velocity, of R Lyrae, 85
—— —, variations, of W Geminorum, U Aquilae, DT Cygni, 279
Radiation, lunar, 21
Spectra, band, evidence for existence of carbon isotope of mass 13, 251
———, of europium, gadolinium, terbium, dysprosium, holmium, temperature classification, 373
———, of long-period variable stars, behavior of bright lines, 177
———, of ten bright-line stars of classes B and A, 315
Spectral energy-curve, of sun-spots, 121
Spectrographic objective, Rayton short-focus, 229
Spectrohelioscope, work, 55
Spectrum, of columbium, temperature classification, 441
———, solar, multiplet intensities, 361
Star clusters, proper motion of N.G.C. 2264; 293
Stars, bright-line, of classes B and A, spectra, 315
———, Cepheid variable, radial-velocity variations of W Geminorum, U Aquilae, DT Cygni, 279
———, distribution of absolute magnitudes, 93, 329
———, faint, proper motion, 345
———, K- and M-type, distribution of absolute magnitudes, 105, 335, 467
———, long-period variable, behavior of bright spectral lines, 177
———, variable, photometric and spectrographic orbits of TT Aurigae, 481
———, ———, radial velocity of R Lyrae, 85
———, ———, spectrographic orbit of RS Canum Venaticorum, 273
———, ———, spectrographic study of U Sagittae, 235
Stellar parallaxes, photographic determination with the 60- and 100-inch reflectors, 1
Sun, multiplet intensities in spectrum, 361
Sun-spots, spectral energy-curve, 121
Temperature classification, of spectra of europium, gadolinium, terbium, dysprosium, holmium, 373
———, of spectrum of columbium, 441
Temperatures, lunar, 21
Terbium, spectrum, temperature classification, 373
Variable stars. *See* Stars, variable
Velocities, angular and linear peculiar, distributions used to determine distribution of stellar absolute magnitudes, 93
———, parallactic and peculiar, used to determine distribution of absolute magnitudes among K and M stars, 335, 467
———, peculiar, used to determine distribution of absolute magnitudes among K and M stars, 105
———, radial, distribution, used to determine distribution of stellar absolute magnitudes, 329
Velocity, radial, of R Lyrae, 85
———, ———, variations, of W Geminorum, U Aquilae, DT Cygni, 279

522 19 C28 V18

MOUNT WILSON OBSERVATORY CONTRIBUTION

INSERT BOOK
MASTER CARD
FACE UP IN
FRONT SLOT
OF S.R. PUNCH

MASTER CARD

UNIVERSITY OF ARIZONA
LIBRARY

GLOBE 901144-0

20001 006937307b